Synthesis and Biomechanistic Studies of Quinocarcin and Structural Analogs

Submitted by

Mark Edward Flanagan

Department of Chemistry

In partial fulfillment of the requirements

for the degree of

Doctor of Philosophy

Colorado State University

Fort Collins, Colorado

Spring, 1995

Colorado State University

March 6, 1995

WE HEREBY RECOMMEND THE DISSERTATION PREPARED UNDER OUR SUPERVISION BY MARK E. FLANAGAN ENTITLED "SYNTHESIS AND BIOMECHANISTIC STUDIES OF QUINOCARCIN AND STRUCTURAL ANALOGS" BE ACCEPTED AS FULFILLING IN PART THE REQUIREMENTS FOR THE DEGREE OF DOCTOR OF PHILOSOPHY.

Graduate Research Committee Members

ADVISER

DEPARTMENT HEAD

ABSTRACT OF DISSERTATION

SYNTHESIS AND BIOMECHANISTIC STUDIES OF QUINOCARCIN AND STRUCTURAL ANALOGS

The formal total synthesis of the antitumor antibiotic quinocarcin is presented. The synthesis is characterized by a novel NBS oxidative azomethine ylide cycloaddition reaction for the diastereoselective construction of the tetracyclic framework of this substance.

A novel mechanism for the reduction of molecular oxygen that results in the O_2-dependent cleavage of DNA by quinocarcin, tetrazomine and synthetic structural analogs is presented. The results are discussed in the context of a redox self-disproportionation of the oxazolidine moieties of these compounds which produces superoxide by a previously unrecognized mechanism discovered herein.

Stereoelectronic control elements of superoxide production have been elucidated through the use of structural analogs prepared by total synthesis. The synthesis of a structurally less complex water soluble analog of quinocarcin which exhibits most of the physical properties associated with the parent compound is presented. By covalently attaching known DNA binding molecules to this substance, the ability to vary the mechanism and DNA-cleavage specificity of this compound has been demonstrated and is presented herein along with a proposed binding model derived from molecular mechanics.

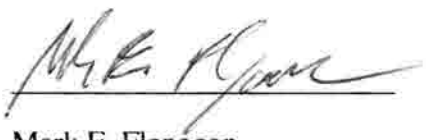

Mark E. Flanagan

Department of Chemistry

Colorado State University

Fort Collins, Colorado 80523

Acknowledgments

The author would like to take this opportunity to thank the faculty and staff of the Department of Chemistry, Colorado State University for supporting him during his tenure as a graduate student. The author would like to personally thank Mr. Donald Dick and Dr. Chris Rithner of the Central Instrument Facility (Department of Chemistry) for mass spectral data and NOE experiments. Also to be acknowledged are the author's thesis committee members for their involvement in his graduate career at Colorado State University. A special token of gratitude is extended to Prof. Frank R. Stermitz and Prof. Robert Woody for taking the time out of their busy schedules to do such a thorough and professional job in critiquing this manuscript. The author would also like to thank Prof. Marc M. Greenberg, Prof. Albert I. Meyers and Dr. Stephen Marburg (Merck & Co., Inc.) for the important role they played in helping him secure a postdoctoral position and funding. The following other faculty members are also acknowledged: Prof. Samuel J. Danishefsky (Memorial Sloan Kettering) for providing authentic comparison spectra of the methyl ester of synthetic quinocarcinamide; Prof. Jack R. Norton for providing access to facilities for manipulating $^{18}O_2$; and Prof. Tony K. Rappe' for performing molecular mechanics calculations on synthetic quinocarcin analogs.

The author would like to thank the Kyowa Hakko Kogyo Co., Ltd. and the Yamanouchi Pharmaceutical Co. for their generous gifts of natural quinocarcin and tetrazomine used in these studies.

The author wishes to extend a special token of gratitude to all of his colleagues (past and present) in the Williams research group for their friendship and for creating an interesting and stimulating work environment. The following individuals made significant contributions to this body of work through direct experimental input and/or helpful scientific discourse: Ms. Tricia L. Cecil, Dr. Timothy Cushing, Dr. Paul P. Ehrlich, Dr. Andrew Fray, Ms. Renee Gallegos, Dr. Tomasz Glinka, Dr. Richard H. Hutchings,

Dr. Gregory F. Miknis, Dr. Mathew Peterson, Mr. Scott R. Rajski, Mr. Samuel B. Rollins, Mr. Steven M. Rubenstein, Dr. Peter J. Sinclair (Merck & Co., Inc.) and Mr. Tracy N. Tippie.

The author would like to pay a special thanks to Prof. Robert M. Williams for providing laboratory space and maintaining an intellectual environment conducive to independent thought and creativity. The author also acknowledges the support that Prof. Williams has given him over the years which has set the foundation for a challenging and potentially rewarding career in chemistry.

Finally, the author would like to thank his family, in particular his father and mother Mr. and Mrs. Edward J. Flanagan for their support and for always believing in him and his abilities. Without their unremitting patience and encouragement none of this work would have been possible.

...This manuscript is dedicated to my loving wife Diana and daughter Natalie for their constant support, encouragement and inspiration which helped make this work possible. Thank you.

Table of Contents

Table of Contents Continued...

List of Figures, Schemes and Tables

Schemes Page

Tables Page

Chapter 1
Quinocarcin and Related Compounds

The naphthyridinomycins, bioxalomycins, saframycins, quinocarcins and tetrazomine constitute an important, structurally related group of antitumor antibiotic alkaloids produced by *Actinomycetes* microoganisms. These compounds are characterized by a tetracyclic core containing a bicyclic piperazine ring system. In spite of these basic similarities, this family of compounds exhibits a great diversity of structural features which is, at least in part, responsible for the broad range of physical properties and biological activities observed for these substances.

The antitumor activity displayed by these compounds results from their ability to inhibit nucleic acid synthesis and/or oxidatively damage these macromolecular targets. All of these materials have been proposed to associate with DNA *in vivo* (non-covalently or covalently), rendering the DNA template unsuitable for replication, thereby creating a cytotoxic state. Like most antitumor agents, the members of this family of compounds suffer from non-specific cytotoxicity problems which undermine their efficacy as chemotherapeutic treatments. As a result, efforts are underway in a number of research groups to: (1) better understand the mechanism by which these compounds inflict cellular damage on cancerous tissues; (2) elucidate sources of non-specific toxicity to healthy cells; and (3) develop new drugs, synthetically or semi-synthetically so as to attenuate undesirable side effects, producing more selective and less toxic materials.

Much of the discussion over the following chapters involves the elucidation of a mechanism by which the title compound and tetrazomine cause oxidative damage to DNA (*in vitro*), which is an attribute that *may* be associated with the non-specific host toxicity of these substances. Through the use of synthetic chemistry, structural analogs of these

compounds have been prepared. From examination of the physical properties of these synthetic materials, structural features of quinocarcin which give rise to this DNA-damaging potential have been discovered, along with preliminary means to attenuate and/or more specifically direct this activity. Additionally, a new synthetic approach to access advanced intermediates toward the total synthesis of quinocarcin will be presented.

The remainder of the information in this chapter is separated into three sections as follows: the first section is intended to present a broad overview of the physical characteristics exhibited by the members of this family of compounds, indicating features of the individual molecules important to their biological activities; the second section provides a review of the major synthetic efforts toward the total synthesis of quinocarcin; and the last section includes a presentation of the efforts to prepare semi-synthetic derivatives of quinocarcin with improved chemotherapeutic efficacy.

1.1. Physical Properties/Structure-Reactivity Relationships

Naphthyridinomycin (**1**) is characterized by a substituted quinone A ring and the bridged oxazolidine functionality between C-13b and C-4. Naphthyridinomycin is a ruby red crystalline compound produced by *Streptomyces lusitanus*.[1] The structure of naphthyridinomycin was determined by x-ray analysis by Sygusch, *et al.* in 1974 and later (1975) revised to the structure depicted in Figure 1 (**1**).[2] This compound exhibits broad spectrum antibiotic activity against both gram-negative and gram-positive. The promising antitumor activities exhibited by both naphthyridinomycin and cyanocycline A (**2**) have been proposed to result primarily from inhibition of DNA synthesis.[3] This proposal was based on data demonstrating the ability of these compounds to cause 50% inhibition of incorporation of tritiated thymidine into *E. coli* DNA suggesting inactivation of DNA-polymerase as a likely mode of action. Despite these promising biological activities, though, naphthyridinomycin has proven too toxic for clinical use.

Figure 1. The naphthyridinomycins

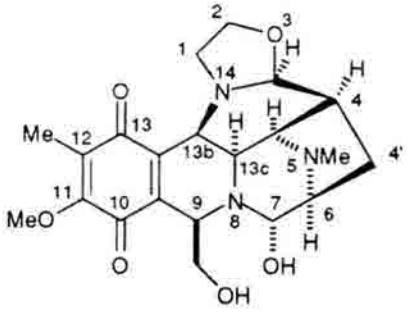

Naphthyridinomycin, **1**

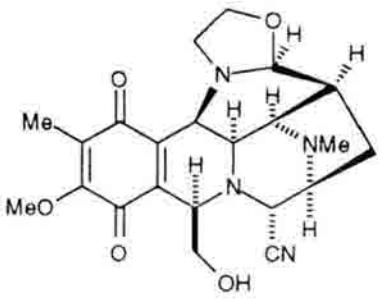

Cyanocycline A, **2**

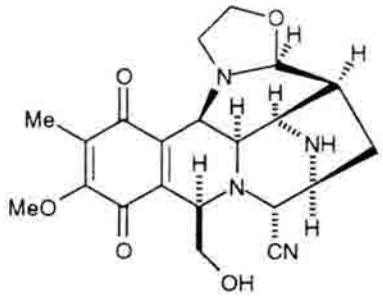

Cyanocycline B, **3**

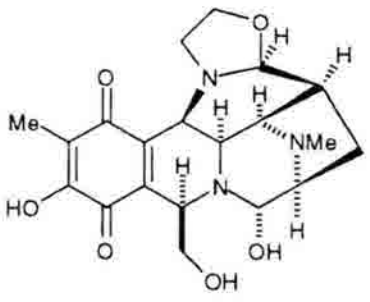

SF-1739 HP, **4**

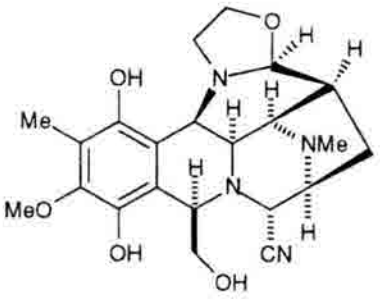

5a

Cyanocycline A, which differs from naphthyridinomycin by the cyano group at C-7 is three times less toxic than **1**.[1] This substance still retains significant, broad spectrum antibiotic activity in addition to strong antitumor activity in *in vitro* and *in vivo* assays against various tumor cell lines.[4] The cyano group is thought to provide stability to the

molecule, therefore attenuating non-selective host toxicity of this substance as compared to **1**. It has also been proposed that the cyano group of **2** may assist in the passage of the compound through the cell membrane, but comes off before interacting with DNA.[5] In doing so, iminium **6** would be generated (Scheme 1) which is believed to be the species responsible for cytotoxicity *via* DNA-alkylation. As will be seen throughout this class of

Scheme 1. Proposed DNA-alkylation mechanism for **1** and **2**

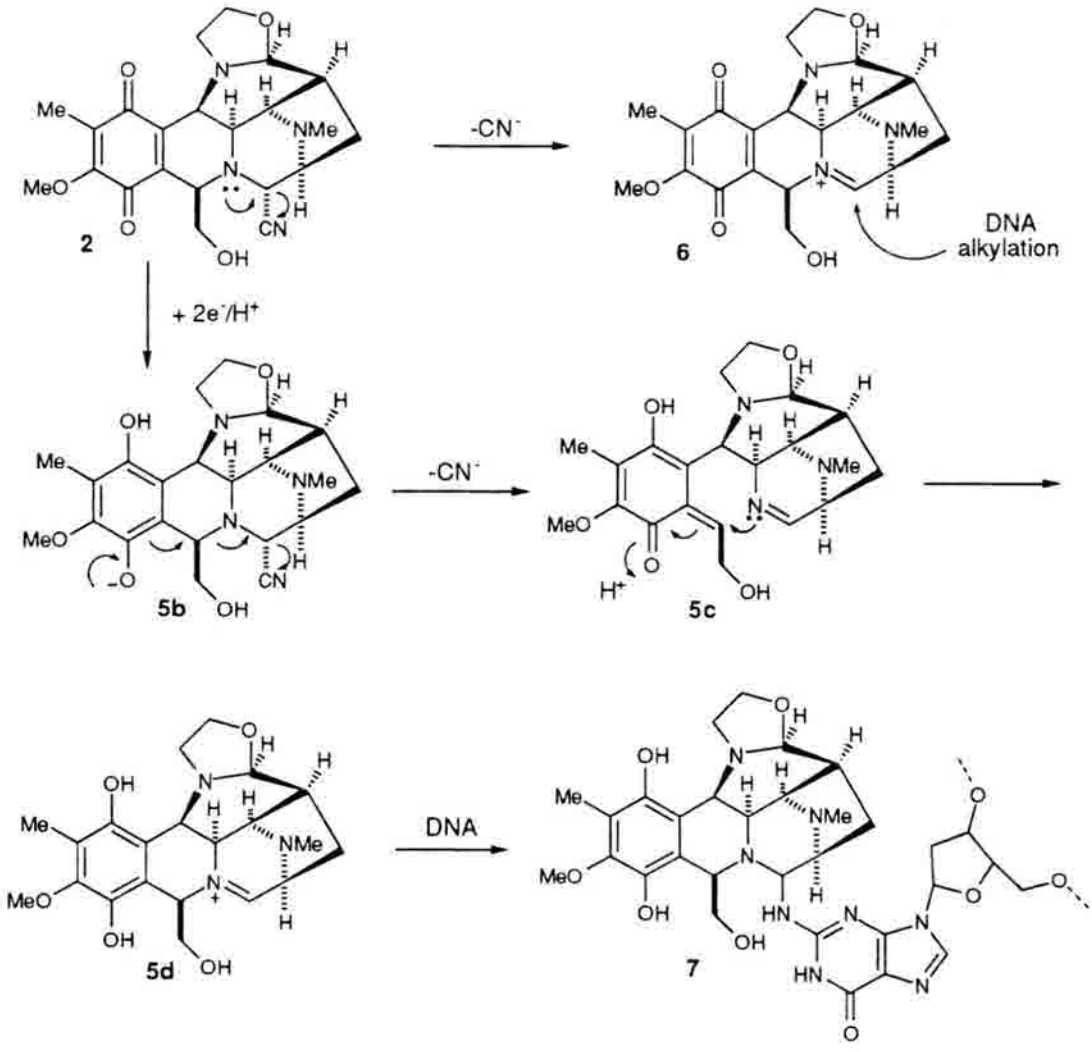

compounds, the oxidation state and substituents on C-7 play a principal role in the biological activities exhibited by these substances.

Both of these compounds (**1** and **2**) have been shown to be more potent antitumor agents if first reduced as illustrated in Scheme 1.[3a] This process is likely to involve the intermediacy of hydroquinone **5b** (in the case of **2**), which is believed to facilitate the expulsion of cyanide resulting in more efficient formation of iminium **5d**. Experiments in which DNA was incubated with radioactively labeled **1** and **2** showed only small amounts of covalently bound material following dialysis. However, when these compounds were first reduced, substantial irreversible binding of the drugs was consistently observed.[5] Similar mechanisms involving the bioreductive activation of quinone moieties to facilitate DNA alkylation have been proposed for nalidixic acid[6] and mitomycin C.[7]

Cyanocycline B (**3**) which is derived form *N*-desmethylnaphthyridinomycin and SF-1739 (**4**), inwhich the methoxy at C-11 of **1** is replaced with a hydroxyl group, are compounds structurally related to **1** and **2**. However, little has been reported concerning their biological activities. Hydroquinone **5a** has not received extensive evaluation, but would be expected to display increased activity compared to **1** and **2** for reasons previously discussed.

Bioxalomycins α1, α2, β1 and β2 (**8** - **11**, Figure 2) were recently isolated from the fermentation broths of *Streptomyces viridostaticus* and in preliminary antimicrobial and antitumor assays have exhibited potent activity.[8] The bioxalomycins bear striking similarities to naphthyridinomycin which calls into question the natural structures of these substances. The bioxalomycins are characterized by the presence of the C-7, C-9 oxazolidine moiety, but resemble the naphthyridinomycins by all other physical measurements. The question of whether the bioxalomycins are the true natural forms of these antitumor antibiotics was recently raised by Ellestad and coworkers.[8] Using a mildly

acidic isolation protocol, the Ellestad group observed that the primary isolate from *Streptomyces viridostaticus* was bioxalomycin α2 (**9**), with a small amount of β2 (**11**) also

Figure 2. The bioxalomycins

Bioxalomycin α1, **8**

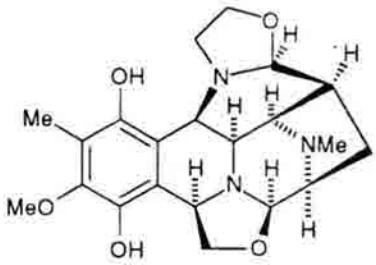

Bioxalomycin α2, **9**

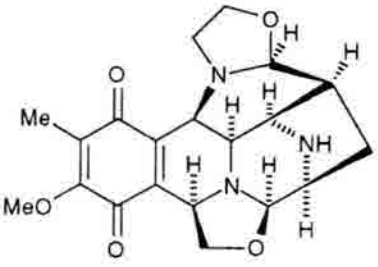

Bioxalomycin β1, **10**

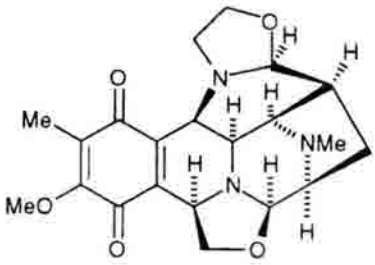

Bioxalomycin β2, **11**

being produced. When the same isolation procedure was employed with fermentation broths of *Streptomyces lusitanus* (the *Streptomyces* strain from which the naphthyridinomycins were originally reported to be isolated[1]), the Ellestad group isolated α2 (**9**) and β2 (**11**), with β2 being the primary isolate. The crucial observation however,

was that no naphthyridinomycins (oxazolidine ring-opened adducts) were afforded by these broths. It has been shown that cyanocycline A can be prepared semi-synthetically from naphthyridinomycin.[4b] Similar results were obtained upon reaction of β2 with sodium cyanide.[8] Since many antibiotic isolation procedures involve cyanide- containing buffers,

Figure 3. The Saframycins

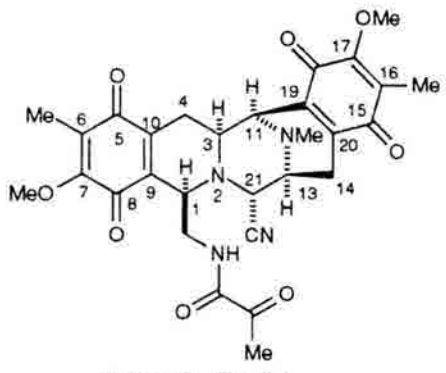

Saframycin A, **12**

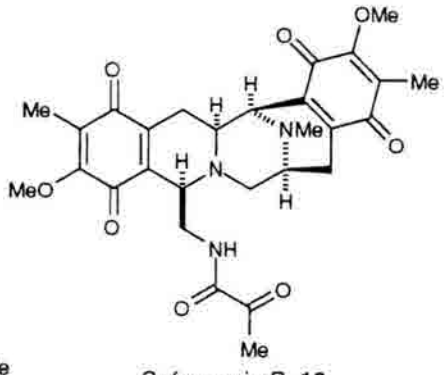

Saframycin B, **13**

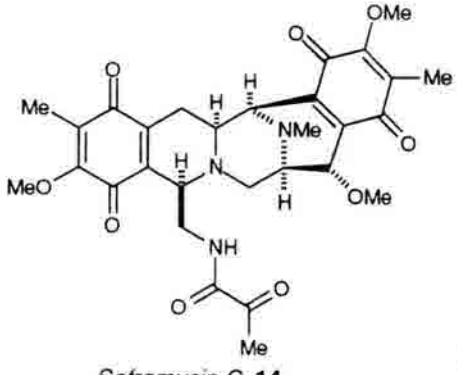

Saframycin C, **14**

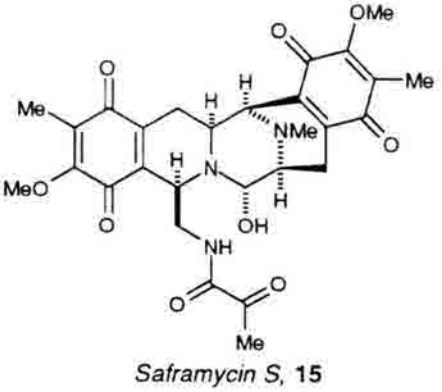

Saframycin S, **15**

these observations suggest that cyanocycline A and B may actually be derived from β2 and β1 respectively during isolation. Taken together, these results support the Ellestad hypothesis that the bioxalomycins are the natural forms of these compounds and that naphthyridinomycin and the cyanocyclines are artifacts of the isolation procedures employed. Furthermore, it has also been suggested that the original structure of naphthyridinomycin, elucidated by x-ray analysis, may actually have resulted from a transitory effect of the highly acidic isolation protocol (0.1 N HCl) used to obtain this substance. These questions and further biological studies concerning these new and novel antitumor antibiotics are currently under investigation.

Saframycin A (**12**) is an antitumor antibiotic produced by *Streptomyces lavendulae* and is characterized by the [3.3.1] bicyclic C, D ring system and twin quinone moieties.[9] Saframycin A exhibits broad antimicrobial activity and strong antitumor activity against L1210 and P388 leukemias and Ehrlich's sarcoma. Antitumor assays with L1210 leukemia cells indicate inhibition of nucleic acid synthesis to be the primary mode of action.[10,11] Similar to the naphthyridinomycins, DNA alkylation has been invoked in this process and an analogous mechanism to that shown in Scheme 1, involving bioreductive activation, has been proposed for saframycin A. Reactions of radiolabeled saframycin A with DNA show a covalent association of the label with the DNA over time. On the other hand, saframycin A labeled with ^{14}C-cyanide showed an increase in radiolable dispersion into solution when incubated with DNA under the same conditions, pointing to C-21 (saframycin A numbering) as the biologically relevant functional group.[10]

The structurally similar saframycins B (**13**) and C (**14**) have also been shown to associate with DNA in the minor groove and inhibit DNA replication, although to a much lesser extent than that observed for saframycin A. The diminished activity of these compounds as compared to saframycin A, coupled with the lack of the cyanide leaving

group at C-21, again points to this functional group as being critical for DNA-alkylation and the ensuing biological activity observed for saframycin A.

Saframycins A and C have also been shown to cause oxidative damage to supercoiled plasmid DNA which is dependent upon bioreductive activation.[11] Similar oxidative DNA-cleavage activity has been observed for numerous quinone containing compounds and is well recognized to be associated with semiquinone radical-mediated reduction of molecular oxygen. Reduced oxygen species such as hydroxyl radical are well documented to cause oxidative lesions to DNA. The subject of oxidative damage to DNA will be discussed in depth in Chapter 4, including proposed mechanisms of O_2 activation by saframycin A.

Quinocarcin (**16**) is a natural secondary metabolite produced by *Streptomyces melanovinaceus* and is the simplest member of this class of antitumor agents.[14] Quinocarcin has been shown to display weak antimicrobial activity against several Gram-positive microbes but is inactive toward Gram-negative bacteria. As its citrate salt, quinocarcin (named quinocarmycin citrate or KW2152) displays promising antitumor activity against several lines of solid mammalian carcinomas including St-4 gastric carcinoma; Co-3 human colon carcinoma; MX-1 human mammary carcinoma; M5076 sarcoma; B16 melanoma and P388 leukemia.[15] This substance and semi-synthetic derivatives discussed later in this chapter are currently under evaluation in human clinical trials by the Kyowa Hakko Kogyo Co. Recently, the structurally related antitumor antibiotic tetrazomine (**20**) was isolated from *Saccharothrix mutabilis* subsp. *chichijiimaensis* and is reported to display good antimicrobial activity against both Gram-positive and Gram-negative organisms in the 0.78-50 μg/mL range and also shows potent activity towards P-388 and L1210 leukemia *in vitro*.[16] Additionally, **20** showed promising activity against P388 leukemia *in vivo*.

Figure 4. The quinocarcins and tetrazomine

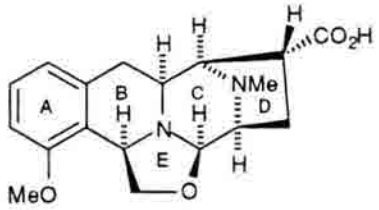

Quinocarcin, DC-52, **16**

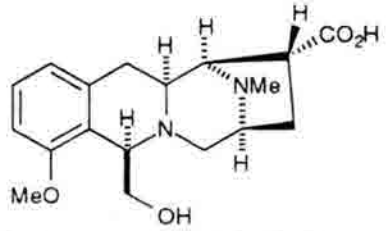

Quinocarcinol, DC-52-d, **17**

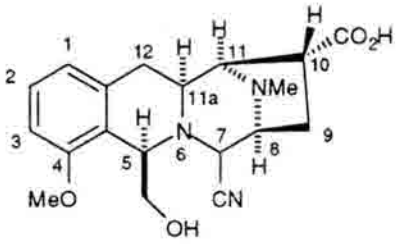

DX-52-1, **18**

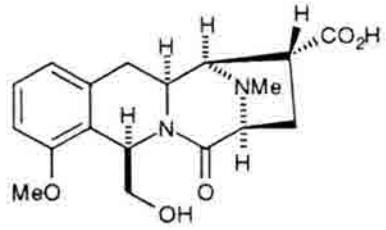

Quinocarcinamide, **19**

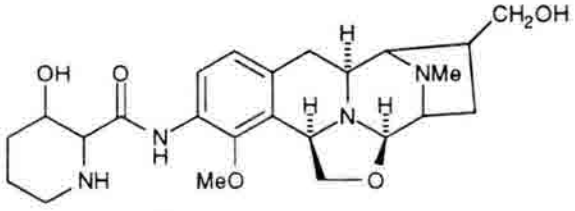

Tetrazomine, **20**

Interest in quinocarcin (**16**) was stimulated by a report by Tomita, *et al.* that recorded the remarkable observation that **16** cleaves plasmid DNA in an O_2-dependent fashion that was reported: (1) to *not* be stimulated by the addition of metal ions (Fe^{2+} or

Cu^{2+}); (2) to be stimulated by dithiothreitol; (3) to be inhibited by oxygen free radical scavengers such as methanol, *tert*-butanol, α-tocopherol,β-carotene and; (4) to be inhibited by superoxide dismutase (SOD) and catalase.[14a] Quinocarcin blocks RNA synthesis in preference to DNA and protein synthesis in P388 leukemia cells. On the other hand, in *Bacillus subtilis*, quinocarcin inhibited [^{3}H] thymidine incorporation suggesting inhibition of DNA polymerase; therefore, DNA synthesis is thought to be preferentially inhibited in *Bacillus subtilis*. It has been proposed that quinocarcin alkylates DNA in the minor groove through the ring-opened form of the oxazolidine in a similar manner to that proposed for **1** and **12**.[17] Indirect support for the involvement of the oxazolidine ring in the above context comes from the lack of antitumor activity displayed by quinocarcinol (**17**, DC-52-d) which is co-produced with **16** by *Streptomyces melanovinaceus*. The oxazolidine moieties of quinocarcin and tetrazomine also appear to be associated with the capacity of these compounds to cause the oxidative damage to DNA as observed by Tomita.[14a] A proposed mechanism for this behavior including discussion and full supporting details will be presented in Chapter 4.

As will be discussed in depth in Chapter 4, quinocarcinol (**17**) and quinocarcinamide (**19**) have been found to be produced from the anaerobic decomposition of quinocarcin. Since **17** is co-produced with **16** by *Streptomyces melanovinaceus*, it is interesting to question its creation as arising by a genetically-encoded biosynthetic pathway, or by a secondary and endogenous microbial reduction. The ability of these substances (**16** and **20**) to undergo spontaneous redox disproportionations is suspected as providing the thermodynamic driving force behind the ability of these compounds to activate molecular oxygen, ultimately leading to the oxidative damage of DNA.

1.2. Synthetic Studies Toward the Total Synthesis of Quinocarcin

While quinocarcin is considered to be the simplest member of this class of antitumor antibiotics, it does possess a number of challenging structural attributes causing many researchers to pursue its synthesis. The highly unstable oxazolidine functionality of quinocarcin presents just one of the challenging obstacles to the synthetic preparation of this compound. Also of considerable interest are the six stereocenters that must be set in forming the B, C, D, E bicyclic ring system of quinocarcin.

The first attempted synthesis of quinocarcin was undertaken by Danishefsky, *et al.* Due to difficulties encountered in forming the oxazolidine ring of **16**, however, this synthesis was eventually reported as the total synthesis of (±)-quinocarcinol methyl ester.[18] In spite of these difficulties, this synthetic approach to the A, B, C, D tetracyclic core of quinocarcin was very effective and provided the first totally synthetic approach to both redox decomposition products produced by quinocarcin (**17** and **19**, Figure 4). Details of the semi-synthetic preparation of **17** and **19** from quinocarcin will be discussed in Chapter 4.

As outlined in scheme 2, starting from *m*-hydroxybenzaldehyde (**21**), reaction with allyl bromide produced allyl ether **22** in 93% yield. The Claisen rearrangement (N,N-dimethylaniline, 230°C) proceeded to afford the 1,2,3-substituted material (**23**) as the predominant product. Following methylation (NaH, MeI), the methoxy aromatic compound **23** was afforded in 84% yield from **22**. Addition of cyanide to the aldehyde functionality of **23** followed by lithium aluminum hydride reduction produced the corresponding amino alcohol which was sequentially protected affording **24** in 68% overall yield from **23**. At this point, the double bond of **24** was isomerized into conjugation upon reaction with Pd-$(MeCN)_2$ generating **25** as a 3.5:1 mixture of E/Z isomers. The very elegant tetrahydroisoquinoline-forming cyclization reaction was facilitated by reaction of **25**

Scheme 2. Danishefsky synthesis of (±)-quinocarcinol methyl ester

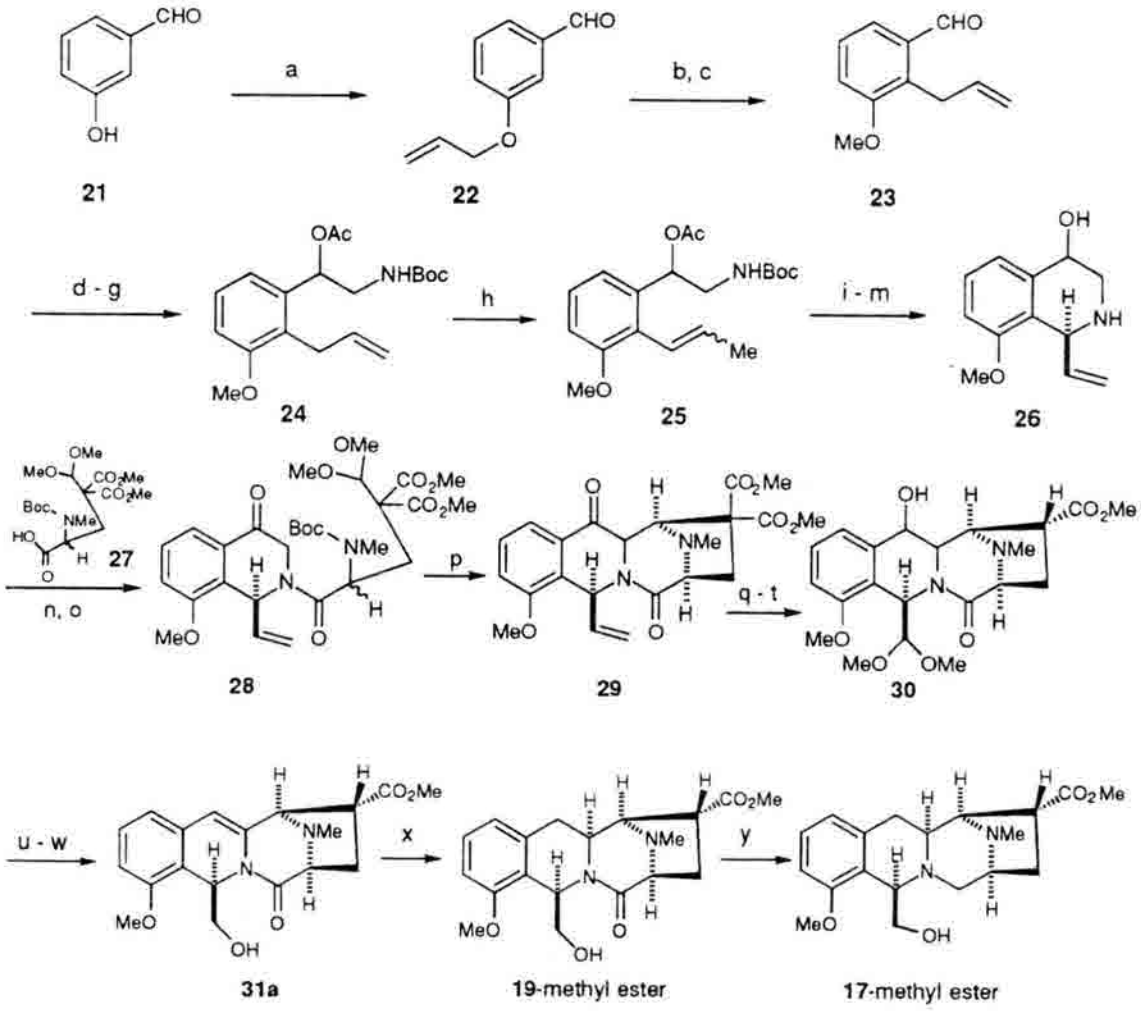

Key: (a) NaH, allyl bromide; (b) *N,N*-dimethylaniline, 230°C; (c) NaH, MeI; (d) TMS-CN, KCN, 18-crown-6; (e) $LiAlH_4$; (f) $(t\text{-}BuOCO)_2$; (g) Ac_2O, DMAP; (h) $PdCl_2\text{-}(MeCN)_2$; (i) *N*-phenylselenophthalimide, CSA; (j) mCPBA; (k) $HNiPr_2$, Δ; (l) TFA; (m) K_2CO_3, methanol; (n) BOP-Cl, Et_3N; (o) DMSO, $(COCl)_2$, Et_3N, -78°C; (p) $BF_3\text{-}Et_2O$, chloroform, reflux; (q) zinc borohydride, dichloromethane; (r) OsO_4, $NaIO_4$, dioxane/H_2O; (s) trimentyl orthoformate; (t) NaCN, DMSO, 140°C; (u) TFA; (v) $Et_3NSO_2NCO_2Me$ (Burgess reagent); (w) $NaBH_4$, methanol; (x) Raney-Ni W2, H_2 (1600 psi), 60°C; (y) BH_3-THF.

with N-phenylselenophthalimide[19], whereupon sequential deprotections afforded the hydroxy-tetrahydroisoquinoline **26** in approximately 50% overall yield from **25**. Acylation of **26** with the racemic γ-carboxyglutamate derivative **27** was achieved by reaction of **26** and **27** in the presence of *bis*-(oxo-oxazolidonyl) phosphinic chloride (BOP-Cl) to furnish amide **28** as a mixture of diastereomers following Swern oxidation. The key cyclization reaction to produce the tetracyclic piperazine framework of quinocarcin was then achieved by reaction of **28** with BF_3-Et_2O affording **29**. It was found that only the diastereomer of **28** exhibiting the quinocarcin relative stereochemical configuration underwent cyclization, the other diastereomer being inappropriately oriented for the required ring closure. Reduction of the aryl ketone followed by oxidation of the olefin (OsO_4, $NaIO_4$) and acetal protection of the resulting aldehyde then allowed for the selective decarboxylation (NaCN, DMSO, 140°C, 20 min) at C-10 affording the exo-carboxymethyl compound **30**. Dehydration of **30** with Burgess reagent ($Et_3NSO_2NCO_2Me$) followed by sequential deprotection and reduction of the aldehyde afforded the unsaturated product **31** in 43% yield from **30**. Reduction of the double bond occurred cleanly upon reaction of **31** with H_2 (1600 psi) and W2 Raney-Ni (60°C, 5 h) producing lactam **32** as a single diastereomer, the result of selective reduction from the α-face of **31**. Over-reduction of the amide (**32**) in efforts to form the oxazolidine *via* reduction to the aldehyde oxidation state yielded quinocarcinol methyl ester.

In an effort to circumvent some of the problems encountered by Danishefsky, researchers devised alternate approaches to forming the quinocarcin oxazolidine. One such strategy, reported by Williams *et al.*, involved the intramolecular condensation of an aldehyde with an amino alcohol, generating the oxazolidine ring in the final step of the synthesis.[21] To test this idea, the model study illustrated in Scheme 3 was conducted. Starting with 2-bromoanisol, lithiation followed by addition of (N-methoxy-N-methyl)-

Scheme 3. Williams C-11a *anti*-analog synthesis

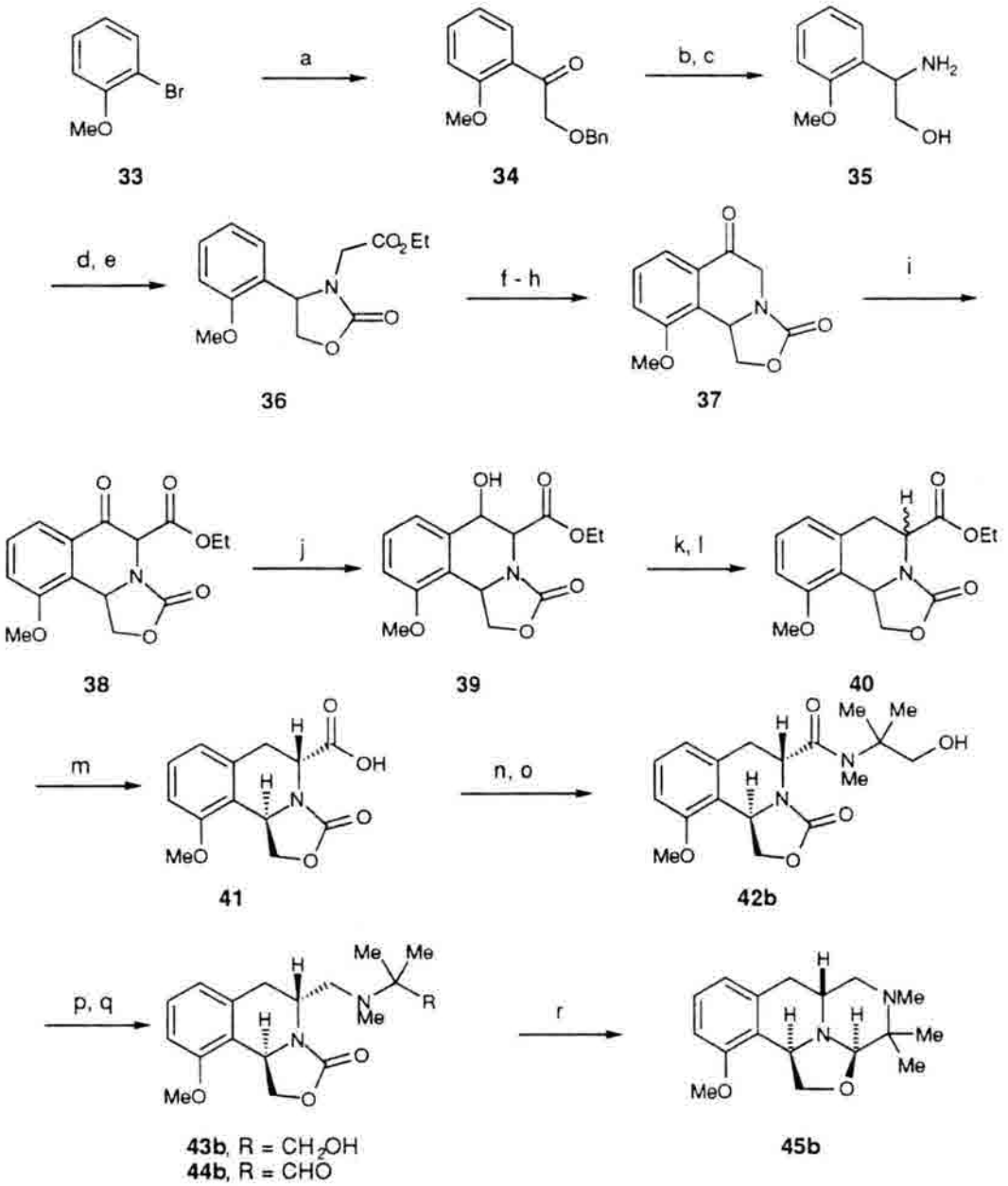

Key: (a) *n*-BuLi, (MeO)MeN(O)CCH$_2$OBn; (b) NH$_4$OAc, NaBH$_3$CN; (c) Pd/C, H$_2$; (d) ethyl bromoacetate; (e) carbonyldiimidazole; (f) LiOH, ethanol; (g) SOCl$_2$, PhH, reflux; (h) AlCl$_3$, Cl$_2$CH$_2$CH$_2$Cl$_2$; (i) KN(Me$_3$Si)$_2$, EtO$_2$CCN; (j) NaBH$_3$CN, AcOH; (k) Ph$_3$P, CCl$_4$, Et$_3$N; (l) Pd/C, H$_2$; (m) LiOH, ethanol; (n) SOCl$_2$, PhH, reflux; (o) N-methyl 2-amino-2-methyl-1-propanol; (p) BH$_3$-THF; (q) DMSO, (COCl)$_2$, Et$_3$N, -78^{o}C; (r) LiOH, ethanol, reflux.

benzyloxy acetamide furnished ketone **34** in 90% yield. Reductive amination followed by removal of the *O*-benzyl group generated amino alcohol **35** in 53% yield on the two steps. This amino alcohol was to eventually be the moiety involved in the oxazolidine-forming condensation reaction in the final step of the synthesis. However, for the duration of the synthesis, this group was protected as the oxazolidinone. Reaction of **35** with ethyl bromoacetate followed by carbonyldiimidazole afforded oxazolidinone ethyl ester **36** in 58% yield. Saponification and acid chloride formation with thionyl chloride produced the precursor to the crucial intramolecular Friedel-Crafts acylation ($AlCl_3$, tetrachloroethane) which proceeded in 65% yield affording isoquinolone **37**.[20] C-Homologation of the enolate of **37** with ethyl cyanoformate furnished β-ketoester **38** which was subsequently reduced to the β-hydroxy ethyl ester (**39**) by reaction with sodium cyanoborohydride. Elimination to form the intermediate α,β-unsaturated ethyl ester was accomplished by reaction of **39** with triphenylphosphine, carbontetrachloride and triethylamine. Palladium-catalyzed hydrogenolysis of this material produced two diastereomers of **40** in a 10:1 ratio (*syn* / *anti*). The desirable stereochemical outcome for this hydrogenation was precluded by the subsequent saponification reaction which afforded only the undesired epimerized *anti*-carboxylic acid **41**. As a result, this approach would never prove amenable to the synthetic preparation of **16**. However, the synthesis of **44b** was continued in order to test the crucial oxazolidine forming final step. Condensation of **41** with *N*-methyl-2-amino-2-methyl-1-propanol was achieved *via* the acid chloride to afford amide **42b**. Reduction of the amide with BH_3-THF followed by Swern oxidation furnished the precursor (**43b**) to the penultimate oxazolidine-forming step. Closure of the C and E rings was achieved by reaction of **43b** with lithium hydroxide in refluxing ethanol which removed the oxazolidinone, furnishing compound **44b** in 25% yield.[21] Although the yield of this reaction was low, it did suggest that this methodology offered a viable means of quinocarcin oxazolidine construction.

The geminal dimethyl group at C-8 of **44b** was found to be necessary for product isolation. While the analogous cyclization with the methylene-containing substrate proceeded with initial product formation, the tetracyclic product was reported to quickly decompose upon silica gel purification. The stability provided by the geminal dimethyl group was proposed to prevent decomposition of the molecule *via* tautomerization of the ring-opened iminium form of the oxazolidine to the enamine.[21] A similar mechanism of decomposition for quinocarcin was not considered possible since tautomerization to the enamine for **16** would require formation of a bicyclic bridgehead double bond. This reasoning suggests that the bicyclic system inherent to the oxazolidine-containing compounds (bioxalomycins, quinocarcin and tetrazomine), may do little more than provide stability to the biologically important oxazolidine functional group such that this moiety can remain "intact" long enough for the compounds to interact with their macromolecular hosts.

Concurrent with the Williams work, Fukuyama and coworkers were pursuing a synthetic approach to quinocarcin which employed a similar oxazolidine-forming step toward the end of the synthesis. These efforts ultimately resulted in the first stereocontrolled total synthesis of (±)-quinocarcin (Scheme 4).[22] This synthesis is characterized by a key diastereoselective Pictet-Spengler reaction to form the tetrahydroisoquinoline portion of quinocarcin. Condensation of aldehyde **45** with the enolate of diketopiperazine **46**, followed by elimination, amminolysis and protection afforded **47**. Partial reduction of the amide carbonyl followed by acryliminium ion-mediated cyclization ($HgCl_2$, CSA, CH_3CN/H_2O) produced bicyclic monoketopiperazine **48** in 59% yield from **47**. Protection and installation of the aryl bromide yielded compound **49**. The bromine at the *para*-position mandates that only the desired regioisomer from the Pictet-Spengler step would be obtained. Following amide protection, partial reduction of the amide resulted in ring opening to pyrrolidine **50** upon treatment

Scheme 4. Fukuyama synthesis of (±)-quinocarcin

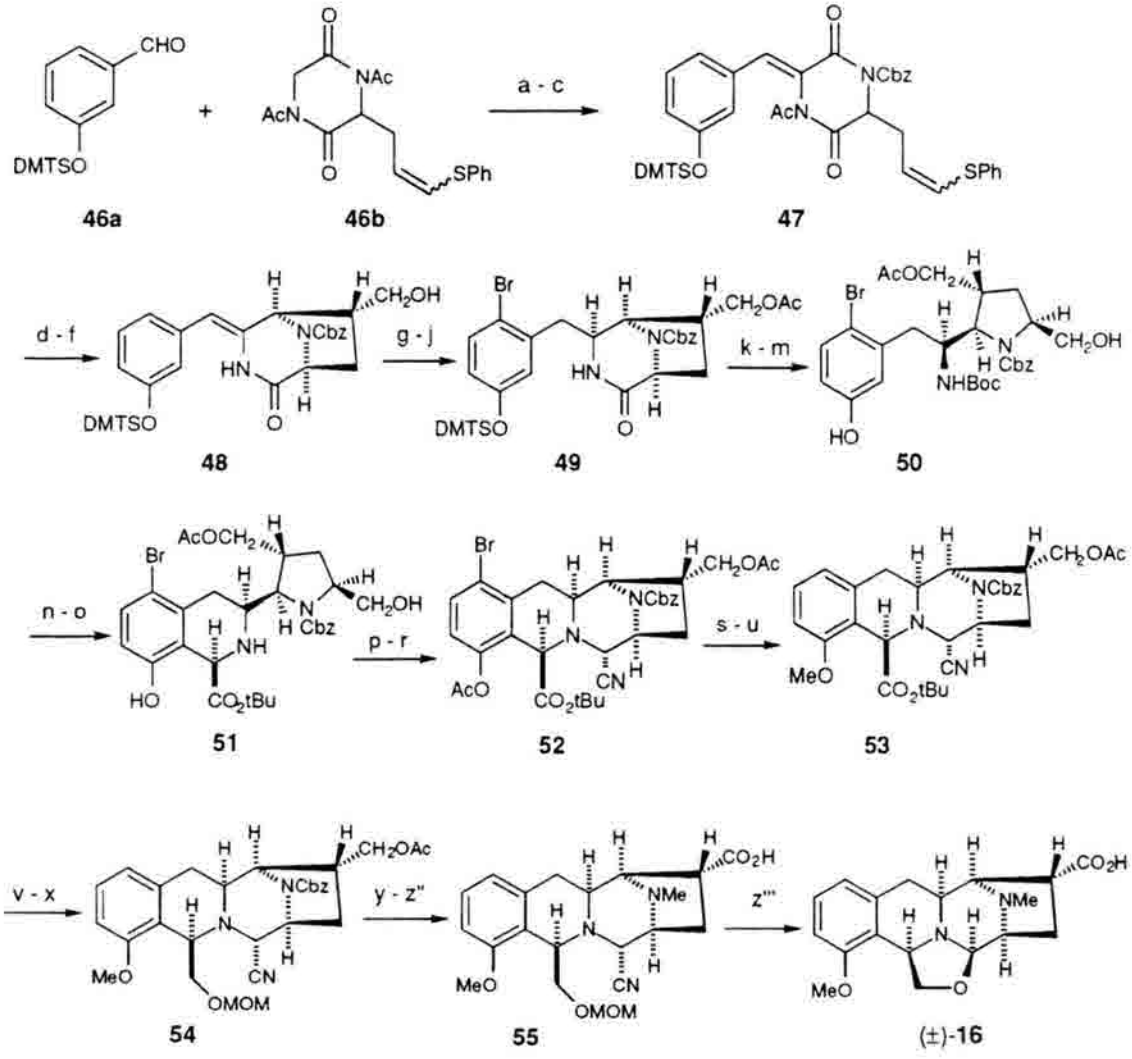

Key: (a) *t*-BuOK, THF; (b) NH_3, methanol; (c) Cbz-Cl, DMAP; (d) $NaBH_4$, methanol; (e) $HgCl_2$, CSA, $MeCN/H_2O$; (f) NaBH4, methanol; (g) Raney-Ni W2, H_2 (2000 psi), ethanol; (h) Cbz-Cl, $NaHCO_3$; (i) Br_2, dichloromethane; (j) Ac_2O, pyridine; (k) $(t\text{-BuOCO})_2$, DMAP; (l) $NaBH_4$, methanol; (m) *n*-Bu_4NF, THF; (n) TFA; (o) *t*-BuOCOCHO, methanol; (p) Ac_2O, K_2CO_3; (q) DMSO, $(COCl)_2$, Et_3N, -78°C; (r) Me_3SiCN, $ZnCl_2$; (s) $NaHCO_3$, methanol; (t) MeI, K_2CO_3, acetone; (u) Bu_3SnH, AIBN, PhH; (v) TFA; (w) *i*-BuOCOCl, Et_3N, dichloromethane; (x) MOM-Cl, Et_3N, dichloromethane; (y) 3 N NaOH, methanol; (z) Pd/C, H_2; (aa) MeI, *i*-Pr_2NEt; (bb) Jones reagent, acetone; (cc) Me_3SiCl, NaI, MeCN; $AgNO_3$, methanol/H_2O.

with *n*-Bu_4NF. Deprotection of the amine then allowed the crucial Pictet-Spengler reaction with *tert*-butyl glyoxylate to proceed, resulting in an 8:1 mixture of products displaying a preference for the diastereomer exhibiting the *syn*, quinocarcin stereochemistry (**51**).

From isoquinoline **51**, oxidation to the aldehyde under Swern conditions produced the cyclized hemi-aminal intermediate which was trapped as the cyano adduct (**52**). Rather than generate the oxazolidine at this point, it was considered beneficial to carry on the more stable amino nitrile for the duration of the synthesis, then form the E ring in the last step. Conversion to the aromatic methoxy group and reduction (Bu_3SnH, AIBN) of the aryl bromide afforded **53**. Following a series of transformations depicted in Scheme 4, carboxylic acid **55** was prepared, which served as the precursor to the final oxazolidine ring-forming step. Deprotection of the MOM ether generated DX-52-1 (**18**) *in situ*, whereupon addition of silver nitrate ultimately furnished (±)-**16** in 70% isolated yield.

The first asymmetric synthesis of (-)-quinocarcin was published by Garner, *et al.* in 1992 (Scheme 5).[23] This synthesis showcased azomethine ylide cycloaddition methodology developed specifically for the stereocontrolled synthesis of the quinocarcin pyrrolidine.[24] Starting with benzaldehyde derivative **56**, homologation *via* the α-methylthiosulfinylmethyl sulfide afforded carboxylic acid **57** in 66% yield. Formation of the Evans oxazolidinone[25] **58** followed by asymmetric azidation and reduction ($NaBH_4$) furnished aryl amino alcohol **59** in 58% yield (the Mosher amide of this material indicated >99% purity of a single enantiomer by NMR). Reaction of **59** with maleic anhydride followed by dehydration with acetic anhydride afforded maleimide **60** in 40% yield on the two steps. Reaction of **60** with methyl azide formed the triazoline intermediate which underwent a photo-induced rearrangement furnishing aziridine **61** in 89% yield from **60**. The key pyrrolidine-forming step then occurred *via* photo-induced dipole formation of **61** in the presence of chiral acryloyl sultam **62** affording the optically pure pyrrolidine cycloadduct as a result of double asymmetric induction.[26] The next step involved an

Scheme 5. Garner synthesis of (-)-quinocarcin

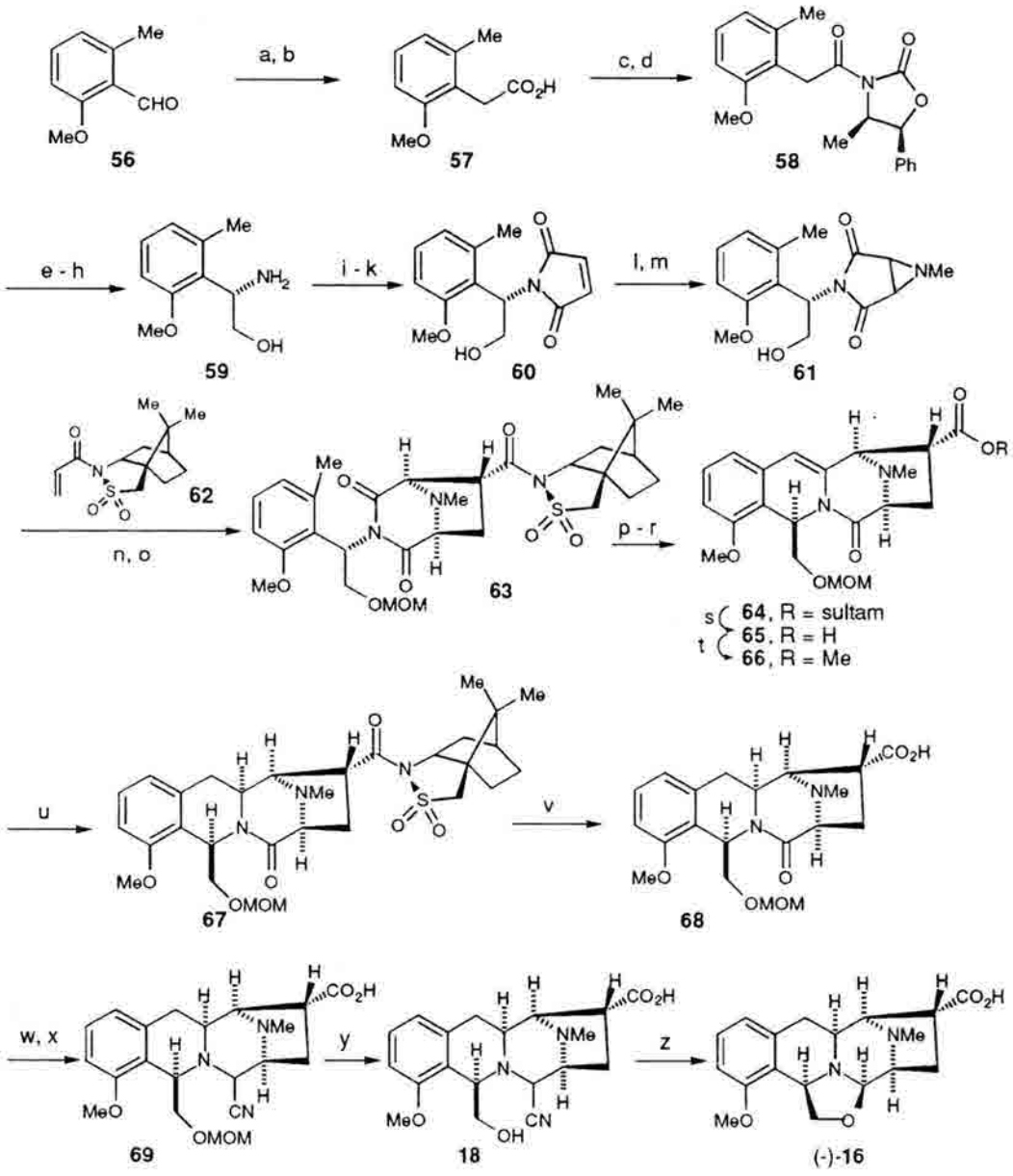

Key: (a) $MeSCH_2S(O)Me$, Triton B, THF; (b) HCl-Et_2O, reflux; (c) *t*-BuCOCl, Et_3N, THF; (d) lithium salt of oxazolidinone; (e) $KN(Me_3Si)_2$, THF, -78°C; (f) trisyl azide, AcOH; (g) $NaBH_4$, THF/H_2O; (h) Pd/C, H_2; (i) maleic anhydride; (j) Ac_2O, NaOAc, 120°C; (k) 5 N HCl-THF; (l) MeN_3, $PhCH_3$; (m) hν (Pyrex); (n) hν (2537Å), dioxane; (o) MOM-Cl, *i*-Pr_2NEt, dichloromethane; (p) NBS, chloroform, hν; (q) Ph_3P, chloroform; (r) *t*-BuOK, $HCONMe_2$, 120°C; (s) LiOH, THF/H_2O; (t) CH_2N_2, Et_2O-CH_2Cl_2; (u) Raney-Ni, H_2 (1400 psi), ethanol, 65°C; (v) LiOH, THF/H_2O; (w) Li/NH_3, THF, -33°C; (x) NaCN, H_2O; (y) Me_3SiCl, NaI, MeCN; (z) $AgNO_3$, methanol/H_2O.

unprecedented intramolecular imide olefination *via* the phosphonium ylide to generate olefin **64** as a single diastereomer. Rigorous structural assignment of **64** was secured through extensive NMR experiments (NOE, COSY) with methyl ester **66**. This material was prepared by saponification of sultam **64** followed by treatment of the intermediate acid (**65**) with diazomethane. Acid **68** was then accessed by reduction from the α-face (H_2 (1400 psi), Raney-Ni W2) furnished amide **67** as a single diastereomer. However, about 50% over-reduction of this substrate to the corresponding alcohol was observed. Amide **67** was then converted to acid **68** upon treatment with LiOH in THF/H_2O (30% yield from **64**).

At this point, Garner and coworkers faced the same problem of partial amide reduction of **68** as that originally faced by Danishefsky. To solve this problem, Garner again turned to methodology developed by Evans, *et al.* and employed in their total synthesis of cyanocycline A. Evans found that dissolving lithium reduction followed by trapping of the incipient hemi-aminal with cyanide effectively furnished cyanocycline A from the corresponding lactam.[27] Applying this methodology to intermediate **68**, Garner and coworkers were able to effect the analogous reaction, resulting in formation of compound **69** in moderate yield (56% yield). Removal of the MOM protecting group afforded DX 52-1 (**18**) which subsequently furnished (-)-quinocarcin upon treatment with silver nitrate.

The most recent synthesis of (-)-quinocarcin was reported[28] by Terashima, *et al.* This synthesis is characterized by a novel pyrrolidine synthesis starting from optically pure glutamic acid (Scheme 6). Pyrrolidine **74** was then coupled to the rest of the molecule and from this coupled product (**77**) to **16**, this synthesis closely resembles the racemic synthesis reported by Fukuyama, *et al.*

Pyrrolidine **74** was prepared as outlined in Scheme 6.[28a] Starting with (S)-glutamic acid (**70**), cyclization and reduction followed by a series of chemical manipulations afforded γ-lactam **71** in 16% yield from **70**. Diastereoselective alkylation of

71 generated lactam **72** in 61% yield. The hemi-aminal generated by partial reduction of **72** with sodium borohydride resulted in the diastereoselective condensation with cyanide to afford pyrrolidine **73**. Diisobutylaluminumhydride (DIBAL) reduction of this substance then furnished pyrrolidine **74** in 63% yield.

Separately, bromoanisole derivative **75** was lithiated and condensed with 4-*O*-benzyl-2,3-isopropylidine-D-threose to produce **76** following oxidation under Collins conditions (Scheme 7). The coupling of pyrrolidine **74** followed by Jones oxidation afforded compound **77** which spontaneously cyclized in the presence of ammonia to isoquinoline **78**. Perhaps the most noteworthy step in the Terashima synthesis is the

Scheme 6. Terashima synthesis of optically pure quinocarcin pyrrolidine

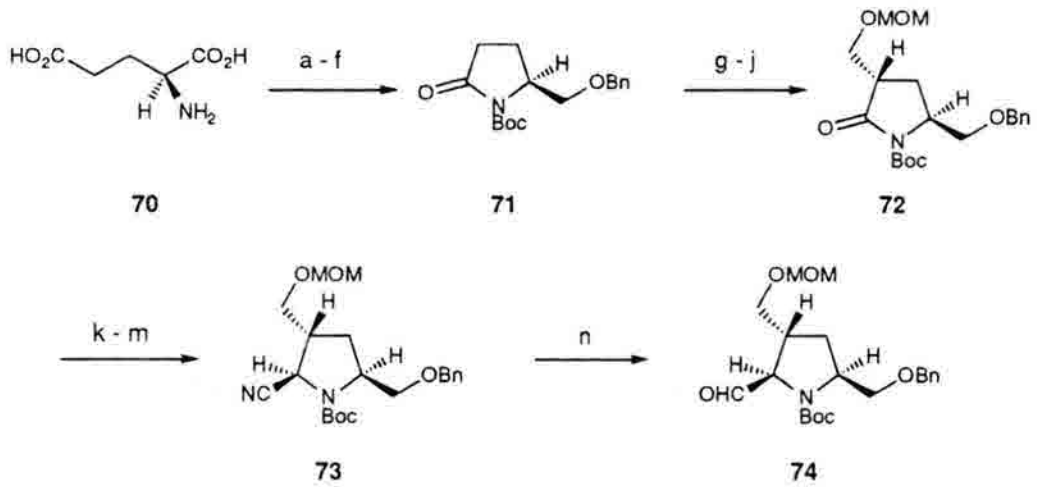

Key: (a) *p*-anisaldehyde, 2 N NaOH, $NaBH_4$; (b) $SOCl_2$, ethanol; (c) $LiBH_4$, ethanol-THF; (d) BnBr, NaH, DMF; (e) CAN, MeCN-H_2O; (f) $(t\text{-BuOCO})_2O$, DMAP, Et_3N, MeCN; (g) $(Me_2N)_2CHO^tBu$, 75°C; (h) 1 N HCl-THF; (i) $NaBH_3CN$, AcOH-THF; (j) MOM-Cl, *i*-Pr_2NEt, dichloromethane; (k) DIBAL, THF, -78°C; (l) PPTS, methanol; (m) Me_3SiCN, BF_3-Et_2O, dichloromethane; (n) DIBAL, $PhCH_3$, -78°C.

subsequent diastereoselective reduction (methanolic HCl, $NaBH_3CN$) of **78** to furnish tetrahydroisoquinoline **79** in 98% yield. From **79**, a series of chemical manipulations

Scheme 7. Terashima synthesis of (-)-quinocarcin

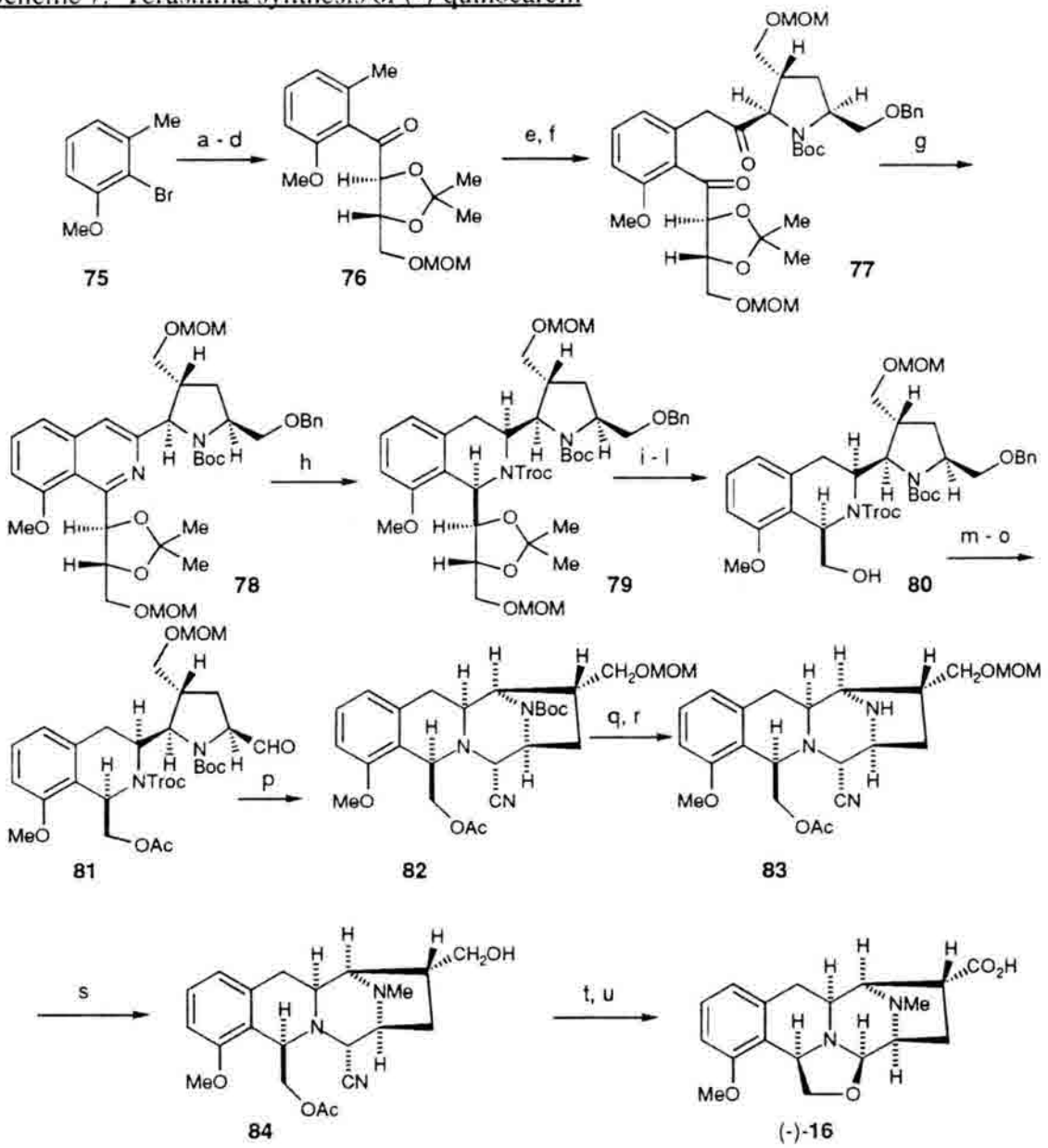

Key: (a) BuLi, -78oC, 4-O-benzyl-2,3-isopropylidine-D-threose; (b) Collins oxidation; (c) $Pd(OH)_2$, H_2, methanol; (d) MOM-Cl, *i*-Pr_2NEt, dichloromethane; (e) LDA, THF, -78^oC; TMEDA, **74**; (f) Jones oxidation; (g) 14 N NH_3, THF; (h) $NaBH_3CN$, 0.1 N HCl-methanol; (i) Troc-Cl, pyridine; (j) $FeCl_3$-SiO_2, chloroform; (k) $NaIO_4$, methanol-H_2O; (l) $NaBH_4$, methanol-H_2O; (m) Ac_2O, DMAP, pyridine; (n) Pd/C, H_2, EtOAc; (o) DMSO, $(COCl)_2$, Et_3N, -78^oC; (p) Zn, THF/AcOH/H_2O; (q) Me_3SiCN, $ZnCl_2$, dichloromethane; (r) TFA, dichloromethane; (s) 37% HCHO, $NaBH_3CN$, methanol; (t) Jones oxidation; (u) $AgNO_3$, methanol.

afforded compound **80** which was converted to amino nitrile **84** in an analogous manner to that described by Fukuyama. The final steps involved oxidation to the carboxylic acid under Jones conditions followed by treatment with silver nitrate, affording (-)-**16** in 76% yield from **84**.

As indicated, all of the syntheses described contain certain attractive features and key reactions. However, when examined in overall terms the net efficiency of these procedures is readily apparent. The Danishefsky synthesis, although not successful at producing quinocarcin could now be considered a formal synthesis since the problem of partial reduction of lactam **68** (Scheme 5) has now been solved by Garner *et al.* The Danishefsky synthesis is one of the more effective procedures for constructing the quinocarcin framework, accessing quinocarcinamide methyl ester and finally quinocarcinol methyl ester in 0.8% overall yield on 25 steps. The Fukuyama synthesis is the longest of the syntheses discussed in terms of steps. In spite of this fact though, the Fukuyama synthesis is the highest yielding procedure, generating (±)-quinocarcin in just over 2% yield on 29 steps. Of the asymmetric syntheses, the Garner procedure is clearly the most efficient. As discussed, the Terashima synthesis is highlighted by several attractive steps, such as the diastereoselective reduction of isoquinoline **78** to tetrahydroisoquinoline **79** in 98% yield (Scheme 7). The overall synthesis by Terashima, however, is precluded by the lengthy and low yielding pyrrolidine synthesis, producing pyrrolidine **74** in just 2.7% yield on 14 steps (Scheme 6). As a convergent synthesis, this approach generates optically pure (-)-quinocarcin in 0.02% overall yield on 35 steps. On the other hand, the Garner synthesis benefits from a highly efficient pyrrolidine forming step *via* an enantioselective cycloadditive strategy followed by a novel phosphonium ylide imide-olefination resulting in the rapid construction of the tetracyclic core of quinocarcin (Scheme 5). This synthesis subsequently accesses optically pure (-)-quinocarcin in 0.27% overall yield on 24 steps.

The formal synthesis presented in Chapter 3 is capable of accessing (±)-quinocarcin in 1.0% overall yield on 26 steps. Specific features of this synthesis will be discussed in detail in Chapter 3.

To date there has not been a reported synthesis of tetrazomine (**20**); a proposed synthesis will be presented at the end of Chapter 3. This proposed synthesis is an extension of the formal synthesis of (±)-quinocarcin presented in Chapter 3.

Antitumor Activity for Semi-Synthetic Derivatives of Quinocarcin

Like many antitumor antibiotics, quinocarcin suffers from non-specific toxicity problems which have halted further clinical trials for this substance. Since it is not known just what physical attributes of **16** impart this host toxicity, a great variety of structural modification strategies have been devised in an effort to prepare more efficacious chemotherapeutic drugs. Most of these approaches result in modifications of the A and E rings of quinocarcin. However, the first approach that will be discussed involves modifications of the D ring.

Evaluation of the drugs prepared in this section was based on their performance in two antitumor assays. Compounds exhibiting cytotoxicity in preliminary screens were first tested *in vitro* against HeLa S_3 cells and IC_{50} values assigned based on their abilities to inhibit the growth of these cells by 50%. Optimal drug doses were then determined based on the general toxicity of the compounds and their corresponding IC_{50} values, which were subsequently used for *in vivo* assays against P388 murine leukemia cells. The ILS values reported represent the increased life span for the mice that received chemotherapy as compared to those mice infected with P388 leukemia, but did *not* receive treatment. The ILS values reported in Tables 1 through 5 represent single dose effects. Most of the compounds described herein were also tested in assays consisting of five consecutive treatments. Although these data are not reported in Tables 1 through 5, any meaningful

differences that were observed from sequential treatments as compared to single dose responses will be discussed in the text.

As part of their overall synthetic studies, the Terashima group also prepared the following D ring congeners of quinocarcin (Schemes 8 and 9).[29] Treatment of **16** with sodium cyanide afforded amino nitrile DX-52-1 (**18**) which, as will be seen, is ubiquitous to semi-synthetic strategies in order to preserve the highly unstable oxazolidine E ring during functional group elaboration. Following acetate protection, the 2-mercaptopyridine-

Scheme 8. Preparation of 10-decarboxyquinocarcin

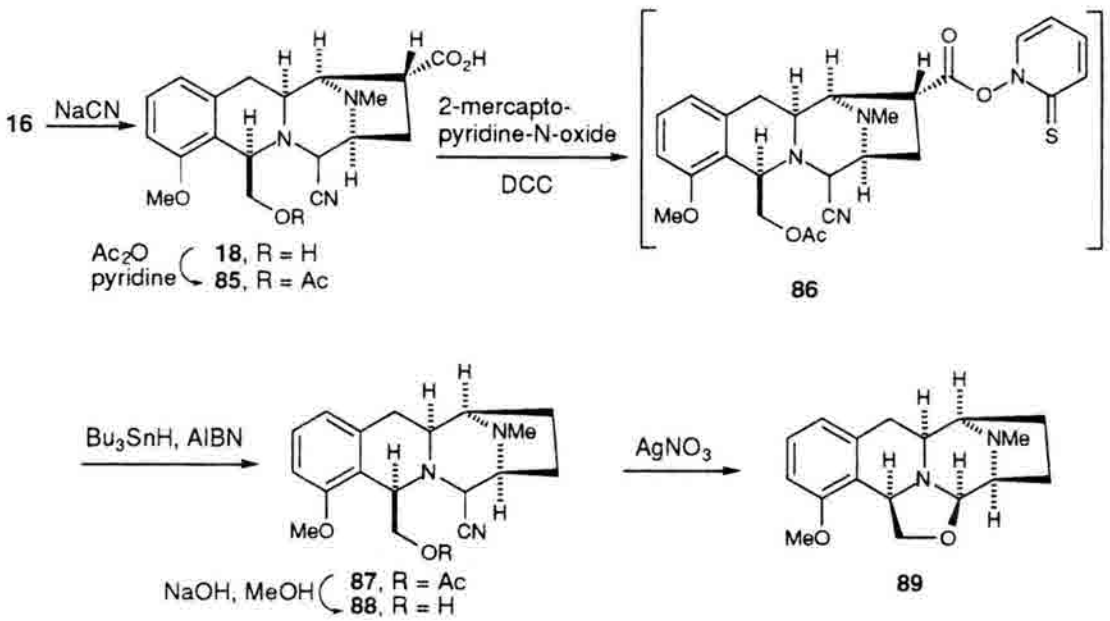

N-oxide ester was prepared by dicyclohexylcarbodiimide (DCC) coupling, which was subsequently reduced (Bu_3SnH, AIBN) to afford the 10-decarboxy derivative **87** (Scheme 8). After acetate removal, treatment with silver nitrate furnished 10-decarboxyquinocarcin **89**. Similarly, the isopropylcarbonate of **85** and **90** were prepared (Scheme 9), whereupon treatment with sodium borohydride produced the 10-hydroxymethyl compounds **84** and **93** respectively. Acetate removal of **84** afforded amino nitrile **94**

Scheme 9. Other D ring quinocarcin congeners

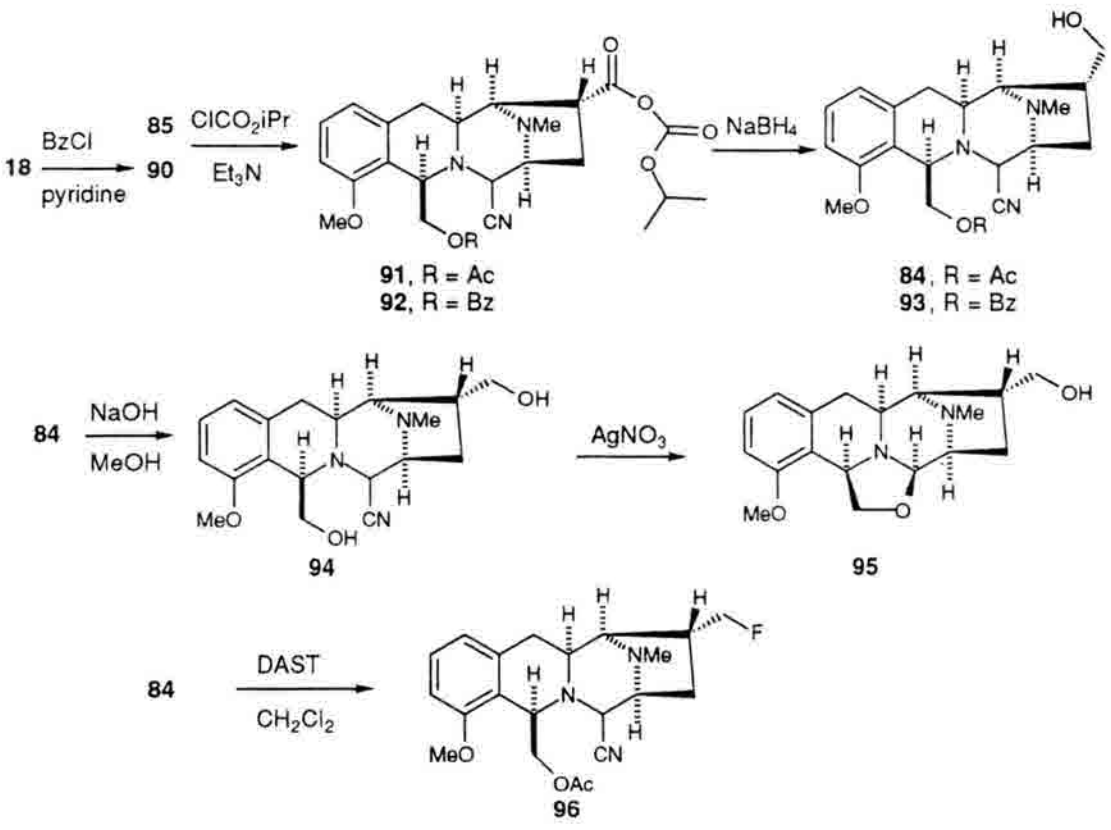

Table 1. Antitumor activity of quinocarcin congeners against P388 murine leukemia cells.[29]

Compound No.	HeLa S3 cells IC_{50} (μg/mL)	optimal dose (mg/kg)	ILS (%)
16	1.0×10^{-1}	25.0	33-39
87	6.4×10^{-2}	12.5	6
88	7.5×10^{-2}	12.5	8
89	5.4×10^{-2}	6.25	20
93	3.6×10^{-2}	25.0	27
95	4.1×10^{-2}	3.13	17
96	5.0×10^{-1}	25.0	12

which subsequently furnished 10-hydroxymethyl quinocarcin analog **95**. Also, treatment of **84** with diethylamino sulfur trifluoride (DAST) generated fluoro compounds **96**.

From Table 1 it can be seen that all of the compounds prepared showed some antitumor activity, although none were as potent as the parent compound (**16**). In consecutive treatments, all of the compounds exhibited some increase in the ILS values measured except for fluoro compound **96**. Although none of the compounds in this study were outstanding in terms of antitumor activity, these data do, however suggest that the C-10 carboxyl group of **16** is not crucial for antitumor activity.

The remainder of the compounds studied were prepared by the Kyowa Hakko Kogyo Co. Ltd. and are characterized by various A ring derivatizations. The first strategy involves the preparation of A ring aromatic substituted quinocarcin congeners (Schemes 10 and 11).[30] Starting from **18**, treatment with boron tribromide afforded C-4 demethylated compound **97** which furnished C-4 desmethyl quinocarcin (**98**). Halogenation of **18** produced the *para*-chloro, bromo and iodo compounds **99**, **100** and **101** respectively, thus affording the corresponding halogenated quinocarcin derivatives **102**, **103** and **104** upon treatment with silver nitrate. Dibromophenol **105** was prepared by acidic bromination of **97** and the nitro derivatives **106** and **107** were furnished upon reaction of **18** and **97** respectively, with nitric acid in acetic acid.

Scheme 10. A ring substituted quinocarcin congeners

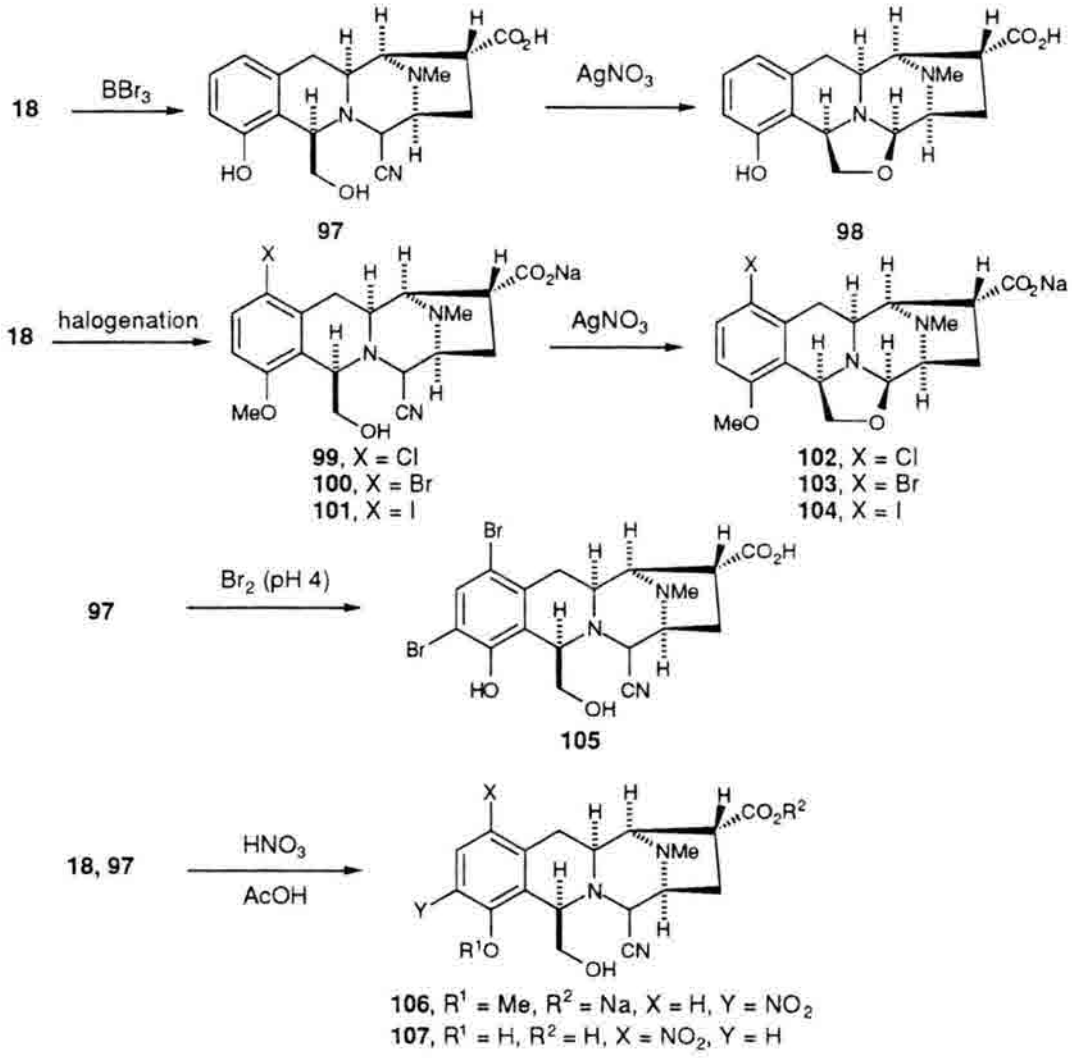

Scheme 11. Other aromatic substituted quinocarcin derivatives

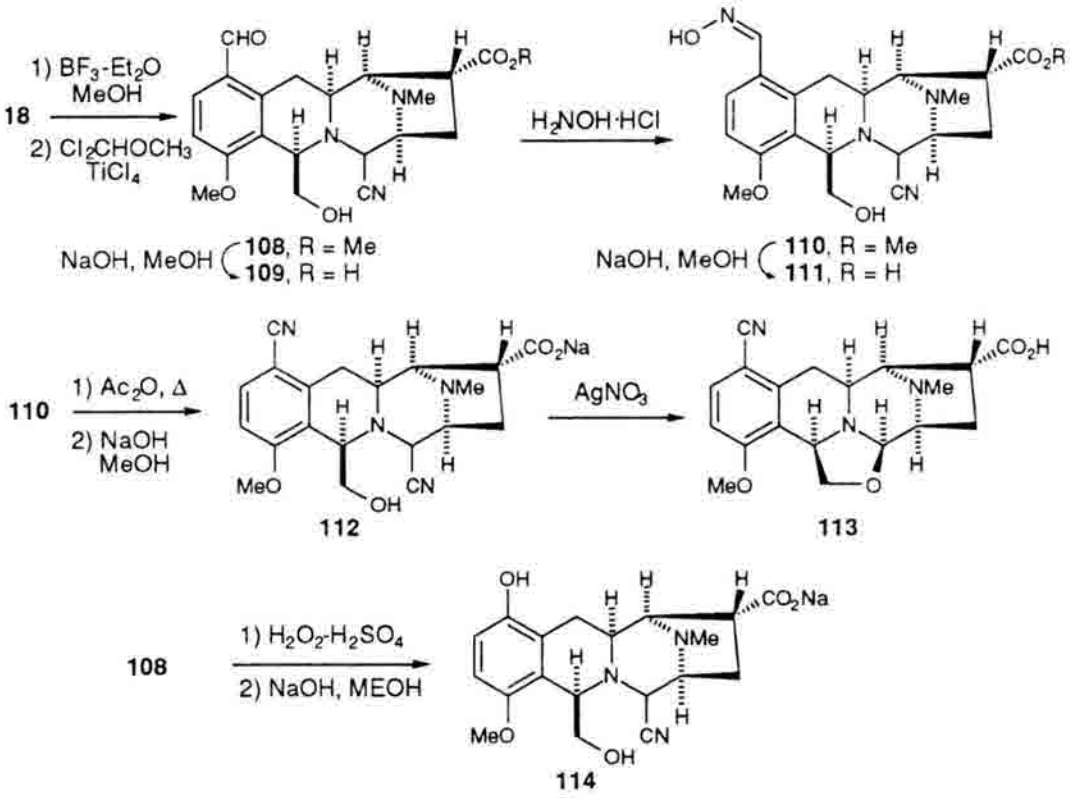

More complex aromatic substituents were prepared as outlined in Scheme 11. Methyl ester formation of **18** followed by aromatic formylation with dichloromethylmethyl ether and titanium tetrachloride afforded **108**, then **109** after saponification. Treatment of **108** with hydroxylamine hydrochloride subsequently furnished oxime **110**, then **111** following saponification. Oxime dehydration with acetic anhydride followed by

Table 2. Antitumor activity of aromatic-substituted quinocarcin congeners against P388 murine leukemia cells.[30]

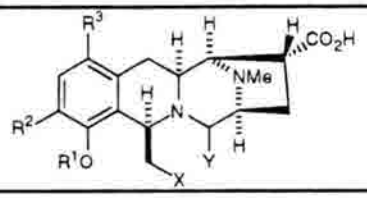

No.	R^1	R^2	R^3	X	Y	[a]HeLa IC_{50}	dose mg/kg	[b]ILS (%)
16	Me	H	H	-O-		0.1	25.0	33-39
18	Me	H	H	OH	CN	0.05	20.0	26
97	H	H	H	OH	CN	5.32	3.13	18
98	H	H	H	-O-		3.03	6.25	14
99	Me	H	Cl	OH	CN	0.042	12.5	23
101	Me	H	I	OH	CN	0.11	50	31
102	Me	H	Cl	-O-		0.04	12.5	40
103	Me	H	Br	-O-		0.048	12.5	50
104	Me	H	I	-O-		0.04	25	24
105	H	Br	Br	OH	CN	0.80	25	28
106	Me	NO_2	H	OH	CN	0.47	5	17
107	H	H	NO_2	OH	CN	0.99	100	27
109	Me	H	CHO	OH	CN	0.56	200	38
111	Me	H	CH=N-OH	OH	CN	1.1	200	38
112	Me	H	CN	OH	CN	0.30	25	40
113	Me	H	CN	-O-		0.51	20	22
114	Me	H	OH	OH	CN	1.7	12.5	30

[a] Drug concentration (μg/mL) required to inhibit the growth of HeLa S_3 cells by 50%. [b] Increased life span of mice that received chemotherapy. Boxed entries represent highly active compounds that received additional testing.

saponification produced cyano compound **112**, which furnished quinocarcin derivative **113** upon treatment with silver nitrate. Finally, hydrogen peroxide oxidation of **108** followed by saponification produced the hydroxylated compound **114**. The results of

antitumor assays for these compounds appear in Table 2. Most of the compounds prepared showed only moderate activity as compared to quinocarcin (**16**) and DX-52-1 (**18**). The exceptions to this trend were chloro and bromo compounds **102** and **103**. These compounds showed better activity than **16** at lower doses. The nitro derivatives (**106** and **107**) were somewhat disappointing, exhibiting poor activity or requiring very high dosages. Also requiring very high doses were formyl compound **109** and oxime **111**. Cyano compound **112** and hydroxyl compound **114** both showed significant activity on single administration, but activity diminished over several administrations.

The promising activity of chloro-**102** was found to extend to assays against MX-1 and B-16 melanoma. In general, these results suggest that the aromatic (A ring) electron density may have some effect on antitumor activity, though these effects appear to be functional group specific.

The next series of compounds involved A ring quinone derivatives.[31] As previously described, several members of this family of natural products contain quinone moieties which may play some role in the antitumor activities exhibited. It was felt, as suggested earlier, that should the electron density of the A ring have an effect on antitumor activity, the presence of a quinone A ring could have interesting consequences.

The first derivatives prepared from **97** were the methyl, and diphenylmethyl esters (**115** and **116** respectively) by oxidation with Fremy's salt to the corresponding quinones **117**, **118** and **119** (Scheme 12). Further elaboration of these compounds with

Scheme 12. Preparation of quinocarcin quinone congeners

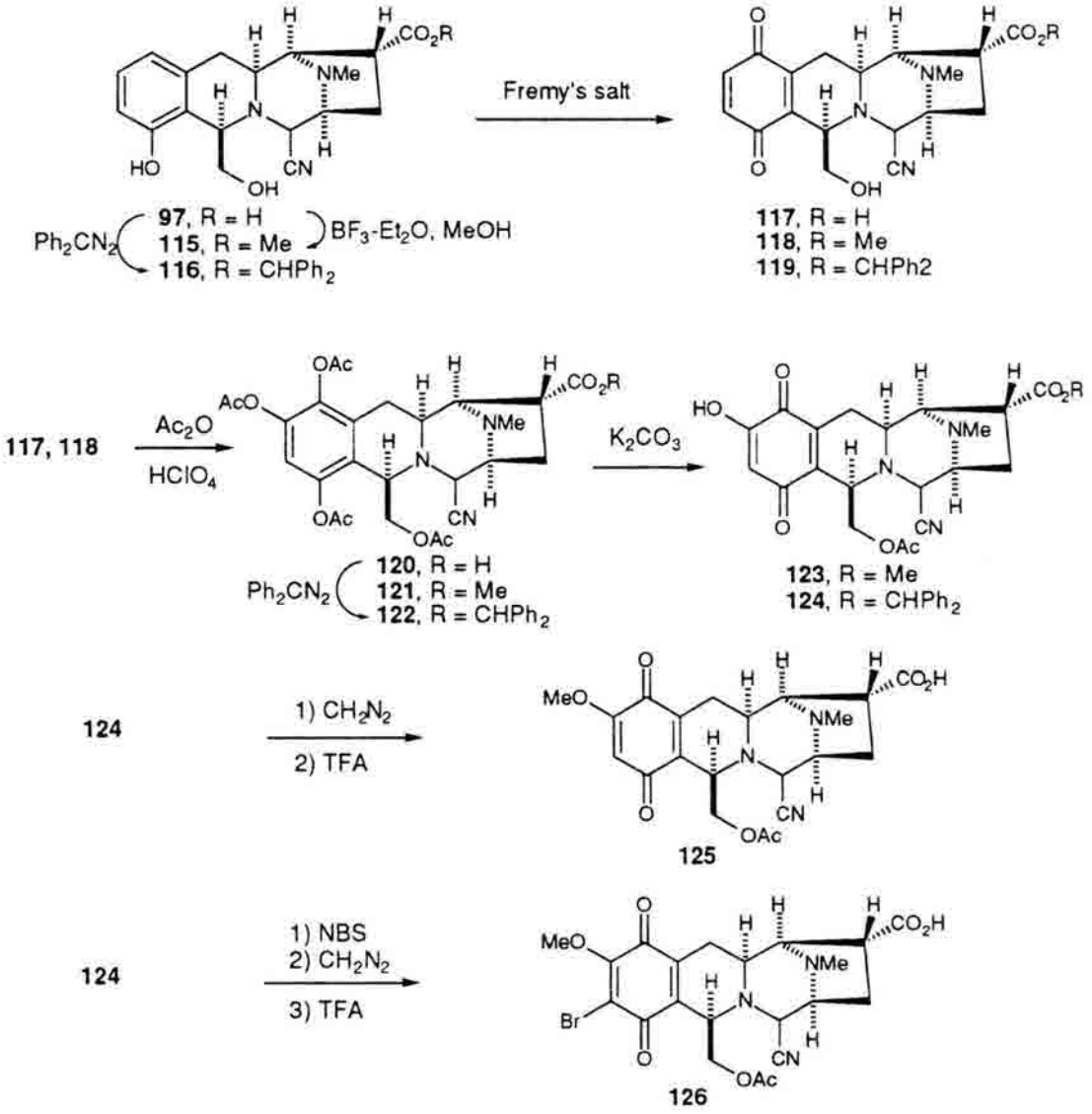

acetic anhydride and perchloric acid produced triacetyl compounds **120** to **122**. Base treatment of **121** and **122** afforded hydroxyquinones **123** and **124**. Additional chemical manipulations of **124** produced methoxyquinone **125** and bromomethoxyquinone **126**.

Compounds **117** and **119** then served as starting points for further quinone substitution strategies as outlined in Scheme 13. Direct addition of dimethylamine with

Scheme 13. Preparation of substituted-quinone congeners of quinocarcin

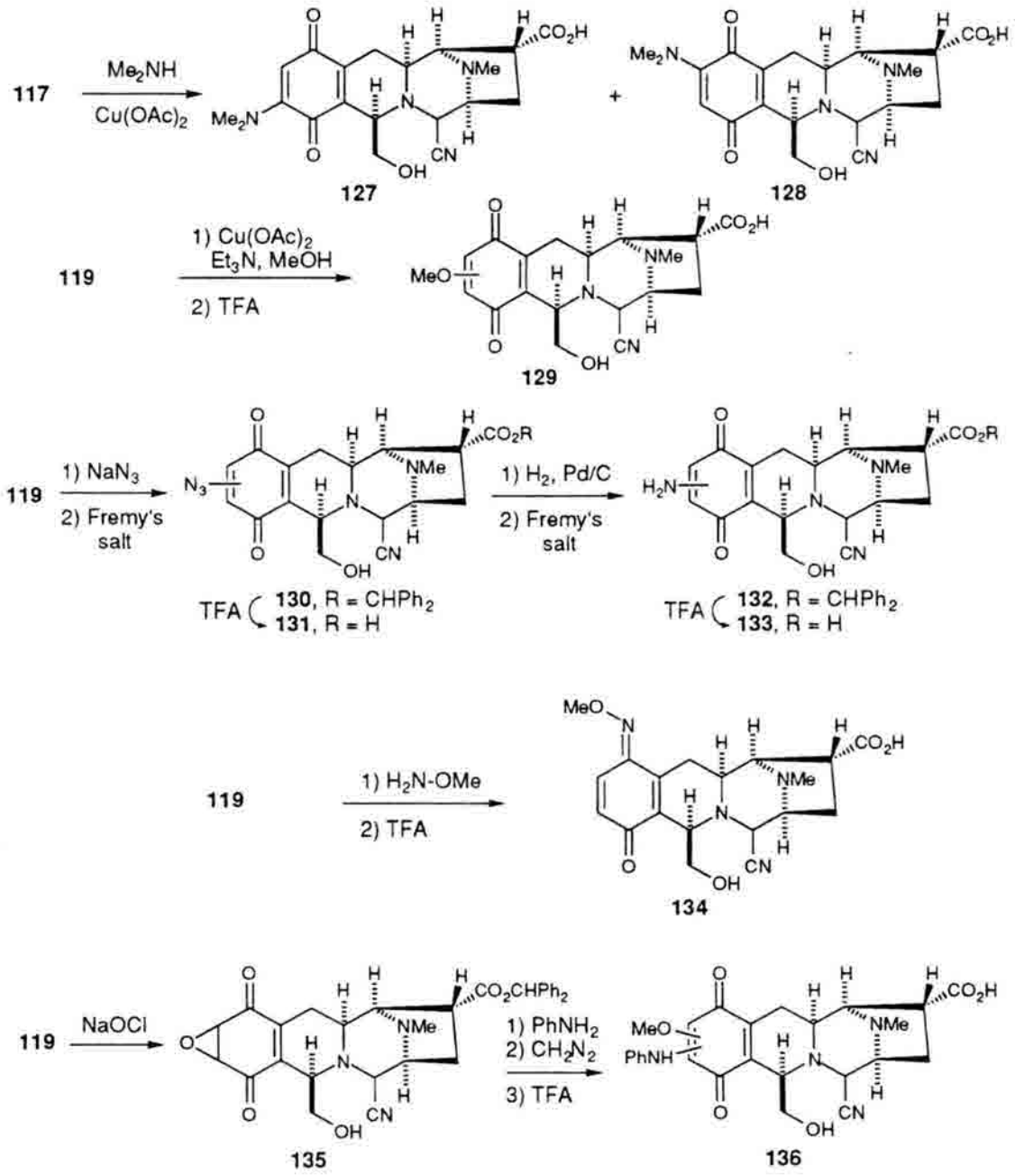

quinone **117** in the presence of copper (II) acetate afforded aminoquinones **127** and **128** which were separable by chromatography. Reaction of **119** with methanol and triethylamine in the presence of copper (II) acetate produced a mixture of methoxy

substituted quinones (**129**). Similarly, treatment of **119** with sodium azide followed by oxidation produced **130** which furnished amino-substituted quinone **132** upon palladium-catalyzed hydrogenolysis. The diphenyl esters of these latter two compounds were removed with trifluoroacetic acid to afford the corresponding acids **131** and **133**. Imine **134** was prepared from **119** by treatment with methanolamine and finally epoxide **135**

Table 3. Antitumor activity of quinocarcin quinone congeners against P388 murine leukemia cells.[31]

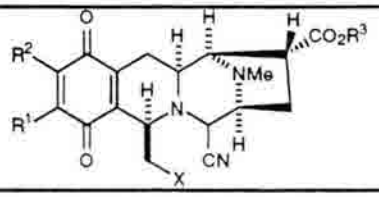

No.	R1	R2	R3	X	[a]HeLa IC_{50}	dose mg/kg	[b]ILS (%)
16					0.1	25.0	33-39
118	H	H	Me	OH	0.12	20	18
123	H	OH	Me	OAc	>10	100	14
125	H	OMe	H	OAc	>10	25	22
126	Br	OMe	H	OAc		9.38	20
127	NMe_2	H	H	OH	0.92	6.25	12
128	H	NMe_2	H	OH	0.79	3.13	15
129	OMe/H		H	OH	>10	3.13	20
131	N_3/H		H	OH	>10	3.13	2
133	NH_2/H		H	OH	>10	1.56	4
134	see structure		H	OH	3.0	25	24
136	PhNH/OMe		H	OH	>10	6.25	15

[a] Drug concentration (μg/mL) required to inhibit the growth of HeLa S_3 cells by 50%. [b] Increased life span for mice that received chemotherapy.

and the disubstituted quinone **136** were prepared sequentially by first reacting **119** with sodium hypochlorite, followed by addition of aniline and diazomethane to provide **136** after removal of the diphenylmethyl ester (TFA).

As shown in Table 3, all of these compounds were less efficient antitumor agents than **16**. The methoxy-substituted compounds **125** and **129** did exhibit some activity. However, upon multiple administrations, these compounds were almost devoid of activity. This activity does, however, follow the trend recognized for the other members of this class of antitumor compounds. For both naphthyridinomycin and saframycin A, the

Scheme 14. Preparation of alkylthiol-substituted quinone congeners of quinocarcin

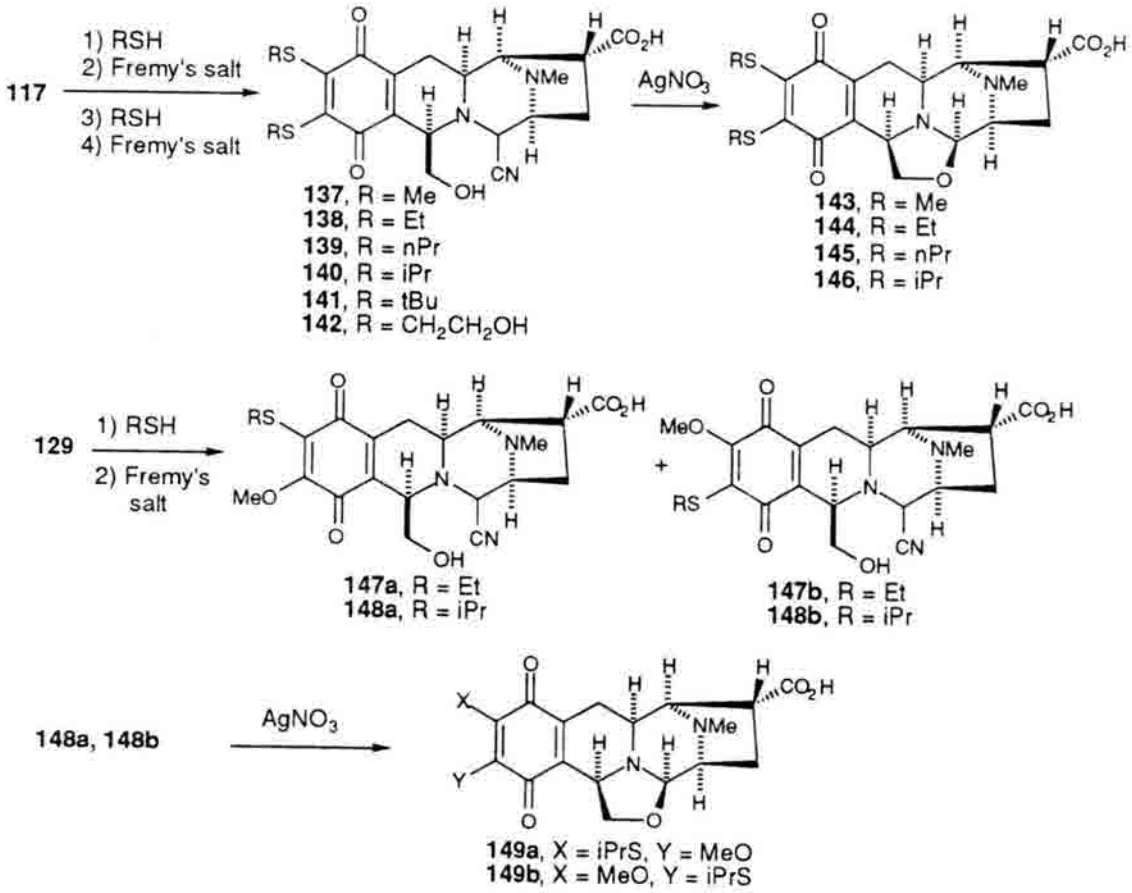

quinone forms of these molecules were weak antitumor compounds, but upon reduction to the hydroquinones, they displayed a high level of cytotoxicity. From these data it seems that the quinones are less active than the corresponding *mono*-methoxy aromatic

compounds (**16** and **18**). As will be seen, this trend will also hold for the hydroquinone-quinocarcin congeners described in Table 5.

Table 4. Antitumor activity of quinocarcin alkylthiol-substituted quinone congeners against P388 murine leukemia cells.[32]

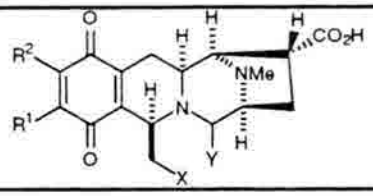

No.	R1	R2	X	Y	[a]HeLa IC_{50}	dose mg/kg	[b]ILS (%)
16					0.1	25	33-39
137	MeS	MeS	OH	CN	0.13	12.5	53
138	EtS	EtS	OH	CN	0.11	12.5	50
139	nPrS	nPrS	OH	CN	0.05	25	56
140	iPrS	iPrS	OH	CN	0.012	25	65
141	tBuS	tBuS	OH	CN	0.004	25	48
142	$HOCH_2CH_2S$		OH	CN	2.47	12.5	26
143	MeS	MeS	-O-		0.019	6.25	48
144	EtS	EtS	-O-		0.08	6.25	64
145	nPrS	nPrS	-O-		0.03	12.5	58
146	iPrS	iPrS	-O-		0.0019	6.25	69
147a	MeO	EtS	OH	CN	2.42	6.25	29
147b	EtS	MeO	OH	CN	2.88	25	31
148a	MeO	iPrS	OH	CN	1.12	12.5	21
148b	iPrS	MeO	OH	CN	0.56	12.5	17
149a	MeO	iPrS	-O-		0.79	6.25	31
149b	iPrS	MeO	-O-		2.37	6.25	30

[a] Drug concentration (μg/mL) required to inhibit the growth of HeLa S_3 cells by 50%. [b] Increased life span for mice that received chemotherapy. Boxed entries represent highly active compounds that received additional testing.

In an effort to investigate the influence of quinone electron density on antitumor activity, a series of thioalkyl-substituted quinones were prepared and tested (Scheme 14 and Table 4).[32] From quinone **117**, sequential reaction of alkyl mercaptans followed by oxidation with Fremy's salt produced alkylthio-substituted quinone congeners **137** through **142**. Further reaction of the methyl, ethyl, *n*-propyl and isopropyl compounds (**137** through **140** respectively) with silver nitrate furnished the thio-substituted quinocarcin analogs **143** through **146**.

Scheme 15. Preparation of hydroquinone congeners of quinocarcin

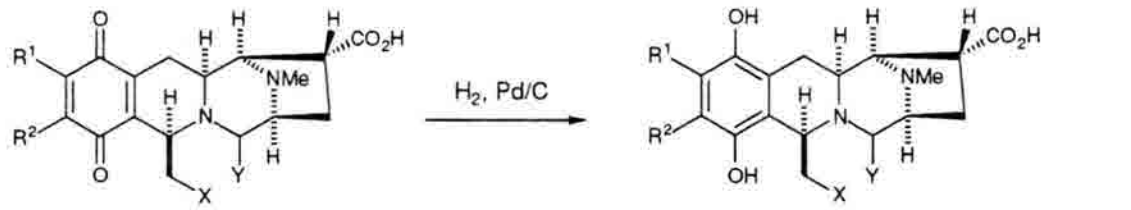

150, R^1 = R^2 = H, X = OH, Y = CN
151, R^1 = R^2 = MeS, X = OH, Y = CN
152, R^1 = R^2 = iPrS, X = OH, Y = CN
153, R^1 = R^2 = MeS, X, Y = -O-
154, R^1 = EtO_2CCH_2S, R^2 = MeS, X = OH, Y = CN
155, R^1 = $HOCH_2CH_2S$, R^2 = MeS, X = OH, Y = CN
156, R^1 = EtS, R^2 = MeO, X = OH, Y = CN

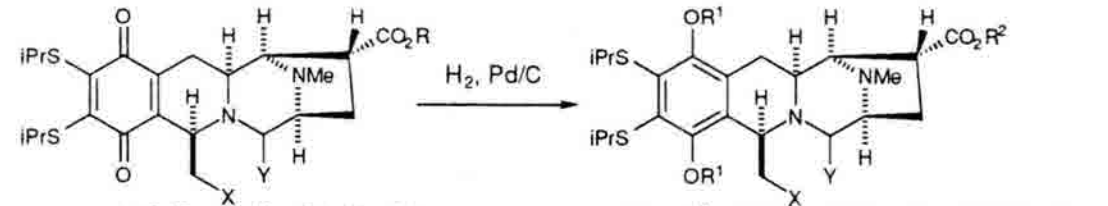

Ph_2CN_2 → **140**, R = H, X = OH, Y = CN
Ph_2CN_2 → **157**, R = $CHPh_2$, X = OH, Y = CN
Ph_2CN_2 → **146**, R = H, X, Y = -O-
Ph_2CN_2 → **158**, R = $CHPh_2$, X, Y = -O-

MeI → **159a**, R^1 = H, R^2 = $CHPh_2$, X = OH, Y = CN
MeI → **159b**, R^1 = Me, R^2 = $CHPh_2$, X = OH, Y = CN
TFA → **160a**, R^1 = Me, R^2 = H, X = OH, Y = CN
$AgNO_3$ → **160b**, R^1 = Me, R^2 = H, X, Y = -O-

Since the methoxy-substituted quinone compound **129** displayed the greatest activity from the last series, it was deemed desirable to construct a mixed thiol, methoxy-substituted congener. This was accomplished by reaction of **129** with ethyl and isopropyl

mercaptans followed by oxidation to afford **147a,b** and **148a,b**. Further elaborations of **148a** and **b** involved silver nitrate treatment to furnish the corresponding quinocarcin derivatives.

Table 5. Antitumor activity of quinocarcin hydroquinone congeners against P388 murine leukemia cells.[32]

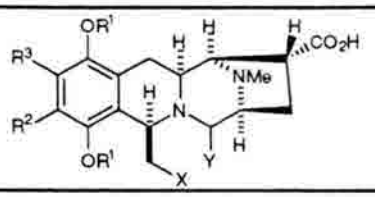

No.	R^1	R^2	R^3	X	Y	[a]HeLa IC_{50}	dose mg/kg	[b]ILS (%)
16						0.1	25.0	33-39
150	H	H	H	OH	CN	6.10	12.5	23
151	H	MeS	MeS	OH	CN	0.09	6.25	47
152	H	iPrS	iPrS	OH	CN	<0.03	12.5	51
153	H	MeS	MeS	-O-		0.13	12.5	65
154	H	MeS	EtO_2C-CH_2S	OH	CN	>10	200	37
155	H	MeS	$HOCH_2$-CH_2S	OH	CN	3.24	6.25	18
156	H	MeO	EtS	OH	CN	1.18	12.5	28
160a	Me	iPrS	iPrS	OH	CN	0.17	50	7
160b	Me	iPrS	iPrS	-O-		0.05	37.5	9

[a] Drug concentration (μg/mL) required to inhibit growth of HeLa S_3 cells by 50%. [b] Increased life span for mice that received chemotherapy. Boxed entries represent highly active compounds that received additional testing.

As illustrated in Table 4, all of the dithioalkyl compounds showed improved activity over **16** which was either a function of A ring electron density or the lipophilicity gained from addition of the alkylthio groups. In spite of the moderately promising results obtained

for methoxy compound **129**, the mixed alkylthio, methoxy compounds **147a,b** and **148a,b** showed minimal activity. The regiochemistry of these substituents also seemed to have little effect on the efficacy on these materials.

Preparation of the hydroquinone derivatives of these materials was conducted by palladium-catalyzed hydrogenolysis as outlined in Scheme 15. Similarly, treatment of the diisopropylthiol compounds **140** and **146** with diazodiphenylmethane afforded the corresponding diphenylmethyl esters **157** and **158**. Reduction of these substances followed by sequential reaction with methyl iodide and trifluoroacetic acid generated the bis-methoxy, diisopropylthiol-substituted compounds **160a** and **160b**.

The antitumor evaluations for these compounds are collected in Table 5. The activities for these compounds appeared to be comparable to those exhibited by the alkylthiol-substituted quinones. The bis-methoxy compounds **160a** and **b**, however, did not perform well. Of the thiol-substituted compounds appearing in Tables 4 and 5, the following substances were selected for further evaluation based on excellent performance. Compounds **137**, **140**, **143**, **146**, **147a** and **151** were chosen and tested against a panel of tumor types including S-180, MX-1, LC-06, St-4 and Co-3. Many of these compounds exhibited significant activity against these tumor types, though these tests did not give rise to any clear structure-reactivity relationship. One interesting example was illustrated by hydroquinone **151**, which displayed good activity against human mammary carcinoma, whereas its quinone counterpart (**137**) was inactive. Compound **137**, however, did perform very well in the murine leukemia assay.

These results indicate that, though some general trends associating functional groups and antitumor activity are observed, it is still difficult to recognize features that lend themselves to predictable chemotherapeutic efficacy. Since the majority of the compounds

discussed in this section were the result of A ring elaborations of **16**, attention should now turn to other portions of this molecule for chemical manipulations.

Of considerable interest should be the oxazolidine (E ring) moiety. This is especially relevant since the E ring of quinocarcin is well recognized to be central to the antitumor activity exhibited by this substance. As will be presented over the following chapters, work in the Williams research group has demonstrated the ability to alter the E ring conformation in synthetic analogs which has caused significant changes in the mode of *in vitro* activity for the compounds prepared. Just what ramifications these altered behaviors will have on antitumor activity is yet to be determined. However, the work presented herein should support the argument for the relevance of continued research in this area.

Chapter 2
Synthetic Model Studies

The emphasis of this chapter will focus on the development of methodologies for the preparation of the A, B, C, E tetracyclic core structure of quinocarcin giving particular attention to various aspects of stereocontrol. As discussed in Chapter 1, Williams, *et al.* demonstrated the ability to synthesize a tetracyclic analog of quinocarcin which resulted in the formation of the unstable oxazolidine E ring in the penultimate step.[21] This compound suffered from the fact that it exhibited the C-11a-*anti* stereochemistry not observed for quinocarcin. Therefore, one initial objective that will be addressed in this chapter is the synthesis of the C-11a-*syn* compound (**45a**). In an effort to improve the physical

Figure 5. Quinocarcin and synthetic structural analogs

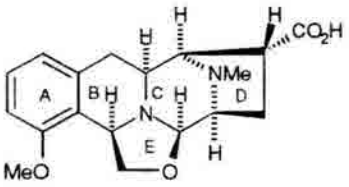

Quinocarcin, DC-52 (**16**)

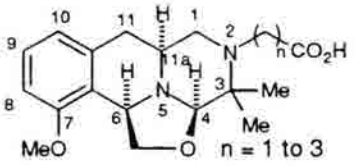

160

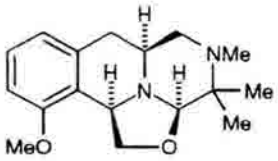

45a

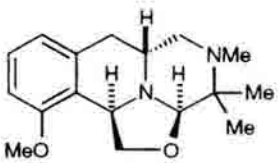

45b

characteristics of these compounds (**45a** and **b**) for later DNA-cleavage studies (Chapter 4), the synthesis of the water-soluble carboxylate-containing analog (**160**) will also be presented herein. Since the compounds targeted in this chapter were also being pursued in order to study mechanistic questions as to the mode of action of this class of compounds,

considerable efforts were made to recognize important structural features and physical properties exhibited by the compounds prepared.

For the purpose of clarity, the numbering of compounds described in this chapter will be based on the benzo [*b*] quinolizine numbering system illustrated by compound **160** (Figure 5). This designation will change in Chapter 3 when the C, D bicyclic ring system is being constructed.

As a starting point for these syntheses, a revised synthesis of the previously prepared isoquinolone **37** was undertaken, the results of which ultimately allowed for the multi-gram preparation of this important, synthetic intermediate. The details of this study are discussed below.

2.1. Modified Synthesis of Isoquinolone 37

The preparation of the key isoquinolone **37** is detailed in Scheme 16 and was made by modification of the known procedure presented in Chapter 1.[20] Ortho-anisaldehyde (**161**) was treated with trimethylsulfonium iodide under phase-transfer conditions to afford the epoxide **162** in high yield. The epoxide was regioselectively opened with phosgene as a 20% solution in toluene to afford the chloroformate **163** in 98% yield. A catalytic amount of water was found to expedite this reaction presumably by generating (*in situ*) a small amount of hydrochloric acid which initiates formation of reactive intermediate **167**. From

Figure 6. Regiochemical bias for reactivity of **162**

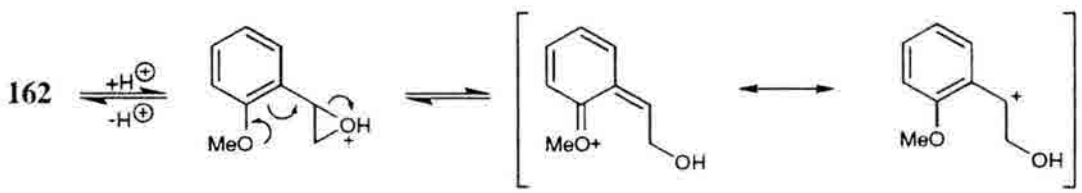

166 **167**

this proposed structure (**167**), the regiochemical outcome of this reaction is also readily apparent (Figure 6). Without purification, **163** was subjected to acylation under Schotten-Baumann conditions to provide the carbamate **164** in quantitative yield. Treatment of **164** with potassium *tert*-butoxide in THF at 0°C effected cyclization to oxazolidinone **36** in 92% yield. This substance was then saponified to the corresponding acid and following recrystallization, was carried on to acid chloride **165** by reaction with oxalylchloride in the presence of a catalytic amount of DMF (76% yield on the two steps). Intramolecular

Scheme 16. Modified synthesis of isoquinolone **37**

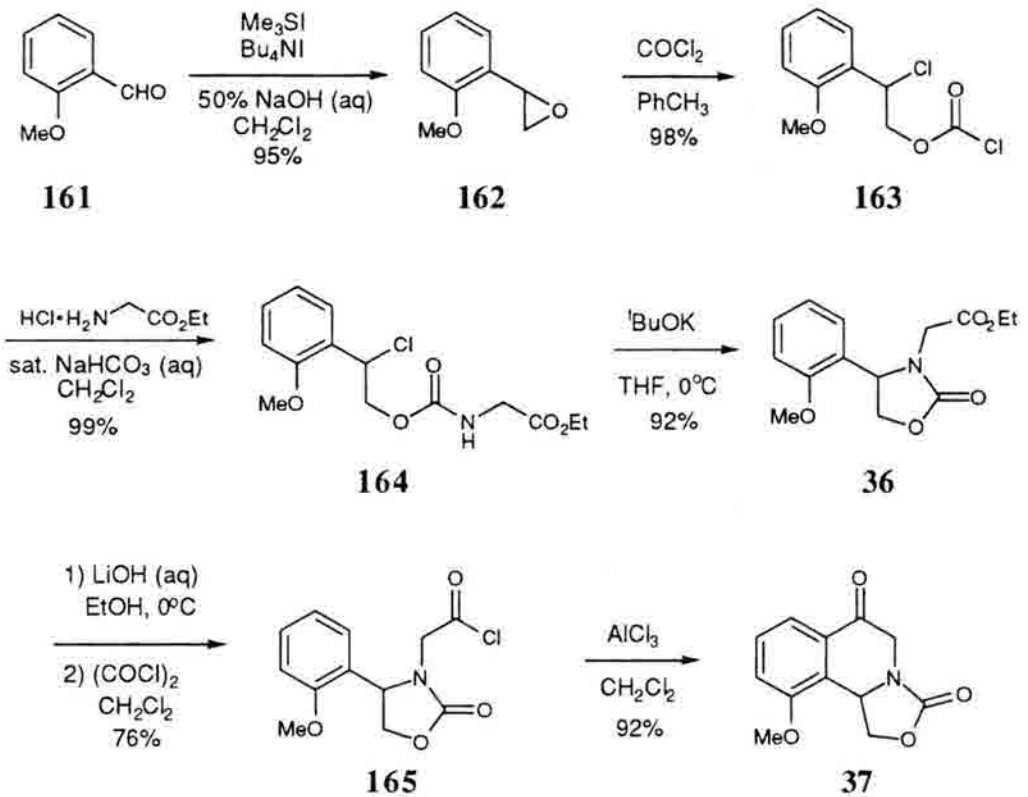

Friedel-Crafts acylation then provided isoquinolone **37** in 92% yield from **165**.[33]

The high yields observed for this sequence and its amenability to scale-up allowed for multi-gram accumulation of **37** which served as a valuable intermediate from which the

syntheses of quinocarcin analogs began. As will be seen in the next chapter, this intermediate also proved useful as a starting point for synthetic studies directed toward the total synthesis of quinocarcin.

2.2. Synthesis of *N*-2-Methyl-C-11a-*syn* Analog 45a

In proceeding toward a C-11a-*syn* analog of quinocarcin it was first necessary to affect C-homologation of **37** *via* the ketone enolate. Due to the propensity of the ketone enolate to undergo O-acylation, this task proved to be somewhat troublesome requiring an extensive examination of electrophiles and reaction conditions . Table 6 lists several attempts at alkylating this substrate. As indicated in entries 7, 9 and 10, it was eventually found that use of a lithium enolate or sodium hydride in DMF with alkyl cyanoformates

Table 6. Attempted C-homologations of isoquinolone **37**.

Entry	Conditions (base, solvent, electrophile)	Results
1	LDA, THF, ethyl chloroformate, -78°C	Decomposition
2	$LiN(SiMe_3)_2$, THF, ethyl chloroformate, 0°C	No Reaction
3	$LiN(SiMe_3)_2$, DMF, ethyl chloroformate, -78-0°C	Decomposition
4	NaH, DMF, ethyl chloroformate, 0°C	Decomposition
5	NaH, DMF, ethyl formate, 0°C	Decomposition
6	Mannich conditions	Decomposition
7	LDA, HMPA/THF, ethyl cyanoformate, -78°C	80% Yield (**38**)
8	NaH, THF, ethyl cyanoformate, -78°C and 0°C	No Reaction
9	NaH, DMF, ethyl cyanoformate, 0°C	88% Yield (**38**)
10	NaH, DMF, methyl cyanoformate, 0°C	77% Yield (**38**)

afforded β-ketoesters in moderate to good yields. As illustrated in Scheme 17, β-ketoethyl ester **38** was reduced with sodium cyanoborohydride giving a single diastereomer (**39**) of unknown relative stereochemistry. This substance served as the key substrate from which the stereoselective synthesis of **45b** (C-11a-*anti*) was prepared as previously described (Scheme 3).[21] By the non-stereoselective route shown in Scheme 17 however, it was found that two parallel approaches could be used for the preparation of both **45a** and **b**. Saponification of **39** afforded the corresponding acid which was carried on to the acid chloride by reaction with thionyl chloride in refluxing toluene. In addition to generating the acid chloride, these conditions also effected an elimination reaction generating the α,β-unsaturated acid chloride *in situ*. Reaction of this intermediate with *N*-methyl-2-amino-2-methyl-1-propanol afforded α,β-unsaturated amide **169** in 48% overall yield. Hydrogenation of this substance provided both **42a** to **42b** in a 2.5 : 1 ratio in 74% total yield. These were isolated on silica gel and carried on separately. Selective borane reduction of the amides allowed for the preparation of the corresponding tertiary amines without significant loss of stereochemical integrity. Following Swern oxidation of these amino alcohols, the crucial oxazolidine-forming step proved somewhat difficult, but could be achieved in 44% yield (in the case of the C-11a-*syn* compound) by refluxing **44a** with ten equivalents of LiOH in ethanol for 48 hours. Silica gel purification and crystallization furnished a single oxazolidine diastereomer of **45a** for which a single crystal x-ray analysis was secured for comparison to that previously obtained for **45b** (Figures 7 and 8).[33]

As is evident from the crystal structures, **45a** and **45b** differ with respect to the orientation of the oxazolidine nitrogen lone pair relative to the adjacent oxazolidinyl methine at C-4. Substance **45a** positions the nitrogen lone pair *trans*-antiperiplanar to this methine, whereas **45b** positions the nitrogen lone pair *trans*-antiperiplanar to the oxazolidine C-O bond (Figure 3). These conformations are exactly those predicted from examination of

Scheme 17. Preparation of *N*-2-methyl tetracyclic quinocarcin analogs **45a** and **45b**

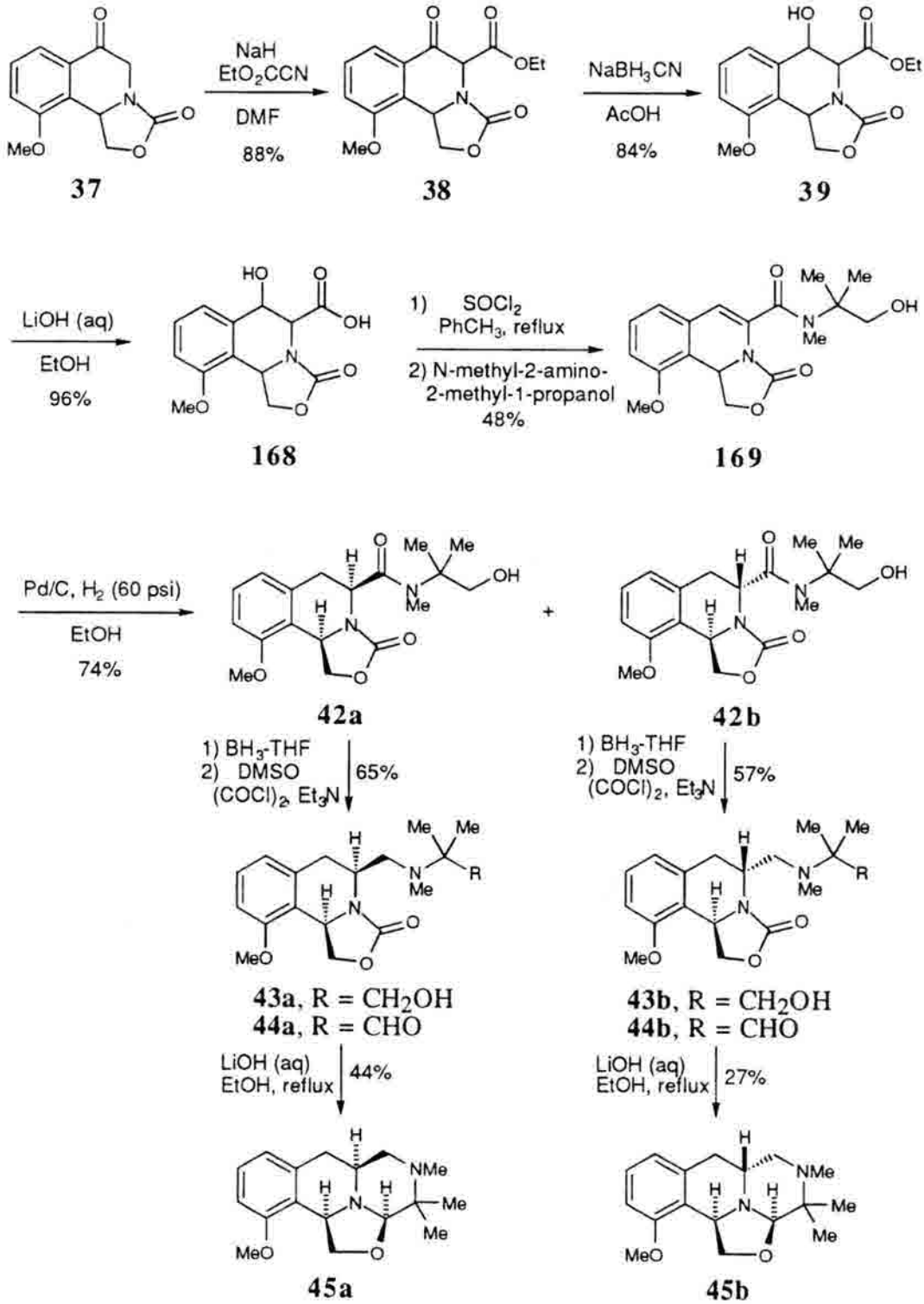

Figure 7. Molecular structure of C-11a-*syn* quinocarcin analog **45a** as determined by single crystal x-ray diffraction analysis

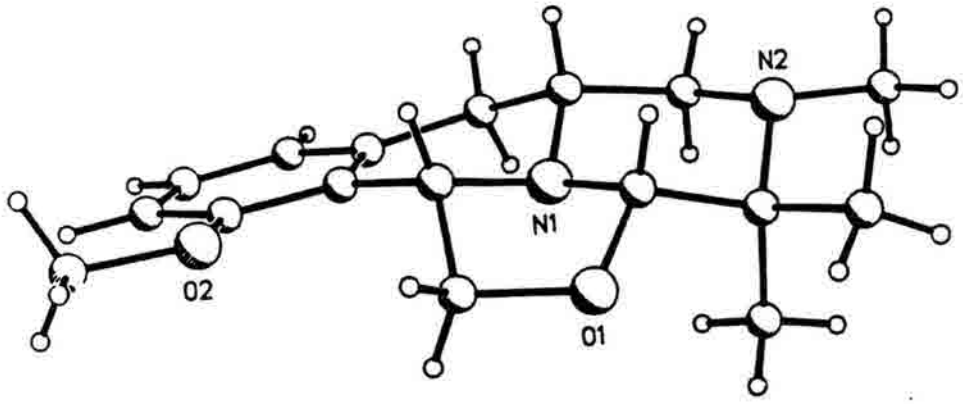

Figure 8. Molecular structure of C-11a-*anti* quinocarcin analog **45b** as determined by single crystal x-ray diffraction analysis[21]

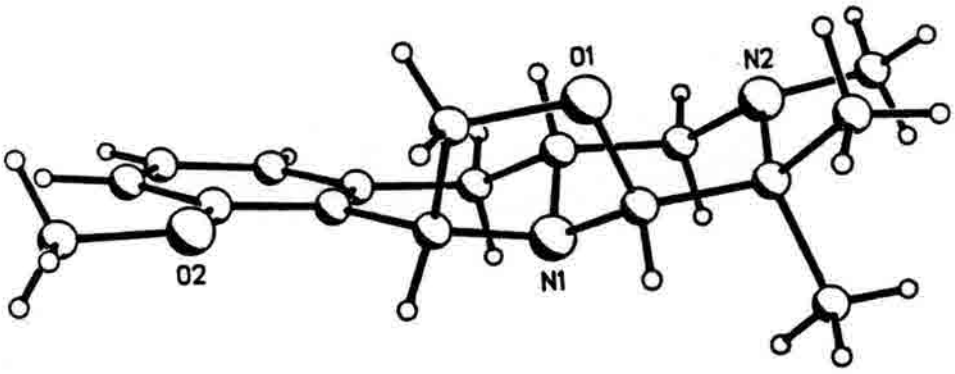

Figure 9. Conformation of **45a** as predicted by molecular mechanics calculations

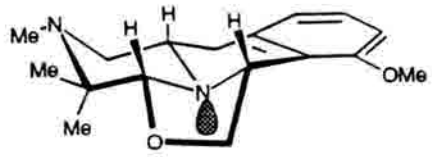

45a

TOTAL ENERGY = 87.8 kcal
BOND STRAIN = 5.1 kcal
ANGLE STRAIN = 31.8 kcal
TORSIONAL STRAIN = 7.4 kcal
N INVERSION = 1.3 kcal
van der WAALS STRAIN = 32.0 kcal
ELECTROSTATIC = 10.2

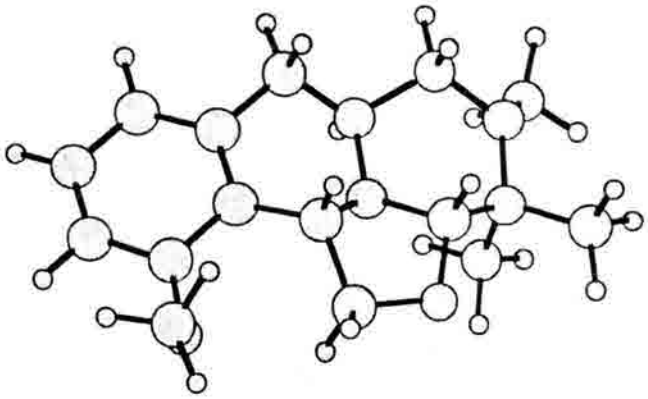

Figure 10. Conformation of **45b** as predicted by molecular mechanics calculations

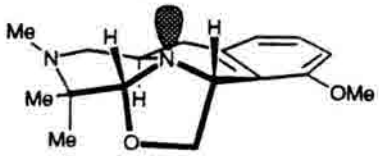

45b

TOTAL ENERGY = 72.8 kcal
BOND STRAIN = 5.0 kcal
ANGLE STRAIN = 15.5kcal
TORSIONAL STRAIN = 8.3 kcal
N INVERSION = 0.57 kcal
van der WAALS STRAIN = 32.9 kcal
ELECTROSTATIC = 10.5

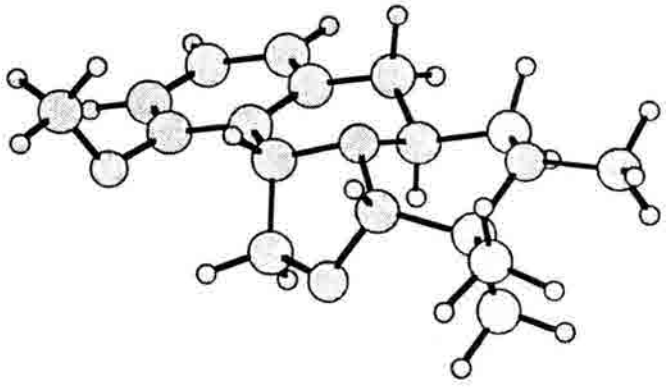

Figure 11. ^{1}H NMR spectrum (300 MHz) ($CDCl_3$) of **45a**

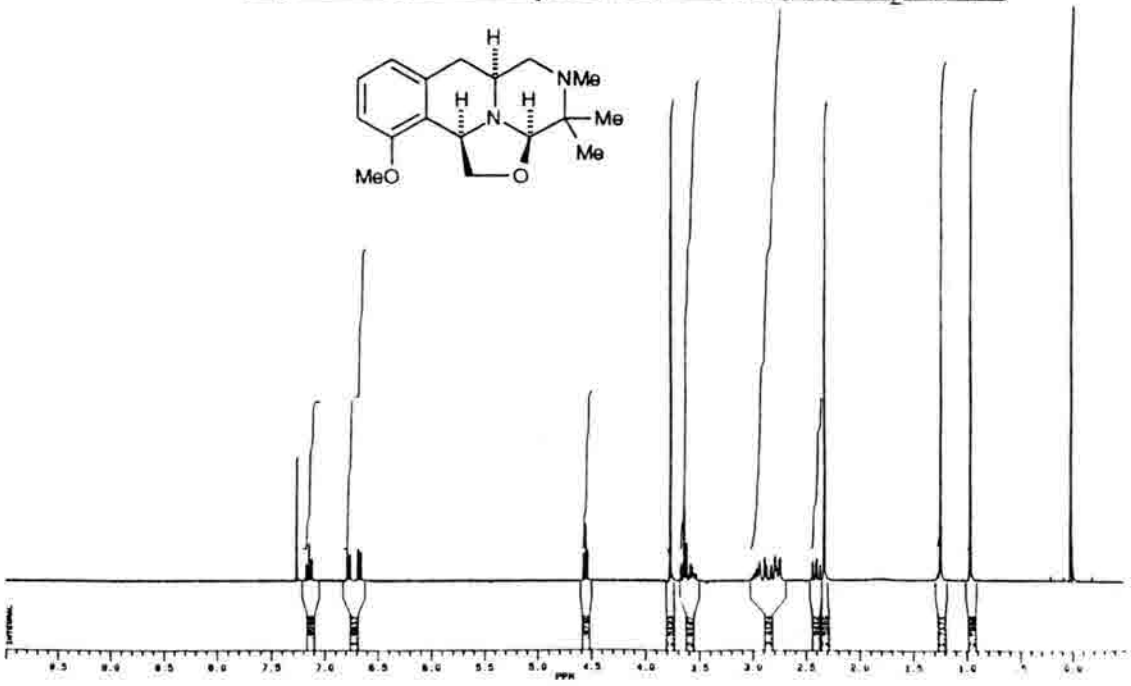

Figure 12. ^{1}H NMR spectrum (270 MHz) ($CDCl_3$) of **45b**

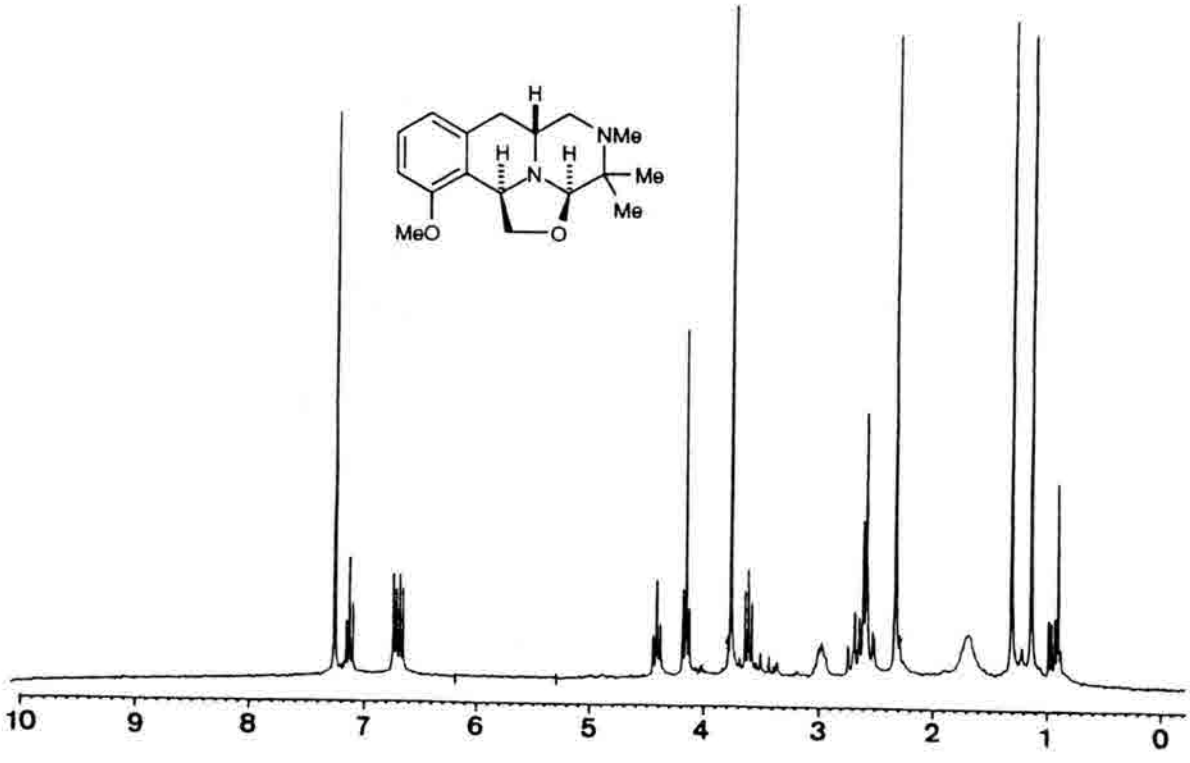

Dreiding molecular models and the molecular mechanics calculations depicted in Figures 9 and 10. As will be discussed in depth in Chapter 4, the different relative configurations about the oxazolidine rings observed in these compounds will have significant ramifications in terms of the mode of action for these substances.

2.3. Synthesis of *N*-2-Carboxymethyl-C-11a-*syn* Analog 160

Although much was learned synthetically and mechanistically from the *N*-2-methyl model system, these compounds do suffer from one major drawback, that being poor water solubility. This solubility problem forced aqueous experimentation with these substances

Scheme 18. Initial approach to water soluble quinocarcin analogs

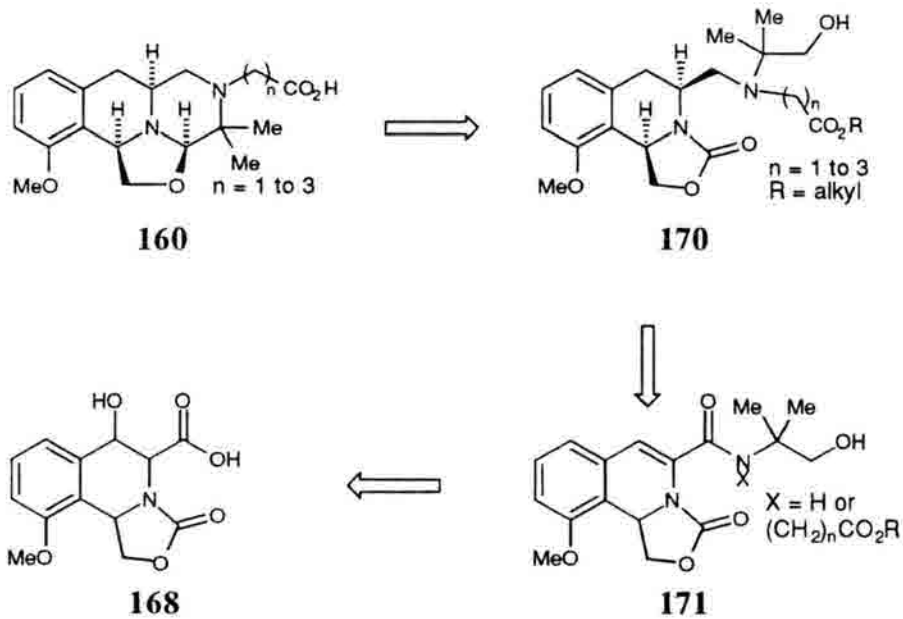

to be conducted at low concentrations or low pH (so as to protonate one or both of the amines present) or in water/alcohol mixtures, limiting further studies with this system. The stereochemical insights elucidated from the analog systems (**45a** and **45b**) and the water-soluble nature of quinocarcin, a zwitterionic amino acid, were taken into consideration as

functionally significant constructs in the design and synthesis compound **160**. By incorporation of a carboxylate moiety such as that depicted in Scheme 18, it was predicted that **160** would take on the water soluble characteristics displayed by quinocarcin.

The initial synthetic approach to **160** was analogous to that just described for **45a** and **b**, the retrosynthetic analysis of which is presented in Scheme 18. By replacement of the methyl group at N-2 with an ester-containing alkyl group, compounds represented by **170** were proposed to cyclize *via* the aldehyde, affording tetracyclic compound **160** under

Scheme 19. Attempted synthesis of C-11a-*syn* amino alcohol **174a**

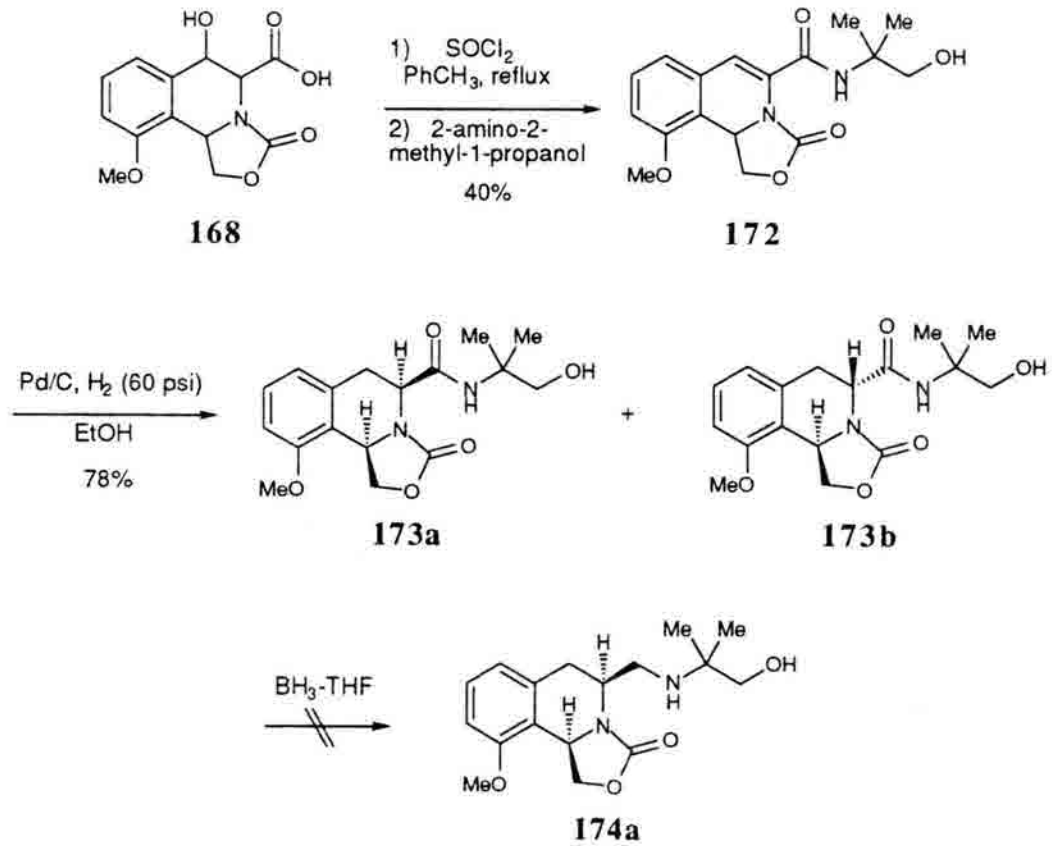

168 **172** **173a** **173b** **174a**

conditions previously described. Preparation of amino alcohol **170** was also envisioned to occur in a similar manner to that described for the previous synthesis resulting from hydrogenation of **171** and subsequent reduction of the amide. The alkyl ester component

of **171** was to be installed in one of two ways. First, where X = H (**171**), N-alkylation would occur following the hydrogenation and amide reduction steps; or second, preparation of the α,β-unsaturated amide would employ a secondary amine in the Schotten-Baumann step thus forming **171** where X already contained the carboxyalkyl group. Since the latter approach suffers from the fundamental problem of reducing an amide in the presence of an ester functionality, the former strategy was attempted first.

Starting from β-hydroxy acid **168**, formation of the α,β-unsaturated amide **172** proceeded in 40% yield on the two steps (Scheme 19). Hydrogenation of this substrate produced diastereomers **173a** and **b** in 78% yield, in a ratio comparable to that observed for the N-methyl case (approximately 3:1). Subsequent borane reduction of the amide failed for the following reasons. Upon reaction with borane, reduction of the N-methyl substrate (**42a**) produced a small amount of the over-reduced oxazolidinone, though not enough to constitute a major problem with the overall yield. On the mono-substituted substrate (**173a**), which reacted somewhat more slowly, this side reaction proved devastating, allowing only small quantities of the desired amine **174a** to be isolated. On the basis of the reactivity exhibited by these substances toward borane reduction, it was decided to attempt the alternate approach involving reduction of the tertiary amide with the ester functionality already installed (**171** where X = $(CH_2)_nCO_2R$, Scheme 18).

Figure 13. Preparation of amino alcohol **176**

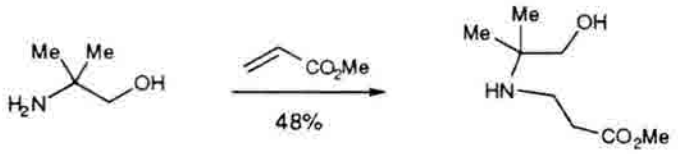

175 **176**

To test this idea, amino alcohol **176** (Figure 13) was first prepared by reaction of 2-amino-2-methyl-1-propanol (**175**) (neat) with methylacrylate affording the Michael

adduct **176** in 48% isolated yield. Again, starting with β-hydroxy acid **168**, amino alcohol **176** was reacted with the acid chloride intermediate under Schotten-Baumann

Scheme 20. Revised approach *via* tertiary amide intermediate **178a**

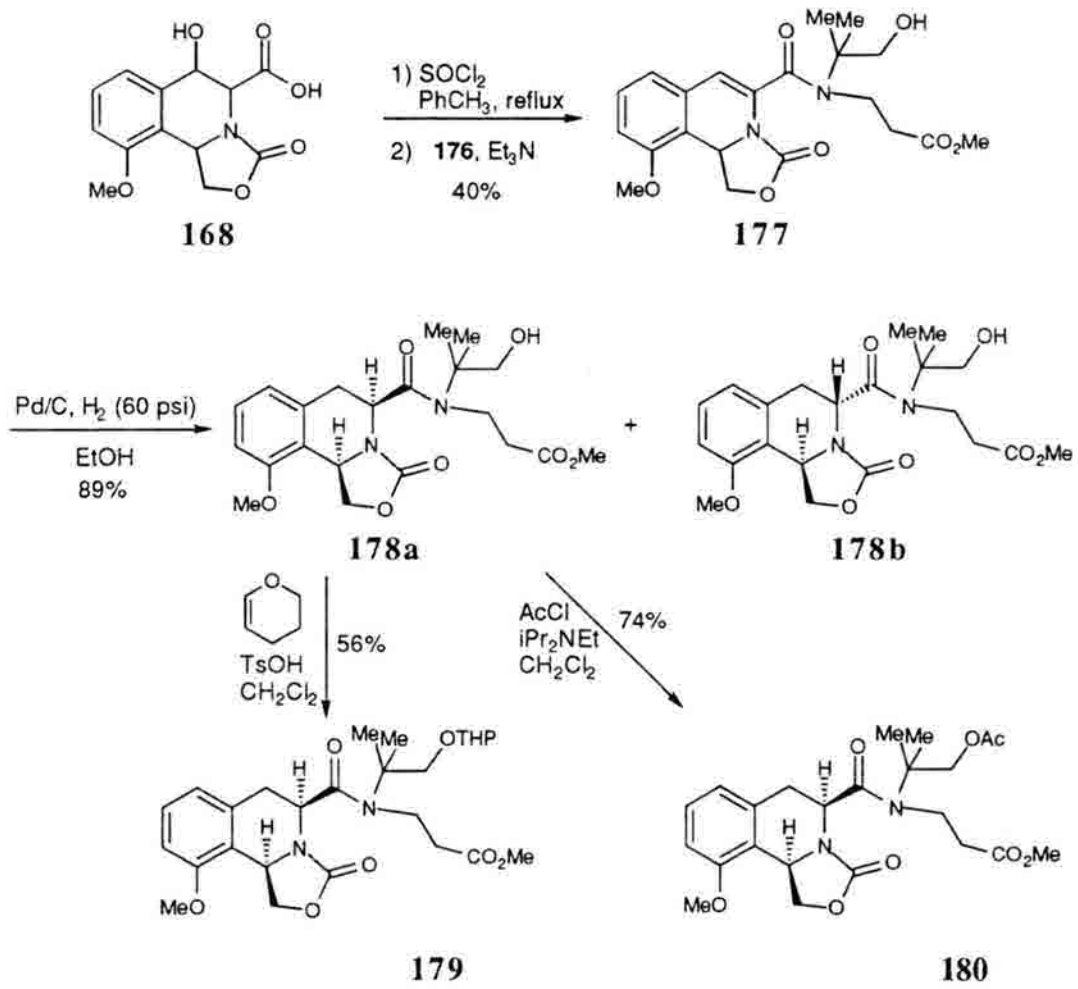

168 **177** **178a** **178b** **179** **180**

conditions affording amide **177** in 40% isolated yield (Scheme 20). Hydrogenation of this substrate afforded a 10:1 ratio of diastereomers (**178a** to **178b**) in 89% yield which were separable by chromatography. Not surprisingly, attempts to selectively reduce the amide of **178a** with borane resulted in over-reduction of the ester or complete decomposition of the substrate. However, in a procedure published[34] by Borch *et al.*, the reductions of secondary and tertiary amides were successfully reduced under mild conditions by first

generating the imidates of the amides studied by reaction with trimethyloxonium tetrafluoroborate. In a facile second step, the imidates were then reduced to the corresponding amines by reaction with sodium borohydride. Applying this procedure to **178a** proceeded with imidate formation, but the unprotected alcohol cyclized to form proposed intermediate **182** (Scheme 21). Although the ester moiety was ultimately found to be inert to the reduction conditions employed, attempts to reduce this intermediate never proceeded beyond formation of oxazolidine **183**. In an effort to circumvent this problem, the alcohol of **178a** was first protected as illustrated in Scheme 20. Under the strong Lewis acidic condition of imidate formation though, both the tetrahydropyran (THP) and even the acetate protecting groups were removed. In the case of **179**, a small amount of the desired amino alcohol product was isolated. When applied to **180**, the only product

Scheme 21. Proposed formation of oxazolidine **183** from **178a**

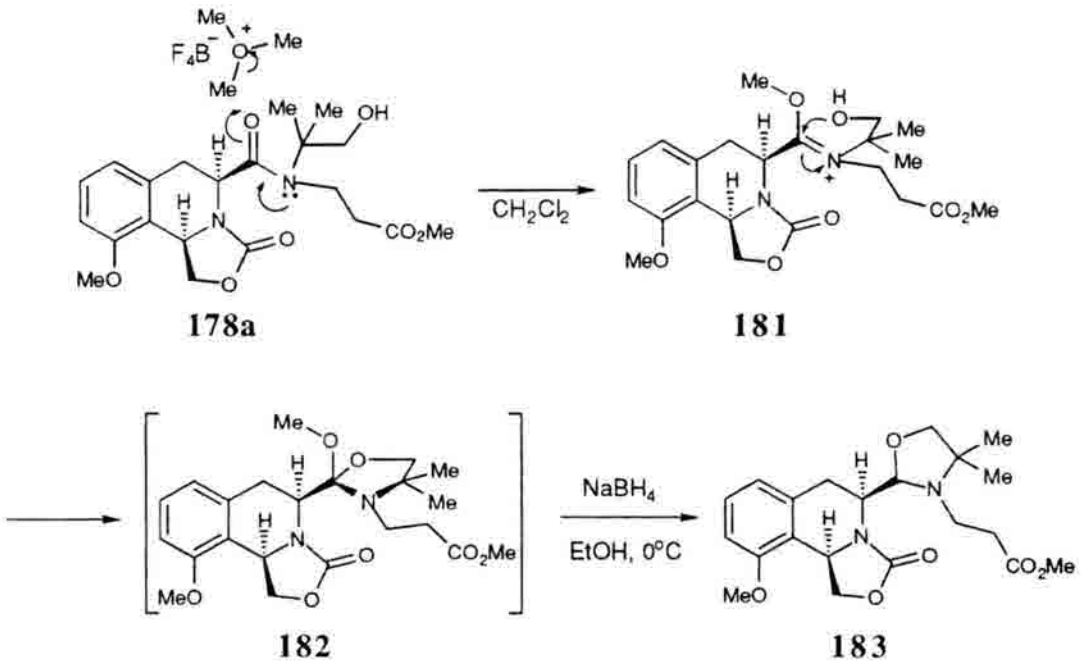

178a **181**

182 **183**

isolated from this two-step procedure was again oxazolidine **183**. Furthermore, the presence of these highly electron deficient intermediates caused as much as 20%

epimerization at C-11a, rendering this approach impractical even if the yields for this two step process could be improved.

During this time two alternative approaches were conceived which were designed to avoid the problems associated with an amide intermediate. These two approaches would access allylic amine **184** directly, as illustrated in the retrosynthetic plan in Scheme 22. From α,β-unsaturated aldehyde **185**, allylic amines represented by **184** were to be prepared by reductive amination. Alternatively, these amines should readily be prepared from allylic alcohol **186** by converting the alcohol to a good leaving group and proceeding *via* a nucleophilic substitution strategy. The uncertainty of these approaches was a

Scheme 22. Alternate retrosynthetic plan bypassing amide **171**

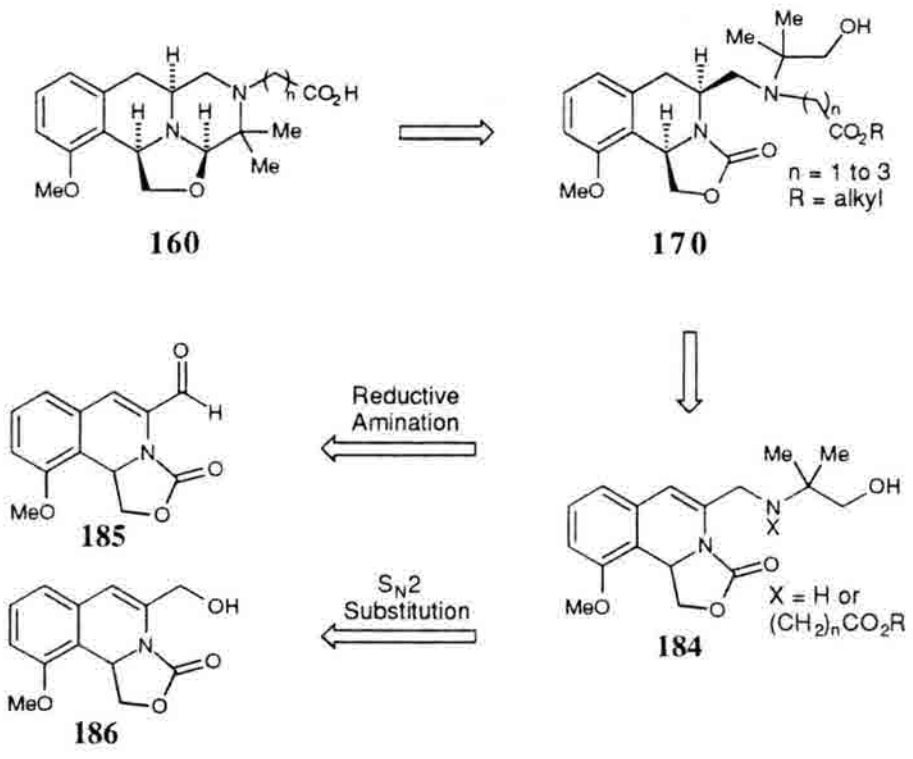

160 **170** **185** **186** **184**

manifestation of the difficulty in predicting the variablility in X (**184**) that either of these strategies would allow due to the highly hindered neopentyl nature of this amine. To attempt to answer this question, the two substrates were first prepared as described in

Scheme 23. From β-hydroxy acid **168**, the α,β-unsaturated acid chloride intermediate **187** was reduced to aldehyde **185** with tributyltin hydride in the presence of a catalytic amount of palladium *tetrakis*-triphenylphosphine as described by Guibe, *et al.* [35] Alternatively, Swern oxidation of allylic alcohol **186** afforded aldehyde **185** in high yield. This method proved to be superior to the tin hydride reduction since, the product (**185**)

Scheme 23. Preparation of aldehyde **185** and allylic alcohol **186**

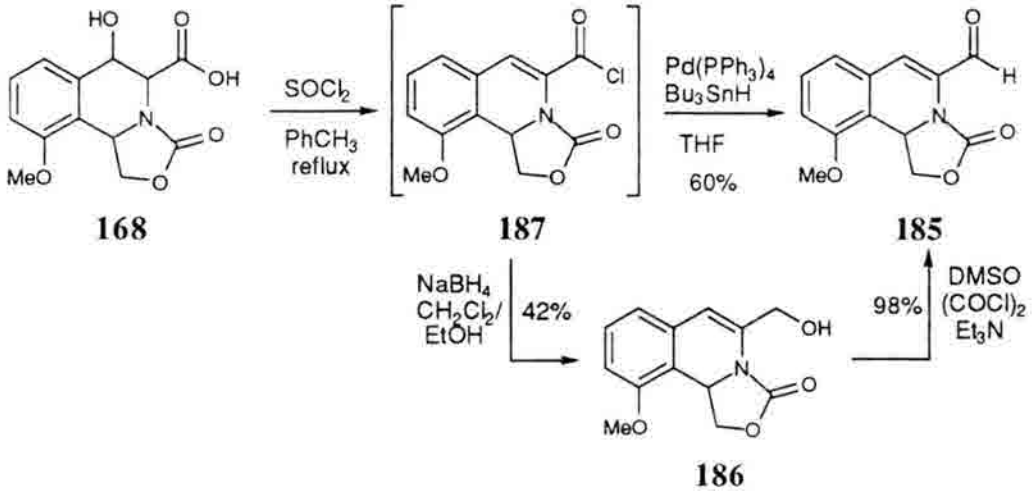

proved easier to purify from the Swern oxidation. Allylic alcohol **186** was generated *via* the acid chloride intermediate (**187**) by sodium borohydride reduction resulting in a stable, chromatographable intermediate (**186**).

The reductive amination approach to **184** proved to be very limited, allowing only 2-amino-2-methyl-1-propanol (where X = H, **175**, Figure 13) to be coupled in 25% yield. All attempts to couple secondary amines by this method proved unsuccessful, resulting only in reduction of aldehyde **185** to the corresponding alcohol (**186**). Reaction of allylic alcohol **186** with methanesulfonyl chloride and triethylamine followed by addition of 2-amino-2-methyl-1-propanol also produced **184** in an improved 46% yield. Aliquots taken from the first step of this process revealed, by ^{1}H NMR, that the reactive intermediate in this reaction was actually allylic chloride **188** (Scheme 24). The reaction presumably

proceeds with mesylate formation followed by displacement of the mesylate anion by chloride. This behavior has been observed for other allylic alcohols when reacted with

Scheme 24. Stereoselective synthesis of amino alcohol **174a**

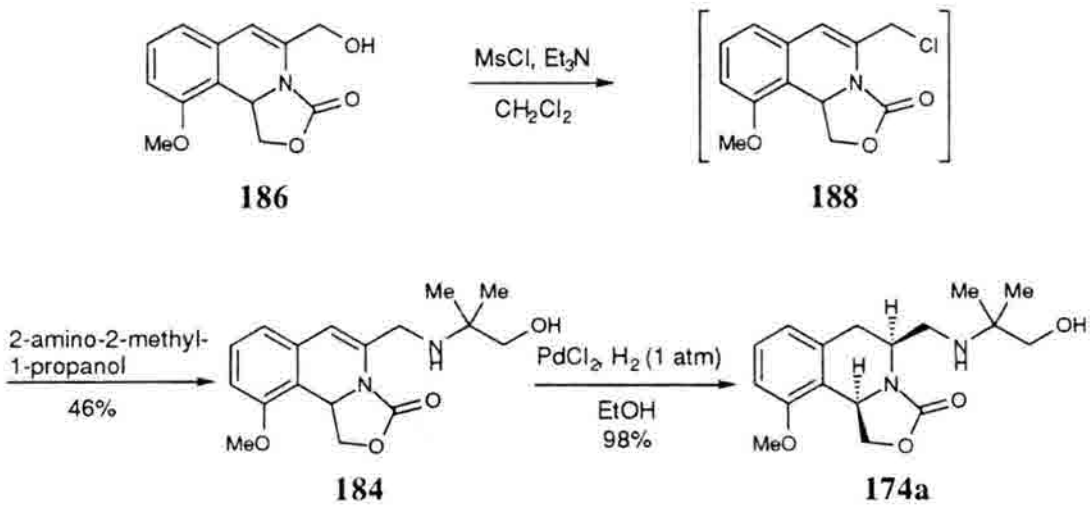

186 **188** **184** **174a**

mesyl chloride.[36] Chloride however, proved to be a sufficiently good leaving group to allow the subsequent amine substitution step to proceed, forming **184** in moderate yield (Scheme 24). Though this procedure only allowed the coupling of amines where X = H or methyl, it did represent a viable procedure for accessing allylic amine **184**. The diastereoselective reduction of this material was then achieved by reacting **184** with one equivalent of palladium chloride under one atmosphere of hydrogen affording **174a** as a single diastereomer in 98% yield (Scheme 24). The relative stereochemistry of **174a** was determined by reacting an aliquot with trimethyloxonium tetrafluoroborate, thus producing **43a**. Comparison of the physical data for this compound with those for the *N*-methyl amino alcohol (**43a**) prepared in the previous synthesis (Scheme 17), for which an x-ray analysis of a subsequent compound was obtained[33] (Figure 7), provided unambiguous proof for the relative stereochemistry of **174a** indicated in Scheme 24. In addition to

providing structural elucidation for **174a**, by intersecting the former synthesis, this also represents a stereocontrolled formal synthesis of **45a**.

With the desired C-11a *syn* stereochemistry installed, the next step involved the *N*-alkylation of this substance with a carboxylate-containing group. The difficulty of this task was realized when **174a** did not react with methyl iodide in attempting to prepare *N*-methylamine **43a** for structural elucidation. Although this compound was eventually obtained by reaction with trimethyloxonium tetrafluoroborate as just described, this proved to be just the first example of the inertness of **174a** toward reactive electrophiles. Table 7 lists several examples of electrophiles tried and the results observed. Attempts to obtain the

Table 7. Attempted N-alkylations of amino alcohol **174a**.

Entry	Conditions	Results
1	Methyl iodide, DMF, 25°C	No Reaction
2	Me_3OBF_4, methylene chloride, 25°C	49% Yield to **43a**
3	methyl acrylate, DMF, 60°C	No Reaction
4	Methyl 4-bromobutyrate, DMF, 25°C	No Reaction
5	Methyl 4-iodobutyrate, DMF, 25°C to 60°C	No reaction and decomposition of iodide
6	Ethyl bromoacetate, DMF, 25°C	Formation of **191**
7	Allyl iodide, DMF, 25°C	30% Yield to **190**

Michael adduct (entry 3) were unsuccessful, as were reactions with most ester- containing alkyl halides. The exception to this trend was ethyl bromoacetate which did react with this substrate, though formation of lactone **191** could not be controlled. Converting **191** (Figure 14) to the desired product would have been problematic in addition to the fact that the regiochemistry of this compound (**191**) was never unambiguously determined.

Reaction with allyl iodide (entry 7), on the other hand, did provide the first potentially useful adduct, since the olefinic product **190** (Figure 14) could likely be ozonolized and further oxidized to the ester or carboxylic acid. The low yield of this reaction though, was likely to be an obstacle to the success of this approach, since there were still several steps remaining in order to obtain the target compound.

Figure 14. N-Alkylation products from **174a**

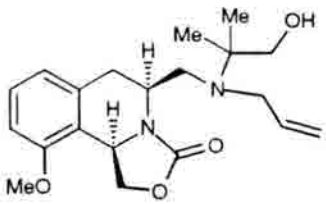

190

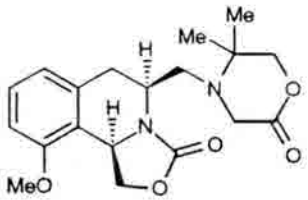

191

As previously suggested, the lack of reactivity of **174a** as a nucleophile is primarily due to the neopentyl nature of this amine. Another feature of this substrate that probably exacerbates this problem is the position of the carbonyl oxygen from the oxazolidinone, putting this atom in close proximity to the nucleophilic center, further hindering reactivity of the amine. To eliminate this problem, a final and ultimately successful strategy was pursued which involved attempting the N-alkylation step after formation of tetracycle **193** as shown in Scheme 25. Closure of the C and E rings to form tetracyclic intermediate **193** was achieved by first oxidizing **174a** under Swern conditions, affording aldehyde **192**; followed by treatment with lithium hydroxide in refluxing ethanol which deprotected the oxazolidinone, allowing the subsequent condensation step to proceed, furnishing **193** in 22% isolated yield. As envisioned, N-alkylation of **193** with ethyl bromoacetate in the presence of sodium bicarbonate proceeded affording ethyl ester **194** in 81% yield. The target compound (**160**) was then isolated on silica gel in 82% yield, following saponification of **194** with lithium hydroxide (Scheme 25).

Scheme 25. Preparation of water-soluble quinocarcin analog **160**

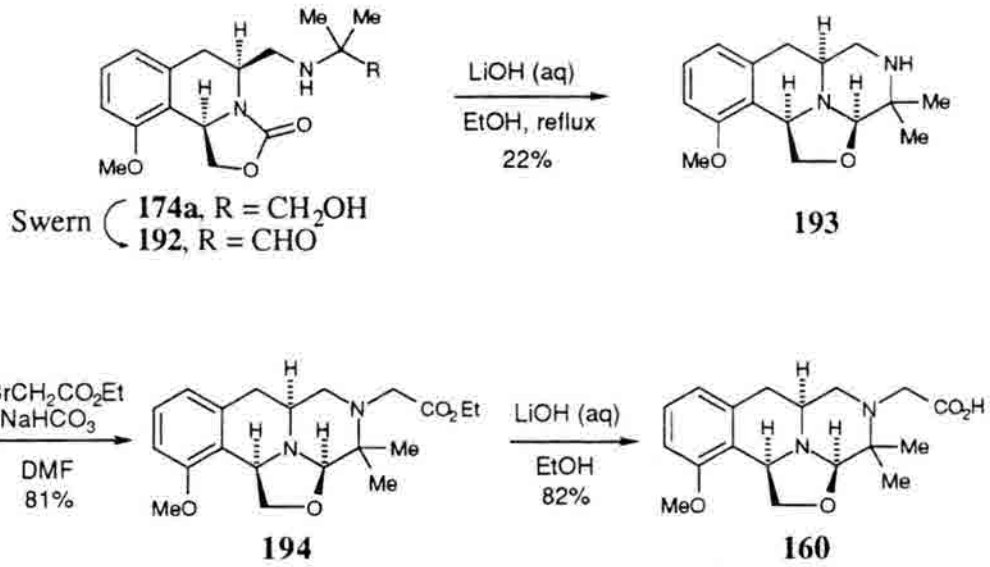

In summary, the various model studies described demonstrate the ability to construct the A, B, C, E ring system of quinocarcin and have overcome previous stereochemical limitations. A non-stereoselective method has allowed the preparation of both the C-11a-*syn* and C-11a-*anti* compounds (**45a** and **b**), whereas the development of a stereoselective approach has led to an alternate synthesis of **45a** and the water-soluble variant **160**. With the information gained from this study, attention was turned to the development of new methods for applying this information to the construction of the bicyclic ring system of quinocarcin. Details of these efforts will be discussed in the next chapter.

Figure 15. ^{1}H NMR spectrum (300 MHz) ($CDCl_3$) of **160**

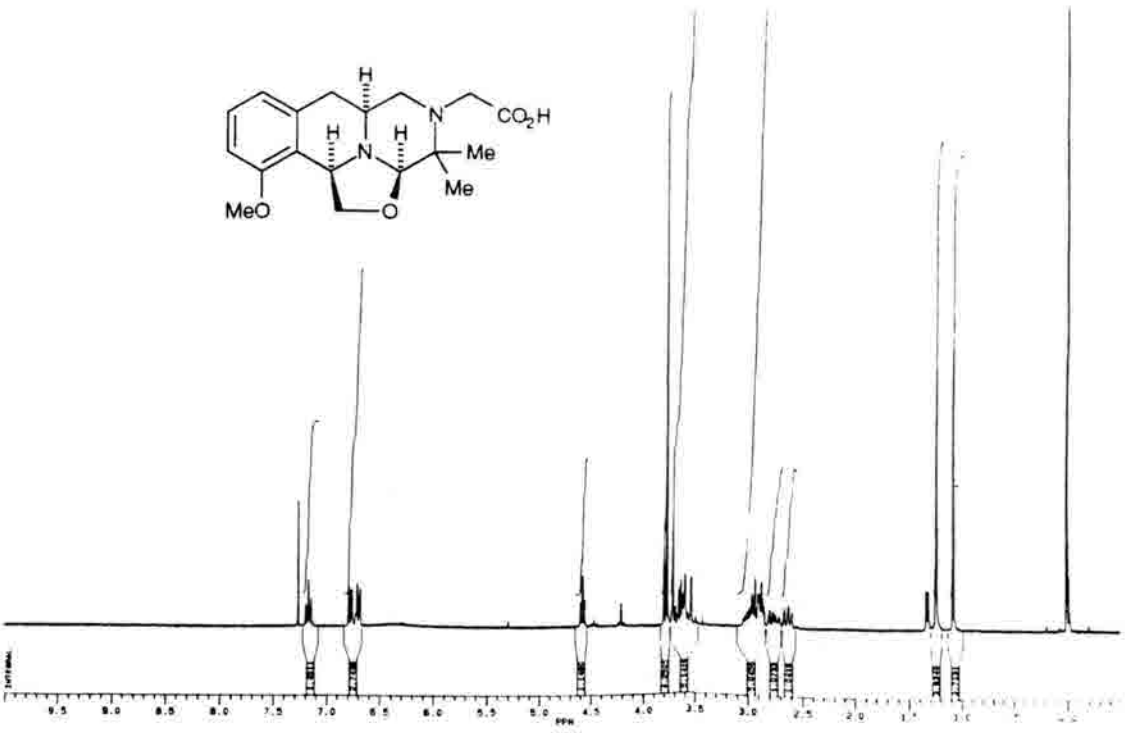

Chapter 3
The Formal Total Synthesis of (±)-Quinocarcin

Studies toward the total synthesis of quinocarcin commenced following consideration of methods for the incorporation of a pyrrolidine C, D ring component into the aforementioned analog synthesis. As discussed in Chapter 1, a number of different synthetic strategies have been devised for forming the quinocarcin pyrrolidine ring. Arguably, the most efficient was the [3 + 2] dipole cycloadditive strategy employed

Scheme 26. Garner model system for quinocarcin pyrrolidine synthesis

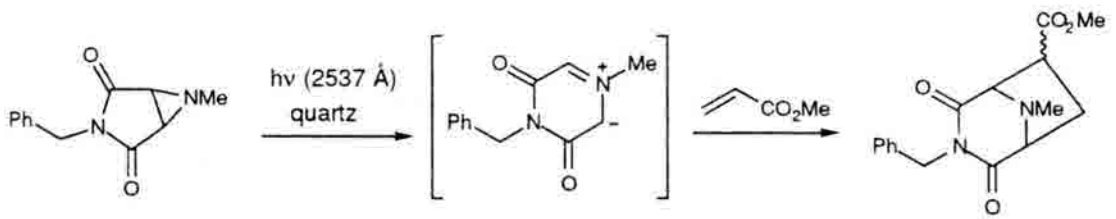

195 **196** **197**

by Garner *et al.*, which generated the pyrrolidine ring *via* a photo-generated azomethine ylide (Scheme 26).[24] This approach had the obvious advantage of making two carbon-carbon bonds in a single chemical step resulting in formation of the pyrrolidine ring. For this reason, two cycloadditive strategies will be pursued in this chapter in an effort to construct the complex ring system of quinocarcin, while attempting to employ previously developed methodology from the model studies.

The numbering of compounds in this chapter will be based on the 8,11-iminoazepino [1,2-*b*] isoquinoline ring system used for DX-52-1 (**18**) and is illustrated by compound **198** in Scheme 27.

3.1. Initial Approach Based on Model Studies

Taking the information gained from the model studies and applying it to a total synthesis of quinocarcin resulted in the basic retrosynthetic plan presented in Scheme 27. Scheme 27a illustrates the previously described methodology for forming the tetracyclic analog **45a** resulting from deprotection of the oxazolidinone under basic conditions which

Scheme 27. Retrosynthetic plan to quinocarcin

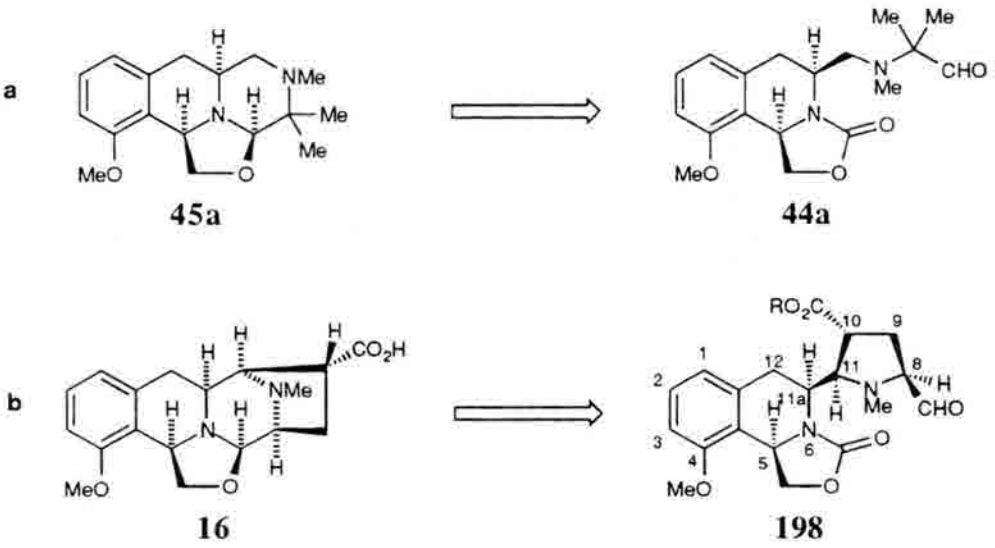

allowed the subsequent oxazolidine-forming step to occur. Applying this to the synthesis of **16**, which posesses the bicyclic C, D ring system required formation of a pyrrolidine ring exhibiting the regiochemistry and relative stereochemistry indicated by **198**. Following the installation of an aldehyde or chemical equivalent at C-8, cyclization to **16** was then envisioned as outlined in Scheme 27b. If a dipole cycloadditive strategy was to be employed for generating the pyrrolidine ring of **198**, the challenge was then to determine which mode of azomethine ylide formation would be most compatible with the intermediates available from the model study.

The literature describes a rich array of procedures for generating azomethine ylides. The most widely recognized methods for their preparation are illustrated in Figure 16.

These involve: (1) deprotonation of iminium salts;[37] (2) rhodium-catalyzed rearrangements of α-diazo ketones;[38] (3) the base-mediated decomposition of tertiary amine N-oxides;[39] (4) the entropy-driven decarboxylation of α-amino acid iminium salts;[40] (5) fluoride desilylation of silylmethyliminium salts;[41] and (6) the photo or thermal ring-opening of

Figure 16. Common methods for generating azomethine ylides

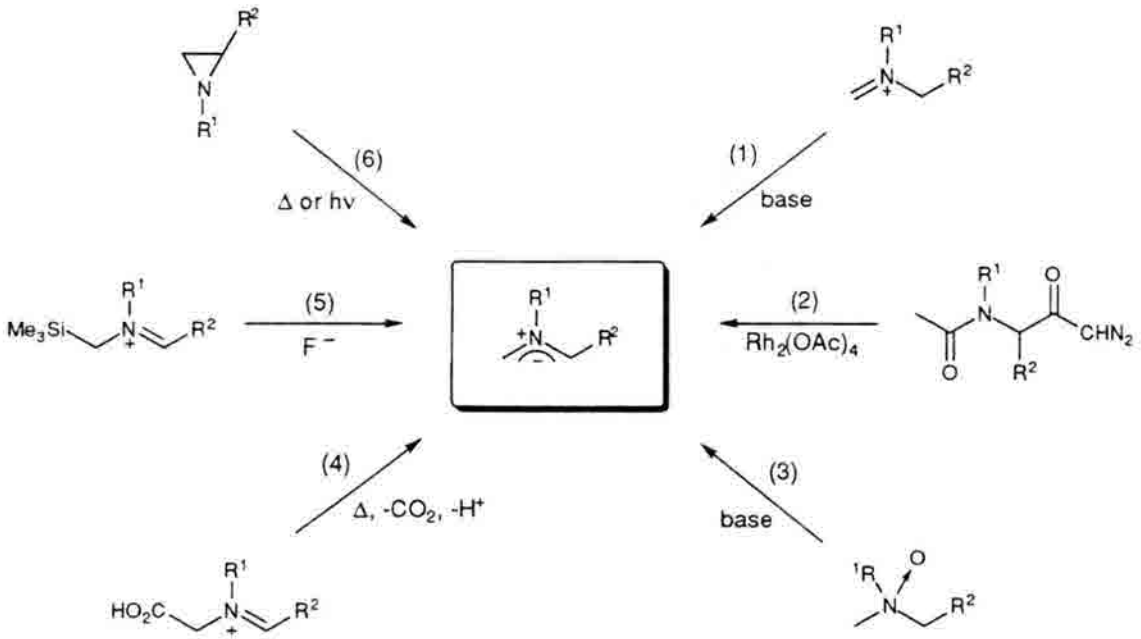

aziridines.[37] Of these procedures, the seemingly most applicable approach for intersecting the analog synthesis was *via* the deprotonation method (1). Confalone *et al.* demonstrated that sarcosine ethyl ester (*N*-monomethyl glycine ethyl ester) can be condensed with an aldehyde thereby generating the iminium species *in situ*.[42] Treating this iminium with base afforded the dipole which subsequently underwent a [3 + 2] cycloaddition reaction. Since an iminium salt could conceivably be generated by condensation of the previously prepared aldehyde **185** with a sarcosine ester, the simplest method to test this approach initially was that envisioned in Scheme 28. Condensation of the sarcosine ester (**199**) with **185** was expected to generate the iminium ion *in situ*, whereupon deprotonation with base was

envisioned to generate the intermediate azomethine ylide. Subsequent [3 + 2] cycloaddition with an acrylate ester (**200**) was proposed to afford pyrrolidines displaying the regiochemical configuration illustrated by **201**. This regiochemistry was predicted based

Scheme 28. Initial cycloadditive approach to quinocarcin

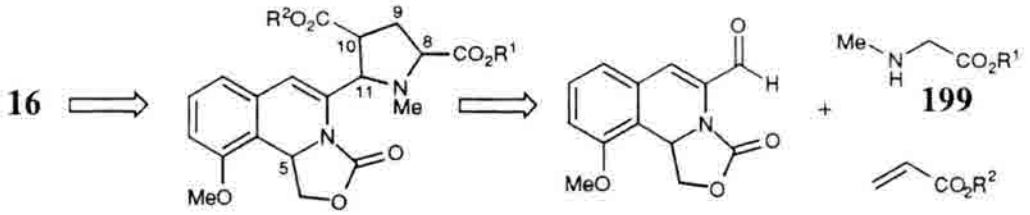

on the ability to stabilize negative charge α to the ester moiety of the sarcosine resulting in a larger HOMO coefficient at that center. If the proper relative stereochemistry in the pyrrolidine ring was obtained from the cycloaddition (particularly at C-8 and C-11) then

Scheme 29. Pyrrolidines *via* a deprotonation approach

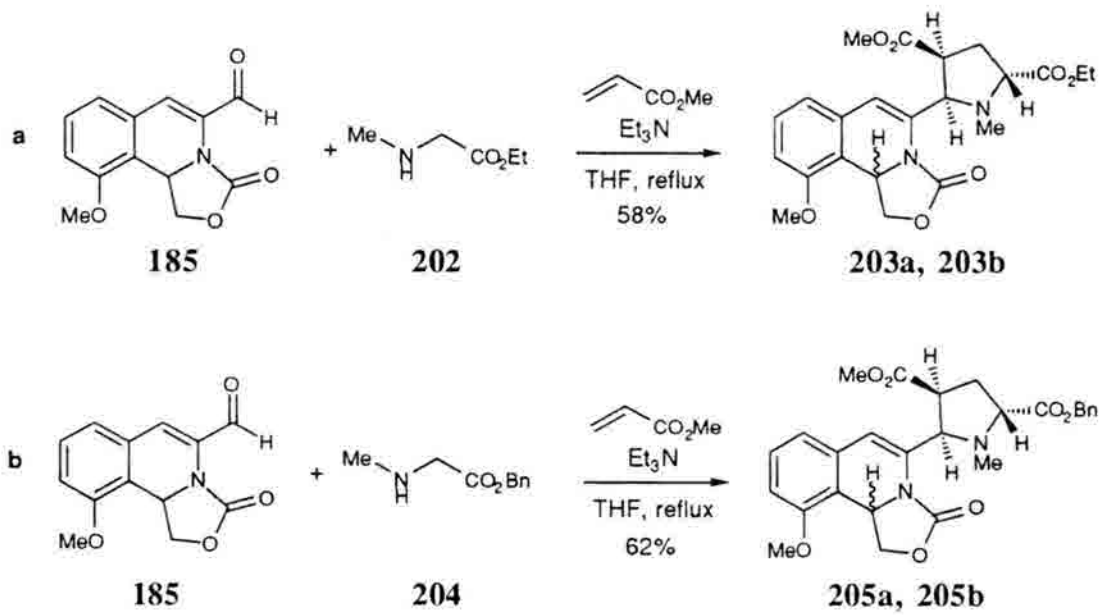

Figure 17. ^{1}H NMR spectrum (300 MHz) ($CDCl_3$) of cycloadduct **205a**

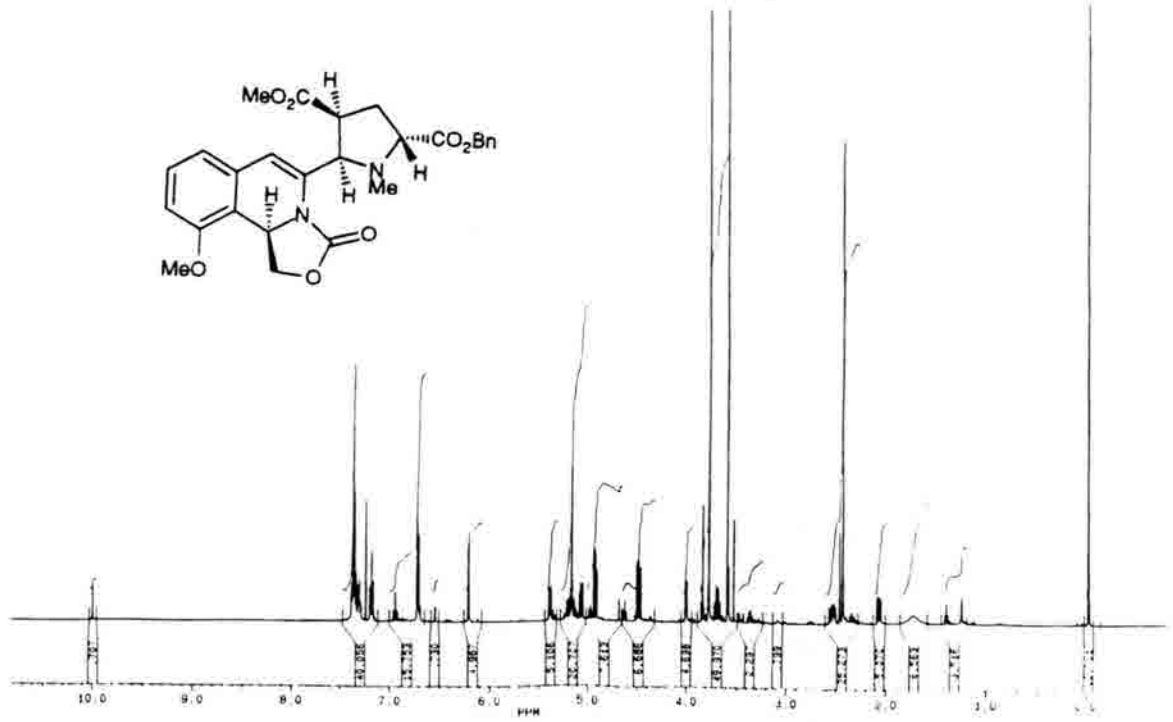

Figure 18. ^{1}H NMR spectrum (300 MHz) ($CDCl_3$) of cycloadduct **205b**

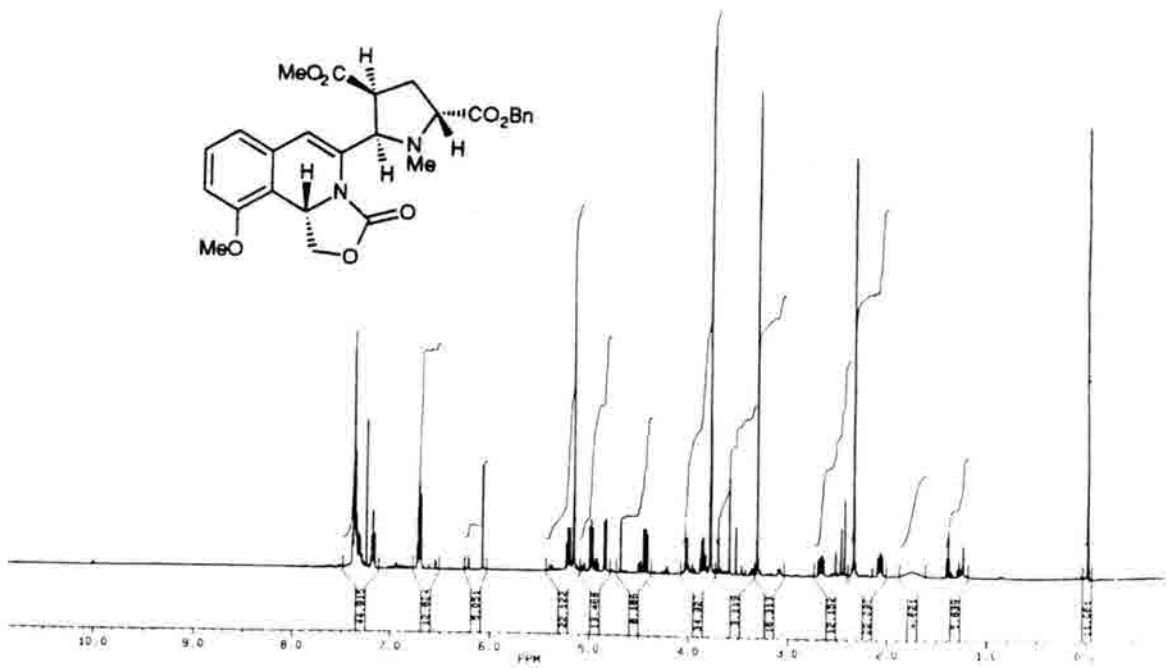

conversion of this substrate to **16** was proposed to occur by first reducing the double bond, then allowing condensation of the deprotected amino alcohol with the aldehyde resulting from selective reduction of the sarcosine ethyl ester as per the analog synthesis (see Scheme 27).

To test this approach, aldehyde **185** was first prepared as described in Chapter 2 (Scheme 23). The cycloaddition reaction was then carried out by reacting **185** with five equivalents of sarcosine ethyl ester, ten equivalents of methylacrylate and 0.1 equivalents of triethylamine (Scheme 29a). After refluxing in THF for 24 h, a 1.5:1 mixture of pyrrolidine products (**203a** and **b**) were isolated in 58% yield. The physical data obtained for these compounds confirmed pyrrolidine formation. Additionally, homonuclear decoupling experiments indicated the regiochemistry predicted in Scheme 28 for both diastereomers. Due to the inability to crystallize these substances or to identify all of the pyrrolidine proton signals in the ^{1}H NMR it was not possible to determine if the desired relative stereochemistry was obtained for either compound. In an effort to answer this question, sarcosine benzyl ester (**204**) prepared by the procedure described by Patel,[43] was employed in the cycloaddition reaction. The reaction was run under the same

Figure 19. Results of homonuclear decoupling and NOE experiments for **205a** and **b**

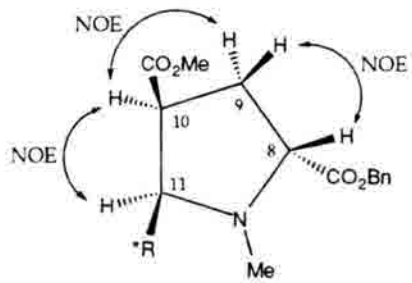

conditions and again two pyrrolidine diastereomers were isolated from the reaction mixture, this time in a 1: 1 ratio (Scheme 29b). The benzyl ester methylene ^{1}H NMR signal, however, was shifted downfield from that of the ethyl ester, which allowed for all

of the pyrrolidine proton signals for each diastereomer of **205** to be assigned. As a result, homo-decoupling and NOE experiments demonstrated that both diastereomers of **205** exhibited the regiochemistry and relative stereochemistry in the pyrrolidine rings illustrated in Figure 19 resulting from two diastereomers about C-5. By chemical correlation it was clear that the same two diastereomers were observed for the ethyl ester cycloadducts in Scheme 29a.

Scheme 30. Rationale for stereochemical outcome of cycloadditions

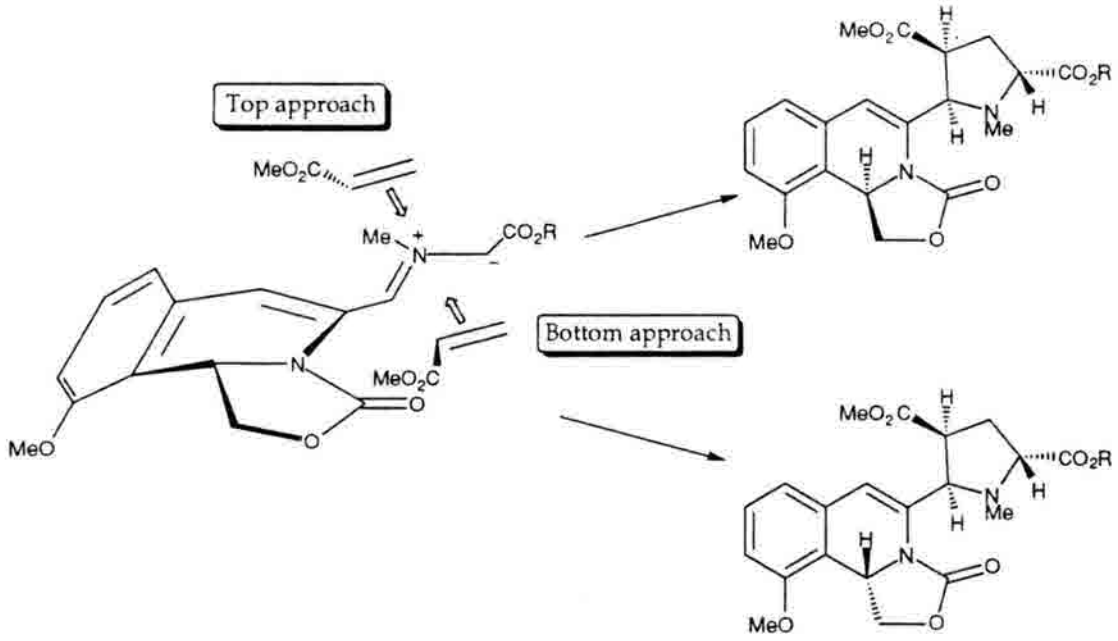

The stereochemistry observed was the likely result of the dipole reacting through the "W" configuration as shown in Scheme 30, with dipolarophile approach coming from each face, giving rise to the two diastereomers.[40a] This results in the same relative stereochemistry for each pyrrolidine diastereomer, the two compounds just differing about C-5. As a result, only one of these diastereomers in each case (Scheme 29a or 29b) could have possessed the correct relative stereochemistry at C-11 (the non-epimerizable center) which meant that the incorrect stereochemistry was afforded at C-8 and C-10 for these

substances. Due to the undesired stereochemical outcome for these reactions, and the problem of oxidation state for the substituent at C-8, which still had to be converted to an aldehyde, a somewhat different approach was pursued that was designed to address these problems.

The reactions in Scheme 29 were the result of ylide formation by deprotonation of an α-amino ester-iminium salt. As illustrated in Figure 16 (4), azomethine ylides can also be generated by decarboxylation of the structurally similar α-amino acid iminium salts.[40] Therefore, as shown in Scheme 31, condensation of an aldehyde (**206**) with an α-amino

Scheme 31. Proposed mechanism for dipole formation *via* decarboxylation

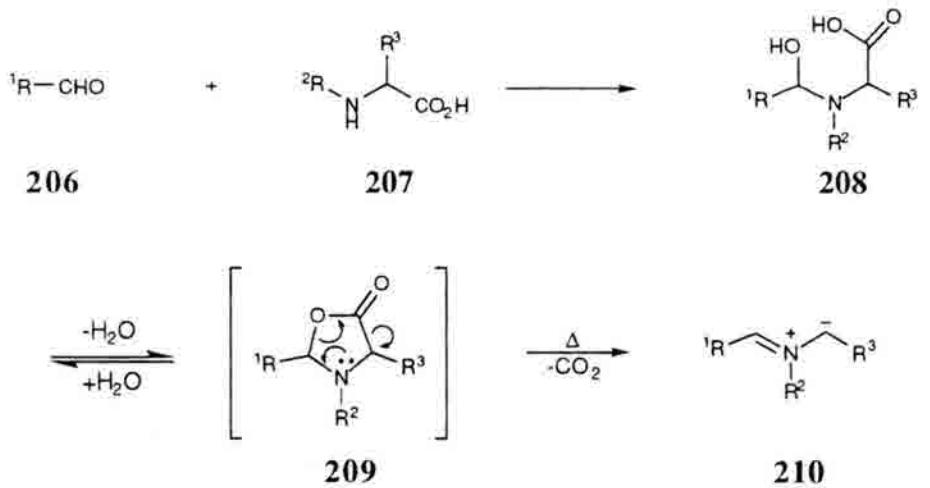

206 **207** **208** **209** **210**

acid results initially in formation of hemi-aminal **208**. Following loss of water, the proposed 5-oxazolidinone **209** decarboxylates upon heating to afford dipole **210**. The advantage that this process offered was the potential for variability in R^3 which represented the substituent that would ultimately appear on C-8 of the pyrrolidine. It was believed that this would more readily provide the necessary aldehyde oxidation state for this moiety. Also, generating the ylide by a different mechanism might affect the stereochemical outcome for the cycloadditive process. The caveat however, was that by lacking the ester moiety at R^3 of the ylide, the regiochemical outcome for cycloadditions would be less

predictable. In spite of this potential drawback, the possibility for success was considered adequate; therefore this approach was explored.

The first example tried was with sarcosine in the ylide-forming step (where R^2 = Me and R^3 = H). Therefore as outlined in Scheme 32, reaction of aldehyde **185** with five equivalents of sarcosine, ten equivalents of methyl acrylate and 0.1 equivalents of triethylamine in refluxing THF produced two pyrrolidine products (**212a** and **b**). While the

Scheme 32. Decarboxylation cycloaddition using sarcosine

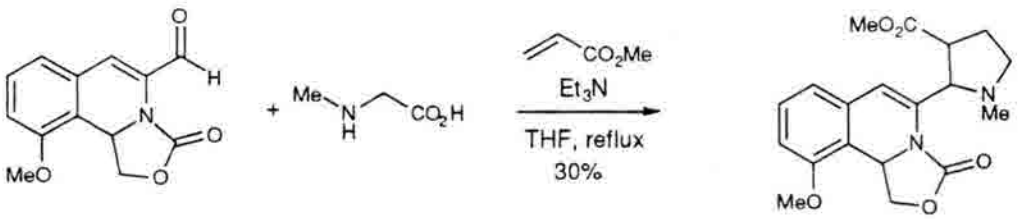

185 **211** **212**

^{1}H NMR data on compound **212b** were difficult to interpret, decoupling experiments on **212a** revealed the regiochemistry indicated in Scheme 32. This success prompted a strategy for generating pyrrolidines by this method which would have a protected aldehyde at C-8 (R^3 = masked aldehyde).

In order to apply this idea, the α-amino acid containing the masked aldehyde had to be prepared. Following the procedure[44] described by David and Veyrieres for the preparation of β-ethoxy-*O*-ethyl serine ethyl ester, amino acid **217** was prepared as outlined in Scheme 33. N-formylation of sarcosine followed by reaction with thionyl chloride in ethanol produced ethyl ester **213** in 83% overall yield. Formylation followed by reaction with sodium ethoxide and ethyl formate in benzene generated the intermediate sodium salt **214** as a gel. This material was then converted to ethyl ester **216** by reaction with dry hydrochloric acid in anhydrous ethanol for 48 hours at room temperature (46% yield from **213**). Amino acid **217** was then isolated from DOWEX 50 ion exchange resin

(H^+ form) following saponification of **216** with LiOH. It is noteworthy that in generating the diethyl acetal **216** over a 48 hour period, the N-formyl protecting group was removed

Scheme 33. Synthesis of amino acid **217**

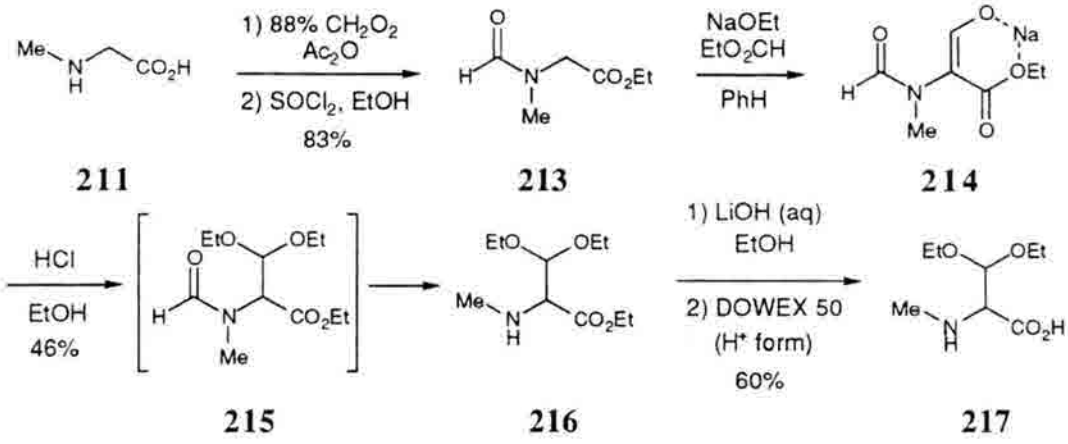

211 **213** **214**

215 **216** **217**

in a slower step. By letting this reaction go for just 2 hours as opposed to 48 hours, intermediate **215** could be isolated preferentially. This compound was to be used later to synthesize the methyl acetal analog of **217**.

With the necessary pieces in hand, the first cycloaddition reactions were attempted. Reaction of aldehyde **185** with **217** under the usual conditions afforded pyrrolidine cycloadducts **218a** and **218b** (Scheme 34a). Again, the two diastereomers isolated

Figure 20. Resonance contributors for azomethine ylide

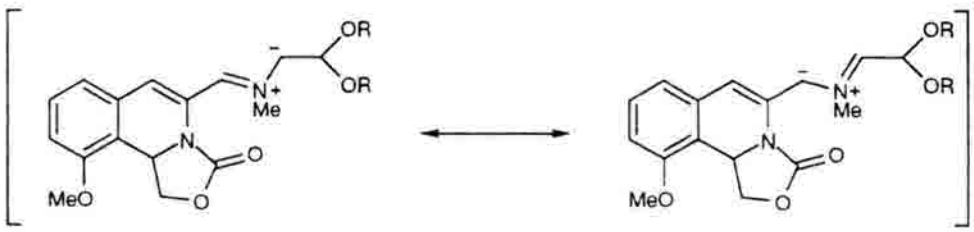

222 **223**

exhibited the regiochemistry depicted in Scheme 34a as determined by homonuclear decoupling experiments. As alluded to previously, this regiochemical outcome was difficult to predict, but might be rationalized by considering the relative contribution of the resonance structures depicted in Figure 20 for the azomethine ylide. Structure **223** puts negative charge on the allylic carbon which is conjugated to an electron rich aromatic system and is therefore highly delocalized. On the other hand, structure **222** puts the negative charge β to two oxygens which can be stabilized through induction.

Scheme 34. Cycloadditions with acetal-containing amino acid substrates

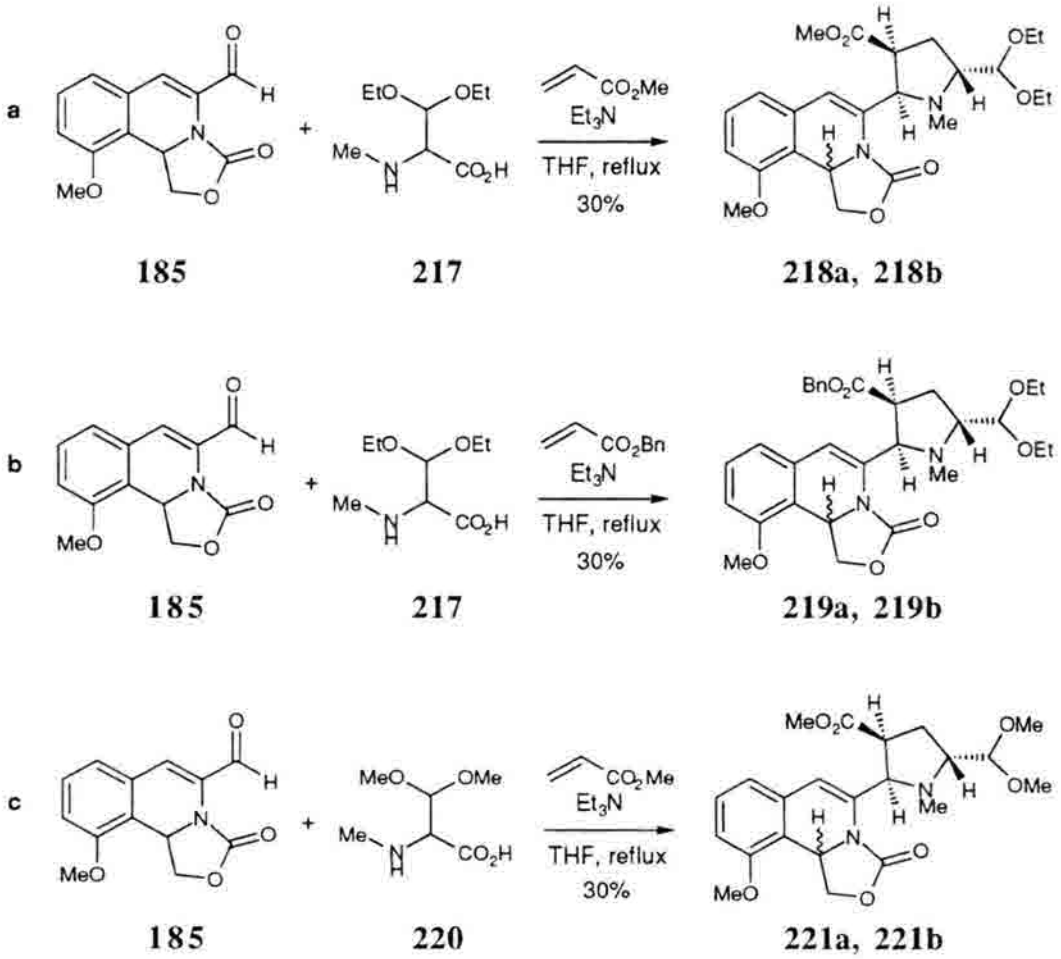

Figure 21. ^{1}H NMR spectrum (300 MHz) ($CDCl_3$) of cycloadduct **218a**

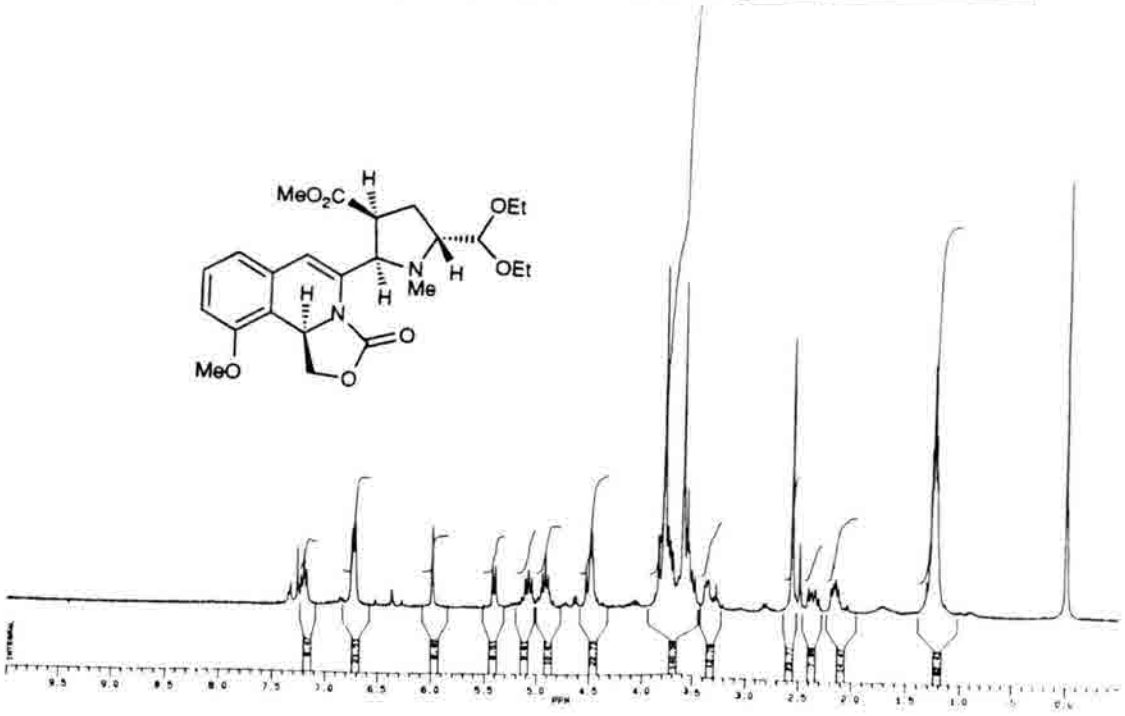

Figure 22. ^{1}H NMR spectrum (300 MHz) ($CDCl_3$) of cycloadduct **218b**

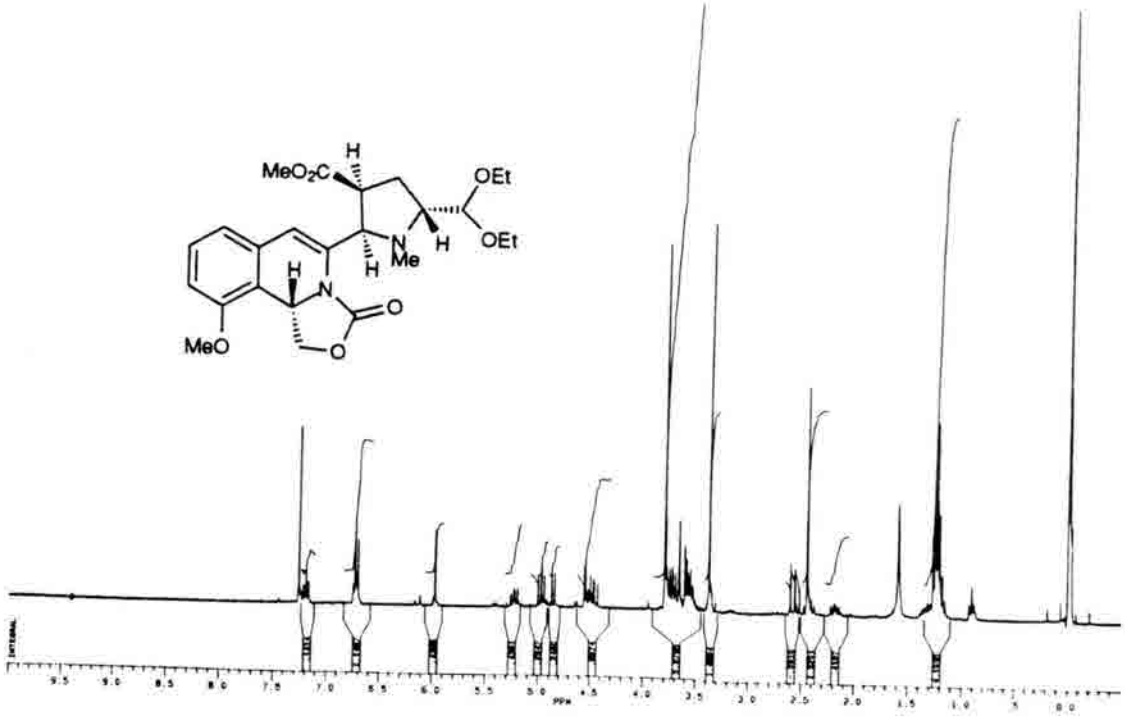

From the outcome of this reaction it appears that the latter must have been the major contributor, though it's worth pointing out that a third, minor isomer was detected in the crude reaction mixture. Although this material was not characterizable due to its minor contribution to the material balance, the possibility remains that this substance may have been a different regioisomer. By chemical correlation it was again determined that these cycloadducts displayed the same relative stereochemistry observed previously, which as stated before, indicates the wrong stereochemistry at C-8 and C-10 for **218a** (diastereomer

Table 8. Summary of cycloaddition reactions from aldehyde **185**.

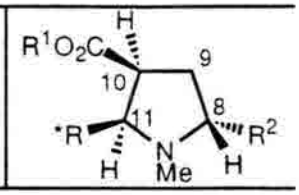

Entry	R^1	R^2	Ratio of diastereomers	Yield
1[a]	Me	H	2:1 (**212a** : **212b**)	30%
2[a]	Me	CH_2OBn	3:1 (**228a** : **228b**)	34%
3[a]	Me	$CH(OEt)_2$	2.5:1 (**218a** : **218b**)	32%
4[b]	Bn	$CH(OEt)_2$	2:1 (**219a** : **219b**)	30%
5[a]	Me	$CH(OMe)_2$	2:1 (**221a** : **221b**)	25%
6	Me	CO_2Et	1.5:1 (**203a** : **203b**)	58%
7	Me	CO_2Bn	1:1 (**205a** : **205b**)	62%

[a] Minor diastereomer not fully characterizable. [b] Third minor diastereomer observed, but not characterizable.

exhibiting the correct stereochemistry at C-11). In another attempt to alter this stereochemisty, the substituents for the intermediate ylide were varied as indicated in Schemes 34b and 34c. In 34b, methyl acrylate was replaced by benzyl acrylate, prepared

by reaction of acryloyl chloride with benzyl alcohol. Also, the dimethyl acetal analog of **217**, prepared by reaction of **215** with dry hydrochloric acid in anhydrous methanol, was employed as illustrated in Scheme 34c. In both cases, the same diastereomers were isolated and no new compounds were detected. In addition, the ratio of usual products changed only slightly. By examination of the whole set of reactions in Table 8, it can be seen that little variability in diastereoselectivity was ever realized. The only prominent trend was the superior yields observed for the deprotonation reactions (entries 6 and 7) versus the decarboxylation reactions (entries 1 through 5).

Scheme 35. Acetal deprotection study

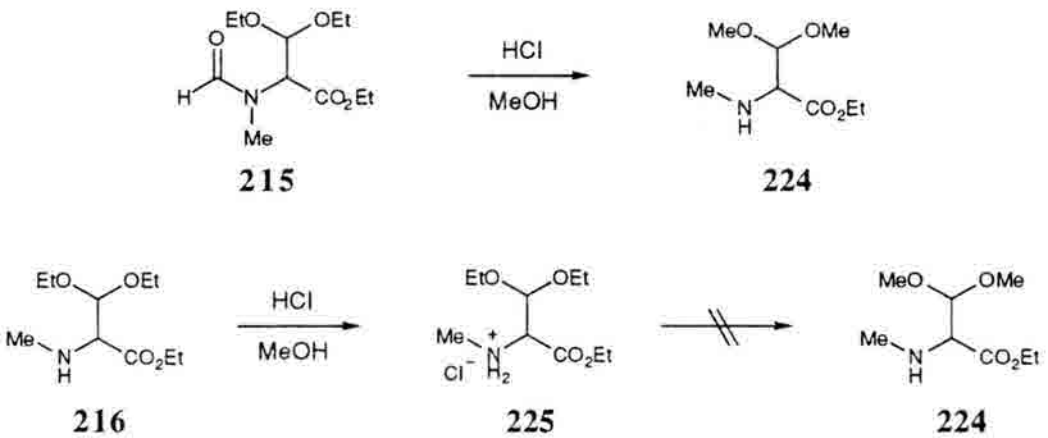

In another attempt to correct the stereochemistry of the cycloadducts prepared, efforts were made to deprotect the acetal functionality of **218a** with the intention of epimerizing the center at C-8. This was envisioned to occur either under the acidic conditions of acetal deprotection or by treatment of the unprotected aldehyde with base. In attempting this, however, a surprising result was obtained in that, even under highly acidic deprotection conditions, no acetal removal was observed. To understand this phenomenon better, the following study was conducted.

As discussed previously, **220** was prepared by reaction of **215** with dry hydrochloric acid in anhydrous methanol followed by saponification of ethyl ester **224** (Scheme 35). However, when the deformylated ethyl acetal **216** was treated under the same conditions, no exchange of ethoxy groups was detected by ^{1}H NMR. Even when reacted for two days with saturated methanolic hydrochloric acid or under reflux conditions, no exchange occurred. The best explanation for this behavior would be that for the latter example, formation of the hydrochloride salt occurs in an instantaneous first step and the resulting cation, in close proximity to the acetal inhibits positive charge development necessary for exchange or deprotection to occur.

Scheme 36. Cycloaddition with a serine based substrate

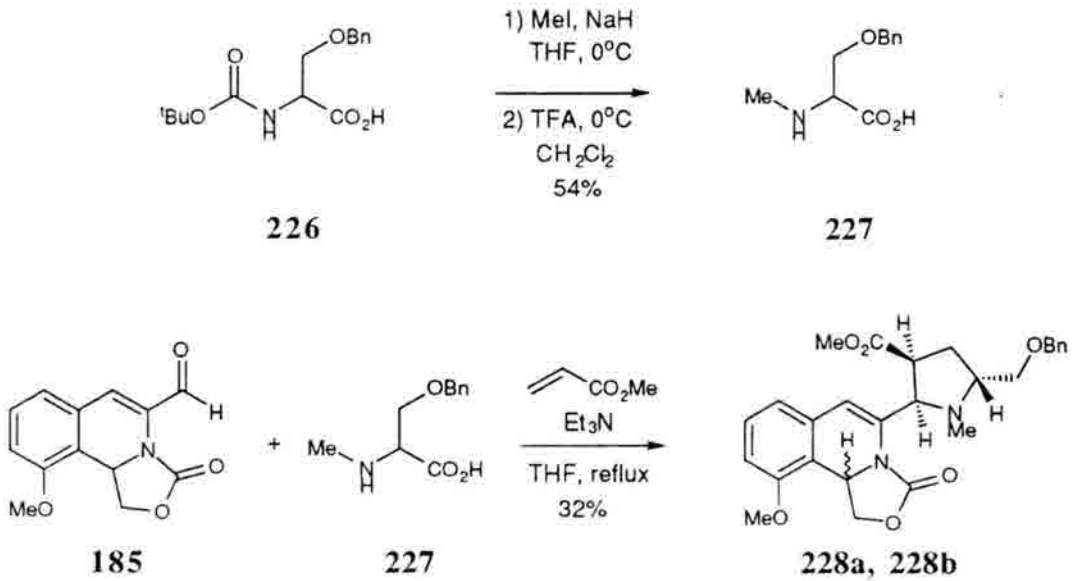

226 **227**

185 **227** **228a, 228b**

Another approach attempted in an effort to generate an aldehyde functionality at C-8 involved using *N*-methyl-*O*-benzyl serine as the α-amino acid substrate (**227**). This material was prepared as outlined in Scheme 36 from commercially available *N*-^{t}BOC-*O*-benzyl serine (**226**).[45] The cycloaddition step proceeded in 34% yield affording

cycloadducts **228a** and **b** in a 3:1 ratio (Scheme 36). Unfortunately, repeated attempts to debenzylate **228a** resulted in decomposition to an uncharacterizable mixture.

In a final effort to convert pyrrolidine cycloadducts into quinocarcin, the three step process outlined in Scheme 37 was employed. Palladium-catalyzed hydrogenolysis of cycloadducts **218a** and **219a** produced complex mixtures which were carried on crude. By deprotecting the oxazolidinones with LiOH followed by acidic work-up, it was

Scheme 37. Attempts to directly convert cycloadducts to **16**

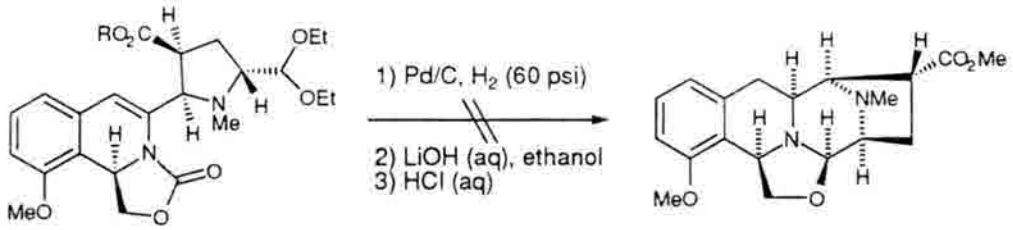

218a, R = Me
219a, R = Bn

16

anticipated that epimerization might occur at C-8 and/or C-10 resulting in the possiblility of some bicyclic product formation. However, due to the problem of deprotecting the acetals discussed above and the appearent instability of the intermediates to these conditions, no natural product was ever isolated by this procedure. Due to these failures, and as a result of encouraging results that were beginning to unfold for two modified approaches to this synthetic problem, this route was finally abandoned.

Though eventually deemed unsuccessful as an approach to the total synthesis of quinocarcin, the synthetic methodology presented in this section does however, represent a potentially useful extension of the cycloadditive technology employed. Table 8 demonstrates the versatility of these condensation reactions which involves the participation of three separate chemical entities. In doing so, these reactions result in the: (1) formation of a carbon-nitrogen bond and two carbon-carbon bonds; (2) formation of pyrrolidines

diastereoselectively and of one regiochemical configuration in a single step; and (3) presenting a choice of oxidation states for at least one of the pyrrolidine cycloadduct substituents. As part of an overall synthetic approach that could take advantage of the diastereoselectivity exhibited by these reactions, this chemistry might be potentially useful.

3.2. Modified Approach: Control of Pyrrolidine Stereochemistry

The inability to control stereochemistry at C-8 observed for the previous synthetic approach was due to the propensity of the ylides prepared to adopt a "W" configuration (**229**) prior to the cycloaddition step. To obtain the quinocarcin relative stereochemistry would require a 180° rotation of a bond in the dipole thereby producing **230** as the reactive

Figure 23. Dipole conformation interconversion

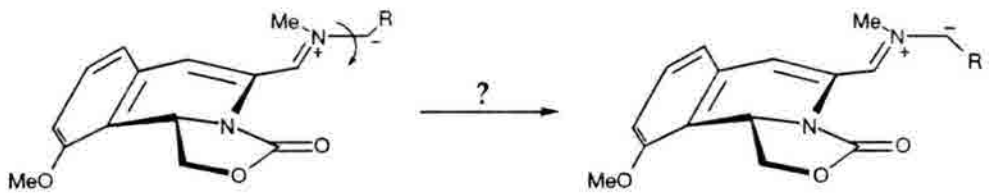

229 **230**

species. By the previous approach it was difficult if not impossible to effect such a conversion due to the acyclic nature of the dipoles formed which presumably assumes the "W" configuration so as to limit steric interactions between the various substituents.

One strategy that has been shown to circumvent this stereocontrol problem which could still utilize the intermediates generated from the model studies is that described by Joule *et al.* (Scheme 38).[46] In addition to obtaining the correct relative stereochemistry between C-8 and C-11 (DX-52-1 (**18**) numbering), the desired exo-configuration at C-10 exhibited by quinocarcin was also obtained.

Scheme 38. Joule cycloadditive approach

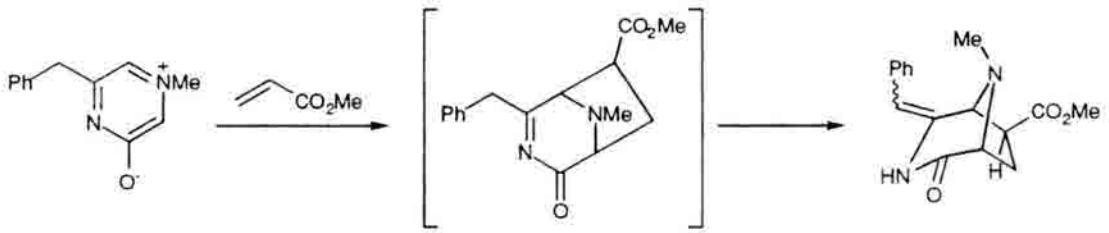

231 **232** **233**

To adopt this strategy the following two proposed synthetic approaches were envisioned and are presented by retrosynthetic analysis in Scheme 39. Obtaining intermediate **68** which, as described in Chapter 1 (Scheme 5), can be converted to quinocarcin would represent a formal synthesis. As such this intermediate was targeted. To carry out a cycloaddition analogous to that described by Joule would necessitate formation of ylide **242** which should readily be prepared by deprotonation of iminium **241** (Scheme 39). The first proposed synthesis of **241** involves formation of α,β-unsaturated amide **172** as described in Chapter 2 (Scheme 19). From this substrate, formation of oxazoline **237** was envisioned to occur by cyclization of amido alcohol (**172**) and subsequent deprotection of the oxazolidinone. The oxazoline protecting group was chosen on the basis of its base stability (necessary for deprotection of the oxazolidinone), and conversion to the corresponding aldehyde is well precedented.[47] N-acylation was then envisioned with 9-fluorenylmethyloxycabonyl (FMOC)-protected sarcosine to produce

Scheme 39. Retrosynthetic plan for revised approaches

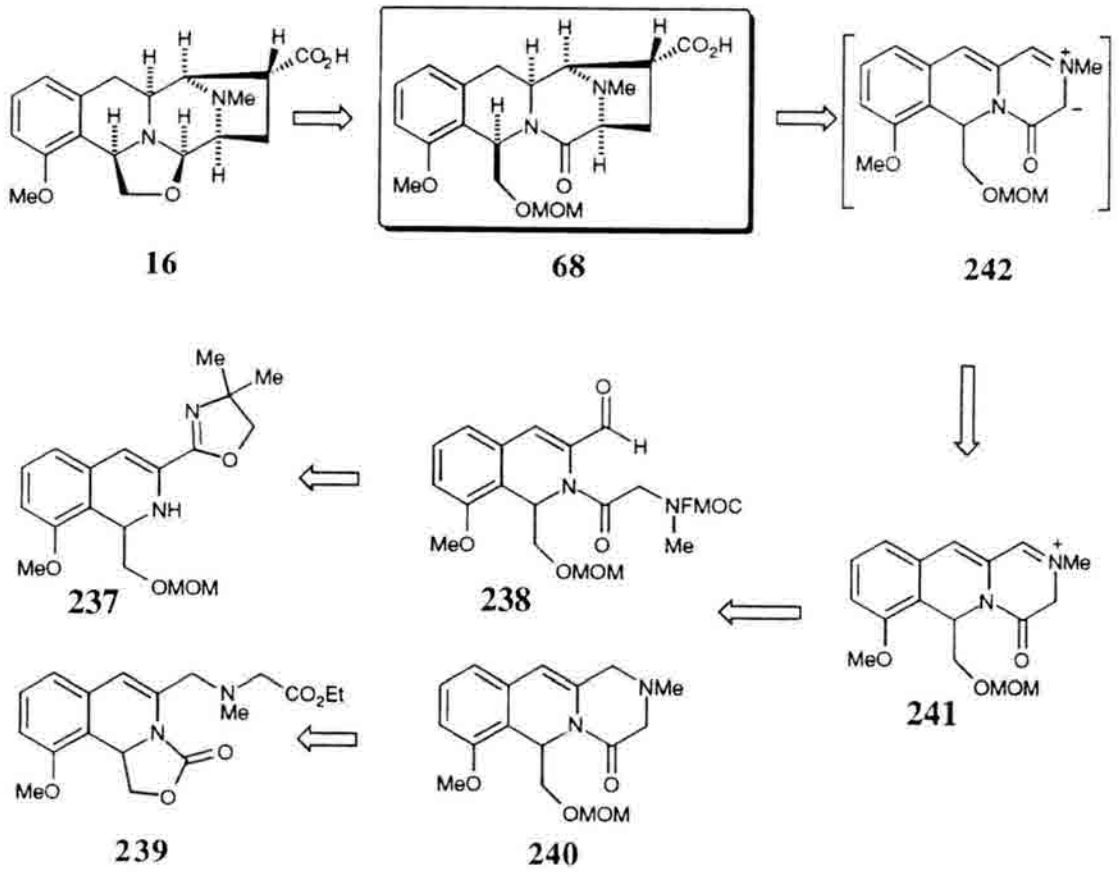

238. Under basic conditions, this substance should readily form iminium **241** by first deprotecting the base labile FMOC group followed by intramolecular cyclization. Under basic conditions this intermediate should spontaneously form ylide **242**.

The alternative approach to **242** was envisioned as occurring by reaction of allylic alcohol **186** with methanesulfonyl chloride followed by substitution with sarcosine ethyl ester to afford allylic amine **239**. Following oxazolidinone deprotection and saponification, this intermediate should be amenable to lactam formation thus producing tricyclic monoketopiperazine **240**. Oxidation of this substance to iminium **241** should then allow access to ylide **242**.

As planned, oxazoline **234** was prepared from amido alcohol **172** by reaction with thionyl chloride.[47] As a test for the utility of this functional group for this application the oxazoline was converted to aldehyde **185** in 60% overall yield by the standard protocol described by Meyers *et al.*[47a] With this aspect of oxazoline utility established, deprotection

Scheme 40. Synthesis of oxazolidinone deprotected substate for *N*-acylations

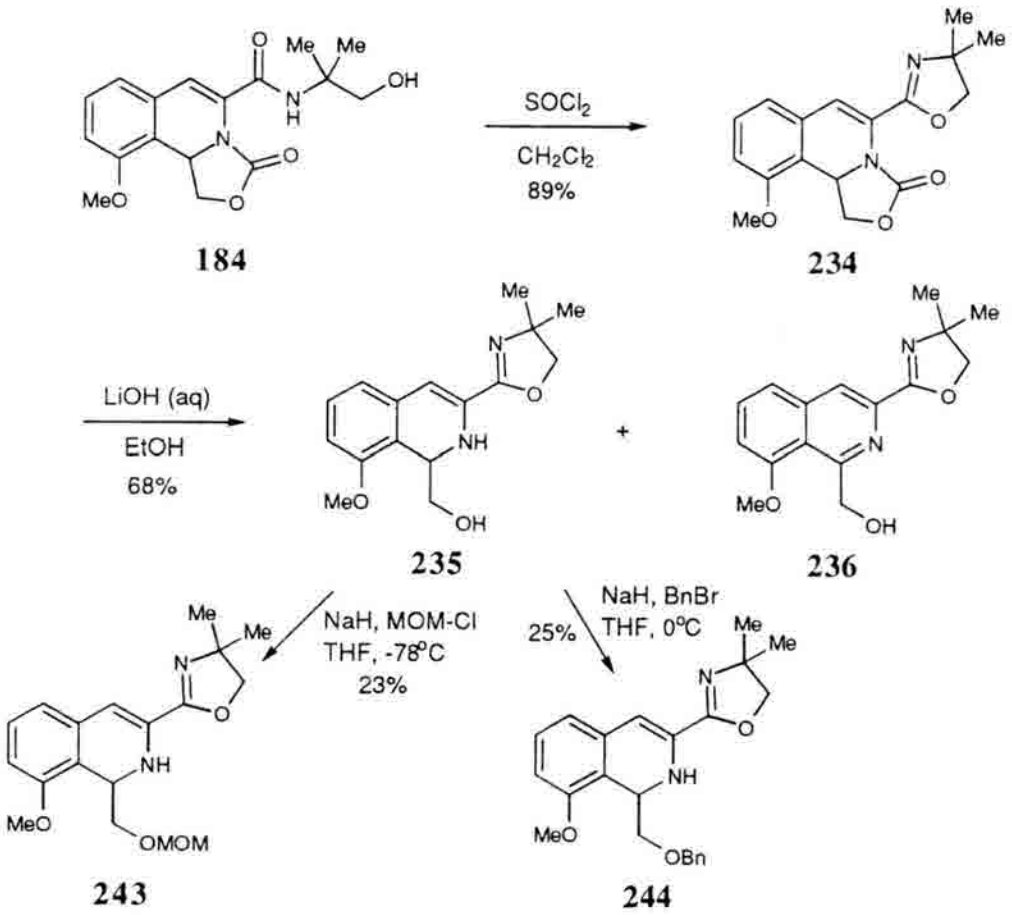

of the oxazolidinone of **234** was accomplished by reaction with LiOH (aq) in ethanol affording amino alcohol **235** and the oxidized isoquinoline **236** in approximately a 1:1 ratio (Scheme 40). Alcohol protection of amino alcohol **235** with MOM-Cl and benzyl bromide was conducted; the low yields observed were the result of oxidation to the

corresponding isoquinolines. As illustrated in Scheme 41, attempts to N-acylate these substrates with FMOC-sarcosine were unsuccessful presumably due to the highly hindered

Scheme 41. Attempted *N*-acylations of **235**, **243** and **244**

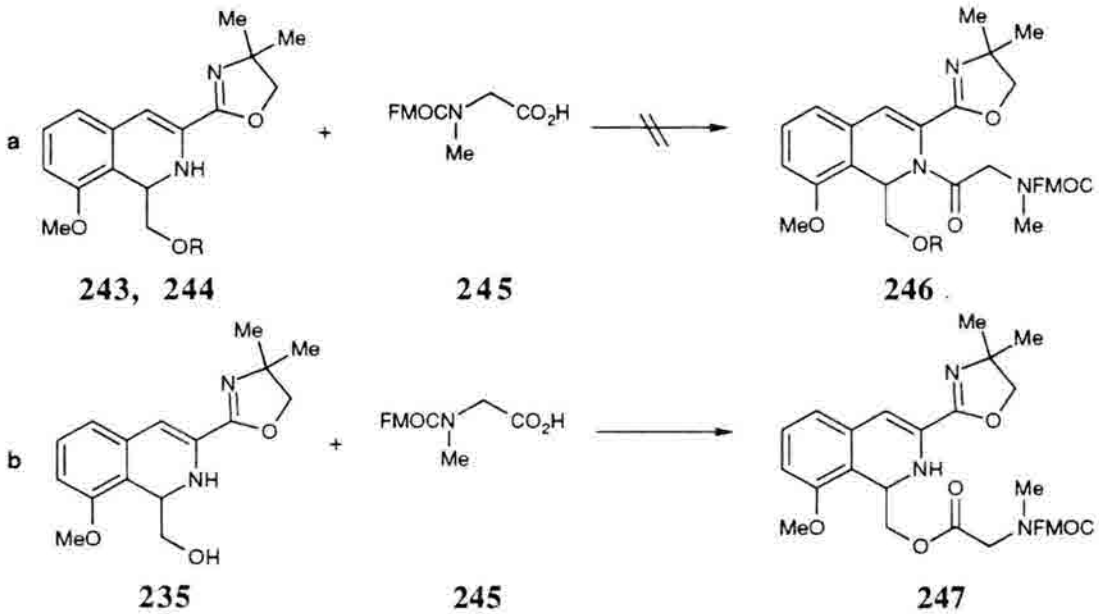

approach of the amine. Table 9 outlines the various acylation methods employed in this study. From entries 1 through 5 it can be seen that both carbodiimide and *bis*-(oxo-oxazolidonyl) phosphinic chloride (BOP-Cl) coupling strategies failed. The highly reactive ketene, generated as described by Evans *et al.*, also failed to react with the MOM-protected substrate.[48] In an effort to reduce the amount of steric crowding around the site of desired N-acylation, the alcohol protecting groups were removed. Although this should have made the amine more accessible, this also had the effect of producing another nucleophilic moiety on the substrate which, as can be seen in Table 9 (entries 6 and 7), resulted exclusively in formation of ester **247** as opposed to the desired amide. Repeated attempts to N-acylate this compound were unsuccessful. Other protecting group strategies were also examined in place of the oxazoline. The MOM- and benzyl-protected allylic alcohols were prepared,

though attempts to deprotect the oxazolidinone in the presence of these groups, even in a carefully purged argon atmosphere, led almost exclusively to the isoquinoline by-products.

Table 9. Attempts to N-acylate **235**, **243** and **244**.

Entry	Substrate	Conditions	Results
1	**244**	DCC, methylene chloride	No reaction
2	**244**	[a] BOP-Cl, Et_3N, methylenechloride	No reaction
3	**243**	DCC, methylene chloride	No reaction
4	**243**	[a] BOP-Cl, Et_3N, methylenechloride	No reaction
5[b]	**243**	Ketene	No reaction
6	**235**	DCC, methylene chloride	22% yield to **247**
7[b]	**235**	Ketene	40% yield to **247**

[a] *bis*-(oxo-oxazolidonyl) phosphinic chloride. [b] Ketene prepared as described by Evans *et al.* and Hegedus *et al.* by addition of Et_3N to the acid chloride at -78°C.[48]

Additionally, attempts to protect the α,β-unsaturated aldehyde **185** as an acetal were unsuccessful, leading only to decomposition.

The inability to N-acylate this substrate prompted an investigation of the alternate route to azomethine ylide **242** *via* the monoketopiperazine. This was accomplished by first preparing tricyclic monoketopiperazine **248** as outlined in Scheme 42. From allylic alcohol **186**, reaction with methanesulfonyl chloride followed by addition of sarcosine ethyl ester afforded allylic amine **239** in 96% yield on the two steps. Saponification of the ethyl ester and deprotection of the oxazolidinone afforded the intermediate amino alcohol. This material was then carried on without purification by cyclization with 1,3-

dicyclohexylcarbodiimide (DCC) and N-hydroxybenzatriazole (HOBT) producing **248** in 53% isolated yield on the two steps. At this point, a number of procedures were tried in an

Scheme 42. Formal total synthesis of (±)-quinocarcin

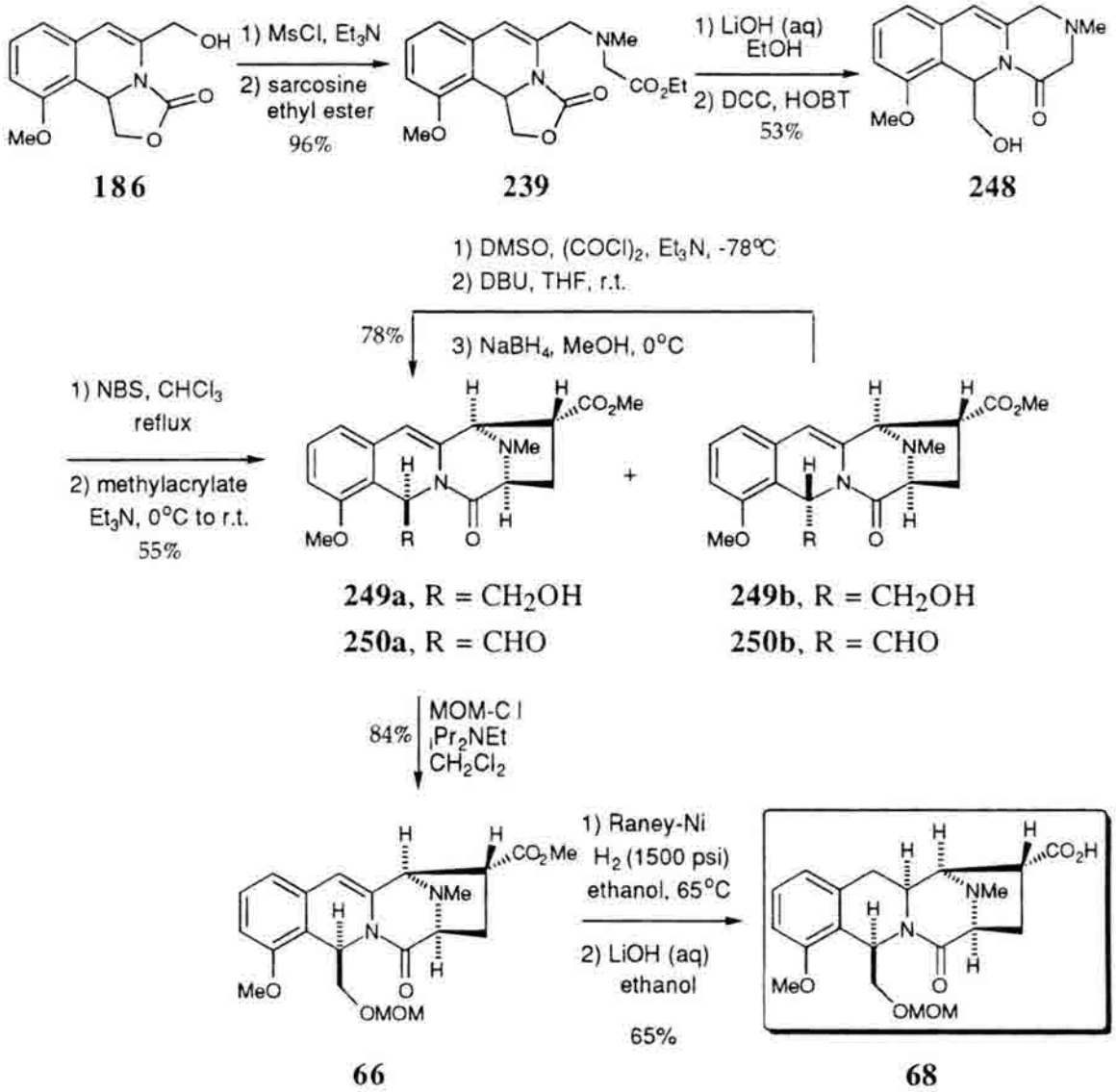

effort to introduce a double bond in the C ring by oxidation, thus generating the iminium precursor to azomethine ylide **242**. Attempts to generate the dipole *via* the N-oxide led to decomposition of the substrate. Attempts to employ other oxidants such as 2,3-dichloro-

5,6-dicyanoquinone (DDQ) and *tert*-butyl hypochlorite also resulted in the decomposition of this substance. Reaction of **248** with one equivalent of N-bromosuccinimide (NBS) in

Figure 24. ^{1}H NMR spectrum (300 MHz) ($CDCl_3$) of **68**

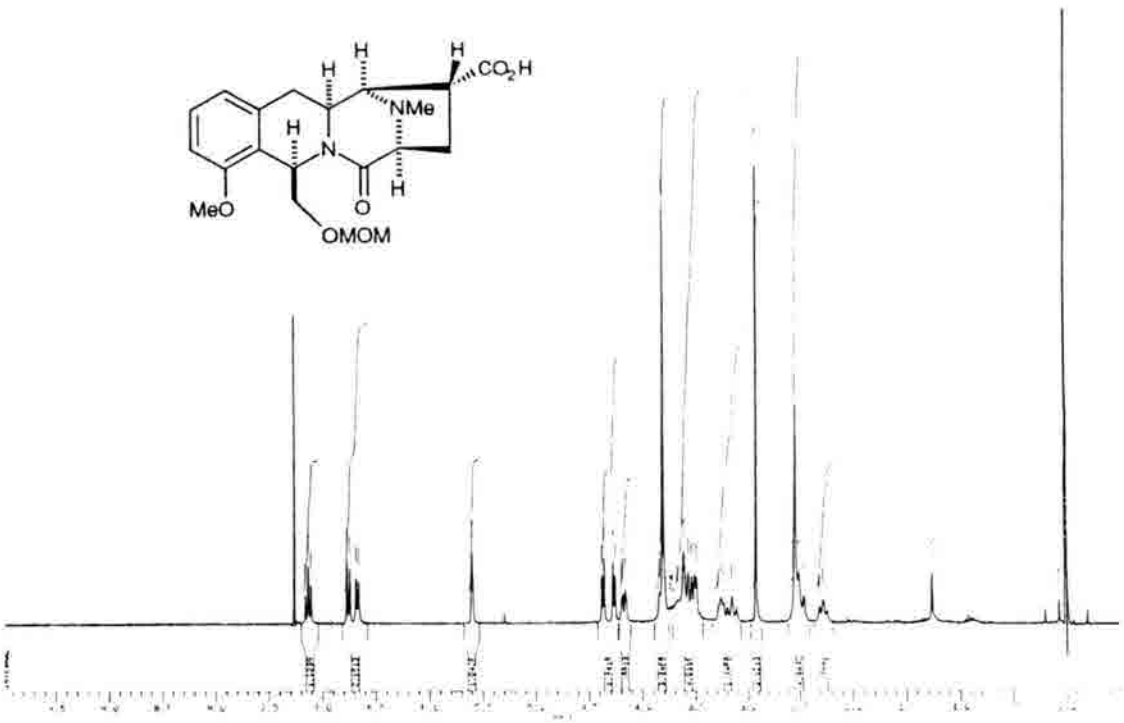

refluxing chloroform however, did result in formation of the dark green iminium salt. Upon addition of triethylamine at 0°C to this mixture resulted in a dark blue solution which upon warming to room temperature in the presence of methyl acrylate resulted in the formation of a 5:1 ratio of cycloadducts **249b** and **249a** respectively (55% yield on the two steps which is comparable to yields observed by Joule *et al.* on their substrate).[46] This ratio presumably resulted from a preference for approach of the dipolarophile from the least hindered face. No other cycloadducts were isolated from the reaction mixture. Compounds **249a** and **b** were again diastereomeric about C-5; both possessed the desired pyrrolidine regiochemistry, relative stereochemistry and exo configuration at C-10. Since

the desired product (**249a**) was the minor diastereomer from the cycloaddition, **249b** was subsequently epimerized to **249a** in the following manner (see Scheme 42). Amido alcohol

Scheme 43. Synthesis of saturated tricyclic monoketopiperazine **257**

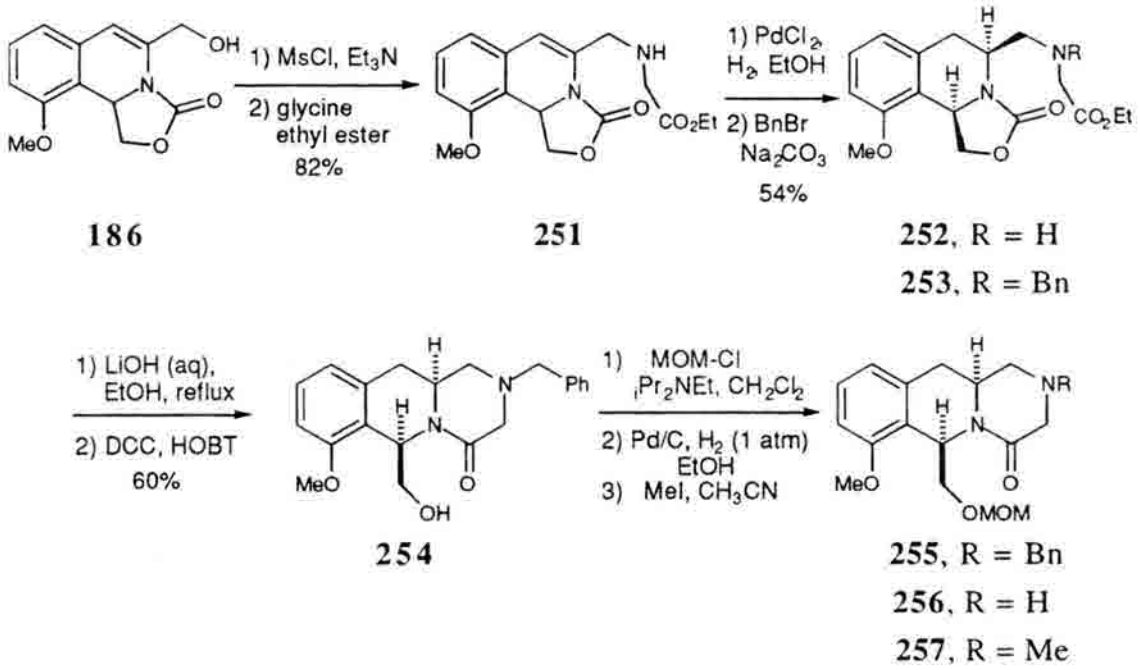

186 **251** **252**, R = H; **253**, R = Bn

254 **255**, R = Bn; **256**, R = H; **257**, R = Me

249b was first oxidized under Swern conditions to **250b** in 94% yield. Next, **250b** was reacted with one equivalent of 1,8-diazobicyclo [5.4.0] undec-7-ene (DBU) in THF at room temperature for 3 h resulting in 80% conversion to aldehyde **250a**. The $NaBH_4$ reduction of **250a** to **249a** is a reaction that was first described in the total synthesis of quinocarcinol methyl ester[18] by Danishefsky *et al.* (Chapter 1, Scheme 2) which completed the conversion of **249b** to **249a** in 78% overall yield (based on 20% recovery of **250b**). The alcohol of compound **249a** was then protected by reaction with chloromethyl methyl ether and N,N-diisopropylethylamine affording **66** in 84% yield; this substrate had been previously prepared by Garner.[23] This substance (**66**) was then converted to **68** via Raney-Ni (W2) reduction (1500 psi H2) followed by saponification of the methyl ester affording **68** in 65% yield based on recovered starting material form the Raney-Ni

reduction. As described in Chapter 1 (Scheme 5), **68** can now be converted to **18** by partial reduction of the amide by dissolving lithium reduction and trapping with cyanide. The target compound (**16**) is then generated from DX-52-1 (**18**) under acidic or Lewis-acidic conditions.

The Raney-Ni reduction step in this sequence represents the most cumbersome reaction to carry out, requiring special equipment and harsh conditions. These conditions have been reported to result in overreduction and unwanted side reactions in some cases.[23b] As an extension to the synthetic approach outlined in Scheme 42, the following exercise was conducted in an effort to bypass the Raney-Ni reaction, thus intersecting the Garner synthesis at a more advanced intermediate. By coupling glycine ethyl ester to allylic alcohol **186** in an analogous manner to that just described for sarcosine ethyl ester, allylic amine **251** was afforded (Scheme 43). This substance was easily reduced diastereoselectively to amino ester **252** in high yield. This was accomplished by reacting **251** with one equivalent of palladium chloride, under one atmosphere of hydrogen in ethanol for 16 hours. It is important to point out that these conditions did not reduce the corresponding double bond of **66**. Following benzyl protection of the amine, deprotection of the oxazolidinone followed by lactam formation generated the saturated monoketopiperazine **254** in 60% yield on the two steps (Scheme 43). This substance was sequentially MOM-protected and benzyl-deprotected affording **256** in 66% yield overall. Finally, the N-methyl derivative of this compound (**257**) was generated by reaction with iodomethane in acetonitrile.

Attempts to generate the corresponding azomethine ylide *via* the NBS oxidative process were unsuccessful yielding no detectable cycloadducts. This result forced the conclusion that the ability of NBS to carry out this transformation on **248** may be peculiar to this type of substrate, the implication being the requirement for an sp^2 hybridized center at C-11a (DX-52-1 (**18**) numbering) in order for the bromination reaction to proceed.

Bromination presumably occurs on the allylic carbon, initially forming **258**, which is immediately followed by elimination of the bromide, producing **259** (Scheme 44). Aliquots of the reaction mixture after just 10 minutes reveal a new singlet in the ^{1}H NMR at 10.00 ppm indicative of the iminium methine. Also the resulting deep green color observed is the likely result of extended conjugation upon formation of **259**. The regiochemical

Scheme 44. Proposed mechanism for NBS mediated ylide formation

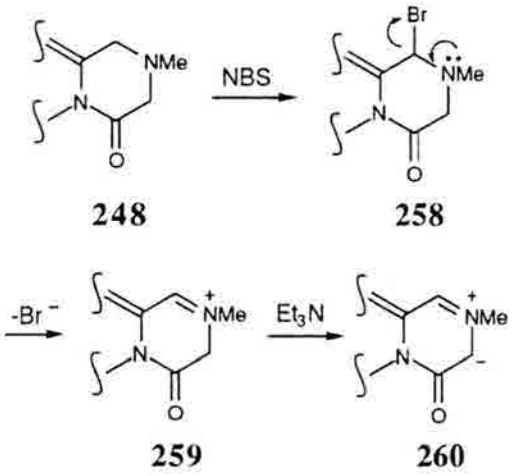

248 **258** **259** **260**

outcome of the cycloaddition reaction results from **260** being the major resonance contributor to the azomethine ylide. As with the previous cycloaddition reactions, this is the result of negative charge being effectively stabilized on the carbon α to the amide carbonyl. As dictated by the cyclic nature of **260**, the cycloadducts formed are forced into the desired relative stereochemical configuration between C-8 and C-11.

Although formation of an ylide on the saturated substrate (**257**) could not be generated by the NBS oxidative approach, a number of procedures for dipole formation on this substrate could still be attempted such as those proposed in Scheme 45. Oxidation of the secondary amine to imine **261** followed by quaternization may lead to dipole formation. Alternatively, the ylide may be accessed *via* the methylamine *N*-oxide (**263**).[39] Success

with either approach would have obvious advantages and therefore represent areas of synthetic research that should continue.

Scheme 45. Proposed methods of ylide formation for saturated substrate

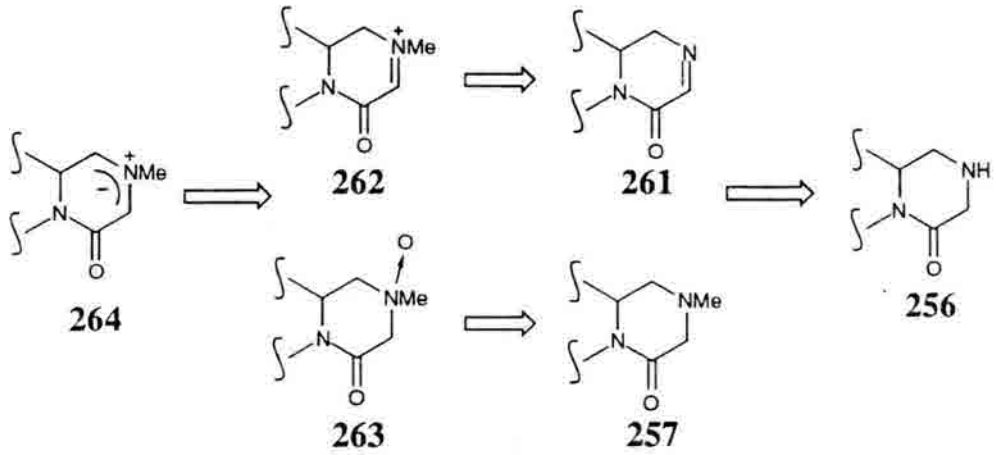

In summary, the methodology described in this section represents a new synthetic approach to access advanced intermediates toward the total synthesis of quinocarcin which should have utility enroute to the other members in this class of antitumor antibiotics. This approach is particularly attractive because it involves the use of common, readily available shelf reagents, and all of the steps described are amenable to large scale chemistry. Although an epimerization is necessary, this three-step process benefits from a thermodynamically favored epimerization reaction. A number of steps in this synthesis should also be amenable to the development of asymmetric variants which would result in a very effective synthetic approach to these natural products.

3.3. Future Directions

3.3.a. Proposed total synthesis of tetrazomine. To date there has not been a published synthesis of tetrazomine despite the remarkable structural similarities between **20** and **16**. The original structure elucidation of **20** was presented without any indication of

relative stereochemistry. Based on this report, the major structural differences between **20** and **16** were twofold. First, the oxidation state of the carbon attached to C-10'; and second, the presence of the β-hydroxypipecolinic acid moiety acylated *via* a nitrogen on C-3'.

Figure 25. Structures of quinocarcin and tetrazomine

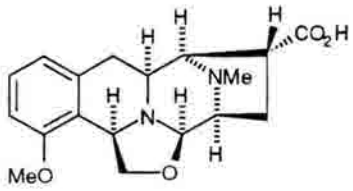

Quinocarcin, **16**

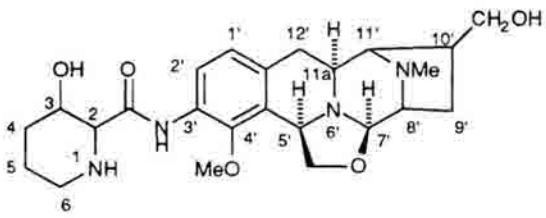

Tetrazomine, **20**

Results presented in Chapter 4 illustrate the ability of tetrazomine to generate superoxide, an ability shared by quinocarcin.[49,50] This redox behavior has been shown to require a *trans*-antiperiplanar relationship between the oxazolidine nitrogen lone pair and the adjacent methine. As indicated by the results obtained in the model studies, the three dimensional structure elucidation of **45a** and **45b** suggests that this oxazolidine conformation can only exist if the C-11a (C11a' for **20**) *syn* stereochemistry exhibited by quinocarcin is present.[33] On the basis of this stereoelectronic requirement and the similar redox behavior exhibited by both **16** and **20**, it is likely that **20** possesses the same relative stereochemistry at C-5', C-7' and C-11a' as that for **16**. Therefore, it is logical to propose the total synthesis of **20** starting from intermediate **68** prepared in the aforementioned formal synthesis.

Scheme 46. Synthesis of **269** *via* Williams lactone methodology

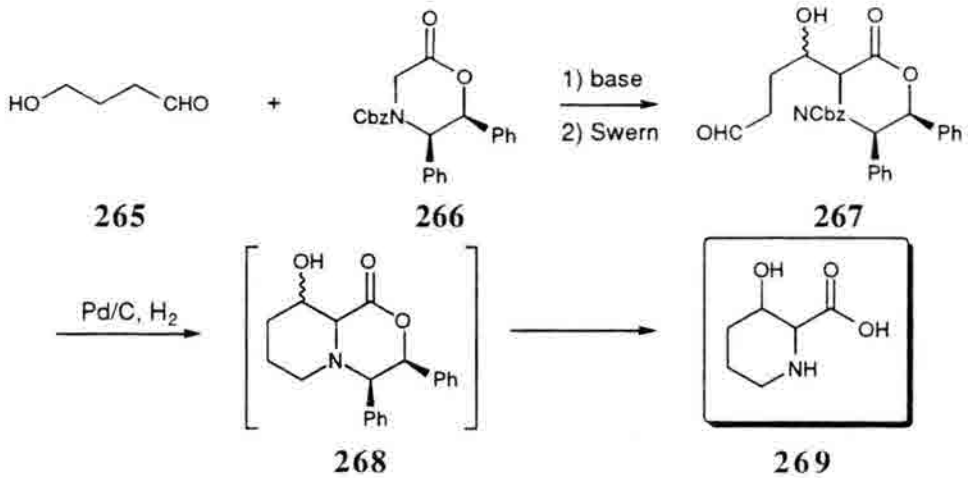

265 **266** **267** **268** **269**

In addition to the methodology presented in this chapter which demonstrates the accessibility of DX-52-1 (**18**), the following unpublished results from the Williams research group have also demonstrated the ability to access other features exhibited by **20**.

Scheme 47. Precedence for C-3' derivatization

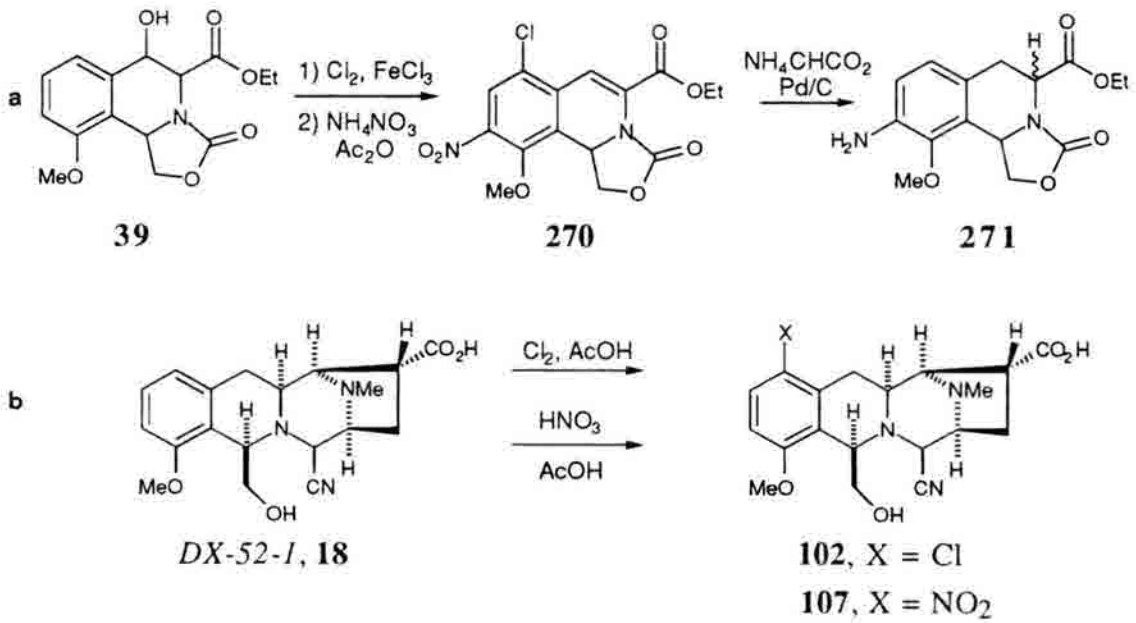

39 **270** **271**

DX-52-1, **18**

102, X = Cl

107, X = NO_2

These include constructing the β-hydroxypipecolinic acid residue (**269**) *via* the Williams electrophilic glycinate methodology[51] as outlined in Scheme 47, and the development of methodology for the selective functionalization of C-3' (Scheme 47a).[52] From the information presented in Chapter 1 and outlined in Scheme 47b involving the semi-synthetic derivatization of **16**, the precedent for carrying out the three-step procedure outlined in Scheme 47a on **18** is well established (Scheme 47b).[30] Based on this assumption, the following total synthesis of **20** is envisioned as outlined by retrosynthetic analysis (Scheme 48).

Scheme 48. Proposed total synthesis of (±)-tetrazomine

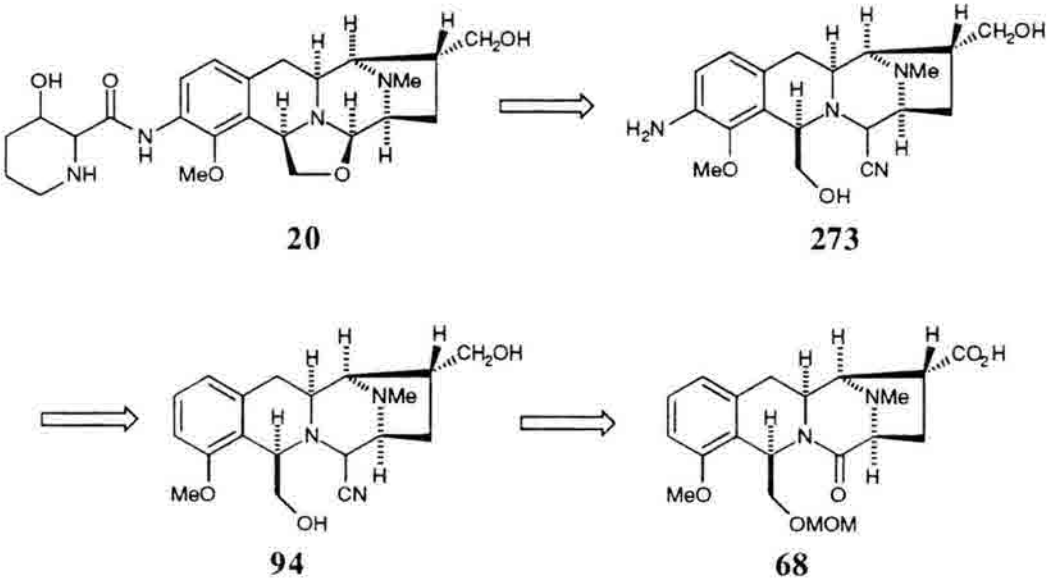

20 **273**

94 **68**

Starting with intermediate **68** prepared as described herein, **94** should be readily obtainable via **18** (prepared in three steps as shown by Garner) by sodium borohydride reduction of the isopropyl carbonate on C-10 as illustrated in Scheme 9, Chapter 1.[29] The incorporation of the amine at C-3 is then envisioned *via* the steps described in Scheme 47a to obtain **273**. Finally acylation with **269** followed by deprotections as necessary should

furnish **20** upon generation of the oxazolidine ring by one of the known procedures (acid or $AgNO_3$).[30-32]

Chapter 4
The O_2-Dependent Cleavage of DNA by Quinocarcin, Tetrazomine and Synthetic Structural Analogs

4.1 Background

It is now widely recognized[53] that a variety of clinically significant antitumor antibiotics can mediate oxygen-dependent cleavage of the ribose-phosphate backbone of cellular DNA and RNA. An enormous structural array of interesting natural products and semi-synthetic and totally synthetic substances mediate oxidative strand scission of nucleic acids through metal-mediated activation of O_2 ultimately producing hydroxyl radical or other reactive oxygen species.[54-61] Many readily oxidizable organic substances such as semi-quinone radical anions, thiols and ascorbate are capable of reducing molecular oxygen resulting in the production of superoxide.

Superoxide is well documented to mediate DNA strand breakage *via* dismutation to hydrogen peroxide followed by Fenton-mediated generation of the diffusable and highly reactive hydroxyl radical.[13] The dismutation of superoxide is known to be facilitated by a variety of iron chelates (Haber-Weiss cycle), which turns out to be the only kinetically significant step in the overall reduction of dioxygen to hydroxyl radical (Scheme 49).[62] With iron-ethylenediaminetetraacetic acid (EDTA), k_2 represents the rate determining step at neutral pH resulting in a steady state of Fe(II)EDTA since $k_1 > k_3 >> k_2 > k_{-1}$.[62c] In the absence of metal chelators such as EDTA which, have the effect of accelerating the Fenton reaction, the rate determining step becomes the reduction of H_2O_2 by Fe(II) (Fenton reaction, 76 M^{-1} s^{-1}, step 3, Scheme 49).[62d] Since essentially all of the O_2-dependent

DNA-damaging reactions described herein are conducted in the absence of such metal chelators, this latter rate constant (76 M^{-1} s^{-1}) is the most relevant.

Production of hydroxyl radical can be monitored by examining its reaction with reporter molecules such as deoxyribose. This process has been shown to be inhibited: (1) by superoxide dismutase (SOD), illustrating the superoxide-dependence for the overall process since superoxide is responsible for generating Fe(II) in the rate determining step;

Scheme 49. Haber-Weiss / Fenton cycling

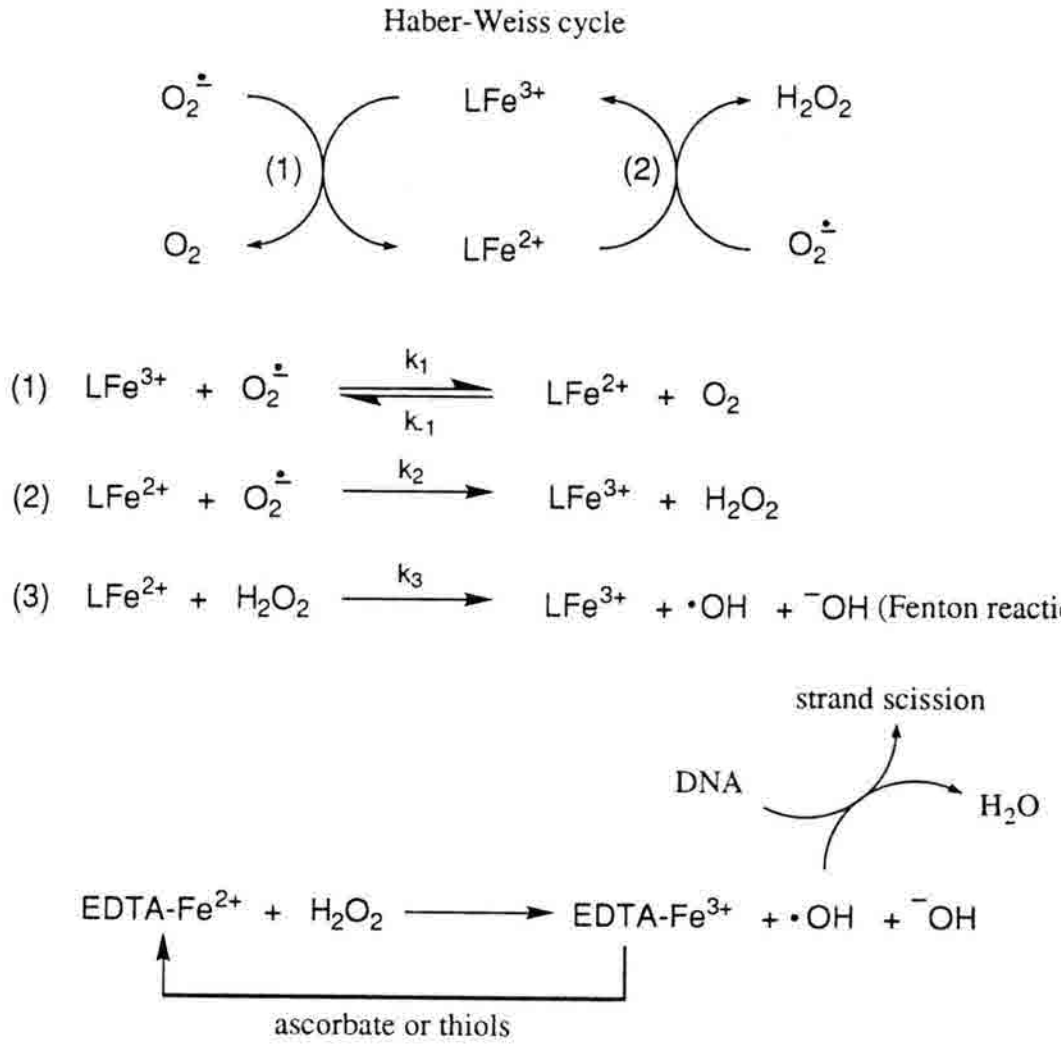

(2) by catalase to a lesser extent than SOD, but still demonstrating the role of hydrogen peroxide in this process; and (3) by formate, picolinate,[63] thiourea and mannitol, which are known hydroxyl radical scavengers.

The ability of hydroxyl radical to abstract hydrogen atoms from deoxyribose is at the basis of its ability to cause oxidative damage to DNA and RNA. Since hydroxyl radical is a short-lived, high energy, diffusable species, the damage caused to nucleic acids is random, resulting in strand scission at any base pair site. This process can be activated by addition of reducing agents such as ascorbate and thiols which provide a constant source of Fe(II) as well as superoxide thereby facilitating the DNA-cleavage process (Scheme 49).[56a] It's important to point out here that other activated oxygen species have been invoked in the DNA-cleavage process. Based on certain thermodynamic considerations, it has been suggested that the product, or one of the products (produced in addition to hydroxyl radical) from the Fenton reaction may actually be an Fe(IV)EDTA-oxo species.[64] Although spin-trapping of hydroxyl radical in the EPR does indicate its presence, it does not disprove the presence of a reactive Fe(IV) complex since the hydroxyl radical detected may result from hydrolysis of the putative Fe(IV)EDTA-oxo compound. Although this point is still being debated in the literature, for the purpose of this discussion it is merely a point of edification since the outcome of this debate should have little consequence as to the mechanism by which the compounds described herein generate superoxide.

The damage incurred by DNA upon reaction with hydroxyl radical (or activated oxygen species) has been shown to occur *via* two predominate pathways.[54] The first, illustrated in Scheme 50, results from hydroxyl radical abstraction of the C-1' hydrogen from the deoxyribose producing radical **275**. Upon radical coupling of **275** with another equivalent of hydroxyl radical, the hydroxylated product **276** suffers base release in a pH-dependent step affording lactone **277**. As a result of activation of the α-protons, a second base dependent step causes strand scission and formation of the unsaturated lactone **278**.

Scheme 50. C-1' hydrogen atom abstraction

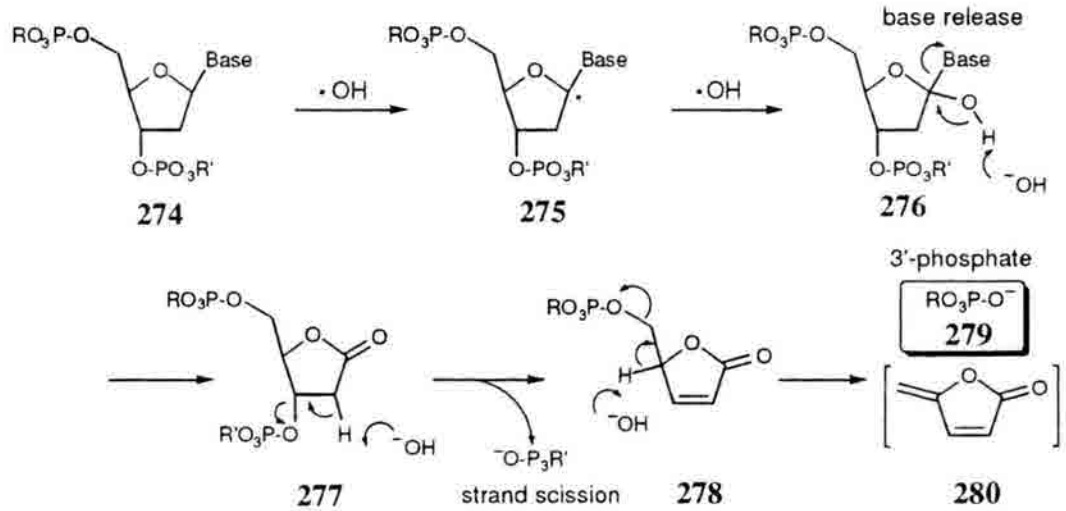

In a final base-mediated step, the 3'-phosphate product (**279**) is afforded in addition to the putative intermediate **280** (never actually isolated as a result of its high reactivity under these conditions). The other fate of the DNA comes from abstraction of the C-4' hydrogen

Scheme 51. C-4' hydrogen atom abstraction

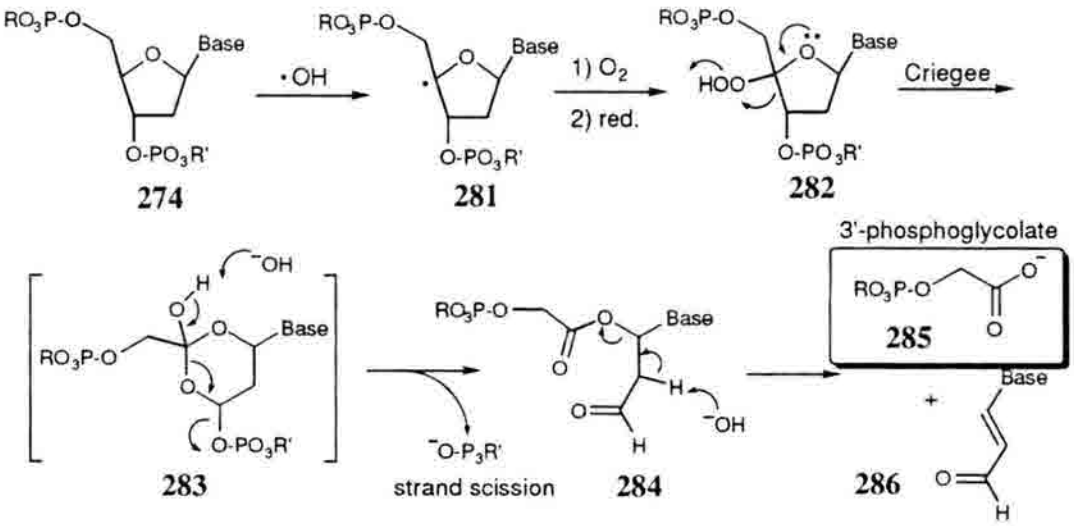

resulting in ribosyl radical **281** as outlined in Scheme 51. Reaction of this species with molecular oxygen followed by single electron reduction results in hydroperoxide **282**.

This structure is then proposed to undergo a Criegee rearrangement affording the alkaline labile intermediate **283** which decomposes to aldehyde **284** resulting in strand scission. In a final base-mediated step, the 3'-phosphoglycolate product (**285**) is formed in addition to the base propenal (**286**).

Reaction of hydroxyl radical with 5'-^{32}P-labeled DNA causes a statistical mixture of degradation products resulting from cleavage occurring at every base pair. Autoradiograms of electrophoresis gels display the characteristic "ladder" indicative of this non-selective cleavage process. In addition to the ladder, doublets ("Tullius bands") are produced at every base pair cleavage site which correspond to the two 3'-products (3'-phosphate (**279**) and 3'-phosphoglycolate (**285**)) produced by the two pathways just described.[56,57] As a result of elucidation of these two mechanisms (Schemes 50 and 51), this pattern has become very diagnostic of hydroxyl radical-mediated damage to DNA.

Scheme 52. Production of superoxide by thiols

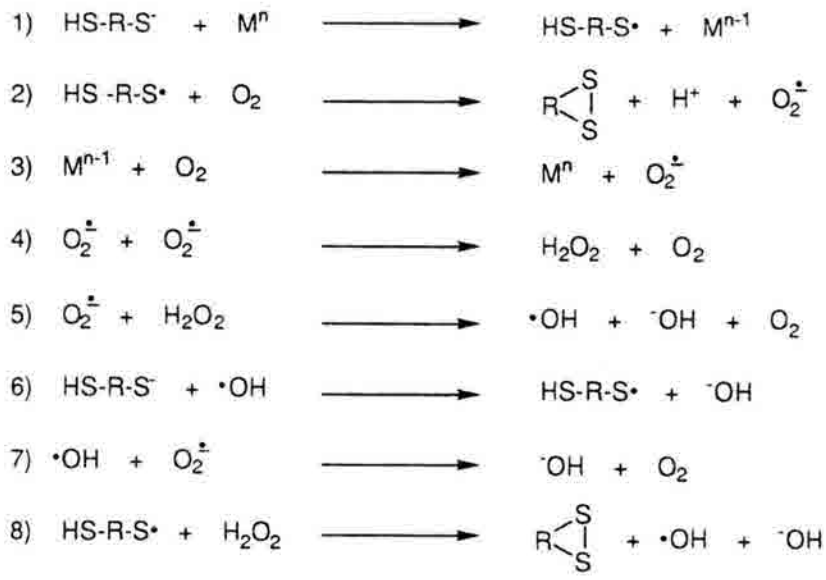

Organic molecules that damage nucleic acids by a metal-dependent activation of molecular oxygen are numerous. The following examples represent the most highly studied mechanisms of O_2 activation.

Thiols are well known to produce reduced forms of molecular oxygen.[65] In a stepwise process thiols are converted to disulfides in the presence of oxygen resulting in the concomitant reduction of molecular oxygen to superoxide. This process is believed to involve metal [Fe^{3+} or Cu^{2+}] reduction in the first step producing the M^{n-1} species plus the thiyl radical (Scheme 52). A single electron transfer from this radical to molecular oxygen affords superoxide with the disulfide being produced in the process. The resulting M^{n-1}

Figure 26. Structures of the anthracyclines and bleomycins

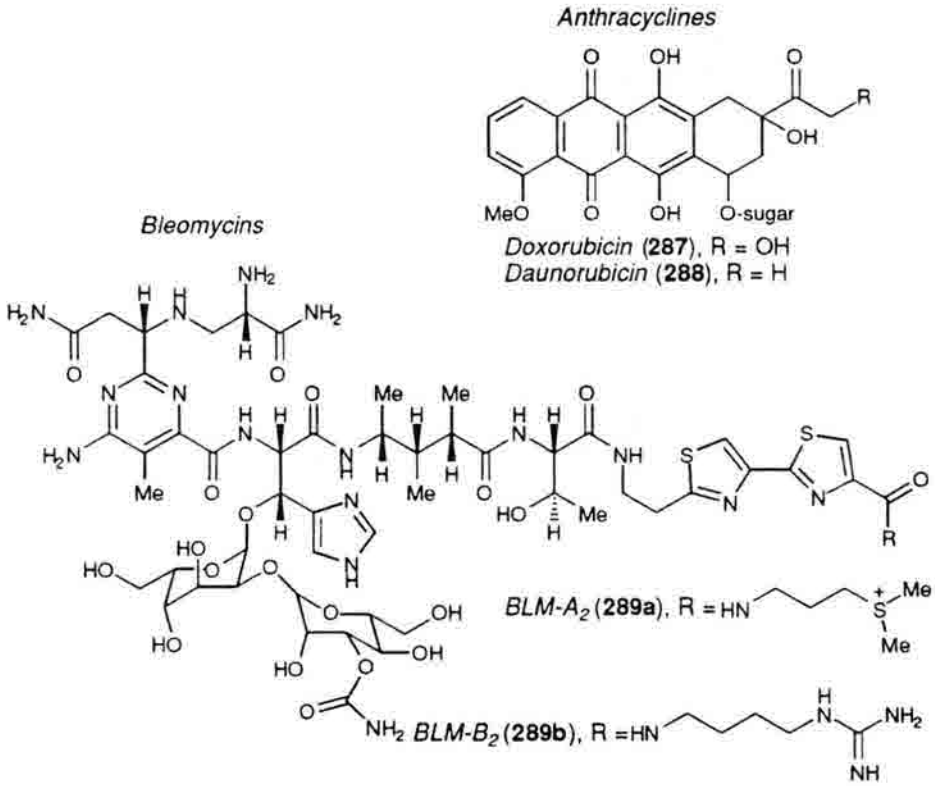

metal is then capable of reducing another equivalent of oxygen producing a second superoxide and regenerating M^n. Misra has proposed the additional steps (4 through 8)

shown in Scheme 52, which can be thought of as chain propagation steps resulting in further reduction of superoxide to hydroxyl radical.

One of the most highly studied classes of antitumor antibiotics capable of causing O_2-dependent cleavage of DNA are the bleomycins (**289a** and **b**).[54,55] The bleomycins contain a coordination pocket which has been shown to possess a high affinity for Fe(III) forming a pentacoordinate complex. As illustrated in Scheme 53, a single electron reduction of this complex [Fe(III)-BLM] by reducing agents such as ascorbate or DTT (*in vitro*) or NADPH-cytochrome-*P*-450 reductase (*in vivo*), followed by binding of oxygen to the unoccupied coordination site affords the Fe(II)-BLM-O_2 complex. A second reduction step then produces "activated BLM" which is believed to possess an Fe-oxo species. Upon binding to DNA this moiety is presented juxtaposed to the C-4' hydrogen of the deoxyribose, resulting in its abstraction, producing the corresponding ribosyl radical. As a result, this cleavage is characterized by the 3'-phosphoglycolate end product formed in

Scheme 53. Bleomycin activation and DNA strand scission cycle

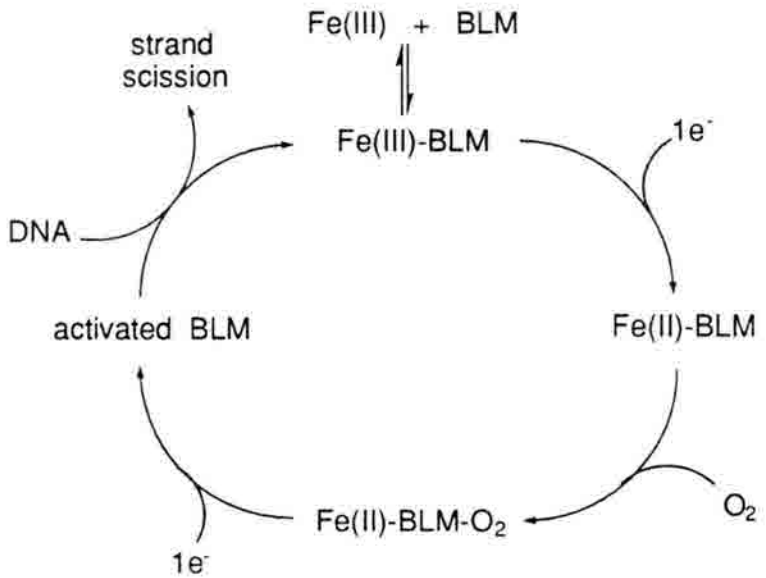

addition to base propenal release. In fact, much of the mechanistic information presented in Scheme 51 on base propenal formation resulting from C-4' hydrogen atom abstraction was a consequence of studies of bleomycin-DNA interactions.[54a]

Another important class of compounds are the quinone-containing anthracyclines (**287** and **288**) (Figure 26).[12] In an initiation step similar to that proposed for bleomycin involving a single electron reduction, hydroquinone radical **290** is produced which is then believed to reduce molecular oxygen to superoxide as shown in Scheme 54. The

Scheme 54. Superoxide production by doxorubicin

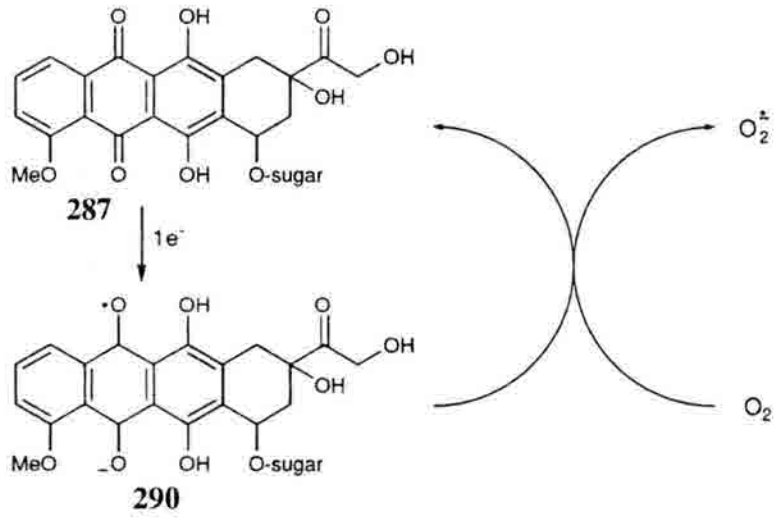

superoxide can then be processed to an activated species by the aforementioned metal-dependent process (Scheme 49), ultimately resulting in damage to DNA. Similar mechanisms for O_2-activation resulting in DNA-damage have been proposed for adriamycin, streptonigrin and mitomycins B and C, all of which contain analogous quinone moieties.

Figure 27. Structures of quinocarcin and related compounds

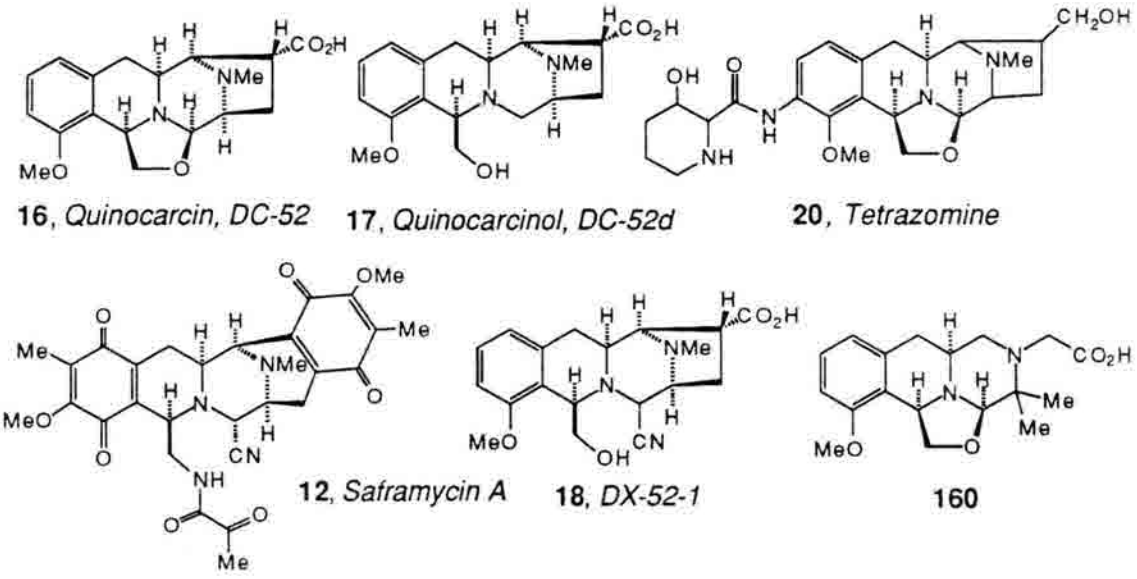

The first example of this type of process involving one of the quinocarcin-related antitumor compounds came from a report in 1982 by Lown, *et al.*, which recorded the ability of saframycins A and C to cause single-stranded lesions to supercoiled plasmid DNA.[11a] Due to the quinone moieties that these compounds contain, and the dependence on reducing agents exhibited, the same mechanism (i.e., *via* semi-quinone radical anion-mediated reduction of molecular oxygen) was initially proposed for DNA-cleavage by the saframycins as that just described for the anthramycins. As presented in Chapter 1, the DNA-alkylating ability of saframycin A was enhanced upon reduction to the hydroquinone. The surprising finding that the hydroquinone retained DNA-cleavage activity was explained as follows. Since hydroquinone formation with concomitant loss of cyanide producing iminium **292** was invoked in the DNA-alkylation process (Scheme 55), it was therefore proposed that this iminium could suffer an additional one electron reduction producing carbon-centered radical **293**. Following binding of molecular oxygen, the proposed

peroxy radical intermediate (**294**) was envisioned to expel a molar equivalent of superoxide thus regenerating iminium **292**.[11b]

Scheme 55. Proposed mechanism for superoxide production by saframycin A

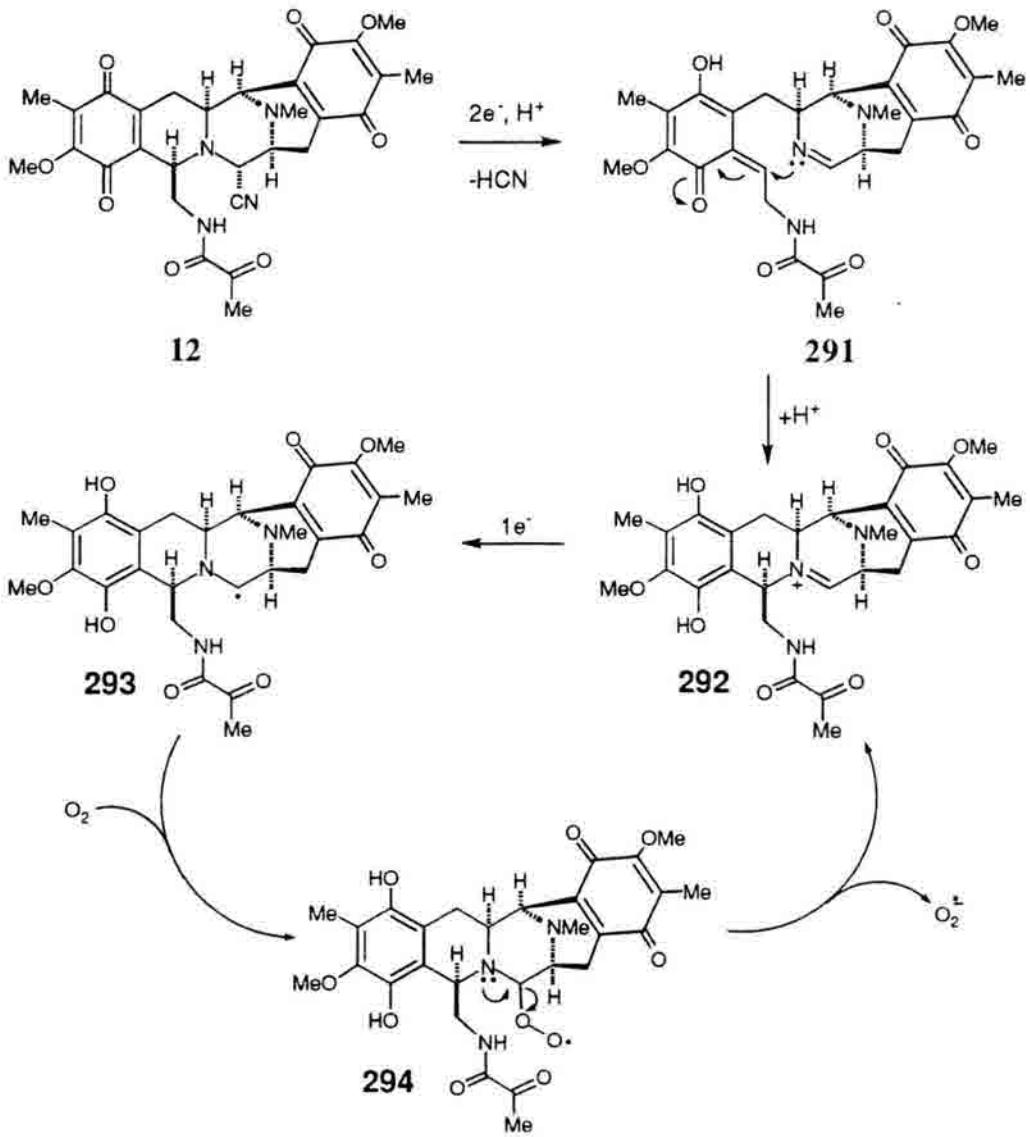

A similar mechanism for superoxide production by quinocarcin and tetrazomine is presented below. In the case of these substances, the intermediacy of a carbon-centered radical such as **293** would be required for superoxide production since these compounds

lack the quinone moiety which is typically associated with the activation of molecular oxygen.

4.2 Mechanistic Details of Superoxide Production by Quinocarcin and Structural Analogs

Superoxide production by quinocarcin was first reported by Tomita, *et al.*, but a mechanistic explanation was not offered.[14a] This study reported the remarkable finding that **16** was able to cleave plasmid DNA in an O_2-dependent fashion, which was (1) inhibited by addition of oxygen free radical scavengers such as methanol and *tert*-butanol; (2) was inhibited by superoxide dismutase and catalase; (3) was facilitated by addition of the reducing agents, but did *not* require them; and (4) was *not* stimulated by addition of metal ions (Fe^{2+} or Cu^{2+}). These intriguing findings, coupled with the observation that quinocarcin contained no readily recognizable functional group such as a quinone that is typically associated with superoxide production, prompted much of the work that will be discussed in this chapter.

The ability exhibited by quinocarcin and tetrazomine to inhibit nucleic acid biosynthesis has been proposed to occur *via* alkylation of DNA in the minor groove through the ring-opened iminium form of the oxazolidine moieties of these compounds.[17] Similar DNA alkylation mechanisms have been invoked for naphthyridinomycin and saframycin A. Indirect support for the involvement of the oxazolidine ring in the above context comes from the lack of antitumor activity displayed by quinocarcinol (**17**, DC-52-d) which is co-produced with **16** by *Streptomyces melanovinaceus*.[15] Importantly, quinocarcinol also did not cleave plasmid DNA, which forced the conclusion that the oxazolidine moiety of **16** was responsible for the oxidative degradation of DNA by some previously unrecognized mechanism.

Scheme 56. Proposed disproportionation of quinocarcin and superoxide production

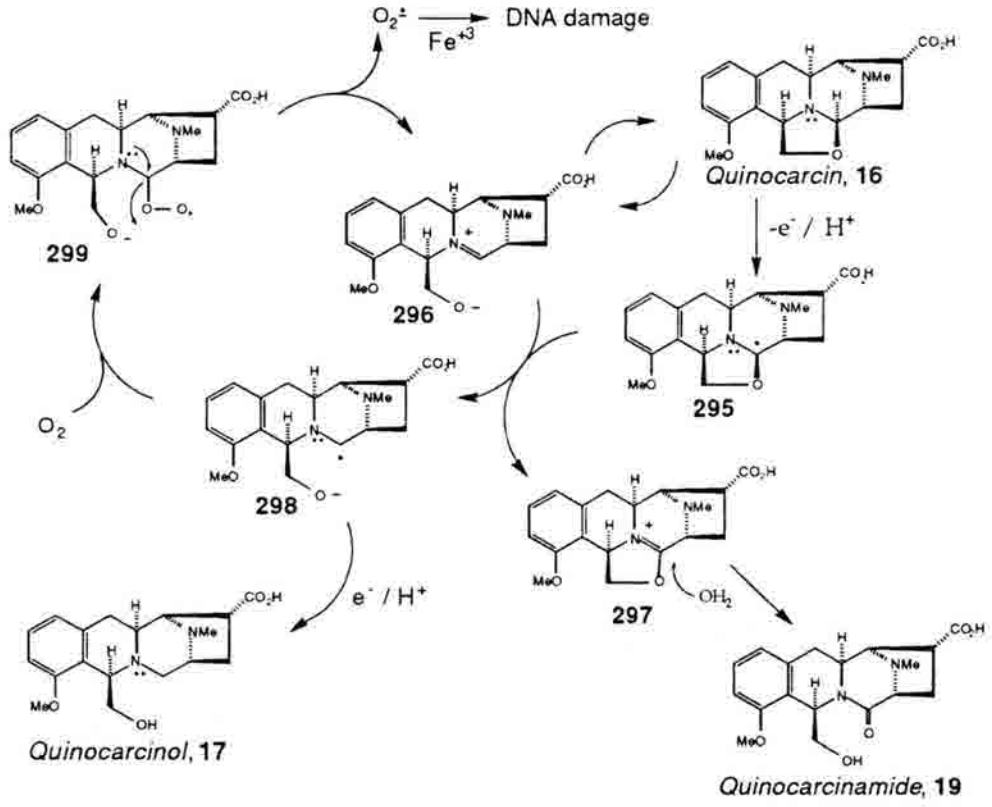

4.2.a. Disproportionation of quinocarcin and tetrazomine. Subsequent experimental evidence obtained, demonstrated that this oxygen-dependent mechanism was linked to the ability of these compounds to undergo disproportionation reactions of their oxazolidine moieties which under anaerobic conditions led to the redox products quinocarcinol (**17**) and quinocarcinamide (**19**) (in the case of **16**, Scheme 56). However, under aerobic conditions, oxygen is proposed to bind to an intermediate carbon-centered radical which, with participation of the adjacent nitrogen lone pair, results in the subsequent expulsion of a molar equivalent of superoxide.[50] When natural quinocarcin was allowed to stand in carefully deoxygenated water at 25°C, two new products were produced as monitored by HPLC (see Figure 29). The slower eluting peak was isolated and identified as quinocarcinol (**17**); preparation of an authentic sample of **17** from **16** by NaBH4

reduction[14a] rigorously confirmed this assignment. The faster eluting peak was later identified as quinocarcinamide (**19**) based on IR, mass spectra , fully decoupled ^1H NMR and ^{13}C NMR spectroscopy. Esterification of **19** with diazomethane in aqueous dioxane

Figure 28. Features of quinocarcin disproportionation

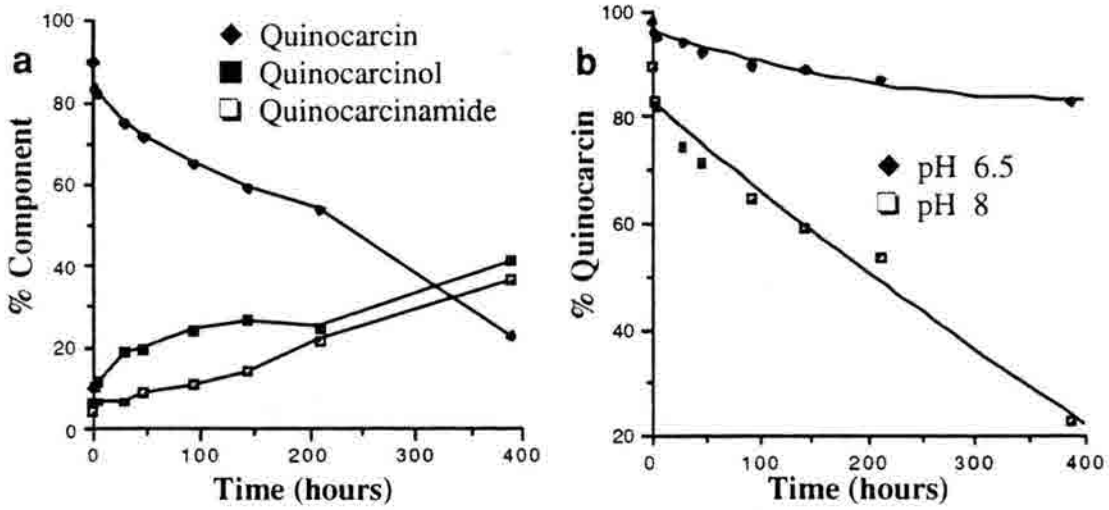

produced a substance whose ^1H NMR and IR spectra were identical to those of authentic, synthetic material[18] providing final, rigorous structural confirmation. As can be seen in Figure 28a, following this reaction by HPLC revealed that as the concentration of the quinocarcin diminished, a steady and complementary increase in the other components were observed. In the presence of oxygen, however, the disproportionation proceeds with superoxide formation, ultimately generating hydroxyl radical which has the effect of decomposing the disproportionation components as illustrated in Figure 30.

Similar behavior was also observed for tetrazomine, which under analogous conditions generated two new compounds.[49,52] These were subsequently identified as the oxidized tetrazaminamide (**300**) by high resolution mass spectrometry, and the reduced component tetraziminol (**301**), identified by mass spectrometry and ^1H NMR. Additional structural verification for the latter came from comparison of **301**, isolated from the

Figure 29. HPLC traces from anaerobic disproportionation

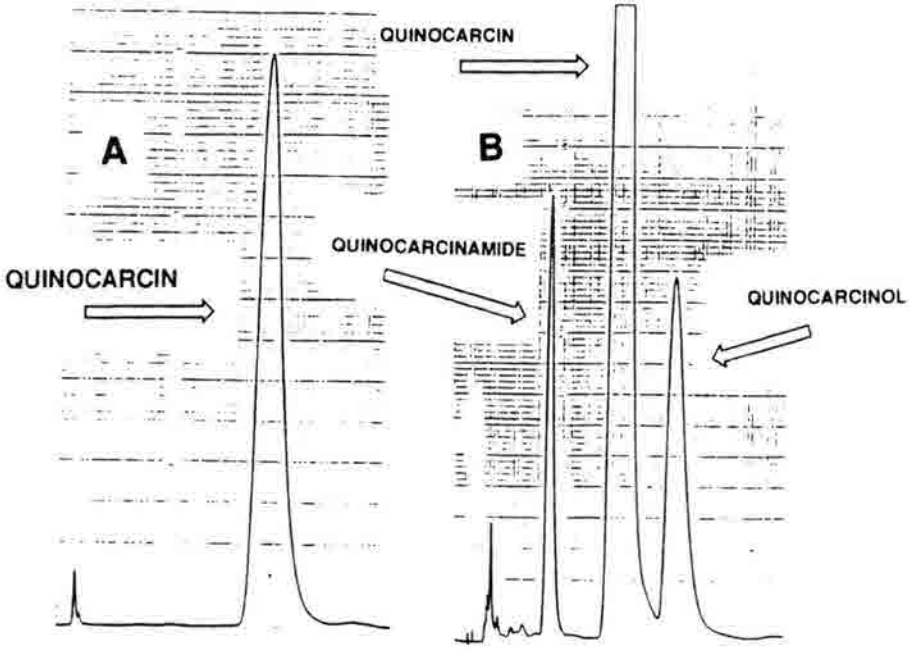

Key: **A**. HPLC purified quinocarcin (**16**). **B**. Decomposition of **16** after 3 weeks under anaerobic conditions.

Figure 30. HPLC traces from aerobic disproportionation

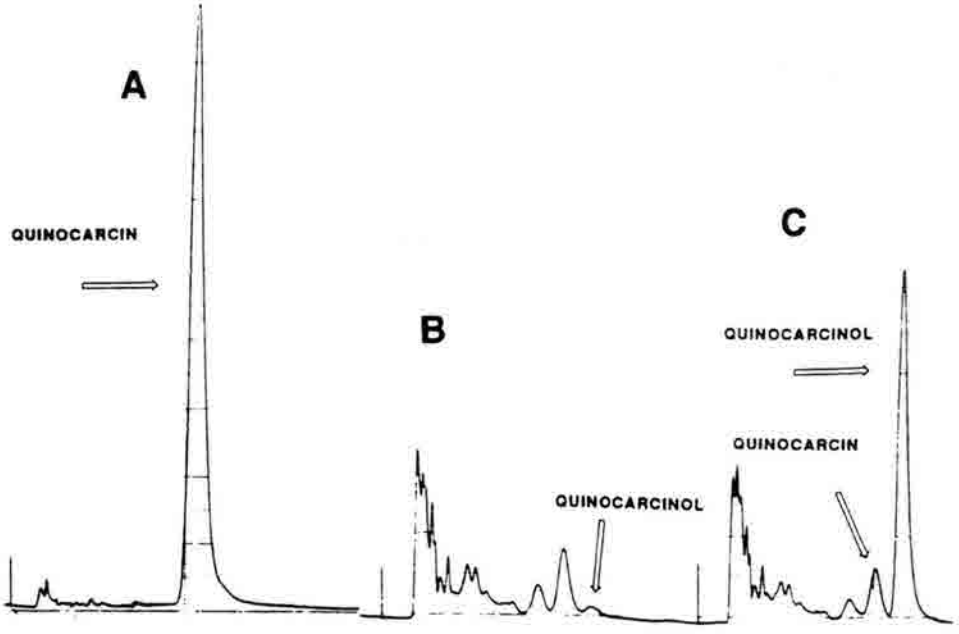

Key: **A**. HPLC purified quinocarcin (**16**). **B**. Decomposition of **16** after 3 weeks under aerobic conditions. **C**. Aerobic decomposition mixture spiked with quinocarcinol (**17**).

disproportionation just described, with authentic material prepared by $NaBH_4$ reduction of **20**.

The identification of these anaerobic redox products rigorously supports the proposal that **16** and **20** undergo Cannizzaro-like self-redox disproportionations; i.e., quinocarcin and tetrazomine serve as their own reductants. Therefore, as suggested in Scheme 56, single electron transfer from **16** with concomitant proton loss from the oxazolidine nitrogen to the ring-opened tautomer (**296**) would furnish radical anion **298** and the oxazolidinyl radical **295.** Radical **295** should be capable of reducing a second equivalent of **296** ultimately becoming oxazolidinium ion **297** which should hydrolyze to quinocarcinamide (**19**). Evidence for the intermediacy of **297** was secured by running the

Scheme 57. Anaerobic diproportionation of quinocarcin conducted in $^{18}OH_2$

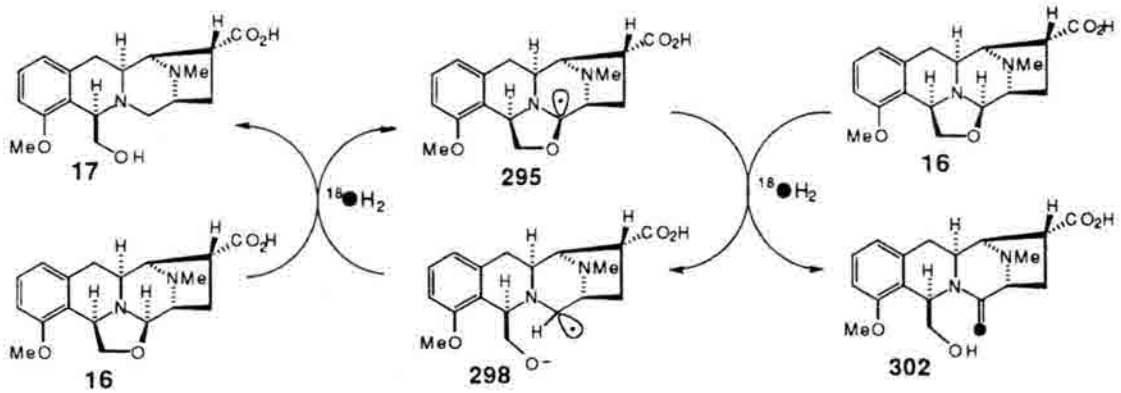

anaerobic disproportionation in 98% $^{18}OH_2$ and analyzing the product (**302**) by mass spectroscopy; greater than 40% ^{18}O was incorporated at the amide carbonyl (Scheme 57). Under anaerobic conditions, radical anion **298** subsequently abstracts a hydrogen atom (presumably from **16**) resulting in formation of quinocarcinol (**17**) and regenerating radical **295**. Evidence for this hydrogen atom transfer came from disproportionation reactions in D_2O which indicated by no incorporation of deuterium on C-7 of **17** isolated from the reactions by ^1H NMR (Scheme 58).

It is important to point out that the same result could be observed from direct hydride transfer from **16** to **296** in the disproportionation step without incorporation of deuterium occurring at C-7. However, eliminating the intermediacy of a carbon-centered radical such as **298** would make it difficult to explain the production of superoxide. Therefore Scheme 56 presents the most reasonable mechanism to explain superoxide production and still be consistent with the observed redox characteristics of these compounds.

Scheme 58. Anaerobic diproportionation of quinocarcin conducted in D_2O

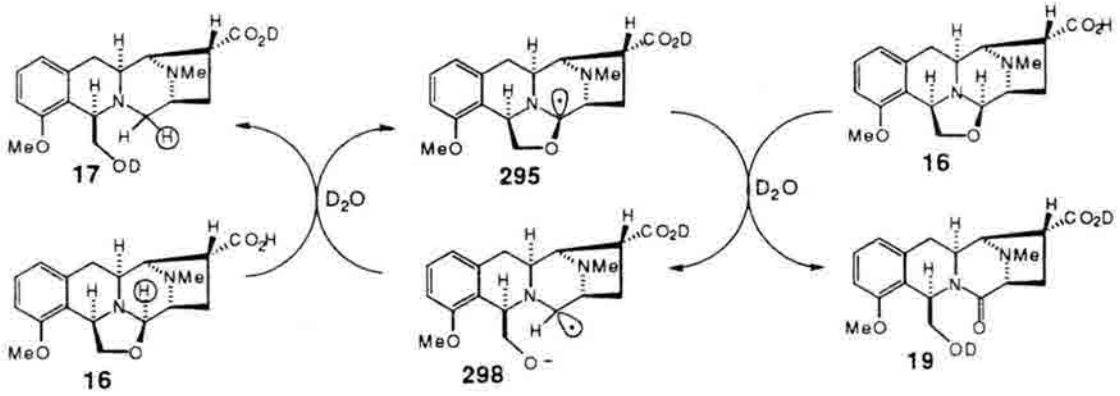

Under aerobic conditions, radical anion **298** can react with molecular oxygen to produce peroxy radical anion **299** which ,with nitrogen participation, expels one molar equivalent of superoxide, regenerating **296** (Scheme 56). It is also mechanistically plausible that the putative peroxy radical anion **299** could fragment directly to amide **19** *via* homolysis of the O-O bond and directly generate hydroxyl radical. Such a scenario would have been in accordance with the Tomita result which claimed an apparent metal-*independent* DNA-cleavage process. Therefore if quinocarcin is able to generate hydroxyl radical directly in this way, metals would not have been necessary to carry out Fenton/Haber-Weiss cycling in order to generate hydroxyl radical. A labeling experiment however, demonstrated that this pathway is unlikely. Disproportionation of pure **16** was

carried out in water as described above under an atmosphere of 98% $^{18}O_2$. Quinocarcinol (**17**) and quinocarcinamide (**19**) were isolated by reverse phase HPLC and subjected to mass spectral analysis following diazomethane esterification. The fragmentation pattern of **19** at m/e = 329 showed no significant enhancement at the M + 2 peak (m/e = 331) that would have been diagnostic for ^{18}O incorporation at the amide carbonyl by the peroxide homolysis possibility alluded to above. The authentic ^{18}O-labeled amide **302** obtained as described above from anaerobic disproportionation in $^{18}OH_2$, showed no propensity to exchange with $^{16}OH_2$ after several days at room temperature as evidenced by the same mass spectral analytical protocol.

Another noteworthy observation from the disproportionation was the pH dependence exhibited. Figure 28b depicts the rate of change of quinocarcin concentration during the disproportionation process. As can be seen, by buffering the reaction at pH 8 a marked increase in the rate of disappearance of quinocarcin was observed as compared to reactions carried out below pH 7. This result is consistent with the proposed mechanism in Scheme 56 since this process would require that the oxazolidine nitrogen be deprotonated. As will be seen in the upcoming sections, this pH trend will manifest itself in other behaviors exhibited by these compounds.

4.2.b. Superoxide production as measured by reduction of nitroblue tetrazolium (NBT). Superoxide production by quinocarcin, tetrazomine and several other compounds was carefully measured by following the reduction of nitroblue tetrazolium (NBT). This assay has been used extensively for the detection of superoxide and for the subsequent accumulation of rate data.[65,66] In this two electron process, NBT (colorless) is reduced to the monoformazan compound **304** which can be detected spectrophotometrically in the visible range (Scheme 59).

Reactions were run by adding the substrate to an aerated solution of NBT in 20 mM phosphate buffer containing one percent Triton X-100 detergent. The optical absorbances at 500 nm were then measured over a 30 minute period, and the ΔOD was the

Scheme 59. Superoxide reduction of NBT

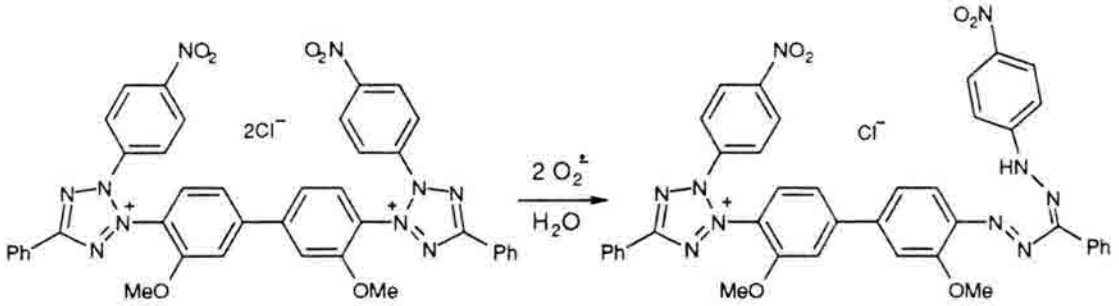

Nitroblue tetrazolium (NBT), **303** *Monoformazan*, **304**

average slope for the linear change in optical density over the reaction time. The rates of superoxide production were calculated from the molar extinction coefficient of **304** at 500 nm (12,200)[66b] and by assuming that the $[O_2]$ did not appreciably change over this time period (*pseudo*-zero order in O_2).

It was found that these reactions were completely inhibited by superoxide dismutase (SOD); the results are collected in Table 10. Importantly, the formation of superoxide by quinocarcin and tetrazomine was extremely slow ($10^4 \sim 10^5$ times slower) relative to the rate-limiting step of the Haber-Weiss/Fenton reaction which is 76 M^{-1} s^{-1} for the reduction of H_2O_2 by Fe(II). The slow production of superoxide by these compounds is likely the overall rate limiting step in the DNA-cleavage process.

Just as was observed for the disproportionation reactions, the reductions of NBT by quinocarcin and structural analogs were pH-dependent, exhibiting an increased rate of reduction as the pH was raised (Table 10 entries 1 through 3). This behavior directly paralleled the pH-dependency for the DNA cleavage reactions described in the next section (4.2.c).

Table 10. Rates of superoxide production as measured by spectraphotometric monitoring of the reduction of nitroblue tetrazolium (NBT).

Entry	Substrate	pH	rate ($M\ s^{-1} \times 10^{-9}$)
1	1.0 mM quinocarcin	6	0.0
2	1.0 mM quinocarcin	7	4.20
3	1.0 mM quinocarcin	8	11.0
4	1.0 mM quinocarcin + 10 µg/mL SOD	8	0.0
5	1.0 mM quinocarcinol (**17**)	8	0.0
6	1.0 mM quinocarcinamide (**19**)	8	0.0
7	1.0 mM tetrazomine	6	2.46
8	1.0 mM tetrazomine	7	10.6
9	1.0 mM tetrazomine	8	17.5
10	1.0 mM tetrazomine + 10 µg/mL SOD	8	0.0
11	2.0 mM N-2-carboxymethyl analog (**160**)	6	0.21
12	2.0 mM N-2-carboxymethyl analog (**160**)	7	0.82
13	2.0 mM N-2-carboxymethyl analog (**160**)	8	0.99
14	5.0 mM N-2-carboxymethyl analog (**160**)	8	1.56
15	1.0 mM DX-52-1 (**18**)	8	0.0
16[a]	1.0 mM N-2-methyl-*syn* analog (**45a**)	8	0.41
17[a]	1.0 mM N-2-methyl-*anti* analog (**45b**)	8	0.0
18	20 mM phosphate buffer (control)	8	0.0

All reactions run in 1% Triton X100 and 20 mM phosphate buffer at the indicated pHs. [a] Reactions run in 5 % methanol.

Remers conducted molecular mechanics calculations on quinocarcin by docking the drug in the minor groove.[17] These calculations suggested that the lowest energy conformer of **16** orients the piperazine ring in a chair-like conformation which therefore places the oxazolidine nitrogen lone pair in an antiperiplanar orientation to the oxazolidine methine. Ring opening of the oxazolidine to the iminium species (Scheme 60) requires nitrogen pyrimidal inversion to a higher energy twist boat conformer that was calculated to lie ~10 kcal mol^{-1} above the other conformer. In this situation, the oxazolidine nitrogen lone pair is *syn*- to the methine and antiperiplanar to the C–O bond. It was postulated that the iminium species should be a good alkylator for N-2 of guanine in the minor groove of the sequence $d(ATGCAT)_2$. Based on the similarity to naphthyridinomycin and saframycin, this is a very reasonable expectation. In the context of superoxide production and the capacity to oxidatively damage DNA a different question regarding the conformational significance of the oxazolidine moiety was asked. As shown in Scheme 60, the initial step in the electron-transfer between the oxazolidine and the iminium species involves 1-electron loss from the oxazolidine nitrogen with loss of the oxazolidine methine as a proton producing a radical. It is reasonable to expect that the trans, antiperiplanar arrangement of the oxazolidine methine and nitrogen lone pair in the lower energy conformer predicted by these calculations should also be the most favorable geometry for a 1-electron oxidation and concomitant proton loss in the redox self-disproportionation, since this arrangement provides maximum overlap in the transition state. Similar stereoelectronic effects have been observed[82] for the oxidation of other amines such as the example shown in

Scheme 60. Stereoelectronic control elements of superoxide production

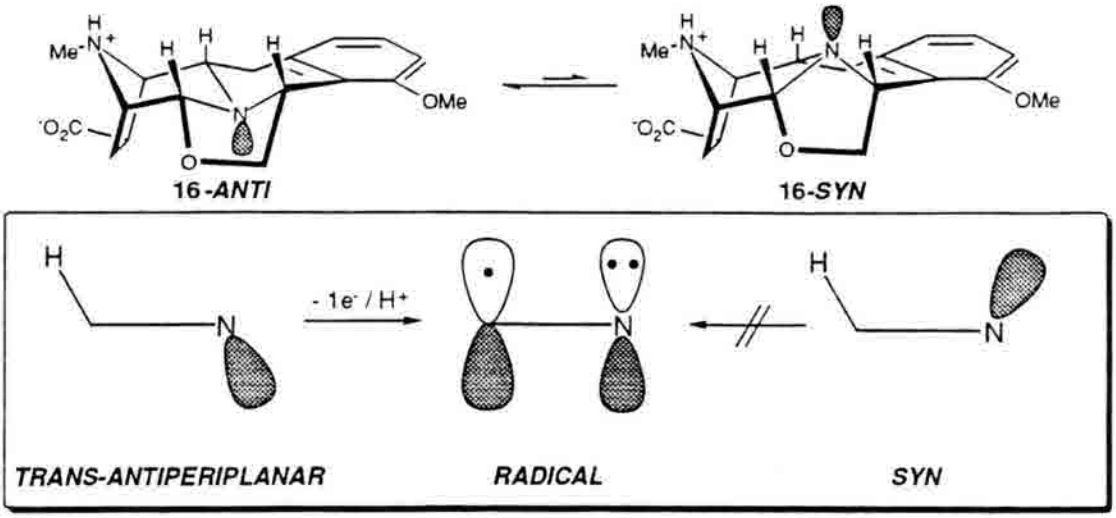

45a 45b

Scheme 61. Precedent for stereoelectronic effect[82a]

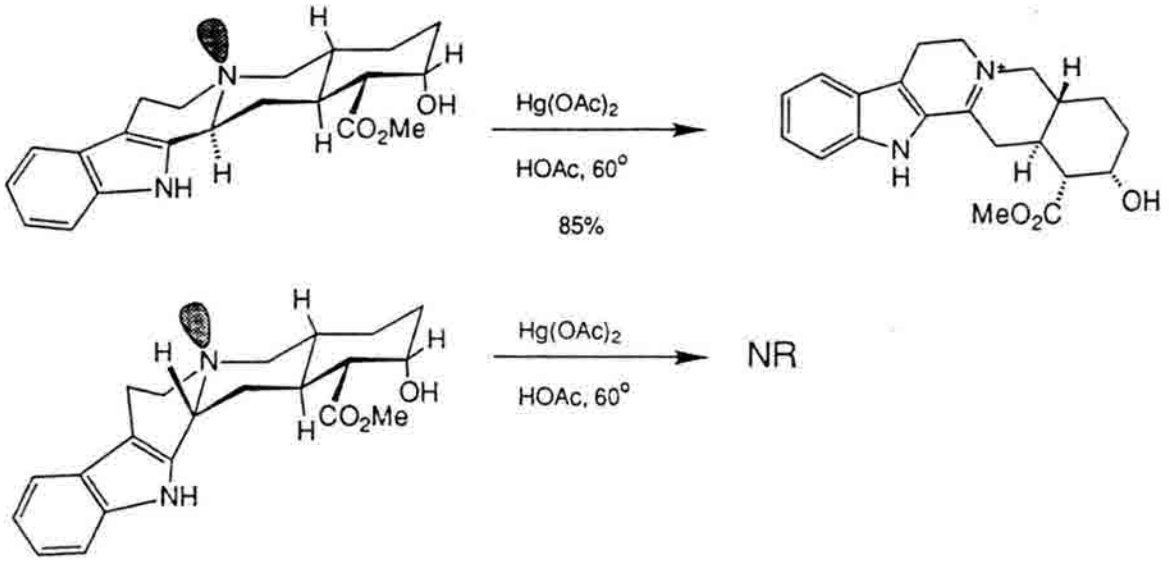

Scheme 61. Synthetic analogs **45a** and **45b** in Scheme 60 have the conformations depicted as determined by the single crystal x-ray analyses presented in Chapter 2.[33] Compound **45b** mimics the *syn*-conformer of quinocarcin, while **45a** mimics the *anti*-conformer of quinocarcin. The relative difference in the capacity of synthetic analogs **45a** and **b** to effect both superoxide production (Table 10, entries 16 and 17) as well as DNA cleavage (as will be discussed in the next section, 4.2.c), supports the hypothesis that stereoelectronic control elements of the oxazolidine ring system are intimately related to the biological activities of these substances. Additionally, neither quinocarcinol (**17**), quinocarcinamide (**19**) nor the semi-synthetic cyano derivative of quinocarcin (DX-52-1, **18**) produced superoxide, as evidenced by their complete lack of NBT reduction ability (Table 10, entries 5, 6 and 15), which further supports the notion that the oxazolidine moiety of these compounds must be "intact" and in the quinocarcin ground-state relative stereochemical configuration in order for superoxide production to proceed.

4.2.c. Cleavage of supercoiled plasmid DNA. Examination of the interaction of these compounds with DNA initially involved reactions of the purified materials with supercoiled plasmid DNA (pBR 322) between pH 5 and 9 phosphate buffer (20 mM) at 37°C for 2 hours in the presence of air. Salient experimental results are collected in Tables 11, 12 and 13 and Figure 31. Cleavage of the DNA was detected by loading the reaction mixtures onto 1% agarose gels containing 0.4 μg/mL ethidium bromide, followed by electrophoresis. The gels were then immediately visualized on a UV transilluminator which revealed by scanning densitometry the relative abundance of the three forms of plasmid caused by cleavage of the supercoiled substrate upon reaction with the drugs. The mean number of single strand scissions (*S*) per supercoiled DNA substrate was calculated using the Poisson distribution.[57a] When only forms I (supercoiled) and forms II (nicked open circular) are present, the equation simplifies to $S = -\ln f_I$, where f_I is the fraction of form I molecules from the densitometry data. In those cases where form III (linear) DNA was

Figure 31. Representative agarose gels depicting various amounts of DNA-cleavage in the presence of additives for **16**, **20**, **160** and conjugates (**314** and **315**)

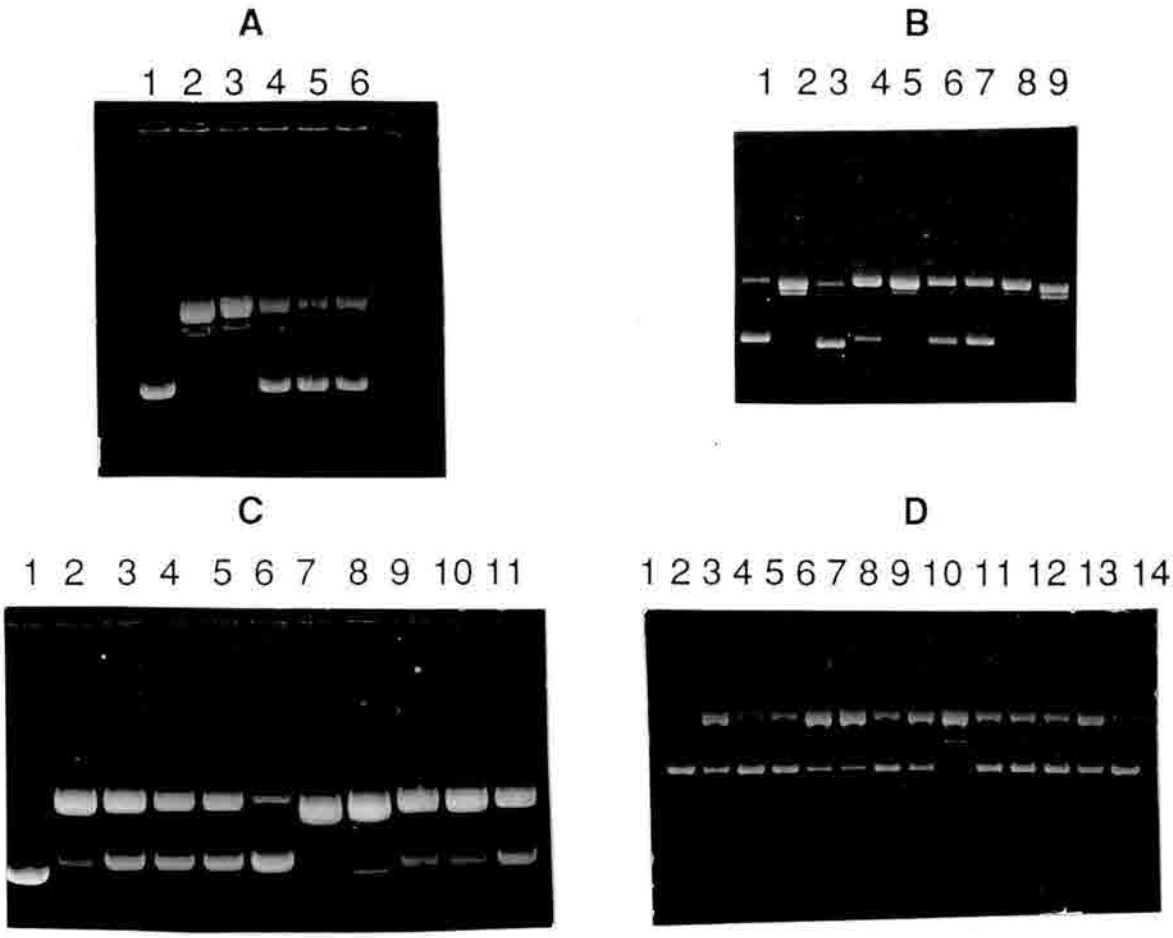

Key: **A**. Lane 1, supercoiled DNA (ΦX 174); lane 2, 1.0 mM quinocarcin (**16**); lane 3, 1.0 mM Tetrazomine (**20**); lane 4, 1.0 mM water soluble analog **160**; lane 5, 1.0 mM netropsin conjugate (**314**); lane 6, 1.0 mM spermine dimer (**315**). **B**. Lane 1, supercoiled plasmid DNA (pBR 322); lane 2, 1.0 mM **16** + 0.1 mM H_2O_2; lane 3, 0.1 mM H_2O_2; lane 4, 1.0 mM **16** + 0.1 mM Fe(III) + 1.0 mM desferal; lane 5, 1.0 mM **16** + 0.1 mM Fe(III); lane 6, 1.0 mM **16** + 1.0 mM desferal; lane 7, 1.0 mM **16** + 0.2 mM desferal; lane 8, 1.0 mM **16** + 0.1 mM desferal; lane 9, 1.0 mM **16**. **C**. Lane 1, Supercoiled plasmid DNA (pUC 19); lane 2, 1.0 mM tetrazomine (**20**); lane 3, 1.0 mM **20** (deoxygenated); lane 4, 1.0 mM **20** + 10 μg/mL catalase; lane 5, 1.0 mM **20** + 100 μg/mL catalase; lane 6, 1.0 mM **20** + 10 μg/mL SOD; lane 7, 1.0 mM **20** + 0.1 mM H_2O_2; lane 8, 0.1 mM **20** + 0.1 mM H_2O_2; lane 9, 1.0 mM **20** + 0.1 mM Fe(II); lane 10, 1.0 mM **20** + 0.1 mM Fe(III); lane 11, 1.0 mM **20** + 0.1 mM Cu(II). **D**. Lane 1, Supercoiled DNA (ΦX 174); lane 2, 1.0 mM **160**; lane 3, 1.0 mM **160** + 10 μg/mL SOD; lane 4, 1.0 mM **160** + 100 μg/mL catalase; lane 5, 1.0 mM **160** + 0.1 mM H_2O_2; lane 6, 0.1 mM **315**; lane 7, 0.1 mM **315** + 10 μg/mL SOD; lane, 8, 0.1 mM **315** + 100 μg/mL catalase; lane 9, 0.1 mM **315** + 0.1 mM H_2O_2; lane 10, 0.1 mM **314**; lane 11, 0.1 mM **314** + 10 μg/mL SOD; lane 12, 0.1 mM **314** + 100 μg/mL catalase; lane 13, 0.1 mM **314** + 0.1 mM H_2O_2; lane 14, 0.1 mM H_2O_2.

present, S was calculated from $f_I + f_{II} = [1-S(2h+1)/2L]^{S/2}$ where h is the distance between hits on opposite strands to produce a linear molecule (16 base pairs) and L is the total number of base pairs in the plasmid (4363 base pairs for pBR 322).

Table 11. Cleavage of supercoiled plasmid DNA by **16**, **20**, and synthetic analogs.

Entry	Substrate and Concentration	S^a
1	0.1 mM quinocarcin	0.3
2	1.0 mM quinocarcin	7.8
3	0.1 mM tetrazomine	0.4
4	1.0 mM tetrazomine	10.0
5	0.1 mM N-2-carboxymethyl analog (**160**)	0.25
6	1.0 mM N-2-carboxymethyl analog (**160**)	0.73
7	1.0 mM N-2-methyl-*syn* analog (**45a**), citrate salt	0.17
8	5.0 mM N-2-methyl-*syn* analog (**45a**), citrate salt	0.49
9	1.0 mM N-2-methyl-*anti* analog (**45b**), citrate salt	0.0
10	5.0 mM N-2-methyl-*anti* analog (**45b**), citrate salt	0.08
11	5.0 mM DX-52-1 (**18**)	0.0
12	1.0 mM quinocarcinol (**17**)	0.0
13	1.0 mM quinocarcinamide (**19**)	0.0

Each reaction contained 0.5 µg of supercoiled plasmid DNA pBR 322 in a total volume of 10 µL. All reactions were run in 20 mM phosphate buffer (pH 8) at 37°C for 2 hours. [a] The S value for a DNA control reaction represented the amount of nicked open cirular DNA present in the starting plasmid and was subtracted from the S values calculated for the individual cleavage reactions.

Quinocarcin and tetrazomine showed significant cleavage of the DNA at 0.1 mM concentration (Table 11, entries 1 and 3) at pH 8 without the addition of any external reductants.[49,50] Again, the reactions were found to be pH dependent, optimal cleavage being observed between pH 8-9. Figure 32 illustrates the pH profile for DNA-cleavage by quinocarcin, tetrazomine and water soluble analog **160**. At lower pH values, (pH 5-7) nicking was observed, but was significantly less than at higher pH. As alluded to previously, this is consistent with the obligate participation of the unprotonated oxazolidine nitrogen atom in the redox cycle. Quinocarcin analog **160** cleaved plasmid DNA, but as illustrated in Table 11, quinocarcin and tetrazomine were considerably more effective at the

Figure 32. Effects of pH on plasmid cleavage

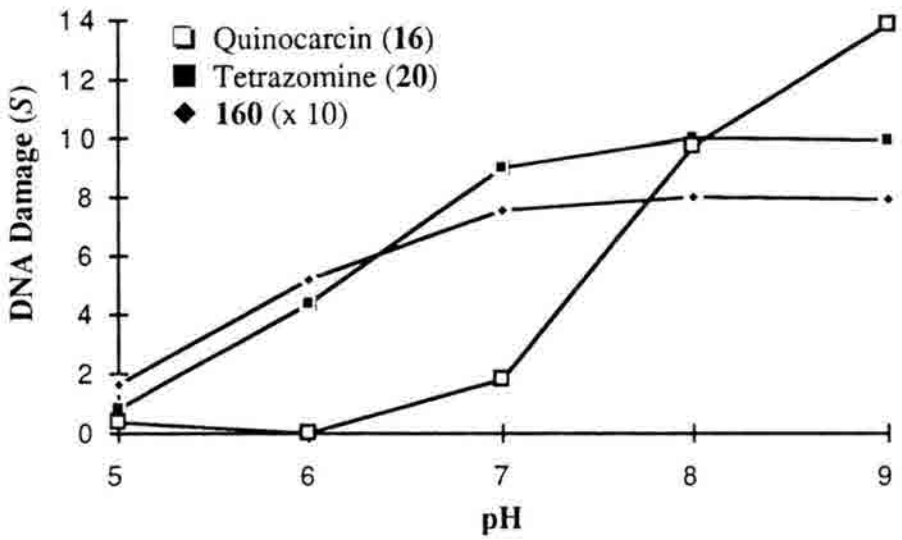

same concentrations. From the data collected in Table 14, it appears likely that compound **160** produces superoxide by the same mechanism proposed for quinocarcin and tetrazomine. DNA cleavage mediated by compound **160** is affected by the addition of SOD and catalase which inhibit DNA strand scission. As expected, the addition of hydrogen peroxide had a stimulatory effect on DNA cleavage. Compound **160** displays parallel pH trends for DNA damage and superoxide release (as evidenced by the reduction

Table 12. Effects of additives on DNA-cleavage by quinocarcin.

Entry	Conditions[a]	[Quinocarcin]	% inhibn	% enhancemt
1	0.1 mM Fe(III)	1.0 mM	0	0
2	0.1 mM Fe(III) + 0.1 mM desferal	1.0 mM	27	
3	0.1 mM Fe(III) + 1.0 mM desferal	1.0 mM	91	
4	0.1 mM desferal	1.0 mM	24	
5	1.0 mM desferal	1.0 mM	87	
6	10 mM desferal	1.0 mM	>99	
7	deoxygenated[b]	1.0 mM	84	
8	0.1 mM H_2O_2	0.1 mM		143
9	0.1 mM H_2O_2	1.0 mM		141
10	1.0 mM picolinic acid	1.0 mM	22	
11	10 mM picolinic acid	1.0 mM	94	
12	10 μg/mL catalase	1.0 mM	33	
13	100 μg/mL catalase	1.0 mM	83	
14	10 μg/mL SOD	1.0 mM	>99	

[a] All reactions were mixed at ice bath temperature and brought to a final volume of 10 μL. All reactions were then incubated for 2 h at 37°C in 20 mM phosphate buffer (pH 8) with 0.5 μg of supercoiled plasmid DNA (pBR 322). [b] Reactants were mixed at ice bath temperature, purged with argon gas then brought to 37°C.

of nitroblue tetrazolium (NBT)) to both quinocarcin and tetrazomine (Figure 32 and Table 10).

Table 13. Effects of additives on DNA-cleavage by tetrazomine.

Entry	Conditions[a]	[Tetrazomine]	% inhibn	% enhancemt
1	0.1 mM Fe(II)	1.0 mM	0	0
2	0.1 mM Fe (III)	1.0 mM	5	
3	0.1 mM desferal	1.0 mM	0	
4	1.0 mM desferal	1.0 mM	37	
5	10 mM desferal	1.0 mM	94	
6	deoxygenated[b]	1.0 mM	80	
7	0.1 mM H_2O_2	0.1 mM		68
8	0.1 mM H_2O_2	1.0 mM		29
9	1.0 mM picolinic acid	1.0 mM	28	
10	10 mM picolinic acid	1.0 mM	71	
11	10 μg/mL catalase	1.0 mM	55	
12	100 μg/mL catalase	1.0 mM	54	
13	10 μg/mL SOD	1.0 mM	94	

[a] All reactions were mixed at ice bath temperature and brought to a final volume of 10 μL. All reactions were then incubated for 2 h at 37°C in 20 mM phosphate buffer (pH 8) with 0.5 μg of supercoiled plasmid DNA (pBR 322). [b] Reactants were mixed at ice bath temperature, purged with argon gas then brought to 37°C.

Due to poor water solubility, **45a** did not exhibit potent DNA-cleavage, but, it did exhibit some DNA damaging potential as the citrate salt (Table 11, entries 7 and 8). As a

result of the stereoelectronic control requirement alluded to previously, the *anti* analog **45b** was dormant under these conditions. Additionally, DX-52-1 (**18**), quinocarcinol (**17**), and quinocarcinamide (**19**) all failed to exhibit any significant DNA-cleavage by this assay.

Exclusion of oxygen significantly inhibited DNA-cleavage for both quinocarcin and tetrazomine as expected (Table 12, entry 7 and Table 13, entry 6). Superoxide dismutase completely inhibited DNA cleavage (Table 12, entry 14 and Table 13, entry 13), consistent with both the capacity of these compounds to generate superoxide and the corresponding DNA cleavage event to be exclusively superoxide-dependent. Catalase also inhibited the reactions, but not as potently as SOD (Table 12, entries 12 and 13; Table 13, entries 11 and 12). Addition of hydrogen peroxide to drug / DNA reactions had a potent stimulatory effect on DNA cleavage over control reactions containing hydrogen peroxide at the same concentrations (Table 12, entries 8 and 9; Table 13, entries 7 and 8). Addition of picolinic acid to reaction mixtures of DNA with quinocarcin and tetrazomine at 1 mM and 10 mM showed increasing inhibition (Table 12, entries 10 and 11; Table 13, entries 9 and 10). Picolinic acid is known to be a very potent scavenger of hydroxyl radical and inhibitor of the Fe(II)/Fe(III) redox couple.[63] Taken together, the above results point strongly to Fenton-type chemistry being responsible for the scission of DNA. Tomita had reported that the addition of iron or copper salts had no stimulatory effects on the ability of quinocarcin to cleave DNA; these findings have been corroborated, the results appear in Table 12. The addition of the potent iron chelator desferal did, however, exhibit significant inhibition of DNA cleavage for both quinocarcin and tetrazomine, particularly at high concentrations (Table 12, entries 2-6; Table 13, entries 3-5). Desferal is known to have a high affinity for Fe(III) (log kf = 30.7), forming a hexa-coordinate complex that excludes iron-associated water and uncouples the oxidation of Fe(II) from the formation of hydroxyl radical (Fenton reaction).[13] These results support the notion that adventitious metals in a number of possible oxidation states in these reaction mixtures can be activated by the slow

release of superoxide and cause Fenton-related damage to DNA. Thus, these results indicate that , in contrast to the conclusions of Tomita, the DNA cleavage is indeed metal-dependent and that the low concentration of adventitious Fe^{+3} present is already in excess of that required to effect Fenton-mediated cleavage of the DNA; addition of excess iron would therefore not be expected to have any additive effect. Thus, the data support a hypothesis wherein the limiting reagent in DNA cleavage mediated by these compounds is the slow production of superoxide.

4.2.d. Reactions with 5'-^{32}P-labeled synthetic oligonucleotides. Further evidence for this redox behavior was obtained from analysis of the reaction of quinocarcin and tetrazomine with a small synthetic oligonucleotide by high resolution polyacrylamide gel electrophoresis. A synthetic 45 base pair oligonucleotide of random composition end-labeled with ^{32}P and annealed to its complement, was reacted with quinocarcin and tetrazomine in the absence of any additional reducing agents (37°C, 5 hours, 20 mM phosphate buffer, pH 8). The result was non-sequence specific cleavage at every nucleotide as evidenced by denaturing 20% polyacrylamide gel electrophoresis (Figure 33, lanes 3-6). Furthermore, every cleavage band appeared as a doublet which is characteristic of the 3'-phosphate and 3'- phosphoglycolate ends resulting from non-selective Fenton-mediated cleavage.[56,57] A similar cleavage pattern was observed from incubating the duplex with 1.0 mM Fe(II)EDTA under aerobic conditions (Figure 33, lane 7). The 3'-phosphate products were unambiguously identified by band shift assay upon treatment of drug-damaged DNA reaction mixtures with T4 polynucleotide kinase.[67] The enzymatically modified DNA bands corresponding to the 3'-phosphate products were shifted to a slower moving product, as illustrated in Figure 34, due to the absence of the one negative charge associated with the phosphate removed. Another noteworthy observation from Figure 33 is the change in relative ratios of the two 3' base pair products (phosphate versus phosphoglycolate) observed when comparing DNA-cleavage from tetrazomine, quinocarcin

Figure 33. Reactions of **16**, **20** and Fe(II)EDTA with 5'-P^{32}-labeled 45mer

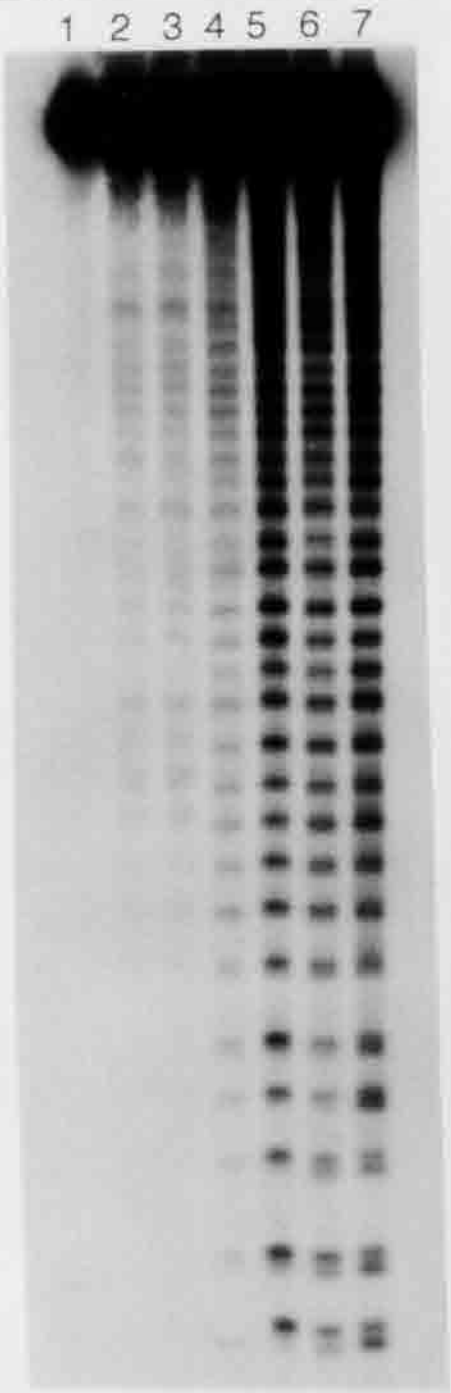

Figure 34. Band shift assay by enzymatic phosphate removal

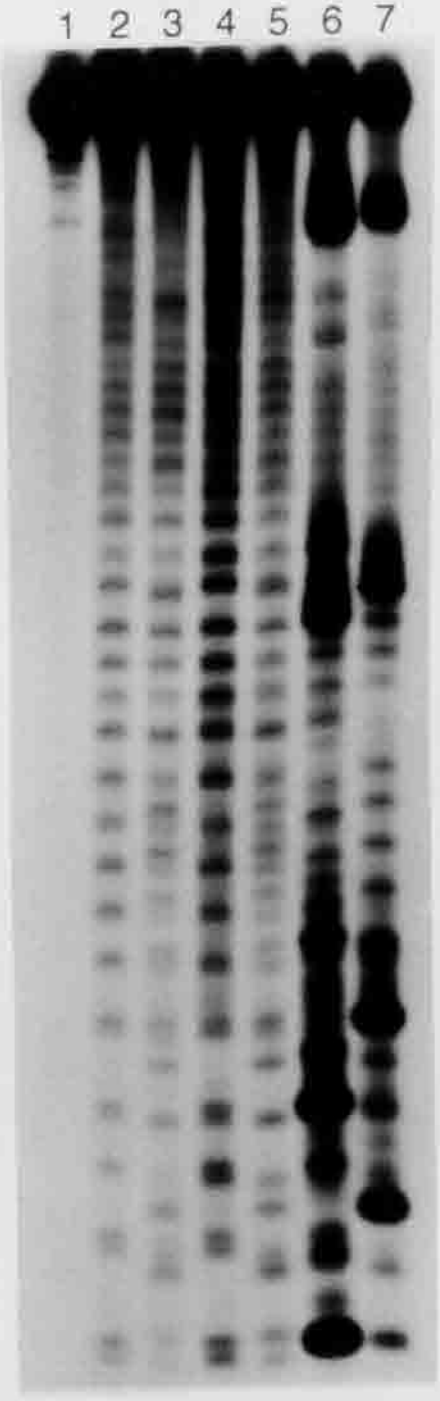

5' ^{32}P-TTAATTAAGACGTAACATCCAGCTACAAACTATCTTCGATAACCA 3'

3' AATTAATTCTGCATTGTAGGTCGATGTTTGATAGAAGCTATTGGT 5'

Figure 33: Lane 1, 5'-^{32}P-labeled standard.

Lane 2, control.

Lane 3, 0.1 mM tetrazomine.

Lane 4, 1.0 mM tetrazomine.

Lane 5, 10 mM tetrazomine.

Lane 6, 10 mM quinocarcin.

Lane 7, 1.0 mM Fe(II)EDTA.

Figure 34: Lane 1, DNA standard.

Lane 2, 5 mM quinocarcin.

Lane 3, 5 mM quinocarcin followed by T4 polynucleotide kinase.

Lane 4, 1.0 mM Fe(II)EDTA.

Lane 5, 1.0 mM Fe(II)EDTA followed by T4 kinase.

Lane 6, Maxam and Gilbert G reaction.

Lane 7, Maxam and Gilbert G reaction followed by T4 kinase.

All reactions run in 20 mM phosphate buffer (pH 8) at 37°C for 10 hours.

and Fe(II)EDTA (Figure 35). By scanning densitometry, the relative ratios for phosphate to phosphoglycolate are 8:2 for tetrazomine, 6:4 for quinocarcin, and 4:6 for Fe/EDTA (Figure 35, lanes 5, 6, and 7 respectively).[49] One plausible explanation for this behavior could be that tetrazomine, and to a lesser extent quinocarcin, non-covalently or covalently associated within the minor groove of DNA may protect the DNA from the drug's own oxidative damaging potential. From the molecular modeling studies conducted by Remers *et al.*, it was proposed that quinocarcin docks in the minor grove and may alkylate the DNA through the ring opened iminium form. The effect of **16** and **20** associated to DNA in this manner might, therefore, protect the ribose-phosphate backbone from oxidative damage by blocking sites in the minor grove. Evidence for this comes from experiments which show an increased resistance to Fe(II)EDTA cleavage for DNA that was first incubated with tetrazomine (10 mM) for 5 hours followed by ethanol precipitation (Figure 36, lane 2). However, when the order of reagents was reversed (i.e. treated with Fe/EDTA followed by 10 mM tetrazomine) significantly more cleavage was consistently observed (Figure 36, lane 3). Furthermore, the apparent lack of the 3'-phosphoglycolate product observed in Figure 36 (lane 2) even though this DNA was eventually exposed to Fe(II)EDTA, underlies the hypothesis that the difference in relative ratios of the two 3'-products shown in Figure 35 for quinocarcin and tetrazomine may be associated with a protective property for C-4' hydrogen atom abstraction exhibited by these compounds. This assertion is based on the assumption that a diffusable species (i.e. ·OH) is responsible for the DNA-damage observed. Therefore the drugs associated in the minor groove may partially inhibit abstraction of the C-4'-hydrogen which ultimately leads to the 3'-phosphoglycolate product.

Figure 35. Ratios of 3'-products afforded by **16**, **20** and Fe(II)EDTA

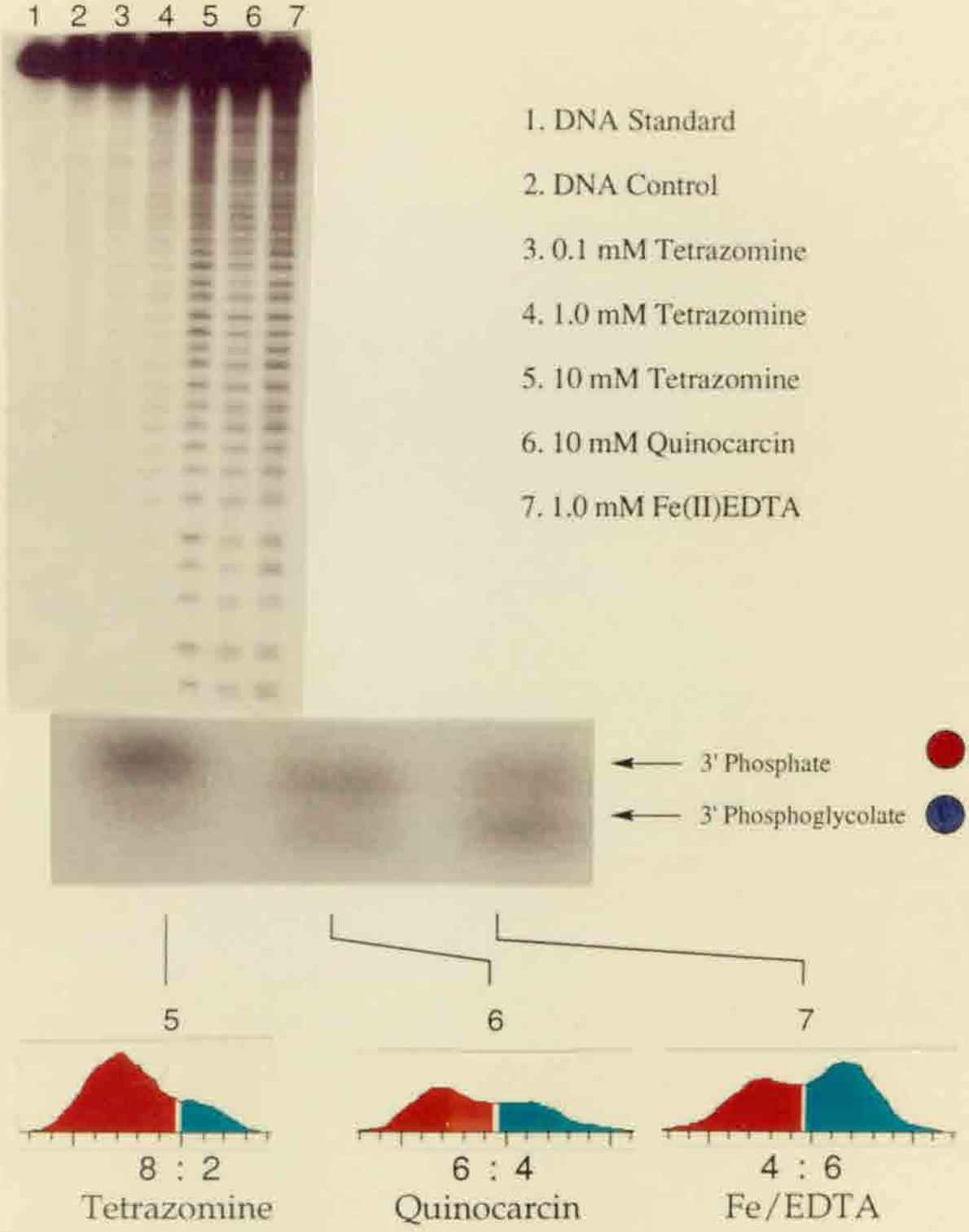

Figure 36. Effects of reaction order (**20** and Fe(II)EDTA)

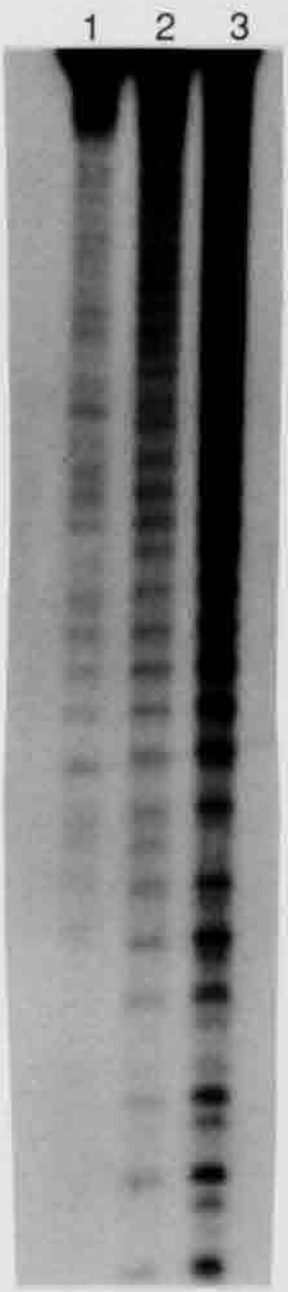

5' ^{32}P-TTAATTAAGACGTAACATCCAGCTACAAACTATCTTCGATAACCA 3'

3' AATTAATTCTGCATTGTAGGTCGATGTTTGATAGAAGCTATTGGT 5'

Key: Lane 1, DNA control (10 h, 37°C, 20 mM phosphate buffer (pH 8); lane 2, 10 mM **20** followed by 1.0 mM Fe(II)EDTA; lane 3, 1.0 mM Fe(II)EDTA followed by 10 mM **20**.

4.3. Manipulation of DNA-Cleavage with Synthetic Derivatives of 160

Netropsin and other distamycin-like peptides are well recognized to bind in the minor groove in AT rich regions of DNA.[68-70] The flat, slightly curved structures of these compounds coupled with their positive charge facilitates preferential binding in these regions of the minor groove.[71] A variety of DNA-cleaving compounds have been covalently attached to distamycin peptides in an effort to achieve affinity cleaving. Such complexes include the highly studied distamycin and P5-Fe/EDTA complexes.[72] More recently, other DNA cleaving compounds have been successfully linked to these peptides which have altered their capacity to damage DNA. Reactive DNA-damaging structures

Scheme 62. Preparation of activated ester of **306**

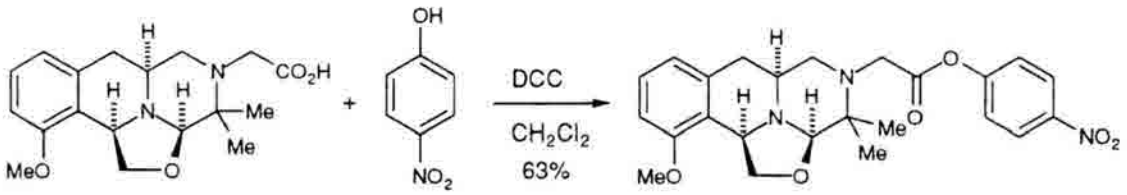

160 **305** **306**

such as enediynes and other radical-forming moieties have been successfully employed.[73,74] It is well known that polyamines such as spermidine and spermine are good DNA binding molecules. These basic substances are protonated at physiological pH enabling them to strongly associate to the negatively charged phosphodiester regions of DNA and engage in hydrogen bonding interactions in both the major and minor grooves.[75,76]

4.3.a. Preparation of netropsin-1 conjugate (314) and spermine dimer (315). Conjugations of **160** to these DNA binding molecules were carried out by first reacting compound **160** with *para*-nitrophenol and dicyclohexyl carbodiimide (DCC) to afford the activated *para*--nitrophenyl ester **306** (Scheme 62). The dipeptide **312** was

Scheme 63. Preparation of netropsin analog **313**

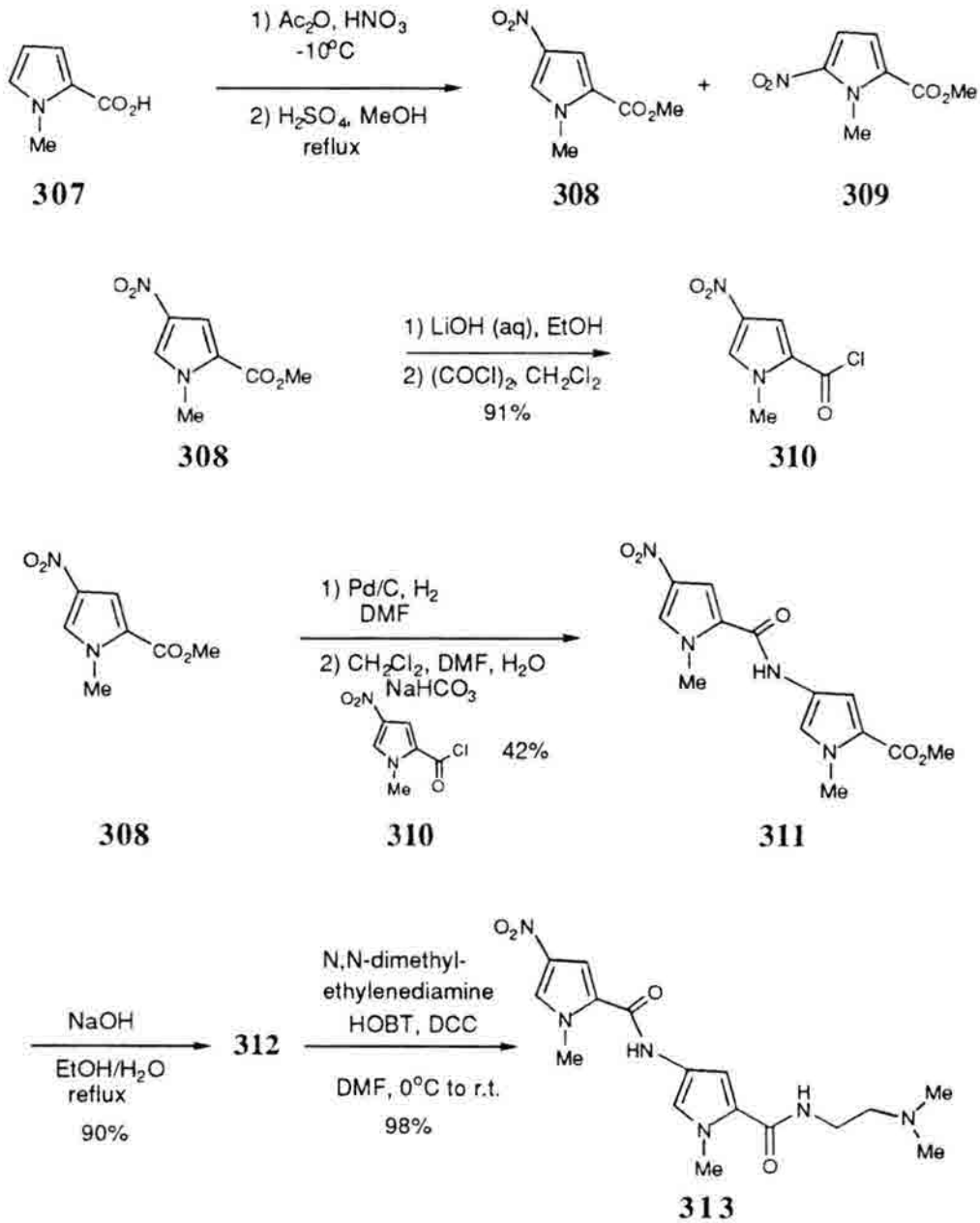

prepared as described by Bailer with minor modifications (Scheme 63).[77] Reaction of saponified **312** with N,N-dimethylethylenediamine, DCC and N-hydroxybenzotriazole

Scheme 64. Preparation of **160**-conjugates

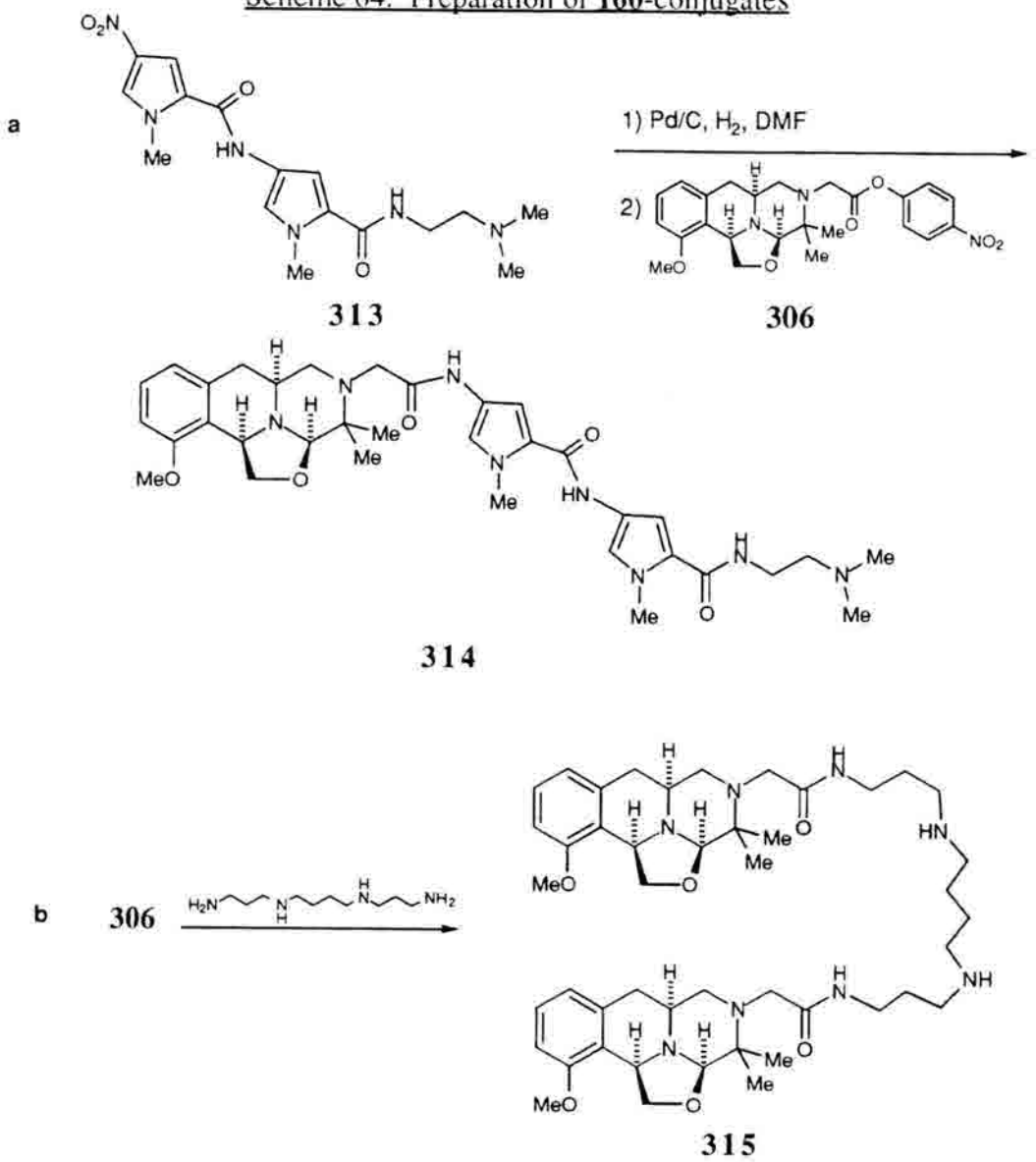

(HOBT) afforded **313** in 98% yield. Reduction of the nitro group by catalytic hydrogenolysis followed by immediate reaction with **306** produced netropsin conjugate

Figure 37. ^{1}H NMR spectrum (300 MHz) ($CDCl_3$) of netropsin conjugate **314**

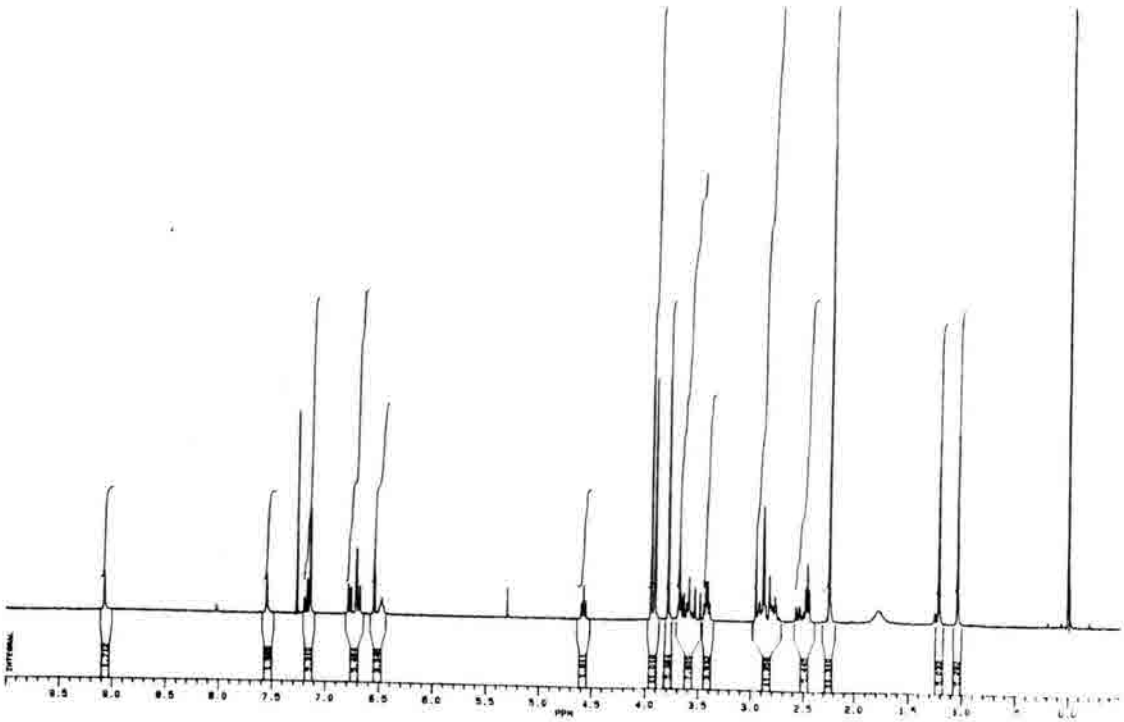

Figure 38. ^{1}H NMR spectrum (300 MHz) ($CDCl_3$) of spermine dimer **315**

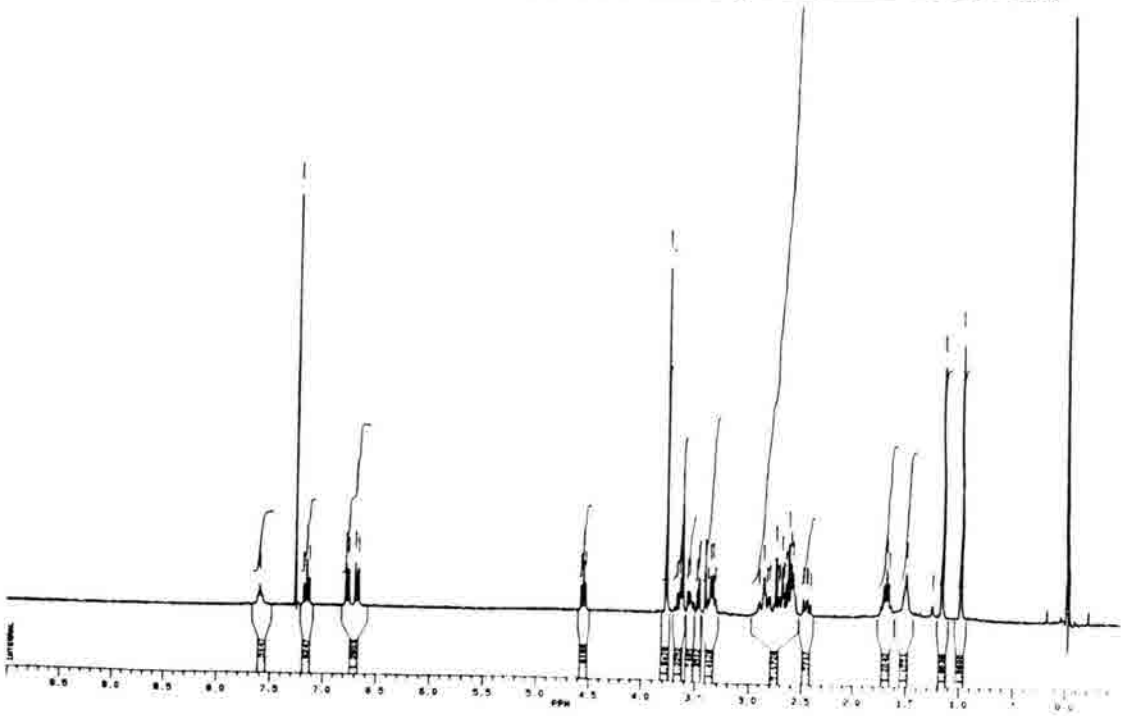

Figure 39. Effects of concentration on DNA-cleavage for **16**, **20**, **160** and conjugates

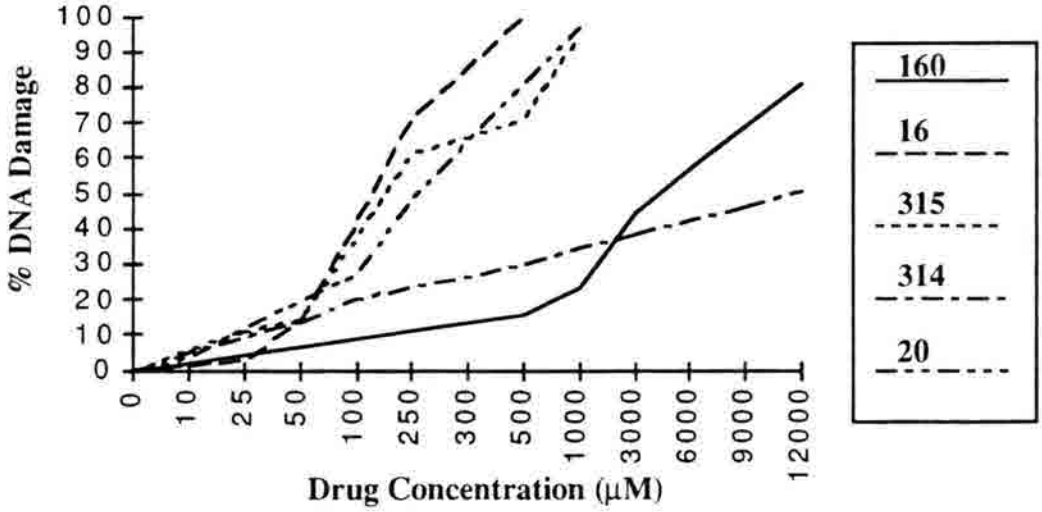

Table 14. Effects of additives on DNA-cleavage by **160** and conjugates.

Entry	Substrate	Conditions	% inhibn	% enhancemt
1	1.0 mM **160**	10 μg/mL SOD	85	
2	1.0 mM **160**	100 μg/mL catalase	65	
3[a]	1.0 mM **160**	0.1 mM H_2O_2		19
4	200 μM **314**	10 μg/mL SOD	0	0
5	200 μM **314**	100 μg/mL catalase	3	
6[a]	200 μM **314**	0.1 mM H_2O_2		95
7	200 μM **315**	10 μg/mL SOD	83	
8	200 μM **315**	100 μg/mL catalase	32	
9[a]	200 μM **315**	0.1 mM H_2O_2		289

All reactions run in 20 mM phosphate buffer (pH 8) at 37°C. [a] Values corrected for background cleavage due to H_2O_2 by subtraction of control.

314 in 52% yield after chromatography. Similarly, spermine dimer **315** was prepared by reaction of two equivalents of **306** with spermine in DMF at 4°C. Compound **315** probably exists as a mixture of diastereomers (one set of enantiomers plus the *meso*-compound) since **160** was prepared as a racemate. The physical data collected for **315** (^{1}H NMR and ^{13}C NMR), however, are consistent with the production of a single diastereomer, but a rigorous stereochemical assignment could not be made.

4.3.b. DNA-cleavage by conjugates. To study the effectiveness of these compounds as DNA-cleaving agents, compounds **1, 2, 3** and the conjugates were reacted under various conditions with supercoiled plasmid DNA (ΦX 174). Compound **160** was observed to effect the cleavage of plasmid DNA. However, as illustrated in Figure 39, quinocarcin and tetrazomine are considerably more effective at the same concentrations.

As shown in Figure 39, covalently linking compound **160** to spermine (forming dimer **315**), resulted in a greater than ten-fold increase in DNA cleavage activity as compared to compound **160** alone. These data and those illustrated in Figure 40 suggests that this increase in activity renders compound **315** as potent as quinocarcin or tetrazomine. As expected, DNA cleavage by compound **315** was inhibited by the addition of SOD and catalase (Table 14, entries 7 and 8) and enhanced by the addition of hydrogen peroxide (Table 14, entry 9).

Compared with other antitumor substances that cause oxidative damage to DNA, quinocarcin and tetrazomine are rather modest in terms of the rate at which they damage DNA. This is a direct manifestation of the slow production of superoxide by these substances. However, one interesting feature of the DNA-cleavage reactions for **16** and **20** is that they are vastly more efficient in effecting DNA cleavage per equivalent of superoxide generated than other superoxide-generating systems, such as DTT and ascorbate. For a qualitative comparison, the nicking efficiency (*NE*) of DNA cleavage as a

function of the rate of superoxide produced (as measured by NBT reduction) for all the compounds appearing in Figure 39 have been calculated, the results appear in Table 15.

Table 15. Nicking efficiency (*NE*) for superoxide producing compounds including conjugates.

$$NE = \frac{\eta}{(\sigma/3)n_{\text{superoxide}}}$$

Entry	Substrate	[a] Nicking Yield η (mol)	[b] Superoxide Produced (mol)	% *NE* (*NE* x 10^2)
1	dithiothreitol	1.20×10^{-14}	1.41×10^{-7}	2.6×10^{-5}
2	ascorbic acid	2.32×10^{-13}	3.02×10^{-7}	2.3×10^{-4}
3	quinocarcin	3.16×10^{-13}	2.38×10^{-10}	0.40
4	tetrazomine	1.54×10^{-13}	3.78×10^{-10}	0.12
5	**160**	2.15×10^{-14}	1.07×10^{-11}	0.60
6	**315**	1.54×10^{-13}	1.07×10^{-11}	2.16[c]
7	**314**	4.72×10^{-14}	1.07×10^{-11}	1.32[c]

[a] Total number of moles of DNA lesions calculated ($S \times n_{\text{DNA substrate}}$). [b] Theoretical yield of superoxide (mol) based on rate data presented in Table 1. [c] Value based on rate of superoxide production for **160**. The value (σ/3) is a stoichiometric factor which takes into account the number of molecules of superoxide theoretically necessary to produce one molecule of hydroxyl radical. σ represents the number of superoxide producing oxazolidines per molecule (1 for all compounds studied except for the spermine dimer (**315**)).

Quinocarcin is over 1,000 times more efficient in effecting DNA cleavage *per mole of superoxide* than ascorbate and more than 10,000 times more efficient than DTT. Tetrazomine and synthetic analog **160** are similar in efficiency to quinocarcin. Since these compounds all produce superoxide very slowly as compared to DTT and ascorbate, the

relative efficiency of DNA-cleavage, as a function of the rate of superoxide produced by these oxazolidine-containing substances appears to be a direct manifestation of their abilities to associate with DNA. Therefore, the reactive intermediates are delivered in close proximity to the DNA resulting in more DNA-cleavage per mole of superoxide produced. Further evidence for this came from the efficiencies calculated for the two conjugates. In spite of producing superoxide at less than one tenth the rate observed for quinocarcin and tetrazomine, the conjugates were an order of magnitude more efficient in causing damage to DNA.

As illustrated in Figure 39, the DNA-cleavage concentration profiles for the compounds studied display distinct behavior. At low concentrations (below 25 uM) a slow increase in DNA-cleavage was observed for all compounds. For compounds **16**, **20** and **315**, a marked increase in DNA damage occurs above 25 μM; for compound **160**, this change occurs above 1000 μM. The exception to this trend seems to be compound **314** which maintains a slow increase in DNA-cleavage activity over the entire concentration range. These data suggest that the preferred AT-rich regions of the DNA substrate might be saturated by **314** at low drug concentration, and increasing the drug concentration thus, only has a moderate effect. Further evidence for sequence-selective cleavage by **314** and characterization of the cleavage sites was conducted with ^{32}P-end-labeled restriction fragments, the results of which are described below.

A 516 base pair restriction fragment from pBR 322 was employed. Initially, the 3'-^{32}P-end-labeled fragment was used which was prepared by linearization of the purified, supercoiled substrate with Eco RI restriction endonuclease. Following 3'-labeling a second restriction digest with Rsa I produced the desired 3'-^{32}P-end-labeled 516mer which was subsequently gel purified. Figure 40 depicts the sequence random nature of cleavage of this substrate mediated by quinocarcin (Figure 40, lane 2). As previously shown using the

Figure 40. Reactions of **16**, **160**, **314** and **315** with 5'-labeled 516mer

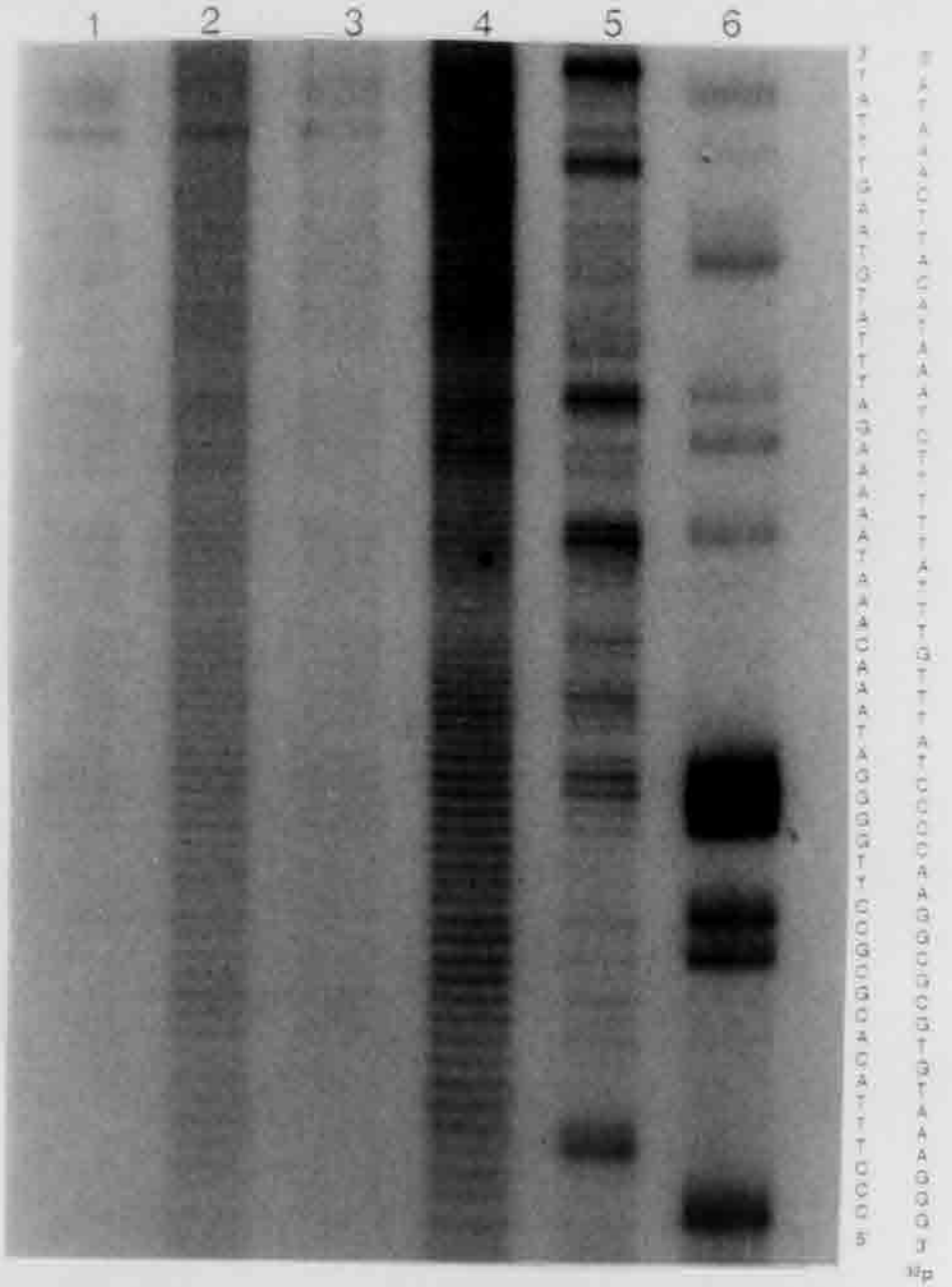

Key: Lane 1, DNA standard; lane 2, 200 μM **16**; lane 3, 200 μM **160**; lane 4, 200 μM **315**; lane 5, 200 μM **314**; lane 6, Maxam and Gilbert G reactions. All reactions run in 10 mM phosphate buffer (pH 8) at 37°C for 10 hours.

Figure 41. Reactions of **314** with 3' and 5'-labeled 516 bp restriction fragments

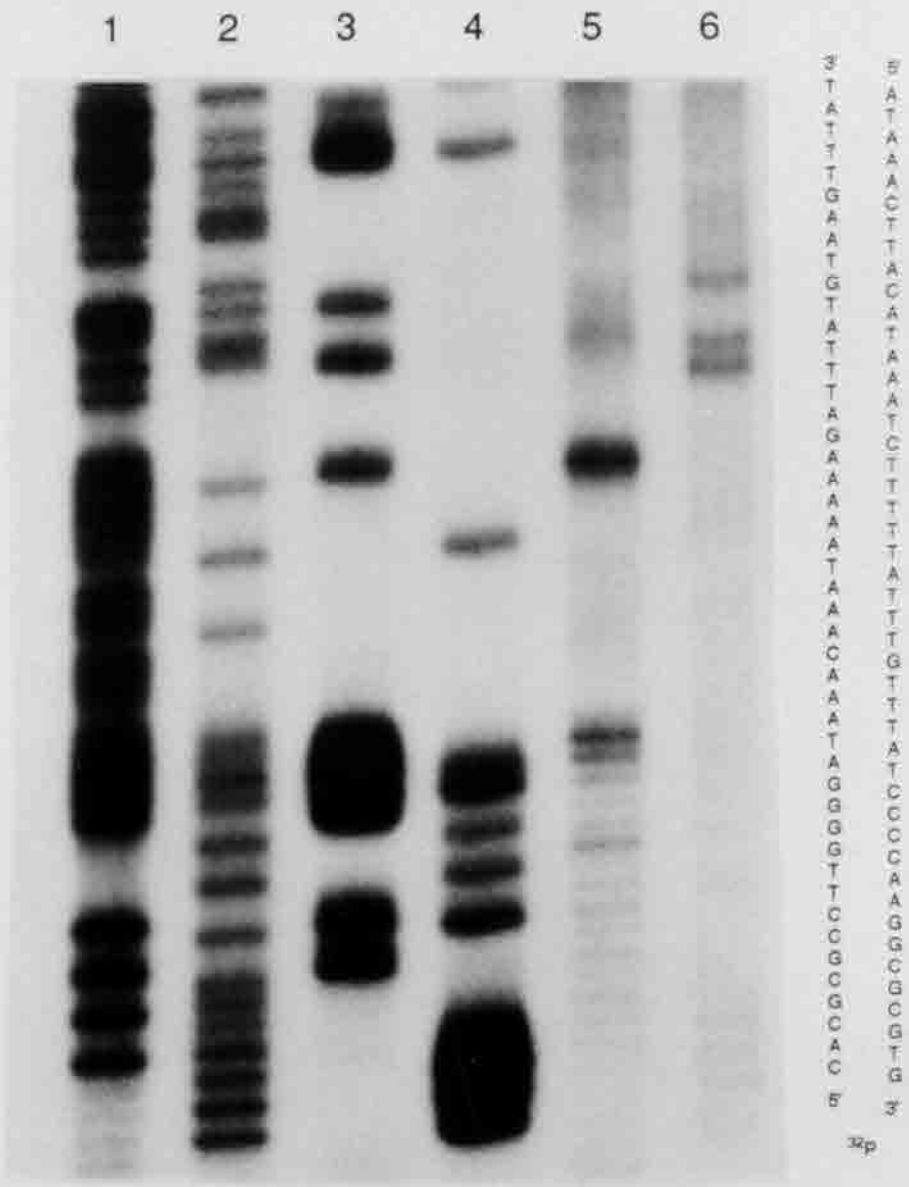

Key: Lane 1, 3'-Maxam and Gilbert G + A reaction; lane 2, 5'-Maxam and Gilbert G + A reaction; lane 3, 3'-Maxam and Gilbert G reaction; lane 4, 5'-Maxam and Gilbert G reaction; lane 5, 3'-labled DNA + 200 μM **314**; lane 6, 5'-labled DNA + 200 μM **314**. All reaction run in 10 mM phosphate buffer (pH 8) at 37°C for 10 hours.

supercoiled plasmid cleavage assay, quinocarcin is a significantly more effective DNA-cleaving agent than **160** (lane 3). However, as can be seen in lanes 3 and 4 (Figure 40), covalent attachment of spermine to **160** (producing **315**) causes a marked increase in cleavage activity although there was no indication of any sequence-specific nature to this damage. The netropsin conjugate (**314**) (Figure 40, lane 5) however, does exhibit a definite sequence-selective DNA-cleavage pattern.

In order to fully elucidate the pattern of DNA damage exhibited by compound **314**, the 516 base pair substrate was also labeled (5'-^{32}P) in an analogous manner to that described for the 3'-labeling process. Having the 516 base pair substrate labeled on both the 3' and 5' ends allowed for the determination of cleavage activity occurring on each individual strand of the double helix. The results of this double labeling experiment are illustrated in Figure 41. Lanes 5 and 6 (Figure 41) illustrate reactions of compound **314** with the 3'-^{32}P-labeled and 5'-^{32}P-labeled DNA respectively. The data from this experiment are summarized on the histograms in Figure 42; the highest frequency of cleavage occurred around the 5'-d(ATTT)-3' sequence (NMR NOESY experiments have revealed similar sequence specificity for Distamycin A complexed with the dodecamer d(CGCAAATTTGCG)$_2$[78]). The actual sites of cleavage however, were two bases to the 3' end of this four-base recognition site. There is also evidence from the histograms (highlighted in boxes, Figure 42), that in some cases, the drug may be able to bind in two orientations, which would also affect cleavage two bases to the 3' end of the 5'-d(AAAT)-3' recognition sequence. Such an observation is not unexpected since it has been shown that many of the distamycin peptides actually bind in two orientation in the minor groove in a 1:1 or 2:1 drug to DNA ratio.[77,78] It is also significant to note the apparent directional preference for cleavage exhibited by compound **314**, since little or no cleavage was observed around 3'-d(ATTT/TAAA)-5' sequences.

Analysis of the data indicates that lesions caused by compound **314** do not necessarily occur on the complementary DNA strands at proximal Watson-Crick base pairs. Proximal double-strand damage is observed in the case of the distamycin-Fe/EDTA affinity cleaving agents.[72] In these systems, the metal that mediates the Fenton-type

Figure 42. Histograms indicating selective cleavage for netropsin conjugate **314**

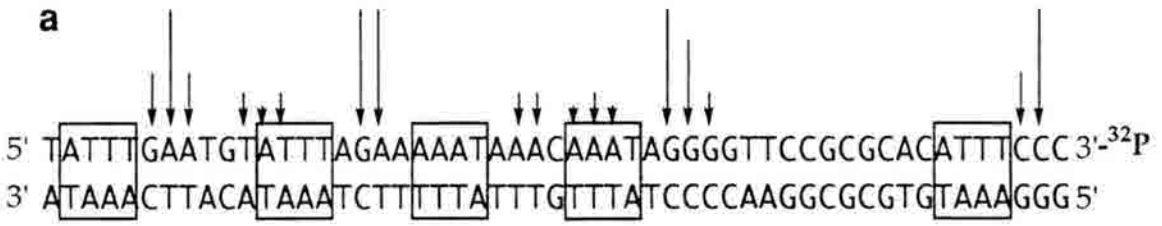

Histogram for Figure 40, lane 5.

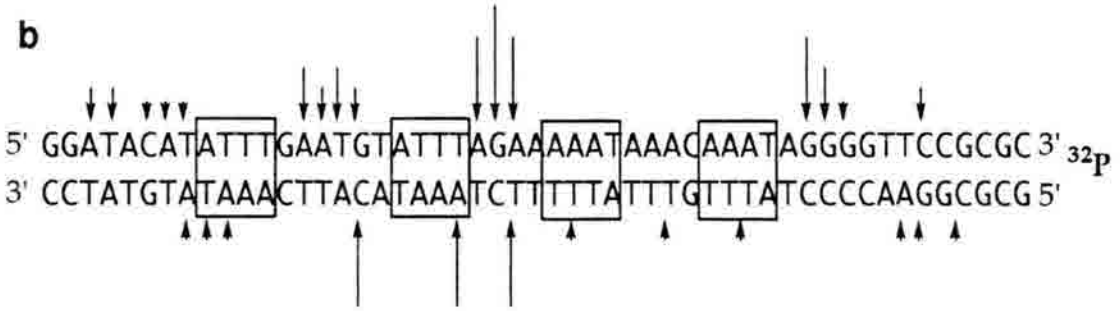

Histogram for Figure 41, lanes 5 and 6.

production of hydroxyl radical is held proximal to the DNA as a consequence of being complexed to the EDTA moiety. If the redox-active oxazolidine portion of DNA-*bound* **314** is generating a (non-diffusable) proximal reactive oxidant, or a highly reactive diffusable oxidant (such as hydroxyl radical) one would expect cleavage to occur on one or both strands of the DNA in close proximity to the site where the drug is bound to the recognition sequence. Alternatively, if superoxide is the only initial species produced by

bound drug, the superoxide molecule must diffuse away from the drug to interact with Fe(III) in solution to initiate the Haber-Weiss / Fenton cycling of hydroxyl radical. In this case, sequence-random cleavage would be expected and a "footprint" of the bound drug might be anticipated. Examination of the autoradiogram and histogram (Figure 42b) for **314** suggests that an alternative mode of DNA damage may be operating. One plausible explanation for the observed cleavage pattern would be that compound **314** is also operating *via* a direct hydrogen atom abstraction mechanism. Superoxide production by this class of compounds is proposed to occur as a result of the attack of molecular oxygen on a carbon-centered radical (Scheme 56, **295** or **298**) derived from the auto-redox disproportionation of the oxazolidine ring or by exogenous reduction of **314** (Scheme 56) followed by expulsion of superoxide. It is therefore possible that proper orientation of the drug as dictated by the netropsin moiety, might position the radical in the proper geometry to abstract a hydrogen atom from the phosphoribose backbone that, in the presence of oxygen, would ultimately result in scission of the DNA. Experimental support for this hypothesis is presented in Table 14 (entries 4 and 5) which shows that DNA damage caused by compound **314** is not readily inhibited by the addition of SOD and catalase; this situation is in marked contrast to quinocarcin (Table 12, entries 12 through 14); tetrazomine (Table 13, entries 11 through 13) compound **160** (Table 14, entries 1 and 2) and compound **315** (Table 14, entries 7 and 8), whose DNA cleavage chemistry all display sensitivity to SOD and catalase. These data strongly suggest the involvement of a superoxide-*independent* mechanism in the DNA cleavage exhibited by compound **314**. An issue of further intrigue in the case of **314**, involves the exact mechanism for the reduction of the bound or unbound drug and the presentation of the reduced species to the DNA substrate.

Based on the observed DNA-cleavage chemistry of compound **314**, it was considered whether it was possible from a structural viewpoint, for **314** to bind in the

minor groove to a four base recognition sequence and adopt the requisite geometry to abstract a hydrogen atom two bases to the 3'-side. To attempt to answer this question, molecular modeling was employed by docking the "natural" enantiomer of **314** into the

Figure 43. Proposed hydrogen bonding interaction for **314** with the d(ATTT) binding site based on published interactions exhibited by netropsin

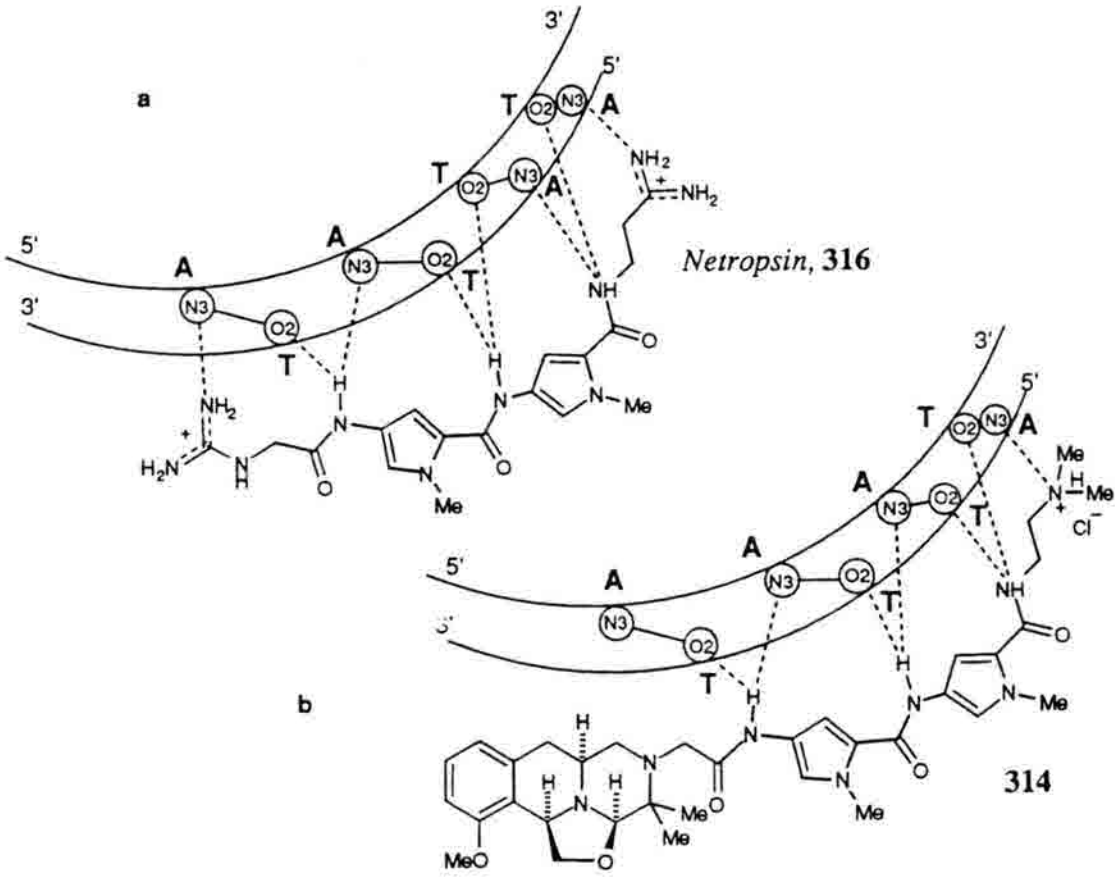

dodecamer d(CGCAAATTTGCG)$_2$ which contains the 5'-d(ATTT/TAAA)-3' sequence of interest. By taking advantage of known hydrogen-bonding interactions exhibited by netropsin (Figure 43a)[80,81] and applying these parameters to the binding of **314** (Figure 43b), it was possible to obtain the minimized structure depicted in Figure 44. It can be seen from this model, which involves contact with all four bases of the recognition site, that C-7 of the oxazolidine ring of compound **314** is oriented to fall within ~ 3 Å of the

Figure 44. Molecular model of **314** bound to the 5'-d(ATTT/TAAA)-3' sequence

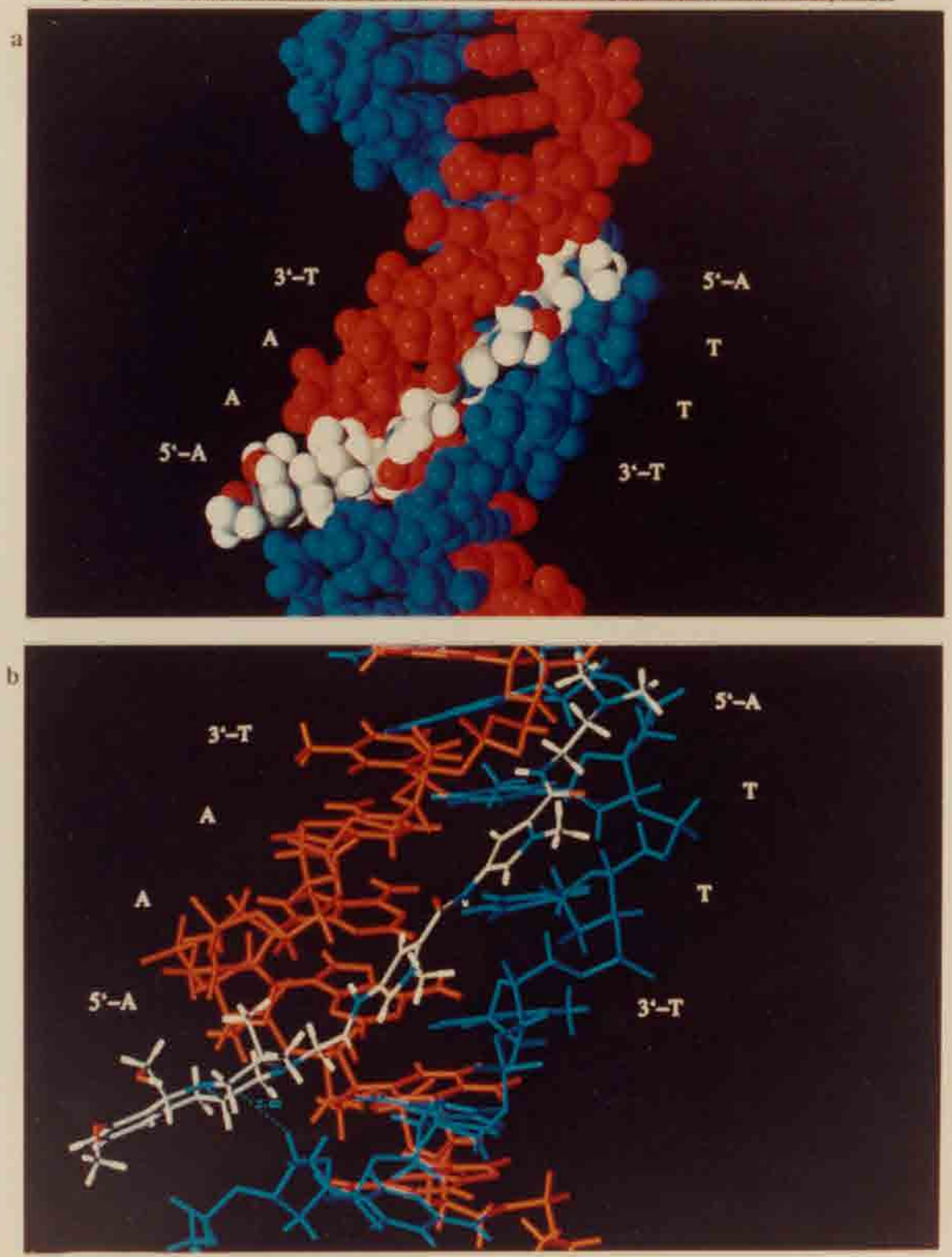

C-4' hydrogen atom of the deoxyribose ring two base pairs to the 3'- end of this sequence. As a corollary to this, preliminary data have suggested that there may be a preference for C-4' hydrogen atom abstraction for this cleavage. Reaction of compound **314** with the 5'-^{32}P-labeled restriction fragment gave DNA products that, upon reaction with T4 polynucleotide kinase resulted in no apparent band shift, suggesting that the 3'-phosphoglycolate product may be formed preferentially (as predicted by the model in Figure 44) in these reactions. These results are preliminary; however, future studies with appropriate small oligonucleotides should verify these results.

4.3.c. Antimicrobial activity. The new, synthetic compounds (**160**, **314** and **315**) were assayed for *in vitro* antibacterial activity against the following organisms by the agar disc-diffusion assay: *Bacillus subtilis, Staphylococcus aureus, Micrococcus luteus, E. coli, Pseudomonas aeruginosa, Klebsiella pneumoniae, Serratia marcescens, Candida albicans, Saccharomyces cerevisae, Mycobacteria peregrinum, Mycobacteria smegmatis, Mycobacteria fortuitum* and *Mycobacteria chelonei*. Only compound **315** displayed weak anti-microbial activity against *Bacillis subtilis* (at 1 mg / mL) and *Mycobacteria smegmatis* (at 10 mg / mL). Control assays with spermine and compound **160** showed no activity against *Mycobacteria smegmatis*.

4.4. Conclusion

In summary, a previously unrecognized reaction for the reduction of molecular oxygen by a simple heterocyclic ring system has been presented. This reduction is driven by the inherent intermolecular redox chemistry of the drugs themselves, requiring no exogenous reductants. The ability to produce superoxide enables quinocarcin and tetrazomine to affect oxidative damage of DNA. While it is not yet clear whether the antitumor properties of these substances are a manifestation of the oxidative DNA-cleavage ability they possess or their ability to inhibit nucleic acid synthesis (or some combination

thereof), it was of interest to study this O_2-dependent DNA-cleavage mechanism since there were no readily recognizable functionalities associated with these compounds that would give rise to this activity.

The capacity of many antitumor antibiotics to cause oxidative damage to DNA in cancerous tissues is typically inseparable from the non-specific damage inflicted on healthy cells by reduced oxygen species and is widely recognized to be associated with the undesirable host toxicity of many antitumor drugs. Although quinocarcin exhibits very promising antitumor activity, it does suffer from non-specific cytotoxicity problems. Chemical means to attenuate the production of the reactive intermediates, or to direct the activity of the drugs more specifically, is deemed highly desirable.

The ability to prepare a structurally less complex analog of quinocarcin which exhibits most of the physical properties associated with the parent compound has been demonstrated. By covalently attaching known DNA binding molecules it has been possible to vary the mechanism and DNA cleavage specificity of this class of antitumor antibiotics. Through the use of synthetic chemistry, it has been possible to identify unique stereoelectronic control elements of the oxazolidine ring, which is the biologically significant functional group responsible for the production of reactive oxidants that ultimately causes damage to nucleic acids. This has allowed for the preparation of the first totally synthetic analog (**314**) of this class of compounds that has markedly different DNA damaging chemistry than the natural products or the other synthetic analogs. It should now be possible to apply the insights gained from this study to the semi-synthetic alteration of the natural products themselves with the objective of decreasing their non-specific cytotoxicity, thereby increasing their potential efficacy as chemotherapeutic agents.

Chapter 5
Experimental Section

5.1. General Procedures

Compounds were prepared by standard laboratory procedures. Chromatography for compound isolations employed Selectoscientific silica-gel (32-63) or EM Science TLC plates (silica-gel 60, F254, 20 x 20 cm x 250 μm). Radial chromatography employed a Chromatotron Model 7924 using 2 or 4 mm silica plates as needed. HPLC separations were carried out using a Waters 6000 pump equipped with a variable wavelength UV detector (Waters). ^{1}H NMR and ^{13}C NMR data was collected using a Bruker AC-300 or 270 MHz FT NMR spectrometer and chemical shifts reported relative to TMS. ^{1}H NMR data collected in methanol-d4 were reported relative to the methanol peak at 3.30 and data collected in DMSO-d6 were reported relative to the DMSO peak at 2.49. IR data was collected on a Perkin Elmer 1600 FTIR.

Unless otherwise stated, all chemical tranformations were carried out in flame-dried glassware under an atmosphere of argon or nitrogen. Tetrahydrofuran and diethyl ether were dried over sodium/benzophenone while dichloromethane and toluene were dried over calcium hydride. Following distillation, transfer of solvents was conducted using oven-dried syringes.

Caution! Reactions involving phosgene, thionyl chloroide, oxalyl choride and other toxic materials that created an inhalation hazard were carried out in a well ventilated fume hood. Experiments involving ^{32}P-enriched ATP of dATP were handled behind a β-shield whenever possible and appropriate personal protection (gloves, goggles, ect...) used.

Disproportionation of 16 and HPLC analysis of products.

Solutions of citrate free **16** were made up in 10 mM phosphate buffer at the indicated pHs (D_2O and $^{18}OH2$ were also employed as indicated) which had been deoxygenated under freeze-thaw vacuum purging with nitrogen. An aliquot was then analyzed by HPLC (C18 Resolve Pack Column (Waters); 5% methanol/5% acetonitrile in 6mM potassium phosphate pH 6.8 (isocratic); and detected by UV at 270nm) which revealed only the peak at 16min. corresponding to **16**. The solution was then allowed to age at 25°C under anaerobic conditions with aliquots being taken periodically and analyzed by HPLC for quinocarcin and formation of **19** and **17**, retention times 10min. and 22min. respectively. Authentic quinocarcinol (**17**) was obtained from quinocarcin by $NaBH_4$ reduction according to Tomita. The authentic sample of quinocarcinol was identical to that obtained by the disproportionation of **16** described above by ^1H NMR, IR, and TLC (silica gel; 10% H_2O in ethanol).

Analytical data for quinocarcinamide (19).

^1H NMR (300 MHz) (D_2O) δ HOD: 2.34 (1 H, dd, J = 13.6 Hz, J = 9.9 Hz); 2.38 (3 H, s); 2.59 (1 H, ddd, J = 13.6 Hz, J = 7.0 Hz, J = 7.0 Hz); 2.78 (1 H, m); 3.03 (1 H, m); 3.22 (1 H, dd, J = 7.0 Hz, J = 10.3 Hz); 3.58 (1 H, d, J = 6.6 Hz); 3.70 (1 H, dd, J = 11.4 Hz, J = 3.9 Hz); 3.79 (1 H, m); 3.82 (1 H, Br. s); 3.87 (3 H, s); 3.93 (1 H, dd, J = 11.4 Hz, J = 4.4 Hz); 5.45 (1 H, t, J = 4.0 Hz); 6.94 (1 H, d, J = 7.8 Hz); 7.04 (1 H, d, J = 7.8 Hz); 7.33 (1 H, d, J = 7.8 Hz).

IR (KBr): 3601, 3430, 2929, 2340, 2020, 1897, 1792, 1626, 1580, 1388, 1079 cm^{-1}. Additional structural verification was secured through esterification to quinocarcinamide methyl ester as follows. To 2.0 mL of 1 M NaOH was added 5 mg of 1-methyl-3-nitro-1-nitrosoguanidine (Aldrich). The diazomethane formed was carried via nitrogen pressure bubbling through a 2.0 mL solution of dioxane/H_2O (1:1) containing 1 mg of **19**. Once the dioxane solution had turned yellow, the flask was then sealed and the

mixture was allowed to stand at room temperature for 30 min. The mixture was then concentrated to dryness affording 1 mg of the corresponding methyl ester whose ^1H NMR matched that of a synthetic sample kindly provided by Prof. S.J. Danishefsky. This procedure was also utilized for aliquoting the ^{18}O experiments for mass spectral determinations.

Reductions of Nitroblue Tetrazolium (NBT).

Each reaction was performed in triplicate by adding an appropriate amount of drug stock solution to an aerated solution of nitroblue tetrazolium (0.12 mM) in 20 mM phosphate buffer (at the indicated pH) containing 1% Triton X100 detergent and the final volumes brought to 750μL with deionized water. The optical absorbance was measured at 25°C over a 30min. period at 500 nm (Varian DMS 80 UV/vis. spectrophotometer) and the ΔOD was the average slope for the linear OD change over the reaction time. The rates for superoxide production were calculated by assuming that $[O_2]$ does not appreciably change over this time period and is in excess (zero order in oxygen). The rates (reported in Table 1, Chapter 4) were calculated from the ΔOD measurements and based on a molar extinction coefficient (ε_O) of 12,200 for the monoformazan product of NBT at 500 nm.

Preparation of supercoiled plasmid DNA (pBR 322).

To 40 μL of electro-competent cells (*E. coli.*; MC 1061) was added 1 μL (1 μg) of pBR 322 plasmid DNA (New England Biolabs), the mixture agitated, and aged in an ice-bath for 1 min. The mixture was then transferred to an ice cooled, 0.1 cm electroporation cuvette and the material pulsed (BioRad Gene Pulser) at 25 μF, 200 Ω and 1.1 kV. The cells were then quickly transferred to 1 mL of sterile SOC broth (20 mM glucose, 20 g bacto-tryptone (Difco), 5 g bacto-yeast (Difco), 1 g $MgCl_2$, 0.5 g NaCl, and 186 mg KCl to 1.0 L) and incubated at 37°C, with agitation (200 rpm), for 1h. The mixture was

transferred to a sterile Eppendorf tube and centrifuged (14 K, 5 min., room temperature). The supernatant was discarded and the cells resuspended in 400 μL of sterile SOC broth. Dilutions were made to 10^2, 10^4, 10^6, 10^8 (400 μL each), and 100 μL of each plated onto LB agar plates containing 30 μg/mL ampicillin (in duplicate). The plates were inverted and incubated at 37°C for 18 h at which time colonies were counted and a yield of 10^{10} transformants assessed. Resistant colonies were then grown in 3.0 L of sterile LB broth (10 g bacto-tryptone, 5 g bacto-yeast extract, and 10 g NaCl to 1.0 L) containing 30 μg/mL ampicillin, at 37°C for 18 h until an OD (optical density) of 0.800 to 0.900 was achieved. Chloramphenicol (170 μg/mL final concentration) was added and the incubation continued for an additional 18 h. The cells were pelleted by centrifugation (5K, 10min., 4°C), and the plasmid DNA (pBR 322) isolated following the Qiagen maxi-prep kit procedure.

Purification of supercoiled plasmid DNA used in DNA-cleavage assays.

Supercoiled plasmid DNA (pBR 322) from plasmid preparations or ΦX 174 (purchased from New England Biolabs) used in plasmid nicking assays were purified on 1% agarose gels. The gels were electrophoresed at 75 V for 2 h, then the bands corresponding to supercoiled DNA, as visualized by hand held ultra violet (UV) light on a preparative TLC plate (EM Science Silica Gel 60, F254, 20 x 20 cm, x 250 μm) background were excised and the DNA removed from the gel with a Schleicher & Schuell Elutrap electroeluter at 150 V (3 h). The DNA was then concentrated and desalted on Microcon 30 membranes (Amicon Inc.).

Cleavage of supercoiled plasmid DNA (pBR 322 and ΦX 174).

DNA-cleavage reaction mixtures were made up by addition at 0°C of appropriate amounts of reagent stock solutions to a stock solution of pBR 322 DNA plasmid containing 0.5 μg DNA per reaction. The total volumes of the reaction mixtures were brought up to

10 μL with distilled and deionized water when necessary and the reaction mixtures were incubated at 37°C for 2 h in tightly capped plastic Eppendorf tubes. Stock solutions for experiments including DNA were prepared using distilled, deionized water and commercially available reagents: DTT - Sigma; sodium phosphate monobasic - EM Science; sodium phosphate dibasic, 30% hydrogen peroxide - Malinckrodt; superoxide dismutase, beef liver catalase (suspension in water) - Boehringer Mannheim Biochemical. Desferal was the generous gift from Ciba-Geigy Co. The cleavage of plasmid DNA was detected by loading the reactions onto 0.8% agarose gels (containing 0.4 μg/mL ethidium bromide) and electrophoresed for 2 h at 55 V. The electrophoresis gels were immediately visualized on a UV transilluminator and photographed using black and white instant films (Polaroid T667). The measurements of the relative intensities of DNA bands were performed on the photographs using the Dell System 325 computer and Technology Resources Inc. image processing software. The film used to photograph the gels was confirmed to have a linear response to the range of DNA quantities used. The mean number of single strand scissions (*S*) per supercoiled DNA substrate was calculated using the Poisson distribution (see Chapter 4.2.c). All reactants were mixed at ice bath temperature and brought to a final volume of 10 μL. All reactions were then incubated for 2h at 37°C in the indicated buffer with 0.5 ug pBR 322 plasmid DNA.

Labeling (5'-^{32}P) of synthetic oligonucleotides for high resolution polyacrylamide gel electrophoresis.

To a solution of the synthetic deoxyoligonucleotide (100 pmol) in 74μL of deionized water was added 20 μL of polynucleotide kinase buffer, 4 μL (40 units) of T4 polynucleotide kinase (New England Biolabs) and 1 μL (10 μCi) of γ-^{32}P ATP (Dupont). The reaction was incubated for 60 min at 37°C and 10 min at 70°C. The solution was loaded onto a 2 mL column of Sephadex G-50 and eluted with deionized water. The first

radioactive fraction was collected and precipitated with ethanol/ 3M NaOAc (pH 5.2), and dried. Annealing was performed by mixing equimolar amounts of the 5'-^{32}P-end-labeled strand and the complimentary strand in deionized water to a final volume of 100 µL and heated to 65°C for 30 min. and slowly cooled to 0°C.

Reactions with 5'-^{32}P-labeled oligonucleotides and electrophoresis of products.

Reactions were made up by additions at 0°C of appropriate amounts of stock solutions to 3 µL of labeled DNA (~5 pmol). The total volume of the reactions was brought to 10 µL with deionized water and enough 100 mM phosphate buffer (at indicated pH) such to achieve a final concentration of 20 mM phosphate. Each reaction was incubated at 37°C for 5 h (none of the reactions contained any additional reducing agents such as DTT). To the reaction mixtures were then added 1 µL of 3M NaOAc (pH 5.2) and 60µL of ethanol and the resulting solutions aged at -70°C for 10 min. The tubes were centrifuged at 14 K for 10 min. at 4°C , the supernatants discarded and the DNA pellet dried under reduced pressure. To each dried pellet of DNA, was added 10 µL of loading buffer (formamide, 10 mM EDTA, pH 8, 0.025% xylenecyanol FF and 0.025% bromophenol blue) then heated to 90°C for 2 min., placed on ice and immediately loaded (20,000 CPM/lane as measured using a Packard scintillation counter) onto 20% denaturing (urea) polyacrylamide gels and run for ~6h at 1300 V. The bands were then visualized by autoradiography using Kodak X-OMAT AR (35 x 43 cm) film.

Band shift assays by enzymatic 3'-phosphate removal.

To DNA-cleavage reactions redissolved in 10 µL of deionized water were added 2 µL of 10 x T4 kinase buffer and the mixtures heated to 90°C for 2 min. After cooling to 0°C, 20 units of T4 polynucleotide kinase (New England Biolabs.) were added, the

reactions mixed and incubated at 37°C for 1 h. The reaction mixtures were then ethanol precipitated, the pellets washed with 70% ethanol, dried under reduced pressure then redissolved in tracking dye (formamide, 10 mM EDTA, pH 8, 0.025% xylenecyanol FF and 0.025% bromophenol blue) and loaded to polyacrylamde gels and run as described above.

Preparation and ^{32}P-labeling of pBR 322 restriction fragments.

Supercoiled plasmid DNA (pBR 322) was linearized with Eco R1 restriction endonuclease (Boehringer Mannheim) and split into two portions. The first portion was labeled (3'-^{32}P) by addition of DNA polymerase (Klenow enzyme, labeling grade - Boehringer Mannheim) and α ^{32}P-dATP (Dupont) for 30 min at 25°C. Additional Klenow enzyme was then added followed by *cold*, 100 mM dATP (New England Biolabs) and the reaction aged at 25°C for an additional 30 min to insure complete fill-in. The enzyme was heat denatured at 65°C for 15 min then purified by Sephadex G-50 size exclusion chromatography. The first radioactive fraction was ethanol precipitated and dried under reduced pressure (Savant Speed-Vac, SVC-100). The residue was dissolved in deionized water and phenol/chloroform extracted, 24:1 chloroform/isoamylalcohol extracted and ethanol precipitated. Separately, the second portion was labeled (5'-^{32}P) by first phenol/chloroform and 24:1 chloroform/isoamylalcohol extracting the Eco RI linearized plasmid. The ethanol precipitated, dried pellet was then dephosphorylated with calf intestinal alkaline phosphatase (CIP - New England Biolabs) as directed by the manufacturer, the enzyme deactivated by heating at 70°C followed by phenol/chloroform and 24:1 chloroform/isoamylalcohol extractions and ethanol precipitation. The dried pellet was treated with 10 to 20 μCi of γ ^{32}P-ATP (Dupont) in the presence of 40 units of T4 polynucleotide kinase (New England Biolabs) for 60 min, the enzyme deactivated by heat denaturation at 70°C for 10 min and loaded to a 2 mL sephadex G-50 column. The first

radioactive fraction was ethanol precipitated and dried under reduced pressure. In both cases (3' and 5'-labeled material) the dried pellets were redissolved in deionized water and restriction cut a second time with Rsa I (Boehringer Mannheim), the reaction mixtures ethanol precipitated, dried under reduced pressure, redissolved in tracking dye (formamide, 10 mM EDTA, pH 8, 0.025% xylenecyanol FF and 0.025% bromophenol blue) and loaded to 15% preparative, non-denaturing polyacrylamide gels. The gels were electrophoresed at 400 V until the xylenecyanol reached the bottom of the gels. The bands corresponding to the 167 and 516 base pair restriction fragments, as indicated by autoradiography, were excised from the gels and isolated by extraction into 500 mM ammonium acetate/1.0 mM EDTA (pH 8) followed by *n*-butanol extraction and ethanol precipitation.

Reactions with ^{32}P-labeled restriction fragments.

Reactions were made up by additions at 0°C of appropriate amounts of reagent stock solutions (stock solution of **314** was prepared as the hydrochloride salt) to 3 μL of ^{32}P-labeled DNA (approximately 100 μM base pairs final concentration). The total volume of the reactions were brought to 10 μL with deionized H_2O and enough 100 mM phosphate buffer (pH 8) such to achieve a final concentration of 10 mM phosphate. Each reaction was incubated at 37°C for 10 h. To the reaction mixtures were then added 1 μL of 3 M NaOAc (pH 5.2) and the reaction mixture ethanol precipitated and dried under reduced pressure. To each pellet was added 10 μL of loading buffer (formamide, 10 mM EDTA, pH 8, 0.025% xylenecyanol FF and 0.025% bromophenol blue) then heated to 90°C for 5 min and immediately loaded (10,000 CPM/lane as measured by a Packard 1500 liquid scintillation analyzer) to 20 x 40 cm, 15% denaturing (urea) polyacrylamide gel containing 20% formamide and run at 1300 V until the xylenecyanol reached the bottom of the gel. The gels were then fixed in 5% acetic acid, 15% methanol (aq), dried on a Bio-Rad 583 gel

dryer and the bands visualized by autoradiography using Kodak X-OMAT AR (35 x 43 cm) film.

Molecular modeling.

Molecular mechanics were carried out using DRIEDING forcefield in the molecular modeling package BIOGRAF (Molecular Simulations, Inc., 16 New England Executive Park, Burlington, MA 01803-5297). Netropsin conjugate **314** was manually docked in the minor groove into the 5'-d(ATTT)$_2$-3' sequence of the 5'-d(CGCAAATTTGCG)$_2$-3' dodecamer and minimized. The dodecamer 5'-d(CGCAAATTTGCG)$_2$-3' was obtained from the Brookhaven Protein Data Bank.

5.2. Preparation of compounds

161 **162**

(2-Methoxyphenyl)oxirane (162).

A non-homogenous mixture of *O*-anisalkehyde (**161**) (20 g/0,147 mol), 500 mL of dichloromethane. aqueous NaOH (50%, 330 mL), tetra-*n*-butylammonium iodide (0.52 g/0.0014 mol) was vigorously stirred at room temperature for 5 days. After dilution with water the organic layer was separated, washed with water, dried over Na_2SO_4, concentrated in vacuum and the residue was Kugelrohr distilled to yield 20.4 g of the pure product in the form of a colorless liquid. 93% yield.

^{1}N NMR (270 MHz) $CDCl_3$) δ TMS: 2.69 (1 H, q, J = 2.4 Hz), 3.12 (1 H, q, J = 4.6 Hz), 3.85 (3 H, s), 4.20 (1 H, t, J = 2.7 Hz), 6.91 (2 H, m), 7.15 (1 H, q, J = 1.6 Hz), 7.25 (1 H, m).

IR (NACl): 3051, 3002, 2941, 2838, 1689, 1602, 1496, 1466, 1439, 1391, 1287, 1256, 1103, 1048, 1027, 989, 880, 775 cm^{-1}.

162 **164**

***O*-2-Chloro-2-(2'-methoxyphenyl)-N-ethoxyacetyl carbamate (164).**

A solution of epoxide **162** (0.69 g/4.60 mmol) and 10 mL of a 20% phosgene solution in toluene (Fluka) was sealed in a flask and stirred at room temperature for 60 h. The excess phosgene was then removed by nitrogen purge through a caustic scrubber for 2h. The reaction mixture was then concentrated under reduced pressure producing chloroformate **163** as on oil. This material was then redissolved in dichloromethane (15 mL) and a solution of saturated $NaHCO_3$ (15 mL) added followed by a solution of glycine ethyl ester hydrochoride dissolved in a small volume of water. The resulting two phase reaction then stirred vigorously at room temperature for 20 min, at which time the layers were separated and the organic layer (bottom) washed with water, dried over Na_2SO_4 and concentrated to dryness in vacuo affording 1.4 g of **164**. 96% Yield. Crystals from isopropanol, mp = 61 - 63°C.

163. ^{1}H NMR (300 MHz) ($CDCl_3$) δ TMS: 3.85 (3 H, s), 4.55 (1 H, dd, *J* = 11.3 Hz, *J* = 5.0 Hz), 4.67 (1 H, dd, *J* = 11.3 Hz, *J* = 7.9 Hz), 5.62 (1 H, dd, *J* = 5.0 Hz), 6.90 (1 H, d, *J* = 8.3 Hz), 6.98-7.03 (1 H, m), 7.30-7.36 (1 H, m), 7.48 (1 H, dd, *J* = 7.6 Hz, *J* = 1.6 Hz).

163. IR (NaCl): 1779, 1492, 1252, 1145, 775 cm^{-1}.

164. ^{1}H NMR (300 MHz) ($CDCl_3$) δ TMS: 1.28 (1 H, t, *J* = 7.2 Hz), 3.85 (3 H, s), 3.95 (2 H, d, *J* = 5.5 Hz), 4.21 (2 H, q, *J* = 7.2 Hz), 4.44-4.48 (2 H, m), 5.32 (1 H, br

s), 5.58 (1 H, t, J = 6.3 Hz), 6.88 (1 H, d, J = 8.4 Hz), 6.98 (1 H, t, J = 7.2 Hz), 7.3 (1 H, m), 7.48 (1 H, dd, J = 7.7 Hz, J = 1.6 Hz).

164. IR (NaCl): 3357, 1729, 1533, 1495, 1252, 1201, 1052, 1026, 757 cm^{-1}.

Anal. calcd for $C_{14}H_{18}ClNO_5$: C, 53.25; H, 5.74; N, 4.43. Found: C, 53.40; H, 5.81; N, 4.39.

164 **36**

1-(Carboethoxy)methyl-5-(2'-methoxy)phenyloxazolidin-2-one (36).

To a solution of **164** (15.7 g,50.0 mmol) in THF (150 mL) cooled to 0°C a solution of potassium *t*-butoxide (6.13 g, 55.0 mmol) in THF (75 mL) was added slowly with stirring. After 0.5 h the reaction mixture was diluted with water, slightly acidified with dilute HCl and extracted with dichloromethane. The organic extract was dried over Na_2SO_4, filtered and concentrated in vacuum to yield 14 g **36** as an oil. 98% Yield.

^{1}H NMR (270 MHz) ($CDCl_3$) δ TMS: 1.26 (3 H, t, *J* = 7.0 Hz), 3.43 (1 H, d, *J* = 18.0 Hz), 3.85 (3 H, s), 4.17 (3 H, m), 4.35 (1 H, d, *J* = 18.0 Hz), 4.74 (1 H, t, *J* = 8.5 Hz), 5.35 (1 H, m), 6.99 (2 H, m), 7.31 (2 H, m).

IR (NaCl): 2960, 2920, 2820, 1750, 1600, 1580, 1485, 1460 cm^{-1}.

36 **165**

1-(Carbochloro)methyl-5-(2'-methoxy)phenyloxazolidin-2-one (165).

To a stirred solution of **36** (14 g/49.0 mmol) in 150 mL of ethanol was added LiOH monohydrate (2.8 g, 66.7 mmol) in water (60 mL) at 0°C. After 0.5 h the reaction mixture was concentrated under reduced pressure to a half volume at room temperature, diluted with water, acidified and extracted with ethyl acetate. The extract was dried over Na_2SO_4, filtered and concentrated. From the oily residue the pure acid intermediate was obtained by crystallization from ethyl acetate (9.3 g, 74%), mp = 165 - 166°C. Physical data matched those reported in the liturature. This material was then slurried in 250 mL of dry dichloromethane and to this solution was added 9.2 g (73 mmol) of oxalyl chloride. The reaction mixture then stirred at room temperature for 2 h at which time the reaction was concentrated under reduced pressure affording 12 g of acid choride **165**. 73% Overall yield.

^{1}H NMR (270 MHz) ($CDCl_3$) δ TMS: 3.78 (1/2 H, s), 3.85 (3.5 H, s), 4.25 (1 H, dd, J = 8.5 Hz, J = 8.9 Hz), 4.72-4.76 (2 H, m), 5.32 (1 H, d, J = 9.0 Hz), 6.95-6.98 (2 H, m), 7.27 (2 H, m).

IR (NaCl): 3060, 3020, 2940, 2830, 1800, 1760, 1600, 1590, 1460, 1420 cm^{-1}.

165 **37**

1-Hydroxymethyl(2,2'-carbonyl)-4-keto-8-methoxy-tetrahydroisoquinolone (37).

To a solution of acid chloride **165** (14.4 g/48 mmol) in 100mL of dichloromethane and cooled to 0°C was added aluminum chloride (26 g/192 mmol) as a solid over a 15 min period. The resulting mixture stirred at 0°C for 30 min followed by stirring at room temperature for an additional 3 h. The reaction mixture was then poured onto ice and once melted was extracted 3 x 100mL with dichloromethane, the organic layers combined, dried over $MgSO_4$, filtered through Celite and concentrated to dryness in vacuo. The crude was then taken up in 3:1 ethylacetate/hexane and passed through a short column of silica and then concentrated to dryness in vacuo affording 10.4 g of isoquinolone **37**. 92% Yield. Crystals from ethyl acetate/hexanes, mp = 159°C (dec).

^{1}H NMR (300 MHz) ($CDCl_3$) δ TMS: 3.85 (1/2 ABq, *J* = 20.2 Hz), 3.91 (3 H, s), 4.25 (1, t, *J* = 9.4 Hz), 4.68 (1/2 ABq, *J* = 20.2 Hz), 5.01 (1 H, t, *J* = 9.9 Hz), 5.23 (1 H, t, *J* = 9.6 Hz), 7.15 (1 H, d, *J* = 9.2 Hz), 7.45 (1 H, t, *J* = 9.3 Hz), 7.73 (1 H, d, *J* = 9.0 Hz).

IR (NaCl): 3080, 3020, 2940, 2870, 1765, 1695, 1595, 1580, 1430 cm^{-1}.

Figure 45. ^{1}H NMR spectrum (300 MHz) ($CDCl_3$) of isoquinolone **37**

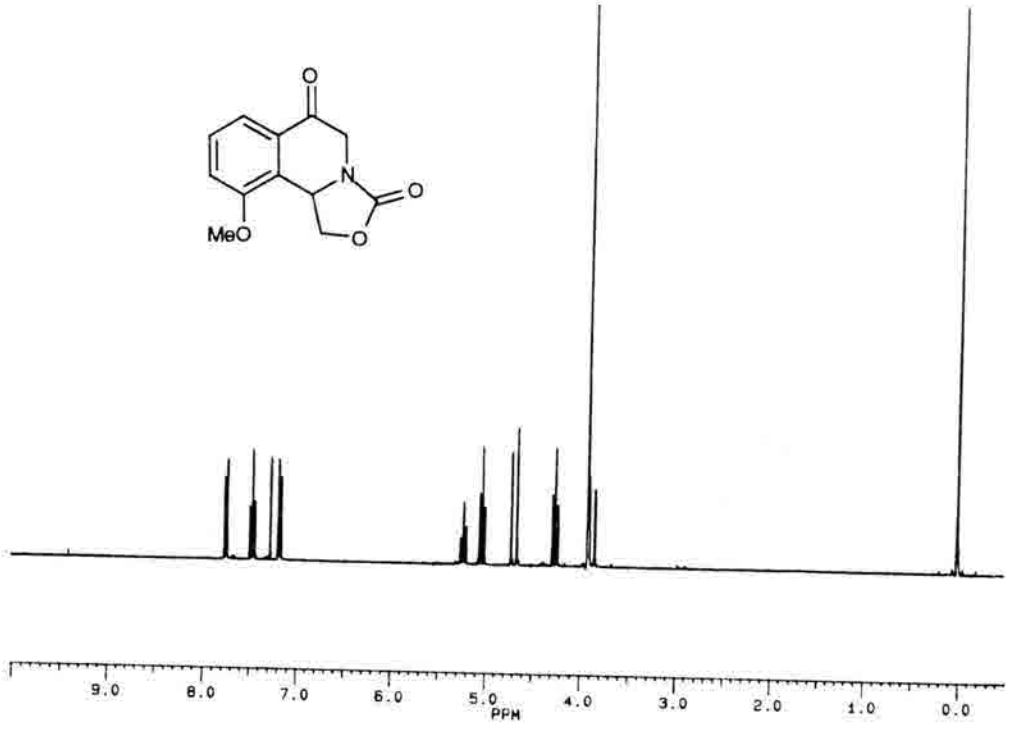

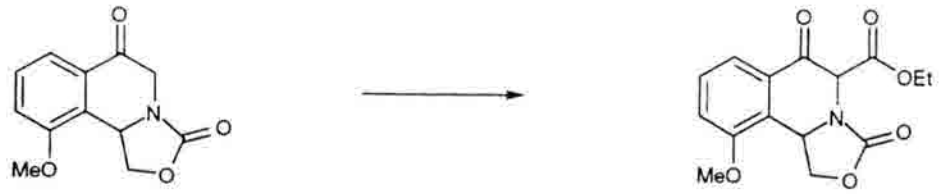

37 **38**

3-Carboethoxy1-1-hydroxymethyl(2,2'-carbonyl)-4-oxo-8-methoxytetrahydroisoquinoline (38).

To a stirred solution of **37** (15 g, 0.064 mol) in DMF (375 mL) was added 2.3 g (0.096 mol) of sodium hydride as a solid (slowly) and the resulting mixture stirred at room temperature for 15 min. The reaction mixture was then cooled to 0°C and to this mixture added 7.0 g (0.07 mol) of ethylcyano formate and the resulting solution stirred at 0°C for 30 min at which time the reaction was poured onto ice and the resulting slurry acidified with 1 N HCl (aq). The mixture was diluted with dichloromethane and washed with water and brine. The organic layer was dried over $MgSO_4$, filtered, evaporated and the residue was chromatographed on silica gel (hexane/ethyl acetate - 3/2) yielding **38** as an amorphous solid (15.6 g, 80%), mp = 91 - 92°C.

^{1}H NMR (270 MHz) ($CDCl_3$) δ TMS: 1.24 (3 H, t, *J* = 8.2 Hz), 3.87 (3 H, s); 4.11-4.25 (3 H, m); 5.05 (1 H, t, *J* = 8.5 Hz); 5.32 (1 H,s); 5.57 (1 H, t, J = 8.5 Hz), 7.16 (1 H, d, J = 7.7 Hz), 7.43 (1 H, t, *J* = 8.0 Hz); 7.71 (1 H, d, J = 7.8 Hz).

IR (NaCl): 1765, 1750, 1700, 1250 cm^{-1};

Mass spectrum, m/z = 305 (100), 233 (12).

38 **39**

1-Hydroxymethyl(2,2'-carbonyl)-3-carboethyoxy-4-hydroxy-8-methoxytetrahydroisoquinoline (39).

To a solution of ketoester **38** (19 g, 0.062mol) dissolved in 300 mL of glacial acetic acid was added $NaBH_3CN$ (7.8 g, 0.124 mol) and the reaction mixture stirred at room temperature for 18 h. After diluting with dichloromethane the organic layer was washed with water, Na_2CO_3 solution, water and dried over Na_2SO_4. Evaporation of the solvent yielded yellowish oily product which crystallized on standing (16 g, 84%). Analytical sample was obtained by recrystallization from ethyl acetate/hexane mp = 119-121°C.

^{1}H NMR (270 MHz) ($CDCl_3$) δ TMS: 1.23 (3 H, t, *J* = 7.0), 3.83 (3 H, s), 4.03 (1 H, t, *J* = 8.8 Hz), 4.92-5.18 (4 H, m), 6.18-6.84 (1, H, m), 7.26-7.37 (2 H, m).

^{13}C NMR (300 MHz) ($CDCl_3$) δ: 13.90, 50.27, 53.95, 55.37, 61.92, 66.35, 70.19, 109.11, 118.04, 120.89, 129.05, 137.36, 155.03, 156.80, 169.48.

IR (KBr pellet): 3520, 1753, 1717, 1413, 1221.

Anal. calcd for $C_{15}H_{17}NO_6$: C, 58.62; H, 5.57; N, 4.56. Found: C, 58.72; H, 5.60; N, 4.44.

39 **169**

1-Hydroxymethyl(2,2'-carbonyl)-3-(*N*-methyl-*N*-2,2-dimethylethoxy)-carboxamide-8-methoxydihydroisoquinoline (169).

To a solution of crude β-hydroxyester **39** (148 mg, 0.48 mmol) in ethanol (5.0 mL) aqueous LiOH (2.0 M, 0.36 mL, 0.72 mmol) was added at room temperature. After 0.5 h at room temperature the reaction mixture was diluted with water and washed with dichloromethane. The aqueous layer was acidified with HCl (2.0 M, 0.4 mL) and extracted with dichloromethane. Drying of the organic extract over Na_2SO_4 and evaporation of the solvent yielded slightly yellowish solid (105 mg) which was refluxed in toluene (2.0 mL) with thionyl chloride (134 mg, 1.13 mmol) for 3 h. The reaction mixture was concentrated in vacuum, the oily residue was redissolved in dry dichloromethane and excess of *N*-methyl-2-amino-2-methyl-1-propanol (118 mg, 1.13 mmol, 3.0 eq., obtained from 2-amino-2-methyl-1-propanol by treatment with methyl chloroformate and subsequent reduction of the methylurethane with excess of lithium aluminum hydride) in dichloromethane (2.0 mL) was added with ice-water cooling. After 1 h at room temperature the reaction mixture was washed with water and the hydroxyamide **169** (63 mg, 48%) was isolated by radial chromatography on silica gel (ethyl acetate/hexane - 2/1) as a crystalline colorless solid. Analytical sample was obtained by recrystallization from methanol mp = 188-190°C.

^{1}H NMR (270 MHz) ($CDCl_3$) δ TMS: 1.43 (3 H, s), 3.06 (3 H, s), 3.83 (3 H, s), 3.80-3.92 (2 H, m), 4.56 (1 H, dd, J = 10.8, J = 9.3 Hz), 5.09 (1 H, dd, J = 8.8 Hz,

J = 8.1 Hz), 5.39 (1 H, dd, J = 10.9 Hz, J = 8.2 Hz), 6.03 (1 H, br s), 6.77-6.85 (2 H, m), 7.23-7.30 (1 H, m).

IR (NaCl): 3500, 1755, 1633, 1575 cm^{-1}.

Anal. calcd for $C_{18}H_{22}N_2O_5$: C, 62.41; H, 6.40; N, 8.09. Found: C, 62.21; H,6.44; N, 7.89.

Figure 46. ^1H NMR spectrum (300 MHz) ($CDCl_3$) of hydroxamide **169**

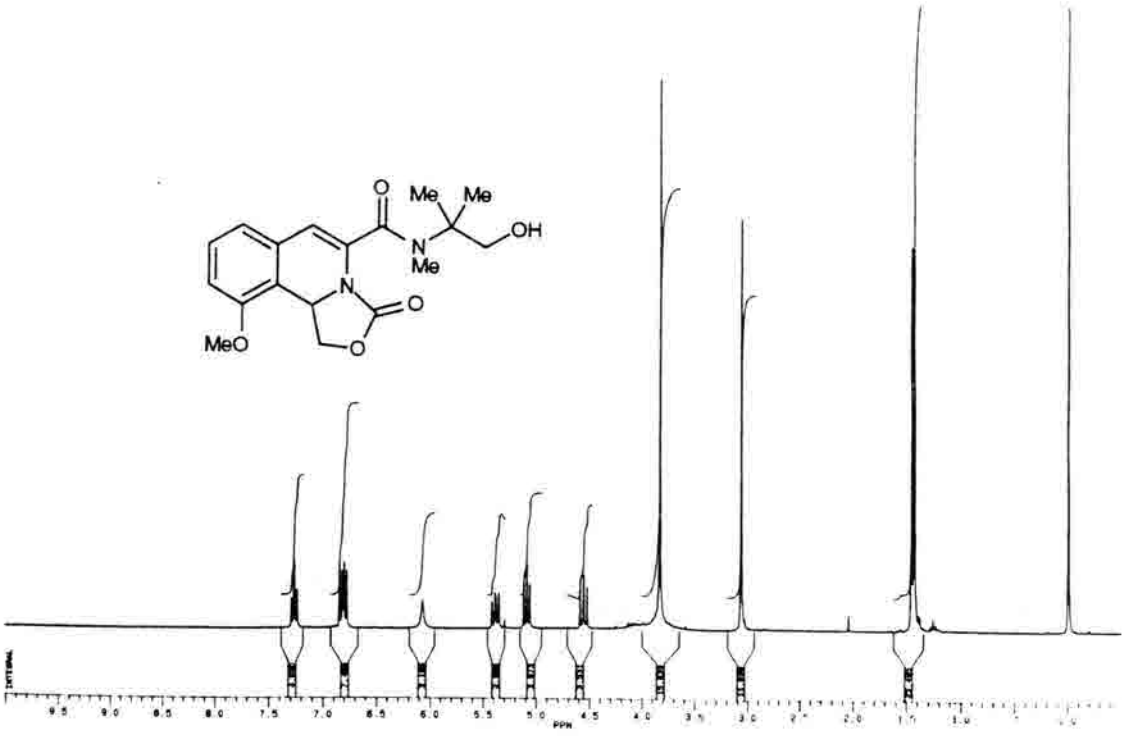

169 **42a, 42b**

***cis*-1-Hydroxymethyl-(2,2'-carbonyl)-3-(*N*-methyl-*N*-2,2-dimethylethoxy) carboxamide-8-methoxytetrahydroisoquinoline (42a) and *trans*-1-hydroxymethyl-(2,2'-carbonyl)-3-(*N*-methyl-*N*-2,2-dimethylethoxy)-carboxamide-8-methoxytetrahydroisoquinoline (42b).**

A solution of unsaturated amide **169** (252 mg, 0.728 mmol) in ethanol (100 mL) was hydrogenated under 60 psi H_2 at room temperature with 5% palladium on charcoal catalyst (240 mg) for 12 h. The mixture of diasteroisomeric products was separated by PTLC chromatography on silica gel (dichloromethane/THF - 20/1) to yield amides **42a** (131 mg, 52%) and **42b** (55mg, 22%) as colorless oils. Analytical samples were obtained by recrystallization. **42a** (ethyl acetate) mp= 197.5-198.5°C; **42b** (ethyl acetate/hexane) mp = 131-132°C.

42a. ^{1}H NMR (270 MHz) ($CDCl_3$) δ TMS: 1.39 (3 H, s), 1.42 (3 H, s), 2.88 (1 H, dd, J = 16.9 Hz, J = 3.5 Hz), 3.06 (3 H,s), 3.20 (1 H, br s), 3.41 (1 H, dd, J = 16.3 Hz, J = 11.6 Hz), 3.83 93 H, s), 4.12 (1 H, dd, J = 11.3 Hz, J = 3.6 Hz), 4.23 (1 H, dd, J = 9.0 Hz, J = 6.3 Hz), 4.63 (1 H, dd, J = 11.4 Hz, J = 1.2 Hz), 4.85 (1 H, t, J = 8.9 Hz), 5.14-5.20 (1 H,m), 6.75-6.82 (2 H,m), 7.20-7.27 (1 H, m).

42a. IR (NaCl): 3474, 1731, 1645, 1583 cm^{-1}.

42a. Anal. calcd for $C_{18}H_{24}N_2O_5$: C, 62.05; H, 6.94; N, 8.04. Found: C, 61.92; H, 6.75; N, 7.73.

42b. **^{1}HNMR** (270 MHz) ($CDCl_3$) δ $CHCl_3$: 1.22 (3 H, s), 3.02 (3 H, s), 2.98-3.12 (2 H, m), 3.59 (2 H, br s), 3.78 (3 H, s), 3.87-3.94 (1 H, m), 4.09 (1 H, t, J = 8.7 Hz), 4.90 (1 H, t, J = 8.8 Hz), 5.66 (1 H, dd, J = 7.5 Hz, J = 4.6 Hz), 5.18 (1 H, t, J = 8.6 Hz), 6.68 (1 H, d, J = 8.2 Hz), 6.75 (1 H, d, J = 8.2 Hz), 7.16 (1 H, t, J = 7.9 Hz).

42b. **IR** (NaCl): 3459, 1745, 1648, 1591, 1084, 731 cm^{-1}.

42b. **Anal.** calcd for $C_{18}H_{24}N_2O_5$: C, 62.05; H, 6.94; N, 8.04. Found: C, 61.99; H, 6.86; N, 7.82.

Figure 47. ^{1}H NMR spectrum (300 MHz) ($CDCl_3$) of *cis*-amidoalcohol **42a**

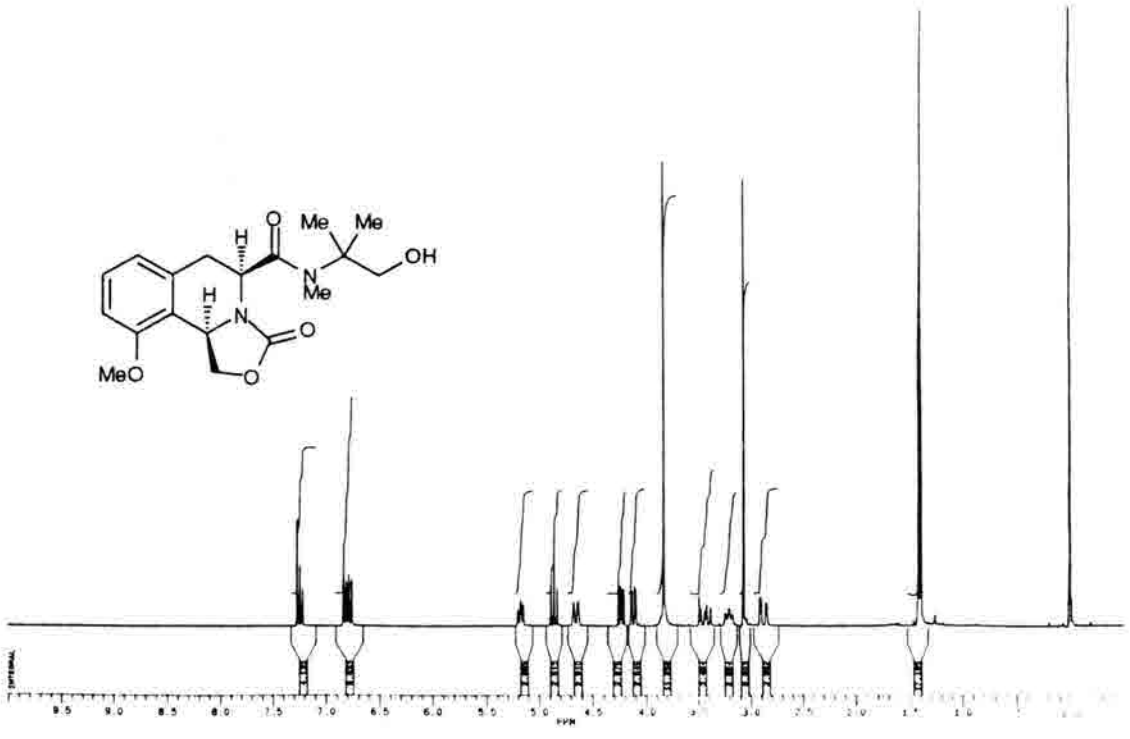

42a **43a**

***cis*-1-Hydroxymethyl-(2,2'-carbonyl)-3-(*N*-methyl-*N*-2,2-dimethylethoxy)-aminomethyl-8-methoxytetrahydroisoquinoline (43a).**

To a suspension of **42a** (129 mg, 0.37 mmol, 1.0 eq.) in dry THF (10 mL) solution of borane in THF (1.0 M, 1,85 mL) was added at room temperature under N_2. After 5 h at room temperature 1.0 M aqueous $(NH_4)_2CO_3$ was added and stirring was continued for another 5 h. The reaction mixture was concentrated and partitioned between water and methylene chloride. Separation on silica gel by radial chromatography (dichloromethane/MeOH - 10/1) yielded starting amide (13 mg, 10%) and amine **43a** (80 mg, 65%) as colorless oil.

^{1}H NMR (300 MHz) ($CDCl_3$) δ TMS: 1.03 (3 H, s), 1.07 (3 H, s), 2.31 (3 H, s), 2.70 (1 H, br s), 2.76-2.85 (2 H, m), 3.06 (1 H, dd, *J* = 15.8 Hz, *J* = 8.8 Hz), 3.16 (1 H, dd, *J* = 13.3 Hz, *J* = 5.3 Hz), 3.30 (1 H, 1/2 ABq, *J* = 10.8 Hz), 3.45 (1 H, 1/2 ABq, *J* = 10.8 Hz), 3.58-3.67 (1 H, m), 3.82 (3 H, s), 4.31 (1 H, dd, *J* = 9.0 Hz, *J* = 6.6 Hz), 4.76 (1 H, t, *J* = 8.7 Hz), 5.00 (1 H, d, *J* = 8.1 Hz), 6.82 (1 H, d,*J* = 7.6 Hz), 7.23 (1 H, t, *J* = 8.1 Hz).

IR (NaCl): 3457, 1747, 1586, 1070 cm^{-1}.

Figure 48. ^{1}H NMR spectrum (300 MHz) ($CDCl_3$) of *cis*-amino alcohol **43a**

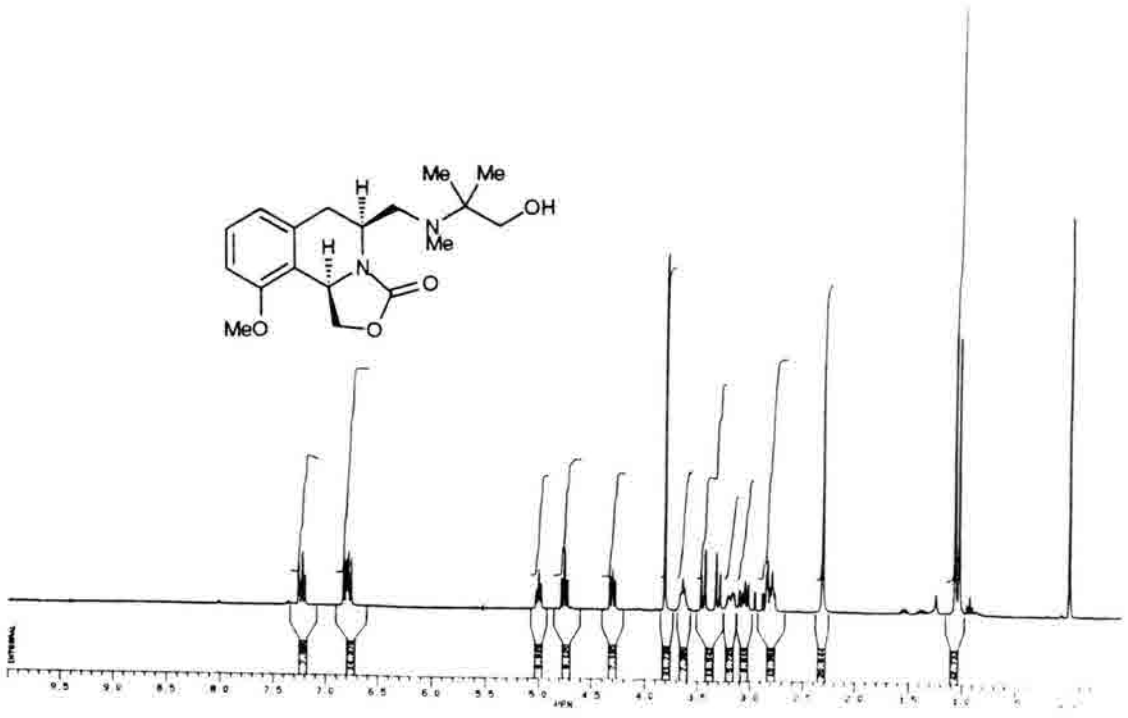

42b **43b**

***trans*-1-Hydroxymethyl-(2,2'-carbonyl)-3-(*N*-methyl-*N*-2,2-dimethylethoxy)-aminomethyl-8-methoxytetrahydroisoquinoline (43b).**

To a suspension of **42b** (110 mg, 0.32 mmol) in dry THF (10 mL) a solution of borane in THF (1.0 M, 1.58 mL) was added at room temperature under N_2. After 5 h at room temperature 1.0 M aqueous $(NH_4)_2CO_3$ was added and stirring was continued for another 5 h. The reaction mixture was concentrated and partitioned between water and methylene chloride. Separation on silica gel by radial chromatography (dichloromethane/MeOH - 10/1) yielded amine **43b** (92 mg, 88%) as colorless oil.

^{1}H NMR (270 MHz) ($CDCl_3$) δ TMS: 0.89 (3 H, s), 2.24-2.34 (1 H, m), 2.29 (3 H, s), 2.53 (1 H, dd, *J* = 13.1 Hz, *J* = 8.8 Hz), 2.71 (1 H, d *J* = 12.9 Hz), 3.05-3.25 (3 Hm), 3.80 (3 H, s), 4.10 (1 H, t, *J* = 7.9 Hz), 4.35-4.43 (1 H, m), 4.90 (1 H, t, *J* = 8.1 Hz), 4.96-5.02 (1 H, m), 6.71-6.75 (2 H, m), 7.18 (1 H, t, *J* = 8.0 Hz).

IR (NaCl): 3455, 1751, 1587, 1077 cm^{-1}.

Mass spectrum m/z = 335 (MH+), 333, 303, 263.

43a **44a**

***cis*-1-Hydroxymethyl-(2,2'-carbonyl)-3-(*N*-methyl-*N*-2,2-dimethyl-2-formyl)-aminomethyl-8-methoxytetrahydroisoquinoline (44a).**

To a stirred solution of DMSO (10 mg/0.09 mmol.) in 2.0 mL of dichloromethane and cooled to -78°C was added 5.7 mg (0.045 mmol) of oxalyl chloride and the resulting solution stirred at -78°C for 15 min. Separately, 11 mg (0.03 mmol) of aminoalcohol **43a** were dissolved in a small volume of dichloromethane and introduced to the reaction vessel and the resulting mixture stirred at -78°C for 30 min. At this time, 30 mg (0.30 mmol) of triethylamine were added and stirring continued at -78°C for an additional 30 min. The reaction mixture was then warmed to 25°C and concentrated under reduced pressure. The residue was redissolved in dichloromethane (20 mL), washed with water, dried over Na_2SO_4 and concentrated to dryness in vacuo affording 11 mg of aldehyde **44a**. Quant. yield.

^{1}H NMR (300 MHz) ($CDCl_3$) δ TMS: 1.09 (3 H, s), 1.12 (3 H, s), 2.30 (3 H, s), 2.70 (1 H, dd, *J* = 13.3 Hz, *J* = 9.2 Hz), 2.88 (1 H, dd, *J* = 15.7 Hz, *J* = 4.1 Hz), 3.02 (1 H, dd, *J* = 13.2 Hz, *J* = 4.5 Hz), 3.09 (1 H, dd, *J* = 15.8 Hz, *J* = 8.1 Hz), 3.62-3.68 (1 H, m), 3.82 (3 H, s), 4.30 (1 H, dd, *J* = 8.9 Hz, *J* = 7.2 Hz), 4.77 (1 H, dd, *J* = 9.0 Hz, *J* = 8.1 Hz), 4.98 (1 H, t, *J* = 7.4 Hz), 6.78 (1 H, d, *J* = 8.3 Hz), 6.82 (1 H, d, *J* = 7.7 Hz), 7.24 (1 H, t, *J* = 7.7 Hz), 9.47 (1 H, s).

IR (NaCl): 1730, 1586, 1470, 1070 cm^{-1}.

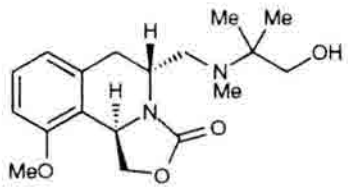

43b

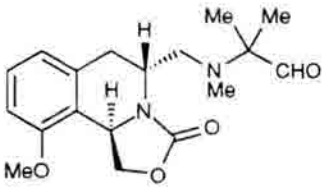

44b

***trans*-1-Hydroxymethyl-(2,2'-carbonyl)-3-(*N*-methyl-*N*-2,2-dimethyl-2-formyl)-aminomethyl-8-methoxytetrahydroisoquinoline (44b).**

To a stirred solution of DMSO (10 mg/0.09 mmol.) in 2.0 mL of dichloromethane and cooled to -78°C was added 5.7 mg (0.045 mmol) of oxalyl chloride and the resulting solution stirred at -78°C for 15 min. Separately, 11 mg (0.03 mmol) of aminoalcohol **43a** were dissolved in a small volume of dichloromethane and introduced to the reaction vessel and the resulting mixture stirred at -78°C for 30 min. At this time, 30 mg (0.30 mmol) of triethylamine were added and stirring continued at -78°C for an additional 30 min. The reaction mixture was then warmed to 25°C and concentrated under reduced pressure. The residue was redissolved in dichloromethane (20 mL), washed with water, dried over Na_2SO_4 and concentrated to dryness in vacuo affording 7 mg of aldehyde **44b**. 65% Yield.

^{1}H NMR (300 MHz) ($CDCl_3$) δ TMS: 0.93 (3 H, s), 0.99 (3 H, s), 2.23-2.42 (5 H, m), 2.88 (1 H, d, J = 16.3 Hz), 3.06 (1 H, dd, J = 16.2 Hz, J = 5.8 Hz), 3.8 (3 H, s), 3.98-4.07 (1 H, m), 4.37-4.45 (1 H, m), 4.86-4.94 (1 H, m), 6.71-6.75 (2 H, m), 7.20 (1 H, t, J = 7.9 Hz), 9.25 (1 H, s).

IR (NaCl): 1756, 1587, 1472, 1258, 1078 cm^{-1}.

44a **45a**

4α,6α,11aα-2-Aza-7-methoxy-5,4-oxazolo-1,3,4,6,11,11a-hexahydro-2,3,3-trimethyl-2*H*-benzo[*b*]quinolizine (45a).

To a stirred solution of aldehyde **44a** (11 mg/0.03 mmol) in 2 mL of ethanol was added 0.2 mL of 2 M LiOH (aq) and the resulting mixture degassed by purging with nitrogen. The solution then was heated at reflux with stirring for 48 h. After cooling to room temperature, the reaction mixture was concentrated under reduced pressure. Water (2 mL) was added, the mixture extracted 3 x 10 mL with dichloromethane, the dichloromethane layers combined, dried over Na_2SO_4 and concentrated to dryness in vacuo. The components were separated by PTLC (silica; 10:1 dichloromethane/methanol) affording 4.2 mg of oxazolidine **45a**. 44% Yield. Crystals from pentane, mp = 111-113°C.

^{1}H NMR (300 MHz) ($CDCl_3$) δ TMS: 0.95 (3 H, s), 1.23 (3 H, s), 2.32 (3 H, s), 2.39 (1 H, dd, *J* = 11.5 Hz, *J* = 9.5 Hz), 2.73-2.98 (4 H, m), 3.52-3.67 (3 H, m), 3.77 (3 H, s), 4.55 (1 H, t, *J* = 6.2 Hz), 6.67 (1 H, d, *J* = 8.2 Hz), 6.77 (1 H, d, *J* = 7.6 Hz), 7.14 (1 H, t, *J* = 8.1 Hz). See Figure 4, Chapter 2.

IR (NaCl): 1581, 1470, 1260, 1087, 1018, 779 cm^{-1}.

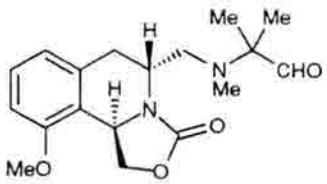

44b

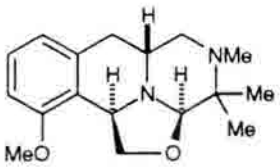

45b

4α,6α,11aβ-2-Aza-7-methoxy-5,4-oxazolo-1,3,4,6,11,11a-hexahydro-2,3,3-trimethyl-1,3,4,6,11,11a-hexahydro-2*H*-benzo[*b*]quinolizine (45b).

To a stirred solution of aldehyde **44a** (10 mg/0.027 mmol) in 2 mL of ethanol was added 0.2 mL of 2 M LiOH (aq) and the resulting mixture degassed by purging with nitrogen. The solution then was heated at reflux with stirring for 48 h. After cooling to room temperature, the reaction mixture was concentrated under reduced pressure. Water (2 mL) was added, the mixture extracted 3 x 10 mL with dichloromethane, the dichloromethane layers combined, dried over Na_2SO_4 and concentrated to dryness in vacuo. The components were separated by PTLC (silica; 10:1 dichloromethane/methanol) affording 2.2 mg of oxazolidine **45b**. 27% Yield. Crystals from ethyl acetate/hexanes, mp = 159-160°C.

^{1}H NMR (300 MHz) ($CDCl_3$) δ TMS: 1.16 (3 H, s), 1.33 (3 H, s), 2.34 (3 H, s), 2.52-2.75 (4 H, m), 2.95-3.05 (1 H, m), 3.62 (1 H, d, *J* = 7.3 Hz), 3.77 (3 H, s), 4.16 (2 H, t *J* = 7.4 Hz), 4.42 (1 H, t, *J* = 7.7 Hz), 6.71 (1 H, d, *J* = 7.5 Hz), 6.74 (1 H, d, *J* = 7.6 Hz), 7.18 (1 H, t, *J* = 7.0 Hz). See Figure 5, Chapter 2.

IR (NaCl): 1588, 1473, 1260, 1018, 786, 744 cm^{-1}.

39 **172**

1-Hydroxymethyl-(2,2'-carbonyl)-3-(*N*-2,2-dimethylethoxy)-carboxamide-8-methoxydihydroisoquinoline (172).

To a solution of crude β-hydroxyester **39** (120 mg, 0.42 mmol) in ethanol (5.0 mL) aqueous LiOH (2.0 M, 0.36 mL, 0.72 mmol) was added at room temperature. After 0.5 h at room temperature the reaction mixture was diluted with water and washed with dichloromethane. The aqueous layer was acidified with HCl (2.0 M, 0.4 mL) and extracted with dichloromethane. Drying of the organic extract over Na_2SO_4 and evaporation of the solvent yielded slightly yellowish solid which was refluxed in toluene (2.0 mL) with thionyl chloride (150 mg, 1.30 mmol) for 3 h. The reaction mixture was concentrated in vacuum, the oily residue was redissolved in dry dichloromethane and excess of 2-amino-2-methyl-1-propanol (236 mg, 2.0 mmol) in dichloromethane (2.0 mL) was added with ice-water cooling. After 1 h at room temperature the reaction mixture was washed with water and the hydroxyamide **169** (55 mg, 40%) was isolated by radial chromatography on silica gel (ethyl acetate/hexane - 2/1) as crystalline colorless solid.

^{1}HNMR (300 MHz)($CDCl_3$) δ TMS: 1.38 (6 H, s), 3.74 (2 H, m), 3.84 (s, 3H), 4.67 (1 H, dd, J = 9.9 Hz, J = 9.3 Hz), 5.08 (1 H, dd, J = 8.6 Hz, J = 8.0 Hz), 5.37 (1 H, dd, J = 8.3 Hz), 6.50 (1 H, s), 6.90 (2 H, d, J = 7.2 Hz), 7.29 (1 H, t, J = 7.6 Hz).

IR (NaCl): 3500, 1755, 1633, 1575 cm^{-1}.

Mass spectrum m/z (relative intensity) 332 (0.6) (MH^+), 314 (21.9), 301(16.0), 299 (8.2), 244 (16.5), 186 (14.4), 158 (14.7), 115 (5.8).

Figure 49. ^{1}H NMR spectrum (300 MHz) ($CDCl_3$) of hydroxyamide **172**

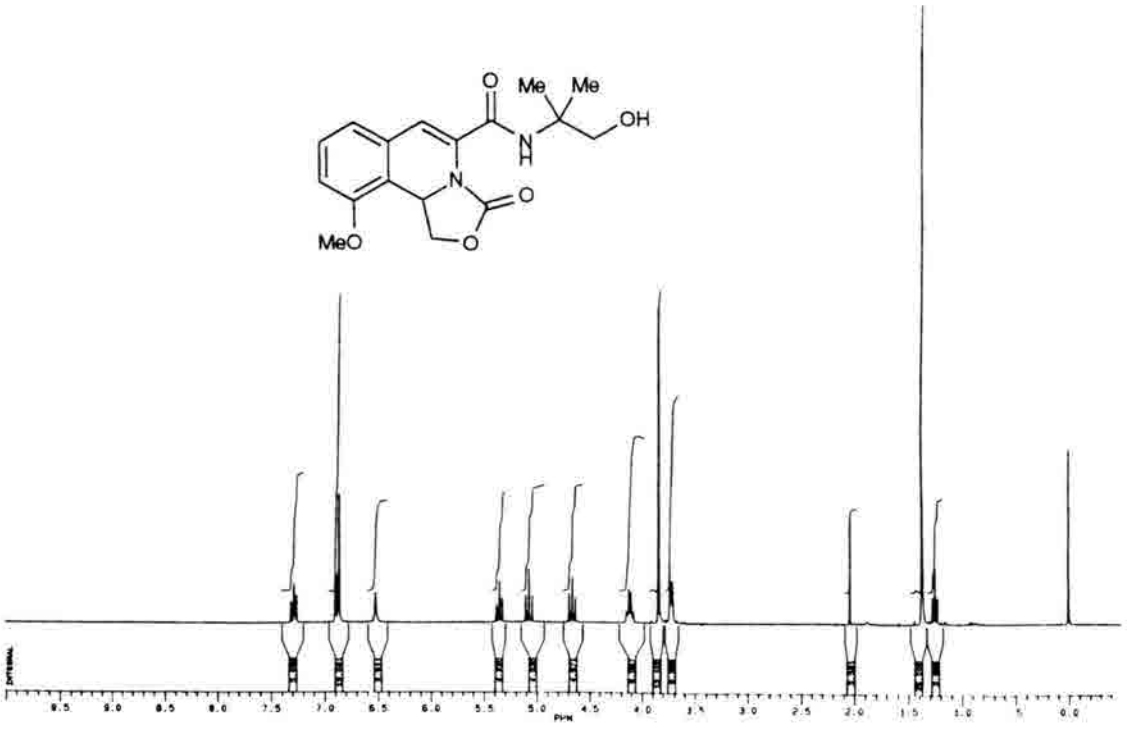

172 **173a, 173b**

***cis*-1-Hydroxymethyl-(2,2'-carbonyl)-3-(*N*-2,2-dimethylethoxy)-carboxamide-8-methoxytetrahydroisoquinoline (173a).**

Compound **172** (59 mg/0.18 mmol.), dissolved in 25 mL of ethanol was charged to a hydrogenation bomb with 50 mg of 5% Pd on carbon. This mixture stirred at room temperature (r.t.) under an atmosphere of H_2 (60 psi) for 16 h. The resulting mixture was filtered through Celite and concentrated to dryness in vacuo. The diastereomers were then separated by PTLC (7:1 CH_2Cl_2/THF), the faster eluting spot corresponding to the *cis*-diastereomer (33 mg, 56%). The *trans*-product was not characterizable due to impurities.

173a. **^{1}H NMR** (300 MHz) ($CDCl_3$) δ TMS: 1.28 (3 H, s), 1.36 (3 H, s), 3.01-3.06 (1 H, m), 3.22-3.35 (2 H, m), 3.84 (3 H, s), 3.93 (1 H, q, J = 4.2 Hz), 4.08 (1 H, d, J = 11.0 Hz), 4.43 (1 H, dd, J = 8.4 Hz, J = 4.2 Hz), 4.79 (1 H, dd, J = 8.7 Hz), 5.08 (1 H, dd, J = 3.3 Hz), 6.02 (1 H, s), 6.77-6.85 (2 H, m), 7.23-7.28 (1 H, m).

IR (NaCl): 3359, 2947, 1730, 1586, 1470, 1070 cm^{-1}.

Figure 50. ^{1}H NMR spectrum (300 MHz) ($CDCl_3$) of *cis*-hydroxyamide **173a**

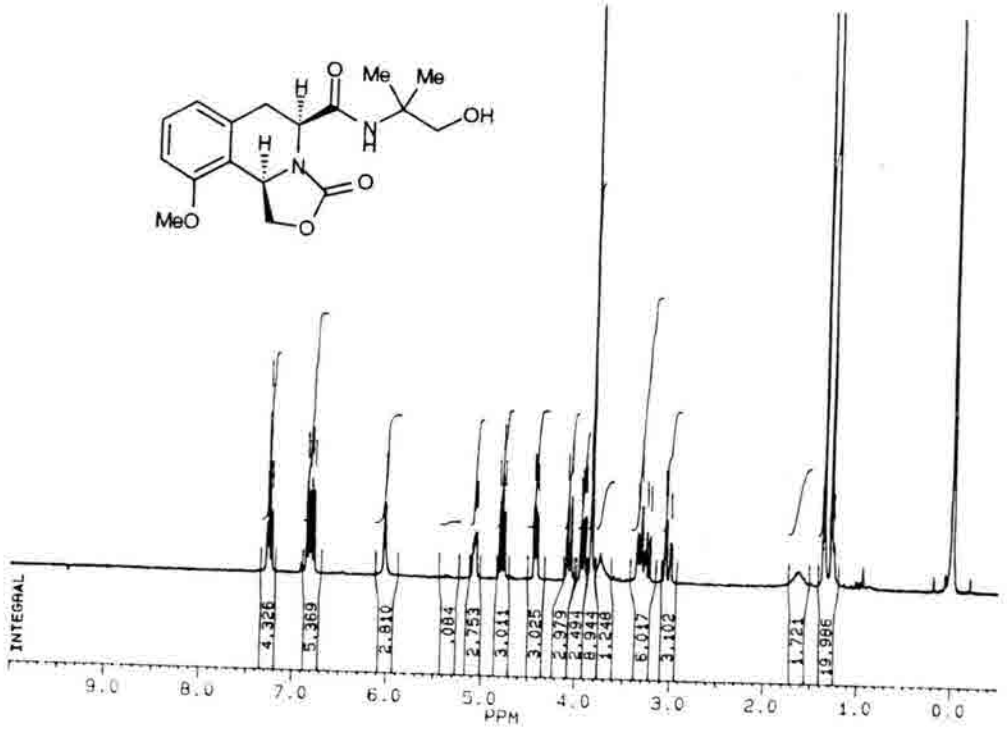

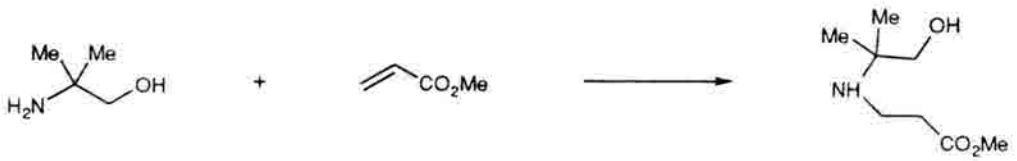

175 **176**

Methyl N-2,2-dimethylethoxy-3-aminopropionate (176).

To a stirred solution of 2.0 g (22 mmol) 2-amino-2-methyl-1-propanol (**175**) in 20 mL of CH_2Cl_2 was added 2.0 mL (1.9 g, 22 mmol) of methyl acrylate and 0.5 mL of triethylamine. The resulting mixture then stirred at room temperature for 3 days at which time it was concentrated to dryness in vacuo. The crude was then taken up in 20mL of $CHCl_3$,washed with 2 x 20 mL H_2O, the organic layer dried over Na_2SO_4, filtered through celite and concentrated to dryness in vacuo affording pure amine **176** (1.28 g, 36%).

^{1}H NMR (300MHz) ($CDCl_3$) δ TMS: 1.07 (6H, s), 2.50 (2H, t, J = 6.3), 2.79 (2H, t, J = 6.3), 3.32 (2H, s), 3.70 (3H, s).

^{13}C NMR (300 MHz) $CDCl_3$) δ: 24.00 (q), 24.17 (q), 35.12 (t), 37.18 (t), 51.56 (q), 53.50 (s), 67.77 (t).

IR (NaCl): 3302, 2967, 2872, 1737, 1438, 1363, 1320, 1174, 1097, 1056, 902, 843 cm^{-1}.

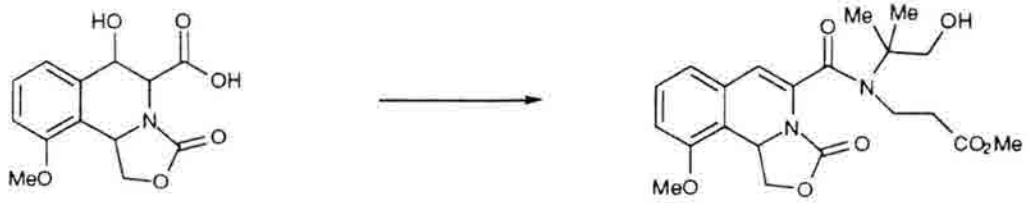

168 **177**

1-Hydroxymethyl-(2,2'-carbonyl)-3-(N-2-carboxymethylethyl-N-2,2-dimethylethoxy)-carboxamide-8-methoxydihydroisoquinoline (177).

Carboxylic acid **168** (1.2 g, 4.19 mmol)was refluxed in toluene (20 mL) with thionyl chloride (1.5 g, 12.6 mmol) for 3 h. The reaction mixture was concentrated in vacuum, the crude acid chloride redissolved in dry dichloromethane (10 mL) and cooled to 0°C. To this solution was then added 827 mg (4.7 mmol) of amino alcohol **176** and 756 mg (5.9 mmol) of triethylamine as a mixture in 8 mL of dichloromethane. The resulting mixture stirred at 0°C for one hour then at room temperature for an additional three h. Water (10 mL) was then added, the layers separated and the water layer backwashed with 10 mL of dichloromethane. The dichloromethane layers were then combined, dried over Na_2SO_4 and concentrated to dryness in vacuo affording crude **177** which was then purified by flash chromatography (silica; 3:1 ethylacetate/hexanes) producing 630 mg of pure **177**. 40% Yield.

^{1}HNMR (300 MHz) ($CDCl_3$) δ TMS: 1.47 (6 H, s), 2.68 (2 H, t, *J* = 8.0 Hz), 3.60 (3 H, s), 3.65-3.75 (2 H, m), 3.82 (2 H, s), 3.82 (3 H, s), 4.57 (1 H, t, *J* = 10.6 Hz), 5.09 (1 H, t, *J* = 8.2 Hz), 5.42 (1 H, t, *J* = 9.5 Hz), 6.16 (1 H, br. s), 6.78 (1 H, d, *J* = 7.5 Hz), 6.83 (1 H, d, *J* = 8.2 Hz), 7.26 (1 H, t, *J* = 7.8 Hz). **^{13}CNMR** (300MHz) ($CDCl_3$) δ: 14.1 (s), 20.9 (q), 21.3 (q), 36.1 (t), 51.7 (q), 55.5 (q), 60.3 (t), 62.5 (s), 71.0 (t), 110.9 (d), 117.9 (s), 119.2 (d), 129.6 (d), 130.7 (s), 155.0 (s), 171.0 (s), 171.2 (s). **IR** (NaCl): 3506, 2950, 1753, 1643, 1476, 1412, 1265, 1094 cm^{-1}.

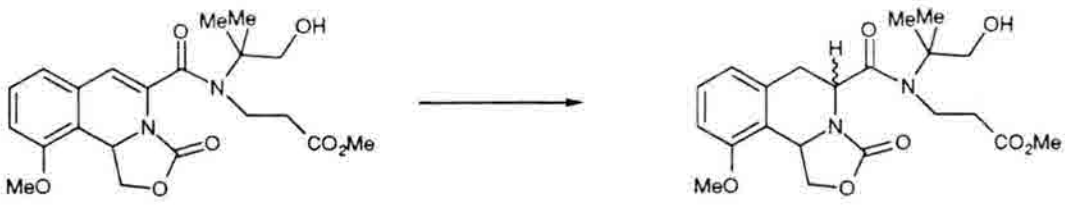

177 **178a, 178b**

***cis* and *trans*-1-Hydroxymethyl-(2,2'-carbonyl)-3-(N-2-carboxymethylethyl-N-2,2-dimethylethoxy)-carboxamide-8-methoxytetrahydroisoquinoline (178a and 178b).**

To **177** (540 mg/1.29 mmol) dissolved in 58 mL of ethanol was added 412 mg of 5% Pd on carbon and the solution saturated with H_2. The resulting mixture then stirred at room temperature in a hydrogenation bomb under 60 psi H_2 for 48 h. The reaction mixture was then filtered through Celite and concentrated to dryness in vacuo affording 490 mg of a 4:1 mixture (*cis / trans*) of diastereomers. The *cis* diastereomer (**178a**) was isolated by flash chromatography (silica; 7:1 dichloromethane/THF, R_f = 0.49) producing 360 mg of pure **178a**. 66% Yield.

^{1}H NMR (300 MHz) ($CDCl_3$) δ TMS: 1.40 (3 H, s), 1.44 (1 H, s), 2.51-2.62 (1 H, m), 2.74 (1 H, dd, *J* = 5.7 Hz, *J* = 4.9 Hz), 2.85 (1 H, dd, *J* = 3.4 Hz, *J* = 13.8 Hz), 3.08 (1 H, t, *J* = 11.2 Hz), 3.43 (1 H, dd, *J* = 11.5 Hz, *J* = 5.1 Hz), 3.63-3.73 (1 H, m), 3.68 (3 H, s), 3.83 (3 H, s), 3.96-4.12 (1 H, m), 4.19 (1 H, dd, *J* = 3.5 Hz, *J* = 7.6 Hz), 4.27 (1 H, dd, *J* = 5.9 Hz, *J* = 3.1 Hz), 4.70 (1 H, dd, *J* = 4.0 Hz, *J* = 7.7 Hz), 4.84 (1 H, t, *J* = 8.9 Hz), 5.23 (1 H, t, *J* = 7.7 Hz), 6.79 (2 H, t, *J* = 8.5 Hz), 7.24 (1 H, t, *J* = 7.9 Hz).

^{13}C NMR (300 MHz) ($CDCl_3$) δ: 23.4 (q), 25.3 (q), 30.3 (t), 36.7 (t), 40.7 (t), 51.9 (q), 54.0 (d), 54.8 (d), 55.3 (q), 62.5 (s), 67.0 (t), 69.6 (t), 108.3 (d), 121.7 (d), 122.5 (s), 128.7 (d), 135.2 (s), 155.7 (s), 157.3 (s), 167.3 (s), 171.6 (s).

IR (NaCl): 3488, 2952, 1740, 1655, 1587, 1474, 1412, 1259, 1070 cm^{-1}.

Anal. calcd for $C_{21}H_{28}N_2O_7$: C, 59.99; H, 6.71; N, 6.66. Found: C, 59.70; H, 6.80; N, 6.65.

Figure 51. ^1H NMR spectrum (300 MHz) ($CDCl_3$) of *cis*-hydroxyamide **178a**

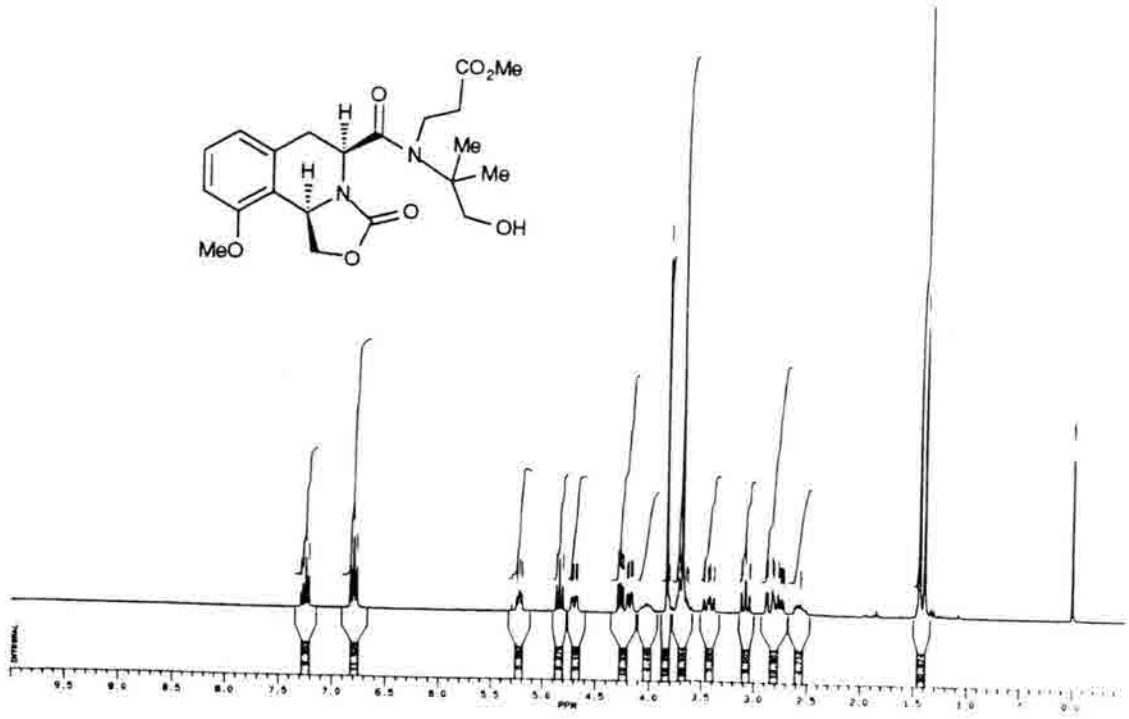

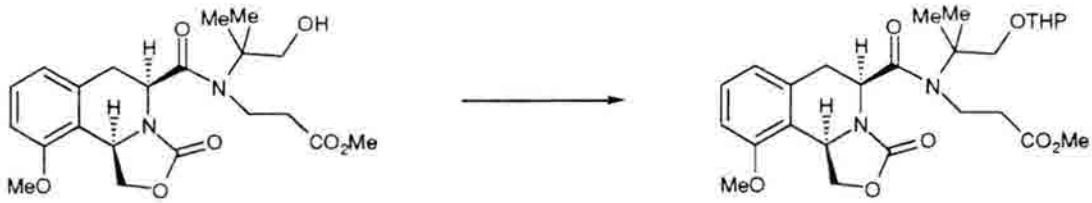

178a **179**

***cis*-1-Hydroxymethyl-(2,2'-carbonyl)-3-(N-2-carboxymethylethyl-N-2,2-dimethylethoxy-O-2-tetrahydropyran-2-yl)-carboxamide-8-methoxytetrahydroisoquinoline (179).**

To a stirred solution of **178a** (45 mg/0.107 mmol) in 2 mL of dichloromethane containing 1 mg (0.005 mmol) of *p*-toluenesulfonic acid and cooled to 20°C was added 45 mg (0.532 mmol) of dihydropyran and the resulting solution stirred at 20°C for 1.5 h. Ether (10 mL) was added and the reaction mixture washed with 5 mL of sat. $NaHCO_3$, 5 mL sat. brine, 5 mL water, the organic layer (top) dried over Na_2SO_4, decanted and concentrated to dryness in vacuo affording 55 mg of crude **179** which was purified by PTLC (silica; 3:1 ethylacetate/hexanes; R_f = 0.45) producing 29 mg of pure **179**. 56% Isolated yield.

^{1}H NMR (300 MHz) ($CDCl_3$) δ TMS: 1.38 (1.5 H, s), 1.43 (1.5 H, s), 1.48 (3 H, s), 1.51-1.66 (4 H, m), 1.68-1.83 (2 H, m), 2.88-2.97 (3 H, m), 3.31 (1 H, q, *J* = 8.0 Hz), 3.46-3.51 (1 H, m), 3.68 (1.5 H, s), 3.69 (1.5 H, s), 3.66-3.84 (2 H, m), 3.81 (3 H, s), 4.36 (2 H, q, *J* = 7.5 Hz), 4.55 (1 H, dd, *J* = 2.0 Hz, *J* = 9.4 Hz), 4.83 (1 H, ddd, *J* = 1.9 Hz, *J* = 6.7 Hz, *J* = 1.9 Hz), 5.12 (1 H, q, *J* = 7.5 Hz), 6.75-6.80 (2 H, m), 7.21 (1 H, t, *J* = 7.9 Hz). **^{13}C NMR** (300 MHz) ($CDCl_3$) δ: 19.8, 23.8, 24.7, 25.4, 30.5, 31.0, 36.4, 40.5, 51.7, 53.4, 54.1, 55.2, 60.7, 62.1, 62.4, 69.7, 72.4, 89.9, 99.6, 108.6, 121.4, 122.9, 128.5, 155.5, 155.6, 172.3. **IR** (NaCl): 2945, 1760, 1661, 1587, 1475, 1439, 1408, 1378, 1260, 1201, 1174, 1066, 1034, 903, 766, 731 cm^{-1}.

178a **180**

***cis*-1-Hydroxymethyl-(2,2'-carbonyl)-3-(N-2-carboxymethylethyl-N-2,2-dimethylethoxy-O-acetyl)-carboxamide-8-methoxytetrahydroisoquinoline (180).**

To a stirred solution of **178a** (67 mg/0.159 mmol) dissolved in 5 mL of dichloromethane and cooled to 0°C was added 31 mg (0.239 mmol) of N,N-diisopropylethylamine followed by 19 mg (0.239 mmol) of acetyl chloride. The resulting mixture was then allowed to warm to room temperature and stir for 2 h. The reaction mixture was then diluted with dichloromethane (20 mL), washed with water, dried over $MgSO_4$, filtered through Celite and concentrated to dryness in vacuo. The crude was then purified by radial PTLC (silica; 3:1 ethylacetate/hexanes affording 25 mg of product **180**. 34% Yield.

^{1}H NMR (300MHz) ($CDCl_3$) δ TMS: 1.40 (3 H, s), 1.50 (3 H, s), 2.07 (3 H, s), 2.56-2.72 (1 H, m), 2.83-2.91 (1 H, m), 2.93 (1 H, dd, *J* = 4.1 Hz, *J* = 12.2 Hz), 3.33 (1 H, dd, *J* = 8.8 Hz, *J* = 4.2 Hz), 3.70 (3 H, s), 3.82 (3 H, s), 4.30 (1 H, 1/2 ABq, *J* = 11.0 Hz), 4.34 (1 H, dd, *J* = 7.0 Hz, *J* = 1.7 Hz), 4.53 (1 H, 1/2 ABq, *J* = 11.0 Hz), 4.82 (1 H, t, *J* = 8.5 Hz), 5.13 (1 H, t, *J* = 7.7 Hz), 6.76 (1 H, d, *J* = 5.0 Hz), 6.79 (1 H, d, *J* = 4.3 Hz), 7.21 (1 H, t, *J* = 7.9 Hz).

178a **183**

***cis*-1-Hydroxymethyl-(2,2'-carbonyl)-3-(2-N-2-carboxymethylethyl-3,3-dimethyloxazolidin-2-yl)-carboxamide-8-methoxytetrahydroisoquinoline (183).**

To a stirred solution of **178a** (7 mg/0.015 mmol) in dichloromethane (1 mL) and cooled to 0°C was added 11 mg (0.076 mmol) of trimethyloxonium tetrafluoroborate, the resulting mixture warmed to room temp. and stirred for 2 h. The reaction mixture was then cooled to 0°C and an ice-bath cooled slurry of 5.7 mg (0.150 mmol) of sodium borohydride in 1 mL of ethanol was added. The resulting mixture then stirred at 0°C for 30 min. then at room temperature for an additional 2 h. The reaction was then quenched with 1 N HCl (aq) and the reaction mixture concentrated under reduced pressure. Dichloromethane (20 mL) were added, the mixture washed with $NaHCO_3$ (sat.), dried over Na_2SO_4, decanted and concentrated to dryness in vacuo. The reaction mixture was separated by PTLC (silica; 3:1 ethylacetate/hexanes) affording 4 mg of undesired product **183**.

^{1}H NMR (300MHz) ($CDCl_3$) δ TMS: 1.08 (3 H, s), 1.15 (3 H, s), 2.53 (2 H, t, J = 7.1 Hz), 2.76-2.93 (2 H, m), 3.05-3.23 (2 H, m), 3.17 (1 H, 1/1 ABq, J = 5.8 Hz), 3.22 (1 H, 1/2 ABq, J = 5.8 Hz), 3.66 (3 H, s), 3.65-3.73 (1 H, m), 3.79 (3 H, s), 4.33 (1H, t, J = 9.2 Hz), 4.84 (1 H, t, J = 7.5 Hz), 4.96 (1 H, t, J = 9.4 Hz), 5.07 (1 H, d, J = 2.4 Hz), 6.74 (1 H, d, J = 8.2 Hz), 6.81 (1 H, d, J = 7.6 Hz), 7.20 (1 H, t, J = 7.8 Hz).

IR (NaCl): 2965, 1747, 1687, 1474, 1384, 1263, 1201, 1070, 766 cm^{-1}.

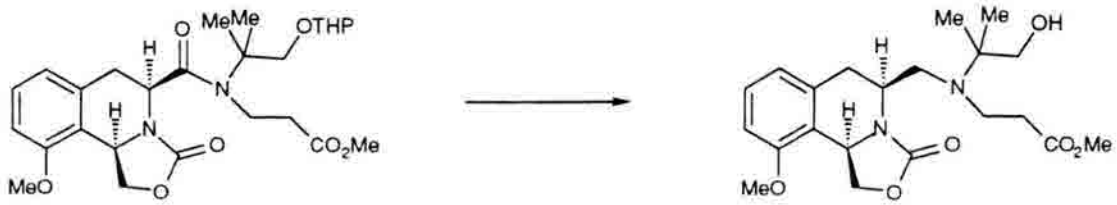

179 **170**

***cis*-1-Hydroxymethyl-(2,2'-carbonyl)-3-(N-2-carboxymethylethyl-N-2,2-dimethylethoxy)-aminomethyl-8-methoxytetrahydroisoquinoline (170).**

To a stirred solution of **179** (30 mg/0.059 mmol) dissolved in 2.5 mL of dichloromethane and cooled to 0°C was added 44 mg (0.297 mmol) of Me_3OBF_4 and the resulting solution immediately warmed to room temperature where it stirred for 2.5 h. The reaction mixture was then cooled to 0°C and to it added 2.5 mL of ice-bath cooled ethanol containing 9 mg (0.236 mmol) of sodium borohydride. The resulting mixture stirred at 0°C for 30 min. followed by stirring at room temperature for an additional two h. Water (5 mL) was then added and the mixture extracted 2 x 10mL with dichloromethane, the dichloromethane layers combined, dried over Na_2SO_4 and concentrated to dryness in vacuo affording 24 mg of crude **170** which was purified by PTLC (silica; 3:1 ethylacetate/hexanes; $R_f = 0.07$) producing 8 mg of pure **170**. 35% Yield.

^{1}H NMR (300MHz) ($CDCl_3$) δ TMS: 1.08 (6 H, s), 2.48 (2 H, t, *J* = 6.8 Hz), 2.79 (2 H, t, *J* = 6.8 Hz), 3.08 (1 H, dd, *J* = 4.9 Hz, *J* = 11.3 Hz), 3.35 (1 H, dd, *J* = 8.1 Hz, *J* = 8.0 Hz), 3.66-3.73 (1 H, m), 3.68 (3 H, s), 3.80-3.84 (1 H, m), 3.83 (3 H, s), 4.03 (2 H, d, *J* = 4.7 Hz), 4.34 (1 H, dd, *J* = 4.9 Hz, *J* = 3.0 Hz), 4.43 (1 H, dd, *J* = 7.1 Hz, *J* = 1.8 Hz), 4.88 (1 H, t, *J* = 8.2 Hz), 5.08 1 H, t, *J* = 7.7 Hz), 6.81 (2 H, t, *J* = 7.4 Hz), 7.23 (1 H, t, *J* = 8.0 Hz).

IR (NaCl): 3344, 2949, 1740, 1587, 1474, 1438, 1396, 1262, 1171, 1087, 1028 cm^{-1}.

168 **185**

3-Formyl-1-hydroxymethyl (2,2'-carbonyl)-8-methoxydihydroisoquinoline (185).

Carboxylic acid **168** (326 mg, 1.17 mmol) was refluxed in toluene (7 mL) with thionyl chloride (418 mg, 3.51 mmol) for 3 h and concentrated in vacuum. The residue was slurried in 4 mL of dry THF, under a nitrogen atmosphere, and to this mixture was added 2 mg (0.08 mmol) of palladium *tetrakis*-triphenylphosphine. Tributyltin hydride (224 mg/0.77 mmol) was then added over a period of 10 min. The resulting mixture stirred for 30 min. at which time the reaction mixture was concentrated under reduced pressure. The residue was triturated 3 x with 10 mL of hexanes, dissolved in ethyl acetate, passed through a plug of silica and concentrated to dryness in vacuo. This material was again triturated 2 x with 10 mL of hexanes affording 171 mg of a yellow amorphous solid. 60% Yield.

^{1}H NMR (300 MHz) ($CDCl_3$) δ TMS: 3.84 (3 H, s), 4.65 (1 H, t, J = 9.0 Hz), 5.15 (1 H, dd, J = 9.0 Hz, J = 8.4 Hz), 5.39 (1 H, t, J = 9.0 Hz), 6.94 (1 H, s), 6.97 (1 H, s), 7.00 (1 H, s), 7.31-7.36 (1 H, m), 10.02 (1 H, s).

^{13}C NMR (300 MHz) ($CDCl_3$) δ: 53.40, 55.60, 71.52, 112.96, 121.33, 121.44, 121.87, 129.81, 133.04, 155.12, 156.03, 185.72.

IR (NaCl, dichloromethane): 2928, 1752, 1695, 1610, 1475, 1260, 1094 cm^{-1}.

168 **186**

1-Hydroxymethyl-(2,2'-carbonyl)-3-hydroxymethyl-8-methoxydihydroisoquinoline (185).

To a stirred solution of **168** (2.6 g/9.35 mmol) in 52 mL of dry toluene was added 3.3 g (28 mmol) of thionyl chloride and the resulting mixture heated at reflux with stirring for 3 h. The reaction mixture was then cooled to room temperature and concentrated under reduced pressure. Dichloromethane (106 mL) was added, the mixture cooled to -78°C and to this mixture was added, over a 5 min period, an ice-bath cooled slurry of 2.8 g (74 mmol) of sodium borohydride in 80 mL of ethanol. The resulting mixture was then warmed to room temperature and stirred for 2 h. After quenching the reaction with 1 N HCl (aq), the reaction mixture was concentrated under reduced pressure. The residue was redissolved in dichloromethane (150 mL), washed with water, dried over Na_2SO_4 and concentrated to dryness in vacuo. The residue was then purified by flash chromatography (silica; 3:1 ethylacetate/hexanes) affording 860 mg of allylic alcohol **186**. 42% Yield.

^{1}H NMR (300MHz) ($CDCl_3$) δ TMS: 3.81 (3 H, s), 4.39 (1 H, dd, J = 6.6 Hz, J = 7.0 Hz), 4.50-4.61 (1 H, m), 4.54 (1 H, dd, J = 9.2 Hz, J = 2.3 Hz), 5.06 (1 H, dd, J = 7.9 Hz, J = 1.3 Hz), 5.28 (1 H, dd, J = 7.9 Hz, J = 3.6 Hz), 5.93 (1 H, s), 6.73 (1 H, d, J = 7.1 Hz), 6.78 (1 H, d, J = 8.3 Hz), 7.23 (1 H, t, J = 7.6 Hz).

^{13}C NMR (300MHz) ($CDCl_3$) δ: 54.8 (d), 55.4 (q), 61.6 (t), 70.6 (t), 110.0 (d), 111.7 (d), 117.5 (s), 118.4 (d), 129.1 (s), 129.5 (d), 132.0 (s), 136.0 (s), 154.9 (s).

IR (NaCl): 3450, 2938, 2841, 1756, 1645, 1602, 1576, 1477, 1446, 1401, 1284, 1263, 1220, 1094, 1019, 942, 834, 791, 748 cm^{-1}. **Anal.** calcd for $C_{13}H_{13}NO_4$: C, 63.15; H, 5.30; N, 5.67. Found: C, 63.40; H, 5.24; N, 5.60.

Figure 52. ^1H NMR spectrum (300 MHz) ($CDCl_3$) of aldehyde **185**

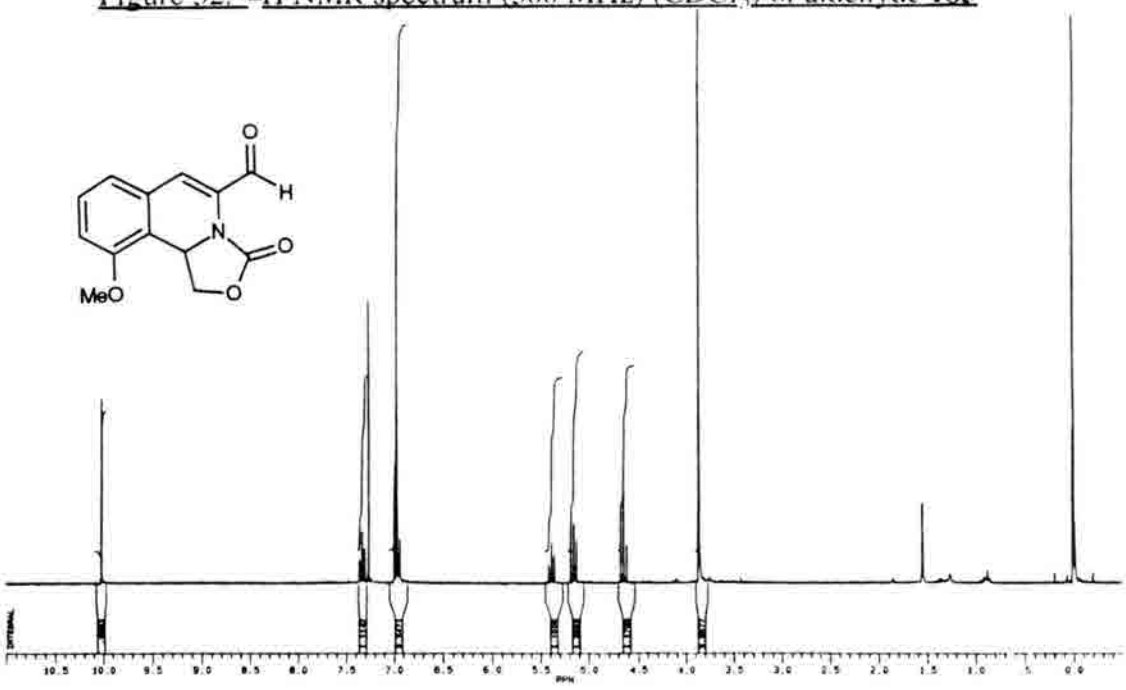

Figure 53. ^1H NMR spectrum (300 MHz) ($CDCl_3$) of allylic alcohol **186**

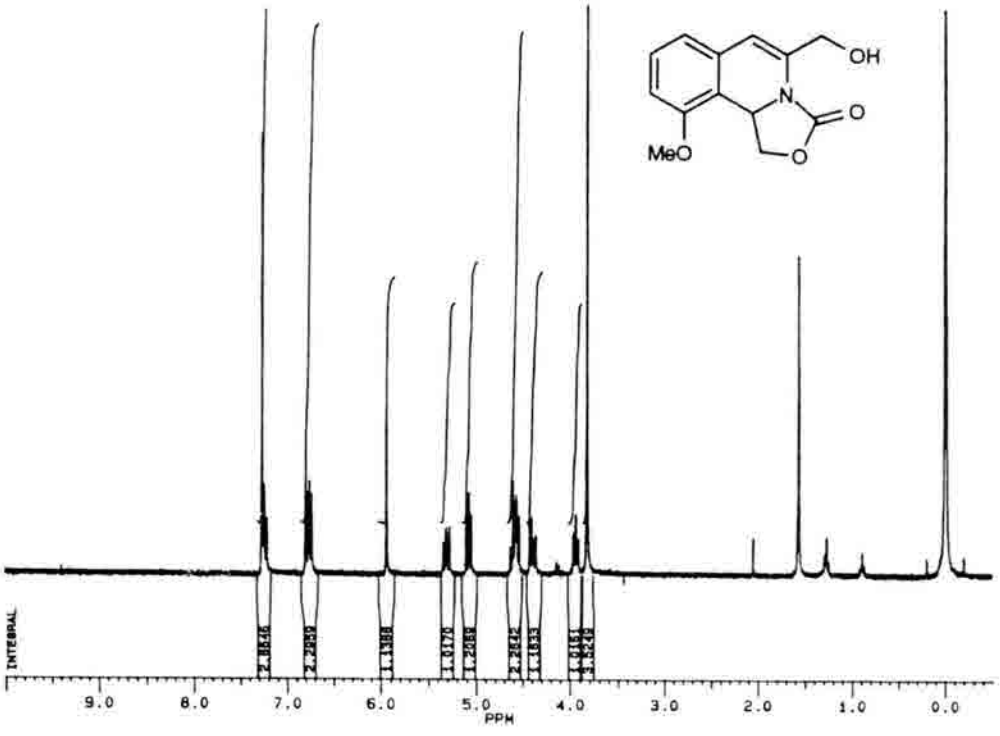

186 **185**

3-Formyl-1-hydroxymethyl-(2,2'-carbonyl)-8-methoxydihydroisoquinoline (185).

To a stirred solution of of DMSO (87 mg/1.11 mmol.) in 4.5 mL of dry dichloromethane, cooled to -78°C, was added 70 mg (0.55 mmol) of oxalyl chloride and the resulting solution stirred at -78°C for 15 min. Allylic alcohol **186** (64 mg/0.277 mmol) dissolved in 1 mL of dichloromethane was then introduced via canula and the resulting mixture stirred at -78°C for 1.5 h. At this time, 358 mg (2.77 mmol) of triethylamine were added and stirring continued at -78°C for an additional 30 min. The reaction mixture was then warmed to room temperature and concentrated under reduced pressure. The residue was redissolved in dichloromethane (20 mL), washed with 5 mL of water, dried over Na_2SO_4 and concentrated to dryness in vacuo affording 67 mg of aldehyde **185**. 98% Yield. Physical data reported above.

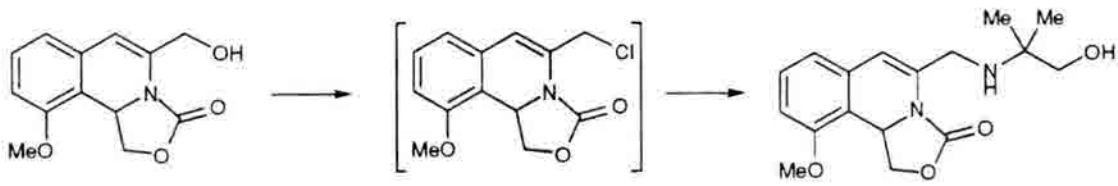

186 **188** **184**

1-Hydroxymethyl-(2,2'-carbonyl)-3-(*N*-2,2-dimethylethoxy)-aminomethyl-8-methoxydihydroisoquinoline (184).

To a stirred solution of **186** (0.5 g/2.02 mmol) in 18 mL of dichloromethane and cooled to 0°C was added 695 mg (6.07 mmol) of methanesulfonyl chloride followed by 1 g (10.1 mmol) of triethylamine and the resulting mixture stirred at 0°C for 30min. At this point, 1.8 g (20.2 mmol) of 2-amino-2-methyl-1-propanol (Aldrich) were added to the allylic clhoride **188** (generated *in situ*) and the reaction mixture warmed to room temperature and stirred for 16 h. The reaction mixture was then diluted with 100 mL of dichloromethane, washed with $NaHCO_3$ (sat.), dried over Na_2SO_4 and concentrated to dryness in vacuo. The crude product was purified by flash chromatography (silica; 10:1 dichloromethane/methanol) affording 296 mg of pure **184**. 46% Yield on the two steps.

188. **^{1}H NMR** (300MHz) ($CDCl_3$) δ TMS: 3.82 (3 H, s), 4.30 (1 H, 1/2 ABq, J = 8.6 Hz), 4.51 (1 H, dd, J = 7.6 Hz, J = 1.8 Hz), 5.03 (1 H, t, J = 6.8 Hz), 5.26 (1 H, 1/2 ABq, J = 8.6 Hz), 5.31 (1 H, dd, J = 6.4 Hz, J = 2.3 Hz), 6.12 (1 H, s), 6.74 (1 H, d, J = 7.2 Hz), 6.79 (1 H, d, J = 7.0 Hz), 7.25 (1 H, t, J = 6.7 Hz).

184. **^{1}H NMR** (300MHz) ($CDCl_3$) δ TMS: 1.14 (3 H, s), 1.16 (3 H, s), 3.34 (1 H, 1/2 ABq, J = 11.2 Hz), 3.46 (1 H, 1/2 ABq, J = 11.2 Hz), 3.49 (1 H, 1/2 ABq, J = 13.3 Hz), 3.81 (3 H, s), 4.00 (1 H, 1/2 ABq, J = 13.3 Hz), 4.52 (1 H, dd, J = 9.2 Hz, J = 2.0 Hz), 5.03 (1 H, dd, J = 8.2 Hz, J = 1.0 Hz), 5.30 (1 H, dd, J = 8.3 Hz, J = 2.9 Hz), 6.00 (1 H, s), 6.72 (1 H, d, J = 7.6 Hz), 6.76 (1 H, d, J = 8.4 Hz), 7.22 (1 H, t, J = 7.7 Hz).

^{13}C NMR (300Mz) ($CDCl_3$) δ: 22.39 (q), 22.86 (q), 34.82 (s), 42.29 (t), 54.64 (d), 55.28 (q), 66.87 (t), 69.96 (t), 110.15 (d), 118.21 (s), 118.27 (d), 118.34 (d), 129.19 (d), 131.58 (s), 132.67 (s), 154.76 (s), 155.06 (s).

IR (NaCl): 3469, 3327, 2966, 1754, 1645, 1602, 1576, 1477, 1400, 1282, 1097, 748 cm^{-1}.

Anal. calcd for $C_{17}H_{22}N_2O_4$: C, 64.13; H, 6.97; N, 8.80. Found: C, 64.12; H, 6.80; N, 8.76.

Figure 54. ^{1}H NMR spectrum (300 MHz) ($CDCl_3$) of allylic amine **184**

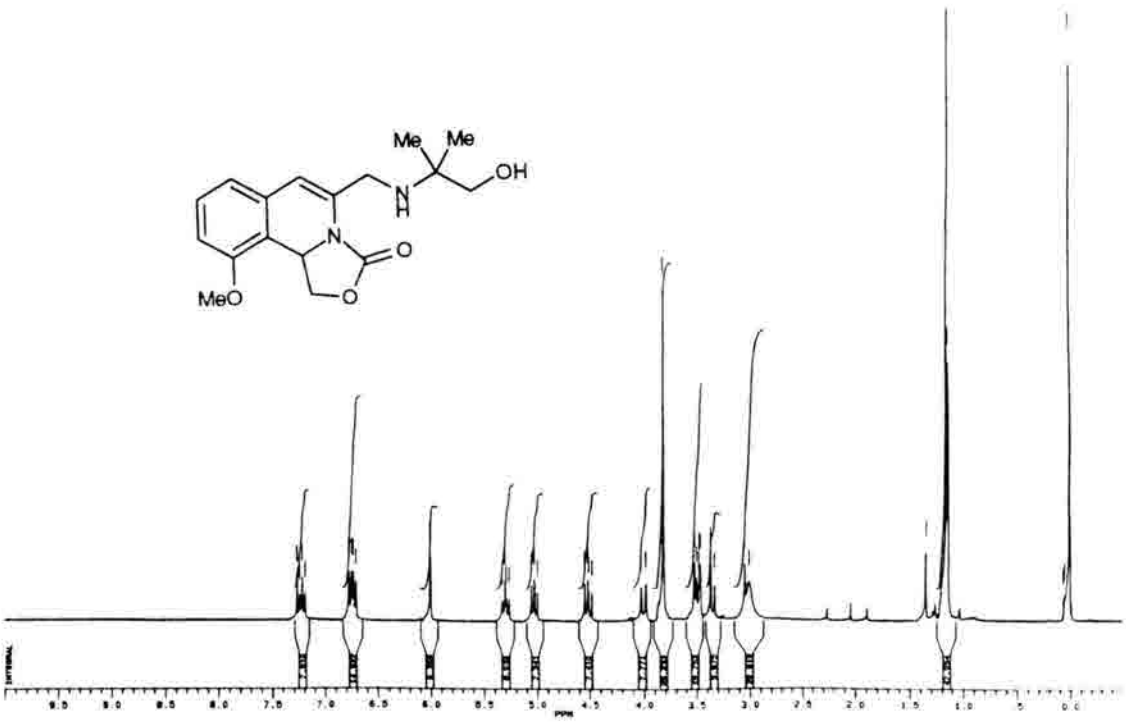

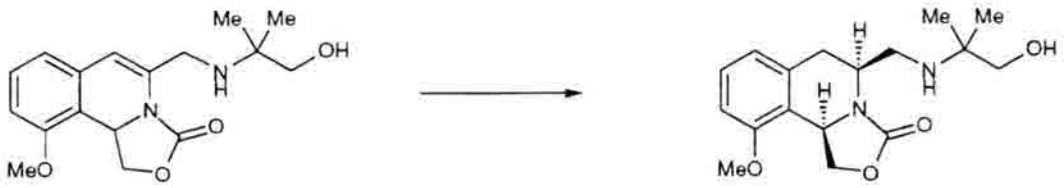

184 **174a**

***cis*-1-Hydroxymethyl-(2,2'-carbonyl)-3-(*N*-2,2-dimethylethoxy)-aminomethyl-8-methoxytetrahydroisoquinoline (174a).**

To a stirred solution of **184** (250 mg/0.785 mmol) dissolved in 18 mL of ethanol and purged with nitrogen was added 139 mg (0.785 mmol) of palladium chloride (Aldrich). The reaction mixture was then saturated with hydrogen and stirred at 25°C under 1 atmosphere of hydrogen for 18 h. The reaction mixture was then purged with nitrogen, filtered through Celite and concentrated under reduced pressure. The residue was redissolved in 100 mL of dichloromethane, washed with $NaHCO_3$ (sat.), dried over Na_2SO_4 and concentrated to dryness in vacuo affording 246 mg of **174a**. 98% Yield.

^{1}H NMR (300MHz) ($CDCl_3$) δ TMS: 1.07 (3 H, s), 1.13 (3 H, s), 2.68-2.76 (2 H, m), 3.00 (1 H, dd, J = 10.7 Hz, J = 2.2 Hz), 3.24 (1 H, 1/2 ABq, J = 11.2 Hz), 3.52 (1 H, 1/2 ABq, J = 11.2 Hz), 3.48-3.56 (1 H, m), 3.82 (3 H, s), 4.18 (1 H, dd, J = 6.7 Hz, J = 2.2 Hz), 4.82 (1 H, t, J = 8.9 Hz), 5.04 (1 H, t, J = 8.0 Hz), 6.76 (2 H, d, J = 8.0 Hz), 7.22 (1 H, t, J = 7.9 Hz).

^{13}C NMR (300MHz) ($CDCl_3$) δ: 23.56, 25.09, 32.53, 42.70, 53.74, 54.85, 55.30, 55.67, 67.10, 69.10, 108.32, 121.51, 123.40, 128.57, 135.57, 155.84, 157.04.

IR (NaCl): 3246, 2973, 1742, 1586, 1477, 1407, 1260, 1099, 1072 cm^{-1}.

Anal. calcd for, $C_{17}H_{24}N_2O_4$: C, 63.73; H, 7.55; N, 8.74. Found: C, 63.55; H, 7.24; N, 8.47.

Figure 55. ^{1}H NMR spectrum (300 MHz) ($CDCl_3$) of *cis*-amino alcohol **174a**

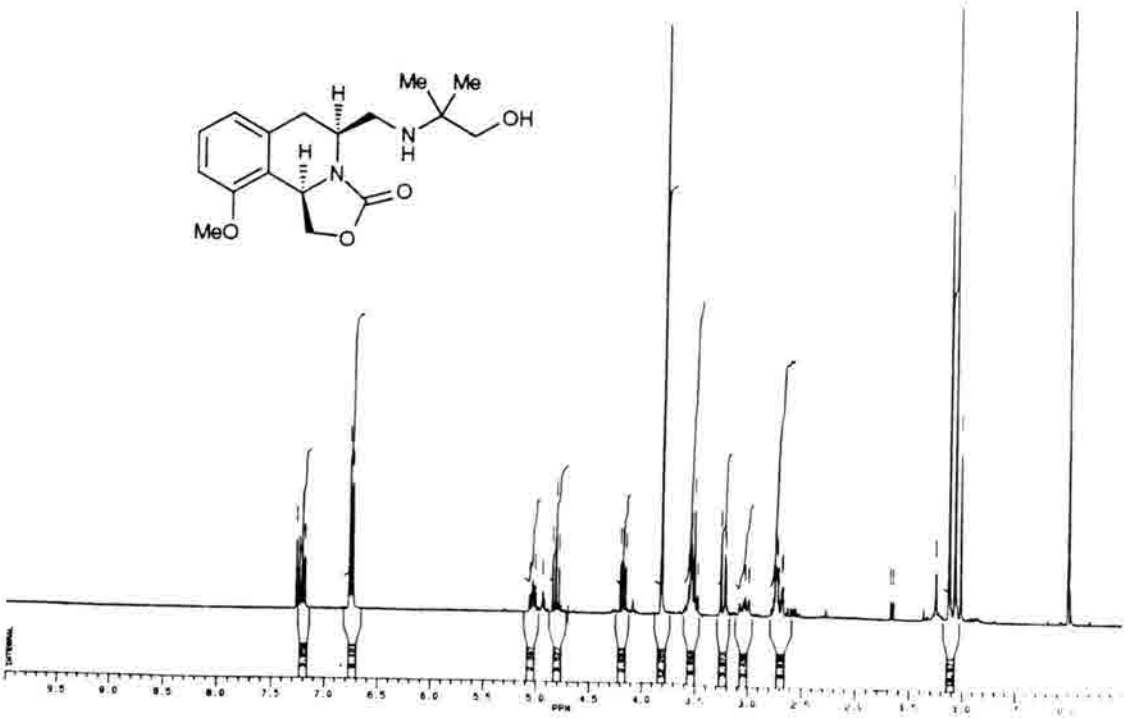

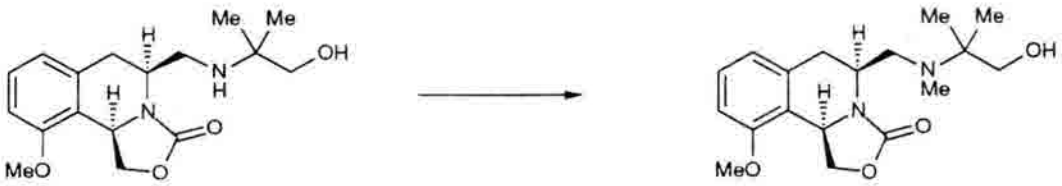

174a **43a**

***cis*-1-Hydroxymethyl-(2,2'-carbonyl)-3-(*N*-methyl-*N*-2,2-dimethylethoxy)-aminomethyl-8-methoxytetrahydroisoquinoline (43a).**

To a stirred solution of **174a** (4 mg/0.012 mmol) in 0.5 mL of dichloromethane and cooled to 0°C was added 2.2 mg (0.015 mmol) of trimethyloxonium tetrafluoroborate, the resulting mixture warmed to room temperature and stirred for 5 h. The reaction mixture was then concentrated under reduced pressure, redissolved in dichloromethane (10 mL), washed with water, dried over Na_2SO_4, decanted and concentrated to dryness in vacuo. The residue was then purified by PTLC (silica; 10:1 dichloromethane/methanol) affording 2 mg of **43a**. 49% Yield. Physical data reported above.

174a **190**

***cis*-1-Hydroxymethyl-(2,2'-carbonyl)-3-(*N*-propene-3-yl-*N*-2,2-dimethylethoxy)-aminomethyl-8-methoxytetrahydroisoquinoline (190).**

To a stirred solution of **174a** (19 mg/0.059 mmol) in 1.0 mL of dichloromethane and cooled to 0°C was added 12 mg (0.071 mmol) of allyl iodide, the resulting mixture warmed to room temperature and stirred for 24 h. The reaction mixture was then concentrated under reduced pressure, redissolved in dichloromethane (15 mL), washed with $NaHCO_3$ (sat.), dried over Na_2SO_4 and concentrated to dryness in vacuo. The residue was then purified by PTLC (silica; 10:1 dichloromethane/methanol) affording 6 mg of olefin **190** ($R_f = 0.76$). 30% Yield.

^{1}H NMR (300MHz) ($CDCl_3$) δ TMS: 1.08 (3 H, s), 1.10 (3 H, s), 2.80 (1 H, dd, J = 3.9 Hz, J = 12.0 Hz), 2.87 (1 H, dd, J = 7.9 Hz, J = 5.7 Hz), 3.05 (1 H, dd, J = 9.6 Hz, J = 6.4 Hz), 3.26-3.43 (5 H, m), 3.50-3.61 (1 H, m), 3.82 (3 H, s), 4.31 (1 H, dd, J = 6.1 Hz, J = 2.8 Hz), 4.73 (1 H, t, J = 8.9 Hz), 4.95 (1 H, dd, J = 4.8 Hz, J = 2.1 Hz), 5.06 (1 H, d, J = 10.0 Hz), 5.19 (1 H, d, J = 15.8 Hz), 5.88-5.93 (1 H, m), 6.77 (1 H, d, J = 8.0 Hz), 6.82 (1 H, d, J = 7.4 Hz), 7.20-7.25 (1 H, m).

IR (NaCl): 3461, 2969, 2929, 1749, 1586, 1473, 1383, 1259, 1069, 919, 765 cm^{-1}.

174a **191**

***cis*-1-Hydroxymethyl-(2,2'-carbonyl)-3-(5,5-dimethyl-2-oxo-morphalino-4-yl)-aminomethyl-8-methoxytetrahydroisoquinoline (191).**

To a stirred solution of **174a** (12 mg/0.037 mmol) in 0.5 mL of DMF was added 63 mg (0.370 mmol) of ethyl bromoacetate followed by 31 mg (0.370 mmol) of sodium bicarbonate and the resulting mixture stirred at room temperature for 18 h. The reaction mixture was then dilluted with 10 mL of dichloromethane, the mixture washed with water, dried over Na_2SO_4, decanted and concentrated under reduced pressure. The residue was then purified by PTLC (silica; 10:1 dichloromethane/methanol) affording 8 mg of lactone **919**.

^{1}H NMR (300MHz) ($CDCl_3$) δ TMS: 1.12 (3 H, s), 1.15 (3 H, s), 2.82-3.06 (3 H, m), 3.11 (1 H, dd, *J* = 4.8 Hz, *J* = 8.4 Hz), 3.45 (1 H, 1/2 ABq, *J* = 18.6 Hz), 3.49-3.54 (1 H, m), 3.60 (1 H, 1/2 ABq, *J* = 18.6 Hz), 3.82 (3 H, s), 4.05 (2 H, d, *J* = 3.1 Hz), 4.31 (1 H, dd, *J* = 6.5 Hz, *J* = 2.4 Hz), 4.77 (1 H, t, *J* = 8.6 Hz), 4.98 (1 H, t, *J* = 7.2 Hz), 6.79 (1 H, d, *J* = 8.2 Hz), 6.80 (1 H, d, *J* = 7.7 Hz), 7.23 (1 H, t, *J* = 7.9 Hz).

174a **192**

***cis*-1-Hydroxymethyl-(2,2'-carbonyl)-3-(*N*-2,2-dimethyl-2-formyl)-aminomethyl-8-methoxytetrahydroisoquinoline (192).**

To a stirred solution of DMSO (153 mg/1.96 mmol.) in 13 mL of dichloromethane and cooled to -78°C was added 124 mg (0.980 mmol) of oxalyl chloride and the resulting solution stirred at -78°C for 15 min. Separately, 157 mg (0.490 mmol) of amino alcohol **174a** were dissolved in 30 mL of dry ether and through this solution bubbled dry HCl, precipitating the hydrochloride salt. This mixture was then concentrated to a dry solid in vacuo. This material was then redissolved in 3 mL of dichloromethane and introduced to the reaction vessel via cannula and the resulting mixture stirred at -78°C for 1.5 h. At this time, 496 mg (4.90 mmol) of triethylamine were added and stirring continued at -78°C for an additional 30 min. The reaction mixture was then warmed to 25°C and concentrated under reduced pressure. The residue was redissolved in dichloromethane (30 mL), washed with 10 mL of water, dried over Na_2SO_4 and concentrated to dryness in vacuo affording 151 mg of aldehyde **192**. 97% Yield.

^{1}H NMR (300MHz) ($CDCl_3$) δ TMS: 1.21 (3 H, s), 1.24 (3 H, s), 2.65-2.73 (2 H, m), 3.03 (1 H, dd, J = 11.0 Hz, J = 8.5 Hz), 3.41-3.59 (2 H, m), 3.82 (3 H, s), 4.14 (1 H, dd, J = 7.5 Hz, J = 1.4 Hz), 4.83 (1 H, t, J = 8.8 Hz), 5.04 (1 H, t, J = 7.8 Hz), 6.76 (2 H, d, J = 8.2 Hz), 7.21 (1 H, t, J = 8.0 Hz), 9.49 (1 H, s).

^{13}C NMR (300Mz) ($CDCl_3$) δ: 21.53, 32.20, 44.33, 54.64, 55.26, 55.36, 60.84, 65.39, 68.97, 108.24, 121.47, 123.20, 128.37, 128.43, 135.48, 155.76, 204.53.

IR (NaCl): 3316, 2974, 2923, 1747, 1586, 1473, 1258, 1071 cm^{-1}.

Figure 56. ^{1}H NMR spectrum (300 MHz) ($CDCl_3$) of *cis*-amido aldehyde **192**

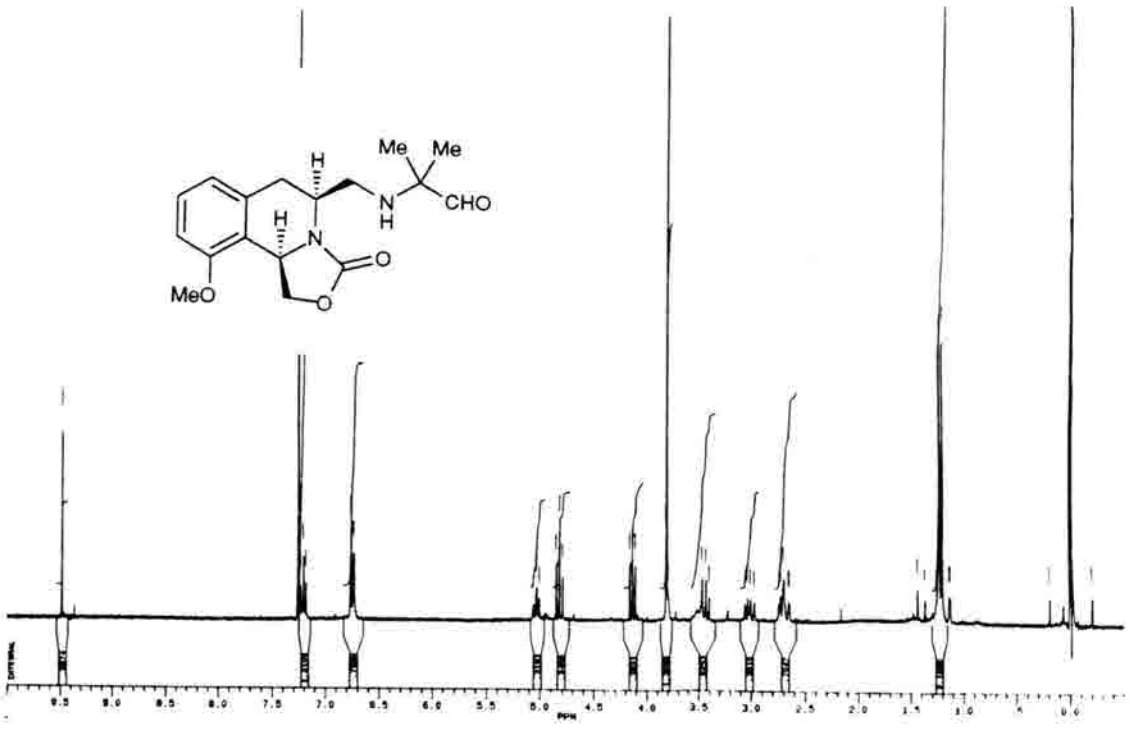

192 **193**

4α,6α,11aα-2-Aza-3,3-dimethyl-7-methoxy-5,4-oxazolo-1,3,4,6,11,11a-hexahydro-2*H*-benzo[*b*]quinolizine (193).

To a stirred solution of aldehyde **192** (150 mg/0.471 mmol) in 23 mL of ethanol was added 2.3 mL of 2M LiOH (aq) and the resulting mixture degassed by purging with nitrogen. The solution then was heated to reflux with stirring for 18 h. After cooling to room temperature, the reaction mixture was concentrated under reduced pressure. Water (15 mL) was added, the mixture extracted 3 x 25 mL with dichloromethane, the dichloromethane layers combined, dried over Na_2SO_4 and concentrated to dryness in vacuo. The components were separated by PLC (silica; 10:1 dichloromethane/methanol) affording 28 mg of tetracycle **193** (R_f = 0.38). 22% Yield.

^{1}H NMR (300MHz) ($CDCl_3$) δ TMS: 1.17 (6 H, s), 2.62-2.77 (3 H, m), 2.88 (1 H, t, *J* = 8.6 Hz), 3.01 (1 H, dd, *J* = 2.6 Hz, *J* = 9.9 Hz), 3.53-3.63 (2 H, m), 3.77 (3 H, s), 3.82 (1 H, s), 4.53 (1 H, t, *J* = 6.4 Hz), 6.68 (1 H, d, *J* = 8.2 Hz), 6.78 (1 H, d, *J* = 7.7 Hz), 7.15 (1 H, t, 8.0 Hz).

^{13}C NMR (300MHz) ($CDCl_3$) δ: 17.15 (q), 26.93 (q), 33.15 (t), 35.25 (s), 40.93 (q), 47.09 (t), 54.50 (d), 55.36 (d), 58.72 (d), 70.45 (t), 95.91 (d), 107.57 (d), 109.11 (s), 120.90 (s), 123.26 (d), 127.48 (s).

IR (NaCl): 3284, 2957, 2837, 1749, 1681, 1583, 1472, 1440, 1256, 1088, 1029, 951, 776, 743 cm^{-1}.

HRMS (FAB), calcd for $C_{16}H_{23}N_2O_2$ (MH^+): 275.1760. Found: 275.1762.

193 **194**

4α,6α,11aα-2-Aza-3,3-dimethyl-2-ethoxyacetyl-1,3,4,6,11,11a-hexahydro-7-methoxy-5,4-oxazolo-2-*H*-benzo[*b*]quinolizine (194).

To a stirred solution of **193** (25 mg/0.091 mmol) in 1.0 mL of DMF was added 46 mg (0.273 mmol) of ethylbromoacetate (Aldrich) followed by 38 mg (0.455 mmol) of sodium bicarbonate and the resulting mixture stirred at 25°C for 12 h. The reaction mixture was then diluted with 20 mL of dichloromethane, the mixture washed with water, dried over Na_2SO_4 and concentrated under reduced pressure. The residue was then purified by PTLC (silica; 10:1 dichloromethane/methanol) affording 26 mg of **194** (R_f = 0.83). 81% Yield.

^{1}H NMR (300MHz) ($CDCl_3$) δ TMS: 0.97 (3 H, s), 1.23 (3 H, s), 1.28 (3 H, t, *J* = 4.7 Hz), 2.43 (1 H, t, *J* = 11.0 Hz), 2.77-3.04 (5 H, m), 3.53-3.64 (3 H, m), 3.66 (1 H, s), 3.77 (3 H, s), 4.19 (2 H, q, *J* = 7.1 Hz), 4.54 (1 H, t, *J* = 5.9 Hz), 6.67 (1 H, d, *J* = 8.2 Hz), 6.77 (1 H, d, *J* = 7.7 Hz), 7.14 (1 H, t, *J* = 7.9 Hz).

IR (NaCl): 1753, 1581, 1470, 1260, 1087, 1018, 779 cm^{-1}.

Figure 57. ^{1}H NMR spectrum (300 MHz) ($CDCl_3$) of tetracycle **193**

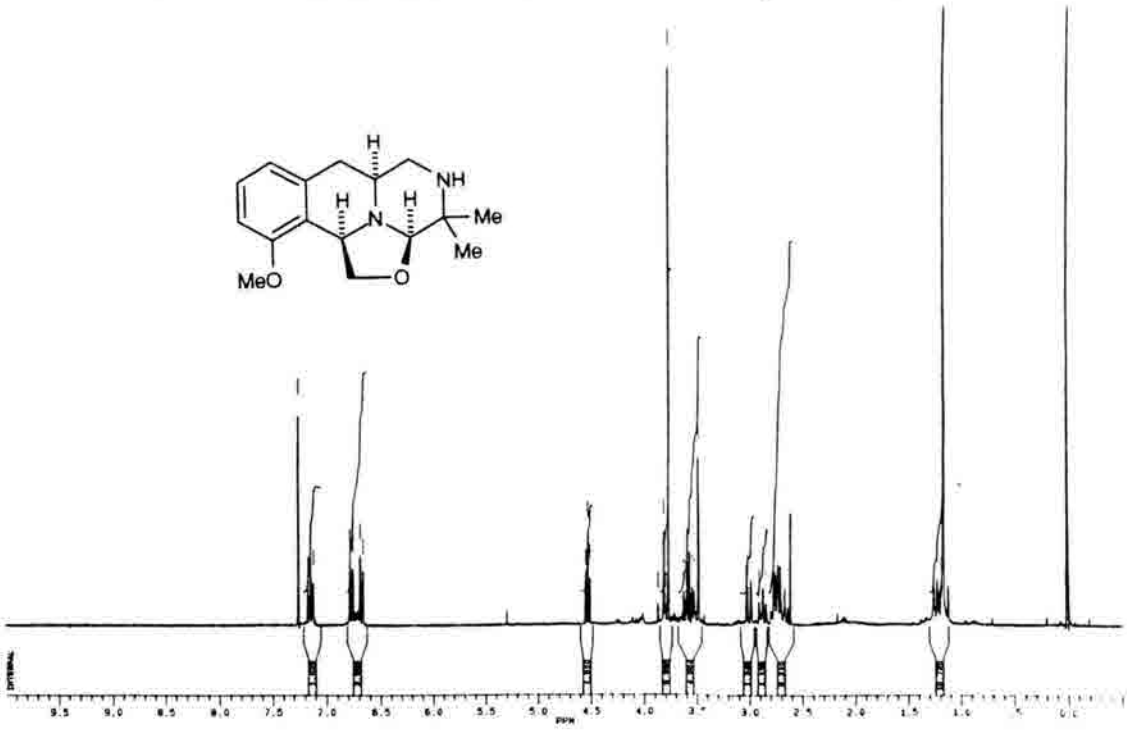

Figure 58. ^{1}H NMR spectrum (300 MHz) ($CDCl_3$) of tetracyclic ethyl ester **194**

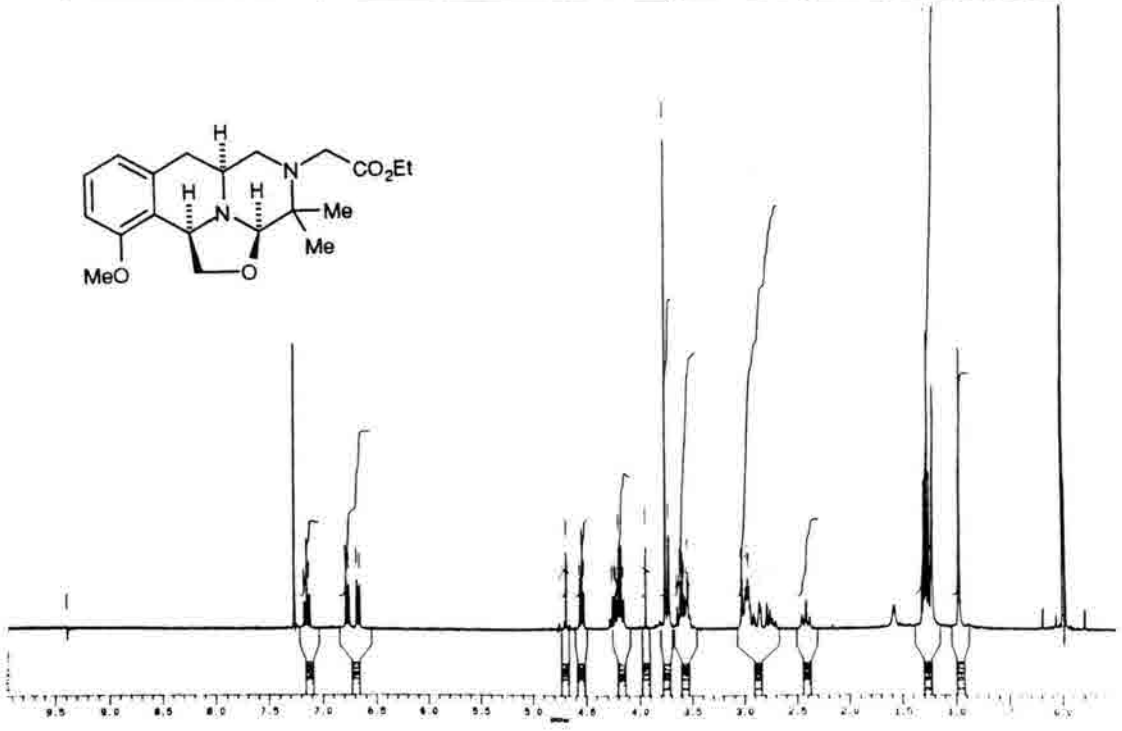

194 **160**

4α,6α,11aα-2-Aza-2-carboxyacetyl-1,3,4,6,11,11a-hexahydro-7-methoxy-5,4-oxazolo-3,3-dimethyl-2*H*-benzo[*b*]quinolizine (160).

To a stirred solution of **194** (15 mg/0.042 mmol) in 4 mL of ethanol was added 420 μL of 2M LiOH (aq), the resulting mixture degassed by purging with nitrogen and stirred at 25°C for 2 h. The reaction mixture was concentrated under reduced pressure and the components separated by PLC (silica; 10:1 dichloromethane/methanol) affording 11 mg of carboxymethyl tetracycle **160** ($R_f = 0.17$). 82% Yield.

^{1}H NMR (300MHz) ($CDCl_3$) δ TMS: 1.09 (3 H, s), 1.27 (2 H, s), 2.63-2.78 (2 H, m), 2.95 (3 H, br.d, *J* = 17.3 Hz), 3.60-3.68 (2 H, m), 3.77 (3 H, s), 4.57 (1 H, t, *J* = 5.5 Hz), 6.68 (1 H, d, *J* = 8.2 Hz), 6.76 (1 H, d, *J* = 7.8 Hz), 7.15 (1 H, t, *J* = 7.8 Hz). See Figure 6, Chapter 2.

^{13}C NMR (300MHz) ($CDCl_3$) δ: 12.48, 23.49, 32.50, 51.26, 51.66, 55.30, 58.31, 58.65, 67.97, 71.37, 94.92, 107.76, 121.21, 122.64, 127.82, 134.92, 156.02, 171.00.

IR (NaCl): 2975, 2836, 1719, 1637, 1582, 1471, 1376, 1259, 1090, 952, 899, 775, 736 cm^{-1}.

HRMS (FAB), calcd for $C_{18}H_{25}N_2O_4$ (MH^+): 333.1814. Found: 333.1816.

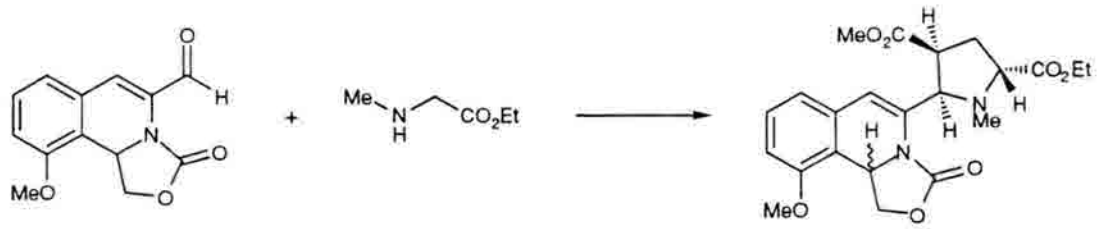

185 **202** **203a, 203b**

(1α)-1-Hydroxymethyl-(2,2'-carbonyl)-3-[(2α,4β,5α)-2-carboxyethyl-4-carboxymethyl-1-methylpyrolidin-5-yl]-8-methoxydihdroisoquinoline (203a) and (1β)-1-hydroxymethyl-(2,2'-carbonyl)-3-[(2α,4β,5α)-2-carboxyethyl-4-carboxymethyl-1-methylpyrolidin-5-yl]-8-methoxydihdroisoquinoline (203b).

To aldehyde **185** (35 mg/0.14 mmol) dissolved in 3.0 mL of THF was added 88 mg (0.56 mmol) of sarcosine ethyl ester hydrochloride, 71 mg (0.014 mmol) of triethylamine and 121 mg (1.4 mmol) of methyl acrylate. The resulting mixture was then refluxed for 10 h. At this time the reaction mixture was cooled to room temperature and concentrated under reduced pressure. The residue was redissolved in dichloromethane, washed with sat. NaHCO3 (aq), dried over Na2SO4 and concentrated to dryness in vacuo affording 62 mg of a light yellow oil. This material was then purified by PTLC (silica; 3:1 ethylacetate/hexane, $R_f = 0.85$) affording 35 mg of a diastereomeric mixture. 58% Yield. The two diastereomers were then separated by PTLC (silica; 12% acetonitrile in toluene, **203a**, $R_f = 0.40$, **203b**, $R_f = 0.30$).

203a. **^{1}H NMR** (300 MHz) ($CDCl_3$) δ TMS: 1.31 (3 H, t, J = 6.5 Hz), 2.09 (1 H, q, J = 7.7 Hz), 2.47 (3 H, s), 2.50 (1 H, m), 3.63 (3 H, s), 3.72 (1 H, q, J = 8.7 Hz), 3.80 (3 H, s), 3.97 (2 H, d, J = 7.6 Hz), 4.19-4.24 (2 H, m), 4.51 (1 H, t, J = 10.1 Hz), 4.94 (1

H, t, J = 8.0 Hz), 5.09 (1 H, t, J = 10.5 Hz), 5.38 (1 H, d, J = 9.5 Hz), 6.25 (1 H, s), 6.73-6.77 (2 H, m), 7.21 (1 H, t, J = 8.2 Hz).

IR (NaCl): 2943, 2856, 1760, 1730, 1638, 1600, 1572, 1474, 1371, 1278, 1197, 1164, 1088, 1028 cm^{-1}.

Mass spectrum, m/z (relative intensity) 430 (16.8, M^+), 415 (8.5), 383 (7.7), 357 (100), 355 (12.3), 297 (8.2), 271 (7.0), 250 (7.3), 206 (11.7), 149 (18.3), 127 (33.4), 121 (19.5), 84 (27.0), 57 (68.0), 41 (37.2).

203b. **^{1}H NMR** (300 MHz) ($CDCl_3$) δ TMS: 1.31 (3 H, t, J = 7.1 Hz), 2.10-2.13 (1 H, m), 2.38 (3 H, s), 2.58-2.68 (1 H, m), 3.34 (3 H, s), 3.81 (3 H, s), 3.86 (1 H, t, J = 6.8 Hz), 3.99 (1 H, dd, J = 2.0 Hz, J = 6.4 Hz), 4.16-4.24 (2 H, m), 4.46 (1 H, dd, J = 9.2 Hz, J = 2.2 Hz), 4.83 (1 H, d, J = 8.8 Hz), 5.00 (1 H, dd, J = 7.9 Hz, J = 1.2 Hz), 5.25 (1 H, dd, J = 7.7 Hz, J = 3.4 Hz), 6.10 (1 H, s), 6.73 (2 H, d, J = 8.0 Hz), 7.20 (1 H, t, J = 7.8 Hz).

IR (NaCl): 2921, 2856, 1763, 1725, 1638, 1600, 1572, 1474, 1371, 1278, 1169, 1093, 1028 cm^{-1}.

Mass spectrum, m/z (relative intensity) 430 (14.5, M^+), 415 (15.3), 383 (15.8), 357 (100), 355 (31.1), 339 (6.2), 297 (8.6), 265 (6.9), 127 (32.0), 82 (9.9), 44 (51.3).

Figure 59. ^{1}H NMR spectrum (300 MHz) ($CDCl_3$) of pyrolidine cycloadduct **203a**

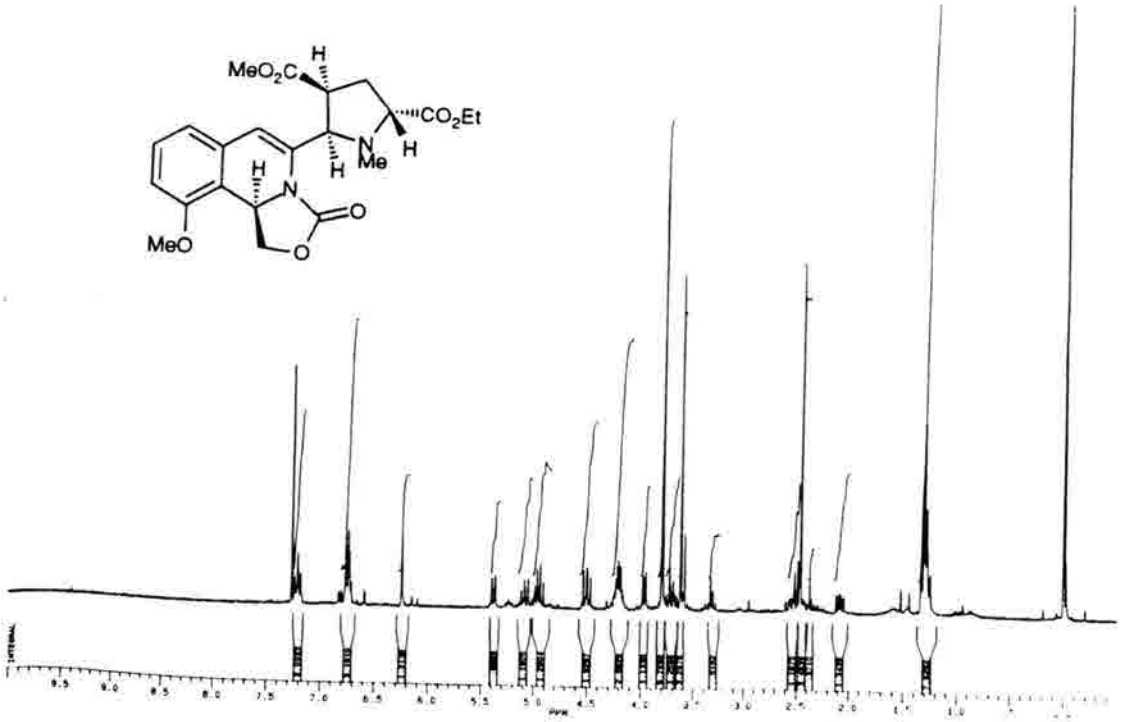

Figure 60. ^{1}H NMR spectrum (300 MHz) ($CDCl_3$) of pyrolidine cucloadduct **203b**

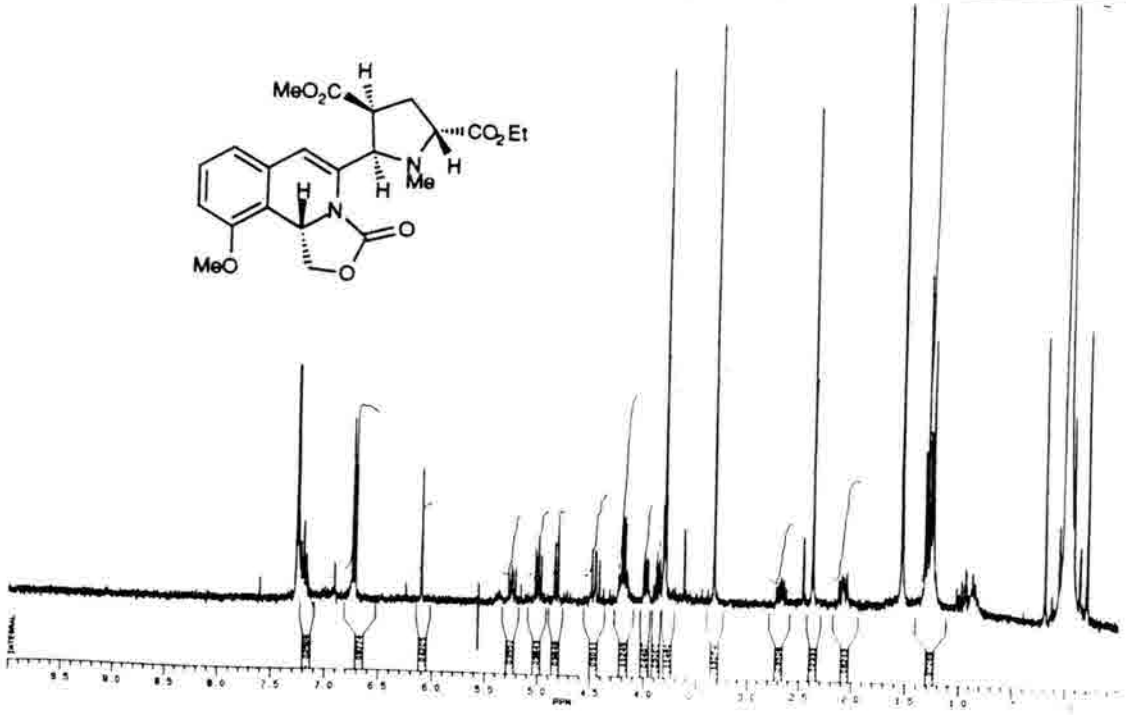

211 **204**

Benzyl *N*-methylaminoacetate (204).

To a suspention of sarcosine (**211**) (1.8 g, 20 mmol.) in 140 mL of benzyl alcohol and cooled to 0°C was added 24 g (200 mmol) of thionyl chloride over a 10 min period. The resulting mixture was then warmed to room temperature and then heated to 100°C for 5 h. The reaction mixture was cooled to 4°C and 70 mL of ether added. After 18 h the crystals formed were collected by filtration and washed with cold ether. The crystals were dissolved in 50 mL of dichloromethane washed with $NaHCO_3$ (sat.), dried over Na_2SO_4, decanted and concentrated to dryness in vacuo affording 1.3 g of benzyl ester **204**. 36% Yield.

^{1}H NMR (300MHz) ($CDCl_3$) δ TMS: 2.45 (3H, S), 3.42 (2H, s), 5.18 (2H, s), 7.35-7.37 (5H, m).

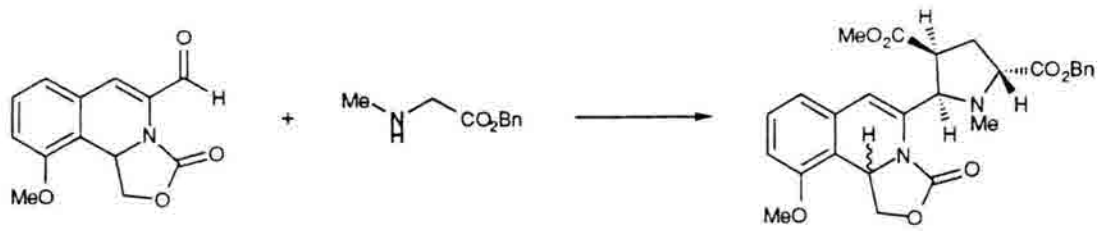

185 **204** **205a, 205b**

(1α)-1-Hydroxymethyl-(2,2'-carbonyl)-3-[(2α,4β,5α)-2-carboxybenzyl-4-carboxymethyl-1-methylpyrolidin-5-yl]-8-methoxydihdroisoquinoline (205a) and (1β)-1-hydroxymethyl-(2,2'-carbonyl)-3-[(2α,4β,5α)-2-carboxybenzyl-4-carboxymethyl-1-methylpyrolidin-5-yl]-8-methoxydihdroisoquinoline (205b).

To a stirred solution of aldehyde **185** (209 mg/0.852 mmol) and 367 mg (4.26 mmol) of methyl acrylate dissolved in 5 mL of THF was added 305 mg (1.70 mmol) of sarcosine benzylester (**204**) followed by 8.6 mg (0.085 mmol) of triethylamine and the resulting mixture stirred at reflux for 24 h (aldehyde consumed as indicated by 2,4-dinitrophenylhydrazine). The reaction mixture was then cooled to room temperature and concentrated under reduced pressure. The residue was then redissolved in ethyl acetate and passed through a short column of silica and concentrated to dryness in vacuo affording a mixture of two diastereomers (260 mg) of pyrrolidine **205** following PTLC (silica; 1:1 ethylacetate/hexanes, $R_f = 0.52$). 62% Yield. The diastereomers were then separated by PTLC (silica; 49:1 dichloromethane/acetone) affording 120 mg of **205a** and 120 mg of **205b**.

205a. **^{1}H NMR** (300 MHz) ($CDCl_3$) δ TMS: 2.08 (1 H, dd, J = 7.7 Hz, J = 13.9 Hz), 2.45 (3 H, s), 2.53-2.59 (1 H, m), 2.95 (1 H, t, J = 7.3 Hz), 3.62 (3 H, s), 3.75 (1 H, q, J = 7.7 Hz), 3.80 (3 H, s), 4.02 (1 H, t, J = 3.7 Hz), 4.51 (1 H, dd, J = 9.2 Hz, J = 10.7

Hz), 4.94 (1 H, t, J = 8.1 Hz), 4.99-5.05 (1 H, m), 5.09 (2 H, d, J = 2.6 Hz), 5.42 (1 H, d, J = 10 Hz), 6.23 (1 H, s), 6.71-6.76 (1 H, m), 7.35-7.40 (7 H, m). See Figure 2, Chapter 3.

^{13}C NMR (300 MHz) ($CDCl_3$) δ: 31.4, 36.0, 47.1, 51.9, 55.2, 55.3, 62.1, 65.5, 66.2, 69.2, 109.7, 111.6, 118.6, 121.4, 128.0, 128.1, 128.3, 128.3, 128.6, 129.2, 132.4, 135.7, 136.8, 154.5, 154.9, 173.1, 173.2.

IR (NaCl): 2948, 2842, 1759, 1642, 1632, 1576, 1476, 1383, 1280, 1259, 1169, 1092, 747 cm^{-1}.

HRMS (FAB), calcd for $C_{27}H_{29}N_2O_7$ (MH^+): 493.1975. Found: 493.1976.

205b. **^{1}H NMR** (300 MHz) ($CDCl_3$) δ TMS: 2.05-2.14 (1 H,m), 2.36 (3 H, s), 2.52 (1 H, d, J = 15 Hz), 2.63-2.73 (1 H, m), 3.33 (3 H, s), 3.81 (3 H, s), 3.84-3.90 (1 H, m), 4.04 (1 H, dd, J = 2.1 Hz, J = 8.7 Hz), 4.46 (1 H, dd, J = 9.2 Hz, J = 11.3 Hz), 4.82 (1 H, d, J = 8.8 Hz), 4.79-5.03 (1 H, m), 5.18 (2 H, s), 5.20-5.27 (1 H, m), 6.09 (1 H, s), 6.72 (2 H, d, J = 7.9 Hz), 7.20 (1 H, t, J = 7.9 Hz), 7.31-7.40 (5 H, m). See Figure 3, Chapter 3.

IR (NaCl): 2948, 1761, 1733, 1637, 1601, 1676, 1476, 1370, 1281, 1260, 1168, 1093, 747 cm^{-1}.

HRMS (FAB), calcd for $C_{27}H_{29}N_2O_7$ (MH^+): 493.1975. Found: 493.1969.

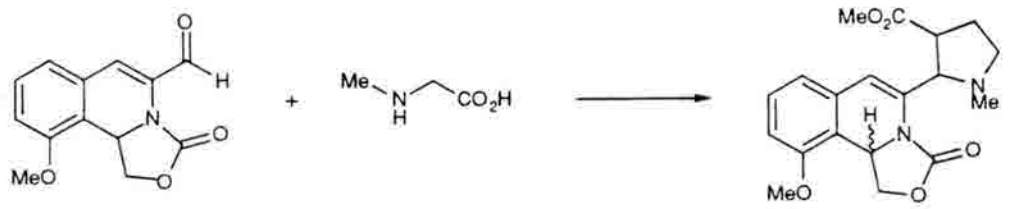

185 **211** **212a, 212b**

1-Hydroxymethyl-(2,2'-carbonyl)-3-(3-carboxymethyl-1-methylpyrrolidin-2-yl)-8-methoxydihdroisoquinoline (212a).

To 25 mg (0.10 mmol) of aldehyde **185** dissolved in 3 mL of ethyl acetate was added 45 mg (0.51 mmol) of sarcosine (**211**) and 4Å molecular sieves. This mixture stirred at 60°C for 1 h at which time 430 mg (5.0 mmol) of methyl acrylate in 5 mL of toluene were added and the resulting mixture heated to reflux (95°C) for 12 h. At this time the reaction mixture was cooled to room temperature, filtered through a plug of silica (eluted with ethylacetate) and concentrated to dryness in vacuo affording 15 mg of crude material, which was further purified by PTLC (silica; 3:1 ethylacetate/hexane; however only one was purified suficiently to be characterized) affording 6 mg of **212a** (R_f = 0.58). 30% Yield.

212a. **^{1}H NMR** (300 MHz) ($CDCl_3$) δ TMS: 2.05 (2 H, m), 2.45 (3 H, s), 2.67 (1 H, q, *J* = 7.9 Hz), 2.91 (1 H, m), 3.16 (1 H, br. t, *J* = 7.7 Hz), 3.71 (3 H, s), 3.81 (3 H, s), 4.44 (1 H, d, *J* = 5.8 Hz), 4.52 (1 H, dd, *J* = 9.3 Hz, *J* = 1.4 Hz), 4.99 (1 H, dd, *J* = 8.2 Hz, *J* = 0.9 Hz), 5.25 (1 H, dd, *J* = 8.5 Hz, *J* = 2.3 Hz), 6.42 (1 H, s), 6.74-6.79 (2 H, m), 7.23 (1 H, t, *J* = 7.7 Hz).

IR (NaCl): 2944, 2841, 2780, 1758, 1574, 1477, 1390, 1277, 1169, 1087 cm^{-1}.

Mass spectrum, m/z (relative intensity) 358 (62.5), 343 (87.7), 311 (57.9), 299 (29.1), 267 (26.9), 142 (100), 141 (26.7), 127 (18.5), 82 (36.8), 69 (24.5), 42 (18.0).

Figure 61. ^{1}H NMR spectrum (300 MHz) ($CDCl_3$) of pyrolidine cycloadduct **212a**

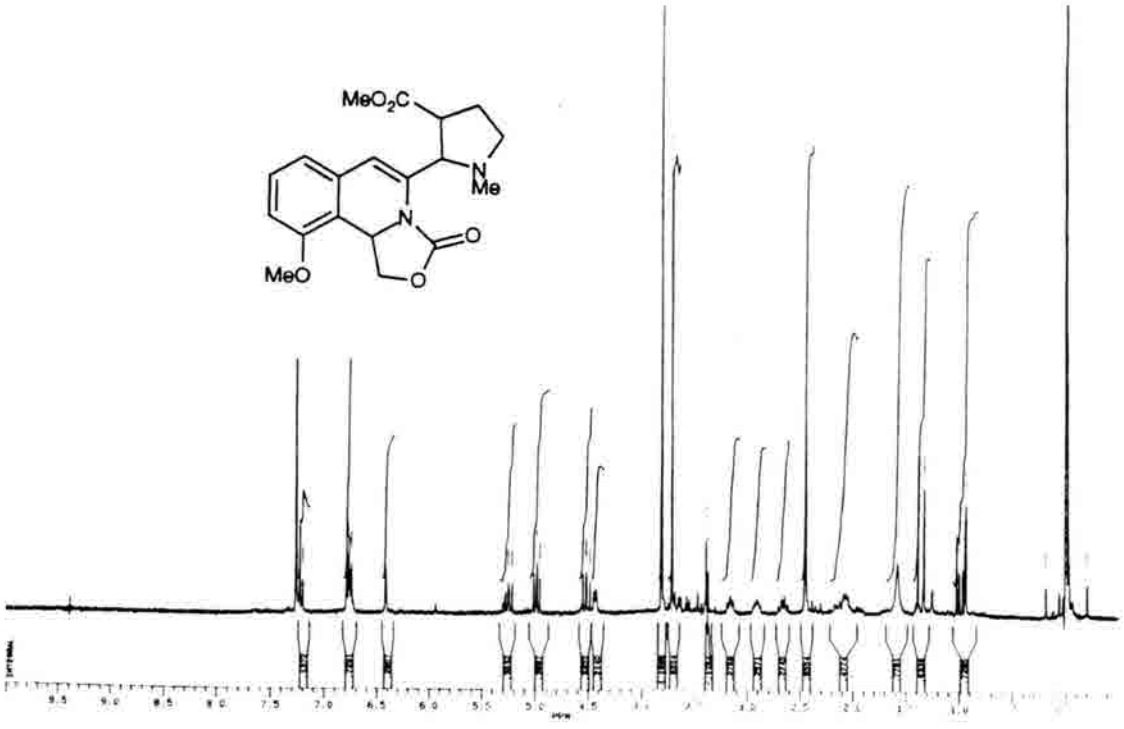

211 **213**

Ethyl *N*-formyl-*N*-methylaminoacetate (213).

To 8.9 g (0.1 mol) of sarcosine (**211**) dissolved in 250 mL of 88% formic acid was added 83 mL of acetic anhydride at a rate such as not to exceed a temperature of 50°C. Once added the reaction mixture stirred at room temperature for 48 h. At this time 300 mL of water were added and the reaction mixture concentrated under reduced pressure affording 11.5 g of the *N*-formyl acid intermediate. To the acid redissolved in 150mL ethanol and chilled to 0°C in an ice-bath was added slowly 17 g (0.15 mol) of thionyl chloride. The resulting mixture stirred at 0°C for 3h, at which time the reaction mixture was concentrated under reduced pressure. The crude product was then redissolved in 100 mL of dichloromethane and washed once with 1 N NaOH then with water. The dichloromethane layer (bottom) was then dried over Na_2SO_4, filtered through Celite and concentrated to dryness in vacuo affording 12 g of **213**. 85% Yield.

Acid intermediate. **^{1}H NMR** (300 MHz) (D_2O) δ HOD: 2.81 (3 H, d, J = 54.0 Hz), 3.99 (2 H, d, J = 23.0 Hz), 7.87 (1 H, d, J = 24.0 Hz).

IR (NaCl): 2932, 2529, 1730, 1638, 1393, 1218, 1088 cm^{-1}.

213. **^{1}H NMR** (300 MHz) ($CDCl_3$) δ TMS: 1.26-1.33 (3 H, m), 3.02 (3 H, d, J = 32.0 Hz), 4.04 (2 H, d, J = 35.0 Hz), 4.20-4.25 (2 H, m), 8.09 (1 H, d, J = 21.0 Hz).

IR (NaCl): 2983, 1746, 1677, 1393, 1207, 1085, 1028, 990, 854 cm^{-1}.

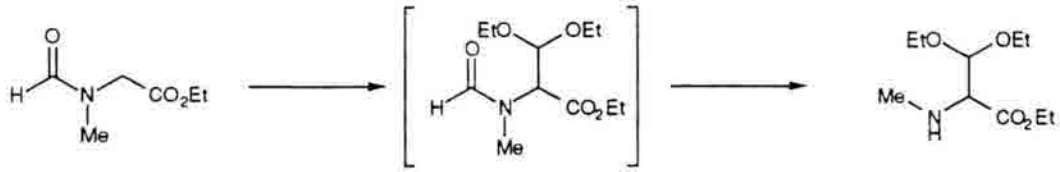

213 **215** **216**

Ethyl 2-methylamino-3,3-diethyoxypropionate (216).

In a 200 mL round bottom flask was slurried 2.7 g (40 mmol) of sodium ethoxide in 30 mL of benzene and the mixture chilled to 0°C in an ice-bath. To this mixture was added 5.8 g (40 mmol) of **213** followed by 5.9 g (80 mmol) of ethyl formate. The reaction mixture stirred at 0°C for 30 min and was then aged at room temperature for 18 h (gel formed). At this time the reaction mixture was concentrated under reduced pressure. The dried gel was then dissoved in 100 mL of 3:1 ethanol/dichloromethane, cooled to 0°C and dry HCl blown through the reaction mixture for 5 min. The reaction vessel was then sealed and stirred at room temperature for 48 h. At 2 h, an aliquot was taken; ^{1}H NMR revieled the formation of intermediate **215**. After the additional time, the reaction mixture was conc. under reduced pressure producing a light yellow oil. The oil was redissolved in dichloromethane, washed with 1 N NaOH, then washed with water. The dichoromethane layer (bottom) was then dried over Na_2SO_4 and concentrated to dryness in vacuo affording 3.5 g of **216**. 41% Overall yield.

215. ^{1}H NMR (270MHz) ($CDCl_3$) δ TMS: 1.14-1.32 (9 H, m), 3.03 (3 H, d, J = 47 Hz), 3.52-3.78 (4 H, m), 4.14 (1 H, d, J = 22 Hz), 4.21-4.26 (2 H, m), 4.98 (1 H, dd, J = 5.8 Hz, J = 8.1 Hz), 8.09 (1 H, d, J = 8.4 Hz).

216. ^{1}H NMR (300 MHz) ($CDCl_3$) δ TMS: 1.16-1.29 (9 H, m), 2.47 (3 H, s), 3.48 (1 H, d, J = 4.2 Hz), 3.52-3.63 (2 H, m), 3.64-3.76 (2 H, m), 4.22 (2 H, q, J = 7.2 Hz), 4.71 (1 H, d, J = 4.0 Hz).

IR (NaCl): 3342, 2978, 1740, 1686, 1446, 1373, 1188, 1115, 1068 cm^{-1}.

Figure 62. ^1H NMR spectrum (300 MHz) ($CDCl_3$) of N-formyl amino ester **215**

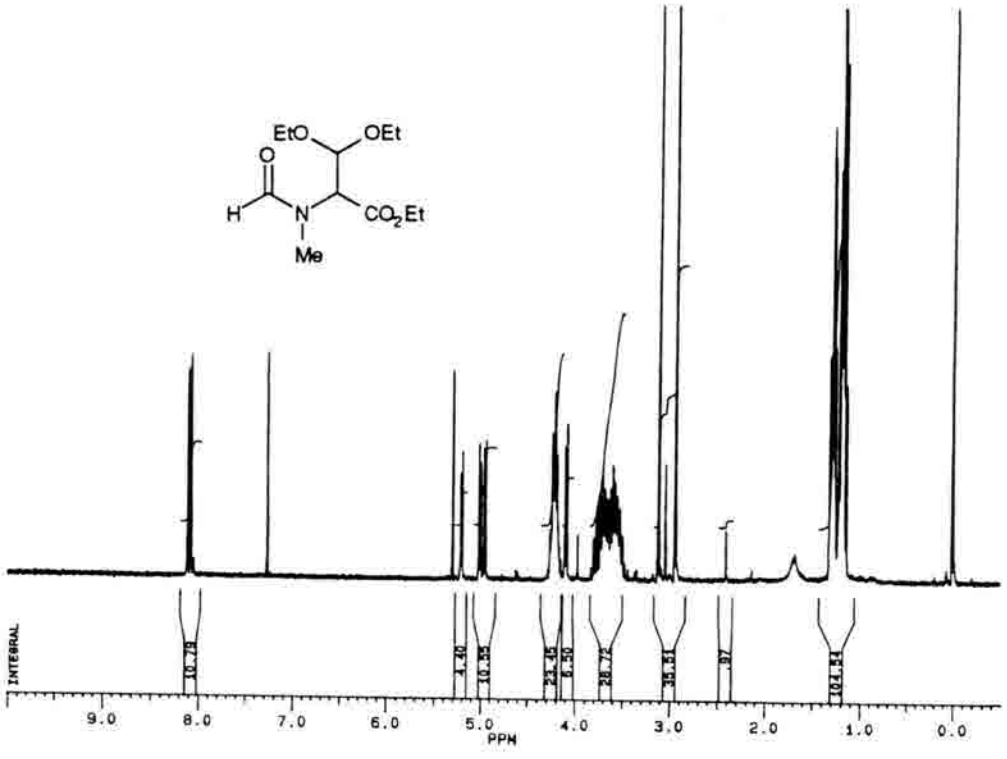

216 **217**

2-Methylamino-3,3-diethoxypropionic acid (217).

To 50 mg (0.23 mmol) of **216** dissolved in 3.5 mL of ethanol and cooled to 0°C in was added 1.2 mL of 2 M LiOH (aq). The resulting mixture stirred at 0°C for 1 h followed by stirring at room temperature for an additional 2 h. At this time the reaction mixture was concentrated under reduced pressure producing a solid. The solid was dissolved in a small volume of water, neutralized with 1 N HCl (aq) and the resulting solution loaded to a 10 mL column of DOWEX 50 (H^+ form). After washing with several volumes of deionized water, the amino acid was eluted with 2 N NH_4OH. Ninhydrin positive fractions were combined, the excess ammonia purged with nitrogen and the resulting solution lyophilized affording 27 mg of pure **217**. 60% Yield.

^{1}H NMR (300 MHz) (D_2O) δ HOD: 0.99-1.09 (6 H, m), 2.54 (3 H, s), 3.42-3.71 (5 H, m), 4.75 (1 H, d, J = 3.3 Hz).

Figure 63. ^{1}H NMR spectrum (300 MHz) ($CDCl_3$) of amino acid **217**

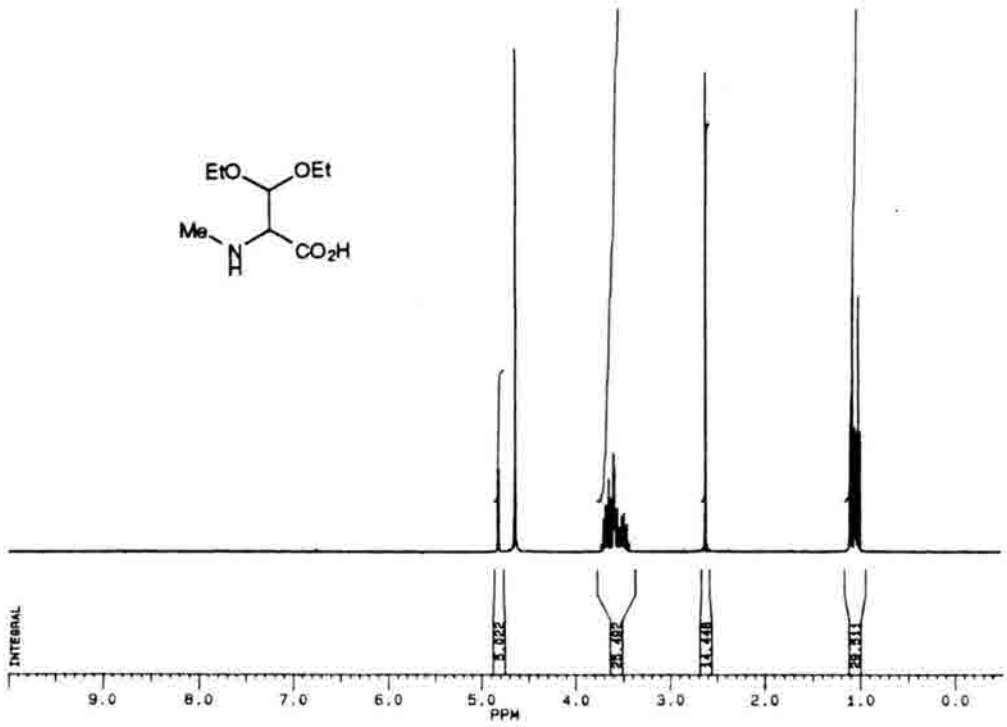

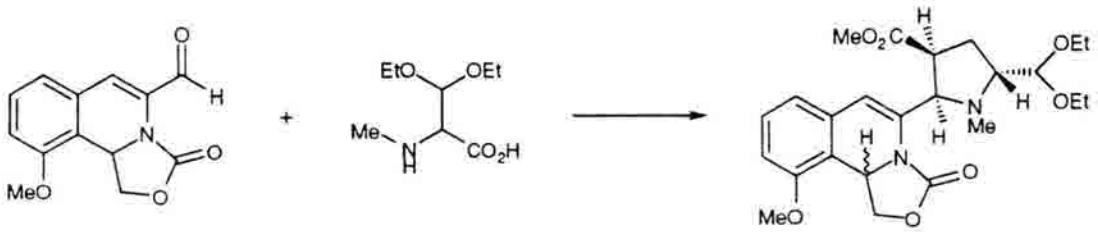

185 **217** **218a, 218b**

(1α)-1-Hydroxymethyl-(2,2'-carbonyl)-3-[(2α,4β,5α)-2-diethoxymethyl-4-carboxymethyl-1-methylpyrolidin-5-yl]-8-methoxydihdroisoquinoline (218a) and (1β)-1-Hydroxymethyl-(2,2'-carbonyl)-3-[(2α,4β,5α)-2-diethoxymethyl-4-carboxymethyl-1-methylpyrolidin-5-yl]-8-methoxydihdroisoquinoline (218b).

To a slurry of aldehyde **185** (113 mg/0.46 mmol) and amino acid **217** (97 mg/0.51 mmol) in 10 mL of dry THF was added 47 mg (0.46 mmol) of triethylamine followed by 198 mg (2.30 mmol) of methyl acrylate and the mixture brought to reflux for 4 h at which time no aldehyde was visible by TLC (silica; 3:1 ethylacetate/hexane; stained with 2,4-dinitrophenylhydrazine). The reaction mixture was cooled to room temperature and concentrated under reduced pressure. The residue was redissolved in ethyl acetate and passed through a plug of silica. PTLC (silica; 13% CH_3CN in toluene) produced two diastereomers. Diastereomer 1, 20 mg (R_f = 0.5); diastereomer 2, 10 mg 0.4.

218a. **^{1}H NMR** (300 MHz) ($CDCl_3$) δ TMS: 1.23-1.32 (6 H, m), 2.16 (1 H, dd, *J* = 7.5 Hz, *J* = 13.0 Hz), 2.36 (1 H, dd, *J* = 9.3 Hz, *J* = 18.8 Hz), 2.57 (3 H, s), 3.37 (1 H, d, *J* = 5.6 Hz), 3.49-3.85 (4 H, m), 3.61 (3 H, s), 3.80 (3 H, s), 4.45-4.54 (2 H, m), 4.93 (1 H, t, *J* = 8.6 Hz), 5.42 (1 H, d, *J* = 8.4 Hz), 6.00 (1 H, s), 6.74 (2 H, d, *J* = 8.5 Hz), 7.21 (1 H, t, *J* = 7.9 Hz). See Figure 5, Chapter 3.

^{13}C NMR (300 MHz) ($CDCl_3$) δ: 15.48 (q), 15.58 (q), 27.94 (t), 35.59 (q), 47.57 (d), 51.71 (d), 55.00 (q), 55.26 (q), 62.83 (d), 64.09 (t), 64.10 (t), 64.71 (d), 69.17 (t), 104.02 (d), 109.71 (d), 112.71 (d), 118.61 (d), 119.14 (s), 121.14 (s), 128.97 (s), 129.20 (d), 132.31 (s), 154.94 (s), 173.51 (s). IR (NaCl): 2974, 1759, 1576, 1476, 1379, 1278, 1169, 1089 cm^{-1}.

Mass spectrum, m/z (relative intensity): 460.2 (2.4, M^+), 385.1 (14.8), 357.1 (100), 355.1 (22.3), 309.1 (13.4), 291.0 (19.9), 277.1 (21.7), 263.1 (14.2), 159.0 (12.0), 103.1 (14.8), 57.1 (18.3), 45.1 (44.3), 30.9 (92.4), 28.1 (82.8).

218b. **^{1}H NMR** (300 MHz) ($CDCl_3$) δ TMS: 1.17-1.25 (6 H, m), 2.15-2.23 (1 H, m), 2.46 (3 H, s), 2.59 (1 H, d, J = 12.1 Hz), 3.38 (3 H, s), 3.51-3.80 (4 H, m), 3.80 (3 H, s), 4.47 (1 H, dd, J = 9.2 Hz, J = 11.3 Hz), 4.55 (1 H, d, J = 3.7 Hz), 4.86 (1 H, d, J = 8.4 Hz), 4.98 (1 H, dd, J = 8.1 Hz, J = 9.1 Hz), 5.23 (1 H, dd, J = 8.3 Hz, J = 11.1 Hz), 5.98 (1 H, s), 6.73 (2 H, d, J = 8.0 Hz), 7.19 (1 H, t, J = 7.4 Hz). See Figure 6, Chapter 3.

^{13}C NMR (300 MHz) ($CDCl_3$) δ 15.49 (q), 15.53 (q), 27.65 (t), 35.23 (q), 48.09 (d), 51.37 (d), 54.67 (q), 55.36 (q), 63.54 (t), 63.97 (t), 64.21 (d), 64.39 (d), 69.51 (t), 103.58 (d), 109.32 (d), 110.64 (d), 118.00 (s), 118.25 (d), 128.40 (s), 129.33 (d), 132.84 (s), 134.20 (s), 153.40 (s), 154.94 (s).

IR (NaCl): 2973, 1760, 1575, 1476, 1376, 1279, 1170, 1064 cm^{-1}.

Mass spectrum, m/z (relative intensity): 460.1 (4.2), 414.1 (5.0), 385.0 (6.3), 357.0 (80.6), 315.0 (33.9), 309.0 (18.5), 268.9 (89.7), 266.9 (64.0), 244.1 (34.1), 213.0 (26.3), 177.0 (23.8), 149.0 (35.9), 103.0 (62.8), 57.1 (100), 30.9 (68.2).

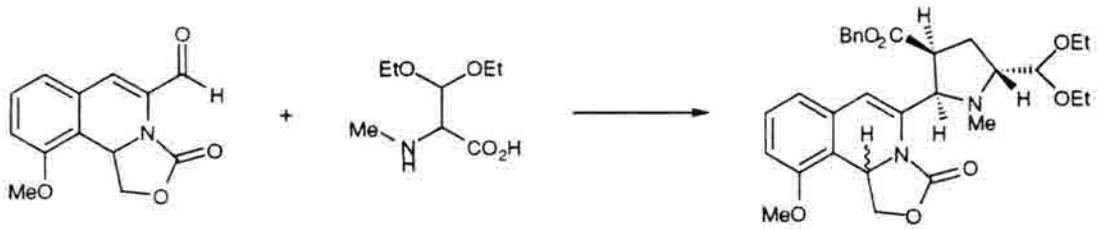

185 **217** **219a, 219b**

(1α)-1-Hydroxymethyl-(2,2'-carbonyl)-3-[(2α,4β,5α)-2-diethoxymethyl-4-carboxybenzyl-1-methylpyrrolidin-5-yl]-8-methoxydihdroisoquinoline (219a) and (1β)-1-hydroxymethyl-(2,2'-carbonyl)-3-[(2α,4β,5α)-2-diethoxymethyl-4-carboxybenzyl-1-methylpyrrolidin-5-yl]-8-methoxydihdroisoquinoline (219b).

To a stirred solution of aldehyde **185** (50 mg/0.20 mmol) and 162 mg (1.00 mmol) of benzyl acrylate dissolved in 5 mL of THF was added 76 mg (0.40 mmol) of finely crushed amino acid **217** followed by 2.6 mg (0.02 mmol) of triethylamine and the resulting mixture stirred at reflux for four hours (aldehyde consumed as indicated by 2,4-dinitrophenylhydrazine). The reaction mixture was then cooled to room temperature and concentrated under reduced pressure. The residue was then redissolved in ethyl acetate and passed through a short column of silica and concentrated to dryness in vacuo affording a crude mixture of diastereomers which were separated by PTLC (silica; 1:1 ethylacetate/hexanes) affording 14 mg of **219a** (R_f = 0.54) and 8 mg of **219b** (R_f = 0.46). 30% yield.

219a. **^{1}H NMR** (300 MHz) ($CDCl_3$) δ TMS: 1.17-1.286 (6 H, m), 2.20 (1 H, dd, *J* = 7.9 Hz, *J* = 5.2 Hz), 2.38-2.48 (1 H, m), 2.56 (3 H, s), 1.9 Hz, *J* = 6.7 Hz), 3.53-3.63 (3 H, m), 3.72-3.81 (2 H, m), 3.80 (3 H, s), 4.40 (1 H, ddd, *J* = 1.2 Hz, *J* = 8.0 Hz, *J* = 1.2 Hz), 4.48 (1 H, d, *J* = 3.9 Hz), 4.65-4.74 (2 H, m), 4.97 (1 H, 1/2 ABq, *J* = 12 Hz),

5.08 (1 H, 1/2 ABq, J = 12 Hz), 5.44 (1 H, d, J = 8.5 Hz), 5.98 (1 H, s), 6.70 (2 H, m), 7.17-7.37 (6 H, m).

^{13}C NMR (300 MHz) ($CDCl_3$) δ: 15.5 (q), 15.6 (q), 28.1 (t), 35.6 (q), 47.7 (d), 54.7 (d), 54.8 (d), 55.3 (q), 62.7 (d), 64.1 (t), 64.7 (d), 66.5 (t), 69.1 (t), 69.3 (t), 104.0 (d), 109.6 (d), 112.7 (d), 118.6 (d), 119.3 (s), 128.1 (d), 128.3 (d), 128.4 (d), 129.1 (d), 129.3 (d), 132.2 (s), 135.7 (s), 136.5 (s), 154.8 (s), 154.9 (s), 173.0 (s).

IR (NaCl): 2973, 1758, 1576, 1476, 1381, 1278, 1164, 1088, 747 cm^{-1}.

Mass spectrum, m/z (relative intensity) 536 (1.4), 490 (4.7), 461 (6.0), 433 (100), 353 (6.3), 297 (7.4), 172 (6.0), 91 (65.0), 45 (42.8), 31 (82.1).

219b. ^{1}H NMR (300 MHz) ($CDCl_3$) δ TMS: 1.21-1.28 (6 H, m), 2.20 (1 H, ddd, J = 2.3 Hz, J = 7.1 Hz, J = 2.8 Hz), 2.42 (3 H, s), 2.47-2.57 (1 H, m), 3.42 (1 H, ddd, J = 2.7 Hz, J = 2.9 Hz, J = 2.8 Hz), 3.51-3.58 (3 H, m), 3.69-3.85 (2 H, m), 3.78 (3 H, s), 4.58 (1 H, d, J = 3.4 Hz), 4.62-4.65 (1 H, m), 4.66 (1 H, 1/2 ABq, J = 12.5 Hz), 4.81 (1 H, 1/2 ABq, J = 12.5 Hz), 4.78-4.87 (1 H, m), 5.06 (1 H, dd, J = 8.1 Hz, J = 3.2 Hz), 5.80 (1 H, s), 6.71 (2 H, d, J = 8.0 Hz), 6.92 (2 H, d, J = 7.2 Hz), 7.05-7.27 (4 H, m).

IR (NaCl): 2965, 1760, 1476, 1362, 1128, 1065 cm^{-1}.

Mass spectrum, m/z (relative intensity) 536 (3.3), 490 (9.1), 461 (8.6), 433 (83.4), 353 (8.3), 297 (13.5), 262 (62.0), 183 (54.5), 103 (20.8), 91 (100), 31 (59.4).

215 **224**

Ethyl 2-methylamino-3,3-dimethoxypropionate (224).

To **215** (1.0 g/4.5 mmol) dissolved in 40 mL of dry methanol was bubbled dry HCl for 5 min. The resulting mixture stirred at room temperature for 24 h. At this time, dry HCl was again bubbled through the reaction mixture for 5 min and the reaction stirred for an additional 24 h. The reaction mixture was then concentrated under reduced pressure, redissolved in 40 mL of dichloromethane, washed 2 x with 20 mL of 1 M NaOH (aq), then with 20 mL water, dried over Na_2SO_4, filtered through Celite and concentrated to dryness in vacuo affording 477 mg of **224**. 55% Yield.

^{1}H NMR (300 MHz) ($CDCl_3$) δ TMS: 1.31 (3 H, t, J = 7.3 Hz), 2.46 (3 H, s), 3.42 (1 H, d, J = 4.3 Hz), 3.43 (3 H, s), 4.25 (2 H, q, J = 7.1 Hz), 4.51 (1 H, d, J = 5.9).

IR (NaCl): 3343, 2979, 1737, 1451, 1371, 1181, 1115, 1071 cm^{-1}.

224 **220**

2-Methylamino-3,3-dimethoxypropionic acid (220).

To 450 mg (2.35 mmol) of ethyl ester **224** dissolved in 20 mL of ethanol and cooled to 0°C was added 10 mL (20.4 mmol) of 2 M LiOH (aq). The resulting solution was then warmed to room temperature and stirred for 4 h. At this time 1.2 mL of acetic acid (glacial) were added and the reaction mixture concentrated under reduced pressure. The solid residue was then redissolved in a small volume of H_2O and loaded onto a 20mL column of DOWEX 50 (H^+ form) and was washed with several volumes of deionized water. Amino acid **220** was then eluted from the resin with 2 M NH_4OH. Ninhydrin possitive fractions were combined and concentrated to dryness in vacuo affording 280 mg of **220**. 73% Yield.

^{1}H NMR (300 MHz) (D_2O) δ HOD: 2.59 (3 H, s), 3.33 (3 H, s), 3.35 (3 H, s), 3.61 (1 H, d, J = 3.0 Hz), 4.63 (1 H, d, J = 1.6 Hz).

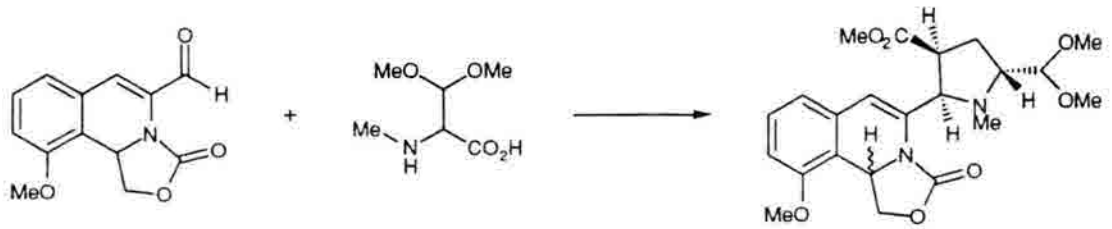

185 **220** **221a, 221b**

(1α)-1-Hydroxymethyl-(2,2'-carbonyl)-3-[(2α,4β,5α)-2-dimethoxymethyl-4-carboxymethyl-1-methylpyrrolidin-5-yl]-8-methoxydihdroisoquinoline (221a) and (1β)-1-hydroxymethyl-(2,2'-carbonyl)-3-[(2α,4β,5α)-2-dimethoxymethyl-4-carboxymethyl-1-methylpyrrolidin-5-yl]-8-methoxydihdroisoquinoline (221b).

To a slurry of aldehyde **185** (230 mg/0.93 mmol) and amino acid **220** (167 mg/1.02 mmol) in 15 mL of dry THF was added 94 mg (0.93 mmol) of triethylamine followed by 400 mg (4.65 mmol) of methyl acrylate and the mixture brought to reflux for 4 h at which time no aldehyde was visible by TLC (silica; 3:1 ethylacetate/hexane; stained with 2,4-dinitro-phenylhydrazine). The reaction mixture was cooled to room temperature and concentrated under reduced pressure. The residue was redissolved in ethyl acetate and passed through a plug of silica. The components were then purified by Chromatotron (silica; 1:1 ethylacetate/hexane) affording 2 diastereomers (40 mg each). 25% Yield.

221a. **^{1}H NMR** (300 MHz) ($CDCl_3$) δ TMS: 2.13 (1 H, dd, *J* = 7.8 Hz, *J* = 3.1 Hz), 2.34 (1 H, t, *J* = 8.0 Hz), 2.57 (3 H, s), 3.36-3.43 (1 H, m), 3.46 (3 H, s), 3.47 (3 H, s), 3.52-3.59 (1 H, m), 3.62 (3 H, s), 3.80 (3 H, s), 4.32 (1 H, d, *J* = 4.1 Hz), 4.51 (1 H, dd, *J* = 9.3 Hz, *J* = 10.3 Hz), 4.93 (1 H, t, *J* = 8.4 Hz), 5.09 (1 H, dd, *J* = 8.3 Hz, *J* = 10.4 Hz), 5.40 (1 H, d, *J* = 8.5 Hz), 5.99 (1 H, s), 6.74 (2 H, d, *J* = 8.1 Hz), 7.21 (1 H, t, *J* = 7.6 Hz).

^{13}C NMR (300 MHz) ($CDCl_3$) δ: 27.86 (t), 35.58 (q), 47.36 (d), 54.94 (d), 55.08 (q), 55.37 (q), 55.81 (q), 55.91 (q), 62.78 (d), 63.99 (d), 69.15 (t), 106.43 (d), 109.72 (d), 112.75 (d), 118.58 (d), 119.12 (s), 129.18 (d), 132.17 (s), 136.37 (s), 148.02 (s), 154.90 (s), 173.32 (s).

IR (NaCl): 2947, 1758, 1575, 1476, 1383, 1278, 1170, 1117, 1082, 783, 747 cm^{-1}.

226 **227**

***O*-Benyzl-*N*-methylserine (227).**

To a stirred solution of N-^{t}Boc-O-benzylserine (1.0 g/3.39 mmol) dissolved in THF and cooled to 0°C was added 3.8 g (27.1 mmol) of methyl iodide followed by 0.244 g (10.2 mmol) of sodium hydride. The resulting mixture was then warmed to room temperature and stirred for 24 h. Ethyl acetate 5 mL was added followed by water (2 mL) and the reaction mixture concentrated under reduced pressure. The residue was slurried with ethyl acetate (25mL) and washed with water (10 mL), then with brine (sat.) and dried over Na_2SO_4. The Celite filtered solution was then concentrated to dryness in vacuo affording 900 mg of crude material. This material was then redissolved in dichloromethane (22 mL) and cooled to 0°C. To this solution was added 3.3 g (29.1 mmol) of trifluoroacetic acid, the resulting mixture stirred at 0°C for 30min. and then concentrated under reduced pressure. The residue was then dissolved in water (2 mL), cooled to 0°C and neutralized with 1 N NaOH (aq). This solution was then loaded to a 10 mL column of DOWEX 50 (H^+ form) and washed with 50 mL of deionized water. The product was then eluted with 2 M NH_4OH and lyophilized affording 330 mg of pure **227**. 54% Yield.

^{1}H NMR (300 MHz) (D_2O) δ HOD: 2.53 (3 H, s), 3.59 (1 H, t, J = 3.9Hz), 3.76 (2 H, d, J = 4.0 Hz), 4.44 (2 H, s), 7.23-7.29 (5 H, m).

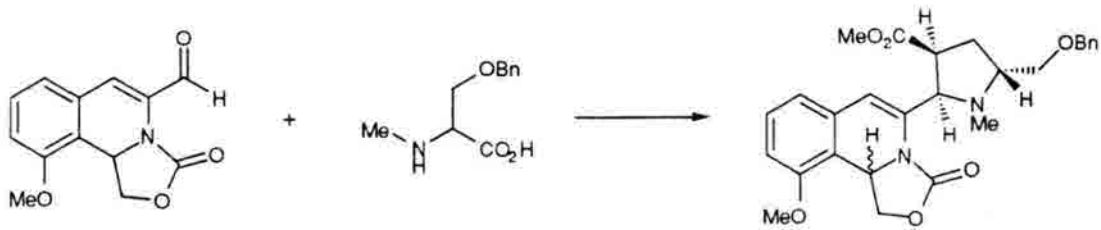

185 **227** **228a, 228b**

(1α)-1-Hydroxymethyl-(2,2'-carbonyl)-3-[(2α,4β,5α)-2-benzylmethoxy-4-carboxymethyl-1-methylpyrrolidin-5-yl]-8-methoxydihdroisoquinoline (228a).

To a suspension of aldehyde **185** (390 mg/1.59 mmol) and amino acid **227** (330 mg/1.57 mmol) in 9 mL of dry THF was added 684 mg (7.95 mmol) of methyl acrylate and the resulting mixture heated to reflux for 18 h. After cooling to room temperature the reaction mixture was concentrated under reduced pressure. The residue was redissolved in ethyl acetate, washed with sat. $NaHCO_3$, dried over $MgSO_4$ and concentrated to dryness in vacuo affording 559 mg of crude material. A mixture of diastereomers was isolated by radial PTLC (silica; 1:1 ethylacetate/hexanes) affording 256 mg of material. The diastereomers were then separated by PTLC (silica; 50:1 dichloromethane/methanol affording pure **228a**. 34% Yield to the mixture of diastereomers.

228a. **^{1}H NMR** (300 MHz) ($CDCl_3$) δ TMS: 2.00 (1 H, q, J = 8.1 Hz), 2.44-2.48 (1 H, m), 2.50 (3 H, s), 3.50-3.59 (3 H, m), 3.61 (3 H, s), 3.79 (3 H, s), 4.44-4.55 (1 H, m), 4.54 (2 H, s), 4.94 (1 H, t, J = 8.7Hz), 5.10 (1 H, dd, J = 8.2 Hz, J = 2.4 Hz), 5.28 (1 H, d, J = 10.0 Hz), 6.15 (1 H, s), 6.73 (2 H, dd, J = 6.3 Hz, J = 2.3 Hz), 7.18-7.36 (6 H, m).

^{13}C NMR (300 MHz) ($CDCl_3$) δ: 30.93 (t), 35.43 (q), 47.29 (d), 51.78 (q), 55.12 (d), 55.35 (q), 61.79 (d), 63.05 (d), 69.20 (t), 70.71 (t), 73.33 (t), 109.64 (d),

111.88 (d), 118.59 (d), 118.73 (s), 127.53 (d), 127.53 (d), 128.24 (s), 128.36 (d), 128.36 (d), 129.20 (d), 129.20 (d), 132.39 (s), 136.81 (s), 138.23 (s), 154.94 (s), 173.60 (s).

IR (NaCl): 2997, 2851, 1758, 1640, 1601, 1576, 1475, 1383, 1364, 1278, 1169, 1090, 746 cm^{-1}.

Figure 64. ^1H NMR spectrum (300 MHz) ($CDCl_3$) of *O*-benzylpyrrolidine **228a**

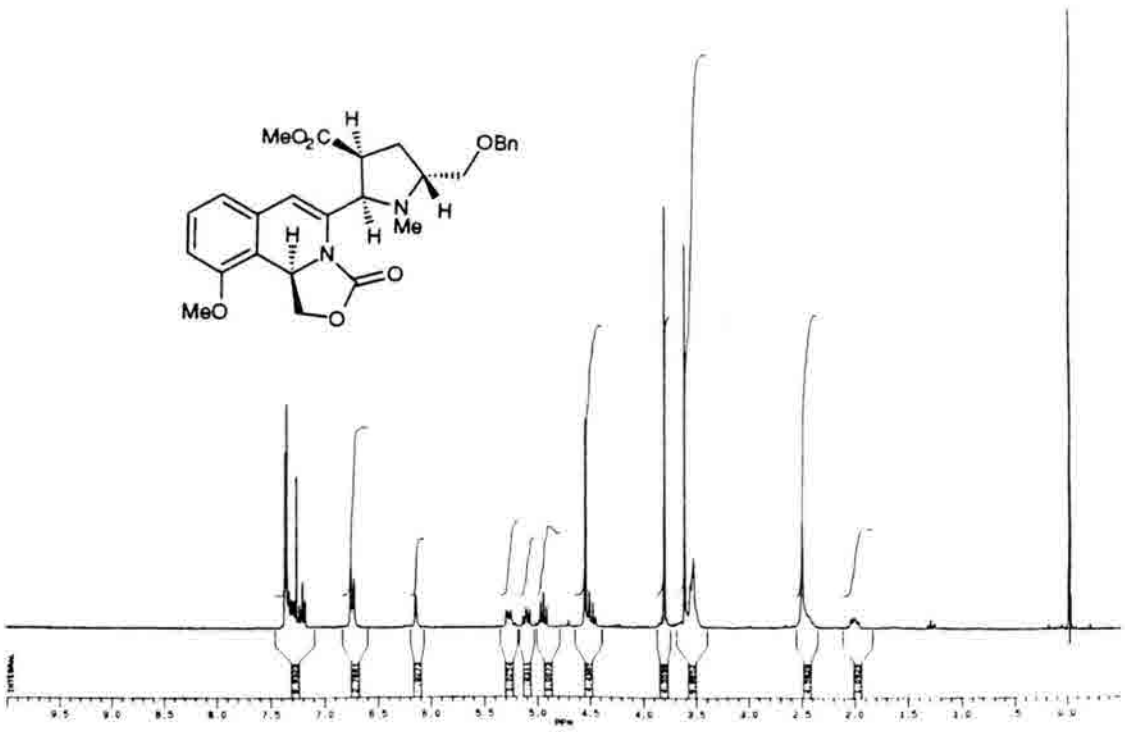

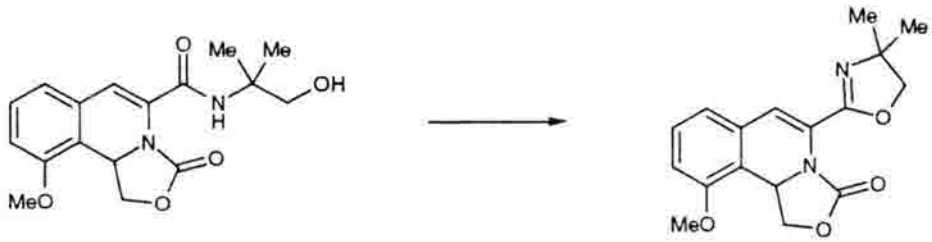

184 **234**

1-Hydroxymethyl-(2,2'-carbonyl)-3-(4,4-dimethyloxazolin-2-yl)-8-methoxydihydroisoquinoline (234).

To 63 mg (0.19 mmol) of amido alcohol **184** dissolved in 2.0 mL of dichloromethane was added 0.45 mL (67 mg/0.6 mmol) of thionyl chloride. The resulting mixture stirred at room temperature for 2 h at which time the reaction mixture was cooled to 0°C and to the reaction added 2.0 mL of cold water and a sufficient amount of 1 N NaOH (aq) to increase the pH of the aqueous phase to 11. The phases were then separated and the aqueous layer extracted 3 x 10 mL with dichloromethane. The dichloromethane extracts were combined, dried over $MgSO_4$, filtered through Celite and concentrated to dryness in vacuo affording 41 mg of oxazoline **234**. 70% Yield.

^{1}H NMR (300 MHz) (CDCl3) δ TMS: 1.37 (3 H, s), 1.41 (3 H, s), 4.12 (2 H, q *J* = 9.0 Hz), 4.67 (1 H, dd, *J* = 9.0 Hz), 5.02 (1 H, dd, *J* = 9.0 Hz), 5.36 (1 H, dd, *J* = 9.0 Hz), 6.81 (1 H, s), 6.84-6.88 (2 H, m), 7.23-7.29 (1 H, m).

^{13}C NMR (300 MHz) ($CDCl_3$) δ: 27.77 (q), 27.85 (q), 53.43 (d), 55.42 (q), 67.69 (s), 70.11 (t), 79.29 (t), 111.60 (d), 111.60 (d), 119.89 (d), 121.39 (s), 124.91 (s), 129.37 (d), 130.60 (s), 155.03 (s), 155.23 (s), 158.06 (s).

IR (NaCl): 2969, 1769, 1654, 1681, 1574, 1476, 1404, 1320, 1296, 1265, 1198, 1081, 786, 723 cm^{-1}.

234 **185**

1-Hydroxymethyl-(2,2'-carbonyl)-3-formyl-8-methoxydihydroisoquinoline (185).

To 50 mg (0.16 mmol) of oxazoline **234** dissolved in 3.5 mL of dichloromethane and chilled to 0°C was added 39 mg (0.24 mmol) of methyl triflate. The resulting solution stirred for 10 min at 0°C, then was warmed to room temperature and stirred for an additional 2 h. At this time the reaction mixture was again cooled to 0°C and to it added a chilled slurry of 147 mg (3.89 mmol) of $NaBH_4$ in 3.5 mL of ethanol. The resulting mixture stirred at 0°C for 45 min at which time the $NaBH_4$ was quenched with sat. NH_4Cl (aq) and the reaction mixture concentrated under reduced pressure. The pale yellow residue was then dissolved in 9 mL of 4:1 THF/H_2O and to it added 282 mg (2.24 mmol) of oxalic acid and the resulting mixture stirred at room temperature for 8 h. At this time 20 mL of water were added and the reaction mixture extracted 2 x 50 mL with 3:1 ethylacetate/ hexane. The organic extracts were then combined, dried over Na_2SO_4, passed through a plug of silica (eluted with 3:1 ethylacetate/hexane) and concentrated to dryness in vacuo affording 25 mg of aldehyde **185**. 64% Yield. Physical data matched that shown above.

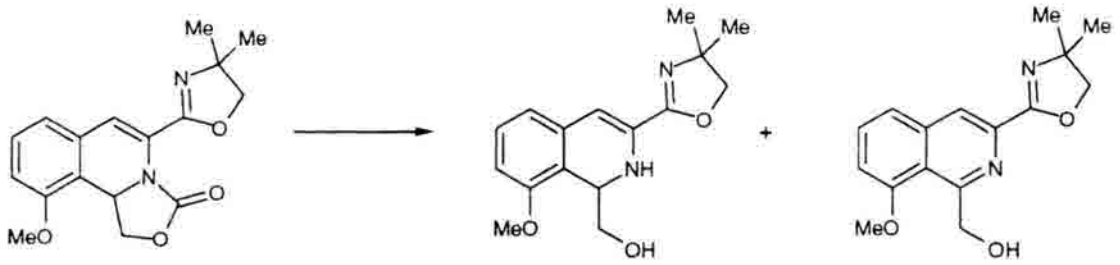

234 **235** **236**

1-Hydroxymethyl-3-(4,4-dimehtyloxazolin-2-yl)-8-methoxy-1,2-dihydroisoquinoline (235) and 1-hydroxymethyl-3-(4,4-dimethyloxazolin-2-yl)-8-methoxyisoquinoline (236).

To a stirred solution of oxazoline **234** (100 mg/0.318 mmol) in 16 mL of ethanol was added 1.6 mL of 2 M LiOH (aq) and the resulting mixture degassed by purging with nitrogen. The solution then was heated at reflux with stirring for 18 h. After cooling to room temperature, 10 mL of water were added, the mixture extracted 3 x 25 mL with dichloromethane, the dichloromethane layers combined, dried over Na_2SO_4, decanted and concentrated to dryness in vacuo affording 93 mg of crude material. The components were separated by PTLC (silica; 3:1 ethylacetate/hexanes) affording 18 mg of II ($R_f = 0.43$) and 16mg of III ($R_f = 0.21$).

235. **^{1}H NMR** (300 MHz) ($CDCl_3$) δ TMS: 1.28 (3 H, s), 1.34 (3 H, s), 3.34 (1 H, dd, *J* = 3.5 Hz, *J* = 7.4 Hz), 3.76 (1 H, dd, *J* = 9.5 Hz, *J* = 1.4 Hz), 3.80 (3 H, s), 4.02 (1/2 ABq, *J* = 8.1 Hz), 4.08 (1/2 ABq, *J* = 8.1 Hz), 4.94-4.99 (1 H, m), 5.21 (1 H, br. s), 6.05 (1 H, d, *J* = 1.2 Hz), 6.66 (1 H, d, *J* = 11.3 Hz), 6.68 (1 H, d, *J* = 12.0 Hz), 7.12 (1 H, t, *J* = 7.9 Hz).

^{13}C NMR (300 MHz) ($CDCl_3$) δ: 28.03, 28.37, 51.66, 55.30, 62.51, 67.22, 79.38, 103.26, 109.01, 109.01, 117.21, 117.87, 128.34, 130.68, 133.79, 155.36.

IR (NaCl): 3395, 2967, 1652, 1604, 1573, 1471, 1370, 1269, 1200, 1104, 1052, 973, 913, 806, 730 cm^{-1}.

236. ^1H NMR (300 MHz) ($CDCl_3$) δ TMS: 1.46 (6H, s), 3.18 (2H, s), 3.99 (3H, s), 4.26 (2H, s), 6.93 (1H, d, J = 8.0Hz), 7.40 (1H, d, J = 7.9Hz), 7.56 (1H, t, J = 6.5Hz), 8.22 (1H, s).

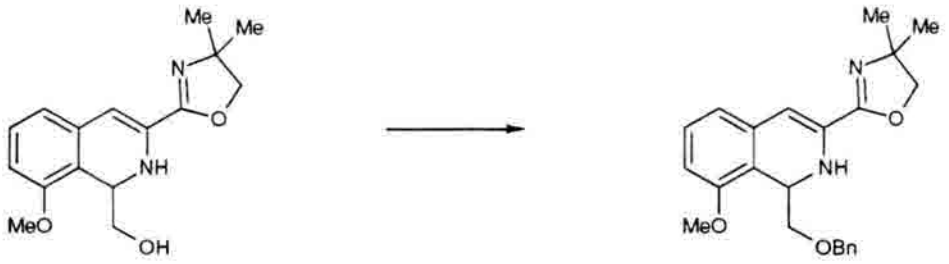

235 **244**

1-O-Benzylhydroxymethyl-3-(4,4-dimethyloxazolin-2-yl)-8-methoxy-1,2-dihydroisoquinoline (244).

To a stirred solution of **235** (31 mg/0.108 mmol) in 1 mL of dry DMF and cooled to 0°C was added 3mg (0.130 mmol) of sodium hydride and the resulting mixture stirred at 0°C for 15 min. At this time 18 mg (0.108 mmol) of benzyl bromide were added and the new mixture stirred at 0°C for 2 h. Methanol (0.5 mL) was added followed by dichloromethane (10 mL) and the mixture washed with 5 mL of water, dried over Na_2SO_4 and concentrated under reduced pressure affording crude **244** which was further purified by PTLC (silica; 5:1 hexanes/ethylacetate) affording 8.8 mg of pure product **244** (R_f = 0.40). 25% Yield.

^{1}H NMR (300 MHz) ($CDCl_3$) δ TMS: 1.38 (3H, s), 1.43 (3H, s), 3.20 (1H, dd, *J* = 3.0Hz, *J* = 6.4Hz), 3.74 (2H, q, *J* = 9.0Hz), 3.77 (3H, s), 4.09-4.18 (2H, m), 4.55 (2H, q, *J* = 12.0Hz), 5.08 (1H, dd, *J* = 2.8Hz, *J* = 6.7Hz), 6.15 (1H, br. s), 6.64 (1H, d, *J* = 7.7Hz), 6.68 (1H, d, *J* = 8.4Hz), 7.11 (1H, t, *J* = 8.2Hz), 7.22-7.36 (5H, m).

IR (NaCl): 2966, 1752, 1707, 1657, 1608, 1471, 1453, 1369, 1270, 1199, 1106, 973, 809, 738, 698 cm^{-1}.

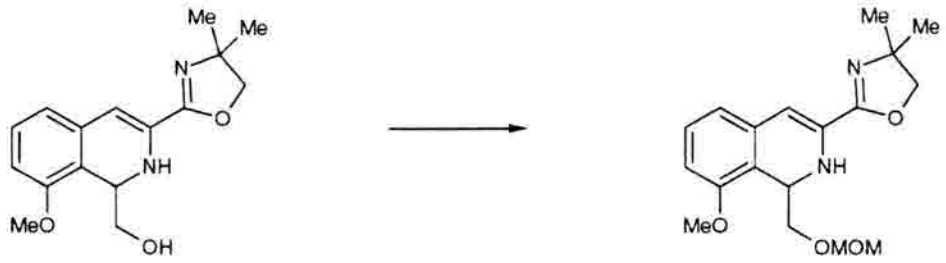

235 **243**

1-Hydroxymethylmethoxylmethyl-3-(4,4-dimethyloxazolin-2-yl)-8-methoxy-1,2-dihydroisoquinoline (244).

To a stirred solution of **235** (31 mg/0.108 mmol) in 1 mL of dry DMF and cooled to 0°C was added 3 mg (0.130 mmol) of sodium hydride and the resulting mixture stirred at 0°C for 15 min. At this time 8.6 mg (0.108 mmol) of chloromethyl methyl ether were added and the new mixture stirred at 0°C for 2h. Methanol (0.5 mL) was added followed by dichloromethane (10 mL) and the mixture washed with 5 mL of water, dried over Na_2SO_4 and concentrated under reduced pressure affording crude **243** which was further purified by PLC (silica; 5:1 hexanes/ethylacetate) affording 8.2 mg of pure product **243** 23% Yield.

^{1}H NMR (300 MHz) ($CDCl_3$) δ TMS: 1.31 (3 H, s), 1.32 (1 H, s), 3.18 (1 H, dd, J = 2.9 Hz, J = 9.6 Hz), 3.35 (3 H, s), 3.77-3.84 (1 H, m), 3.81 (3 H, s), 4.04-4.08 (1 H, m), 4.61 (1 H, 1/2 ABq, J = 9.4 Hz), 4.66 (1 H, 1/2 ABq, J = 9.4 Hz), 5.02 (1 H, dd, J = 2.1 Hz, J = 9.4 Hz), 5.18 (1 H, br s), 6.07 (1 H, s), 6.63 (1 Hd, J = 7.7 Hz, J = 6.67 (1 H, d, J = 8.2 Hz), 7.12 (1 Ht, J = 7.9 Hz).

IR (NaCl): 2968, 1755, 1700, 1657, 1609, 1478, 1451, 1372 cm^{-1}.

211 **245**

9-Fluorenylmethyl-N-carboxymethyl-N-methyl carbamate (245).

To a stirred solution of sarcosine (1.0 g/0.011 mol) in 29 mL of 10% Na_2CO_3 (aq) and cooled to 0°C was added 2.8 g (0.011 mol) of 9-fluorenylmethyl chloroformate dissolved in 20 mL of THF. The resulting mixture warmed to room temperature and stirred for 2 h. The reaction mixture was then poored into 1 L of water, the aqueous layer (bottom) acidified with 1 N HCl and extracted 2 x 300 mL with ethyl acetate. The ethyl acetate layers were combined, dried over $MgSO_4$ and concentrated under reduced pressure affording 3.3 g of **245**. 96% Yield.

^{1}H NMR (300 MHz) ($CDCl_3$) δ TMS: 2.97 (1.5 H, s), 3.01 (1.5 H, s), 3.91 (1 H, s), 4.08 (1 H, s), 4.09-4.28 (1 H, m), 4.43 (2 H, dd, J = 2.8 Hz, J = 3.5 Hz), 7.23-7.41 (4 H, m), 7.51 (1 H, d, J = 7.4 Hz), 7.59 (1 H, d, J = 7.4 Hz), 7.70 (1 H, d, J = 7.5 Hz), 7.74 (1 H, d, J = 7.5 Hz), 10.55 (1 H, br. s).

^{13}C NMR (300 MHz) ($CDCl_3$) δ: 35.35 (q), 47.05 (d), 50.48 (t), 68.01 (t), 119.88 (d), 119.92 (d), 124.73 (d), 124.97 (d), 126.98 (d), 127.02 (d), 127.60 (d), 127.66 (d), 141.22 (s), 143.73 (s), 156.06 (s), 156.87 (s), 174.66 (s), 174.69 (s).

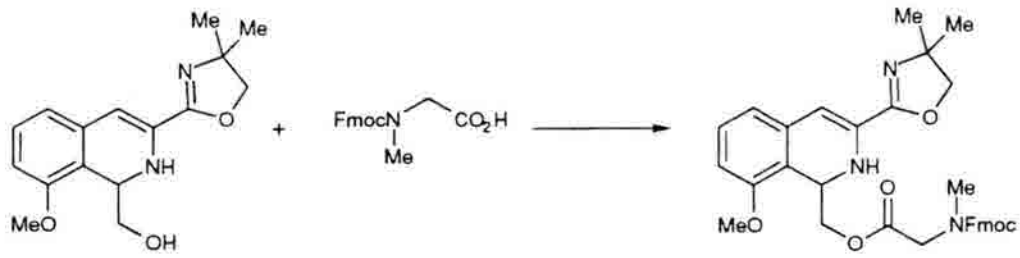

235 **245** **247**

1-[Hydroxymethyl-*O*-(*N*-9-fluorenylmethyloxycarbonyl-*N*-methyl)-aminoacetyl]-3-(4,4-dimethyloxazolin-2-yl)-8-methoxy-1,2-dihydroisoquinoline (247).

To **245** (40 mg/0.13 mmol) dissolved in dichloromethane was added a microdrop of DMF followed by 33 mg (0.26 mmol) of oxalyl choride. The resulting mixture stirred at room temperature for 15 min and the resulting mixture concentrated under reduced pressure. The residue was then redissolved in 2.0 mL of dichloromethane, cooled to -78oC and to this solution added 20 mg (0.195 mmol) of triethylamine and the resulting mixture stirred at -78°C for 15 min, at which time **235** (34 mg/0.118 mmol) dissolved in a small volume of dichloromethane was introduced via cannula. The reaction then warmed to room temperature and stirred for 1 h. The residue following concentration was separated by PTLC (silica; 20:1 dichloromethane/methanol) affording 20 mg of **247**. 40% Yield.

^{1}H NMR (300 MHz) ($CDCl_3$) δ TMS: 1.26 (3 H, s), 1.30 (1.5 H, s), 1.35 (1.5 H, s), 3.03 (3, d, *J* = 9.9 Hz), 3.47 (3 H, s), 3.98-3.82 (3 H, m), 3.85 (1 H, dd, *J* = 3.3 Hz, *J* = 10.7 Hz), 3.98-4.06 (3 H, m), 3.98 (1 H, s), 4.18-4.33 (3 H, m), 4.39 (7.3 Hz), 5.02 (1 H, br s), 5.11 (1 H, d, *J* = 14.6 Hz), 6.11 (1 H, d, *J* = 4.4 Hz), 6.65-6.71 (2 H, m), 7.15 (1 H, t, *J* = 7.9 Hz), 7.26-7.43 (5 H, m), 7.52 (1 H, d, J = 7.4 Hz), 7.62 (1 H, d, *J* = 7.4 Hz), 7.76 (2 H, m).

186 **239**

3-(Ethoxyacetylaminomethyl)-1-hydroxymethyl-(2,2'-carbonyl)-8-methoxydihydroisoquinoline (239).

To a stirred solution of **186** (400 mg/1.62 mmol) dissolved in 14 mL of dichloromethane and cooled to 0°C was added 556 mg (4.85 mmol) of methanesulfonyl chloride followed by 820 mg (8.10 mmol) of triethylamine. The resulting mixture stirred at 0°C for 30 min. at which time 1.2 g (8.10 mmol) of sarcosine ethyl ester hydrochloride (Aldrich) were added, the mixute allowed to come to room temperature and stir for 8 h. The reaction mixture was then concentrated under reduced pressure, redissolved in 25 mL of ethylacetate, passed through a short column of silica (eluted with ethyl acetate) and concentrated to dryness in vacuo affording 588 mg of **239**.

^{1}H NMR (300 MHz) ($CDCl_3$) δ TMS: 1.26 (3 H, t, *J* = 7.3 Hz), 2.53 (3 H, s), 3.43 (1 H, d, *J* = 16.9 Hz), 3.60 (1 H, d, *J* = 14.8 Hz), 3.81 (3 H, s), 4.17 (2 H, q, *J* = 7.1 Hz), 4.33 (1 H, d, *J* = 14.9 Hz), 4.49 (1 H, dd, *J* = 9.2 Hz, *J* = 10.2 Hz), 4.98 (1 H, t, *J* = 8.5 Hz), 5.28 (1 H, dd, *J* = 2.4 Hz, *J* = 8.2 Hz), 6.02 (1 H, s), 6.74 (2 H, t, *J* = 8.4 Hz), 7.22 (1 H, t, *J* = 7.8 Hz).

^{13}C NMR (300 MHz) ($CDCl_3$) δ: 14.23 (q), 41.51 (q), 54.61 (d), 55.38 (q), 56.02 (t), 57.40 (t), 60.27 (t), 69.42 (t), 109.76 (d), 112.83 (d), 118.18 (d), 119.04 (s), 129.27 (d), 132.28 (s), 134.20 (s), 154.57 (s), 154.98 (s), 171.02 (s).

IR (NaCl): 2925, 2853, 1759, 1645, 1576, 1476, 1401, 1280, 1260, 1188, 1091, 747 cm^{-1}.

Anal. calcd for $C_{18}H_{22}N_2O_5$: C, 62.42; H, 6.40; N, 8.09. Found: C, 62.25; H, 6.60; N, 7.93.

Figure 65. ^{1}H NMR spectrum (300 MHz) ($CDCl_3$) of allylic amine **239**

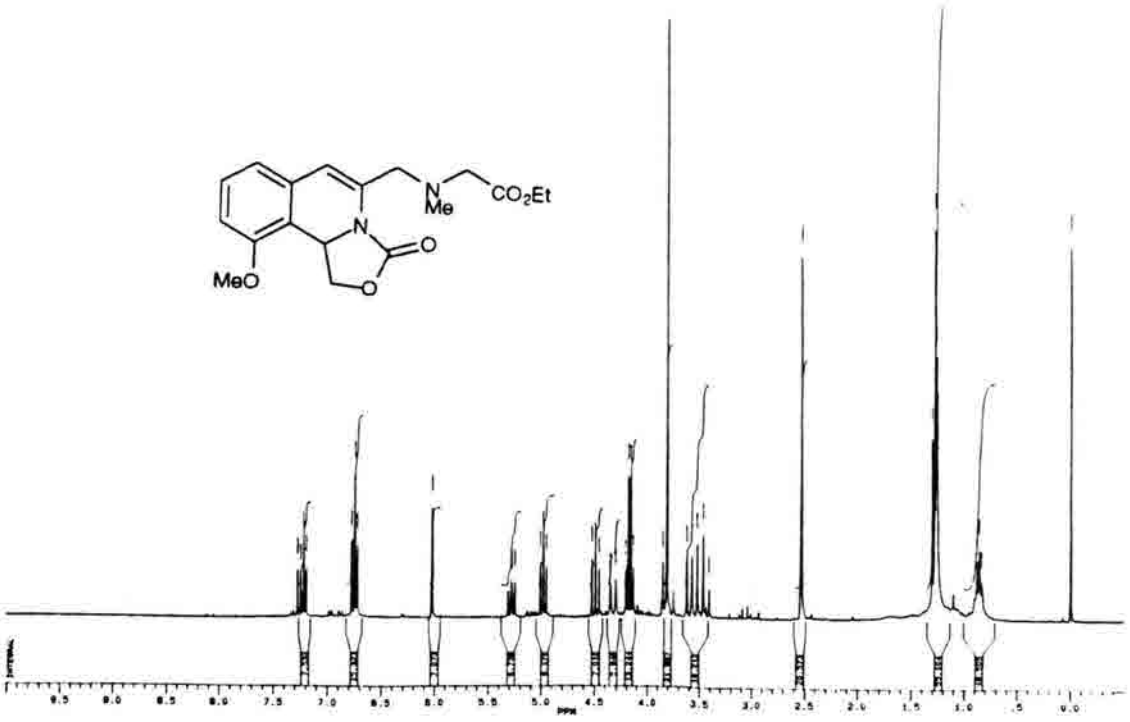

239 **248**

2-Aza-6-hydroxymethyl-7-methoxy-2-methyl-4-oxo-1,3,4,6,11,11a-tetrahydro-2*H*-benzo[*b*]quinolizine (248).

To a stirred solution of **239** (252 mg/0.666 mmol) in 33 mL of ethanol was added 3.3 mL of 2 M LiOH (aq), the reaction mixture degassed by argon purge and the resulting mixture stirred at room temperature for 8 h. The solution was then cooled to 0°C, the pH adjusted to 5 with 6 N HCl (aq) and concentrated to dryness in vacuo. The dry residue was then redissolved in 10 mL of DMF, cooled to 0°C and to this solution added 108 mg (0.799 mmol) of N-hydroxybenzatriazole followed by 165 mg (0.700 mmol) of 1,3-dicyclohexylcarbodiimide. The reaction was stirred at 0°C for 1 h then allowed to come to room temperature and stir for an additional 18 h. After concetrating the reaction mixture under reduced pressure at 35°C, the residue was redissolved in dichloromethane (50 mL), filtered through Celite, washed with sat. $NaHCO_3$ (aq), dried over Na_2SO_4 and concentrated under reduced pressure. The crude material was then purified by flash chromatography (silica; 10:1 dichloromethane/methanol, 0.5% conc. NH_4OH) affording 97 mg of pure **248** (R_f = 0.53). 53% yield.

^{1}H NMR (300 MHz) ($CDCl_3$) δ TMS: 2.42 (3 H, s), 3.39 (1 H, 1/2 ABq, *J* = 13.6 Hz), 3.48 (2 H, s), 3.55 (1 H, 1/2 ABq, *J* = 13.6 Hz), 3.66-3.69 (2 H, m), 3.83 (3 H, s), 5.66 (1 H, s), 6.24 (1 H, dd, *J* = 4.6 Hz, *J* = 7.0 Hz), 6.65 (1 H, d, *J* = 7.6 Hz), 6.74 (1 H, d, *J* = 8.3 Hz), 7.18 (1 H, t, *J* = 8.1 Hz).

^{13}C NMR (300 MHz) ($CDCl_3$) δ: 43.80 (q), 50.10 (d), 55.37 (q), 55.37 (t), 59.06 (t), 64.12 (t), 106.33 (d), 109.30 (d), 116.57 (s), 117.39 (d), 128.87 (d), 131.61 (s), 131.75 (s), 155.19 (s), 166.64 (s).

IR (NaCl): 3184, 2939, 1680, 1643, 1474, 1364, 1274 cm^{-1}.

HRMS (FAB), calcd for $C_{15}H_{19}N_2O_3$ (MH^+): 275.1396. Found: 275.1386.

Figure 66. ^{1}H NMR spectrum (300 MHz) ($CDCl_3$) of tricyclic monoketopiperazine **248**

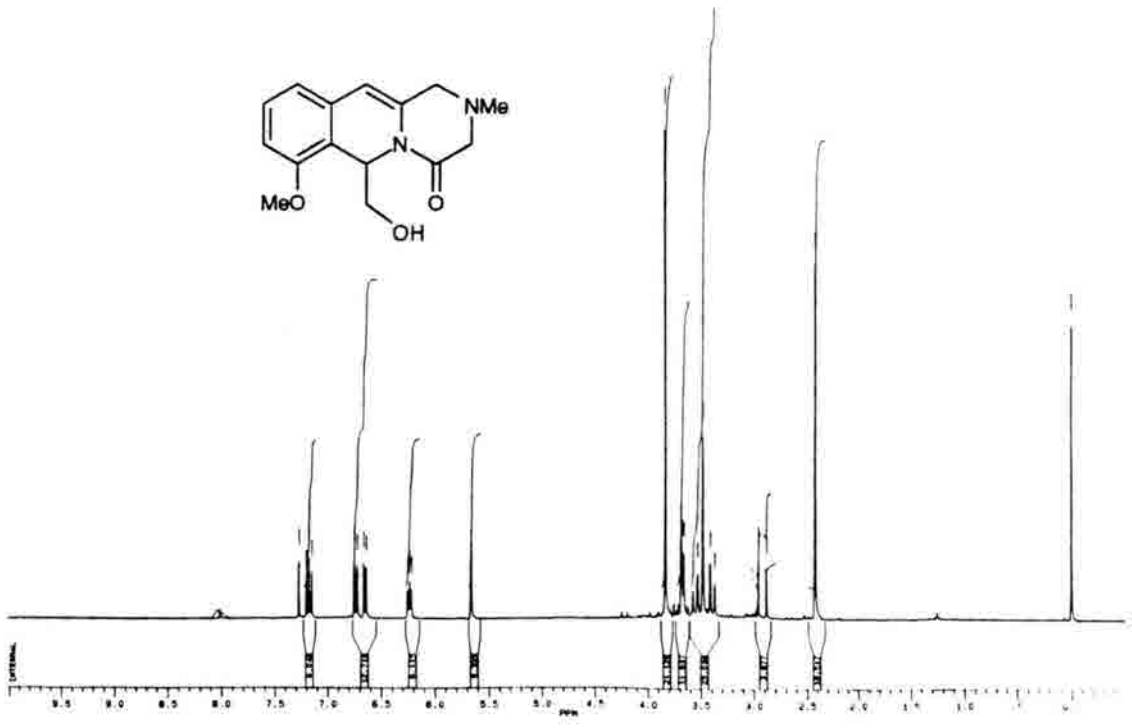

248 **249a, 249b**

Methyl (5α,8β,10β,11β)-5,7,8,9,10,11-hexahydro-4-methoxy-5-hydroxymethyl-13-methyl-7-oxo-8,11-iminoazepino[1,2-*b*]isoquinoline-10-carboxylate (249a) and methyl (5α,8α,10α,11α)-5,7,8,9,10,11-hexahydro-4-methoxy-5-hydroxymethyl-13-methyl-7-oxo-8,11-iminoazepino[1,2-*b*]isoquinoline-10-carboxylate (249b).

To a stirred solution of **248** (44 mg/0.160 mmol) in 11 mL of chloroform was added 28 mg (0.160 mmol) of N-bromosuccinimide and the resulting solution brought to reflux for 1 h (dark green color formed). At this time, the reaction mixture was cooled to 0°C and to the mixture added 687 mg (8.00 mmol) of methylacrylate followed by addition of a solution of 162 mg (1.60 mmol) of triethylamine in 5 mL of chloroform over a 15 min. period (dark blue color formed). The reaction mixture was then allowed to come to room temperature and stir for 1 h. The reaction was then concentrated under reduced pressure, redissolved in dichloromethane, washed with sat. $NaHCO_3$, dried over Na_2SO_4 and concentrated to dryness in vacuo. The crude material was then purified by PLC (silica; 3:1 dichloromethane/THF, 0.25% conc. NH_4OH) affording 5 mg of **249a** ($R_f = 0.38$) and 27 mg of **249b** ($R_f = 0.24$). 55% yield.

249a. ^{1}H NMR (300 MHz) ($CDCl_3$) δ TMS: 1.79 (1 H, br. s), 2.46 (3 H, s), 2.54 (1 H, dd, J = 9.81 Hz, J = 13.0 Hz), 2.61-2.69 (1 H, m), 3.33 (1 H, dd, J = 6.3 Hz, J = 9.8 Hz), 3.59-3.65 (1 H, m), 3.70 (1 H, d, J = 6.5 Hz), 3.76 (3 H, s), 3.84 (3 H, s),

4.04 (1 H, s), 5.70 (1 H, s), 6.18 (1 H, dd, J = 4.0 Hz, J = 8.1 Hz), 6.68 (1 H, d, J = 7.5 Hz), 6.75 (1 H, d, J = 7.9 Hz), 7.20 (1 H, t, J = 8.0 Hz).

^{13}C NMR (300 MHz) ($CDCl_3$) δ: 34.90, 35.65, 47.36, 48.87, 52.45, 55.42, 64.75, 65.33, 66.94, 105.53, 109.40, 116.55, 117.75, 129.06, 131.16, 134.87, 155.25, 170.10, 173.63.

IR (NaCl): 3425, 2951, 2842, 1737, 1683, 1642, 1474, 1363, 1273, 1084 cm^{-1}.

HRMS (FAB), calcd for $C_{19}H_{23}N_2O_5$ (MH^+): 359.1607. Found: 359.1602.

249b. **^{1}H NMR** (300 MHz) ($CDCl_3$) δ TMS: 2.10 (1 H, br. s), 2.17 (1 H, dd, J = 9.9 Hz, J = 13.6 Hz), 2.62 (3 H, s), 2.63-2.70 (1 H, m), 2.88 (1 H, dd, J = 4.8 Hz, J = 10.0 Hz), 3.67-3.76 (1 H, m), 3.76 (3 H, s), 3.85 (3 H, s), 4.23 (1 H, s), 5.67 (1 H, s), 6.25 (1 H, dd, J = 4.1 Hz, J = 7.3 Hz), 6.67 (1 H, d, J = 7.6 Hz), 6.75 (1 H, d, J = 7.6 Hz), 7.21 (1 H, t, J = 8.0 Hz).

^{13}C NMR (300 MHz) ($CDCl_3$) δ: 32.11, 34.84, 50.12, 50.30, 52.50, 55.40, 64.54, 64.90, 65.68, 104.02, 109.20, 115.95, 117.21, 129.07, 132.30, 136.53, 155.33, 171.41, 173.26.

IR (NaCl): 2950, 1734, 1684, 1636, 1474, 1272, 1078 cm^{-1}.

Figure 67. ^{1}H NMR spectrum (300 MHz) ($CDCl_3$) of cycloadduct **249a**

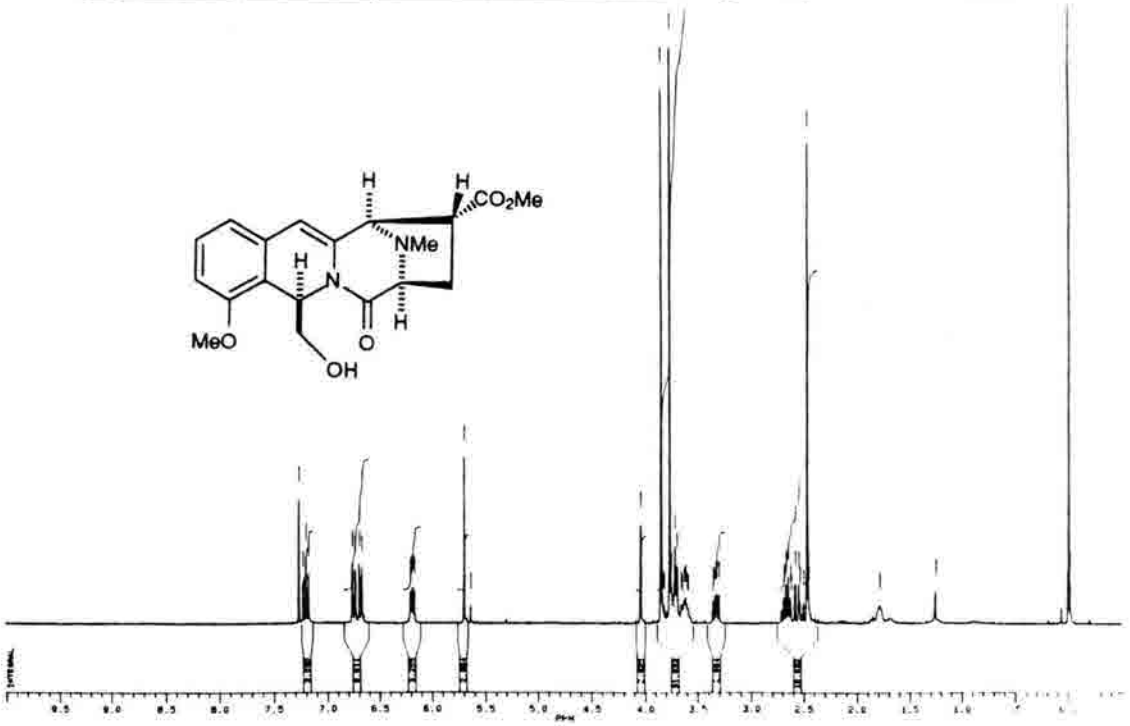

Figure 68. ^{1}H NMR spectrum (300 MHz) ($CDCl_3$) of cycloadduct **249b**

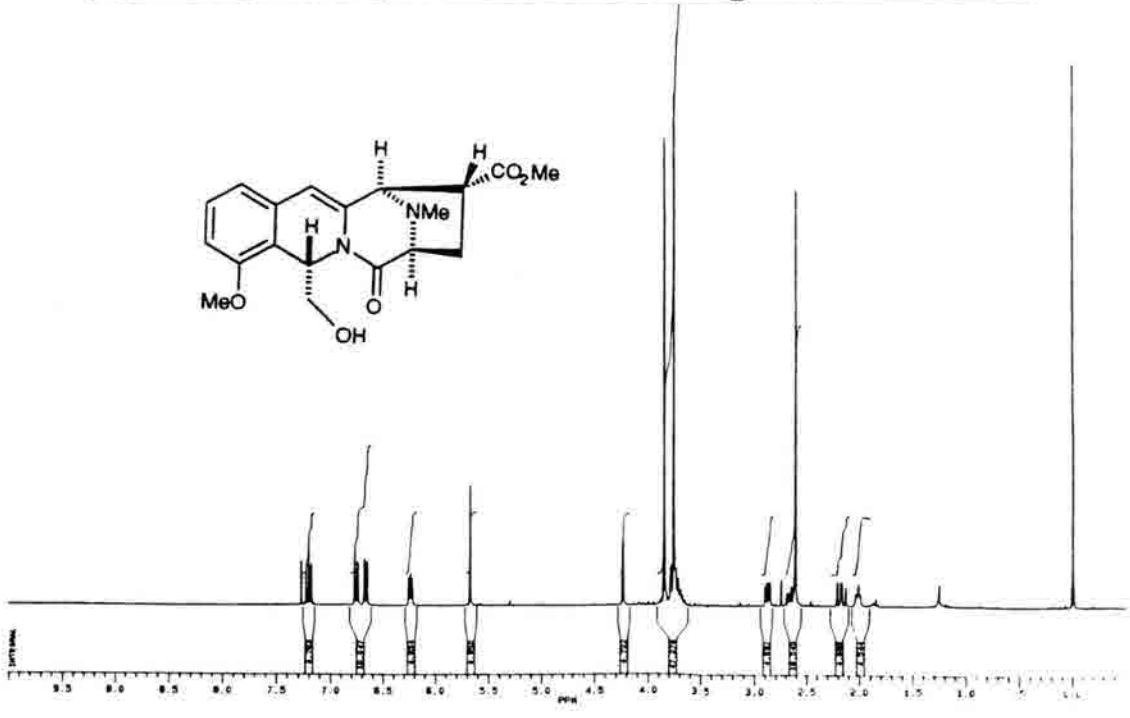

249b **250b**

Methyl (5α,8α,10α,11α)-5,7,8,9,10,11-hexahydro-4-methoxy-5-formyl-13-methyl-7-oxo-8,11-iminoazepino[1,2-*b*]isoquinoline-10-carboxylate (250b).

To a solution of DMSO (31 mg/0.402 mmol) in 2.5 mL of dichloromethane and cooled to -78°C was added 26 mg (0.201 mmol) of oxalyl chloride and the mixture stirred at -78°C for 10 min. A solution of **249b** (36 mg/0.100 mmol) in 1.0 mL of dichloromethane was then added and the resulting solution stirred at -78°C for 1 h, at which time 101 mg (1.00 mmol) of triethylamine were added and the reaction mixture allowed to come to room temperature. The reaction was then concentrated under reduced pressure, redissolved in dichloromethane (20 mL), washed with water, dried over Na_2SO_4 and concentrated to dryness in vacuo affording 34 mg of **250b**. 94% yield.

^{1}H NMR (300 MHz) ($CDCl_3$) δ TMS: 2.22 (1 H, dd, *J* = 9.8 Hz, *J* = 13.5 Hz), 2.62-2.71 (1 H, m), 2.79 (3 H, s), 2.93 (1 H, dd, *J* = 5.0 Hz, *J* = 9.8 Hz), 3.74-3.80 (1 H, m), 3.76 (3 H, s), 4.21 (1 H, s), 5.59 (1 H, s), 6.58 (1 H, s), 6.68 (1 H, d, *J* = 8.3 Hz), 6.80 (1 H, d, *J* = 7.8 Hz), 7.25 (1 H, t, *J* = 8.0 Hz), 9.35 (1 H, s).

^{13}C NMR (300 MHz) ($CDCl_3$) δ: 32.74, 35.03, 49.83, 52.51, 55.61, 58.08, 64.97, 65.32, 102.79, 109.14, 110.79, 117.90, 130.08, 132.10, 137.39, 155.46, 169.62, 173.20, 191.29.

IR (NaCl): 2948, 2852, 1735, 1686, 1645, 1475, 1275 cm^{-1}.

HRMS (FAB), calcd for $C_{19}H_{21}N_2O_5$ (MH^+): 357.1450. Found: 357.1451.

Figure 69. ^{1}H NMR spectrum (300 MHz) ($CDCl_3$) of amido aldehyde **250b**

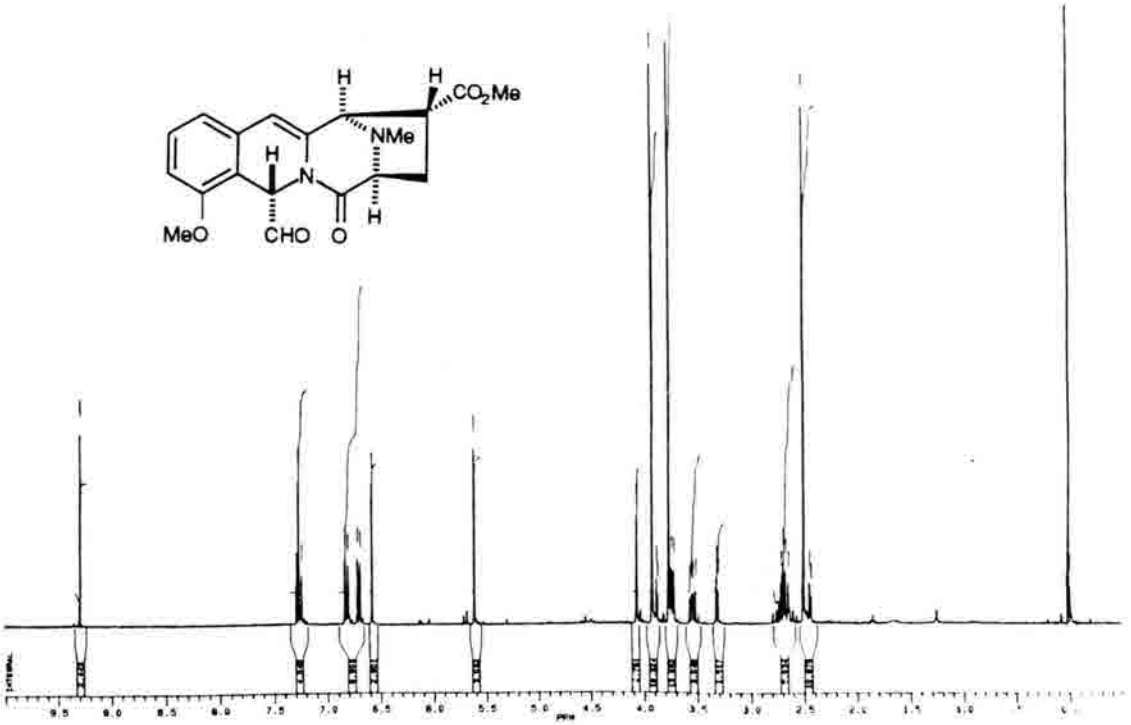

Figure 70. ^{1}H NMR spectrum (300 MHz) ($CDCl_3$) of amido aldehyde **250a**

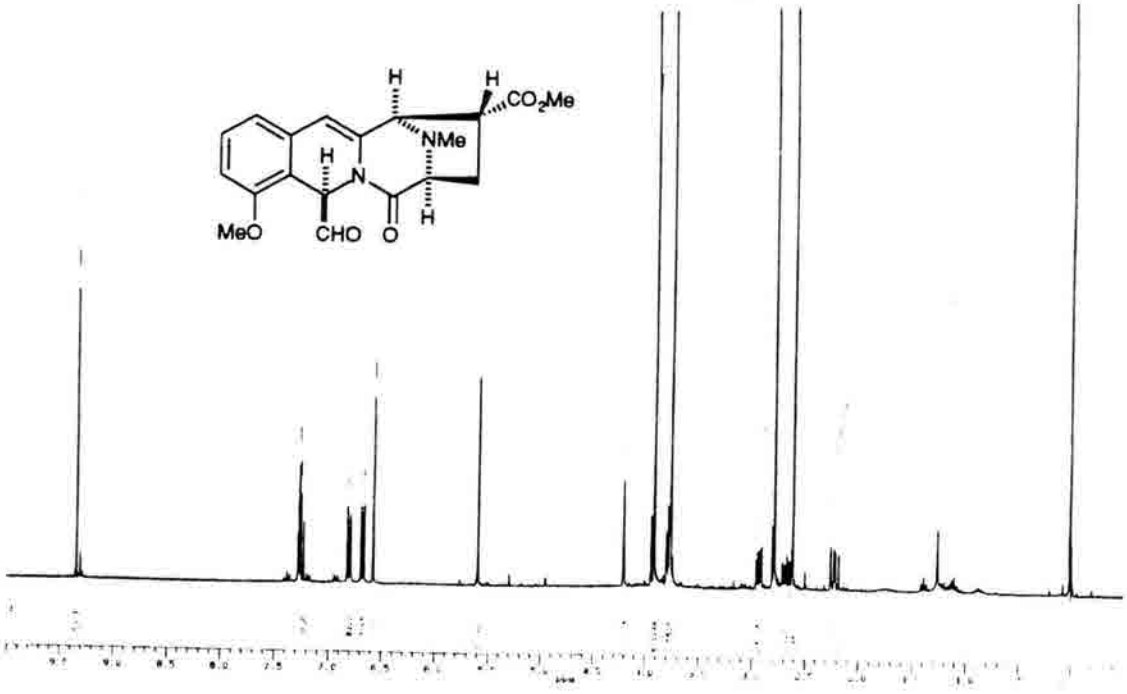

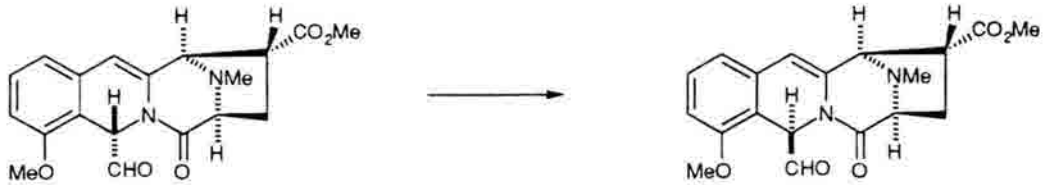

250b **250a**

Methyl (5α,8β,10β,11β)-5,7,8,9,10,11-hexahydro-4-methoxy-5-formyl-13-methyl-7-oxo-8,11-iminoazepino[1,2-*b*]isoquinoline-10-carboxylate (250a).

To a stirred solution of **250b** (30 mg/0.084 mmol) in 10 mL of dry THF was added 13 mg (0.084 mmol) of 1,8-diazobicyclo-[5.4.0]-undec-7-ene and the resulting mixture stirred at room temperature for 3 h. The reaction was then diluted with 25 mL of dichloromethane then washed with sat. $NaHCO_3$ (aq), dried over Na_2SO_4 and concentrated to dryness in vacuo. The crude was then purified by PLC (silica; 3:1 ethylacetate/hexanes) affording 22 mg of **250a** (R_f = 0.41) and 6 mg of **250b** (R_f = 0.50).

250a. **^{1}H NMR** (300 MHz) ($CDCl_3$) δ TMS: 2.50 (3 H, s), 2.64-2.71 (2 H, m), 3.54 (1 H, dd, *J* = 6.4 Hz, *J* = 9.5 Hz), 3.73 (1 H, d, *J* = 6.4 Hz), 3.76 (3 H, s), 3.92 (3 H, s), 4.07 (1 H, s), 5.61 (1 H, s), 6.57 (1 H, s), 6.70 (1 H, d, *J* = 7.5 Hz), 6.82 (1 H, d, *J* = 8.3 Hz), 7.27 (1 H, t, *J* = 8.7 Hz), 9.29 (1 H, s).

^{13}C NMR (300 MHz) ($CDCl_3$) δ: 34.92, 35.63, 47.83, 52.47, 55.64, 56.48, 65.20, 66.55, 104.14, 109.31, 111.22, 118.17, 130.09, 136.02, 155.48, 168.48, 173.78, 192.13.

IR (NaCl): 2951, 2842, 1734, 1687, 1647, 1475, 1776, 172, 1088 cm^{-1}.

HRMS (FAB), calcd for $C_{19}H_{21}N_2O_5$ (MH^+): 357.1450. Found: 357.1465.

250a **249a**

Methyl (5α,8β,10β,11β)-5,7,8,9,10,11-hexahydro-4-methoxy-5-hydroxymethyl-13-methyl-7-oxo-8,11-iminoazepino[1,2-*b*]isoquinoline-10-carboxylate (249a).

To a stirred solution of **250a** (14 mg/0.039 mmol) dissolved in 3 mL of anhydrous methanol and cooled to 0°C was added 6 mg (0.157 mmol) of sodium borohydride (Baker) and the resulting mixture stirred at 0°C for 1 h. The reaction mixture was then carefully quenched by addition of 1 N HCl (aq) until bubbling subsided. This solution was then concentrated under reduced pressure, the residue redissolved in dichloromethane (10 mL), washed with sat. $NaHCO_3$ (aq), dried over Na_2SO_4 and concentrated to dryness in vacuo affording 13 mg of **249a**. 94% yield. Physical data for **249a** reported above.

249a **66**

Methyl (5α,8β,10β,11β)-5,7,8,9,10,11-hexahydro-4-methoxy-5-[(methoxymethoxy)methyl]-13-methyl-7-oxo-8,11-iminoazepino[1,2-*b*]isoquinoline-10-carboxylate (66).

To a stirred solution of **249a** (6 mg/0.017 mmol) dissolved in 2 mL of dichloromethane and cooled to 0°C was added 7 mg (0.051 mmol) of N,N-diisopropylethylamine followed by 3 mg (0.043 mmol) of chloromethyl methyl ether. The resulting mixture stirred at 0°C for 1 h at which time the reaction mixture was allowed to come to room temperature with continued stirring for an addition 16 h. The reaction was then concentrated under reduced pressure and purified by PLC (silica; 3:1 ethylacetate/hexanes) affording 6 mg of **66** (R_f = 0.30). 84% Yield.

^{1}H NMR (300 MHz) ($CDCl_3$) δ TMS: 2.43-2.51 (1 H, m), 2.46 (3 H, s), 2.60-2.66 (1 H, m), 3.22 (3 H, s), 3.28 (1 H, dd, *J* = 9.9 Hz, *J* = 6.1 Hz), 3.57-3.60 (2 H, m), 3.68 (1 H, d, *J* = 6.4 Hz), 3.77 (3 H, s), 3.84 (3 H, s), 4.03 (1 H, s), 4.44 (1 H, 1/2 ABq, *J* = 6.5 Hz), 4.64 (1 H, 1/2 ABq, *J* = 6.5 Hz), 5.70 (1 H, s), 6.22 (1 H, dd, *J* = 4.6 Hz, *J* = 6.6 Hz), 6.66 (1 H, d, *J* = 7.6 Hz), 6.73 (1 H, d, *J* = 8.3 Hz), 7.18 (1 H, t, *J* = 8.0 Hz). See Figure 7, Chapter 3.

^{13}C NMR (300 MHz) ($CDCl_3$) δ: 34.63, 35.68, 46.01, 47.36, 52.47, 55.22, 55.43, 65.48, 66.94, 67.13, 96.07, 105.68, 109.23, 117.21, 117.54, 128.84, 131.46, 134.97, 155.16, 168.85, 173.75.

IR (NaCl): 2949, 1738, 1686, 1546, 1474, 1358, 1274, 1169, 1029 cm^{-1}.

HRMS (FAB), calcd for $C_{21}H_{27}N_2O_6$ (MH^+): 403.1869. Found: 403.1872.

Figure 71. ^1H NMR spectrum (300 MHz) ($CDCl_3$) of **66**

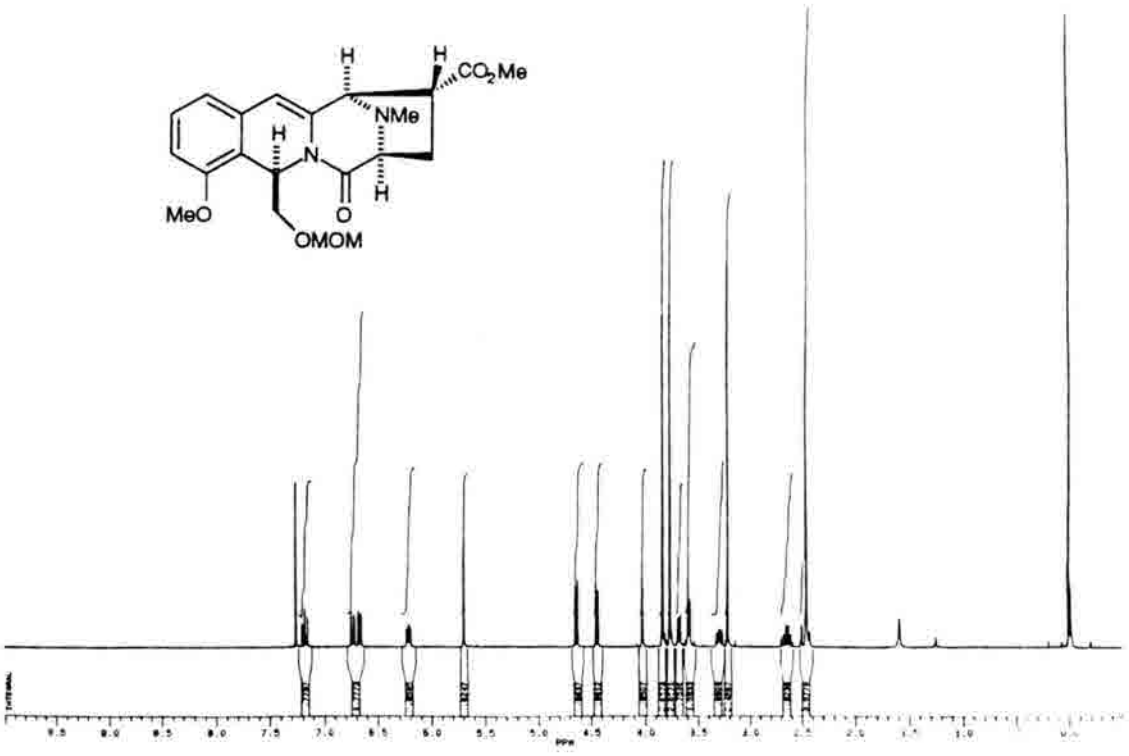

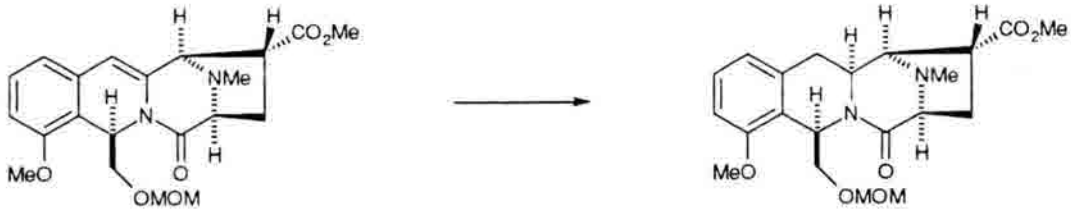

66 **68**-methyl ester

Methyl (5α,8β,10β,11β,11aβ)-5,7,9,10,11,11a,12-octahydro-4-methoxy-5-[(methyoxymethoxy)methyl]-13-methyl-7-oxo-8,11-iminoazepino[1,2-*b*]isoquinoline-10-carboxylate.

To a high pressure hydrogenation bomb was charged 21 mg (0.052 mmol) dissolved in 4 mL of absolute ethanol followed by 200 μL of a slurry of washed W2 Raney-Ni (Aldrich). The mixture was then subjected to high pressure hydrogenolysis (H_2, 1500 psi) for 20 h at 65°C. After cooling, the reaction mixture was then filtered through Celite and concentrated under reduced pressure. The crude mixture was then separated by PTLC (silica; 3:1 ethyl acetate/hexanes) affording 10 mg of pure **68**-methyl ester (R_f = 0.22). 45% Isolated yield.

^{1}H NMR (300 MHz) ($CDCl_3$) δ TMS: 2.29 (1 H, dd, J = 9.6 Hz, J = 13.1 Hz), 2.49 (3 H, s), 2.53 (1 H, dd, J = 2.3 Hz, J = 14.2 Hz), 2.57-2.65 (1 H, m), 2.96 (3 H, s), 3.14 (1 H, t, J = 13.5 Hz), 3.36 (1 H, dd, J = 6.8 Hz, J = 9.6 Hz), 3.53-3.57 (2 H, m), 3.65 (1 H, d, J = 2.6 Hz), 3.76 (3 H, s), 3.82 (3 H, s), 4.23 (1 H, dd, J = 3.0 Hz, J = 9.9 Hz), 4.29 (1 H, 1/2 ABq, J = 6.3 Hz), 4.42 (1 H, 1/2 ABq, J = 6.3 Hz), 5.61 (1 H, t, J = 2.4 Hz), 6.77 (2 H, t, J = 9.1 Hz), 7.18 (1 H, t, J = 7.9 Hz).

^{13}C NMR (300 MHz) ($CDCl_3$) δ: 32.12, 34.45, 37.01, 41.30, 49.37, 52.38, 54.30, 54.68, 55.31, 66.40, 67.10, 68.04, 96.26, 108.66, 119.50, 122.65, 127.85, 138.18, 155.67, 171.02, 174.93.

IR (NaCl): 2949, 1735, 1655, 1474, 1265, 1047 cm^{-1}.

HRMS (FAB), calcd for $C_{21}H_{29}N_2O_6$ (MH^+): 405.2026. Found: 405.2027.

Figure 72. ^{1}H NMR spectrum (300 MHz) ($CDCl_3$) of **68**-methyl ester

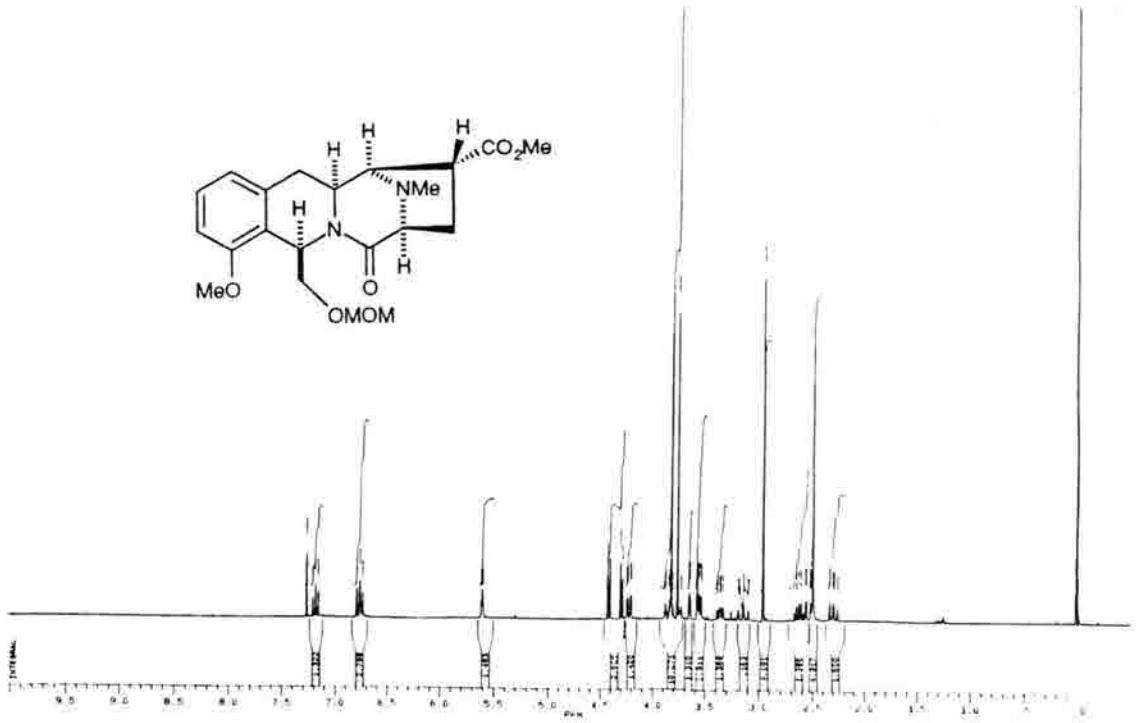

68-methyl ester **68**

(5α,8β,10β,11β,11aβ)-5,7,9,10,11,11a,12-Octahydro-4-methoxy-5-[(methyoxymethoxy)methyl]-13-methyl-7-oxo-8,11-iminoazepino[1,2-*b*]isoquinoline-10-carboxylic acid (68).

To a stirred solution of **68**-methyl ester (10 mg/0.025 mmol) dissolved in 0.5 mL of ethanol was added 0.8 mg (0.037 mmol) of lithum hydroxide in 20 μL of water. The resulting mixture stirred at room temperature for 1.5 h at which time the solution was diluted with water (5 mL), acidified to pH 5 with 1 N HCl (aq) and the mixture extracted 3 x 10 with dichloromethane. The extracts were combined, dried over Na_2SO_4 and concentrated to dryness in vacuo affording 10 mg of crude material. Quant. An aliquot was purified by PTLC (silica; 8:1 chloroform/methanol) producing a pure sample of **68** (R_f = 0.30). **^{1}H NMR** (300 MHz) ($CDCl_3$) δ TMS: 2.28 (1 H, t, J = 9.8 Hz), 2.45-2.53 (2 H, m), 2.54 (3 H, s), 2.92 (3 H, s), 3.11-3.20 (1 H, m), 3.25 (1 H, dd, J = 4.8 Hz, J = 9.6 Hz), 3.49-3.57 (2 H, m), 3.60 (1 H, br s), 3.81 (3 H, s), 3.84 (1 H, d, J = 9.0 Hz), 4.17 (1 H, dd, J = 2.8, J = 10.0 Hz), 4.26 (1 H, 1/2 ABq, J = 6.3 Hz), 4.36 (1 H, 1/2 ABq, J = 6.3 Hz), 5.60 (1 H, br s), 6.67 (1 H, d, J = 7.5 Hz), 6.75 (1 H, d, J = 8.3 Hz), 7.13 (1 H, t, J = 7.9 Hz). **^{13}C NMR** (300 MHz) (CDCl3) δ: 35.18, 49.41, 54.76, 55.34, 67.81, 96.28, 108.78, 119.55, 122.46, 128.12, 138.24, 155.67, 176.28, the rest of the signals were not assignable due to the dilute mixture. **IR** (NaCl): 3448, 2944, 1652, 1591, 1474, 1460, 1265, 1099, 917, 732 cm^{-1}. **HRMS** (FAB), calcd for $C_{20}H_{27}N_2O_6$ (MH^+): 391.1869. Found: 391.1877.

186 **251**

3-(Ethoxyacetylaminomethyl)-1-hydroxymethyl-(2,2'-carbonyl)-8-methoxydihydroisoquinoline (239).

To a stirred mixture of **186** (228 mg/0.922 mmol) dissolved in 9 mL of dichloromethane and cooled to 0°C was added 317 mg (2.77 mmol) of methanesulfonyl chloride followed by 466 mg (4.61 mmol) of triethylamine. The resulting mixture stirred at 0°C for 30 min. at which time 1.5 g (9.22 mmol) of 2-amino-2-methyl-1-propanol were added, the mixture allowed to warm to room temperature and stir for 18 h. The reaction mixture was then diluted with 20 mL of dichloromethane, washed with sat. $NaHCO_3$, dried over Na_2SO_4 and concentrated to dryness under reduced pressure affording crude **239** which was purified by flash chromotography (silica; 10:1 dichloromethane/methanol) affording 180 mg of **251**. 82% Yield.

^{1}H NMR (300MHz) ($CDCl_3$) δ TMS: 1.25 (3 H, t, *J* = 7.0 Hz), 1.37 (3 H, s), 1.38 (3 H, s), 3.60 (1 H, 1/2 ABq, *J* = 14.9 Hz), 3.80-3.86 (4 H, m), 3.98 (1 H, 1/2 ABq, *J* = 14.9 Hz), 4.10 (2 H, q, *J* = 5.1 Hz), 4.48 (1 H, dd, *J* = 9.2 Hz, *J* = 2.1 Hz), 4.99 (1 H, dd, *J* = 9.0 Hz, *J* = .1 Hz), 5.32 (1 H, dd, *J* = 9.4 Hz, *J* = 2.1 Hz), 5.93 (1 H, s), 6.71 (2 H, dd, *J* = 8.4 Hz, *J* = 2.9 Hz), 7.20 (1 H, *J* = 8.1 Hz).

^{13}C NMR (300 MHz) ($CDCl_3$) δ: 14.10, 49.41, 49.58, 54.66, 55.34, 60.66, 69.70, 109.68, 109.68, 111.79, 118.03, 129.31, 132.22, 135.50, 154.61, 154.94, 172.30. **IR** (NaCl): 2980, 1757, 1575, 1476, 1400, 1260, 1141, 1093, 1017, 747 cm^{-1}.

HRMS (CI), calcd for $C_{17}H_{20}N_2O_5$ (MH^+): 332.1372. Found: 332.1370.

251 **252**

***cis*-3-(*N*-Ethoxyacetyl)aminomethyl-1-hydroxymethyl-(2,2'-carbonyl)-8-methoxytetrahydroisoquinoline (252).**

To **251** (100 mg/0.301 mmol) dissolved in 7 mL of ethanol and purged with nitrogen was added 53 mg (0.301 mmol) of palladium chloride and the resulting mixture saturated with H_2. The reaction mixture then stirred at room temperature under 1 atm of H_2 for 16 h. The reaction mixture was then filtered through Celite and concentrated under reduced pressure. The residue was then redissolved in 25 mL of dichloromethane, washed with sat. $NaHCO_3$, dried over Na_2SO_4 and concentrated to dryness in vacuo affording 83 mg of **252**. 82% Yield.

^{1}H NMR (300 MHz) ($CDCl_3$) δ TMS: 1.28 (3 H, t, J = 7.3 Hz), 2.23 (1 H, br s), 2.75 (1 H, dd, J = 1.1 Hz, J = 16.6 Hz), 2.91-3.06 (2 H, m), 3.51-3.68 (2 H, m), 3.81 (3 H, s), 4.15-4.24 (3 H, m), 4.79 (1 H, t, J = 8.9 Hz), 5.02 (1 H, t, J = 7.7 Hz), 6.75 (2 H, dd, J = 3.2 Hz, J = 7.7 Hz), 7.21 (1 H, t, J = 8.0 Hz).

IR (NaCl): 2922, 1743, 1586, 1473, 1258, 1201, 1073 cm^{-1}.

HRMS (CI), calcd for $C_{17}H_{22}N_2O_5$ (MH^+): 334.1529. Found: 334.1524.

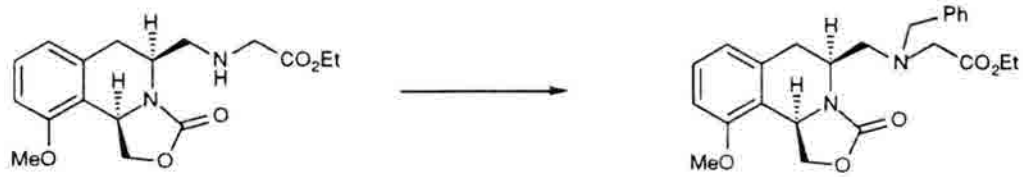

252 253

***cis*-3-(N-Benzyl-N-Ethoxyacetyl)aminomethyl-1-hydroxymethyl (2,2'-carbonyl)-8-methoxytetrahydroisoquinoline (253).**

To **252** (144 mg/0.431 mmol) dissolved in dichloromethane (4 mL) was added benzyl bromide (81 mg/0.474 mmol) followed by a solution of Na_2CO_3 in water. The resulting mixture was rufluxed with vigorous stirring for 5 h at which time the reaction was cooled to room temperature, dilluted with dichloromethane, washed with sat. $NaHCO_3$, dried over Na_2SO_4 and concentrated to dryness in vacuo affording 190 mg of crude material which was purified by PTLC (silica; 1:1 ethylacetate/hexanes) affording 94 mg of pure **253**. 54% Yield.

^{1}H NMR (300 MHz) ($CDCl_3$) δ TMS: 1.26 (3 H, t, *J* = 7.1 Hz), 2.83 (1 H, dd, *J* = 3.4 Hz, *J* = 15.7 Hz), 2.98-3.05 (2 H, m), 3.41 (2 H, d, *J* = 3.0 Hz), 3.53-3.57 (2 H, m), 3.80 (3 H, s), 3.96 (1 H, d, *J* = 13.9 Hz), 4.14 (2 H, q, *J* = 7.2 Hz), 4.25 (1 H, dd, *J* = 6.7 Hz, *J* = 8.9 Hz), 4.73 (1 H, dd, *J* = 8.3 Hz, *J* = 8.8 Hz), 4.90 (1 H, t, *J* = 7.5 Hz), 6.69 (1 H, d, *J* = 7.6 Hz), 6.73 (1 H, d, *J* = 8.2 Hz), 7.18 (1 H, t, *J* = 7.7 Hz), 7.24-7.36 (5 H, m).

IR (NaCl): 2972, 2839, 1750, 1586, 1473, 1383, 1258, 1189, 1070 cm^{-1}.

HRMS (FAB), calcd for $C_{24}H_{29}N_2O_5$ (MH^+): 425.2076. Found: 425.2080.

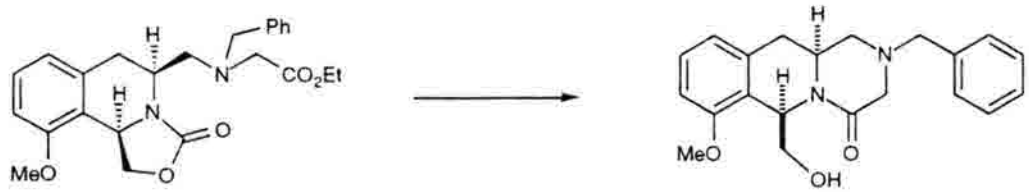

253 254

(6α,11aα)-2-Aza-2-benzyl-6-hydroxymethyl-7-methoxy-4-oxo-1,3,4,6,11,11a-tetrahydro-2*H*-benzo[*b*]quinolizine (254).

To a stirred solution of **253** (380 mg/).895 mmol) dissolved in 45 mL of ethanol was added 4.5 mL of 2 M LiOH (aq), the reaction purged with nitrogen, then heated at reflux for 24 h. After cooling to 0°C, the pH of the reaction was adjusted to 5 with 6 N HCl and the reaction mixture concentrated under reduced pressure. The residue was then redissolved in 15 mL of DMF and the reaction cooled to 0°C. To this solution was then added 145 mg (1.07 mmol) of N-hydroxybenzatriazole followed by 145 mg (1.07 mmol) of DCC, the mixture stirred at 0°C for 1 h then at room temperature for an additional 18 h at which time the reaction mixture was concentrated under reduced pressure. The residue was redissolved in dichloromethane and washed with sat. $NaHCO_3$, dried over Na_2SO_4 and concentrated to dryness in vacuo. The crude material was then purified by flash chromatography (silica; 10:1 dichloromethane/methanol) affording 190 mg of pure **254**. 60% Yield.

^{1}H NMR (300 MHz) ($CDCl_3$) δ TMS: 2.37 (1 H, t, J = 10.8 Hz), 2.58 (1 H, dd, J = 2.4 Hz, J = 14.7 Hz), 2.81 (1 H, t, J = 12.3 Hz), 3.02 (1 H, d, J = 10.7 Hz), 3.13 (1 H, d, J = 16.7 Hz), 3.50-3.64 (5 H, m), 3.81 (3 H, s), 3.95 (1 H, br s), 5.83 (1 H, dd, J = 3.0 Hz, J = 7.0 Hz), 6.70 (1 H, d, J = 7.5 Hz), 6.78 (1 H, d, J = 8.3 Hz), 7.26-7.34 (5 H, m).

^{13}C NMR (300 MHz) ($CDCl_3$) δ: 33.20 (t), 52.81 (d), 55.10 (d), 55.19 (q), 55.33 (t), 57.35 (t), 61.47 (t), 68.31 (t), 108. 95 (d), 119.55 (d), 121.78 (s), 127.43 (d), 128.14 (d), 128.34 (d), 128.34 (d), 128.88 (d), 128.88 (d), 136.71 (s), 136.83 (s), 155.72 (s), 170.04 (s).

IR (NaCl): 3383, 2935, 1627, 1475, 1452, 1422, 1396, 1341, 1264, 1076, 735 cm^{-1}.

HRMS (FAB), calcd for $C_{21}H_{25}N_2O_3$ (MH^+): 353.1865. Found: 353.1881.

254 **255**

(6α,11aα)-2-Aza-2-benzyl-6-hydroxymethylmethoxymethyl-7-methoxy-4-oxo-1,3,4,6,11,11a-tetrahydro-2*H*-benzo[*b*]quinolizine (255).

To a stirred solution of **254** (54 mg/0.153 mmol) dissolved in 3 mL of dichloromethane was added 40 mg (0.306 mmol) of N,N-diisopopylethylamine followed by 19 mg (0.23 mmol) of chloromethyl methylether and the resulting mixture stirred at room temperature for 24 h. After concentrating to room temperature, the residue was separated by flash chromatography (silica; 3:1 ethyl acetate/hexanes) affording 138 mg of pure **255**. 67% Yield.

^{1}H NMR (300 MHz) ($CDCl_3$) δ TMS: 2.33 (1 H, t, *J* = 10.7 Hz), 2.51 (1 H, dd, *J* = 2.5 Hz, *J* = 14.2 Hz), 2.96-3.09 (3 H, m), 2.97 (3 H, s), 3.50-3.66 (5 H, m), 3.80 (3 H, s), 4.19 (1 H, dd, *J* = 3.2 Hz, *J* = 10.0 Hz), 4.28 (1 H, 1/2 ABq, *J* = 6.4 Hz), 4.39 (1 H, 1/2 ABq, *J* = 6.4 Hz), 5.70 (1 H, t, *J* = 2.52 Hz), 6.69 (1 H, d, *J* = 7.5 Hz), 6.76 (1 H, d, *J* = 7.4 Hz), 7.15 (1 H, t, *J* = 7.9 Hz), 7.26-7.32 (5 H, m). See Figure 27.

^{13}C NMR (300 MHz) ($CDCl_3$) δ: 33.58(t), 50.10 (d), 54.21 (d), 54.60 (q), 55.24 (q), 55.70 (t), 57.71 (t), 61.67 (t), 67.95 (t), 95.98 (t), 108.56 (d), 119.27 (d), 122.78 (s), 127.34 (d), 127.70 (d), 128.33 (d), 128.33 (d), 128.88 (d), 128.88 (d), 136.95 (s), 138.08 (s), 155.60 (s), 167.38 (s).

IR (NaCl): 2937, 2879, 2826, 1547, 1475, 1420, 1265, 1149, 1071, 1043 cm^{-1}.

HRMS (FAB), calcd for $C_{23}H_{29}N_2O_4$ (MH^+): 397.2127. Found: 397.2115.

255 **256**

(6α,11aα)-2-Aza-6-hydroxymethylmethoxymethyl-7-methoxy-4-oxo-1,3,4,6,11,11a-tetrahydro-2*H*-benzo[*b*]quinolizine (256).

To a stirred solution of **255** (79 mg/0.199 mmol) dissolved in 6 mL of methanol and purged with nitrogen was added 106 mg of 5% palladium on carbon, the reaction mixture saturated with H_2 and the reaction stirred under 1 atm of H_2 for 3 h. The reaction mixture was then filtered through Celite and concentrated to dryness in vacuo affording 60 mg of pure **256**. 98% Yield.

^{1}H NMR (300 MHz) ($CDCl_3$) δ TMS: 2.59 (1 H, dd, *J* = 2.7 Hz, *J* = 14.3 Hz), 2.91-3.06 (1 H, m), 2.98 (3 H, s), 3.22 (1 H, dd, *J* = 2.5 Hz, *J* = 12.7 Hz), 3.48 (1 H, dd, *J* = 10.2 Hz, *J* = 12.2 Hz), 3.51-3.67 (3 H, m), 3.82 (3 H, s), 4.17 (1 H, dd, *J* = 3.3 Hz, *J* = 10.1 Hz), 4.31 (1 H, 1/2 ABq, *J* = 6.4 Hz), 4.42 (1 H, 1/2 ABq, *J* = 6.4 Hz), 5.77 (1 H, t, *J* = 2.9 Hz), 6.73 (1 H, d, *J* = 7.5 Hz), 6.78 (1 H, d, *J* = 8.3 Hz), 7.18 (1 H, t, *J* = 7.8 Hz).

^{13}C NMR (300 MHz) ($CDCl_3$) δ: 33.36 (t), 49.64 (t), 49.82 (d), 50.20 (t), 54.64 (q), 55.30 (q), 55.73 (d), 68.18 (t), 96.02 (t), 108.64 (d), 119.28 (d), 122.82 (s), 127.82 (d), 137.76 (s), 155.64 (s), 168.23 (s).

IR (NaCl): 3316, 2941, 2903, 2839, 1641, 1475, 1265, 1149, 1052 cm^{-1}.

HRMS (FAB), calcd for $C_{16}H_{23}N_2O_4$ (MH^+): 307.1658. Found: 307.1645.

256 **257**

(6α,11aα)-2-Aza-6-hydroxymethylmethoxymethyl-7-methoxy-2-methyl-4-oxo-1,3,4,6,11,11a-tetrahydro-2*H*-benzo[*b*]quinolizine (257).

To a stirred mixture of **256** (30 mg/0.098 mmol) dissolved in 4 mL of acetonitrile was added 19 mg (0.147 mmol) of N,N-diisopropylethylamine followed by 17 mg (0.118 mmol) of iodomethane and the resulting mixture stirred at room temperature for 4 h. The reaction mixture was dilluted with dichloromethane, washed with sat. $NaHCO_3$, dried over Na_2SO_4 and concentrated to dryness in vacuo affording 18 mg of **257** following purification by PTLC (silica; 3:1 ethyl acetate/hexanes). 60% Yield.

^{1}H NMR (300 MHz) ($CDCl_3$) δ TMS: 2.35 (3 H, s), 2.57 (1 H, dd, *J* = 2.6 Hz, *J* = 14.2 Hz), 2.93-3.07 (2 H, m), 2.99 (3 H, s), 3.54 (1 H, dd, *J* = 1.6 Hz, *J* = 16.4 Hz), 3.64 (1 H, dd, *J* = 2.4 Hz, *J* = 10.1 Hz), 3.82 (3 H, s), 4.18 (1 H, dd, *J* = 3.2 Hz, *J* = 10.0 Hz), 4.29 (1 H, 1/2 ABq, *J* = 6.4 Hz), 4.40 (1 H, 1/2 ABq, *J* = 6.4 Hz), 5.70 (1 H, br s), 6.73 (1 H, d, *J* = 7.6 Hz), 6.78 (1 H, d, *J* = 8.3 Hz), 7.18 (1 H, t, *J* = 8.0 Hz). See Figure 28.

IR (NaCl): 2939, 2885, 2840, 2782, 1646, 1475, 1265, 1150, 1050, 918, 733 cm^{-1}.

Figure 73. ^{1}H NMR spectrum (300 MHz) ($CDCl_3$) of **255**

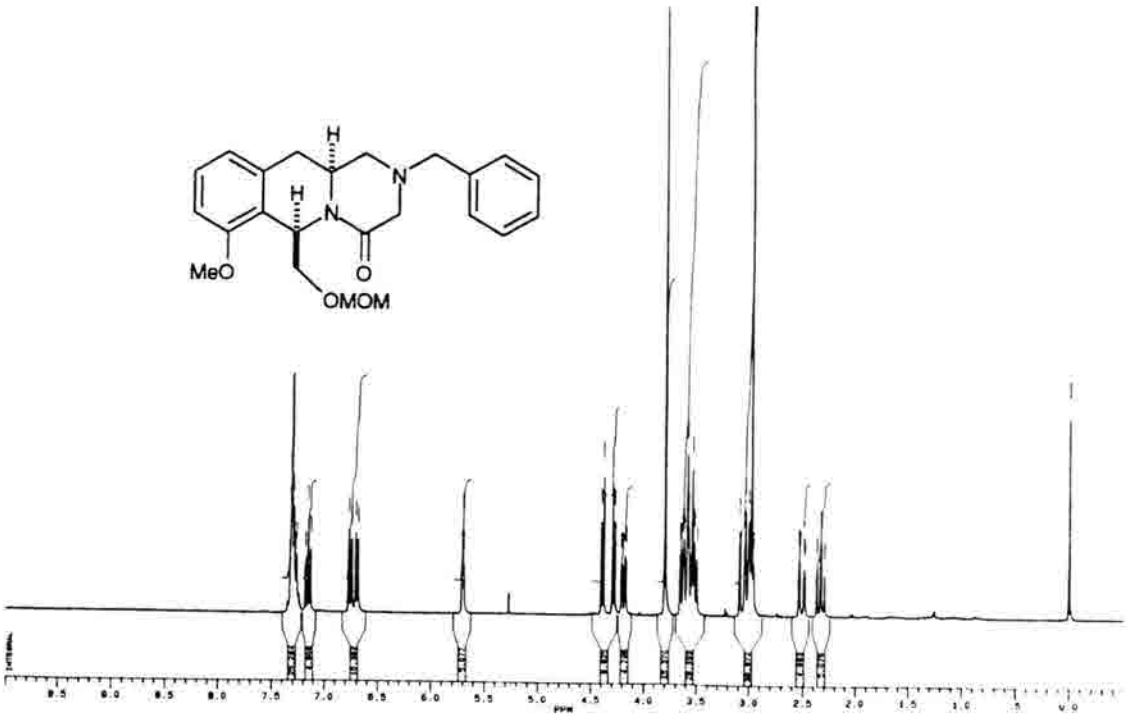

Figure 74. ^{1}H NMR spectrum (300 MHz) ($CDCl_3$) of **257**

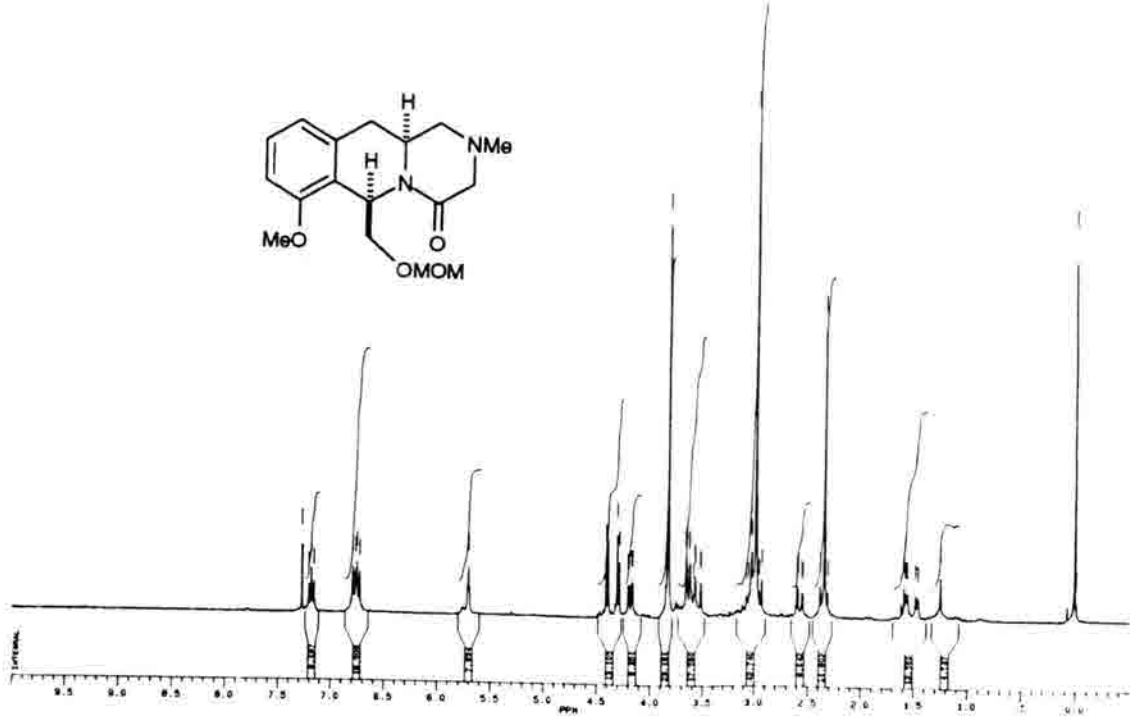

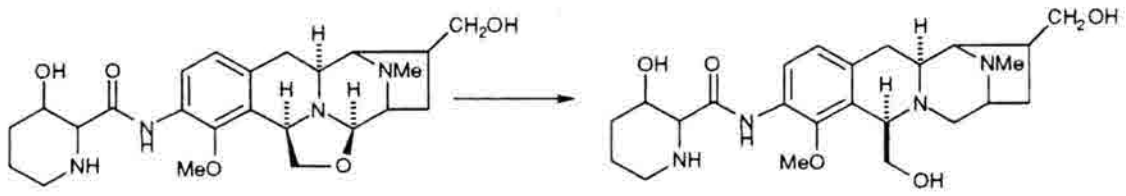

20 **301**

Tetrazominol (301).

To a stirred solution of tetrazomine (**20**) (8 mg/0.017 mmol) dissolved in 1 mL of methanol and cooled to 0°C was added 6.4 mg (0.170 mmol) of sodium borohydride and the resulting mixture stirred at 0°C for 3 h. The reaction was then quenched with sat. NH_4Cl (aq.) then basefide with sat. $NaHCO_3$ (aq.) and concentrated under reduced pressure. The residue was triturated with isopropanol, filtered through Celite and concentrated to dryness in vacuo affording 7 mg of **301**. 95% Yield.

^{1}H NMR (300 MHz) (D_2O) δ HOD: 1.63-1.94 (5 H, m), 2.24 (1 H, t, *J* = 11.4 Hz), 2.48 (1 H, d, *J* = 14.1 Hz), 2.57 (1 H, q, *J* = 11.5 Hz), 2.79-2.89 (5 H, m), 2.96 (1 H, d, *J* = 16.3 Hz), 3.00 (1 H, d, *J* = 12.9 Hz), 3.18 (1 H, br. s), 3.36 (1 H, d, *J* = 13.8 Hz), 3.53-3.68 (5 H, m), 3.60 (3 H, s), 3.84-3.90 (2 H, m), 4.17 (1 H, d, *J* = 1.8 Hz), 4.56 (1 H, s), 6.89 (1 H, d, *J* = 8.2 Hz), 7.33 (1 H, d, *J* = 8.2 Hz).

HRMS (CI), calcd for $C_{24}H_{36}N_4O_5$ (MH+): 460.2696. Found: 460.2696.

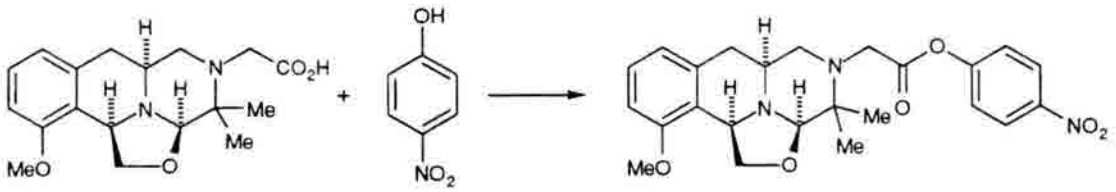

160 **305** **306**

4α,6α,11aα-2-Aza-3,3-dimethyl-1,3,4,6,11,11a-hexahydro-2-(4-nitrophenoxyacetyl)-7-methoxy-5,4-oxazolo-2-*H*-benzo[*b*]quinolizine (306).

To a stirred mixture of **160** (7.0 mg/0.021 mmol) and *para*-nitrophenol (**305**) (3.2 mg/0.023 mmol) in 2 mL of dry dichloromethane and cooled to 0°C was added 5 mg (0.023 mmol) of 1,3-dicyclohexylcarbodiimide (Aldrich). The resulting mixture stirred at 0°C for 1 h, then warmed to 25°C and stirred for an additional 10 h. The reaction mixture was then concentrated under reduced pressure and the residue purified by PLC (silica; 1:1 ethylacetate/hexanes) affording 6 mg of *para*-nitrophenylester **306** (R_f = 0.79). 63% Yield. **^{1}H NMR** (300MHz) ($CDCl_3$) δ TMS: 1.05 (3 H, s), 1.30 (3 H, s), 2.57 (1 H, t, *J* = 11.3 Hz), 2.78 (1 H, dd, *J* = 9.8 Hz, *J* = 7.0 Hz), 2.89 (1 H, d, *J* = 4.1 Hz), 2.96-3.05 (2 H, m), 3.33 (1 H, 1/2 ABq, *J* = 17.3 Hz), 3.55-3.68 (2 H, m), 3.75 (1 H, s), 3.78 (3 H, s), 3.89 (1 H, 1/2 ABq, *J* = 17.3 Hz), 4.57 (1 H, t, *J* = 5.9 Hz), 6.68 (1 H, d, *J* = 8.1 Hz), 6.78 (1 H, d, *J* = 7.7 Hz), 7.16 (1 H, t, *J* = 7.9 Hz), 7.33 (2 H, d, *J* = 9.1 Hz), 8.29 (2 H, d, *J* = 9.0 Hz).

^{13}C NMR (300MHz) ($CDCl_3$) δ: 11.19, 24.17, 32.83, 33.93, 51.06, 51.33, 53.41, 55.28, 57.41, 58.49, 71.10, 94.94, 107.58, 121.30, 122.27, 123.16, 125.22, 125.22, 127.58, 135.62, 145.31, 155.24, 156.08, 169.66.

IR (NaCl): 2933, 1781, 1582, 1523, 1471, 1346, 1258, 1208, 1104, 913, 853, 728 cm^{-1}.

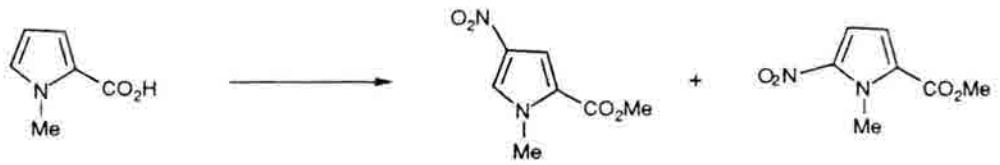

307 **308** **309**

Methyl 1-methyl-4-nitropyrrole-2-carboxylate (308).

To a slurry of 1-methyl-2-pyrrolecarboxylic acid (10 g/0.080 mol) in 60 mL of acetic anhydride and cooled to -10°C was added dropwise over a 15 min period an ice-bath cooled solution of 8 mL of 70% HNO_3 in 40 mL of acetic anhydride. The resulting mixture stirred at -10°C for 30 min. at which time it was poured onto ice. After stirring for 2 h the mixture was then extracted 2 x 50 mL with dichloromethane, dried over Na_2SO_4 and concentrated under reduced pressure. The residue was then redisssolved in 100 mL of methanol and 10 mL of concentrated H_2SO_4 added. The resulting mixture was heated to reflux for 12 h, cooled to room temperature and concentrated to 1/3 its original volume. Water (50 mL) was added and the mixture extracted 2 x 50 mL with chloroform, the extracts combined, dried over Na_2SO_4 and concentrated to dryness in vacuo affording 8 g of crude material which was purified by flash chromotography (silica; 4:1 hexanes/ethylacetate) affording 4 g of pure **308** (R_f = 0.25). 30% Yield.

^{1}H NMR (300MHz) ($CDCl_3$) δ TMS: 3.87 (3H, s), 4.00 (3H, s), 7.42 (1H, d, *J* = 1.9Hz), 7.60 (1H, d, *J* = 2.0Hz).

IR (NaCl): 3252, 3146, 1708, 1499, 1317, 1255, 1195, 1117, 751 cm^{-1}.

308 **310**

1-methyl-4-nitropyrrole-2-carboxylchloride (311).

To a stirred solution of **308** (385 mg/2.09 mmol) in 6 mL of ethanol was added 2.1 mL of 2M LiOH (aq) and the resulting mixture stirred at room temperature for 2 h. The reaction mixture was then acidified with 1 N HCl (aq) and extracted 3 x 20 mL with dichloromethane. The dichloromethane extracts were then combined, dried over Na_2SO_4 and concentrated to dryness in vacuo affording 322 mg of the crude intermediate carboxylic acid. This material was then suspended in 10 mL of dichloromethane, 1 drop of DMF and was followed by 288 mg (2.27 mmol) of oxalyl chloride. The resulting mixture stirred at room temperature for 2 h at which time the reaction mixture was concentrated under reduced pressure producing 356 mg of acid chloride **310** as an amber oil. 91% Yield.

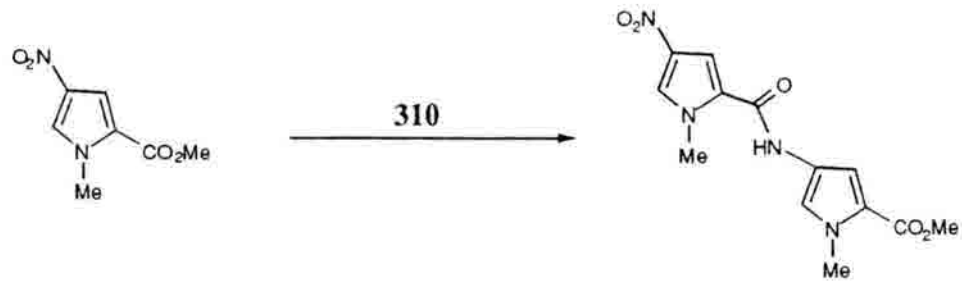

308 **311**

***Di*-pyrrolecarboxamide methyl ester (311).**

To a stirred solution of **308** (289 mg/1.57 mmol) in 3.5 mL of DMF and purged with nitrogen was added 87 mg of 5% Pd on carbon and the mixture saturated with H_2. The resulting mixture then stirred at room temperature under 1atm. of H_2 for 16h. At this time the reaction mixture was filtered through Celite into a solution of acid chloride **310** (356 mg/1.89 mmol) in 10 mL of dichloromethane and the filter cake washed with 5 mL of 1:1 DMF/water. To the new reaction mixture was then added 400 mg (4.76 mmol) of sodium bicarbonate and the resulting mixture stirred vigorously at room temperature for 18 h. The layers were then separated, the organic layer washed with 5 mL of sat. brine, dried over Na_2SO_4 and concentrated to dryness in vacuo. The residue was then separated by flash chromotography (silica; 1:1 ethylacetate/hexanes) affording 200 mg of **311**. 42% Yield.

^{1}H NMR (300 MHz) (DMSO-D6) δ TMS: 3.73 (3H, s), 3.83 (3H, s), 3.94 (3H, s), 6.88 (1H, s), 7.44 (1H, s), 7.54 (1H, s), 8.17 (1H, s), 10.25 (1H, s).

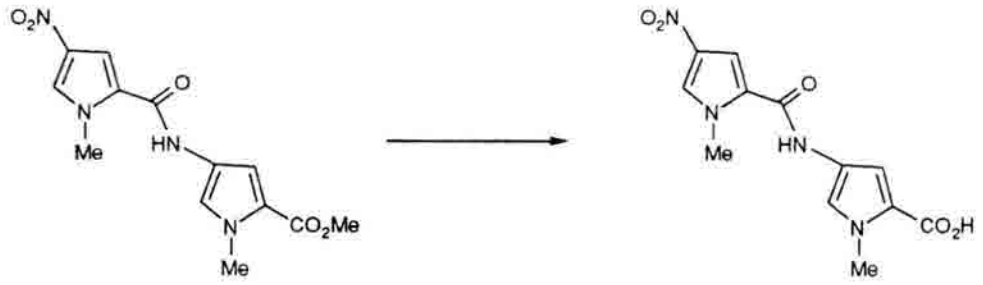

311 **312**

***Di*-Pyrrolecarboxamide (312).**

To a suspension of **311** (125 mg/0.408 mmol) in 8 mL of 1:1 ethanol/water was added 80 mg (2.0 mmol) of sodium hydroxide and the reaction mixture heated to reflux for 30 min. at which time the reaction mixture became homogeneous. The reaction mixture was then cooled to room temperature and acidified with 6 N HCl (aq). The precipitate that formed was filtered off and washed with 1:1 methanol/water and dried affording 107 mg of acid **313**. 90% Yield. Material carried on without further purification.

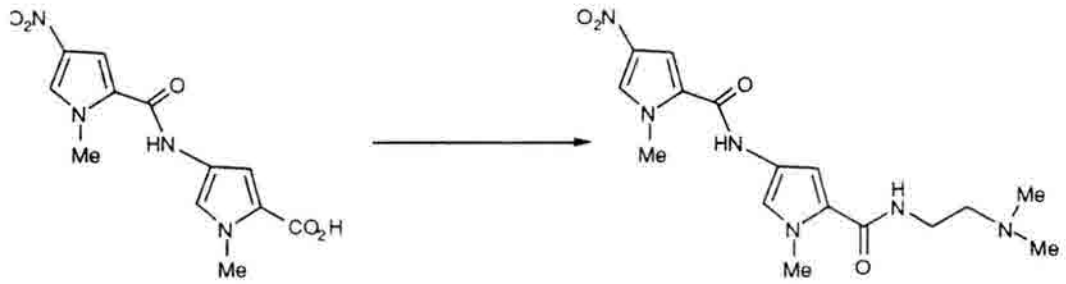

312 **313**

Dimethylethylenediamine-di-pyrrolecarboxamide (313).

To a stirred solution of **312** (100 mg/0.342 mmol) in 2 mL of DMF and cooled to 0°C was added 33 mg (0.376 mmol) of N,N-dimethylethylenediamine followed by 51 mg (0.376 mmol) of N-hydroxybenzatriazole and 78 mg (0.376 mmol) of 1,3-dicyclohexylcarbodiimide. The resulting mixture stirred at 0°C for 1 h followed by stirring at room temperature for 16 h. The reaction mixture was then concentrated under reduced pressure at 35°C and the resulting residue purified by flash chromatography (silica; 3% conc. NH_4OH in methanol) affording 121 mg of **313**. 98% Yield.

^{1}H NMR (300 MHz) (DMSO-d6) δ TMS: 2.18 (6 H, s), 2.38 (2 H, t, J = 6.8 Hz), 3.26 (2 H, q, J = 6.5 Hz), 3.79 (3 H, s), 3.93 (3 H, s), 6.82 (1 H, s), 7.19 (1 H, s), 7.55 (1 H, d, J = 1.7 Hz), 7.93 (1 H, t, J = 5.0 Hz), 8.15 (1 H, s), 10.24 (1 H, s).

^{13}C NMR (300 MHz) ($CDCl_3$) δ: 36.13 (q), 36.13 (q), 36.58 (t), 37.56 (q), 45.20 (q), 58.29 (t), 104.10 (d), 107.63 (d), 118.14 (d), 121.42 (s), 123.23 (s), 126.37 (s), 128.29 (d), 133.88 (s), 156.96 (s), 161.18 (s).

IR (NaCl): 3288, 3130, 2938, 2857, 2821, 2784, 1636, 1575, 1537, 1505, 1463, 1438, 1420, 1402, 1310, 1257, 1208, 1113, 814, 751, 731 cm^{-1}.

Anal. calcd for $C_{16}H_{22}N_6O_4$: C, 53.03; H, 6.12; N, 23.19. Found: C, 53.28; H, 6.18; N, 23.17.

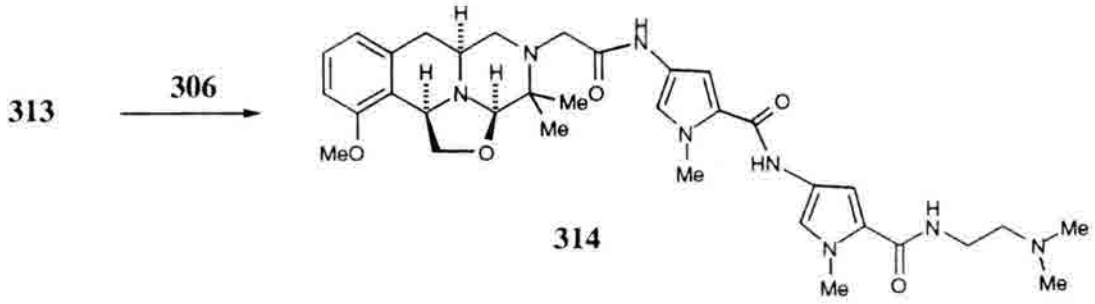

314

Netropsin conjugate (314).

To a stirred solution of **313** (8 mg/0.023 mmol) in 0.5 mL of DMF and degassed with nitrogen was added 5 mg (0.002 mmol Pd) of 5% palladium on carbon (Aldrich) and the resulting mixture saturated with hydrogen. The mixture then stirred at 25°C under 1 atmosphere of hydrogen for 24 h. The reaction mixture was then filtered through Celite into a solution of **306** (7 mg/0.015 mmol) dissolved in 0.5 mL of DMF and the filter cake washed with an additional 2 mL of DMF. To the reaction mixture was then added 7 mg (0.069 mmol) of triethylamine and the resulting solution stirred at 25°C for 7 h. The reaction mixture was then concentrated under reduced pressure and the residue purified by PLC (silica; 3% conc. NH_4OH in methanol) affording 7 mg of netropsin conjugate **314** ($R_f = 0.58$). 47% Yield.

^{1}H NMR (300 MHz) ($CDCl_3$) δ TMS: 1.04 (3 H, s), 1.22 (3 H, s), 2.25 (6 H, s), 2.47 (2 H, t, *J* = 5.8 Hz), 2.51 (1 H, dd, *J* = 8.2 Hz, *J* = 2.3 Hz), 2.74-2.92 (4 H, m), 3.43 (2 H, q, *J* = 5.5 Hz), 3.54-3.69 (5 H, m), 3.79 (3 H, s), 3.91 (3 H, s), 3.94 (3 H, s), 4.58 (1 H, t, *J* = 6.2 Hz), 6.53 (1 H, br. s), 6.57 (1 H, d, *J* = 1.9 Hz), 6.69 (1 H, d, *J* = 8.2 Hz), 6.73 (1 H, d, *J* = 1.8 Hz), 6.78 (1 H, d, *J* = 7.6 Hz), 7.13-7.17 (3 H, m), 7.61 (1 H, s), 9.08 (1 H, s).

^{13}C NMR (300 MHz) ($CDCl_3$) δ: 11.84, 24.04, 32.71, 36.52, 36.58, 36.68, 36.68, 45.16, 51.81, 52.86, 55.31, 57.56, 57.84, 58.49, 71.29, 77.20, 95.74, 103.23, 103.27, 107.68, 118.53, 118.91, 120.99, 121.08, 121.27, 122.89, 123.29, 123.67, 127.71, 135.36, 156.03, 158.82, 161.66, 168.87.

IR (NaCl): 3292, 2937, 2831, 2769, 1650, 1582, 1532, 1469, 1435, 1405, 1260, 1103, 1034, 775 cm^{-1}.

HRMS (FAB), calcd for $C_{34}H_{47}N_8O_5$ (MH^+): 647.3669. Found: 647.3622.

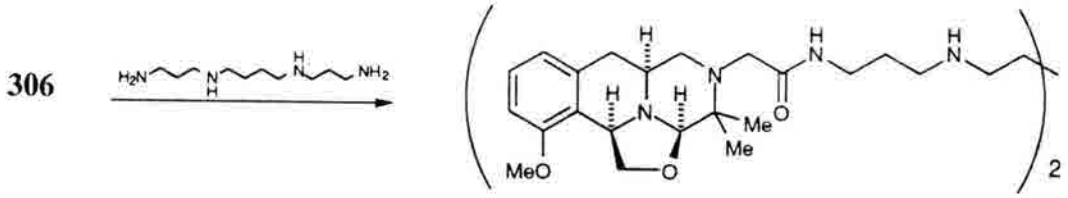

315

Spermine dimer (315).

To a stirred solution of **306** (9 mg/0.020 mmol) dissolved in 1 mL of DMF and cooled to 0°C was added 2 mg (0.010 mmol) of spermine (Aldrich) followed by 6 mg (0.060 mmol) of triethylamine and the resulting mixture stirred at 4°C for 15 h. The reaction mixture was then concentrated under reduced pressure and the residue separated by PTLC (silica; 10% conc. NH_4OH in methanol) affording 4 mg of spermine dimer **315** (R_f = 0.49). 20% yield.

^{1}H NMR (300 MHz) ($CDCl_3$) δ TMS: 0.99 (6 H, s), 1.17 (2 H, s), 1.51 (4 H, br. s), 1.65-1.72 (4 H, m), 2.46 (2 H, dd, *J* = 9.3 Hz, *J* = 2.3 Hz), 2.59-2.75 (10 H, m), 2.82-2.91 (8 H, m), 3.36 (4 H, q, *J* = 6.1 Hz), 3.42-3.67 (8 H, m), 3.63 (2 H, s), 3.78 (6 H, s), 4.56 (2 H, t, *J* = 6.3 Hz), 6.69 (2 H, d, *J* = 8.2 Hz), 6.77 (2 H, d, *J* = 7.7 Hz), 7.16 (2 H, t, *J* = 8.0 Hz), 7.60 (2 H, br. s).

^{13}C NMR (300 MHz) ($CDCl_3$) δ: 11.54, 24.07, 27.95, 30.08, 32.76, 37.12, 47.43, 50.02, 51.69, 52.70, 55.20, 55.30, 57.29, 58.52, 71.20, 95.62, 107.61, 121.27, 122.96, 127.66, 135.46, 156.03, 171.52.

IR (NaCl): 3313, 2933, 2831, 1660, 1581, 1519, 1470, 1259, 1177, 1105, 1087, 953 cm^{-1}.

HRMS (FAB), calcd for $C_{46}H_{71}N_8O_6$: 831.5500. Found: 831.5504.

References

1. Kluepfel, D., Baker, H.A., Piattoni, G., Sehgal, S.N., Sidorowitz, A., Singh, K., and Vezina, C. *J. Antibiot.*, **1975**, *7*, 497.
2. a) Sygusch, J., Brisse, F., Hanessian, S. and Kluepfel, D. *Tetrahedron Lett.* **1974**, 4021. b) Sygusch, J., Brisse, F. and Hanessian, S. *Acta, Cryst.* **1976**, *B32*, 1139.
3. a) Zmijewski, M.J., Miller-Hatch, K. and Goebel, M. *Antimicrob. Agents Chemother.* **1982**, *21*, 787. b) Ishiguro, K., Takahoshi, K., Yazawa, K., Sakiyama, S. and Arai, T. *J. Biol. Chem.* **1981**, *256*, 2162.
4. a) Hayashi, T., Noto, T., Nawata, Y., Okazaki, H., Sawada, M. and Ando, K. *J. Antibiot.* **1982**, *35*, 771. b) Zwijewski, M.J. and Goebel, M. *J. Antibiot.* **1982**, *35*, 524.
5. Arora, S.J. and Cox, M.B. *J. Biomolecular Struc. & Dynamamics* **1988**, *6*, 489.
6. a) Goss, W.A., Deitz, T.M. and Cook, T.M. *J. Bact.* **1964**, *88*, 1112. b) Goss, W. A., Deitz, T.M. and Cook, T.M. *J. Bact.* **1965**, *89*, 1068.
7. Szybalski, W. and Iyer, V.N. *Federation Proc.* **1964**, *23*, 946.
8. Zaccardi, J., Mahender, A., Ashcroft, J., Bernan, V., Korshalla, J.D., Morton, G.O., Siegel, M., Tsao, R., Williams, D.R., Maiese, W. and Ellestad, G.A. *J. Org. Chem.* **1994**, *59*, 4045.
9. a) Arai, T., Takahashi, K. and Kubo, A. *J. Antibiot.* **1977**, *30*, 1015. b) Arai, T., Takahashi, K., Ishiguro, K. and Yazawa, K. *J. Antibiot.* **1980**, *33*, 951.
10. Ishiguro, K., Takahashi, T., Yazawa, K., Sakiyama, S. and Arai, T. *J. Biol. Chem.* **1981**, *256*, 2162.

11. a) Lown, W.J., Joshua, A.V. and Lee, J.S. *Biochemistry* **1982**, *21*, 419. b) Lown, W.J. *Mol. Cell. Biochem.* **1983**, *55*, 17.

12. a) Lown, W.J., Sim, S.-K., Majumdar, K.C. and Chang, R.-Y. *Biochem. Biophys. Res. Commun.* **1977**, *76*, 705. b) Bachur, N.R., Gordon, S.L. and Gee, M.V. *Cancer Res.* **1977**, *38*, 1745.

13. a) Graf, E., Mahoney, J.R., Bryant, R.G. and Eaton, J.W. *J. Biol. Chem.* **1984**, *259*, 3620 . b) Graf, E., Empson K.L. and Eaton, J.W. *J. Biol. Chem.* **1987**, *262*, 11647. c) Ursini, F., Mariorino, M., Hochstein, P. and Ernster, L. *Free Radical Biol. and Med.* **1989**, *6*, 31. d) Halliwell, B. , Gutteridege, J.M.C. , Aruoma, O.I., *Analytical Biochem.* **1987**, *165*, 215. e) Walling, C. *Acc.Chem.Res.* **1975**, *8*, 125. f) Sutton, H.C. and Winterbourn, C.C. *Free Radical Biol. and Med.* **1989**, *6*, 53. g) Lesko, S.A. , Lorentzen R.J. and Ts'o, P.O.P.*Biochemistry* **1980**, *19*, 3023. h) Myers, C. , Gianni, L. , Zweier, J., Muindi, J., Sinha, B.K. and Eliot, H. *Federation Proc.* **1986**, *45*, 2792.

14. a) Tomita, F., Takahashi, K. and Shimizu, K. *J. Antibiotics* **1983**, *36*, 463. b) Takahashi, K. and Tomita, F. *J. Antibiotics* **1983**, *36*, 468. c) Hirayama, M.and Shirahata, K.*J. Chem. Soc. Perkin Trans I* **1983**, 1705.

15. a) Jett, J.R., Saijo, N., Hong, W-S., Sasaki, Y., Takahashi, H., Nakano, H., Nakagawa, K., Sakurai, M., Suemasu, K. and Tesada, M. *Investigational New Drugs* **1987**, *5*, 155. b) Chiang, C-D., Kanzawa, F., Matsushima, Y., Nakano, H., Nakagawa, K., Takahashi, H., Terada, M., Morinaga, S., Tsuchiya, R., Sasaki, Y. and Saijo, N. *J. Pharmacobio-Dyn.* **1987**, *10*, 431. c) Fujimoto, K., Oka, T. and Morimoto, M. *Cancer Research* **1987**, *47*, 1516.

16. a) Suzuki, K., Sato, T., Morioka, M., Nagai, K., Abe, K., Yamaguchi, H., Saito, T., Ohmi, Y. and Susaki, K. *J. Antibiot.*, **1991**, *44*, 479. b) Sato, T., Hirayama, F. and Saito, T. *J. Antibiot.*, **1991**, *44*, 1367.

17. Hill, C.G., Wunz, T.P. and Remers, W.A. *J. Computer-Aided Mol. Design*, 2 **1988**, 91.

18. Danishefsky, S. J., Harrison, P. J., Webb, R. R. and O'Neill, B. T. *J. Am. Chem. Soc.* **1985**, *107*, 1421.

19. Nicolaou, K.C., Claremon, D.A., Barnette, W.E. and Seitz, S.P. *J. Am. Chem. Soc.* **1979**, *101*, 3704.

20. Williams, R.M., Ehrlich, P.P, Zhai, W. and Hendrix, J. *J. Org. Chem.* **1987**, *52*, 2615.

21. Ehrlich, P.P., "Synthetic and Pharmacophoric Studies of Quinocarcin", Ph.D. Dissertation **1990**, Colorado State University.

22. Fukuyama, T. and Nunes, J. J. *J. Am. Chem. Soc.* **1988**, *110*, 5196.

23. a) Garner, P., Ho, W. B. and Shin, H. *J. Am. Chem. Soc.* **1992**, *114*, 2767. b) Garner, P., Ho, W. B. and Shin, H. *J. Am. Chem. Soc.* **1993**, *115*, 10742.

24. a) Garner, P., Suitha, K., Ho, W.B., Youngs, W.J., Kennedy, V.O. and Djebli, A. *J. Org. Chem.* **1989**, *54*, 2041. b) Garner, P. and Ho, W.B. *J. Org. Chem.* **1990**, *55*, 3973. c) Garner, P., Ho, W.B., Grandhee, S.K., Youngs, W.J. and Kennedy, V.O. *J. Org. Chem.* **1991**, *56*, 5893.

25. Evans, D.A., Britton, T.C., Ellman, J.A. and Dorow, R.L. *J. Am. Chem. Soc.* **1990**, *112*, 4011.

26. Vandewalle, M., Van der Eycken, J., Oppolzer, W. and Vullioud, C. *Tetrahedron* **1986**, *42*, 4035.

27. Evans, D. A., Illig, C. R. and Saddler, J. C. *J. Am. Chem. Soc.* **1986**, *108*, 2478.

28. a) Katoh, T., Nagata, Y., Kobayashi, Y., Arai, K., Minami, J. and Terashima, S. *Tetrahedron Lett.* **1993**, *34*, 5743. b) Katoh, T., Kirihara, M., Nagata, Y., Kobayashi, Y., Arai, K., Minami, J. and Terashima, S. *Tetrahedron Lett.* **1993**,

34, 5747. c) Saito, S., Tamura, O., Kobayashi, Y., Matsuda, F., Katoh, T. and Terashima, S. *Tetrahedron* **1994**, *50*, 6193-6258.

29. Katoh, T., Kirhara, M., Yoshino, T., Tamura, O., Ikeuchi, F., Nakatani, K., Matsuda, F., Yamanda, K., Gomi, K., Ashizawa, T. and Terashima, S. *Tetrahedron* **1994**, *50*, 6259.
30. Saito, H., Kobayashi, S., Uosaki, Y., Sato, A., Fujimoto, K., Miyoshi, K., Ashizawa, T., Morimoto, M. and Hirata, T. *Chem. Pharm. Bull.* **1990**, *38*, 1278.
31. Saito, H., Sato, A., Ashizawa, T., Morimoto, M. and Hirata, T. *Chem. Pharm. Bull.* **1990**, *38*, 3202.
32. Saito, H., Hirata, T., Kasai, M., Fujimoto, K., Ashizawa, T., Morimoto, M. and Sato, A. *J. Med. Chem.* **1991**, *34*, 1959.
33. Williams, R. M., Glinka, T., Gallegos, R., Ehrlich, P. P., Flanagan, M. E.; Coffman, H., Park, G.*Tetrahedron* **1991**, *47*, 2629.
34. Borch, R.F. *Tetrahedron Lett.* **1968**, *1*, 61.
35. Four, P. and Guibe, F. *J. Org. Chem.* **1981**, *46*, 4439.
36. Williams, R.M., Glinka, T. and Kwast, E. *J. Am. Chem. Soc.* **1988**, *110*, 5927.
37. Tsuge, O., Ueno, K., Kanemasa, S. and Yorozu, K. *Bull. Chem. Soc. Jap.* **1987**, *60*, 3347.
38. Padwa, A. and Dean, D.C. *J. Am. Chem. Soc.* **1989**, *116*, 6451.
39. a) Beugelmans, R., Negron, G. and Roussi, G. *J. Chem. Soc., Chem. Commun.* **1983**, 31. b) Chastanet, J. and Roussi, G. *J. Org. Chem.* **1985**, *50*, 2910. c) Chastanet, J. and Roussi, G. *Heterocycles* **1985**, *23*, 653. d) Chastanet, J., Fathallah, H., Negron, G. and Roussi, G. *Heterocycles* **1992**, *34*, 1565.
40. a) Grigg, R., Surendrakumar, S., Thianpatanagul, S. and Vipond, D. *J. Chem. Soc., Chem. Commun.* **1987**, 47. b) Grigg, R. *Chem. Soc. Rev.* **1987**, *16*, 89.
41. Vedejs, E. and West, F.G. *Chem. Rev.* **1986**, *86*, 941.

42. Confalone, P.N. and Huie, E.M. *J. Org. Chem.* **1983**, *48*, 2994.

43. Patel, R.P. and Price, S. *J. Org. Chem.* **1965**, *30*, 3575.

44. David, S. and Veyrieres, A. *Carbohyd. Res.* **1969**, *10*, 35.

45. McDermott, J.R. and Benoiton, N.L. *Can. J. Chem.* **1973**, *51*, 1915.

46. a) Kiss, M., Russell-Maynard, J. and Joule, J. A. *Tetrahedron Lett.* **1987**, *28*, 2187. b) Allway, P.A., Sutherland, J. K. and Joule, J. A.*Tetrahedron Lett.* **1990**, *31*, 1012.

47. a) Reuman, M. and Meyers, A.I. *Tetrahedron* **1985**, *41*, 837. b) Warshawsky, A.M. and Meyers, A.I. *J. Am. Chem. Soc.* **1990**, *112*, 8090. c) Meyers, A.I. and Flanagan, M.E. *Org. Syn.* **1993**, *71*, 107.

48. a) Evans, D.A. and Sjogren, E.B. *Tetrahedron Lett.* **1985**, *26*, 3783 and 3787. b) Hegedus, L.S., Montgomery, J., Narukawa, Y. and Snustad, D.C. *J. Am. Chem. Soc.* **1991**, *113*, 5784.

49. Williams, R. M., Flanagan, M. E. and Tippie, T. N. *Biochemistry* **1994**, *33*, 4086.

50. Williams, R. M., Glinka, T., Flanagan, M. E., Gallegos, R., Coffman, H. and Pei, D. *J. Am. Chem. Soc.* **1992**, *114*, 733.

51. Sinclair, P.J., Zhai, D., Reibenspies, J. and Williams, R.M. *J. Am. Chem. Soc.* **1986**, *108*, 1103.

52. Tippie, T.N. "Preparation of Aza-Breveanamide A: Synthetic and Mechanistic Studies of Tetrazomine", Masters Thesis **1995**, Colorado State University.

53. Fisher, J. and Aristoff, P.A. *Progress in Drug Research* **1988**, *32*, 411. Remers, W.A. *J. Nat. Prod.* **1985**, *48*, 173.

54. a) Stubbe, J., and Kozarich, J.W. *Chem. Rev.* **1987**, *87*, 1107. b) Rabow, L.E., Stubbe, J. and Kozarich, J.W. *J. Am. Chem. Soc.* **1990**, *112*, 3196. c) Rabow,

L.E., McGall, G.H., Stubbe, J. and Kozarich, J.W. *J. Am. Chem. Soc.* **1990**, *112*, 3203.

55. a) Natrajan, A., Hecht, S.M., van der Marel, G.A. and van Boom, J.H. *J. Am. Chem. Soc.* **1990**, *112*, 4532. b) Hecht, S.M. *Federation Proc.* **1986**, *45*, 2784.

56. a) Tullius, T.D., Dombroski, B.A., Churchill M.E.A. and Kam, L. *Methods in Enzymology* **1987**, *155*, 537. b) Tullius, T.D.*TIBS* **1987**, *12*, 297. c) Tullius, T.D. and Dombroski, B.A. *Science* **1985**, *230*, 679. d) Latham J.A. and Cech, T.R. *Science* **1989**, *245*, 276.

57. a) Hertzberg, R.P. and Dervan, P.B. *Biochemistry* **1984**, *23*, 3934. b) Dervan, P.B. *Science* **1986**, *232*, 464. c) Dreyer, G.B. and Dervan, P.B. *Proc. Natl. Acad. Sci., USA* **1985**, *82*, 968. d) Moser, H.E. and Dervan, P.B. *Science* **1987**, *238*, 64. e) Chu, B.C.F. and Orgel, L.E. *Proc. Natl. Acad. Sci., USA* **1985**, *82*, 968. f) Vary, C.P.H. and Vournakis, J.N. *Proc. Natl. Acad. Sci., USA* **1984**, *81*, 6978. g) Kean, J.M., White, S.A. and Draper, D.E. *Biochemistry* **1985**, *28*, 1054. h) Tanner, N.K. and Cech,T.R. *Nucl. Acids Res.* **1985**, *13*, 7759. i) Lin, S.B., Blake, K.R., Miller, P.S. and Ts'o, P.O.P. *Biochemistry* **1989**, *28*, 1054.

58. Mack, D.P. and Dervan, P.B. *J. Am. Chem. Soc.*, **1990**, *112*, 4604.

59. a) Chen, C.B. and Sigman, D.S. *J. Am. Chem. Soc.* **1988**, *110*, 6570. b) Sigman, D.S. *Acc. Chem. Res.* **1986**, *19*, 180.

60. Lee, K.S. and Roschenthaler, R. *J. Antibiotics* **1987**, *40*, 692.

61. a) Scannell, R.T., Barr, J.R., Murty, V.S., Reddy, K.S. and Hecht, S.M. *J. Am. Chem. Soc.* **1988**, *110*, 3650.

62. a) Gutteridge, J.M.C. *Free Rad. Commun.* **1990**, *9*, 119. b) Koppenol, W.H. Biochemistry and Bioenergetics **1987**, *18*, 3. c) Brown, E.R. and Mazzrella, J.D.

J. Electroanal. Chem. **1987**, *222*, 173. d) Lesko, S.A., Lorentzen, R.J. and Ts'o, O.P. *Biochemistry* **1980**, *19*, 3023.

63. Sheu, C., Richert, S.A., Cofre, P. B.Ross, Sobkowiak, A., Sawyer D.T. and Kanofsky, J.R. *J.Am. Chem.Soc.* **1990**, *112*, 1936.

64. Sutton, H.C. and Winterbourn, C.C. *Free Radical Biology & Medicine* **1989**, *6*, 53.

65. Misra, H.P. *J. Biol. Chem.* **1974**, *249*, 2151.

66. a) Beauchamp, C. and Fridovich, I. *Biochemistry* **1971**, *44*, 276. b) Tsou, K-C., Cheng, C-S., Nachlas, M.M. and Seligman, A.M. *J. Am. Chem. Soc.* **1956**, 6139.

67. Kopka, M.L., Yoon, C., Goodsell, D., Pjura, P. and Dickerson, R.E. *Proc. Natl. Acad. Sci.* **1985**, *82*, 1376.

68. a) Coll, M., Aymami, J., Marel van der, J.A., van Boom, J.H., Rich, A. and Wang, A.H. *Biochemistry* **1989**, *28*, 310.

69. Coll, M., Frederick, C.A., Wang, A.H. and Rich, A. *Proc. Natl. Acad. Sci.* **1987**, *84*, 8385.

70. Portugal, J. and Waring, M.J. *Eur. J. Biochem.* **1987**, *167*, 281.

71. Zakrzewska, K., Lavery, R. and Pullman, B. *Nucleic Acids Res.* **1984**, *11*, 8825.

72. a) Schultz, P. G., Taylor, J. S. and Dervan, P. B. *J. Am. Chem. Soc.* **1982**, *104*, 6861. b) Schultz, P.G. and Dervan, P.B. *J. Biomol. Struc. Dyn.* **1984**, *1*, 1133. c) Taylor, J. S., Schultz, P. G. and Dervan, P. B. *Tetrahedron* **1984**, *40*, 457.

73. Semmelhack, M. F. and Gallagher, J. J. *J. Org. Chem.* **1994**, *59*, 4357.

74. Bregant, T.M., Groope, J. and Little, R. D. *J. Am. Chem. Soc.* **1994**, *116*, 3635.

75. Jain, S., Zon, G. and Sundaralingam, M. *Biochemstry* **1989**, *28*, 2360.

76. Menger, F.M. and D'Angeio, L.L. *J. Org. Chem.* **1991**, *56*, 3467.

77. Bailer, M., Yagen, B. and Mechoulam, R. *Tetrahedron* **1978**, *34*, 2389.

78. Pelton, J.G. and Wemmer, D.E. *J. Am. Chem. Soc.* **1990**, *112*, 1393.

79. Geierstanger, B.H., Mrksich, M. and Dervan, P.B. *Science* **1994**, *266*, 646.

80. Tabernero, L., *et al.*, *Biochemstry* **1993**, *32*, 8403.

81. Kopka, M.L., Yoon, C., Goodsell, D., Pjura, P. and Dickerson, R.E. *Proc. Natl. Acad. Sci.* **1985**, *82*, 1376.

82. a) Weisenborn, F.L. and Diassi, P.A. *J. Am. Chem. Soc.* **1956**, *78*, 2022. b) Wuest, J.D. and Erhardt, J.M. *J. Am. Chem. Soc.* **1980**, *102*, 6363. c) Schreiber, S.L. *Tetrahedron Lett.* **1980**, *21*, 1027.

Appendix 1
Additional Spectral Data

Appendix 1 contains additional spectral data collected on key synthetic intermediates. The following figures are contained in this appendix:

Figure 1. NOE of cycloadduct **205a** - Control

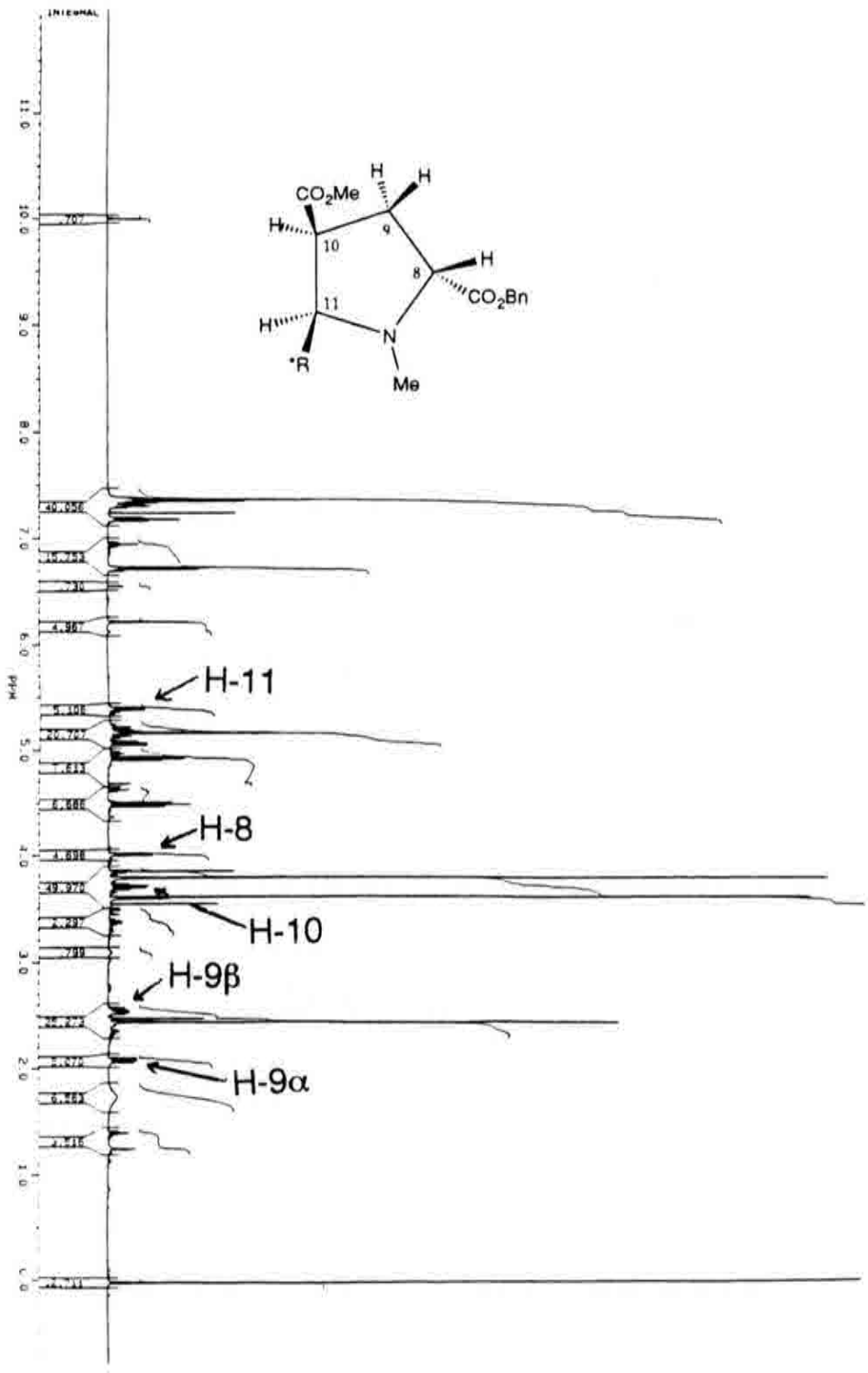

Figure 1 continued - NOE of **205a** irradiation of pyrrolidine methine H-8

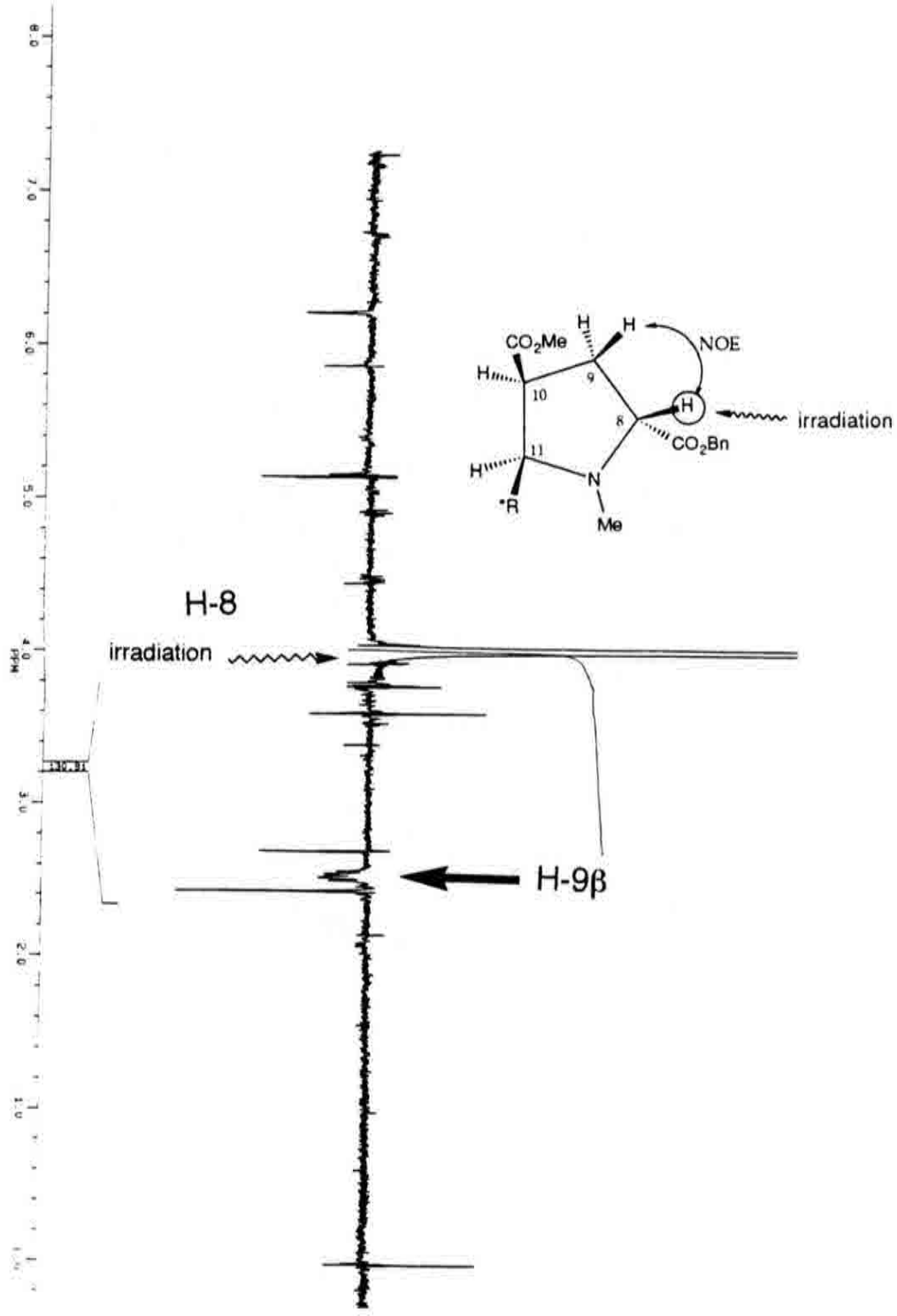

Figure 1 continued - NOE of **205a** irradiation of pyrrolidine methine H-10

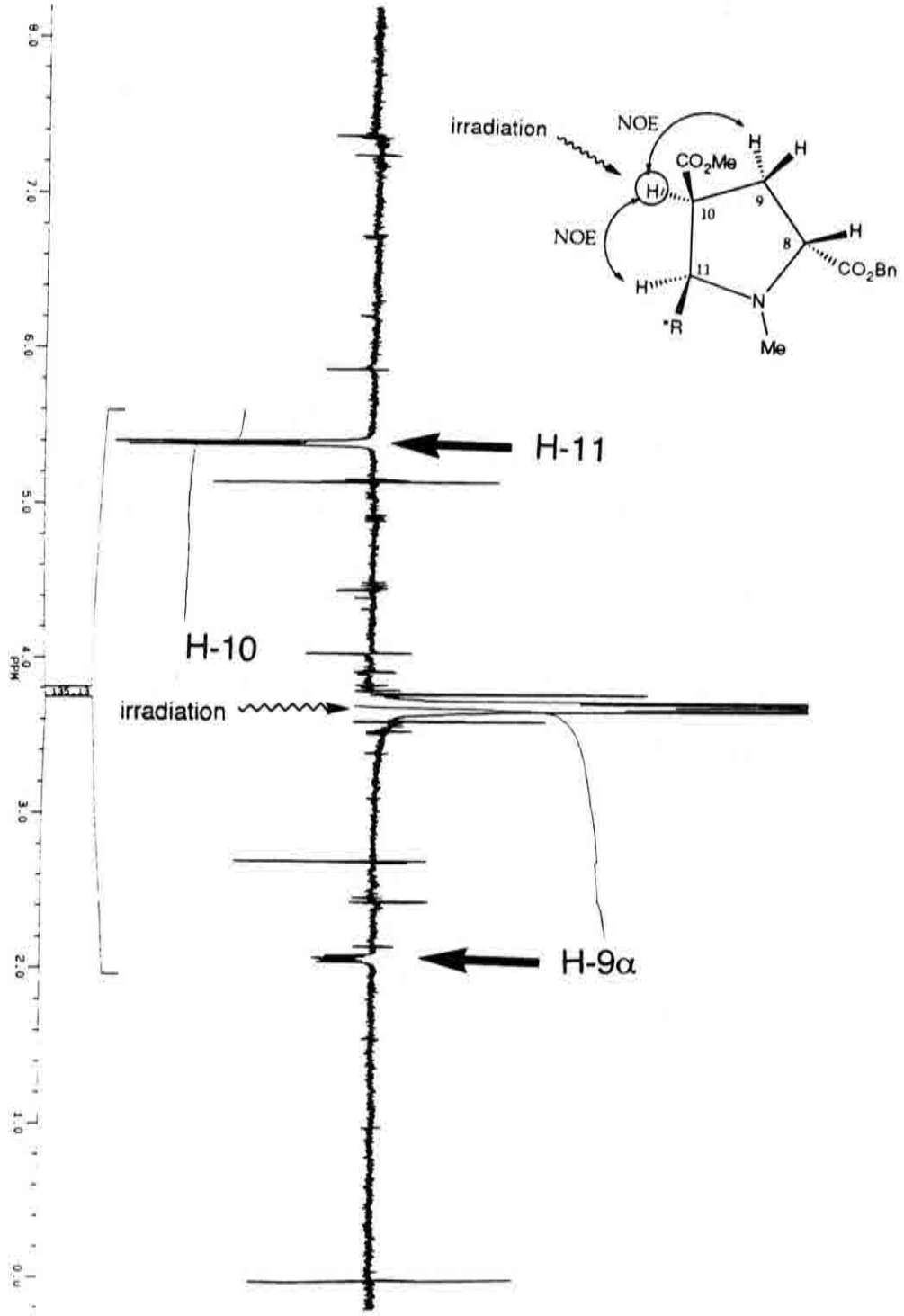

Figure 1 continued - NOE of **205a** irradiation of pyrrolidine methine C-11

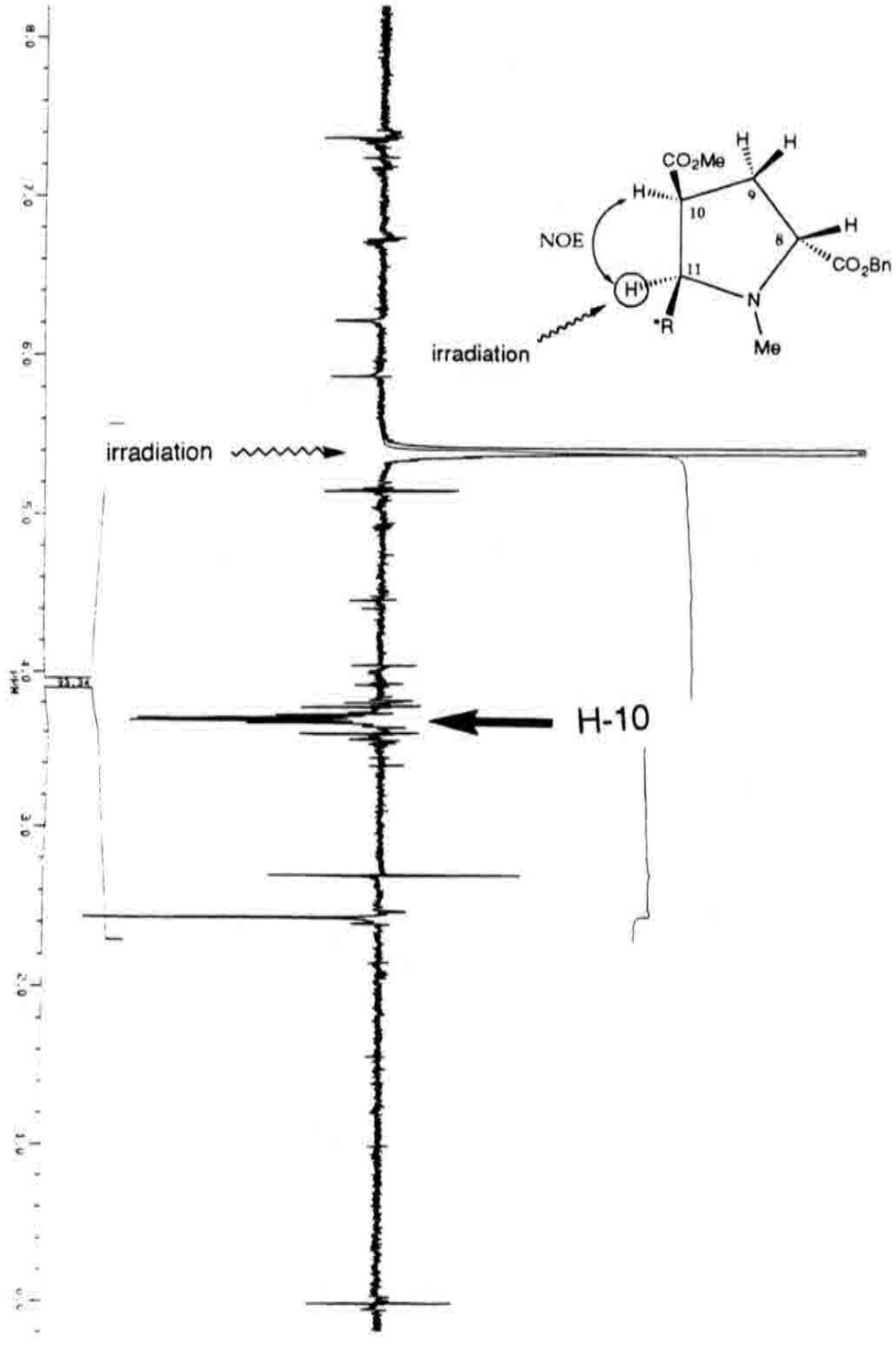

Figure 2. NOE of cycloadduct **205b** - control

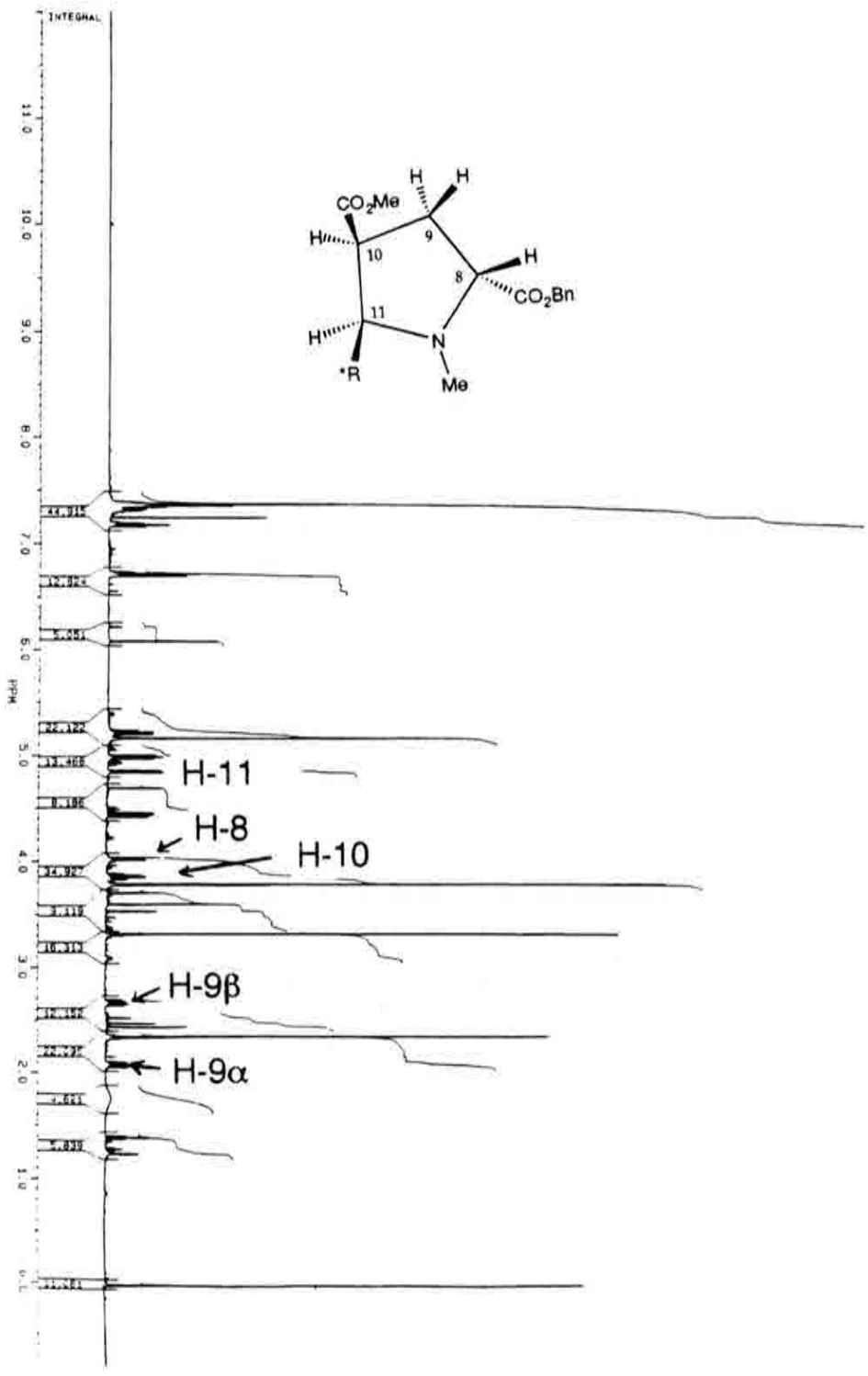

Figure 2 continued - NOE of **205b** irradiation of pyrrolidine methine H-8

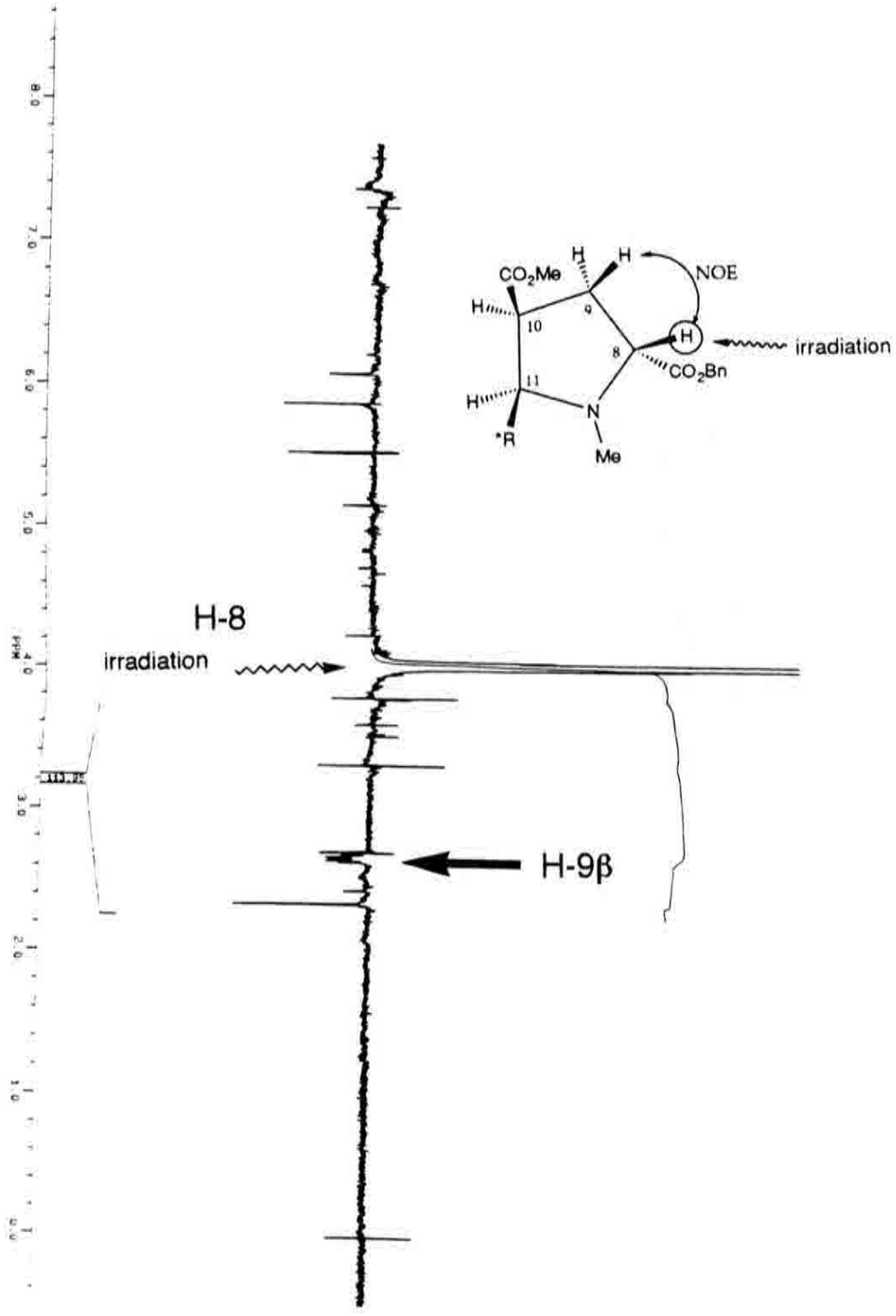

Figure 2 continued - NOE of **205b** irradiation of pyrrolidine methine H-10

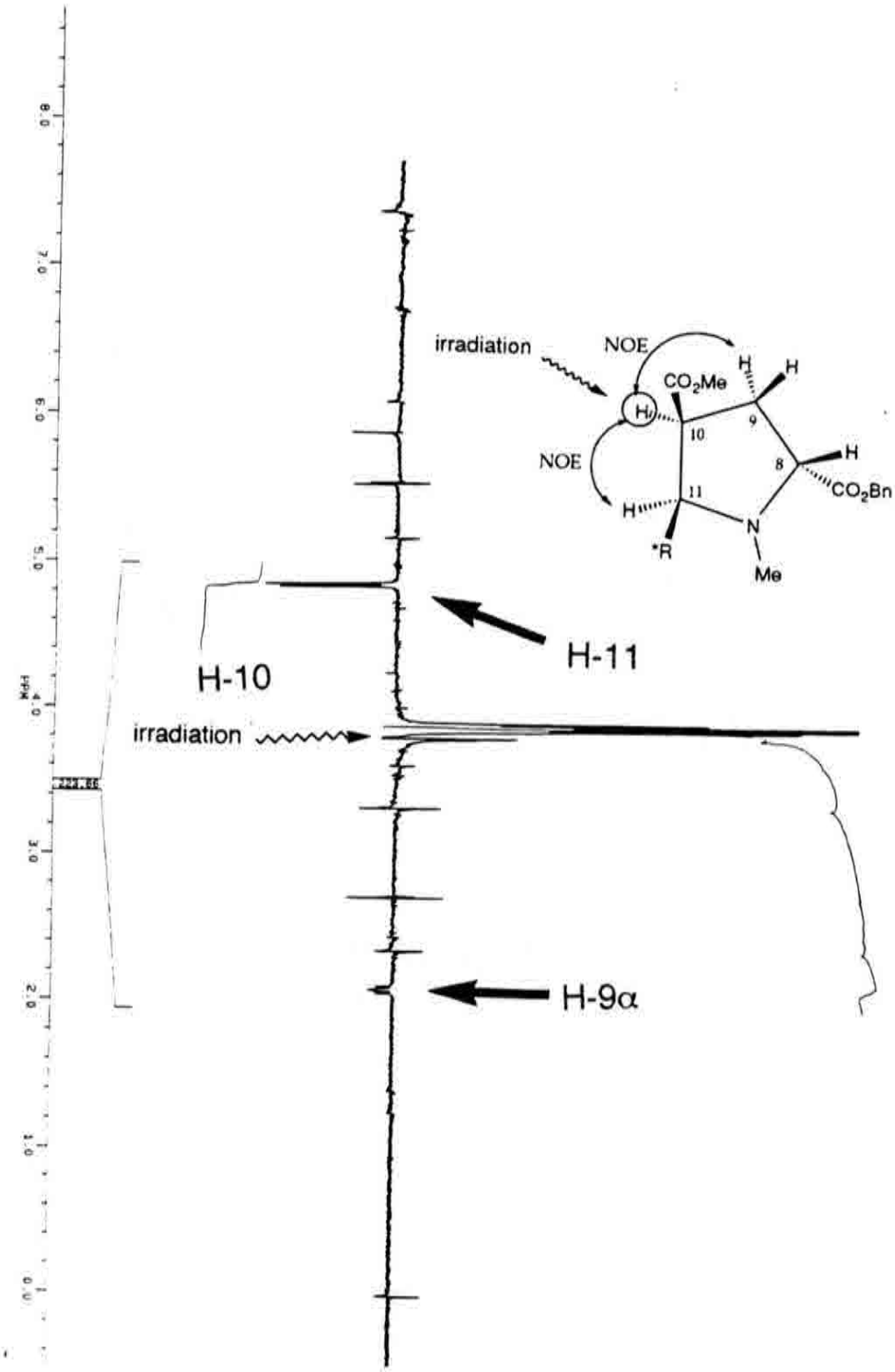

Figure 2 continued - NOE of **205b** irradiation of pyrrolidine methine H-11

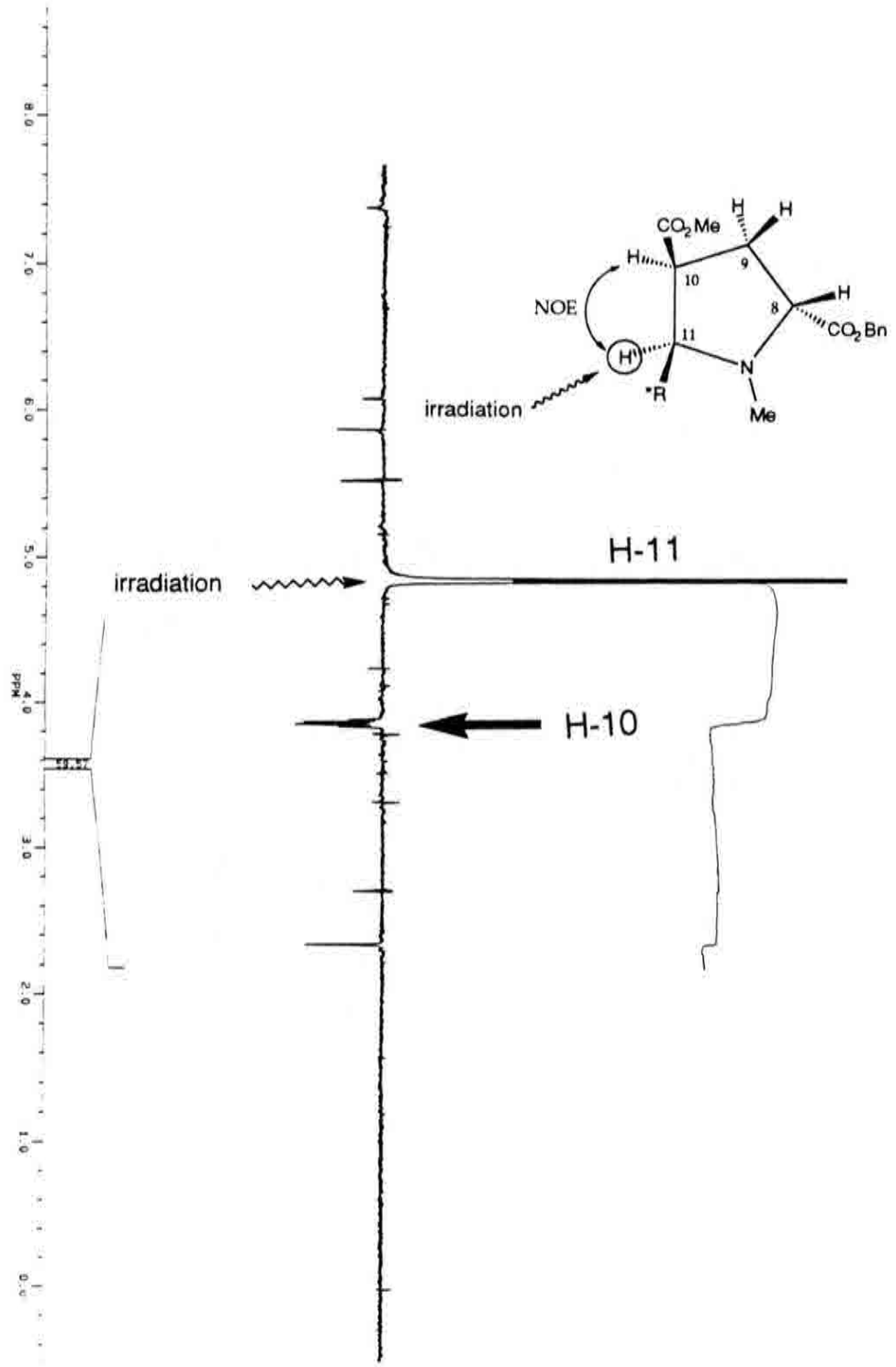

Figure 3. NOE of cycloadduct **249a** - control

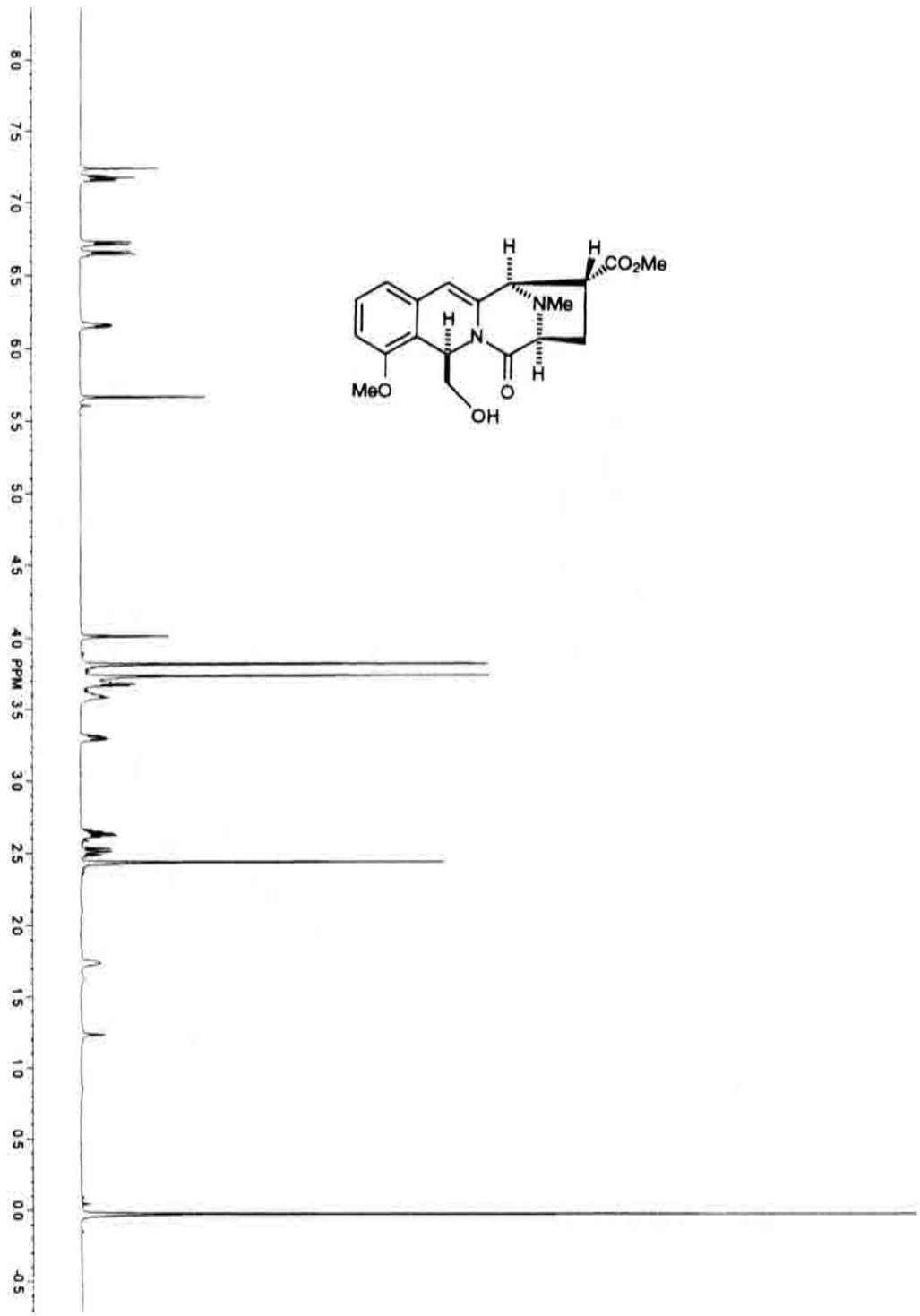

Figure 3 continued - NOE of **249a** - irradiation of vinyl methine

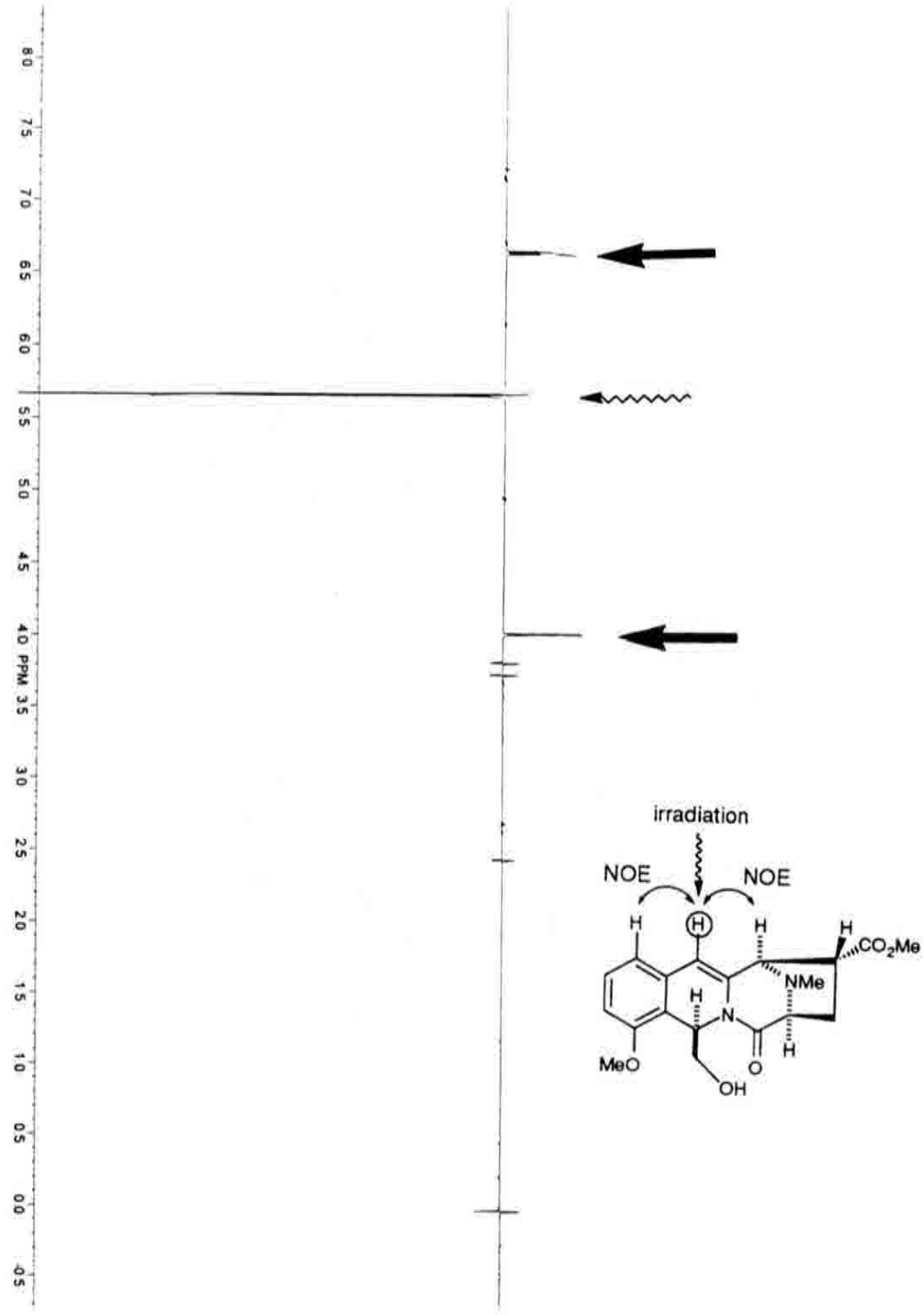

Figure 4. X-Ray coordinates for *N*-2-methyl C-11a-*syn* analog **45a**

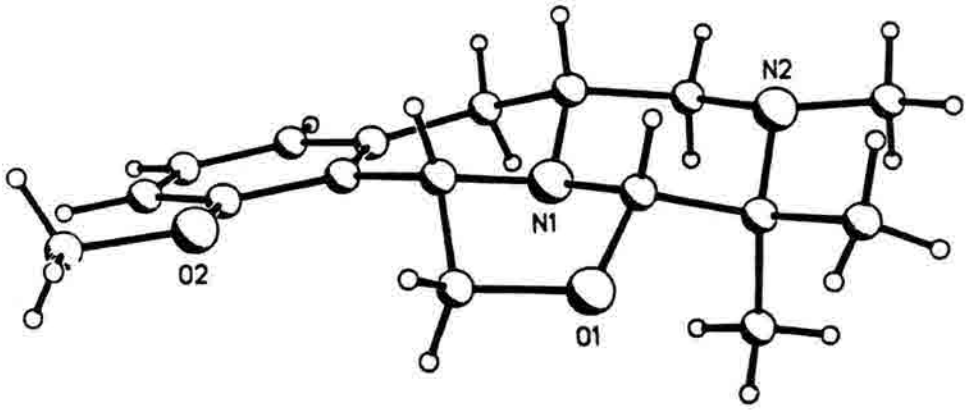

TABLE 1 Atomic coordinates ($x10^4$) and isotropic thermal parameters ($Å^2 x10^3$)[a] for $C_{17}H_{24}N_2O_2$

atom	x	y	z	U^b_{iso}
C1	10641(2)	8316(2)	2293(2)	21(1)*
C2	9948(2)	8834(2)	2656(2)	23(1)*
C3	9373(2)	9360(2)	2054(2)	28(1)*
C4	9511(3)	9371(2)	1054(2)	32(1)*
C5	10194(2)	8877(2)	676(2)	29(1)*
C6	10760(2)	8338(2)	1285(2)	23(1)*
C7	11451(2)	7747(2)	881(2)	26(1)*
C8	11509(2)	7027(2)	1515(2)	21(1)*
C9	12150(3)	6382(2)	1141(2)	29(1)*
C10	12603(2)	5885(2)	2819(2)	24(1)*
C11	12046(2)	6590(2)	3184(2)	21(1)*
C12	11215(2)	7743(2)	2985(2)	20(1)*
C13	9195(3)	9268(2)	4090(3)	41(1)*
C14	10500(2)	7153(2)	3441(2)	24(1)*
C15	12410(3)	5202(2)	3487(2)	32(1)*
C16	13784(2)	6061(2)	2910(2)	32(1)*
C17	12600(3)	5037(2)	1356(3)	40(1)*
N1	12157(2)	5714(1)	1793(2)	26(1)*
N2	11966(2)	7256(1)	2520(2)	19(1)*
O1	11006(2)	6419(1)	3385(1)	24(1)*
O2	9891(2)	8764(1)	3661(1)	29(1)*
C18	5655(2)	9340(2)	2412(2)	20(1)*
C19	4952(2)	8800(2)	2713(2)	20(1)*
C20	4385(2)	8319(2)	2041(2)	23(1)*
C21	4551(2)	8360(2)	1050(2)	27(1)*
C22	5253(2)	8883(2)	740(2)	24(1)*
C23	5809(2)	9379(2)	1416(2)	21(1)*
C24	6541(2)	9972(2)	1086(2)	23(1)*
C25	6614(2)	10655(2)	1789(2)	21(1)*
C26	7317(2)	11297(2)	1511(2)	26(1)*
C27	7660(2)	11726(2)	3228(2)	23(1)*
C28	7075(2)	11002(2)	3499(2)	21(1)*
C29	6232(2)	9865(2)	3175(2)	18(1)*
C30	4223(3)	8221(2)	4069(2)	30(1)*
C31	5511(2)	10435(2)	3666(2)	24(1)*
C32	7423(3)	12380(2)	3922(2)	31(1)*

Figure 4 continued

TABLE 1 (continued)

C33	8841(2)	11544(2)	3393(2)	31(1)*
C34	7782(3)	12625(2)	1832(3)	39(1)*
N3	7284(2)	11942(1)	2197(2)	25(1)*
N4	7013(2)	10370(1)	2788(2)	19(1)*
O3	6021(2)	11171(1)	3660(1)	24(1)*
O4	4874(2)	8794(1)	3712(1)	25(1)*

(a) Estimated standard deviations in the least significant digits are given in parentheses.

(b) For values with asterisks, the equivalent isotropic U is defined as 1/3 of the trace of the U_{ij} tensor.

TABLE 2 Bond lengths (Å)[a] for $C_{17}H_{24}N_2O_2$

C1-C2	1.394(4)	C1-C6	1.399(4)
C1-C12	1.503(4)	C2-C3	1.381(4)
C2-O2	1.384(4)	C3-C4	1.393(5)
C4-C5	1.369(4)	C5-C6	1.395(4)
C6-C7	1.500(4)	C7-C8	1.512(4)
C8-C9	1.510(4)	C8-N2	1.480(3)
C9-N1	1.455(4)	C10-C11	1.525(4)
C10-C15	1.529(4)	C10-C16	1.541(4)
C10-N1	1.479(4)	C11-N2	1.461(3)
C11-O1	1.427(4)	C12-C14	1.549(4)
C12-N2	1.477(4)	C13-O2	1.422(4)
C14-O1	1.432(3)	C17-N1	1.458(4)
C18-C19	1.394(4)	C18-C23	1.395(4)
C18-C29	1.509(4)	C19-C20	1.381(4)
C19-O4	1.376(3)	C20-C21	1.392(4)
C21-C22	1.378(4)	C22-C23	1.395(4)
C23-C24	1.496(4)	C24-C25	1.515(4)
C25-C26	1.507(4)	C25-N4	1.483(3)
C26-N3	1.458(4)	C27-C28	1.526(4)
C27-C32	1.526(4)	C27-C33	1.544(4)
C27-N3	1.481(4)	C28-N4	1.456(4)
C28-O3	1.429(3)	C29-C31	1.555(4)
C29-N4	1.473(4)	C30-O4	1.419(4)
C31-O3	1.433(3)	C34-N3	1.456(4)

(a) Estimated standard deviations in the least significant digits are given in parentheses.

Figure 4 continued

TABLE 3 Bond angles (deg)[a] for $C_{17}H_{24}N_2O_2$

C2-C1-C6	118.6(3)	C2-C1-C12	119.3(3)
C6-C1-C12	122.1(3)	C1-C2-C3	122.2(3)
C1-C2-O2	113.8(2)	C3-C2-O2	124.0(3)
C2-C3-C4	118.0(3)	C3-C4-C5	121.3(3)
C4-C5-C6	120.4(3)	C1-C6-C5	119.5(3)
C1-C6-C7	118.6(2)	C5-C6-C7	121.8(3)
C6-C7-C8	110.0(2)	C7-C8-C9	114.1(2)
C7-C8-N2	107.2(2)	C9-C8-N2	109.6(2)
C8-C9-N1	110.2(2)	C11-C10-C15	107.9(2)
C11-C10-C16	108.2(2)	C15-C10-C16	109.3(2)
C11-C10-N1	108.8(2)	C15-C10-N1	109.6(2)
C16-C10-N1	112.9(2)	C10-C11-N2	115.4(2)
C10-C11-O1	112.6(2)	N2-C11-O1	106.3(2)
C1-C12-C14	114.4(2)	C1-C12-N2	113.9(2)
C14-C12-N2	104.2(2)	C12-C14-O1	105.4(2)
C9-N1-C10	113.0(2)	C9-N1-C17	111.3(2)
C10-N1-C17	114.8(2)	C8-N2-C11	110.8(2)
C8-N2-C12	109.8(2)	C11-N2-C12	100.7(2)
C11-O1-C14	105.6(2)	C2-O2-C13	117.4(2)
C19-C18-C23	119.1(2)	C19-C18-C29	119.0(2)
C23-C18-C29	121.8(3)	C18-C19-C20	121.4(3)
C18-C19-O4	114.8(2)	C20-C19-O4	123.9(3)
C19-C20-C21	118.9(3)	C20-C21-C22	120.6(3)
C21-C22-C23	120.3(3)	C18-C23-C22	119.6(3)
C18-C23-C24	119.3(2)	C22-C23-C24	121.1(3)
C23-C24-C25	109.9(2)	C24-C25-C26	114.2(2)
C24-C25-N4	108.2(2)	C26-C25-N4	108.7(2)
C25-C26-N3	109.9(2)	C28-C27-C32	108.5(2)
C28-C27-C33	107.6(2)	C32-C27-C33	109.0(2)
C28-C27-N3	108.6(2)	C32-C27-N3	109.5(2)
C33-C27-N3	113.4(2)	C27-C28-N4	116.4(2)
C27-C28-O3	111.9(2)	N4-C28-O3	105.9(2)
C18-C29-C31	113.9(2)	C18-C29-N4	114.3(2)
C31-C29-N4	104.2(2)	C29-C31-O3	105.2(2)
C26-N3-C27	112.6(2)	C26-N3-C34	110.8(2)
C27-N3-C34	114.8(2)	C25-N4-C28	110.4(2)
C25-N4-C29	110.2(2)	C28-N4-C29	101.2(2)
C28-O3-C31	105.3(2)	C19-O4-C30	117.2(2)

(a) Estimated standard deviations in the least significant digits are given in parentheses.

Figure 4 continued

TABLE 4 Anisotropic thermal parameters ($Å^2 x 10^3$)[a,b] for $C_{17}H_{24}N_2O_2$

atom	U_{11}	U_{22}	U_{33}	U_{23}	U_{13}	U_{12}
C1	16(2)	20(2)	25(2)	4(1)	-0(1)	-6(1)
C2	18(2)	22(2)	29(2)	2(1)	0(1)	-1(1)
C3	23(2)	21(2)	38(2)	0(1)	-5(1)	1(1)
C4	27(2)	28(2)	38(2)	9(2)	-10(2)	1(1)
C5	28(2)	31(2)	25(2)	10(1)	-4(1)	-4(2)
C6	16(2)	24(2)	28(2)	4(1)	-1(1)	-4(1)
C7	26(2)	33(2)	19(2)	6(1)	-0(1)	-2(1)
C8	16(2)	29(2)	19(2)	1(1)	2(1)	-0(1)
C9	28(2)	36(2)	21(2)	-3(1)	2(1)	0(2)
C10	24(2)	26(2)	20(2)	-1(1)	-1(1)	1(1)
C11	17(2)	25(2)	19(2)	1(1)	-2(1)	-1(1)
C12	20(2)	20(2)	19(1)	-2(1)	-1(1)	-4(1)
C13	39(2)	43(2)	41(2)	-5(2)	7(2)	13(2)
C14	25(2)	21(2)	26(2)	4(1)	6(1)	4(1)
C15	34(2)	28(2)	33(2)	6(1)	0(2)	5(2)
C16	25(2)	35(2)	34(2)	-1(2)	-2(1)	6(2)
C17	50(2)	34(2)	36(2)	-6(2)	-1(2)	10(2)
N1	30(2)	25(1)	22(1)	-4(1)	-0(1)	3(1)
N2	18(1)	20(1)	17(1)	1(1)	-2(1)	1(1)
O1	22(1)	22(1)	28(1)	4(1)	6(1)	2(1)
O2	31(1)	29(1)	26(1)	-1(1)	1(1)	9(1)
C18	19(2)	18(2)	22(2)	1(1)	-1(1)	1(1)
C19	18(2)	19(2)	21(2)	-3(1)	-0(1)	7(1)
C20	20(2)	19(2)	29(2)	-0(1)	-2(1)	-2(1)
C21	29(2)	23(2)	27(2)	-8(1)	-6(1)	1(1)
C22	26(2)	24(2)	21(2)	-3(1)	1(1)	5(1)
C23	20(2)	19(2)	22(2)	-0(1)	1(1)	5(1)
C24	22(2)	27(2)	20(2)	1(1)	3(1)	5(1)
C25	17(2)	25(2)	20(2)	0(1)	1(1)	2(1)
C26	27(2)	30(2)	21(2)	1(1)	4(1)	-2(1)
C27	18(2)	31(2)	21(2)	1(1)	1(1)	-2(1)
C28	17(2)	26(2)	19(1)	-2(1)	-2(1)	-0(1)
C29	18(2)	18(1)	19(1)	1(1)	3(1)	0(1)
C30	29(2)	33(2)	28(2)	-2(1)	6(1)	-8(2)
C31	24(2)	26(2)	24(2)	-6(1)	3(1)	-7(1)
C32	34(2)	28(2)	31(2)	-2(1)	2(1)	-10(2)
C33	22(2)	30(2)	41(2)	1(2)	-2(2)	-6(2)
C34	51(3)	31(2)	36(2)	5(2)	4(2)	-14(2)
N3	32(2)	22(1)	21(1)	1(1)	4(1)	-5(1)
N4	18(1)	21(1)	16(1)	-0(1)	-1(1)	-2(1)
O3	22(1)	23(1)	27(1)	-7(1)	7(1)	-5(1)

Figure 4 continued

TABLE 4 (continued)

O4	27(1)	27(1)	23(1)	-3(1)	5(1)	-9(1)

(a) Estimated standard deviations in the least significant digits are given in parentheses.

(b) The anisotropic thermal parameter exponent takes the form:

$$-2\pi^2(h^2a^{*2}U_{11}+k^2b^{*2}U_{22}+ \ldots +2hka^*b^*U_{12})$$

Figure 4 continued

TABLE 5 Hydrogen coordinates ($x10^4$) and thermal parameters ($Å^2 x10^3$) for $C_{17}H_{24}N_2O_2$

atom	x	y	z	U_{iso}
H3	8892	9708	2316	35
H4	9118	9732	623	39
H5	10285	8901	-14	35
H7A	11170	7616	218	32
H7B	12141	7959	877	32
H8	10814	6823	1503	27
H9A	12854	6558	1120	35
H9B	11853	6236	488	35
H11	12491	6723	3774	21
H12	11559	8080	3480	25
H13A	9232	9128	4775	53
H13B	8491	9207	3783	53
H13C	9406	9798	4036	53
H14A	9819	7143	3071	26
H14B	10436	7284	4117	26
H15A	12568	5376	4157	36
H15B	12870	4785	3364	36
H15C	11698	5026	3384	36
H16A	14172	5637	2681	35
H16B	14021	6161	3593	35
H16C	13888	6514	2525	35
H17A	12549	4599	1781	49
H17B	13316	5109	1242	49
H17C	12180	4948	737	49
H20	3884	7963	2254	28
H21	4172	8021	579	35
H22	5360	8905	54	31
H24A	7221	9747	1078	29
H24B	6284	10146	434	29
H25	5925	10872	1764	27
H26A	7083	11469	852	30
H26B	8021	11108	1537	30
H28	7497	10834	4088	26
H29	6556	9496	3640	22
H30A	4244	8279	4772	36
H30B	4477	7716	3921	36
H30C	3515	8278	3767	36
H31A	5440	10277	4331	29
H31B	4832	10458	3292	29
H32A	7515	12178	4583	37
H32B	6715	12552	3765	37
H32C	7891	12807	3873	37
H33A	9226	11983	3200	38
H33B	9002	11101	3012	38
H33C	9032	11440	4082	38
H34A	7701	13046	2276	47
H34B	7414	12739	1195	47
H34C	8511	12552	1769	47

Figure 5. ^{1}H NMR spectrum (300 MHz) (D_2O) of natural quinocarcinamide (**19**)

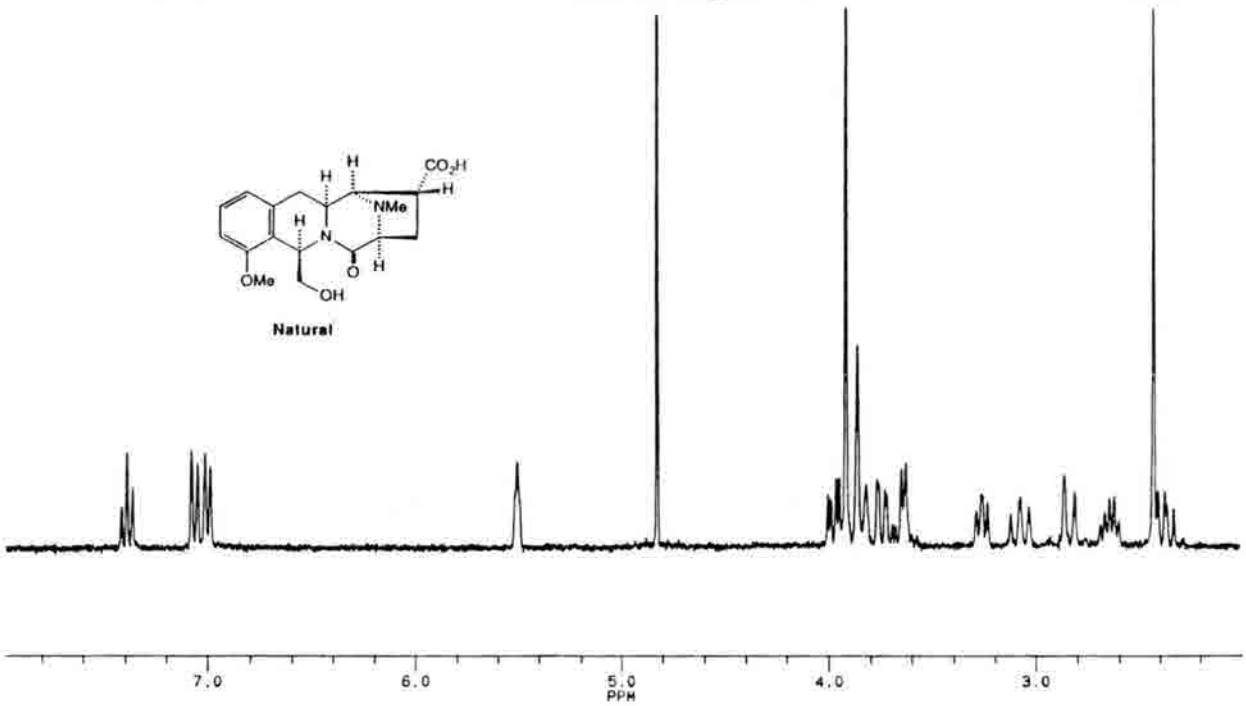

Figure 6. ^{1}H NMR spectrum (300 MHz) ($CDCl_3$) of synthetic quinocarcinamide methyl ester provide by prof. S.J. Danishefsky

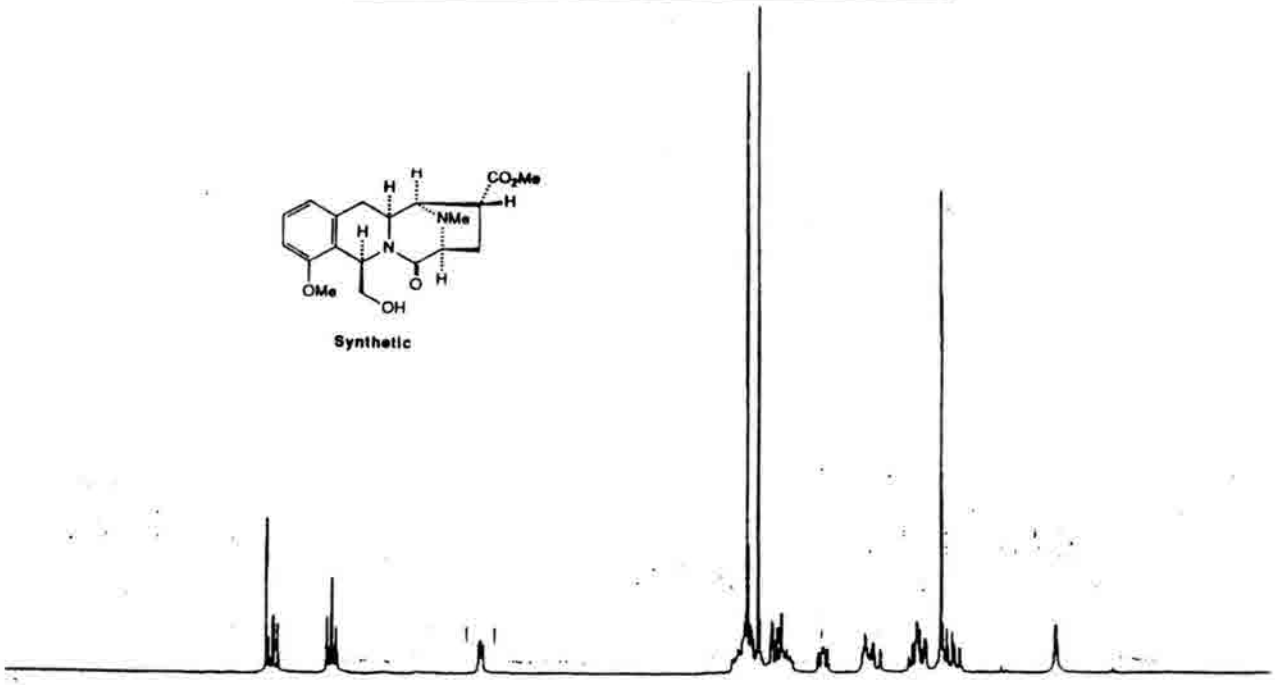

Figure 7. Results of antitumor assay for C-11a-*anti* analog **45b** against P388 leukemia in mice

TEST FOR ANTITUMOR ACTIVITY OF QUINOCARCIN AGAINST [1] P388 LEUKEMIA IN MICE

DRUG [2]	DOSE (MG/KG)	ROUTE	TREATMENT SCHEDULE	MST [3]	%ILS [4]	S/T [5] (DAY +30)
Placebo	----	IP	1,5,9	11.0	Cont.	0/12
Quinocarcin	1.0	IP	1,5,9	11.0	0	0/6
	0.5	IP	1,5,9	9.0	-18	0/6
Cytoxan	60	IP	1,5,9	27.5	+150	3/6

1. BDF1 male mice inoculated IP with $1x10^6$ P388 leukemia cells on day 0 of the test.
2. Drugs administered IP on Days 1, 5 and 9 following tumor inoculation.
   Quinocarcin (1 MG) dissolved in absolute ethanol and further diluted into sterile water for injection containing 0.2% Klucel brand methylcellulose.
3. MST = Median Survival Time in days post tumor inoculation into mice.
4. %ILS = Percent Increase in Lfe Span, relative to placebo treated Controls.
   An ILS = 25% or greater indicates positive antitumor activity.
5. S/T = No. Survivors?No. Treated. 30 days post tumor inoculation.

Test Date: 2/15/90

LL-11373

Appendix 2
Publications

1. Robert M. Williams, Tomasz Glinka, Renee Gallegos, Paul P. Ehrlich, Mark E. Flanagan, Hazel Coffman and Gyoosoon Park. Synthesis, Conformations, Crystal Structures and DNA Cleavage abilities of Tetracyclic Analogs of Quinocarcin. *Tetrahedron* **1991**, *47*, 2629.

2. Robert M. Williams, Tomasz Glinka, Mark E. Flanagan, Renee Gallegos, Hazel Coffman and Deihua Pei. Cannizzaro-Based O_2-Dependent Cleavage of DNA by Quinocarcin. *J. Am. Chem. Soc.* **1992**, *114*, 733.

3. Robert M. Williams, Mark E. Flanagan and Tracy N. Tippie. O_2-Dependent Cleavage of DNA by Tetrazomine. *Biochemistry* **1994**, *33*, 4086.

4. Mark E. Flanagan, Samuel B. Rollins and Robert M. Williams. Netropsin and Spermine Conjugates of a Water Soluble Quinocarcin Analog: Analysis of Sequence Specific DNA Interactions. *Chemistry & Biology* (in press).

Tetrahedron Vol. 47, No. 14/15, pp. 2629-2642, 1991
Printed in Great Britain

0040-4020/91 $3.00+.00

SYNTHESIS, CONFORMATION, CRYSTAL STRUCTURES AND DNA CLEAVAGE ABILITIES OF TETRACYCLIC ANALOGS OF QUINOCARCIN

Robert M. Williams, Tomasz Glinka, Renee Gallegos, Paul P. Ehrlich, Mark E. Flanagan, Hazel Coffman and Gyoosoon Park*

Department of Chemistry, Colorado State University
Fort Collins, Colorado 80523

(*Received in USA* 20 *September* 1990)

Abstract. Two totally synthetic, racemic analogs of quinocarcin have been designed and their crystal structures determined. Both substances effect the modest cleavage of plasmid DNA. Alteration of the conformation of the reactive oxazolidine fused to the piperazine ring by selecting the stereochemistry at C-11a through synthesis drastically attenuates the relative ability of these substances to cleave DNA.

Introduction

Quinocarcin (**1**) is a natural secondary metabolite produced by *Streptomyces melanovinaceus* and is the simplest member of the naphthyridinomycin (**3**)/saframycin (**4**) class of anti-tumor agents.[1,2] Quinocarcin has been shown[1a,3] to display weak antimicrobial activity against several Gram-positive microbes but is inactive toward Gram-negative bacteria. As its citrate salt, quinocarcin (named quinocarmycin citrate or KW2152) displays promising anti-tumor activity[3] against several lines of solid mammalian carcinomas including St-4 gastric carcinoma; Co-3 human colon carcinoma; MX-1 human mammary carcinoma; M5076 sarcoma; B16 melanoma and P388 leukemia. This substance is currently under evaluation in human clinical trials by the Kyowa Hakko Kogyo Co., Japan.

Our interest in this substance stems from a report by Tomita, et. al.[4] that recorded the remarkable observation that **1** cleaves plasmid DNA in an O_2-dependent fashion that was reported: 1) to not require metal ions (Fe^{2+} or Cu^{2+}); 2) to be stimulated by dithiothreitol; 3) to be inhibited by oxygen free radical scavengers such as methanol, *tert*-butanol, α-tocopherol and; 4) to be inhibited by superoxide dismutase (SOD) and catalase. Quinocarcin blocks RNA synthesis in preference to DNA and protein synthesis in P388 leukemia cells.[3d] On the other hand, in *Bacillus subtilis*, quinocarcin inhibited [^{3}H] thymidine incorporation suggesting inhibition of DNA polymerase; therefore, DNA synthesis is thought[4] to be preferentially inhibited in *Bacillus subtilis*. It has also been reasonably proposed[3d,4,5] that quinocarcin alkylates DNA in the minor groove[5] through the ring-opened form of the oxazolidine (imminium **5**); similar DNA alkylation has been invoked for **3** and **4**. Indirect support[3d,4] for the involvement of the oxazolidine ring in the above context comes from the lack of biological activity displayed by quinocarcinol (**2**) which is coproduced with **1** by *Streptomyces melanovinaceus*. Quinocarcinol also does not cleave plasmid DNA[4] which forces the conclusion that the oxazolidine moiety is also responsible for the oxidative degradation of DNA by a unique mechanism.

While it is not yet clear whether the anti-tumor properties of quinocarmycin citrate are a manifestation of only one mode of action (i.e., DNA alkylation) or both (DNA alkylation and oxidative DNA cleavage), we were intrigued by the oxidative cleavage observations of the Kyowa-Hakko group[4] since **1** does not contain any readily recognizable functionality that would be associated with the capacity for oxidative DNA cleavage,[6] such as metal

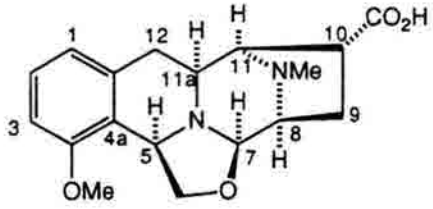

1, *QUINOCARCIN, DC-52*

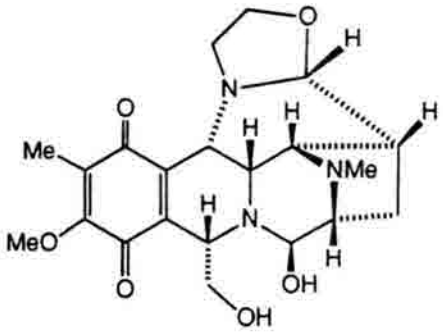

3, *NAPHTHYRIDINOMYCIN*

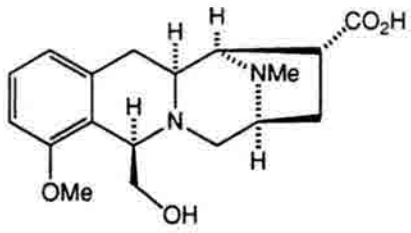

2, *QUINOCARCINOL, DC-52d*

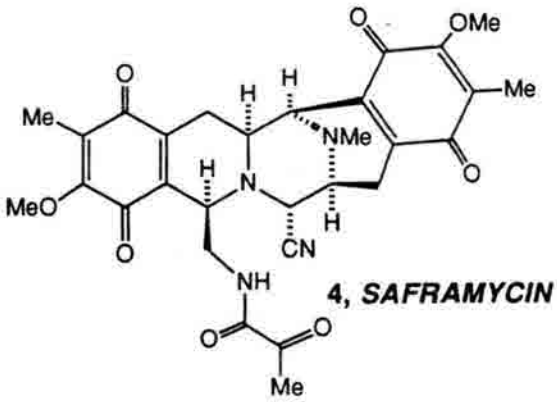

4, *SAFRAMYCIN A*

chelation sites, quinones, and ene-diynes amongst others. Most likely, the efficacy of this drug is a delicate and intimate combination of multiple effects that are brought to bear on its macromolecular targets. We have recently found[7] that quinocarcin undergoes a redox self-disproportionation reaction that we have invoked is coupled to the capacity of this substance to effect the production of superoxide in the presence of molecular oxygen and results, at least in part, to Fenton-mediated lesions in DNA; a mechanism for this process is reviewed[7] in Scheme 1. At the heart of this process, the oxazolidine ring is functioning as its own reductant which ultimately results in the reduction of oxygen and the cleavage of DNA. Such a process would also presumably be relevant to possible oxidative damage to RNA *in vitro* and *in vivo*. In the present study, we wished to examine the intrinsic capacity of simpler oxazolidine-containing analogs to effect the DNA cleavage reaction. Most significantly, we wished to experimentally determine whether pre-designed and synthetically[8] incorporated stereoelectronic control elements into simpler analogs could attenuate the capacity of this ring system to oxidatively damage DNA relative to **1**.

Design Criteria

Remers[5] has conducted molecular mechanics calculations on quinocarcin by docking the drug in the minor groove. From this study, it was concluded that the absolute configuration of quinocarcin is most likely that depicted in Scheme 1. The calculations suggested that the lowest energy conformer of **1** orients the piperazine ring in a chair-like conformation which therefore places the oxazolidine nitrogen lone pair in an antiperiplanar

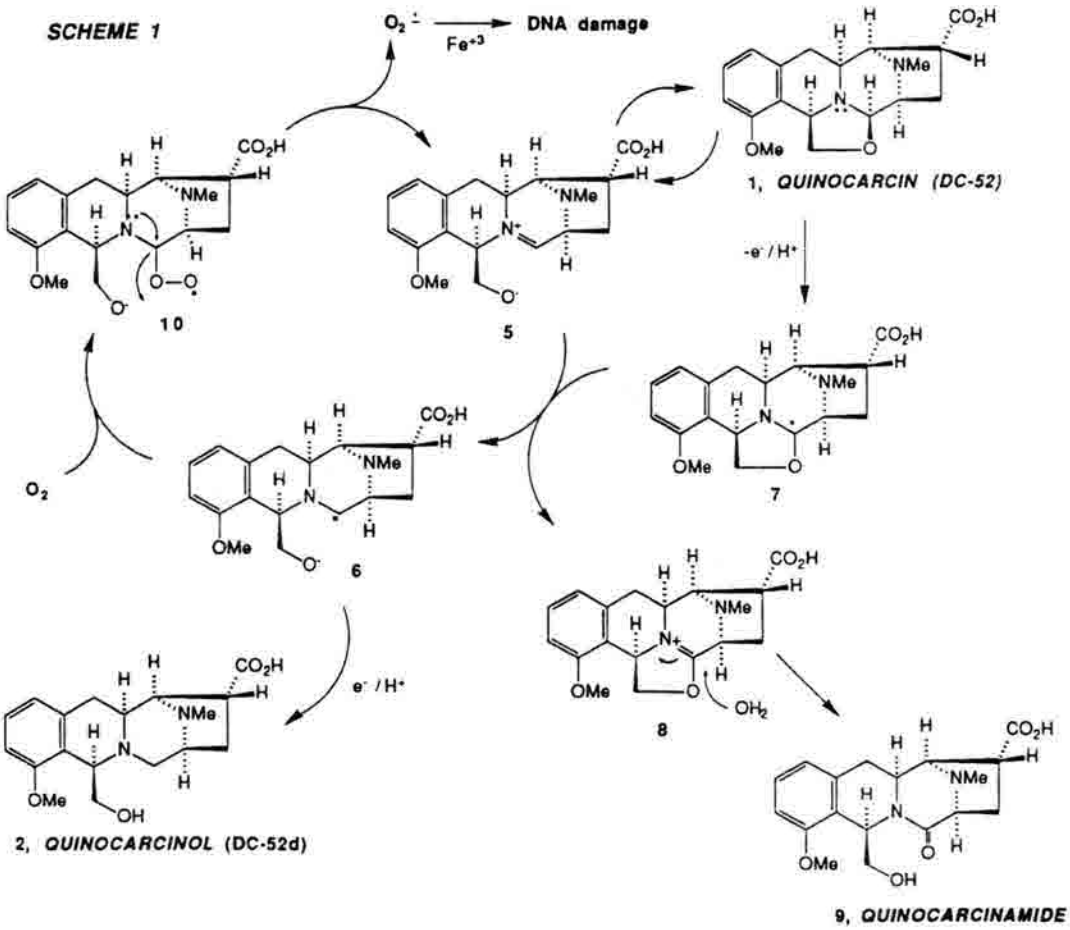

orientation to the oxazolidine methine (Figure 1, *anti*-**1**). Ring opening of the oxazolidine to the imminium species (see **5**, Scheme 1) requires nitrogen pyrimidal inversion to a higher energy twist boat conformer (Figure 1, *syn*-**1**) that was calculated to lie ~10 kcal mol^{-1} above the other conformer. In this situation, the oxazolidine nitrogen lone pair is *syn*- to the methine and antiperiplanar to the C–O bond. It was postulated[5] that the imminium species should be a good alkylator for N-2 of guanine in the minor groove of the sequence $d(ATGCAT)_2$. Based on the similarity to **3** and **4**,[2k] this is a reasonable expectation. In the present study, we wished to ask a different question regarding the conformational significance of the oxazolidine moiety. As shown in Scheme 1, the initial step in the electron-transfer between the oxazolidine and the imminium species involves 1-electron loss from the oxazolidine nitrogen with loss of the oxazolidine methine as a proton producing the reduction and oxidation radicals **6** and **7**, respectively. It is reasonable to expect that the *trans*, antiperiplanar arrangement of the oxazolidine methine and nitrogen lone pair in the lower energy conformer predicted by calculation, should also be the most favorable geometry for concomitant electron and proton loss in the redox self-disproportionation. We hoped to test this idea by synthesizing two simple analogs of quinocarcin that would each mirror one of the two conformational states of the natural product depicted in Figure 1. Thus, analog **23a** which has all three methines

oriented *syn* (same as **1**) would be expected to have the same relative conformation as *anti*-**1** with respect to the oxazolidine and piperazine rings. Analog **23b**, on the other hand, which has inverted stereochemistry at C-11a (quinocarcin numbering) is predicted to exist in a conformation that mirrors *syn*-**1**. Both of these predictions were based on examination of Dreiding stereomodels and molecular mechanics calculations.[9] From this stereoelectronic analysis, **23a** should be much faster at effecting oxidative DNA cleavage relative to **23b**. The synthesis, structures and relative DNA cleavage ability of these materials is presented below.

Results

The preparation of the key isoquinoline **18** is detailed in Scheme 2 and was made by a modification of a known procedure.[10] *Ortho*-anisaldehyde (**11**) was treated with trimethylsulfonium iodide under phase-transfer conditions to afford the epoxide **12** in high yield. The epoxide was regioselectively opened with phosgene as a solution in benzene containing a catalytic amount of water to afford the chloroformate **13**. Without purification, **13** was subjected to acylation under Schotten-Baumann conditions to provide the urethane **14** in 57% overall yield from **12**. Treatment of **14** with potassium t-butoxide in THF at room temperature effected cyclization to the corresponding oxazolidinone which was saponified to the acid[10] **15** (74%, two steps). Acid chloride formation and intramolecular Friedel-Crafts acylation provided the isoquinolone **16** in 74% yield from **15**. The procedure described herein is an optimized preparation (from **15**) based on our previously reported[10] synthesis of **16**. The overall sequence from **11** is considerably more efficient and is amenable to multi-gram scale (10 gm scale is described in the experimental section).

SCHEME 2

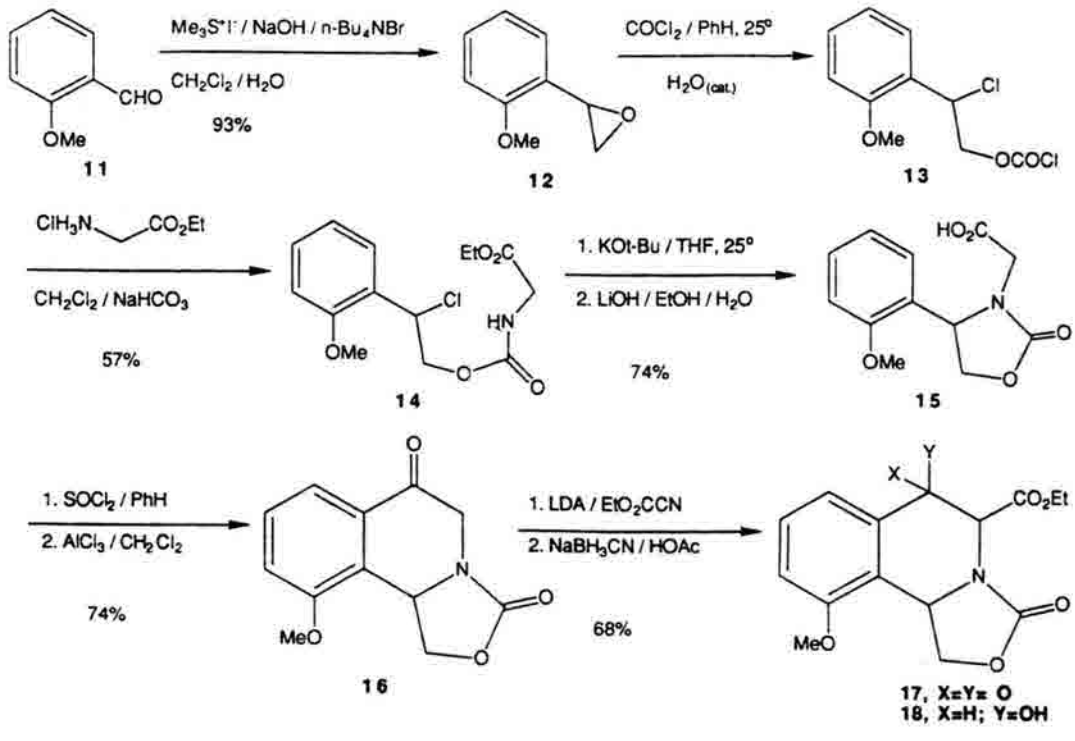

C-Homologation of **16** proved to be troublesome and required extensive examination of various electrophilic species and reaction conditions due to the propensity of the ketone enolate to undergo O-acylation. Eventually, it was found that the lithium enolate condensed smoothly with ethyl cyanoformate to provide the β-ketoester **17**. Reduction of the ketone with sodium cyanoborohydride gave a single diastereomer (**18**) of unknown relative stereochemistry. This substance served as the key substrate from which various stereoselective and non-stereoselective routes to the target oxazolidine analogs (**23**) were examined. We found two parallel,

SCHEME 3

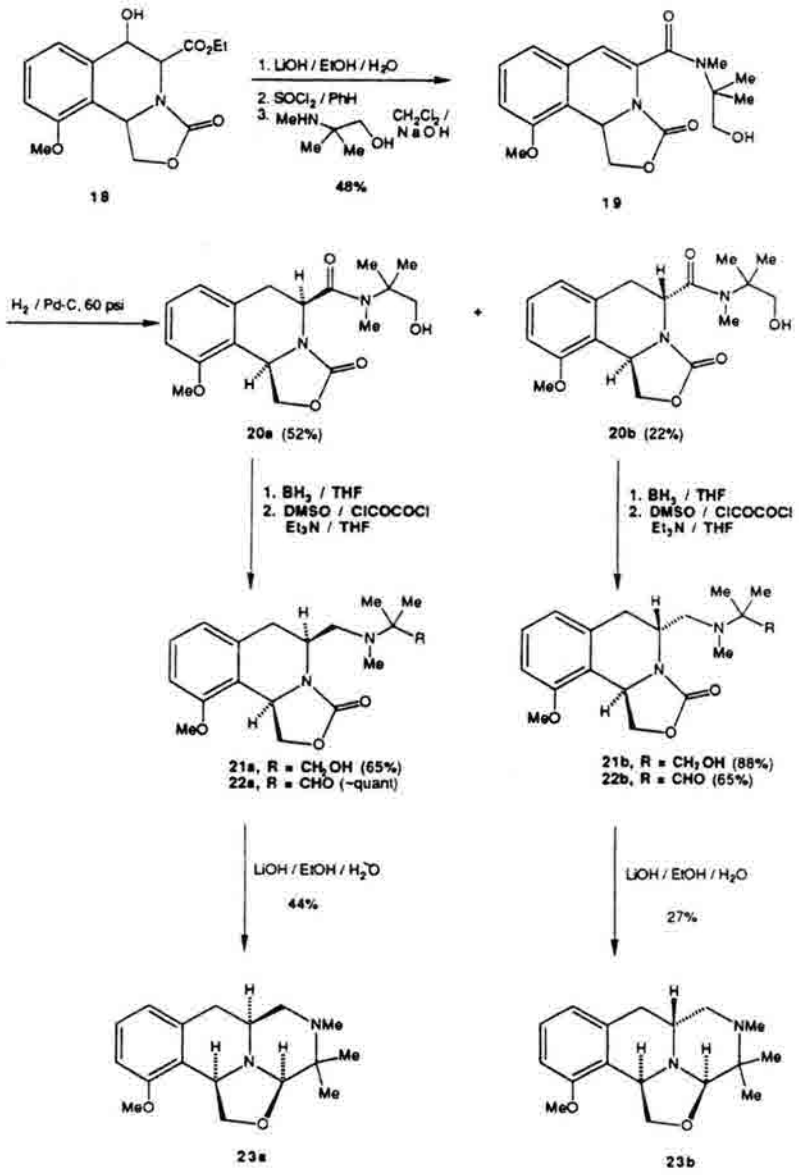

stereoselective routes[11] to **23a** and **23b** from **18**, wherein the relative stereochemistry at C-11a and the oxazolidine methine could be controlled. More recently, we have found it to be more efficient in terms of man-hours, to employ a common, non-stereoselective route that furnishes both stereochemical series and requiring only a simple chromatographic separation as described in Scheme 3.

Saponification of **18** furnished a crude carboxylic acid which was directly treated with thionyl chloride in benzene. The crude product was directly subjected to Schotten-Baumann acylation with 2,2,3-trimethyl ethanolamine to give the unsaturated amide **19** in 48% overall yield from **18**. This substance was then hydrogenated to give 52% of the *syn*-isomer **20a** and 22% of the *anti*-isomer **20b**. These materials were separated by silica gel chromatography and carried on separately to the final oxazolidines.

For **20a**, borane reduction furnished the tertiary amine **21a** in 65% yield without loss of stereochemical integrity. Swern oxidation to the aldehyde **22a** proceeded in essentially quantitative yield. The crucial oxazolidine-forming step proved somewhat capricious, but could be achieved in 44% yield by refluxing **22a** in basic ethanol for two days. Silica gel purification and crystallization furnished a single oxazolidine diastereomer for which a single crystal x-ray analysis[12] has been secured (Figure 2).

Similarly, **20b** was converted into **23b** in modest overall yield. The nicely crystalline **23b** also proved amenable to x-ray crystallographic analysis[12] as shown in Figure 2.

As is evident from the crystal structures, **23a** and **23b** differ with respect to the orientation of the oxazolidine nitrogen lone pair relative to the oxazolidine methine in the crystal. Substance **23a** positions the nitrogen lone pair *trans*-antiperiplanar to the oxazolidine methine; whereas **23b** positions the nitrogen lone pair *trans*-antiperiplanar to the oxazolidine C–O bond. These conformations are exactly those predicted from examination of Dreiding molecular models and molecular mechanics calculations.[9] The inversion of stereochemistry at C-11a (quinocarcin numbering) in **23b** from the all *syn*-situation in **23a** induces sufficient ring strain to favor nitrogen pyramidal inversion and results in a geometry similar to that evident in the crystal structure. These results confirm our predictions alluded to above that **23a** should mirror the ground state conformation (*anti*-**1**, Figure 1) of the oxazolidine for quinocarcin that was postulated in Remers computational study.[5] Similarly, **23b** can be thought of as mirroring the higher energy conformer of quinocarcin (*syn*-**1**, Figure 1) that Remers postulated as being the reactive conformation that precedes oxazolidine ring-opening to the imminium species (see **5**, Scheme 1) which should (quite reasonably) alkylate DNA.

Reactions with DNA

Compounds **23a** and **23b** as the free bases were virtually insoluble in aqueous buffers and were used as either water-soluble citrate or hydrochloride salts. Reaction of these materials with supercoiled plasmid DNA (pBR 322) were examined at various concentrations and conditions; the results are collected in Table 1 and Figure 3. Reactions were conducted in pH 8, 20 mmol phosphate buffer at 37°C for 2 hours and were analyzed by 0.8% agarose gel electrophoresis. The DNA bands were visualized by staining with ethidium bromide after running the gel and were quantitated by scanning densitometry. The supercoiled plasmid (form I, ccc DNA, fastest band) when nicked is first converted to open circular plasmid (form II, cc DNA, slowest band) and after extensive scission, linear DNA (form III, intermediate band) was observed. Both analogs required fairly high concentrations relative to **1** to produce observable damage to the DNA. As predicted, compound **23b** is significantly inferior to **23a** in effecting DNA cleavage and required dithiothreitol (DTT) even at concentrations as high as 5 mmol (entries 2 and 3, Table 1, lanes 2 and 3, Figure 3; compare entry 22). Since **23a** displayed

Figure 1

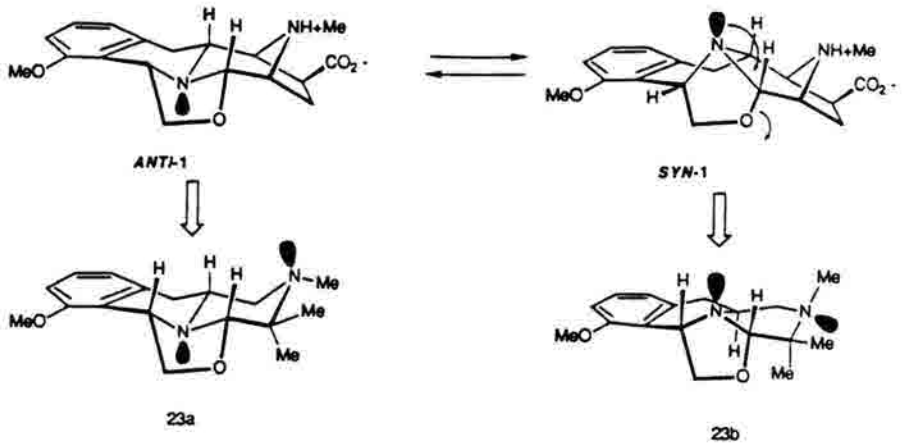

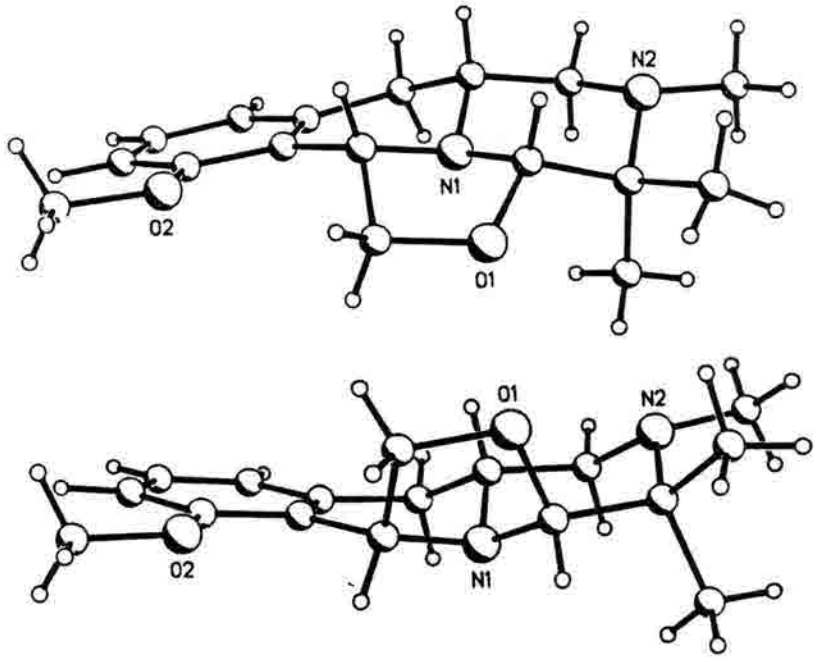

Figure 2. X-Ray Molecular Structures of 23a and 23b. Spheres are of fixed arbitrary radius.

superior DNA cleavage relative to **23b**, the reactivity of this material was examined in more detail and compared to that of **1**. As with quinocarcin, the DNA cleavage by **23a** is enhanced by the addition of DTT (compare entries 7, 16 and 17, Table 1; lanes 7, 16, and 17, Figure 3). It is significant to note that DTT by itself is capable of modest DNA cleavage (entry 17, Table 1, lane 17, Figure 3) *via* Fenton-mediated production of hydroxyl radical; this reaction is a manifestation of superoxide production during thiol autoxidation.[13] The DNA cleavage observed by **23a** in the presence of DTT is at least an order of magnitude greater than DTT alone; the DNA cleavage is thus clearly not due to DTT alone (compare lanes 16 and 17, Figure 3). Superoxide dismutase and catalyse both inhibit

Figure 3. 0.8% Agarose gel electrophoresis of plasmid pBR322 DNA cleavage experiments. Lanes 1-21 correspond to entries 1-21 from Table I. See Table I for visualization details.

the cleavage; SOD being the more potent inhibitor (entries 10 and 11, Table 1; lanes 10 and 11, Figure 3). This is consistent with superoxide production and subsequent Fenton-mediated DNA cleavage.[14] Hydrogen peroxide strongly stimulates the DNA cleavage by **23a** (compare entries 7 and 20, Table 1; lanes 7 and 20, Figure 3). Quinocarcin is significantly better than either **23a** or **23b** at effecting DNA cleavage and gives comparable DNA scission at 1 mmol without external reductants that **23a** gives at 5 mmol with hydrogen peroxide (compare entries 9 and 20, Table 1; lanes 9 and 20, Figure 3).

Quinocarcin has been shown[4,7] to produce superoxide (see Scheme 1) and therefore, Fenton-mediated production of hydroxyl radical with adventitious iron must be invoked for the DNA cleavage event by these molecules. However, hydrogen peroxide alone at 0.1 mmol causes virtually no significant DNA damage (entry 21, Table 1). Since hydrogen peroxide is reduced by Fe(II) in the Fenton reaction, producing hydroxyl radical, the oxazolidine can be functioning indirectly in cycling adventitious Fe(III) to Fe(II) *via* superoxide production or may directly effect the redox cycling of the metal. This point has not yet been addressed. Attempts to sequester adventitious iron and uncouple[15] the presumed Haber-Weiss/Fenton reaction was performed by the addition of the potent Fe(III) chelator desferal (log k_f = 30.7). Addition of desferal to the reaction of **23a** with DNA showed very little inhibition at 0.1 mmol (entry 12, Table 1; lane 12, Figure 3) and partial protection at 10 mmol (entry 14, Table 1; lane 14, Figure 3). However, since the citrate salt of these materials proved to be less effective than the hydrochloride salts in effecting DNA cleavage, we suspect that both citrate and desferal are functioning as competitive CH substrates for the reactive oxidant with DNA (present in very low concentration relative to citrate or desferal) rather than as efficient metal sequestering agents. Additional experimental evidence for direct metal mediation in the DNA cleavage event is not yet available. Ascorbate, a powerful oxygen reductant, is very effective at mediating DNA cleavage which is completely inhibited by catalase (entries 23 and 24, Table 1). The incomplete inhibition of DNA cleavage by **23a** with either catalase of SOD (entries 10 and 11, Table 1) and the incomplete protection afforded by desferal suggests that the mechanism of DNA cleavage by this heterocycle may involve other pathways that are distinct from most recognized DNA oxidants. These possibilities are currently being pursued.

However, indirect experimental evidence points to a significant difference in the capacity of **23a** and **23b** to produce superoxide, paralleling their DNA cleavage abilities. Reduction of nitroblue tetrazolium (NBT)[18] by the HCl salts of **23a** and **23b** were determined at pH 8.0 (20 mM phosphate buffer) containing 1% Triton X-100 at 25°C. For **23a** (1.0 mM) ΔOD_{500nm}/minute = 0.0003 and for **23b** (1.0 mM) ΔOD_{500nm}/minute = 0.0000. For reference[4] 1.0 mM quinocarcin has a ΔOD_{500nm}/minute = 0.002 in the absence of any external reductant

Table I

Entry	Substrate[a]	Concentration [mmol]	% DNA Form I	% DNA Form II	% DNA Form III	S	DNA Cleavage Yield[b] ppm
1	DNA Control		75	25	---	0.29[c]	---
2	**23b** citrate	1.0	77	23	---	-0.03	0.0
3	**23b** citrate	5.0	69	31	---	0.08	0.08
4	**23a** citrate	1.0	63	37	---	0.17	0.85
5	**23a** citrate	5.0	46	54	---	0.49	0.51
6	**23a** hydrochloride	1.0	51	49	---	0.38	2.0
7	**23a** hydrochloride	5.0	19	81	---	1.37	1.4
8	quinocarcin (**1**)	0.1	62	38	---	0.19	9.9
9	quinocarcin (**1**)	1.0	---	84	16	9.5	49
10	**23a** hydrochloride + catalase (10 *ug*/mL)	5.0	39	61	---	0.65	0.68
11	**23a** hydrochloride + SOD (10 *ug*/mL)	5.0	60	40	---	0.22	0.23
12	**23a** hydrochloride + desferal	5.0 0.1	27	73	---	1 0	1.0
13	**23a** hydrochloride + desferal	5.0 1.0	37	63	---	0.70	0.73
14	**23a** hydrochloride + desferal	5.0 10	59	41	---	0.24	0.25
15	DNA Control		81	19	---	0.21[c]	---
16	**23a** hydrochloride + DTT	5.0 0.1	10	87	3	3.8	3.9
17	DTT	0.1	61	39	---	0.28	---
18	DTT + catalase (10 *ug*/mL)	0.1	78	22	---	0.04	---
19	**23a** hydrochloride + DTT + catalase (10 *ug*/mL)	5.0 0.1	32	68	---	0.93	0.97
20	**23a** hydrochloride + H_2O	5.0 0.1	3.5	89	7.5	6.0	6.2
21	H_2O_2	0.1	74	26	---	0.08	---
22	**23b** citrate + DTT	5.0 0.1	50	50	---	0.45	0.47
23	ascorbic acid	0.1	15	79	6	5.4	280
24	ascorbic acid + catalase (10 *ug*/mL)	0.1	80	20	---	0.02	1.0

a. Reaction mixtures were 20 mmol in pH 8 phosphate buffer and contained 0.15 *ug* of pBR 322 plasmid DNA. b. The cleavage yield is expressed by the term S[ccc DNA]/[substrate] and describes the number of single hits per cleavage substrate molecule and allows for a comparison of the relative efficiency of DNA cleavage. c. The S value for the DNA control represents the amount of oc (form II) DNA present in the starting plasmid DNA solution and was subtracted from the S values calculated for the individual cleavage reactions. Measurements of the relative intensity of DNA bands were obtained by scanning densitometry of black and white (Polaroid instant) photographs of the gels (0.8% agarose) visualized by ethidium bromide staining and UV illumination. The mean number of single strang scissions (S)[16] per supercoiled DNA substrate was calculated using the Poisson distribution. When only forms I (ccc or covalently closed circular supercoiled) and forms II (oc or open circular) are present, the equation simplifies to $S = -\ln f_I$, where f_I is the fraction of form I molecules. In those cases where form III (linear) DNA was present, S was calculated from $f_I + f_{II} = [1 - S(2h + 1)/(2L)]^{S/2}$ where h is the distance between hits on opposite strands to produce a linear molecule (16 base pairs)[17] and L is the total number of base pairs in pBR 322 (4362 base pairs). The film used to photograph the gels is assumed to have a linear response to the range of DNA quantities used.[16] Supercoiled DNA is restricted with respect to its ability to bind ethidium bromide and the densitometry values obtained for form I were multiplied by 1.22 as described by Dervan.[16]

(such as DTT). Finally, these substances cleave both double-stranded and single-stranded DNA in a non-sequence specific manner with essentially equal efficacy[7] which argues against the significance of any relative difference in the capacity of these compounds to dock to DNA as a mechanistic determinant relevant to DNA cleavage.

This work demonstrates that simple oxazolidine-containing isoquinolines based on the quinocarcin structure are intrinsically capable of cleaving plasmid DNA and that stereoelectronic elements can markedly attenuate the capacity of these systems to damage nucleic acids. Efforts to attach DNA-binding domains to the synthetic analog nucleus and evaluation of the relative ability of these materials to alkylate DNA as well as their biological activities is under study.

Acknowledgement. This work was supported by the National Institutes of Health (CA43969). We are grateful to Kyowa Hakko Kogyo Co., Japan, for a generous gift of quinocarmycin citrate. We acknowledge Ciba Geigy Corp. and Dr. Peter G. Wuts of the Upjohn Co. for gifts of desferal. We are especially indebted to Professor Tony K. Rappé (CSU) for performing molecular mechanics calculations on **23**. Mrs. Maria Ludwikow and Mr. Robert Hyta are acknowledged for providing technical assistance. Dr. Jed Fisher of the Upjohn Company is thanked for helpful discussions.

EXPERIMENTAL

DNA Nicking Experimentals

DNA nicking reaction mixtures were made up by addition at 0° of appropriate amounts of reagent stock solutions to a stock solution of pBR 322 DNA plasmid (Boehringer-Mannheim Biochemical Co.) containing 0.15 μg DNA per reaction (20 μM base pair concentration). The total volumes of the reaction mixtures were brought up to 10 μl with distilled and deionized water when necessary and the reaction mixtures were incubated at 37° for 2 hours in tightly capped plastic tubes. Stock solutions for DNA including experiments were prepared using distilled, deionized water and commercially available reagents: DTT - Sigma; sodium phosphate monobasic - EM Science; sodium phosphate dibasic, 30% hydrogen peroxide - Malinckrodt; superoxide dismutase, beef liver catalase (suspension in water) - Boehringer Mannheim Biochemical. Desferal was the generous gift from Ciba-Geigy Co. From quinocarcin citrate which was a generous gift from Kyowa Hakko Kogyo Co., Japan, free quinocarcin was obtained by passing it through HP-20 ion exchange resin (Mitsubishi Corp.) at 4°. Citric acid was eluted with water and subsequently free quinocarcin was eluted in methanol/water - 3/1 fraction. Free quinocarcin was further purified by HPLC on C-18 Resolve Column (Waters) using 5% methanol/5% acetonitrile in 6.0mM, pH 6.8 potassium phosphate buffer. To remove the phosphate buffer from lyophilized quinocarcin fraction it was passed through HP-20 column in the same manner as described above.

The degree of DNA nicking was monitored by horizontal gel electrophoresis on 0.8% agarose gel onto which the whole volumes of the reaction mixtures were loaded after prior addition of 3 μl of loading buffer (0.25% bromophenol blue, 40% sucrose). The electrophoreses were run for 2 h at 55V and the gels were submerged for 15 min in ethidium bromide solution. The electrophoresis gels were immediately visualized on a UV transilluminator and photographed using black and white instant films (Polaroid T667). The measurements of the relative intensities of DNA bands were performed on the photographs using the Dell System 325 computer and Technology Resources Inc. image processing software. The average number of nicks per DNA molecule S was calculated according to the method described by Dervan.[16]

Synthesis of Quinocarcin Analogs

(2-Methoxyphenyl)oxirane **12**. A nonhomogenous mixture of o-anisaldehyde (20.0 g, 0.147 mol, 1.0 eq.), trimethylsulfonium iodide (37.0 g, 0.177 mol, 1.2 eq.), tetra n-butylammonium iodide (0.52 g, 0.0014 mol, 0.01 eq.), CH_2Cl_2 (500 mL) and aqueous NaOH (50%, 330 mL) was vigorously stirred at room temperature for 5 days. After dilution with water the organic layer was separated, washed with water, dried over Na_2SO_4, concentrated in vacuum and the residue was Kugelrohr distilled to yield the pure product in form of colorless liquid (20.4 g, 92.5%).

12. ^{1}H NMR (270 MHz) ($CDCl_3$) TMS: 2.69 (1 H, q, J = 2.4 Hz), 3.12 (1 H, q, J = 4.6 Hz), 3.85 (3 H, s), 4.20 (1 H, t, J = 2.7 Hz), 6.91 (2 H, m), 7.15 (1 H, q, J = 1.6 Hz), 7.25 (1 H, m). IR (NaCl, neat):

3051, 3002, 2941, 2838, 1689, 1602, 1496, 1466, 1439, 1391, 1287, 1256, 1103, 1048, 1027, 989, 880, 755 cm^{-1}.

Glycine ethyl ester N-carbamate **14**. A solution of epoxide **12** (0.69 g, 4.60 mmol, 1.0 eq.) and phosgene (0.85 g, 8.58 mmol, 1.86 eq.) in benzene (10 mL) was kept in sealed flask for 48 h. The solvent was removed under reduced pressure (prior to this with larger scale runs the reaction mixture has to be purged with the flux of dry nitrogen and the excessive phosgene should be deactivated by passing through aqueous solution of alkali). The oily residue of crude chloroformate **13** was redissolved in CH_2Cl_2 (15 mL), and a solution of saturated $NaHCO_3$ was added (15 mL), followed by a solution of glycine ethyl ester hydrochloride (0.64 g, 4.6 mmol, 1.0 eq.) in small volume of water. After 10 min of vigorous stirring at room temperature the organic layer was separated, washed with water, dried over $MgSO_4$ and concentrated to yield crude product as yellow oil from which pure **14** was isolated by radial chromatography (CH_2Cl_2/CH_3OH - 10/1) 0.83 g (57%). Analytical sample was obtained by recrystallization from isopropyl alcohol, mp = 61-63°.

13. ^1H NMR (300 MHz) ($CDCl_3$) δ TMS: 3.85 (3 H, s); 4.55 (1 H, dd, J = 11.3 Hz, J = 5.0 Hz); 4.67 (1 H, dd, J = 11.3 Hz, J = 7.9 Hz); 5.62 (1 H, dd, J = 7.9 Hz, J = 5.0 Hz); 6.90 (1 H, d, J = 8.3 Hz); 6.98-7.03 (1 H, m); 7.30-7.36 (1 H, m); 7.48 (1 H, dd, J = 7.6 Hz, J = 1.6 Hz); IR (NaCl, neat): 1779, 1492, 1252, 1145, 755 cm^{-1}.

14. ^1H NMR (270 MHz) ($CDCl_3$) δ TMS: 1.28 (1 H, t, J = 7.2 Hz); 3.85 (3 H, s); 3.95 (2 H, d, J = 5.5 Hz); 4.21 (2 H, q, J = 7.2 Hz); 4.44-4.48 (2 H, m); 5.32 (1 H, br s); 5.58 (1 H, t, J = 6.3 Hz); 6.88 (1 H, d, J = 8.4 Hz); 6.98 (1 H, t, J = 7.2 Hz); 7.30 (1 H, m); 7.48 (1 H, dd, J = 7.7 Hz, J = 1.6 Hz). IR (NaCl, neat): 3357, 1729, 1533, 1495, 1252, 1201, 1052, 1026, 757 cm^{-1}. Anal. Calcd for $C_{14}H_{18}ClNO_5$: C, 53.25; H, 5.74; N, 4.43. Found: C, 53.40; H, 5.81; N, 4.39.

Cyclic urethane **15**. To a solution of **14** (15.7 g, 50.0 mmol, 1.0 eq.) in THF (150 mL) cooled to 0°C a solution of potassium t-butoxide (6.13 g, 55.0 mmol, 1.1 eq.) in THF (75 mL) was added slowly with stirring. After 0.5 h the reaction mixture was diluted with water, slightly acidified with dilute HCl and extracted with CH_2Cl_2. The organic extract was dried over Na_2SO_4, filtered and concentrated in vacuum to yield crude **11**[5] as brownish oil (14.1 g, quant.). Ethanol (150 mL) was added followed by LiOH monohydrate (2.8 g, 66.7 mmol, 1.3 eq.) in water (60 mL) at 0°C. After 0.5 h the reaction mixture was concentrated under reduced pressure to a half volume at room temperature, diluted with water, acidified and extracted with ethyl acetate. The extract was dried over Na_2SO_4, filtered and concentrated. From the oily residue pure **12**[5] was obtained by crystallization from ethyl acetate (9.3 g, 74%).

Isoquinolone **16**. **14** was obtained from acid **12** as previously described.[5] Substituting CH_2Cl_2 for tetrachloroethane as a solvent for Friedel-Crafts cyclization improved the yield to 74% (on 40.0 mmol scale).

β-Ketoester **17**. To a stirred solution of **16** (120 mg, 0.515 mmol, 1.0 eq.) in 10% HMPA/THF (8.8 mL) cooled to -78°C was added $(TMS)_2NLi$ in THF (0.60 mL, 1.0 M, 0.60 mmol, 1.15 eq.). The resulting solution was stirred at -78°C for 45 min when cyanoethylformate (51 mg, 0.515 mmol, 1.0 eq.) was added in one portion. The reaction was stirred at -78°C for 2 h and quenched with saturated aqueous NH_4Cl (0.60 mL, 1.0 M, 1.5 mL), diluted with CH_2Cl_2 (50 mL) and washed with water and brine. The organic layer was dried over $MgSO_4$, filtered, evaporated and the residue was chromatographed on silica gel (hexane/ethyl acetate - 3/2) yielding **17** as an amorphous solid (126 mg, 80%).

17. ^1H NMR (270 MHz) ($CDCl_3$) δ $CHCl_3$: 1.24 (3 H, t, J = 8.2 Hz), 3.87 (3 H, s); 4.11-4.25 (3 H, m); 5.05 (1 H, t, J = 8.5 Hz); 5.32 (1 H, s); 5.57 (1 H, t, J = 8.5 Hz), 7.16 (1 H, d, J = 7.7 Hz), 7.43 (1 H, t, J = 8.0 Hz); 7.71 (1 H, d, J = 7.8 Hz); IR (NaCl, CH_2Cl_2): 1765, 1750, 1700, 1250 cm^{-1}; mass spectrum, $CI(NH_3)$, m/e = 305 (100), 233 (12).

β-Hydroxyester **18**. To a solution of ketoester **17** (267 mg, 0.87 mmol, 1.0 eq.) $NaBH_3CN$ (89 mg, 1.50 mmol, 1.72 eq.) was added at room temperature and the reaction mixture was stirred for 4 h. After diluting with CH_2Cl_2 the organic layer was washed with water, Na_2CO_3 solution, water and dried over Na_2SO_4. Evaporation of the solvent yielded yellowish oily product which crystallized on standing (226 mg, 84%). Analytical sample was obtained by recrystallization from ethyl acetate/hexane mp = 119-121°.

18. ^1H NMR (270 MHz) ($CDCl_3$) δ TMS: 1.23 (3 H, t, J = 7.0); 3.83 (3 H, s); 4.03 (1 H, t, J = 8.8 Hz); 4.92-5.18 (4 H, m); 6.81-6.84 (1 H, m); 7.26-7.37 (2 H, m). IR (KBr pellet): 3520, 1753, 1717, 1413, 1221. Anal. Calcd for $C_{15}H_{17}NO_6$: C, 58.62; H, 5.57; N, 4.56. Found: C, 58.72; H, 5.60; N, 4.44.

Hydroxyamide **19**. To a solution of crude β-hydroxyester **18** (148 mg, 0.48 mmol, 1.0 eq.) in ethanol (5.0 mL) aqueous LiOH (2.0 M, 0.36 mL, 0.72 mmol, 1.5 eq.) was added at room temperature. After 0.5 h at room temperature the reaction mixture was diluted with water and washed with CH_2Cl_2. The aqueous layer was acidified with HCl (2.0 M, 0.4 mL) and extracted with CH_2Cl_2. Drying of the organic extract over Na_2SO_4 and

3.09 (1 H, dd, J = 15.8 Hz, J = 8.1 Hz); 3.62-3.68 (1 H, m); 3.82 (3 H, s); 4.30 (1 H, dd, J = 8.9 Hz, J = 7.2 Hz); 4.77 (1 H, dd, J = 9.0 Hz, J = 8.1 Hz); 4.98 (1 H, t, J = 7.4 Hz); 6.78 (1 H, d, J = 8.3 Hz); 6.82 (1 H, d, J = 7.7 Hz); 7.24 (1 H, t, J = 7.7 Hz); 9.47 (1 H, s). IR (NaCl, neat): 1730, 1586, 1470, 1070 cm^{-1}

By analogous procedure aldehyde **22B** was obtained from **21B** in 65% yield as colorless oil.

22B. ^1H NMR (270 MHz) ($CDCl_3$) δ $CHCl_3$: 0.93 (3 H, s); 0.99 (3 H, s); 2.23-2.42 (5 H, m); 2.88 (1 H, d, J = 16.3 Hz); 3.06 (1 H, dd, J = 16.2 Hz, J = 5.8 Hz); 3.80 (3 H, s); 3.98-4.07 (1 H, m); 4.37-4.45 (1 H, m); 4.86-4.94 (1 H, m); 6.71-6.75 (2 H, m); 7.20 (1 H, t, J = 7.9 Hz); 9.25 (1 H, s). IR (NaCl, neat): 1756, 1587, 1472, 1258, 1078 cm^{-1}.

Quinocarcin analogs **23A,B**. To a solution of crude **22A** (11.0 mg, 0.03 mmol) in ethanol (2 mL) aqueous LiOH solution (2.0 M, 0.2 mL) was added and the mixture was refluxed under N_2 for 48 h. The reaction mixture was diluted with methylene chloride and washed with brine. The organic layer was dried over Na_2SO_4, concentrated and the oily residue was separated by silica gel PTLC (CH_2Cl_2/MeOH - 10/1) to yield starting aldehyde **22A** (2.2 mg, 20%), oxazolidine **23A** (4.2 mg, 44%) and alcohol **21A** (1.0 mg, 10%) as colorless oils. Recrystallization from pentane produced crystalline **23A** mp = 111-113° which was used for X-ray structure determination.

23A. ^1H NMR (300 MHz) ($CDCl_3$) δ TMS: 0.95 (3 H, s); 1.23 (3 H, s); 2.32 (3 H, s); 2.39 (1 H, dd, J = 11.5 Hz, J = 9.5 Hz); 2.73-2.98 (4 H, m); 3.52-3.67 (3 H, m); 3.77 (3 H, s); 4.55 (1 H, t, J = 6.2 Hz); 6.67 (1 H, d, J = 8.2 Hz); 6.77 (1 H, d, J = 7.6 Hz); 7.14 (1 H, t, J = 8.1 Hz). IR (NaCl, neat): 1581, 1470, 1260, 1087, 1018, 779 cm^{-1}.

By analogous procedure **23B** was obtained from **22B** as colorless oil with 27% yield. Recrystallization from ethyl acetate/hexane produced crystalline product mp = 159-160° which was used for X-ray structure determination.

23B. ^1H NMR (270 MHz) ($CDCl_3$) δ TMS: 1.16 (3 H, s); 1.33 (3 H, s); 2.34 (3 H, s); 2.52-2.75 (4 H, m); 2.95-3.05 (1 H, m); 3.62 (1 H, d, J = 7.3 Hz); 3.77 (3 H, s); 4.16 (2 H, t, J = 7.4 Hz); 4.42 (1 H, t, J = 7.7 Hz); 6.71 (1 H, d, J = 7.5 Hz); 6.74 (1 H, d, J = 7.6 Hz); 7.18 (1 H, t, J = 7.9 Hz). IR (NaCl, neat): 1588, 1473, 1260, 1018, 786, 744 cm^{-1}.

References and Footnotes

1. (a) Tomita, F.; Takahashi, K.; Shimizu, K. *J. Antibiotics* (1983) **36**, 463. (b) Takahashi, K.; Tomita, F. *J. Antibiotics* (1983) **36**, 468. (c) Hirayama, M.; Shirahata, K. *J. Chem. Soc. Perkin Trans I* (1983) 1705.

2. Naphthyridinomycin: (a) Kluepfel, D.; Baker, H.A.; Piattoni, G.; Sehgal, S.N.; Sidorowicz, A.; Singh, K.; Vezina, C. *J. Antibiotics* (1975) **28**, 497. (b) Sygusch, J.; Brisse, F.; Hanessian, S.; Kluepfel, D. *Tetrahedron Lett.* (1974) 4021. (c) Sygusch, J.; Brisse, F.; Hanessian, S. *Acta Cryst.* (1976) **332**, 1139. (d) Zimjewski, M.J.; Mikolajczak, M.; Viswanatha, V.; Hruby, V.J. *J. Am. Chem. Soc.* (1982) **104**, 4969. (e) Zimjewski, M.J.; Miller-Hatch, K.; Goebel, M. *Antimicrobial Agents Chemother.* (1982) **21**, 787. (f) Singh, K.; Sun, S.; Kluepfel, D. *Dev. Ind. Microbiol.* (1976) **17**, 209. (g) Zmijewski, M.J.; Goebel, M. *J. Antibiotics* (1982) **35**, 524; Naphthocyanidine: (h) Itoh, J.; Omoto, S.; Inouye, S.; Kodama, Y.; Hisamatsu, T.; Niida, T. *J. Antibiotics* (1982) **35**, 642; Cyanocycline: (i) Hayashi, T.; Noto, T.; Nawata, Y.; Okazak, H.; Sawada, M.; Ando, K. *J. Antibiotics* (1982) **35**, 771; Saframycins: (j) Arai, T.; Takahashi, K.; Kubo, A. *J. Antibiotics* (1977) **30**, 1015. (k) Lown, W.J.;

Joshua, A.V.; Lee, J.S. *Biochem.* (1982) **21**, 419. (l) Ishiguro, K.; Takahashi, K.; Yazawa, K.; Sakiyama, S.; Arai, T. *J. Biol. Chem.* (1981) **256**, 2162. (m) Lown, W.J.; Hanstock, C.C.; Joshua, A.V.; Arai, T.; Takahashi, K. *J. Antibiotics* (1983) **36**, 1184; Safracins: (n) Ikeda, Y.; Idemoto, H.; Hirayama, F.; Yamamoto, K.; Iwao, K.; Asao, T.; Munakata, T. *J. Antibiotics* (1983) **36**, 1279-1294. Reineramycins: (o) Frincke, J.M.; Faulkner, D.J. *J. Am. Chem. Soc.* (1982) **104**, 265.

3. (a) Jett, J.R.; Saijo, N.; Hong, W-S.; Sasaki, Y.; Takahashi, H.; Nakano, H.; Nakagawa, K.; Sakurai, M.; Suemasu, K.; Tesada, M. *Investigational New Drugs* (1987) **5**, 155. (b) Chiang, C-D.; Kanzawa, F.; Matsushima, Y.; Nakano, H.; Nakagawa, K.; Takahashi, H.; Terada, M.; Morinaga, S.; Tsuchiya, R.; Sasaki, Y.; Saijo, N. *J. Pharmacobio-Dyn.* (1987)**10**, 431. (c) Fujimoto, K.; Oka, T.; Morimoto, M. *Cancer Research* (1987) **47**, 1516. (d) For the preparation and *in vitro* anti-tumor evaluation of semi-

synthetic quinocarcin derivatives, see: Saito, H.; Kobayashi, S.; Uosaki, Y.; Sato, A.; Fujimoto, K.; Miyoshi, K.; Ashizawa, T.; Morimoto, M.; Hirata, T. *Chem. Pharm. Bull.* (1990) **38**, 1278.

4. Tomita, F.; Takahashi, K.; Tamaoki, T. *J. Antibiotics* (1984) **37**, 1268.

5. Hill, C.G.; Wunz, T.P.; Remers, W.A. *J. Computer-Aided Mol. Design* (1988) **2**, 91.

6. For several pertinent reviews, see: (a) Lown, J.W. *Mol. and Cell Biochem.* (1983) **55**, 17. (b) Martin, P.G. *Angew. Chem. Int. Ed. Engl.* (1989) **28**, 555. (c) Stubbe, J.; Kozarich, J.W. *Chem. Rev.* (1987) **87**, 1107. (d) Fisher, J.F.; Aristoff, P.A., Progress in Drug Research (1988) **32**, 411.

7. Williams, R.M.; Glinka, T.; Gallegos, R.; Coffman, H.; Flanagan, M., submitted for publication; the structures of both **2** and **9**, resulting from the auto redox disproportionation of **1** have been rigorously confirmed.

8. For synthetic studies on quinocarcin, see: (a) Fukuyama, T.; Nunes, J.J. *J. Am. Chem. Soc.* (1988) **110**, 5196. (b) Danishefsky, S.J.; Harrison, P.J.; Webb, R.R.; O'Neil, B.T. *J. Am. Chem. Soc.* (1985) **107**, 1421. (c) Kiss, M.A.; Russell-Maynard, J.; Joule, J.A. *Tetrahedron Lett.* (1987) **28**, 2187. (d) Saito, H.; Hirata, T. *Tetrahedron Lett.* (1987) **28**, 4065. (e) Garner, P.; Sunitha, K.; Shanthilal, T. *Tetrahedron Lett.* (1988) **29**, 3525. (f) Garner, P.; Sunitha, K.; Ho, W-B.; Youngs, W.J.; Kennedy, V.O.; Djedli, A. *J. Org. Chem.* (1989) **54**, 2041. (g) Garner, P.; Arya, F.; Ho, W-B. *J. Org. Chem.* (1990) **55**, 412. (h) Saito, S.; Tanaka, K.; Nakatani, K.; Matsuda, F.; Terashima, S. *Tetrahedron Lett.* (1989) **30**, 7423. (i) Lessen, T.A.; Demko, D.M.; Weinreb, S.M. *Tetrahedron Lett.* (1990) **31**, 2105. (j) Allway, P.A.; Sutherland, J.K.; Joule, J.A. *Tetrahedron Lett.* (1990) **31**, 4781.

9. The molecular mechanics calculations were carried out using forcefield GENERIC, with partial charges obtained with the QEq method in the molecular modeling package Biograf obtained from the BioDesign subsidiary of Molecular Simulations, Inc., 199 S. Los Robles Avenue, Suite 540, Pasadena, California 91101. After a preminimization of each trial structure 10 cycles of annealed dynamics were carried out from 0K to 600K with a time step of 1.0 fs and a temperature increment of 10 K per 10 fs. With this procedure, minima were obtained for **23**; the results agree with x-ray structures shown in Figure 2. The enantiomorph of the quinocarcin structure is depicted in Figure 1 and was chosen only for the convenience of clarity in rendering the stereoelectronic arguments.

10. Williams, R.M.; Ehrlich, P.P.; Zhai, W.; Hendrix, J. *J. Org. Chem.* (1987) **52**, 2615.

11. Taken in part from the Ph.D. dissertation of Paul P. Ehrlich, Colorado State University, 1990.

12. Details of the x-ray structures will be published elsewhere.

13. Misra, H.P. *J. Biol. Chem.* (1974) **249**, 2151.

14. (a) Lesko, S.A.; Lorentzen, R.J.; Ts'O, P.O. *Biochemistry* (1980) **19**, 3023. (b) Saito, I.; Takayama, M.; Matsuura, T.; Matsugo, S.; Kawanishi, S. *J. Am. Chem. Soc.* (1990) **112**, 883. (c) Halliwell, B.; Gutteridge, J.M.C.; Aruoma, O.I. *Anal. Biochem.* (1987) **165**, 215.

15. (a) Graf, E.; Mahoney, J.R.; Bryant, R.G.; Eaton, J.W. *J. Biol. Chem.* (1984) **259**, 3620. (b) Sutton, H.C.; Winterbourn, C.C. *Free Radical Biol. and Med.* (1989) **6**, 53. (c) Sausville, E.A.; Peisach, J.; Horwitz, S.B. *Biochemistry* (1978) **17**, 2740. (d) Ursini, F.; Maiorino, M.; Hochstein, P.; Ernster, L. *Free Radical Biol. and Med.* (1989) **6**, 31.

16. Hertzberg, R.P.; Dervan, P.B. *Biochemistry* (1984) **23**, 3934.

17. Freifelder, D.; Trumbo, B. *Biopolymers* (1969) **7**, 681.

18. Tsou, K-C.; Cheng, C-S.; Nachlas, M.M.; Seligman, A.M. *J. Am. Chem. Soc.* (1956) **78**, 6139. See also ref. 13.

Reprinted from the Journal of the American Chemical Society, 1992, *114*.

Cannizzaro-Based O_2-Dependent Cleavage of DNA by Quinocarcin

Robert M. Williams,*,† Tomasz Glinka,† Mark E. Flanagan,† Renee Gallegos,† Hazel Coffman,† and Deihua Pei‡

Contribution from the Departments of Chemistry, Colorado State University, Fort Collins, Colorado 80523, and University of California, Berkeley, California 94720.
Received May 28, 1991

Abstract: A novel mechanism for the reduction of molecular oxygen that results in the O_2-dependent cleavage of both single-stranded and double-stranded DNA by quinocarcin (**1**) is presented. The results are discussed in the context of a redox self-disproportionation (Cannizzaro-type) of the oxazolidine moiety of quinocarcin which produces superoxide.

It is now widely recognized[1] that a variety of clinically significant antitumor antibiotics can mediate oxygen-dependent cleavage of the ribose–phosphate backbone of cellular DNA and RNA. An enormous structural array of interesting natural products and semisynthetic and totally synthetic substances mediate oxidative strand scission of nucleic acids through three main families[2] of reactions: (1) metal-mediated activation of O_2 ultimately producing hydroxyl radical or other reactive oxygen species;[3-14] (2) non-metal-dependent generation of reactive carbon radicals[15] that mediate C–H abstraction from the deoxyribose backbone (the resulting deoxyribosyl radical subsequently reacts with molecular oxygen culminating in strand scission), and (3) photolytic production of hydroxyl radical,[16] which does not require metal participation for the DNA cleavage event. A rich array of chemistry can be found in the metal-dependent family of DNA damaging agents. Many readily oxidizable organic substances are capable of reducing molecular oxygen, resulting in the production of superoxide such as semiquinone radical anions, thiols,[17] and ascorbate, among others. Superoxide is well-documented[6,7,18,19] to be capable of mediating DNA strand breakage via dismutation to hydrogen peroxide and reduction of adventitious metals such as Fe(III) to Fe(II) (Haber–Weiss cycling) culminating in the reduction of hydrogen peroxide by Fe(II), generating the highly reactive hydroxyl radical (Fenton reaction).

The capacity of many antitumor antibiotics to cause oxidative damage to DNA in cancerous tissues is typically inseparable from the nonspecific damage inflicted on healthy cells by these reduced oxygen species and is widely recognized to be associated with the

† Colorado State University.
‡ University of California.

(1) Fisher, J.; Aristoff, P. A. *Prog. Drug Res.* **1988**, *32*, 411. Remers, W. A. *J. Nat. Prod.* **1985**, *48*, 173.
(2) Radiolytic decay is an important fourth family but is initiated by a nuclear event rather than a chemical event.
(3) Stubbe, J.; Kozarich, J. W. *Chem. Rev.* **1987**, *87*, 1107. Rabow, L. E.; Stubbe, J.; Kozarich, J. W. *J. Am. Chem. Soc.* **1990**, *112*, 3106. Rabow, L. E.; McGall, G. H.; Stubbe, J.; Kozarich, J. W. *J. Am. Chem. Soc.* **1990**, *112*, 3203.
(4) Natrajan, A.; Hecht, S. M.; van der Marel, G. A.; van Boom, J. H. *J. Am. Chem. Soc.* **1990**, *112*, 4532. Hecht, S. M. *Fed. Proc.* **1986**, *45*, 2784.
(5) Sausville, E. A.; Peisach, J.; Horwitz, S. B. *Biochemistry* **1978**, *17*, 2740.
(6) Graf, E.; Mahoney, J. R.; Bryant, R. G.; Eaton, J. W. *J. Biol. Chem.* **1984**, *259*, 3620. Graf, E.; Empson, K. L.; Eaton, J. W. *J. Biol. Chem.* **1987**, *262*, 11647. Ursini, F.; Mariorino, M.; Hochstein, P.; Ernster, L. *Free Radical Biol. Med.* **1989**, *6*, 31. Halliwell, B.; Gutteridege, J. M. C.; Aruoma, O. I. *Anal. Biochem.* **1987**, *165*, 215. Walling, C. *Acc. Chem. Res.* **1975**, *8*, 125.
(7) Sutton, H. C.; Winterbourn, C. C. *Free Radical Biol. Med.* **1989**, *6*, 53.
(8) Tullius, T. D.; Dombroski, B. A.; Churchill, M. E. A.; Kam, L. *Methods Enzymol.* **1987**, *155*, 537. Tullius, T. D. *TIBS* **1987**, *12*, 297. Tullius, T. D.; Dombroski, B. A. *Science* **1985**, *230*, 679. Latham, J. A.; Cech, T. R. *Science* **1989**, *245*, 276.
(9) Hertzberg, R. P.; Dervan, P. B. *Biochemistry* **1984**, *23*, 3934. Dervan, P. B. *Science* **1986**, *232*, 464. Dreyer, G. B.; Dervan, P. B. *Proc. Natl. Acad. Sci., U.S.A.* **1985**, *82*, 968. Moser, H. E.; Dervan, P. B. *Science* **1987**, *238*, 645. Chu, B. C. F.; Orgel, L. E. *Proc. Natl. Acad. Sci., U.S.A.* **1985**, *82*, 968. Vary, C. P. H.; Vournakis, J. N. *Proc. Natl. Acad. Sci., U.S.A.* **1984**, *81*, 6978. Kean, J. M.; White, S. A.; Draper, D. E. *Biochemistry* **1985**, *28*, 1054. Tanner, N. K.; Cech, T. R. *Nucleic Acids Res.* **1985**, *13*, 7759. Lin, S. B.; Blake, K. R.; Miller, P. S.; Ts'o, P. O. P. *Biochemistry* **1989**, *28*, 1054.

0002-7863/92/1514-733$03.00/0

undesirable host toxicity of most antitumor drugs. The recognition of new mechanisms for the production of such reactive oxygen species and chemical means to attenuate this reactivity without compromising other modes of action often displayed by such substances, such as nucleic acid alkylation, intercalation, and DNA polymerase inhibition, will be essential to designing more specific and efficacious cancer chemotherapeutic agents. In this paper, we report observations that support an entirely new mechanism for O_2 reduction resulting in cleavage of DNA that is based on an auto-redox disproportionation (Cannizzaro-type) of the oxazolidine hemiacetal of **1** (Chart I).

Quinocarcin (**1**) is a natural secondary metabolite produced by *Streptomyces melanovinaceus* and is the simplest member of the naphthyridinomycin (**4**)/saframycin (**5**) class of antitumor agents.[20,21] Quinocarcin has been shown[20,22] to display weak antimicrobial activity against several Gram-positive microbes but is inactive toward Gram-negative bacteria. As its citrate salt, quinocarcin (named quinocarmycin citrate or KW2152) displays promising antitumor activity[22] against several lines of solid mammalian carcinomas including St-4 gastric carcinoma, Co-3 human colon carcinoma, MX-1 human mammary carcinoma, M5076 sarcoma, B16 melanoma, and P388 leukemia. This substance is currently under evaluation in human clinical trials by the Kyowa Hakko Kogyo Co., Japan. Very recently, the structurally related antitumor antibiotic tetrazomine (**3**) was isolated[23] from *Saccharothrix mutabilis* subsp. *chichijiimaensis* and is reported to display good antimicrobial activity against both Gram-positive and Gram-negative organisms in the 0.78–50.0 μg/mL range and also shows potent activity toward P-388 and L1210 leukemia in vitro.

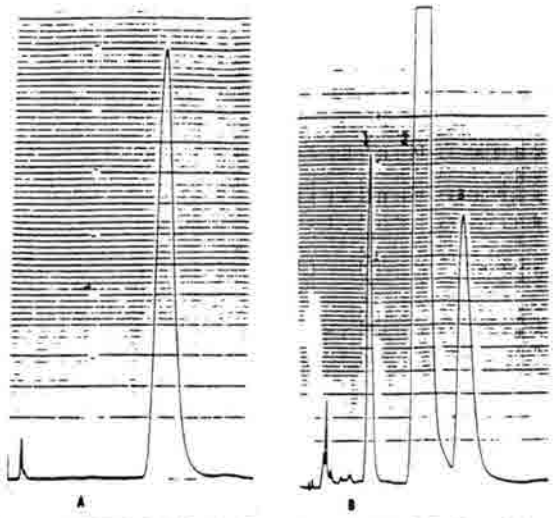

Figure 1. HPLC (C18 Resolve Pack column, 5% MeOH/5% MeCN in 6 mM potassium phosphate (pH 6.8) (isocratic)) of anaerobic quinocarcin (300 mg/mL) at 25 °C: (A) immediately after removal of citrate; (B) after 1 week. Peaks: 1, quinocarcinamide (**10**) 10 min; 2, quinocarcin (**1**) 16 min; 3, quinocarcinol (**2**) 22 min. This corresponds to a rate of disproportionation of $\sim 6 \times 10^{-4}$ M L^{-1} s^{-1}.

(10) Mack, D. P.; Dervan, P. B. *J. Am. Chem. Soc.* **1990**, *112*, 4604.
(11) Chen, C. B.; Sigman, D. S. *J. Am. Chem. Soc.* **1988**, *110*, 6570. Sigman, D. S. *Acc. Chem. Res.* **1986**, *19*, 180.
(12) Lee, K. S.; Roschenthaler, R. *J. Antibiot.* **1987**, *40*, 692.
(13) Scannell, R. T.; Barr, J. R.; Murty, V. S.; Reddy, K. S.; Hecht, S. M. *J. Am. Chem. Soc.* **1988**, *110*, 3650.
(14) Lown, J. W. *Mol. Cell. Biochem.* **1983**, *55*, 17. Lown, J. W.; Joshua, A. V.; Chen, H.-H.; Lown, J. W.; Joshua, A. V.; Lee, J. S. *Biochemistry* **1982**, *21*, 419. Lown, J. W.; Hanstock, C. C.; Joshua, A. V.; Arai, T.; Takahashi, K. *J. Antibiot.* **1983**, *36*, 1184.
(15) Kappen, L. S.; Goldberg, I. H.; Wu, S. H.; Stubbe, J.; Worth, L.; Kozarich, J. W. *J. Am. Chem. Soc.* **1990**, *112*, 2797. Hensens, O. D.; Goldberg, I. H. *J. Antibiot.* **1989**, *42*, 761. Meyers, A. G. *Tetrahedron Lett.* **1987**, *28*, 4493. Meyers, A. G.; Proteau, P. J.; Handel, T. M. *J. Am. Chem. Soc.* **1988**, *110*, 7212. Meyers, A. G.; Proteau, P. J. *J. Am. Chem. Soc.* **1989**, *111*, 1146. Meyers, A. G.; Kuo, E. Y.; Finney, N. S. *J. Am. Chem. Soc.* **1989**, *111*, 8057. Golik, J.; Clardy, J.; Dubay, G.; Groenewold, G.; Kawaguchi, H.; Konishi, M.; Krishnan, B.; Ohkuma, H.; Saitoh, K.; Doyle, T. W. *J. Am. Chem. Soc.* **1987**, *109*, 3461. Golik, J.; Dubay, G.; Groenewold, G.; Kawaguchi, H.; Konishi, M.; Krishnan, B.; Ohkuma, H.; Saitoh, K.; Doyle, T. W. *J. Am. Chem. Soc.* **1987**, *109*, 3462. Lee, M. D.; Dunne, T. S.; Siegel, M. M.; Chang, C. C.; Morton, G. O.; Borders, D. B. *J. Am. Chem. Soc.* **1987**, *109*, 3464. Lee, M. D.; Dunne, T. S.; Chang, C. C.; Ellestad, G. A.; Siegel, M. M.; Morton, G. O.; McGahren, W. J.; Borders, D. B. *J. Am. Chem. Soc.* **1987**, *109*, 3466. Nicolaou, K. C.; Zuccarello, G.; Ogawa, Y.; Schweiger, E. J.; Kumazawa, T. *J. Am. Chem. Soc.* **1988**, *110*, 4866. Nicolaou, K. C.; Ogawa, Y.; Zuccarello, G.; Kataoka, H. *J. Am. Chem. Soc.* **1988**, *110*, 7247. Magnus, P.; Lewis, R. T. *Tetrahedron Lett.* **1989**, *30*, 1905. Magnus, P.; Lewis, R. T.; Bennett, F. *J. Chem. Soc., Chem. Commun.* **1989**, 916. Magnus, P.; Lewis, R. T.; Huffman, J. C. *J. Chem. Soc.* **1988**, *110*, 6921. Magnus, P.; Carter, P. A. *J. Am. Chem. Soc.* **1988**, *110*, 1626. Magnus, P.; Fortt, S.; Herna, T. P.; Snyder, J. P. *J. Am. Chem. Soc.* **1990**, *112*, 4986. Hawley, R. C.; Kiessling, L. L.; Schreiber, S. L. *Proc. Natl. Acad. Sci. U.S.A.* **1989**, *86*, 1105. Zein, N.; Poncin, M.; Nilakantan, R.; Ellestad, G. A. *Science* **1989**, *244*, 697. Snyder, J. P. *J. Am. Chem. Soc.* **1989**, *111*, 7630. Snyder, J. P. *J. Am. Chem. Soc.* **1990**, *112*, 5367. Meyers, A. G.; Dragovich, P. S. *J. Am. Chem. Soc.* **1989**, *111*, 9130. Zein, N.; Sinha, A. M.; McGahren, W. J.; Ellestad, G. A. *Science* **1988**, *240*, 1198. DeVoss, J. J.; Hangeland, J. J.; Townsend, C. A. *J. Am. Chem. Soc.* **1990**, *112*, 4554. Haseltine, J. N.; Danishefsky, S. J.; Schulte, G. *J. Am. Chem. Soc.* **1989**, *111*, 7638. Saito, I.; Kawabata, H.; Fujiwara, T.; Sugiyama, H.; Matsuura, T. *J. Am. Chem. Soc.* **1989**, *111*, 8302. Nagata, R.; Yamanaka, H.; Murahashi, E.; Saito, I. *Tetrahedron Lett.* **1990**, *31*, 2907. Nataga, R.; Yamanaka, H.; Okazaki, E.; Saito, I. *Tetrahedron Lett.* **1989**, *30*, 4995. Shiomi, K.; Iinuma, H.; Naganawa, H.; Hamada, M.; Hattori, S.; Nakamura, H.; Takeuchi, T. *J. Antibiot.* **1990**, *43*, 1000. Konishi, M.; Ohkuma, H.; Tsuno, T.; Oki, T. *J. Am. Chem. Soc.* **1990**, *112*, 3715. Semmelhack, M. F.; Gallagher, J.; Cohen, D. *Tetrahedron Lett.* **1990**, *31*, 1521. Konishi, M.; Ohkuma, H.; Matsumoto, K.; Tsuno, T.; Kamei, H.; Miyaki, T.; Oki, T.; Kawaguchi, H.; Van Duyne, G. D.; Clardy, J. *J. Antibiot.* **1989**, *42*, 1449. Snyder, J. P.; Tipsword, G. E. *J. Am. Chem. Soc.* **1990**, *112*, 4040.
(16) Saito, I.; Takayama, M.; Matsuura, T.; Matsugo, S.; Kawanishi, S. *J. Am. Chem. Soc.* **1990**, *112*, 883 and references cited therein. Zafirou, O. C.; Bonneau, R. *Photochem. Photobiol.* **1987**, *45*, 723.
(17) Misra, H. P. *J. Biol. Chem.* **1974**, *249*, 2151.
(18) Lesko, S. A.; Lorentzen, R. J.; Ts'o, P. O. P. *Biochemistry* **1980**, *19*, 3023.
(19) Myers, C.; Gianni, L.; Zweier, J.; Muindi, J.; Sinha, B. K.; Eliot, H. *Fed. Proc.* **1986**, *45*, 2792.
(20) Tomita, F.; Takahashi, K.; Shimizu, K. *J. Antibiot.* **1983**, *36*, 463. Takahashi, K.; Tomita, F. *J. Antibiot.* **1983**, *36*, 468. Hirayama, M.; Shirahata, K. *J. Chem. Soc., Perkin Trans. 1* **1983**, 1705.
(21) Naphthyridinomycin: Kluepfel, D.; Baker, H. A.; Piattoni, G.; Sehgal, S. N.; Sidorowicz, A.; Singh, K.; Vezina, C. *J. Antibiot.* **1975**, *28*, 497. Syguach, J.; Brisse, F.; Hanessian, S. *Acta Crystallogr.* **1976**, *332*, 1139. Zimjewski, M. J.; Mikolajczak, M.; Viswanatha, V.; Hruby, V. J. *J. Am. Chem. Soc.* **1982**, *104*, 4969. Zimjewski, M. J.; Miller-Hatch, K.; Goebel, M. *Antimicrob. Agents Chemother.* **1982**, *21*, 787. Singh, K.; Sun, S.; Kluepfel, D. *Dev. Ind. Microbiol.* **1976**, *17*, 209. Zmijewski, M. J.; Goebel, M. *J. Antibiot.* **1982**, *35*, 524. Naphthocyanidine: Itoh, J.; Omoto, S.; Inouye, S.; Kodama, Y.; Hisamatsu, T.; Niida, T. *J. Antibiot.* **1982**, *35*, 642. Cyanocycline: Hayashi, T.; Noto, T.; Nawata, Y.; Okazak, H.; Sawada, M.; Ando, K. *J. Anbibiot.* **1982**, *35*, 771. Saframycins: Arai, T.; Takahashi, K.; Kubo, A. *J. Antibiot.* **1977**, *30*, 1015. Lown, W. J.; Joshua, A. V.; Lee, J. S. *Biochemistry* **1982**, *21*, 419. Ishiguro, K.; Takahashi, K.; Yazawa, K.; Sakiyama, S.; Arai, T. *J. Biol. Chem.* **1981**, *256*, 2162. Lown, W. J.; Hanstock, C. C.; Joshua, A. V.; Arai, T.; Takahashi, K. *J. Antibiot.* **1983**, *36*, 1184. Safracins: Ikeda, Y.; Idemoto, H.; Hirayama, F.; Yamamoto, K.; Iwao, K.; Asao, T.; Munakata, T. *J. Antibiot.* **1983**, *36*, 1279–1294. Reineramycins: Frincke, J. M.; Faulkner, D. J. *J. Am. Chem. Soc.* **1982**, *104*, 265.
(22) Jett, J. R.; Saijo, N.; Hong, W-S.; Sasaki, Y.; Takahashi, H.; Nakano, H.; Nakagawa, K.; Sakurai, M.; Suemasu, K.; Tesada, M. *Investigational New Drugs* **1987**, *5*, 155. Chiang, C.-D.; Kanzawa, F.; Matsushima, Y.; Nakano, H.; Nakagawa, K.; Takahashi, H.; Terada, M.; Morinaga, S.; Tsuchiya, R.; Sasaki, Y.; Saijo, N. *J. Pharmacobio-Dyn* **1987**, *10*, 431. Fujimoto, K.; Oka, T.; Morimoto, M. *Cancer Res.* **1987**, *47*, 1516. For the preparation and in vitro antitumor evaluation of semisynthetic quinocarcin derivatives, see: Saito, H.; Kobayashi, S.; Uosaki, Y.; Sato, A.; Fujimoto, K.; Miyoshi, K.; Ashizawa, T.; Morimoto, M.; Hirata, T. *Chem. Pharm. Bull.* **1990**, *38*, 1278. Saito, H.; Sato, A.; Ashizawa, T.; Morimoto, M.; Hirata, T. *Chem. Pharm. Bull.* **1990**, *38*, 3202. Saito, H.; Hirata, T.; Kasai, M.; Fujimoto, K.; Ashizawa, T.; Morimoto, M.; Sato, A. *J. Med. Chem.* **1991**, *34*, 1959.
(23) Suzuki, K.; Sato, T.; Morioka, M.; Nagai, K.; Abe, K.; Yamaguchi, H.; Saito, T.; Ohmi, Y.; Susaki, K. *J. Antibiot.* **1991**, *44*, 479.

Chart I

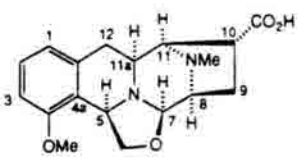

1, *QUINOCARCIN, DC-52*

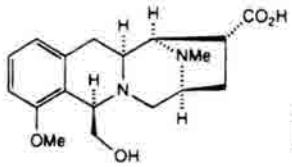

2, *QUINOCARCINOL, DC-52d*

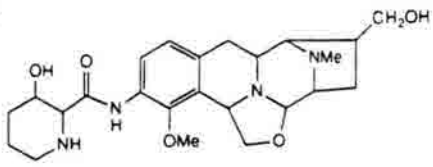

3, *TETRAZOMINE*

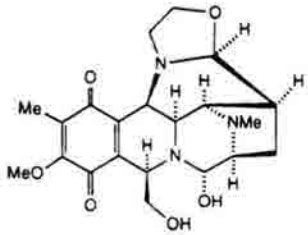

4, *NAPHTHYRIDINOMYCIN*

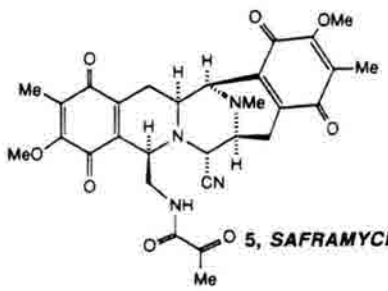

5, *SAFRAMYCIN A*

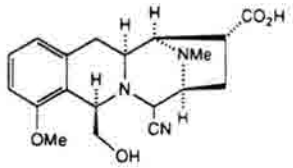

12, DX-52-1

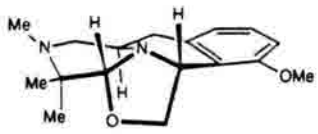

13

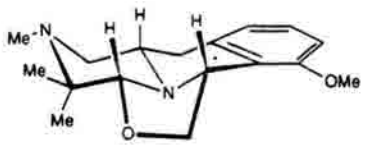

14

Our interest in this substance stems from a report by Tomita et al.[24] that recorded the remarkable observation that **1** cleaves plasmid DNA in an O_2-dependent fashion that was reported (1) *not* to be stimulated by the addition of metal ions (Fe^{2+} or Cu^{2+}), (2) to be stimulated by dithiothreitol, (3) to be inihibited by oxygen-free radical scavengers such as methanol, *tert*-butyl alcohol, α-tocopherol, and β-carotene, and (4) to be inhibited by superoxide dismutase (SOD) and catalase. Quinocarcin blocks RNA synthesis in preference to DNA and protein synthesis in P388 leukemia cells.[22] On the other hand, in *Bacillus subtilis*, quinocarcin inhibited [^{3}H]thymidine incorporation, suggesting inhibition of DNA polymerase; therefore, DNA synthesis is thought[24] to be preferentially inhibited in *B. subtilis*. It has been proposed[22,24] that quinocarcin alkylates DNA in the minor groove[25] through the ring-opened form of the oxazolidine (iminium **6**). Similar DNA alkylation has been invoked for **4** and **5**. Indirect support[22,24] for the involvement of the oxazolidine ring in the above context comes from the lack of antitumor and DNA-damaging activity displayed by quinocarcinol (**2**, DC-52d), which is coproduced with **1** by *Streptomyces melanovinaceus*. Quinocarcinol also does not cleave plasmid DNA,[24] which forces the conclusion that the oxazolidine moiety is also responsible for the oxidative degradation of DNA by a previously unrecognized mechanism.

While it is not yet clear whether the antitumor properties of quinocarcin are a manifestation of only one mode of action (i.e., DNA alkylation) or both (DNA alkylation and oxidative DNA cleavage), we were intrigued by the oxidative cleavage observations of the Kyowa Hakko group[24] since **1** does not contain any readily recognizable functionality that would be associated with the capacity for oxidative DNA cleavage, such as metal chelation sites, quinones, and ene–diynes. Most likely, the efficacy of this drug is a delicate and intimate combination of multiple effects that are brought to bear on its macromolecular targets.

We have obtained experimental evidence presented herein that quinocarcin undergoes a redox self-disproportionation reaction that we propose is coupled to the capacity of this substance to effect the production of superoxide in the presence of molecular oxygen and results, at least in part, to Fenton-mediated lesions in DNA; a mechanism for this process is presented in Scheme I. Natural quinocarcin citrate (quinocarmycin citrate), obtained from Kyowa Hakko Kogyo, was separated from citric acid by ion-exchange chromatography (HP-20) and purified to homogeneity by reversed-phase HPLC. When the purified, colorless antibiotic was allowed to stand in carefully deoxygenated water at 25 °C, two new products are produced by HPLC analysis (Figure 1). The slower eluting peak has been isolated and identified as quinocarcinol (**2**); preparation of an authentic sample[20] from **1** rigorously confirms this assignment. The faster eluting peak has been identified as the amide **10** (herein named quinocarcinamide) based on IR, mass spectra, and fully decoupled ^{1}H NMR and ^{13}C NMR spectroscopy. Esterification of **10** with diazomethane in aqueous dioxane produced a substance whose ^{1}H NMR and IR spectra were identical to those of authentic, synthetic material,[26] providing final, rigorous structural confirmation. The identification of the anaerobic redox products **2** and **10** rigorously supports the proposal that **1** undergoes a Cannizzaro-type self-redox disproportionation; i.e., quinocarcin serves as its own reductant. Therefore, as suggested in Scheme I, single electron transfer from **1** with concomitant proton loss from the oxazolidine nitrogen to the ring-opened tautomer (**6**)[27] would furnish radical anion **7** and the oxazolidinyl radical **8**. Radical **8** should be capable of reducing a second equivalent of **6**, ultimately becoming oxazolidinium ion **9** which should hydrolyze to quinocarcinamide (**10**). Evidence for the intermediacy of **9** was secured by running the anaerobic disproportionation in 98% $^{18}OH_2$ and

(24) Tomita, F.; Takahashi, K.; Tamaoki, T. *J. Antibiot.* **1984**, *37*, 1268.
(25) Hill, C. G.; Wunz, T. P.; Remers, W. A. *J. Computer-Aided Mol. Design* **1988**, *2*, 91.
(26) Danishefsky, S. J.; Harrison, P. J.; Webb, R. R.; O'Neil, B. T. *J. Am. Chem. Soc.* **1985**, *107*, 1421.
(27) It is also conceivable that electron transfer from **1** to molecular oxygen may occur directly or via a metal-mediated process in addition to the transfer shown via **6**.

Table I. Reduction of Nitroblue Tetrazolium by Quinocarcin and DX-52-1[a]

entry	substrate	pH	ΔOD/min at 500 nm (×10⁻⁴)	rate constant, M^{-1} s^{-1}
1	1.0 mM quinocarcin	6	0	0
2	1.0 mM quinocarcin	7.0	3	4.2×10^{-4}
3	1.0 mM quinocarcin	7.4	5	6.8×10^{-4}
4	1.0 mM quinocarcin	8.0	8	1.1×10^{-3}
5	1.0 mM DX-52-1 (**12**)	7.0	0	0
6	1.0 mM DX-52-1 (**12**)	8.0	0	0
7	1.0 mM **13**	8.0	0	0
8	1.0 mM **14**	8.0	3	4.2×10^{4}
9	control phosphate buffer	8.0	0	0

[a] All reductions were carried out in 20 mM phosphate buffer at the indicated pHs. Formation of the furazan product was monitored using a Varian DMS-80 UV/vis spectrophotometer at 500 nm.

Table II. Cleavage of Plasmid Supercoiled DNA (pBR 322)

entry	conditions	[quinocarcin], mM	S[a]
1	pH 5 (20 mM phosphate, 2 h, 37 °C)	1.0	0.3
2	pH 6 (20 mM phosphate, 2 h, 37 °C)	1.0	0.4
3	pH 7 (20 mM phosphate, 2 h, 37 °C)	1.0	1.5
4	pH 8 (20 mM phosphate, 2 h, 37 °C)	1.0	7.8
5	pH 9 (20 mM phosphate, 2 h, 37 °C)	1.0	11.0
6	pH 8 (20 mM phosphate, 4 h, 37 °C)	1.0	19.2
7	H_2O (no buffer, 2 h, 37 °C)	1.0	0.7
8	H_2O (no buffer, 24 h, 37 °C)	1.0	11.4
9	pH 8 (20 mM phosphate, 2 h, 37 °C)	0.1	0.3
10	pH 8 (20 mM Tris, 2 h, 37 °C)	1.0	0.3
11	pH 8 (20 mM phosphate, 2 h, 37 °C)	5.0 (DX-52-1)	0
12	pH 8 (20 mM phosphate, 2 h, 37 °C)	1.0 (quinocarcinamide)	0
13	pH 8 (20 mM phosphate, 2 h, 37 °C)	1.0 (quinocarcinol)	0

[a] The S value for the DNA control represents the amount of nicked open circular DNA present in the starting plasmid and was subtracted from the S values calculated for the individual cleavage reactions. When only forms I (supercoiled) and forms II (nicked open circular) are present, the equation simplifies to $S = -\ln f_I$, where f_I is the fraction of form I molecules. In those cases where form III (linear) DNA was present, S was calculated from $f_I + f_{II} = [1 - S(2h + 1)/2L]^{S/2}$, where h is the distance between hits on opposite strands to produce a linear molecule (16 base pairs) and L is the total number of base pairs in pBR 322 (4362 base pairs).

analyzing the product **10** by mass spectroscopy; greater than 40% ^{18}O was incorporated at the amide carbonyl.[28] Under anaerobic conditions, radical anion **7** subsequently suffers a second electron transfer (presumably from **1** or **8**) with concomitant protonation, resulting in quinocarcinol (**2**). Under aerobic conditions, radical anion **7** can react with molecular oxygen to produce peroxy radical anion **11** which, with nitrogen participation, expels 1 mol equiv of superoxide, regenerating **6**. It is also mechanistically plausible that the putative peroxy radical anion **11** could fragment directly to amide **10** via homolysis of the O–O bond and directly generate hydroxyl radical. A labeling experiment, however, demonstrated that this is not the case. Disproportionation of pure **1** was carried out in water as described above under an atmosphere of 98% $^{18}O_2$. Quinocarcinol (**2**) and quinocarcinamide (**10**) were isolated by reversed-phase HPLC and subjected to mass spectral analysis following diazomethane esterification. The fragmentation pattern of **10** at m/e = 329 showed no significant enhancement at the M + 2 peak (m/e = 331) that would have been diagnostic for

(28) Mass spectral analysis required esterification of the crude products with diazomethane. The base fragment for the corresponding methyl ester of amide **9** was m/e = 329 ($M^+ - CH_2O$); the remainder of the ^{18}O label (~60%) is presumed to reside in the hydroxymethyl moiety due to the ambient electrophilic nature of iminium **8** to hydrolytic capture. Loss of the hydroxymethyl moiety (m/e = 30) is the parent ionization process, generating the corresponding stabilized isoquinolinium amide radical cation (m/e = 329). It was not possible to quantitate ^{18}O incorporation in the hydroxymethyl moiety (m/e = 32) since this appears as a large fragment in both the unlabeled and ^{18}O-labeled samples.

Table III. Effect of Additives on the Cleavage of Plasmid DNA by Quinocarcin[a,b]

entry	reagent	[quinocarcin], mM	% inhibn	% enhancement
1	SOD (10 μg/mL)	1.0	>99	
2	catalase (10 μg/mL)	1.0	33	
3	catalase (100 μg/mL)	1.0	83	
4	deoxygenated mixture[c]	1.0	84	
5	desferal (0.1 mM)	1.0	24	
6	desferal (1.0 mM)	1.0	87	
7	desferal (10 mM)	1.0	>99	
8	Fe(III)/desferal (0.1 mM)	1.0	27	
9	Fe(III)/desferal (1.0 mM)	1.0	91	
10	EDTA (1.0 mM)	1.0	35	
11	DETAPAC (1.0 mM)	1.0	86	
12	picolinic acid (1.0 mM)	1.0	22	
13	picolinic acid (10 mM)	1.0	94	
14	Fe(III) (0.1 mM)	1.0	[d]	
15	H_2O_2 (0.1 mM)	1.0		143
16	H_2O_2 (0.1 mM)	0.1		141
17	DTT (0.1 mM)	1.0	18	
18	DTT (5.0 Mm)	1.0	98	
19	DTT (0.1 mM)	0.1		139
20	DTT (1.0 mM)	0.1		59
21	DTT (5 mM)	0.1	73	

[a] See the Experimental Section. [b] All reactants were mixed at ice bath temperature and brought to a final volume of 10 μL. All reactions were then incubated for 2 h at 37 °C in 20 mM phosphate buffer at pH 8 with 0.15 μg of pBR 322 plasmid DNA. Control reactions for SOD, catalase, iron(III) ammonium sulfate, DTT, desferal, EDTA, DETAPAC (diethylenetriaminepentaacetic acid), H_2O_2, and picolinic acid at the indicated concentrations in the absence of quinocarcin all showed either very marginal or no detectable cleavage of the DNA. [c] The reactants were all mixed at ice bath temperature and then purged with argon gas; the mixture was then brought to 37 °C. [d] No significant inhibition or enhancement of quinocarcin-induced DNA cleavage was observed.

Table IV. Nicking Efficiency as a Function of Superoxide Production (pBR 322 DNA)[a]

entry	reagent	S	ΔΔOD/min[b]	$NE_{superoxide}$
1	ascorbate	5.4	1.653	157
2	DTT	0.28	0.773	19
3	quinocarcin	9.5	0.0013	3.8×10^{4}
4	**14**	0.38	0.0006	3.3×10^{3}

[a] All reactions employed 0.15 μg of pBR 322. [b] SOD concentration was 50 μg/mL for ascorbate and 5 μg/mL for all others.

^{18}O incorporation at the amide carbonyl by the peroxide homolysis possibility alluded to above. The authentic ^{18}O-labeled amide **10** obtained as described above from anaerobic disproportionation in $^{18}OH_2$ showed no propensity to exchange with $^{16}OH_2$ after several days at room temperature as evidenced by the same mass spectral analytical protocol. Neither **2**, **10**, nor the semisynthetic cyano derivative of quinocarcin (DX-52-1, **12**) produce superoxide, as evidenced by the complete lack of nitroblue tetrazolium reduction and their corresponding incapacity to mediate oxidative scission of DNA. On the basis of these observations and the chemical redox chemistry of quinocarcin, we propose the Cannizzaro-driven reduction of molecular oxygen as illustrated in Scheme I.

Superoxide production by quinocarcin was previously reported by Tomita,[24] although a mechanistic explanation was not offered. We have carefully examined superoxide production by quinocarcin and two synthetic analogues,[29] **13** and **14**, by following the reduction of nitroblue tetrazolium (NBT)[17,30] under various pH conditions and find (for **1** and **14**) that this reaction is completely

(29) Williams, R. M.; Glinka, T.; Gallegos, R.; Ehrlich, P. P.; Flanagan, M. E.; Coffman, H.; Park, G. *Tetrahedron* **1991**, *47*, 2629.
(30) Tsou, K-C.; Cheng, C.-S.; Nachlas, M. M.; Seligman, A. M. *J. Am. Chem. Soc.* **1956**, *78*, 6139.

Scheme I

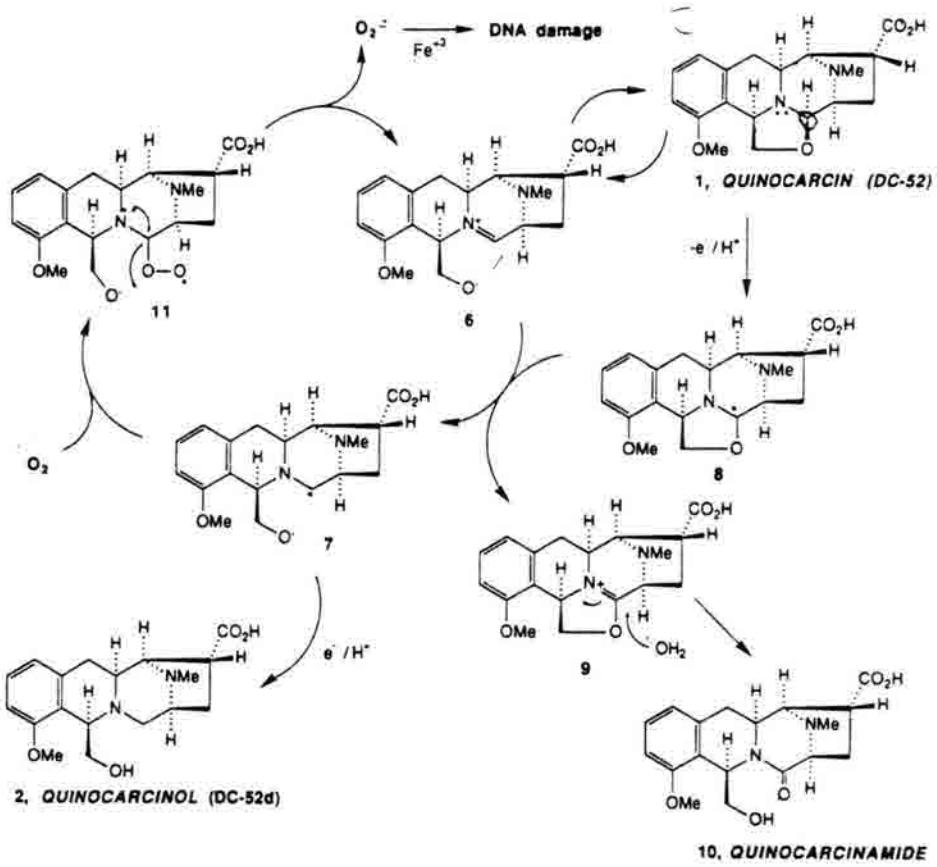

inhibited by SOD; the results are collected in Table I. The reduction of NBT by quinocarcin is pH dependent, exhibiting an increased rate of reduction as the pH is raised. This behavior directly parallels the pH dependency for the DNA cleavage reactions described below.

In order to examine the interaction of quinocarcin with DNA, the pure, colorless antibiotic (0.01–50 mM) was allowed to react with pBR 322 supercoiled plasmid DNA between pH 5 and 9 in phosphate buffer (20 mM) at 37 °C for 2 h in the presence of air. Salient experimental results are collected in Tables II and III. Nicking of the DNA was visualized by 0.8% agarose gel electrophoresis; ethidium bromide solution (0.5 μg/mL) was added to the gel after the gel was run. Quinocarcin showed significant nicking of the DNA at 0.1 mM concentration (Table II, entry 9) at pH 8 without the addition of any external reductants. The reaction was found to be pH dependent, optimal cleavage being observed between pH 8 and 9. At lower pH values (pH 5–7) nicking was observed but was significantly less than at higher pH. This is consistent with the obligate participation of the *unprotonated* oxazolidine nitrogen atom in the redox cycle. Consistent with this behavior, quinocarmycin citrate and DX-52-1, neither of which undergoes the Cannizzaro-type self-redox reaction, displayed a markedly inferior relative ability to nick the DNA at the same concentrations as the purified **1**. Exclusion of oxygen significantly inhibited this reaction (84% inhibition) as expected (Table III, entry 4). DTT at low concentrations enhanced the reaction at low concentrations (0.1 mM) of quinocarcin (Table III, entries 19 and 20) but showed *inhibitory* activity at high concentrations (5 mM; Table III, entries 18 and 21). This is presumably due to the capacity of DTT to serve as a competing CH (or SH) substrate with DNA, which is present in much lower relative concentration. Similar observations on the effect of optimum concentrations of reducing agents on the cleavage of DNA by MPE–Fe(II) have been reported.[9] Independent corroboration of this phenomena was obtained by comparing the relative reactivity of quinocarcin in phosphate and Tris buffers. At 20 mM buffer concentrations, Tris effectively inhibited the cleavage of the plasmid DNA (compare Table II, entries 4 and 10) by quinocarcin. Again, this would indicate that potentially any organic substance can compete with DNA for the Fenton-derived oxidant and that the majority of the reactive oxidant is most likely produced in a non-DNA-associated environment. Superoxide dismutase completely inhibited DNA cleavage (Table III, entry 1), consistent with both the capacity of quinocarcin to generate superoxide and the corresponding DNA cleavage event to be exclusively superoxide dependent. Catalase also inhibits the reaction but is not as potent as SOD (Table III, entries 2 and 3). Addition of hydrogen peroxide to quinocarcin/DNA reactions had a potent stimulatory effect on DNA cleavage over control reactions containing hydrogen peroxide at the same concentrations (Table III, entries 15 and 16). Taken together, the above results point strongly to Fenton-type chemistry being responsible for the scission of DNA. Tomita previously reported[24] that the addition of iron or copper salts had no stimulatory effects on the ability of quinocarcin to cleave DNA; we have corroborated this finding (Table III, entry 14). The addition of the potent iron chelator desferal did, however, lead to significant inhibition of DNA cleavage, particularly at high concentrations (Table III, entries 5–9). Other iron chelators (EDTA, DETAPAC; Table III, entries 10 and 11) also exhibit inhibitory activity. Desferal is known[6] to have a high affinity for Fe(III) (log k_f = 30.7), forming a hexacoordinate complex that excludes iron-associated water and uncouples the oxidation of Fe(II) from the formation hydroxyl radical (Fenton reaction). The participation of higher oxidation states of iron and copper in Fenton reactions and related C–H oxidation chemistry is now well recognized.[7] Picolinic acid is known[31] to be a very potent

Figure 2. Key: lane 1, single-stranded DNA control; lane 2, single-stranded DNA + quinocarcin (1 mM); lane 3, single-stranded DNA + quinocarcin (5 mM); lane 4, single-stranded DNA + quinocarcin (5 mM) followed by T4 kinase; lane 5, single-stranded DNA + $FeSO_4$ (1 mM); lane 6, Maxim–Gilbert G reaction; lane 7, double-stranded DNA control; lane 8, double-stranded DNA + quinocarcin (1 mM); lane 9, double-stranded DNA + quinocarcin (5 mM); lane 10, double-stranded DNA + quinocarcin (5 mM) followed by T4 kinase; lane 11, double-stranded DNA + $FeSO_4$ (1 mM); lane 12, Maxim–Gilbert G reaction. All reactions with quinocarcin are thiol-free. The photograph of the gel was focused on the clearest region to show the double bands (Tullius bands) characteristic of nonselective hydroxyl radical cleavage. There was no significant evidence for any sequence specificity to the cleavage of this substrate (sequence along the gel is therefore superfluous and has been deleted).

scavenger of hydroxyl radical and inhibitor of the Fe(II)/Fe(III) redox couple. Addition of picolinic acid to reaction mixtures of DNA and quinocarcin at 1 and 10 mM showed 22% and 94% inhibition, respectively. These results also support the notion that adventitious metal in these reaction mixtures in a number of possible oxidation states can be activated by the slow release of superoxide and cause Fenton-related damage to DNA. Thus, these results indicate that, in contrast to the conclusions of Tomita,[24] the DNA cleavage is indeed metal dependent and that the low concentration of adventitious Fe^{3+} is already in excess to that required to effect Fenton-mediated cleavage of the DNA; addition of excess iron would therefore not be expected to have any additive effect. Thus, our data support a hypothesis wherein the limiting reagent in the DNA cleavage mediated by quinocarcin is the slow production of superoxide.

Further evidence for a non-DNA-associated oxidant was obtained from an analysis of the reaction of quinocarcin with a small synthetic oligonucleotide by high-resolution polyacrylamide gel electrophoresis. A synthetic 64-base-pair oligonucleotide with the sequence shown in Figure 2 was 5′-end-labeled with ^{32}P, purified by Sephadex G-50 size exclusion chromatography, and annealed to the complementary strand. Reaction of both the duplex 64-mer and the ^{32}P 5′-end-labeled single-stranded oligonucleotide with quinocarcin (1 and 5 mM, without additional reducing agent added) at 37 °C for 5 h resulted in non-sequence-specific cleavage at every single nucleotide as evidenced by denaturing 20% polyacrylamide gel electrophoresis (Figure 2, lanes 2, 3, 8, and 9). Both the double-stranded and single-stranded substrates were cleaved with roughly equal efficiency, a slight preference being noted for single-stranded DNA.[32] Furthermore, every cleavage band appeared as a doublet, which is characteristic of the 3′-phosphate and 3′-phosphoglycolate ends resulting from nonselective Fenton-mediated cleavage.[8,9] We observed the exact same cleavage pattern when the duplex was incubated with 1 mM $FeSO_4$ under aerobic conditions (Figure 2, lanes 5 and 11). Treatment of the quinocarcin-damaged DNA reaction mixtures with T4 polynucleotide kinase in the absence of ATP or ADP exhibited the expected 3-phosphatase gel band shift of the slower moving band of each doublet (Figure 2, lanes 4 and 10) indicative that the slower moving band of each doublet is the 3′-phosphoryl and the faster moving band is the 3′-phosphoglycolate.

Compared with other antitumor substances that cause oxidative damage to DNA, quinocarcin is rather modest in terms of the rate at which DNA cleavage can be measured at a given concentration of drug. This is a direct manifestation of the very slow production of superoxide by quinocarcin. However, one interesting feature of the cleavage reaction of DNA by quinocarcin is that it is vastly more efficient in effecting DNA cleavage *per equivalent of superoxide* generated than other superoxide generating systems, such as DTT and ascorbate. For a qualitative comparison, we have calculated a nicking efficiency ($NE_{superoxide}$) of DNA cleavage as a function of superoxide production (as measured by NBT reduction) for quinocarcin, DTT, and ascorbate. Total superoxide production was estimated by taking the difference between the $\Delta OD/min$ at 500 nm for NBT reduction for each reagent and subtracting the $\Delta OD/min$ under the same conditions in the presence of SOD. The value obtained ($\Delta\Delta OD/min$) can at least be attributed to specific superoxide-mediated reduction of NBT as opposed to direct reduction of the dye by the organic reductant. The equation used was as follows

$$NE_{superoxide} = \frac{(S)(n_{DNA})/n_{substrate}}{(\Delta\Delta OD/min)_{substrate}}$$

where S is the average number of single hits per DNA molecule calculated as described in the footnotes of Table II and n is the number of molecules present. Quinocarcin is 240 times more efficient in effecting DNA cleavage *per superoxide molecule* than ascorbate and 2000 times more efficient than DTT. Synthetic compound **14** is inferior to quinocarcin but is still relatively efficient per superoxide equivalent (21 times versus ascorbate and 173 times versus DTT). The relative differences between quinocarcin and **14** with respect to DNA cleavage are likely a result of the poor solubility of **14** in water; the HCl or citrate salts of **14** were employed in all these studies resulting in protonation of the amines which attenuates the rate of superoxide release (vida infra). Since quinocarcin and synthetic analogue **14** both produce superoxide very slowly compared to DTT and ascorbate, the observed apparent relative efficiency of DNA cleavage as a function of superoxide production for these oxazolidine-containing substances appears to be a direct manifestation of the relative kinetics of superoxide release, although the mechanism for presentation of the oxidant to DNA may be distinct; a detailed explanation cannot be offered at this time. The rate of formation of superoxide by

(31) Sheu, C.; Richert, S. A.; Cofre, P.; Ross, B.; Sobkowiak, A.; Sawyer, D. T.; Kanofsky, J. R. *J. Am. Chem. Soc.* **1990**, *112*, 1936 and referenced cited therein.

(32) Celander D. W.; Cech, T. R. *Biochemistry* **1990**, *29*, 1355. Jezewska, M. J.; Bujalowski, W.; Lohman, T. M. *Biochemistry* **1990**, *29*, 5220.

(33) It should be noted that DX-52-1 and various C-8 and C-10 substituted derivatives maintain significant antitumor activity; see ref 22 (Saito et al., 1990). Hirata, T.; Kobayashi, S.; Takahashi, K.; Morimoto, M.; Saito, H.; Sato, A.; Ashizawa, T. European Patent 128,370, 1984.

quinocarcin[34] (see Table I) is extremely slow (10^4–10^5 times slower) relative to the rate-limiting step[18] of the Haber–Weiss/Fenton reaction, which is 76 M^{-1} s^{-1} for the reduction of hydrogen peroxide by Fe(II). In this context, quinocarcin may prove to be a useful mechanistic tool for studying superoxide-mediated reactions where the slow, controlled release of superoxide would be desired.

Remers[25] has conducted molecular mechanics calculations on quinocarcin by docking the drug in the minor groove. From this study, it was concluded that the absolute configuration of quinocarcin is most likely that depicted in Scheme I. The calculations suggested that the lowest energy conformer of **1** orients the piperazine ring in a chairlike conformation, which therefore places the oxazolidine nitrogen lone pair in an antiperiplanar orientation to the oxazolidine methine (*anti*-**1**). Ring opening of the oxa-

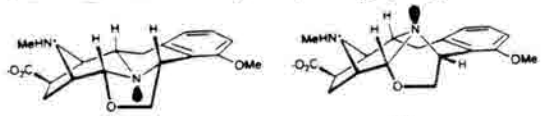

ANTI-1 *SYN-1*

zolidine to the iminium species (see **6**, Scheme I) requires nitrogen pyrimidal inversion to a higher energy twist-boat conformer (*syn*-**1**) that was calculated to lie ~10 kcal mol^{-1} above the other conformer. In this situation, the oxazolidine nitrogen lone pair is syn to the methine and antiperiplanar to the C–O bond. It was postulated[25] that the iminium species[33] should be a good alkylator for N-2 of guanine in the minor groove of the sequence d-$(ATGCAT)_2$. Based on the similarity to **4** and **5**,[21] this is a very reasonable expectation. In the present study, we wished to ask a different question regarding the conformational significance of the oxazolidine moiety. As shown in Scheme I, the initial step in the electron transfer between the oxazolidine and the iminimum species involves one-electron loss from the oxazolidine nitrogen with loss of the oxazolidine methine as a proton producing the reduction and oxidation radicals **7** and **8**, respectively. It is reasonable to expect that the trans, antiperiplanar arrangement of the oxazolidine methine and nitrogen lone pair in the lower energy conformer predicted by calculation should also be the most favorable geometry for concomitant one-electron and proton loss in the redox self-disproportionation, since this arrangement provides maximum overlap in the transition state. Synthetic analogues **13** and **14** have the conformations depicted as determined by single-crystal X-ray analyses.[29] Compound **13** mimics the syn conformer of quinocarcin, while **14** mimics the anti conformer of quinocarcin. The relative difference in the capacity of synthetic analogues **13** and **14** to effect both superoxide production (cf. Table I, entries 7 and 8) as well as DNA cleavage (at 5 mM, **13** cleaves plasmid DNA only one-sixth as efficiently as **14**)[29] supports our hypothesis that stereoelectronic control elements of the oxazolidine ring system are intimately related to the biological activities of these substances.

In summary, we have established a previously unrecognized reaction for the reduction of molecular oxygen by a simple heterocyclic ring system. This reduction is driven by the inherent intermolecular redox chemistry of the drug itself, requiring no exogenous reductants; this reaction can be assisted by external reductants, effectively lowering the concentration of drug required to damage DNA. In this context, it is interesting to question the creation of quinocarcinol (**2**) as arising by a genetically encoded biosynthetic pathway or being an artifact of the secondary redox chemistry of quinocarcin discovered herein or a related secondary and endogenous microbial reduction. Chemical means to attenuate the ability of this class of antitumor drugs to produce reactive oxidants (**13** versus **14**, **12**, stabilizers such as citric acid, stimulators such as DTT and hydrogen peroxide) may contribute to possible approaches to designing more selective and less toxic cancer chemotherapeutic agents. Studies aimed at elucidating the details of the expected covalent interactions of this class of compounds with nucleic acid targets are under investigation in these laboratories.

(34) The rate of superoxide release from quinocarcin is of the same order of magnitude as the rate of redox disproportionation (~6×10^{-6} M L^{-1} s^{-1}) of quinocarcin under anaerobic conditions.

Experimental Section

Purification of 1 from Citric Acid. From quinocarcin citrate, which was a gift from Kyowa Hakko Kogyo, was obtained free quinocarcin by dissolving quinocarcin citrate in water and passing it through HP-20 ion-exchange resin (Mitsubishi Corp.) at 4 °C. Citric acid was eluted with water, and subsequently free quinocarcin was eluted with methanol/water (3/1). Free quinocarcin was further purified by HPLC on a C18 Resolve Pack column (Waters) using 5% methanol/5% acetonitrile in 6.0 mM, pH 6.8 potassium phosphate buffer (isocratic). To remove the phosphate buffer from the lyophilized quinocarcin fraction, the residue was dissolved in water and passed through an HP-20 column in the same manner as described above.

Disproportionation of 1 and HPLC Analysis of Products. A 300 μg/mL solution of citrate-free **1** was made up in deionized water which had been deoxygenated under vacuum followed by purging with nitrogen. A sample was then analyzed by HPLC (C18 Resolve Pack column (Waters); 5% methanol/5% acetonitrile in 6 mM potassium phosphate, pH 6.8 (isocratic); and detected by UV at 270 nm) which revealed only the peak at 16 min corresponding to **1**. The solution was then allowed to age at 25 °C under anaerobic conditions, with aliquots being taken periodically and analyzed by HPLC for quinocarcin and formation of **10** and **2** (retention times 10 and 22 min, respectively). Authentic quinocarcinol (**2**) was obtained from quinocarcin by $NaBH_4$ reduction according to Tomita.[20] The authentic sample of quinocarcinol was identical to that obtained by the disproportionation of **1** described above by ^1H NMR, IR, and TLC (silica gel; 10% H_2O in ethanol). Data for quinocarcinamide (**10**). ^1H NMR (300 MHz) (D_2O) δ HOD: 2.34 (1 H, dd, J = 13.6 Hz, J = 9.9 Hz); 2.38 (3 H, s); 2.59 (1 H, ddd, J = 13.6 Hz, J = 7.0 Hz, J = 7.0 Hz); 2.78 (1 H, m); 3.03 (1 H, m); 3.22 (1 H, dd, J = 7.0 Hz, J = 10.3 Hz); 3.58 (1 H, d, J = 6.6 Hz); 3.70 (1 H, dd, J = 11.4 Hz, J = 3.9 Hz); 3.79 (1 H, m); 3.82 (1 H, br s); 3.87 (3 H, s); 3.93 (1 H, dd, J = 11.4 Hz, J = 4.4 Hz); 5.45 (1 H, t, J = 4.0 Hz); 6.94 (1 H, d, J = 7.8 Hz); 7.04 (1 H, d, J = 7.8 Hz); 7.33 (1 H, d, J = 7.8 Hz). IR (KBr): 3601, 3430, 2929, 2340, 2020, 1897, 1792, 1626, 1580, 1388, 1079 cm^{-1}. Additional structural verification was secured through esterification to quinocarcinamide methyl ester as follows. To 2.0 mL of 1 M NaOH was added 5 mg of 1-methyl-3-nitro-1-nitrosoguanidine (Aldrich). The diazomethane formed was carried via nitrogen pressure bubbling through 2.0 mL of a solution of dioxane/H_2O (1/1) containing 1 mg of **10**. Once the dioxane solution turned yellow, the flask was sealed and the mixture was allowed to stand at room temperature for 30 min. The mixture was then concentrated to dryness, affording 1 mg of the corresponding methyl ester whose ^1H NMR matched that of a synthetic sample provided by Prof. S. J. Danishefsky. This procedure was also utilized for aliquoting the ^{18}O experiments for mass spectral determinations (see ref 28).

Reductions of Nitroblue Tetrazolium by 1 and 12–14. Each reaction was performed in triplicate by adding each substrate to an aerated solution of nitroblue tetrazolium (0.12 mM) in 20 mM phosphate buffer at the indicated pH such that the final concentration of substrate was 1.0 mM. The optical absorbance was measured over a 30-min period at 500 nm, and the ΔOD was the average slope for the linear OD change over the reaction time. Addition of SOD (5 μg/mL) completely inhibited the reduction in all relevant cases (entries 2–4 and 8). The rate constants were calculated by assuming that $[O_2]$ does not appreciably change and is in excess (zero order in oxygen); the reaction is second order with respect to [quinocarcin] or [**14**] (i.e., the only substates that effect the reduction of NBT). The second-order rate constants reported in Table I were calculated from the ΔOD measurements and based on an ϵ_0 of 12 200 for the furazan product of NBT at 500 nm.

Cleavage of Supercoiled Plasmid DNA (pBR322). DNA nicking reaction mixtures were made by addition at 0 °C of appropriate amounts of reagent stock solutions to a stock solution of pBR 322 DNA plasmid (Boehringer-Mannheim Biochemical Co.) containing 0.15 μg of DNA/reaction (20 μM base pair concentration). The total volumes of the reaction mixtures were brought up to 10 μL with distilled and deionized water when necessary, and the reaction mixtures were incubated at 37 °C for 2 h in tightly capped plastic Eppendorf tubes. Stock solutions for experiments including DNA were prepared using distilled, deionized water and commercially available reagents: DTT, Sigma; sodium phosphate monobasic, EM Science; sodium phosphate dibasic, 30% hydrogen peroxide, Malinckrodt; superoxide dismutase, beef liver catalase (suspension in water), Boehringer Mannheim Biochemical. Desferal was the generous gift from Ciba-Geigy Co. The cleavage of plasmid DNA was detected by loading the reactions onto 0.8% agarose gels and staining with ethidium bromide after electrophoresis. The

electrophoreses were run for 2 h at 55 V, and the gels were submerged for 15 min in ethidium bromide solution. The electrophoresis gels were immediately visualized on a UV transilluminator and photographed using black and white instant films (Polaroid T667). The measurements of the relative intensities of DNA bands were performed on the photographs using the Dell System 325 computer and Technology Resources Inc. image-processing software. The film used to photograph the gels was confirmed to have a linear response to the range of DNA quantities used. The mean number of single strand scissions (S) per supercoiled DNA substrate was calculated using the Poisson distribution. All reactants were mixed at ice bath temperature and brought to a final volume of 10 μL. All reactions were then incubated for 2 h at 37 °C in the indicated buffer with 0.15 μg of pBR 322 plasmid DNA.

Labeling (5′, ^{32}P) and Reactions of Synthetic 64-mer for High-Resolution Polyacrylamide Gel Electrophoresis. To a solution of the synthetic deoxyoligonucleotide (200 pmol) in 105 μL of deionized distilled H_2O was added 20 μL of polynucleotide kinase buffer, 4 μL (40 units) of T4 polynucleotide kinase (New England Biolabs), and 2 μL (20 μCi) of [γ†^{32}P]ATP (Du Pont). The reaction was incubated for 90 min at 37 °C and 10 min at 65 °C. The solution was loaded onto a 2-mL column of Sephadex G-50 and eluted with TE buffer (10 mM Tris, 1.0 mM EDTA, pH 8). The first radioactive fraction was collected and precipitated with ethanol/3 M NaOAc (pH 5.2) and dried. Annealing was performed by mixing equimolar amounts of the 5′ ^{32}P-end-labeled strand and the complimentary strand in deionized distilled H_2O to a final concentration of 2 pmol/μL; each was heated to 65 °C for 30 min and slowly cooled to 0 °C. The double-stranded and single-stranded DNA substrates (5 pmol in 3 μL of deionized distilled H_2O) were brought to a final reaction volume of 16 μL in phosphate buffer (20 mM, pH 8). Each reaction was incubated at 37 °C for 5 h. None of these reactions contained any additional reducing agents such as DTT. One microliter of 3 M NaOAc (pH 5.2), 5 μL of t-RNA (1 mg/mL), and 100 μL of ethanol were added, and the mixture was cooled to −70 °C for 10 min. Each tube was centrifuged at 14K (rpm, Eppendorf microfuge) for 10 min at 4 °C, the supernatant decanted, and the DNA pellet dried under reduced pressure. To each sample for lanes 3–5 and 10 was added 10 μL of deionized distilled H_2O followed by heating to 90 °C for 10 min and then cooling on ice. To each reaction tube was added 4 μL of polynucleotide kinase buffer and 4 μL (40 units) of T4 polynucleotide kinase (New England Biolabs). After brief vortexing, each reaction was incubated at 37 °C for 1 h. Each sample was ethanol precipitated, centrifuged, and dried for electrophoresis. To each dried pellet of DNA was added 10 μL of loading buffer (formamide, 10 mM EDTA, pH 8, 0.025% xylenecyanol FF and 0.025% bromophenol blue), and the resultant mixture was then heated to 90 °C for 5 min, placed on ice, and immediately loaded onto a 20% denaturing (urea) polyacrylamide gel. After the gel was run (4 h, 1600 V), it was fixed (acetic acid/methanol, 10% each, aqueous), absorbed onto filter blotting paper, and vacuum dried. The bands were visualized by autoradiography.

Acknowledgment. This research was supported by the National Institutes of Health Grant CA43969. We are indebted to the Kyowa Hakko Kogyo Co., Japan, for the gift of quinocarmycin citrate; Prof. J. R. Norton (Colorado State University) for providing access to facilities for manipulating $^{18}O_2$; Prof. S. J. Danishefsky (Yale University) for providing authentic comparison spectra for the methyl ester of synthetic quinocarcinamide; and Dr. Jed Fisher (The Upjohn Co.), Prof. Peter G. Schultz (University of California, Berkeley), Prof. Jack R. Norton (Colorado State University) and Prof. Mark M. Greenberg (Colorado State University) for helpful discussions.

Reprinted from Biochemistry, 1994, 33.

O_2-Dependent Cleavage of DNA by Tetrazomine†

Robert M. Williams,* Mark E. Flanagan, and Tracy N. Tippie

Department of Chemistry, Colorado State University, Fort Collins, Colorado 80523

Received December 13, 1993; Revised Manuscript Received January 24, 1994•

ABSTRACT: A mechanism for the reduction of molecular oxygen that results in the O_2-dependent cleavage of both single-stranded and double-stranded DNA by the antitumor antibiotic tetrazomine (**1**) is presented. The results are discussed in the context of a redox self-disproportionation of the oxazolidine moiety of tetrazomine. Comparisons are made to the structurally analogous natural product quinocarcin (**2**) in which, like tetrazomine, the oxazolidine moiety is invoked in redox chemistry, which ultimately results in the reduction of molecular oxygen to superoxide.

It is now widely recognized (Fisher & Aristoff, 1988; Remers, 1985) that a variety of clinically significant antitumor antibiotics can mediate oxygen-dependent cleavage of the ribose phosphate backbone of cellular DNA and RNA. An enormous structural array of interesting natural products and semisynthetic and totally synthetic substances mediates oxidative strand scission of nucleic acids through three main families of reactions: (1) metal-mediated activation of O_2, ultimately producing hydroxyl radical or other reactive oxygen species (Stubbe & Kozarich, 1987; Walling, 1975); (2) non-metal-dependent generation of reactive carbon radicals (Myers, 1987; Nicolaou et al., 1988; Magnus et al., 1988; Hawley et al., 1989) that mediate CH abstraction from the deoxyribose backbone (the resulting deoxyribosyl radical subsequently reacts with molecular oxygen, culminating in strand scission); and (3) photolytic production of hydroxyl radical (Saito et al., 1990; Zafirou & Bonneau, 1987), which does not require metal participation for the DNA cleavage event. A rich array of chemistry can be found in the metal-dependent family of DNA-damaging agents. Many readily oxidizable organic substances are capable of reducing molecular oxygen, resulting in the production of superoxide, such as semiquinone radical anions, thiols (Misra, 1974), and ascorbate, among others. Superoxide is well-documented (Lesko & Lorentzen, 1980) to mediate DNA strand breakage via dismutation to hydrogen peroxide followed by Fenton chemistry [in the presence of Fe(III)], generating the highly reactive hydroxyl radical.

Tetrazomine (**1**) is a natural secondary metabolite that was recently isolated from *Saccharothrix mutabilis* subsp. *chichijimaensisi* by Yamanouchi Pharmaceutical Co. (Japan) (Suzuki et al., 1991) and is the most recent member of the quinocarcin (**2**)/naphthyridinomycin/saframycin class of antitumor agents. Tetrazomine has been shown to display broad antimicrobial activity against both Gram-positive and Gram-negative bacteria *in vitro*. Tetrazomine also displays promising *in vitro* antitumor activity (Suzuki et al., 1991) against lymphoid leukemia L1210 and P388 leukemia at 0.0427 and 0.014 μg/mL, respectively. This substance also displayed antitumor activity against P388 leukemia *in vivo*.

Our interest in this substance stems from structural similarities between tetrazomine and the antitumor antibiotic quinocarcin (**2**), which has been the subject of considerable investigation (Williams et al., 1991, 1992). Like quinocarcin, tetrazomine (1) is capable of cleaving both synthetic oligonucleotides and plasmid DNA in an O_2-dependent manner in the absence of external reducing agents such as dithiothreitol (DTT); (2) is not stimulated by the addition of metal ions [Fe(II), Fe(III)]; (3) is inhibited by free radical scavengers such as picolinic acid (Sheu et al., 1990); and (4) is inhibited by superoxide dismutase (SOD[1]) and catalase. We have recently obtained experimental evidence, presented herein, that tetrazomine undergoes a redox self-disproportionation reaction similar to that observed for quinocarcin, which may be coupled to the capacity of this substance to affect the production of superoxide in the presence of molecular oxygen and results, at least in part, in Fenton-mediated lesions in DNA; a proposed mechanism for this process is presented in Figure 2. The rate at which tetrazomine produces superoxide has been carefully examined by following the reduction of nitroblue tetrazolium (NBT) spectrophotometrically under various conditions. It was found that, in addition to being completely inhibited by SOD, these experiments closely paralleled trends observed for the nicking of supercoiled plasmid DNA by tetrazomine.

MATERIALS AND METHODS

Disproportionation of Tetrazomine and Analysis of Products. A 10 mM solution of **1** was prepared in 20 mM phosphate buffer (pH 8.0), which was then deoxygenated by freeze–thaw purging with nitrogen. A sample was then analyzed by HPLC (resolve pack C18 column; 10 mM sodium sulfate, 3% acetonitrile, 0.05% acetic acid, and 0.002% 1-pentanesulfonate sodium salt (isocratic); detected by UV at 254 nm), which revealed only a peak at 5 min corresponding to **1**. The solution was then aged at 4 °C under anaerobic conditions, with aliquots being taken periodically (every third day for 2 weeks), and analyzed by HPLC for tetrazomine and the formation of new products. Approximately 20% conversion of tetrazomine to new products was observed after 2 weeks. These breakdown products were isolated (by HPLC) and desalted by trituration with methanol. Following filtration, the methanol solutions were concentrated under reduced pressure, redissolved in ddH_2O, passed through a column of Dowex 1 (Cl^- form), and lyophilized. One product was identified as the reduced form of tetrazomine, which henceforth will be referred to as tetrazominol (**4**). Authentic tetrazominol was obtained from

† This research was supported by the National Institutes of Health (Grant No. CA 43969).

* Author to whom correspondence should be addressed.

• Abstract published in *Advance ACS Abstracts*, March 1, 1994.

[1] Abbreviations: SOD, superoxide dismutase; NBT, nitroblue tetrazolium; TE, 100 mM Tris base/10 mM EDTA; EDTA, ethylenediaminetetraacetic acid; ddH_2O, double deionized water.

0006-2960/94/0433-4086$04.50/0

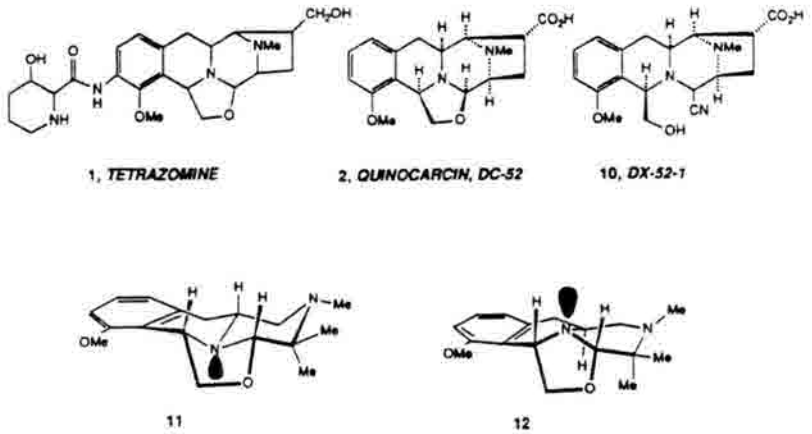

FIGURE 1: Tetrazomine and structural analogs.

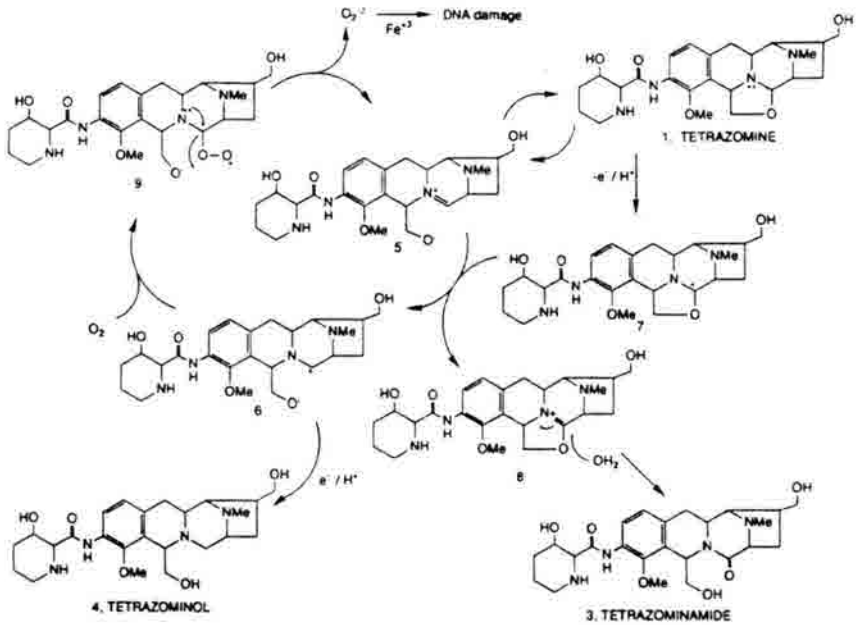

FIGURE 2: Proposed disproportionation of tetrazomine: under anaerobic conditions, resulting in the formation of **3** and **4**; under aerobic conditions, resulting in the production of superoxide.

tetrazomine by reacting 10 mg of the pure drug with 10 equiv of $NaBH_4$ (Baker) in 3 mL of methanol (0 °C) for 3 h. The sample of tetrazominol obtained following isolation by preparative thin-layer chromatography (silica; 4:1 CH_2Cl_2/methanol, $R_f = 0.2$) had the exact same HPLC retention time (8 min) and molecular weight by mass spectrometry as **4** collected from the disproportionation of **1** described above: ^1H NMR (300 MHz) (D_2O) δ (HOD) 1.63–1.94 (5H, m), 2.24 (1H, t, J = 11.4 Hz), 2.48 (1H, d, J = 14.1 Hz), 2.57 (1H, q, J = 11.5 Hz), 2.79–2.89 (5H, m), 2.96 (1H, d, J = 16.3 Hz), 3.00 (1H, d, J = 12.9 Hz), 3.18 (1H, br s), 3.36 (1H, d, J = 13.8 Hz), 3.53–3.68 (5H, m), 3.60 (3H, s), 3.84–3.90 (2H, m), 4.17 (1H, d, J = 1.8 Hz), 4.56 (1H, s), 6.89 (1H, d, J = 8.2 Hz), 7.33 (1H, d, J = 8.2 Hz). MS m/e (M^+): 460.26960 (calcd for $C_{24}H_{36}N_4O_5$, 460.2696). Another product isolated from the disproportionation by HPLC (retention time, 4 min) was identified as the oxidized form of tetrazomine, which henceforth will be referred to as tetrazominamide (**3**): MS m/e (M^+) 475.2578 (calcd for $C_{24}H_{35}N_4O_6$, 475.258). The other material formed was an unidentifiable decomposition product. We were not able to obtain a sufficient quantity of tetrazomine from Yamonouchi Co. to rigorously isolate and characterize this material.

Reductions of Nitroblue Tetrazolium by Tetrazomine. Each reaction was performed in triplicate by adding an appropriate amount of tetrazomine stock solution (20 mM) to an aerated solution of nitroblue tetrazolium (0.12 mM) in 20 mM phosphate buffer (at the indicated pH) containing 1% Triton X-100 detergent with the final volume brought to 750 μL with ddH_2O. The optical absorbance was measured at 25 °C over a 30-min period at 500 nm (Varian DMS 80 UV/vis spectrophotometer), and the ΔOD was the average slope for the linear OD change over the reaction time. The rates for superoxide production were calculated by assuming that $[O_2]$ does not appreciably change over this time period and is in excess (zero order in oxygen). The rates (reported in Table 1) were calculated from the ΔOD measurements and based

Table 1: Rates of Superoxide Production: Measurements by Reduction of Nitroblue Tetrazolium (NBT)

entry	substrate	pH	rate ($\mu s^{-1} \times 10^{-9}$)
1	1.0 mM tetrazomine	6	2.46
2	1.0 mM tetrazomine	7	10.6
3	1.0 mM tetrazomine	8	17.5
4	1.0 mM quinocarcin	8	1.1
5	1.0 mM tetrazomine + 10 μg/mL SOD	8	0.0
6	1.0 mM DX-52-1	8	0.0
7	1.0 mM **11**	8	0.41
8	1.0 mM **12**	8	0.0
9	20 mM phosphate buffer (control)	8	0.0

on a molar extinction coefficient (ϵ_0) of 12 200 for the formazan product of NBT at 500 nm.

Preparation and Purification of Supercoiled Plasmid DNA (pUC 19). To 40 μL of electrocompetent cells (*E. coli*, MC 1061) was added 1 μL (0.35 μg) of pUC 19 plasmid DNA (New England Biolabs), and the mixture was agitated and aged in an ice bath for 1 min. The mixture was then transferred to an ice-cooled, 0.1-cm electroporation cuvette, and the material was pulsed (Bio-Rad gene pulser) at 25 μF, 200 Ω, and 1.1 kV. The cells were then quickly transferred to 1 mL of sterile SOC broth (20 mM glucose, 20 g of bacto-tryptone (Difco), 5 g of bacto-yeast (Difco), 1 g of $MgCl_2$, 0.5 g of NaCl, and 186 mg KCl to 1.0 L) and incubated at 37 °C, with agitation (200 rpm), for 1 h. The mixture was transferred to a sterile Eppendorf tube and centrifuged (14 000 rpm, 5 min, room temperature). The supernatant was discarded, and the cells were resuspended in 400 μL of sterile SOC broth. Dilutions were made to 10^2, 10^4, 10^6, 10^8 (400 μL each), and 100 μL of each plated onto LB agar plates containing 30 μg/mL ampicillin (in duplicate). The plates were inverted and incubated at 37 °C for 18 h, at which time colonies were counted and a yield of 10^{10} transformants was assessed. A resistant colony was then grown in 500 mL of sterile LB broth (10 g of bacto-tryptone, 5 g of bacto-yeast extract, and 10 g of NaCl to 1.0 L) containing 30 μg/mL ampicillin at 37 °C for 18 h. The cells were pelleted by centrifugation (5000 rpm, 10 min, 4 °C). Plasmid DNA (pUC 19) was then isolated following the Promega Magic Maxi-prep kit procedure. The supercoiled plasmid was further purified by low-melt agarose gel electrophoresis (1.2%). The band corresponding to supercoiled plasmid (visualized by 0.4 μg/mL ethidium bromide using a hand-held UV light) was cut from the gel and melted at 75 °C. To this was added 4 vol of 37 °C TE, and the mixture was aged at 37 °C for 1 h. To this solution was then added 1 vol of Tris-equilibrated phenol (pH 8) (room temperature), the tube was mixed gently by rocking, and the layers were separated by centrifugation (4000 rpm, 15 min, room temperature). The aqueous layer (top) was removed and extracted with 2 × 2 vol of butanol (centrifugation was necessary for the separation of layers). To the aqueous layer (bottom) were added 3 vol of ethanol and 50 μL of 3 M NaOAc, pH 5.2, and the solution was mixed gently, aged at −70 °C for 10 min, and centrifuged (20 000 rpm, 30 min, 4 °C). The supernatant was discarded and the pellet resuspended in 200 μL of sterile deionized water. Supercoiled plasmid DNA (pU 19) was recovered in 90% yield from the low-melt gel.

Cleavage of Supercoiled Plasmid DNA (pUC 19). DNA nicking reaction mixtures were made up by the addition at 0 °C of appropriate amounts of reagent stock solutions to a stock solution of supercoiled plasmid DNA (pUC 19), prepared as described above and containing 0.15 μg of DNA per reaction (23 μM base-pair concentration). The total volumes of the reaction mixtures were brought to 10 μL each with distilled, deionized water when necessary, and the reaction mixtures were incubated at 37 °C for 2 h in tightly capped plastic Eppendorf tubes. Stock solutions for experiments including DNA were prepared using distilled, deionized water and commercially available reagents: sodium phosphate, monobasic, EM Science; sodium phosphate, dibasic and 30% hydrogen peroxide, Malinckrodt; superoxide dismutase and beef liver catalase (suspension in water), Boehringer Mannheim Biochemical. Desferal was the generous gift of Ciba-Geigy Co. The cleavage of plasmid DNA was detected by loading the reactions onto 1.2% agarose gels containing 0.4 μg/mL ethidium bromide and running for 2 h at 55 V. The electrophoresis gels were immediately visualized on a UV transilluminator and photographed using black and white instant films (Polaroid T667). The measurements of the relative intensities of DNA bands were performed on the photographs using a Dell System 325 computer and Technology Resources Inc. image processing software. The film used to photograph the gels was confirmed to have a linear response to the range of DNA quantities used. The mean number of single-strand scissions (S) per supercoiled DNA substrate was calculated using the Poisson distribution (Hertzberg & Dervan, 1984), where the value S for the DNA control represents the amount of nicked open circular DNA present in the starting plasmid, and was subtracted from the S values calculated for the individual cleavage reactions. When only forms I (supercoiled) and II (nicked open circular) are present, the equation simplifies to $S = -\ln f_I$, where f_I is the fraction of form I molecules from the densitometry data. In those cases where form III (linear) DNA is present, S is calculated from $f_I + f_{II} = [1 - S(2h + 1)/2L]^{S/2}$, where h is the distance between hits on opposite strands to produce a linear molecule (16 base pairs) and L is the total number of base pairs in pUC 19 (2686 base pairs).

Labeling (5′-^{32}P) and Reactions of Synthetic 45-mer for High-Resolution Polyacrylamide Gel Electrophoresis. To a solution of the synthetic deoxyoligonucleotide (100 pmol) in 74 μL of ddH_2O were added 20 μL of polynucleotide kinase buffer, 4 μL (40 units) of T4 polynucleotide kinase (New England Biolabs), and 1 μL (10 μCi) of [γ-^{32}P]ATP (DuPont). The reaction was incubated for 60 min at 37 °C and for 10 min at 70 °C. The solution was loaded onto a 2-mL column of Sephadex G-50 and eluted with TE buffer. The first radioactive fraction was collected and precipitated with ethanol/3 M NaOAc (pH 5.2) and dried. Annealing was performed by mixing equimolar amounts of the 5′-^{32}P-end-labeled strand and the complementary strand in ddH_2O to a final concentration of 2 pmol/μL; each was heated to 65 °C for 30 min and slowly cooled to 0 °C. Reactions were made up by the additions at 0 °C of appropriate amounts of stock solutions to 3 μL each of labeled DNA (5 pmol). The total volumes of the reactions were brought to 16 μL each with ddH_2O and enough 80 mM phosphate buffer (pH 8) so as to achieve final concentrations of 20 mM phosphate. Each reaction was incubated at 37 °C for 5 h (none of the reactions contained any additional reducing agents, such as DTT). To the reaction mixtures were then added 1 μL of 3 M NaOAc (pH 5.2) and 60 μL of ethanol, and the resulting solutions were aged at −70 °C for 10 min. Each tube was centrifuged at 14 000 rpm for 10 min at 4 °C, the supernatants were discarded, and the DNA pellets were dried under reduced pressure. To each dried pellet of DNA was added 10 μL of loading buffer (formamide, 10 mM EDTA (pH 8), 0.025%

xylenecyanol FF, and 0.025% bromophenol blue), and the sample was then heated to 90 °C for 5 min, placed on ice, and immediately loaded (20 000 cpm/lane as measured using a Packard 1500 liquid scintillation counter) onto a 20% denaturing (urea) polyacrylamide gel and run for 6 h at 1300 V. The bands were visualized by autoradiography.

RESULTS

Disproportionation of Tetrazomine. Natural tetrazomine, obtained from Yamanouchi Pharmaceutical Co., Ltd., was allowed to stand in carefully deoxygenated phosphate buffer (20 mM, pH 8) at 4 °C, with new products being produced. The identification of the anaerobic redox products **3** and **4** supports the proposal that tetrazomine serves as its own reductant, since no other reducing agents were present. Therefore, on the basis of the analogous chemical structure, the observation of anaerobic disproportionation products, and the analogous aerobic behavior (i.e., superoxide production) that tetrazomine shares with quinocarcin, we propose the same Cannizzaro-driven reduction of molecular oxygen for tetrazomine. Therefore, as suggested in Figure 2, single-electron transfer from **1** with concomitant proton loss from the oxazolidine nitrogen to the ring-opened tautomer **5** would furnish radical anion **6** and the oxazolidinyl radical **7**. Radical **7** should be capable of reducing a second equivalent of **5**, ultimately becoming oxazolidinium ion **8**, which would hydrolyze to tetrazominamide (**3**). Under anaerobic conditions, radical anion **6** subsequently suffers a second electron transfer (presumably from **1** or **7**) with concomitant protonation, resulting in tetrazominol (**4**). Under aerobic conditions, radical anion **6** can react with molecular oxygen to produce peroxy radical anion **9** which, with nitrogen participation, expels 1 molar equiv of superoxide, regenerating **5**.

Reductions of Nitroblue Tetrazolium by Tetrazomine. The rate of superoxide production was carefully followed by reduction of NBT (Misra, 1974; Tsou, 1956) under various pH conditions, and it was found that these reactions are completely inhibited by SOD, thus supporting the role of superoxide in this mechanism; the results are collected in Table 1. The reduction of NBT by tetrazomine is pH-dependent, exhibiting an increased rate of reduction as the pH is raised (Table 1, entries 1–3). This behavior directly parallels the pH dependency for the plasmid DNA cleavage reactions described below. Entries 6–8 of Table 1 support the notion that the oxazolidine moiety of tetrazomine must be "intact" and in the quinocarcin configuration, exhibited by synthetic analog **11**, in order for the production of superoxide to proceed.

Cleavage of Supercoiled Plasmid DNA (pUC 19) by Tetrazomine. In order to examine the interaction of tetrazomine with DNA, the pure antibiotic (0.01–10 mM) was allowed to react with supercoiled plasmid DNA (pUC 19) in phosphate buffer (20 mM) between pH 5 and 9 at 37 °C for 2 h in the presence of air. Salient experimental results are collected in Tables 2 and 3. Tetrazomine displayed nicking of the DNA at a 0.1 mM concentration (Table 2, entry 8) at pH 8 without the addition of any external reductants. The reaction was found to be pH-dependent; optimal cleavage occurred at or above pH 7. At lower pH values (below pH 6), nicking was observed, but to a lesser extent (Table 2, entries 1–5). This is consistent with the obligate participation of the *unprotonated* oxazolidine nitrogen atom in the redox cycle. The slightly different pH versus nicking yield (S) profiles for tetrazomine and quinocarcin, illustrated in Figure 3, could therefore be explained by small differences in the pK_a's for the oxazolidine nitrogens. In other words, a slightly higher pH medium is necessary for deprotonation of the quinocarcin oxazolidine nitrogen, which subsequently turns on the redox cycle. Also supporting this notion is the fact that the NBT reductions for tetrazomine and quinocarcin exhibit the same overall trends.

Table 2: Cleavage of Supercoiled Plasmid DNA (pUC 19)

entry	conditions	[tetrazomine or quinocarcin]	S
1	20 mM phosphate, pH 5	1.0 mM tetrazomine	0.9
2	20 mM phosphate, pH 6	1.0 mM tetrazomine	4.4
3	20 mM phosphate pH 7	1.0 mM tetrazomine	9.0
4	20 mM phosphate, pH 8	1.0 mM tetrazomine	10.0
5	20 mM phosphate, pH 9	1.0 mM tetrazomine	10.0
6	20 mM phosphate, pH 8	1.0 mM quinocarcin	9.7
7	20 mM phosphate, pH 8	0.01 mM tetrazomine	0.0
8	20 mM phosphate, pH 8	0.1 mM tetrazomine	0.4

Table 3: Effects of Additives on Plasmid DNA Cleavage

entry	conditions[a]	[tetrazomine] (mM)	% inhibn	% enhancemt
1	0.1 mM $Fe^{II}SO_4$	1.0	0	0
2	0.1 mM $Fe^{III}NH_4SO_4$	1.0	5	
3	0.1 mM desferal	1.0	0	0
4	1.0 mM desferal	1.0	37	
5	10 mM desferal	1.0	94	
6	deoxygenated	1.0	80	
7	0.1 mM H_2O_2	0.1		68
8	0.1 mM H_2O_2	1.0		29
9	1.0 mM picolinic acid	1.0	28	
10	10 mM picolinic acid	1.0	71	
11	10 μg/mL catalase	1.0	55	
12	100 μg/mL catalase	1.0	54	
13	10 μg/mL SOD	1.0	94	

[a] All reactions were run in 20 mM phosphate buffer (pH 8.0).

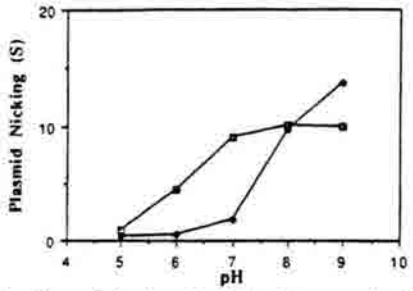

FIGURE 3: pH trends for plasmid nicking of tetrazomine (□) versus quinocarcin (◆). All reactions contained 0.15 μg of supercoiled plasmid DNA (pUC 19) and 1 mM drug and were run in 20 mM phosphate buffer at the indicated pH's (2 h, 37 °C). Values for S were calculated from the Poisson distribution, on the basis of the ratios of forms I (supercoiled), II (nicked open circular), and III (linear) of the DNA from scanning densitometry data of agarose electrophoresis gels following reactions.

Complete removal of oxygen from these experiments during the many manipulations is very difficult; however, partial exclusion of oxygen significantly inhibited this reaction, as expected (Table 3, entry 6). Superoxide dismutase also greatly inhibited DNA cleavage (Table 3, entry 13), which is consistent with both the capacity of tetrazomine to generate superoxide and the corresponding DNA cleavage event to be exclusively superoxide-dependent. Catalase inhibits the reaction, but not as potently as SOD (Table 3, entries 11 and 12). Addition of hydrogen peroxide to tetrazomine/DNA reactions had a potent stimulatory effect on DNA cleavage over control reactions containing hydrogen peroxide at the same concentrations (Table 3, entries 7 and 8). Taken together, the above

results point strongly to Fenton-type chemistry being responsible for the scission of DNA.

Tomita previously reported that the addition of metal ions such as Fe(III) had no stimulatory effect on the ability of quinocarcin to cleave DNA; we have corroborated this finding with tetrazomine, and the results appear in Table 3 (entries 1 and 2). The addition of the potent iron chelator desferal did, however, exhibit significant inhibition of DNA cleavage, particularly at high concentrations (Table III, entries 3–5). Desferal is known to have a high affinity for Fe(III) (log k_f = 30.7), forming a hexacoordinate complex that excludes iron-associated water and uncouples the oxidation of Fe(II) from the formation hydroxyl radical (Fenton reaction). The participation of higher oxidation states of iron and copper in Fenton reactions and related CH oxidation chemistry is now well-recognized (Saito et al., 1990; Zafirou & Bonneau, 1987). Picolinic acid is known (Sheu, 1990) to be a very potent scavenger of hydroxyl radical and inhibitor of the Fe(II)/Fe(III) redox couple. Addition of picolinic acid to reaction mixtures of DNA and tetrazomine at 1 and 10 mM showed 28% and 71% inhibition, respectively. The rate of formation of superoxide by tetrazomine (see Table 1) is extremely slow (10^4–10^5 times slower) relative to the rate-limiting step of the Haber-Weiss/Fenton reaction, which is 76 M^{-1} s^{-1} (Lesko, 1980) for the reduction of hydrogen peroxide by Fe(II). Thus, our data support a hypothesis wherein the limiting reagent in the DNA cleavage mediated by tetrazomine and quinocarcin is the slow production of superoxide. These results also support the notion that adventitious metal in these reaction mixtures in a number of possible oxidation states can be activated by the slow release of superoxide and cause Fenton-related damage to DNA. Thus, these results indicate that DNA cleavage is indeed metal-dependent and that the low concentration of adventitious Fe(III) present is already in excess of that required to effect Fenton-mediated cleavage of DNA; the addition of excess iron therefore would not be expected to have any additive effect. Thus, our data again support the hypothesis wherein the limiting reagent in the DNA cleavage mediated by quinocarcin or tetrazomine is the slow production of superoxide.

Reactions of Tetrazomine with 5′-^{32}P-Labeled Synthetic 45-mer for High-Resolution Polyacrylamide Gel Electrophoresis. Further evidence for a non-DNA-associated oxidant was obtained from analysis of the reaction of tetrazomine with a small synthetic oligonucleotide by high-resolution polyacrylamide gel electrophoresis. A synthetic 45-base-pair oligonucleotide, end-labeled with ^{32}P and annealed to its complement, was reacted with tetrazomine (0.1, 1.0, and 10 mM without any additional reducing agents) at 37 °C for 5 h (20 mM phosphate buffer, pH 8), resulting in non-sequence-specific cleavage at every nucleotide as evidenced by denaturing 20% polyacrylamide gel electrophoresis (Figure 4, lanes 3–5). Furthermore, every cleavage band appeared as a doublet, which is characteristic of the 3′-phosphate and 3′-phosphoglycolate ends resulting from nonselective Fenton-mediated cleavage (Tullius & Dombroski, 1985; Hertzberg & Dervan, 1984). We observed a similar cleavage pattern from incubating the duplex with 10 mM quinocarcin and with 1.0 mM $FeSO_4$/EDTA under aerobic conditions (Figure 4, lanes 6 and 7, respectively). Initially, we found that attenuated cleavage was observed at higher tetrazomine concentrations (10 mM) and was inconsistent with the results obtained by NBT reduction, which shows linear superoxide production over the same concentration range. One explanation for this observation was that in the presence of limited oxygen and high

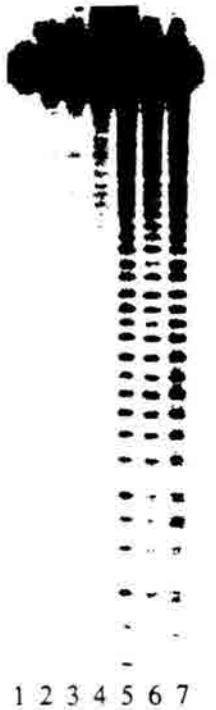

FIGURE 4: Lane 1: 5′-^{32}P-labeled duplex 45-mer. Lane 2: DNA (control). Lane 3: DNA + 0.1 mM tetrazomine. Lane 4: DNA + 1.0 mM tetrazomine. Lane 5: DNA + 10 mM tetrazomine. Lane 6: DNA + 10 mM quinocarcin. Lane 7: DNA + 1.0 mM Fe^{II}/EDTA. There was no significant evidence for any sequence specificity to the cleavage of this substrate (sequence along the gel is therefore superfluous and has been deleted).

tetrazomine concentrations a large portion of the hydroxyl radical produced was not in close proximity to the DNA, therefore exhausting the oxygen source before significant damage to DNA could occur. When reaction mixtures are saturated with oxygen, however, a more linear rate of DNA damage with respect to tetrazomine concentration is observed, as illustrated in Figure 4. An additional factor for this observation could be that tetrazomine, noncovalently or covalently associated within the minor groove of DNA, may protect the DNA from its own oxidative damaging potential. It has been proposed through molecular modeling (Hill et al., 1988) that quinocarcin docks in the minor groove and may alkylate DNA through the ring-opened iminium form (which would be analogous to **5**). The effect of tetrazomine associated to DNA in a similar manner might, therefore, be to protect the ribose phosphate backbone from oxidative damage by blocking sites in the minor groove. Evidence for the latter comes from experiments that show an increased resistance to Fe/EDTA cleavage for DNA that has first been incubated with tetrazomine (10 mM) for 5 h followed by ethanol precipitation (Figure 5, lane 3). However, when the order of reagents is reversed (i.e., treated with Fe/EDTA followed by 10 mM tetrazomine), significantly more cleavage is observed consistently (Figure 5, lane 4).

Another noteworthy observation is the change in relative ratios of the two 3′-base-pair products (phosphate versus phosphoglycolate) observed when comparing tetrazomine to quinocarcin and Fe/EDTA (Figures 4 and 6). By scanning densitometry, the relative ratios for phosphate to phosphoglycolate are 8:2 for tetrazomine, 6:4 for quinocarcin, and 4:6 for Fe/EDTA (lanes 5–7, respectively). Although speculative,

1 2 3 4

FIGURE 5: Lane 1: 5′-^{32}P-labeled duplex 45-mer. Lane 2: DNA (control). Lane 3: DNA + 10 mM tetrazomine followed by 1.0 mM Fe^{II}/EDTA. Lane 4: DNA + 1.0 mM Fe^{II}/EDTA followed by 10 mM tetrazomine. All reactions were carried out in phosphate buffer (pH 8) for 5 h with ethanol precipitations carried out between subsequent reactions.

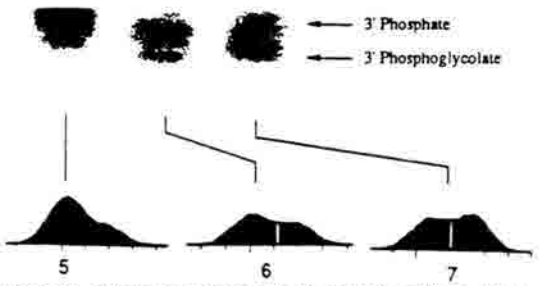

FIGURE 6: Representative base-pair cleavages from Figure 4 (lanes 5–7). Ratios of 3′-phosphate to 3′-phosphoglycolate by scanning densitometry are 8:2, 6:4, and 4:6 for tetrazomine (5), quinocarcin (6), and Fe/EDTA (7), respectively.

these results point to this protective behavior that these compounds exhibit, at least as far as abstraction of the 4′-hydrogen, which ultimately leads to the 3′-phosphoglycolate product, is concerned. This is again supported by the results illustrated in Figure 5, which show virtually no 3′-phosphoglycolate formation upon the treatment of DNA with Fe/EDTA that has first been incubated with tetrazomine.

DISCUSSION

Superoxide production by quinocarcin was previously reported (Tomita et al., 1984), and a mechanistic explanation has now been offered (Williams et al., 1992). Structural determination for tetrazomine (Sato et al., 1991) has revealed a ring system similar to that of quinocarcin, although little is currently known about the stereochemistry of this compound. On the basis of the analogous aerobic behavior that tetrazomine shares with quinocarcin, we now propose the same relative stereochemical configuration of quinocarcin for tetrazomine (with respect to the oxazolidine moiety). This assertion is based on studies (Williams et al., 1991) involving synthetic analogs **11** and **12** in Figure 1 (three-dimensional structures based on X-ray analysis), which suggest the quinocarcin oxazolidine configuration to be necessary for this redox mechanism to operate. When **11**, which has the same configuration as quinocarcin (*syn*), is allowed to stand in phosphate buffer (pH 8) under aerobic conditions at room temperature, it spontaneously produces superoxide (Table 1, entry 7). Under the same conditions, **12**, which is in the *anti* (non-quinocarcin) configuration, does not generate superoxide (Table 1, entry 8). Therefore, since tetrazomine readily produces superoxide under these conditions, this suggests that it possesses the same relative stereochemical configuration illustrated by **11** and quinocarcin, where the nitrogen lone pair is *trans*-antiperiplanar to the adjacent oxazolidinyl methine. This appears to be a requirement for redox chemistry to proceed on the basis of our observations.

The capacity of many antitumor antibiotics to cause oxidative damage to DNA in cancerous tissues is typically inseparable from the nonspecific damage inflicted on healthy cells by these reduced oxygen species and is widely recognized to be associated with the undesirable host toxicity of most antitumor drugs. The recognition of new mechanisms for the production of such reactive oxygen species and the chemical means to attenuate this reactivity without compromising other modes of action often displayed by such substances, such as nucleic acid alkylation, intercalation, and DNA polymerase inhibition, will be essential to designing more specific and efficacious cancer chemotherapeutic agents.

In summary, we have presented another example of a previously unrecognized reaction for the reduction of molecular oxygen by a simple heterocyclic ring system. This reduction is driven by the inherent intermolecular redox chemistry of the drug itself, requiring no exogenous reductants. Chemical means to attenuate the ability of this class of antitumor drugs to produce reactive oxidants (**11** versus **12**, **10**, stabilizers such as citric acid, stimulators such as DTT and hydrogen peroxide) may contribute to possible approaches to designing more selective and less toxic cancer chemotherapeutic agents. Studies aimed at elucidating the details of the expected covalent interactions of this class of compounds with nucleic acid targets are underway. In addition, further mechanistic studies employing synthetic analogs of these compounds are underway in these laboratories.

ACKNOWLEDGMENT

We are grateful to Yamanouchi Pharmaceutical Co. for providing the generous gift of natural tetrazomine. Quinocarcin used in this study was obtained as the generous gift of Kyowa Hakko Kogyo Co. High-resolution mass spectral data was supplied by the Midwest Center for Mass Spectrometry, with partial support by the National Science Foundation, Biology Division (Grant No. DIR9017262).

REFERENCES

Fisher, J., & Aristoff, P. A. (1988) *Prog. Drug Res. 32*, 411.
Hawley, R. C., Kiessling, L. L., & Schreiber, S. L. (1989) *Proc. Natl. Acad. Sci. U.S.A. 86*, 1105.
Hertzberg, R. P., & Dervan, P. B. (1984) *Biochemistry 23*, 3934.
Hill, C. G., Wunz, T. P., & Remers, W. A. (1988) *J. Comput.-Aided Mol. Des. 2*, 91.
Lesko, S. A., & Lorentzen, R. J. (1980) *Biochemistry 19*, 3023.
Magnus, P., Lewis, R. T., & Huffman, J. C. (1988) *J. Chem. Soc. 110*, 6921.

Misra, H. P. (1974) *J. Biol. Chem. 249*, 2151.
Myers, A. G. (1987) *Tetrahedron Lett. 28*, 4493.
Nicolaou, K. C., Zuccarello, G., Ogawa, Y., Schweiger, E. J., & Kumazawa, T. (1987) *J. Am. Chem. Soc. 110*, 4866.
Remers, W. A. (1985) *J. Nat. Prod. 48*, 173.
Saito, I., Takayama, M., Matsuura, T., Matsugo, S., & Kawanishi, S. (1990) *J. Am. Chem. Soc. 112*, 883.
Sato, H., Hirayama, F., & Saito, T. (1991) *J. Antibiot. 44* (12), 1367.
Sheu, C., Richert, S. A., Cofre, P., Ross, B., Sobkowiak, A., Sawyer, D. T., & Kanofsky, J. R. (1990) *J. Am. Chem. Soc. 112*, 1936.
Stubbe, J., & Kozarich, J. W. (1987) *Chem. Rev. 87*, 1107.
Sutton, H. C., & Winterbourn, C. C. (1989) *Free Radical Biol. Med. 6*, 53.
Suzuki, K., Sato, T., Morioka, M., Nagai, K., Abe, K., Yamaguchi, H., Saito, T., Ohmi, Y., & Susaki, K. (1991) *J. Antibiot. 44* (5), 479.
Tomita, F., Takahashi, K., & Tamaoke, T. (1984) *J. Antibiot. 37*, 1268.
Tsou, K.-C., Cheng, C.-S., Nachlas, M. M., & Seligman, A. M. (1956) *J. Am. Chem. Soc. 78*, 6139.
Tullius, T. D., & Dombroski, B. A. (1985) *Science 230*, 679.
Walling, C. (1975) *Acc. Chem. Res. 8*, 125.
Williams, R. M., Glinka, T., Gallegos, R., Ehrlich, P. P., Flanagan, M. E., Coffman, H., & Park, G. (1991) *Tetrahedron 47*, 2629.
Williams, R. M., Glinka, T., Flanagan, M. E., Gallegos, R., Coffman, H., & Pei, D. (1992) *J. Am. Chem. Soc. 114*, 733.
Zafirou, O. C., & Bonneau, R. (1987) *Photochem. Photobiol. 45*, 723.